



bioengineering

Advances in Polyhydroxyalkanoate (PHA) Production, Volume 3

Edited by
Martin Koller

Printed Edition of the Special Issue Published in *Bioengineering*

Advances in Polyhydroxyalkanoate (PHA) Production, Volume 3

Advances in Polyhydroxyalkanoate (PHA) Production, Volume 3

Editor

Martin Koller

MDPI • Basel • Beijing • Wuhan • Barcelona • Belgrade • Manchester • Tokyo • Cluj • Tianjin



Editor

Martin Koller
Research Management and
Service, c/o Institute of
Chemistry, University of Graz
Austria

Editorial Office

MDPI
St. Alban-Anlage 66
4052 Basel, Switzerland

This is a reprint of articles from the Special Issue published online in the open access journal *Bioengineering* (ISSN 2306-5354) (available at: https://www.mdpi.com/journal/bioengineering/special_issues/PHA3).

For citation purposes, cite each article independently as indicated on the article page online and as indicated below:

LastName, A.A.; LastName, B.B.; LastName, C.C. Article Title. <i>Journal Name</i> Year , <i>Volume Number</i> , Page Range.

ISBN 978-3-0365-5039-8 (Hbk)

ISBN 978-3-0365-5040-4 (PDF)

Cover image courtesy of Martin Koller

© 2022 by the authors. Articles in this book are Open Access and distributed under the Creative Commons Attribution (CC BY) license, which allows users to download, copy and build upon published articles, as long as the author and publisher are properly credited, which ensures maximum dissemination and a wider impact of our publications.

The book as a whole is distributed by MDPI under the terms and conditions of the Creative Commons license CC BY-NC-ND.

Contents

About the Editor	vii
Preface to “Advances in Polyhydroxyalkanoate (PHA) Production, Volume 3”	ix
Martin Koller Advances in Polyhydroxyalkanoate (PHA) Production, Volume 3 Reprinted from: <i>Bioengineering</i> 2022, 9, 328, doi:10.3390/bioengineering9070328	1
Evgeniy G. Kiselev, Aleksey V. Demidenko, Natalia O. Zhila, Ekaterina I. Shishatskaya and Tatiana G. Volova Sugar Beet Molasses as a Potential C-Substrate for PHA Production by <i>Cupriavidus necator</i> Reprinted from: <i>Bioengineering</i> 2022, 9, 154, doi:10.3390/bioengineering9040154	9
Young-Cheol Chang, M. Venkateswar Reddy, Kazuma Imura, Rui Onodera, Natsumi Kamada and Yuki Sano Two-Stage Polyhydroxyalkanoates (PHA) Production from Cheese Whey Using <i>Acetobacter pasteurianus</i> C1 and <i>Bacillus</i> sp. CYR1 Reprinted from: <i>Bioengineering</i> 2021, 8, 157, doi:10.3390/bioengineering8110157	29
Xenie Kourilova, Iva Pernicova, Michaela Vidlakova, Roman Krejcirik, Katerina Mrazova, Kamila Hrubanova, Vladislav Krzyzanek, Jana Nebesarova and Stanislav Obruca Biotechnological Conversion of Grape Pomace to Poly(3-hydroxybutyrate) by Moderately Thermophilic Bacterium <i>Tepidimonas taiwanensis</i> Reprinted from: <i>Bioengineering</i> 2021, 8, 141, doi:10.3390/bioengineering8100141	53
Vera Lambauer and Regina Kratzer Lab-Scale Cultivation of <i>Cupriavidus necator</i> on Explosive Gas Mixtures: Carbon Dioxide Fixation into Polyhydroxybutyrate Reprinted from: <i>Bioengineering</i> 2022, 9, 204, doi:10.3390/bioengineering9050204	67
Kenji Tanaka, Kazumasa Yoshida, Izumi Orita and Toshiaki Fukui Biosynthesis of Poly(3-hydroxybutyrate-co-3-hydroxyhexanoate) from CO ₂ by a Recombinant <i>Cupriavidus necator</i> Reprinted from: <i>Bioengineering</i> 2021, 8, 179, doi:10.3390/bioengineering8110179	85
Katharina Meixner, Christina Daffert, Lisa Bauer, Bernhard Drosig and Ines Fritz PHB Producing Cyanobacteria Found in the Neighborhood—Their Isolation, Purification and Performance Testing Reprinted from: <i>Bioengineering</i> 2022, 9, 178, doi:10.3390/bioengineering9040178	95
Philipp Doppler, Christoph Gasser, Ricarda Kriechbaum, Ardita Ferizi and Oliver Spadiut In Situ Quantification of Polyhydroxybutyrate in Photobioreactor Cultivations of <i>Synechocystis</i> sp. Using an Ultrasound-Enhanced ATR-FTIR Spectroscopy Probe Reprinted from: <i>Bioengineering</i> 2021, 8, 129, doi:10.3390/bioengineering8090129	125
Alan Werker, Laura Lorini, Marianna Villano, Francesco Valentino and Mauro Majone Modelling Mixed Microbial Culture Polyhydroxyalkanoate Accumulation Bioprocess towards Novel Methods for Polymer Production Using Dilute Volatile Fatty Acid Rich Feedstocks Reprinted from: <i>Bioengineering</i> 2022, 9, 125, doi:10.3390/bioengineering9030125	135
Milos Kacanski, Lukas Pucher, Carlota Peral, Thomas Dietrich and Markus Neureiter Cell Retention as a Viable Strategy for PHA Production from Diluted VFAs with <i>Bacillus megaterium</i> Reprinted from: <i>Bioengineering</i> 2022, 9, 122, doi:10.3390/bioengineering9030122	161

V. Uttej Nandan Reddy, S. V. Ramanaiah, M. Venkateswar Reddy and Young-Cheol Chang Review of the Developments of Bacterial Medium-Chain-Length Polyhydroxyalkanoates (mcl-PHAs) Reprinted from: <i>Bioengineering</i> 2022, 9, 225, doi:10.3390/bioengineering9050225	173
Lucas Vinicius Santini Ceneviva, Maierwufu Mierzati, Yuki Miyahara, Christopher T. Nomura, Seiichi Taguchi, Hideki Abe and Takeharu Tsuge Poly(3-mercaptopropionate), a Novel α -Methylated Bio-Polythioester with Rubber-like Elasticity, and Its Copolymer with 3-hydroxybutyrate: Biosynthesis and Characterization Reprinted from: <i>Bioengineering</i> 2022, 9, 228, doi:10.3390/bioengineering9050228	197
Liane Meneses, Asiyah Esmail, Mariana Matos, Chantal Sevrin, Christian Grandfils, Susana Barreiros, Maria A. M. Reis, Filomena Freitas and Alexandre Paiva Subcritical Water as a Pre-Treatment of Mixed Microbial Biomass for the Extraction of Polyhydroxyalkanoates Reprinted from: <i>Bioengineering</i> 2022, 9, 302, doi:10.3390/bioengineering9070302	213
Lionel F. Longé, Laurent Michely, Antoine Gallos, Agustin Rios De Anda, Henri Vahabi, Estelle Renard, Michel Latroche, Florent Allais and Valérie Langlois Improved Processability and Antioxidant Behavior of Poly(3-hydroxybutyrate) in Presence of Ferulic Acid-Based Additives Reprinted from: <i>Bioengineering</i> 2022, 9, 100, doi:10.3390/bioengineering9030100	225
Laura Brelle, Estelle Renard and Valerie Langlois Antioxidant Network Based on Sulfonated Polyhydroxyalkanoate and Tannic Acid Derivative Reprinted from: <i>Bioengineering</i> 2021, 8, 9, doi:10.3390/bioengineering8010009	241
Martin Koller and Anindya Mukherjee A New Wave of Industrialization of PHA Biopolyesters Reprinted from: <i>Bioengineering</i> 2022, 9, 74, doi:10.3390/bioengineering9020074	253

About the Editor

Martin Koller

Martin Koller was awarded his PhD degree by Graz University of Technology, Austria, for his thesis on polyhydroxyalkanoate (PHA) production from dairy surplus streams which was enabled by the EU-project WHEYPOL (*“Dairy industry waste as source for sustainable polymeric material production”*), supervised by Gerhart Braunegg, one of the most eminent PHA pioneers. As senior researcher, he worked on bio-mediated PHA production, encompassing development of continuous and discontinuous fermentation processes, and novel downstream processing techniques for sustainable PHA recovery. His research focused on cost-efficient PHA production from surplus materials by bacteria and haloarchaea and, to a minor extent, to the development for PHA for biomedical use.

He currently holds more than 90 Web-of-science listed articles in high ranked scientific journals (h-index 36), authored about 20 chapters in scientific books, edited eight scientific books and seven journal special issues on PHA, gave plenty of invited and plenary lectures at scientific conferences, and supports the editorial teams of several distinguished journals.

Moreover, Martin Koller coordinated the EU-FP7 project ANIMPOL (*“Biotechnological conversion of carbon containing wastes for eco-efficient production of high added value products”*), which, in close cooperation between academia and industry, investigated the conversion of animal processing industry’s waste streams towards structurally diversified PHA and follow-up products. In addition to PHA exploration, he was also active in microalgal research and in biotechnological production of various marketable compounds from renewables by yeasts, chlorophyta, bacteria, archaea, fungi or lactobacilli.

At the moment, Martin Koller is active as research and project manager for the Institute of Chemistry at University of Graz, lecturer at the FH Joanneum (University of Applied Sciences, Graz), and external supervisor for PHA-related projects.

Preface to “Advances in Polyhydroxyalkanoate (PHA) Production, Volume 3”

In 2017, the first Special Issue on “*Advances in Polyhydroxyalkanoate (PHA) Production*” was launched by *Bioengineering*, followed by a second volume in 2019.

At present, the topics and motivations that drove the research presented in these first volumes, namely the growing piles of plastic waste, microplastic formation, increasing atmospheric CO₂ levels, and climate change, have become even more pressing. The global production of highly recalcitrant, full-carbon-backbone plastic of fossil origin already surpasses 400 Mt each year, with insufficient recycling systems and ongoing plastic pollution of the land, rivers, lakes and oceans. In addition to non-degradable macroplastic waste, it was recently scientifically confirmed that micro- and nanoplastic particles not only climb up the food chains and endanger diverse sensitive ecosystems, but are also omnipresent in different organs, tissues and liquids of the human body, with still unpredictable health risks. When incinerated to generate energy, waste from inexpensive plastics releases surplus CO₂, thus fueling global warming and climate change. The consequences of the latter are conspicuous for everybody, with the rapid disappearance of glaciers, growing number of devastating flood disasters, increasing frequency of extensive forest fires, threat of water scarcity connected to the retreat of steppe- and even alpine lakes, and innumerable human heat victims. Finally, the current global political situation, mainly provoked by the Russian Federation’s disgraceful attack on Ukraine, means that fossil feedstock for energy generation, plastic manufacturing, or other applications, is becoming increasingly unaffordable. Accordingly, the reserves of fossil feedstock, the raw materials that global industry rely on, are no longer accessible! This means that biobased alternatives are indispensable, especially on an industrial scale.

All these prevailing issues gave reason to initiate a third Special Issue on the hot topic of microbial biopolyesters. The contributing research groups placed special emphasis on the emerging aspects connected with polyhydroxyalkanoate (PHA) biopolyesters, which are biobased, biosynthesized, biodegradable, compostable, and biocompatible in nature; as guest editor, I am most grateful to all the contributing authors!

Looking at individual articles, it is clear that the current research in PHA biopolyesters focusses on various aspects:

First, microbiology is still at the forefront; the number of new, powerful PHA production strains, isolated from diverse habitats, is steadily increasing. This topic is covered in this Special Issue by a new heterotrophic, thermophilic bacterium, which is cultivable under limited sterility requirements and possesses promising PHA biosynthesis features, as well as a long-term study on the isolation and characterization of new cyanobacteria, which accumulate PHA and other marketable bioproducts based on CO₂ conversion. A separate contribution presents a novel method for the real-time *in situ* monitoring of PHA biosynthesis in growing cyanobacterial cultures, which enables bioprocess intensification. Other autotrophic PHA production processes are described in this issue using a hydrogen-oxidizing, non-phototrophic wild-type strain for PHA homopolyester biosynthesis on explosive gas mixtures, in compliance with safety precautions. Genetically engineered strains with newly constructed PHA biosynthesis pathways were applied to the autotrophic production of PHA heteropolyesters with enhanced material properties.

The utilization of inexpensive waste- and surplus materials as feedstock for PHA production, a central topic in vols. 1 and 2 of this Special Issue series, is still spotlighted, not only as a means of reducing PHA production cost, but also as a way to upcycle existing carbon-rich industrial waste streams, especially those connected to food production. Contributions to the current Special Issue

use by-products of the wine industry, sugar beet processing, and cheese manufacturing as substrates for PHA biosynthesis.

Regarding PHA's material properties, the emerging class of *mcl*-PHA, an elastomeric biopolyester group, is comprehensively covered. Moreover, this issue covers the very first presentation of a new class of biosynthesized branched sulfur-containing polyesters with rubber-like properties. The development of functional PHA-based composited and blends, *post-synthesis* PHA modification, and the manufacturing of high-end PHA-based products with potential applicability in the biomedical field are additional topics of high significance, which are not neglected in this issue.

Advanced bioprocess engineering is explicitly covered by the introduction of a new cell recycling cultivation strategy, which allows for high-throughput PHA production based on highly diluted substrate streams using a Gram-positive production strain. Moreover, the emerging utilization of mixed microbial cultures, such as those present in wastewater treatment plants, is covered by a novel strategy to efficiently produce PHA from mixed cultures using highly diluted fatty acid streams. In the context of PHA recovery from biomass, the central stage of PHA downstream processing, supercritical water is used as an inexpensive, non-toxic agent to replace the hazardous and expensive organic solvents typically used in a contribution to extract these intracellular bioproducts.

Finally, past and current endeavors towards PHA commercialization are presented, focusing on realistic estimations of PHA productivity that could be expected in future. This compilation of industrial PHA production processes is connected to the comparison between the beneficial material features of most promising types of PHA that are available on the market at present, and a critical assessment of expected market prospects.

In their entirety, these contributions draw a holistic and up-to-date picture of the current advancements in the research on microbial PHA biopolyesters. Contributing groups have either been established in the PHA community for a long time, often considered real pioneers, or are among the most ambitious new teams active in this scientific field at present. In future, it will be exciting to observe the progress that is expected to emerge from the hopefully seminal contributions collected in this Special Issue. We should remain optimistic that the presented works will inspire future activities and, most importantly, help to solve the pressing threats mentioned at the beginning of this preface.

Enjoy your reading!

Martin Koller
Editor

Editorial

Advances in Polyhydroxyalkanoate (PHA) Production, Volume 3

Martin Koller^{1,2}

¹ Institute of Chemistry, University of Graz, NAWI Graz, Heinrichstrasse 28/IV, 8010 Graz, Austria; martin.koller@uni-graz.at; Tel.: +43-316-380-5463

² ARENA—Arbeitsgemeinschaft für Ressourcenschonende und Nachhaltige Technologien, Inffeldgasse 21b, 8010 Graz, Austria

Abstract: Steadily increasing R&D activities in the field of microbial polyhydroxyalkanoate (PHA) biopolyesters are committed to growing global threats from climate change, aggravating plastic pollution, and the shortage of fossil resources. These prevailing issues paved the way to launch the third Special Issue of *Bioengineering* dedicated to future-oriented biomaterials, characterized by their versatile plastic-like properties. Fifteen individual contributions to the Special Issue, written by renowned groups of researchers from all over the world, perfectly mirror the current research directions in the PHA sector: inexpensive feedstock like carbon-rich waste from agriculture, mitigation of CO₂ for PHA biosynthesis by cyanobacteria or wild type and engineered “knallgas” bacteria, powerful extremophilic PHA production strains, novel tools for rapid in situ determination of PHA in photobioreactors, modelling of the dynamics of PHA production by mixed microbial cultures from inexpensive raw materials, enhanced bioreactor design for high-throughput PHA production by sophisticated cell retention systems, sustainable and efficient PHA recovery from biomass assisted by supercritical water, enhanced processing of PHA by application of novel antioxidant additives, and the development of compatible biopolymer blends. Moreover, elastomeric medium chain length PHA (*mcl*-PHA) are covered in-depth, inter alia, by introduction of a novel class of bioactive *mcl*-PHA-based networks, in addition to the first presentation of the new rubber-like polythioester poly(3-mercapto-2-methylpropionate). Finally, the present Special Issue is concluded by a critical essay on past, ongoing, and announced global endeavors for PHA commercialization.

Citation: Koller, M. Advances in Polyhydroxyalkanoate (PHA) Production, Volume 3. *Bioengineering* **2022**, *9*, 328. <https://doi.org/10.3390/bioengineering9070328>

Received: 13 July 2022

Accepted: 17 July 2022

Published: 19 July 2022

Publisher’s Note: MDPI stays neutral with regard to jurisdictional claims in published maps and institutional affiliations.



Copyright: © 2022 by the author. Licensee MDPI, Basel, Switzerland. This article is an open access article distributed under the terms and conditions of the Creative Commons Attribution (CC BY) license (<https://creativecommons.org/licenses/by/4.0/>).

Keywords: autotrophs; biopolyesters; CO₂; cyanobacteria; industrialization; *mcl*-PHA; polyhydroxyalkanoate (PHA); polymer processing; polymer recovery; process design

1. Introduction

Waste consisting of contemporarily used full carbon–carbon backbone plastics of fossil origin is very resistant to biodegradation, which generates enduring impairment to the marine and terrestrial environment [1]. Estimates of global emissions of plastic waste to fresh and sea water range from 9 to 23 million metric tons annually, the same order of magnitude as calculated for plastic waste emitted into the land. By 2025, these quantities are expected to double. All conventional plastic ever made either has been incinerated to energy and surplus CO₂, or is still present on our planet; today, roughly 6 Gt of persistent macro-, micro-, and nano-plastic waste are accumulated in our ecosystems, also in living organisms and the trophic chains. These figures impressively illustrate that biobased and biodegradable solutions are indispensable needed [2].

As a potential remedy, so called “bioplastics” are strongly emerging today; however, we should handle this expression with care: Not all “bioplastics” are definitely “green” materials, hence, at the same time biobased, biosynthesized, biodegradable, and biocompatible. Moreover, “plastics”, by definition, are xenobiotic materials not occurring in nature, so the expression “bioplastics” is rather ambiguous. Poly(butylene adipate terephthalate)

(PBAT), poly(lactic acid) (PLA), and thermoplastic starch (TPS) are the current “bioplastic” market leaders; for microbial polyhydroxyalkanoate (PHA) biopolyesters, a current share of not even 2% of the entire bioplastic market, reaching an annual production of not more than approximately 40,000 to 50,000 tons in 2021, is estimated. However, until 2026, the entire “bioplastic” production is expected to increase to about 7.6 million tons, more than twice the value for 2020. In 2026, PHA, the only truly biological (biobased and biosynthesized) and circular (biodegradable and compostable) group of materials among all products commercialized as “bioplastic” will already be among the top 5 “bioplastics”, with an expected share of 6.4% on the “bioplastics” market, which will correspond to about 0.5 million annual tons; hence, the tenfold production quantity of today is expected to be reached in just five years [3]!

With regard to these auspicious prospects, PHA can already be considered typical materials of “Industrial-” or “White Biotechnology”—hence, the large-scale manufacturing of bulk products starting from renewable resources by the action of living organisms (predominantly microbes) or parts thereof (enzymes). Large-scale PHA manufacturing will offer biodegradable materials for diverse packaging purposes in the food and non-food sector, as well as for numerous additional applications, such as in the pharmaceutical and biomedical field, for replacement of petrochemical microplastic in cosmetics, or even for bioremediation [4].

This positive development towards a relevant presence of PHA-based materials on the market in the near future is enabled by the enormous global efforts witnessed today in research and development on these materials. Concerted and synergistic actions of (system) biologists, microbiologists, (computational) biotechnologists, multi-omics experts, chemical engineers, material scientists, and market experts contribute to the rapid development of these microbial materials. The present third Special Issue for *Bioengineering* on advances in PHA production collects exemplary topical studies covering these fields; they give an excellent insight into the global progress in the field of these truly circular biopolyesters.

2. Individual Contributions

Since decades, the exploration of inexpensive feedstock for PHA production is regarded key to decrease the still too high PHA production price [5]. While considerable progress has already been achieved in this field, optimization of PHA production from inexpensive, abundantly available heterotrophic raw materials, especially of agro-industrial origin, from the greenhouse gas methane, and from surplus CO₂, especially from industrial effluent gases, is still ongoing [6].

In the current Special Issue, organic second-generation raw materials from dairy industry, viticulture, and sugar beet processing were studied. Kiselev and colleagues investigated PHA biosynthesis by the wild type bacterial strain *Cupriavidus necator* B-10646 on enzymatic hydrolysates of sugar beet (*Beta vulgaris*) molasses; it was shown that the strain readily converted generated monomeric sugars for biomass growth and PHA biosynthesis. By establishing an optimized feeding strategy and culture medium composition, the authors were able to obtain up to 80 wt.% PHA in biomass. Interestingly, due to minor amounts of components present in hydrolyzed molasses acting as 3-hydroxyvalerate (3HV) precursors, the obtained PHA contained certain amounts of 3HV monomers, in addition to 3-hydroxybutyrate (3HB) as a main building block; composition of such high-quality PHA copolyesters with enhanced processability was finally fine-tuned by co-feeding appropriate amounts of precursor compounds [7].

Chang and colleagues utilized a surplus product from cheese and dairy industry for PHA production: Lactose present in raw cheese whey at a concentration of about 4–5 wt.% was biotechnologically converted in a first step to acetic acid by the aerobic bacterial strain *Acetobacter pasteurianus* C1. In a second step, generated acetic acid was transformed to the PHA homopolymer poly(3-hydroxybutyrate) (P(3HB)) by *Bacillus* sp. CYR-1, a novel Gram-positive PHA production strain. After the removal of excess protein from raw cheese whey, PHA production was increased to more than 400 mg/L. In their conclusion, authors

emphasized that this two-stage process might be beneficial for conversion of such highly diluted feed streams like whey to PHA, without the need for whey pre-treatment by time-, energy-, and material-demanding lactose hydrolysis, and without prior ultrafiltration to concentrate lactose [8].

In the context of novel PHA production strains, such organisms thriving at extreme environmental temperature, salinity, heavy metal load, or pH-value conditions attract increasing attention for PHA biosynthesis under low energy requirements: They can be cultivated under such extreme conditions under restricted sterility precautions without risking the loss of cultivation batches due to microbial contamination [9]. Such concepts are currently termed “Next Generation Industrial Biotechnology” (NGIB) [10], and are already in use for PHA manufacturing by extremophilic engineered strains, mainly halophilic *Halomonas* sp., in inexpensive non-sterile media and simple, open, continuous cultivation batches [11]. In this aspect, Kourilova and co-workers converted aqueous extracts of grape pomace, an agro-industrial waste product from viticulture, to P(3HB); the thermophilic strain *Tepidimonas taiwanensis* LMG 22826 was used as production strain for these cultivation experiments. PHA production capacity of this organism was studied both on the level of phenotype and genotype. It turned out that the strain harbors a Class I PHA synthase similar to other well-known short-chain-length PHA (*scl*-PHA) producers like *C. necator*. Best results for P(3HB) production by this strain were obtained using extract of pomace remaining from pressing Veltliner grapes; here, almost 5 g/L biomass, containing about 48 wt.% P(3HB), were achieved within 72 h of cultivation at a thermophilic cultivation temperature of 50 °C, which is far above the typically mesophilic temperature optimum of established PHA production strains and most potential microbial contaminants [12].

In the context of autotrophic PHA biosynthesis, Lambauer and Kratzer studied P(3HB) homopolymer formation by the well-known aerobic non-phototrophic hydrogen-oxidizing strain *C. necator* H16 on mixtures of the gases H₂, O₂, and CO₂. Special emphasis in this study was dedicated to safety aspects when handling such explosive “knallgas” mixtures according to valid safety standards and Good Laboratory Practice principles; this was realized by operating the process in a simple explosion-proof lab-scale bioreactor placed in a stable and secure way in a fume hood. Cultivations were carried out by supplying the carbon source CO₂ and the reducing agent H₂ in excess, while controlling O₂ availability as the growth-determining factor. Remarkably, best results for P(3HB) biosynthesis were obtained when keeping the gas composition within the explosion limits of O₂/H₂ mixtures. About 13 g/L biomass, containing an expedient P(3HB) mass fraction of 80% was generated during 90 h of cultivation. Notably, no temperature- or pH-control was needed in these cultivation setups. This promising outcome might make this study pioneering for further autotrophic P(3HB) production batches by non-phototrophs, also on larger scale and by using industrial effluent gas [13]. A similar study by Tanaka *et al.* investigated the autotrophic biosynthesis of the readily marine biodegradable PHA copolyester poly(3-hydroxybutyrate-co-3-hydroxyhexanoate) (P(3HB-co-3HHx)), a PHA copolyester of increasing industrial significance to produce various single-use plastic articles, by differently engineered *C. necator* strains. Also in this study, CO₂ was used as the sole carbon source. These cultivations were carried out in simple Erlenmeyer flasks, equipped merely with a sterile filter, a tube, and a pinchcock. P(3HB-co-3HHx) was accumulated at high intracellular fractions, with high molar shares of 3HHx found in obtained copolyester samples. Finally, it was possible to control the 3HHx fraction in P(3HB-co-3HHx) to a value of 11 mol%, which is desired for optimum processability of the material; this was achieved by transforming cells with the plasmid pBPP-crr_{Me}J_{Ac}-emd harboring *A. caviae scl*-PHA specific PhaJ [14]. In addition to non-photoautotrophic “knallgasbacteria” able to build up new biomass from CO₂ and H₂, the oxygenic group of cyanobacteria is able to fix CO₂ phototrophically by resorting to the energy provided by sunlight (“photooxybacteria”). Beside other marketable bio-products like precious pigments (especially phycobilins) or diverse bioactive compounds, many cyanobacteria are also described as proficient photoautotrophic PHA producers [15]. Therefore, the quest for new, robust PHA-accumulating cyanobacteria, adapted to the

most diverse habitats, is steadily ongoing. In a long-term study, Meixner and associated researchers took samples from 25 different locations as remote as a geyser in Iceland, an Argentinian glacier lake, a snow field in Greenland, a wet rock in the Dolomite mountains, and a dammed lake at the Iberian Peninsula. A total of five years was dedicated by the authors to sample collection, strain isolation and purification by sophisticated methods like antibiotics supply and benefitting from cyanobacteria's phototaxis, identification, and characterization of new microbial strains. These isolation studies resulted in a total of 71 primary cultures, 34 of which, containing 19 different cyanobacteria, were thriving in a stable manner after multiple transfers into a fresh medium. Four among these isolated cyanobacteria were shown to accumulate PHA in a simple home-made tubular photobioreactor, and two among them were successfully cultivated even under non-axenic, open cultivation conditions without the need for artificial light supply. Surprisingly, it was strain *Synechocystis* sp. IFA-3, an organism isolated from a fire pond just around the corner of the researchers' institute near Vienna, which turned out to hold highest promise as proficient new PHA producer among all organism isolated by the authors from the magnitude of samples collected all over the world [16]. Also in the nexus of cyanobacteria, Doppler et al. developed a new *in situ* method for fast and reliable determination of PHA in growing phototrophic cultures. Such approaches are of increasing importance for a reliable and *in-real-time* process monitoring and rapid adaptation of process conditions. In this study, spectroscopic probes supported by ultrasound particle traps were used as a viable technology for *in-line*, nondestructive, and real-time process analytics in photobioreactors. In details, spectroscopic attenuated total reflection Fourier-transformed mid-infrared (ATR-FTIR) spectra for P(3HB) and glycogen, two characteristic storage compounds in the selected model cyanobacterium *Synechocystis* sp. PCC 6714, were enhanced by ultrasonic particle manipulation, and used for *in situ* quantification of these compounds throughout the process [17].

Conversion of volatile fatty acids (VFAs), obtained by anaerobic transformation of organic residues, by mixed microbial cultures (MMCs) to PHA is another emerging tool to efficiently produce PHA from various waste streams [18]. Werker and colleagues addressed a well-known shortcoming of this approach: Feed streams of VFAs are typically highly diluted, thus preventing sufficient PHA productivity. To overcome this problem, authors established a novel flow-through bioprocess, which allows a trade-off between a maximum substrate inflow and a maximum substrate-to-PHA conversion (minimum outflow of not utilized substrate). To reach this goal, dynamics of upshift and downshift respiration kinetics were evaluated for MMCs on laboratory and pilot scale. Despite a constant influent substrate flow, biomass recycling into a mixing zone, which was engineered to contain higher substrate concentration, allowed for running the process at optimum PHA productivity, without compromising substrate utilization efficiency [19].

Kacanski and associates also addressed the fact that the typical high dilution of feed streams like VFAs solutions has a negative impact on productivity in fed-batch cultivation setups; the high feed stream volumes to be added into the bioreactor would excessively dilute the cultivation broth, and soon exceed the maximum allowable working volume in the bioreactor [20]. An option to solve this issue is to resort to cell retention systems, as shown before for PHA production on diverse highly diluted substrates in other studies [21–24]. In this *Bioengineering* Special Issue, Kacanski et al. presented a cell recycle fed-batch system for P(3HB) production by the versatile Gram-positive PHA producer *Bacillus megaterium* uyuni S29 from the VFA acetic acid. In this setup, a crossflow microfiltration membrane module was used to recycle active cell biomass (retentate fraction) into the bioreactor, while separating the permeate fraction (substrate-poor supernatant) from the system. An indirect pH-stat feeding regime, coupled to depletion of the substrate acetic acid, was successfully used for feed control in order to keep the substrate (acetate) concentration in an optimum range. A final biomass concentration of 19 g/L, harboring about 70 wt.% P(3HB), was obtained after 72 h of operation using this setup. The authors suggest follow-up studies to optimize the overall productivity by an enhanced nitrogen source feeding regime in order

to further boost the concentration of biocatalytically active *Bacillus* cells for subsequent accumulation of PHA as a secondary, intracellular storage metabolite [20].

In addition to well-described *scl*-PHA, which consist of monomers made up by three to five carbon atoms, another emerging group of PHA biopolyesters was comprehensively reviewed for this Special Issue by Reddy and colleagues: the family of medium-chain-length PHAs (*mcl*-PHA), composed of monomers with six to 14 carbon atoms. Compared to *scl*-PHA, these biopolyesters are characterized by lower degree of crystallinity, glass transition temperature, and melting temperature. Different to *scl*-PHA production by strains like *C. necator*, which resorts to Class I PHA synthases, *mcl*-PHA biosynthesis requires special PHA synthase enzymes from Class II, and, in contrast to most representatives of *scl*-PHA, which have the properties of thermoplastics, *mcl*-PHA typically are elastomeric, latex-like, often sticky materials. Monomers building up *mcl*-PHA can be saturated or unsaturated; the latter, in turn, allows for post-synthetic modification by chemical or enzymatic reactions. The presented review article focuses on different carbon sources and at different operation modes for *mcl*-PHA production, on recent developments of methods for recovery of *mcl*-PHA from biomass, on their particular material properties, challenges during processing, applications in different sectors, and on their realized production on (semi)industrial scale in different global regions [25].

A completely new biopolyester type, structurally strongly related with PHA, was introduced years ago by the group of Alexander Steinbüchel in Münster: so-called poly(thioesters) (PTEs), which are produced by the enzymatic machinery (Class I PHA synthases) of established PHA-accumulating microbes when supplied with chemosynthetically produced mercaptoalkanoic acids [26]. It was demonstrated that, in contrast to PHA's oxoester bonds, thioester bonds in PTEs are highly recalcitrant towards microbial degradation; only hybrid-type poly(oxo-thioesters) like poly(3-hydroxybutyrate-*co*-3-mercaptopropionate) (P(3HB-*co*-3MP)) or poly(3-hydroxybutyrate-*co*-3-mercaptobutyrate), but not PTE homopolyesters like poly(3MP) or poly(3MB) undergo biodegradation by PHA depolymerases, e.g., by depolymerase enzymes from *Schlegelella thermodepolymerans* [27]. In this Special Issue, Ceneviva and colleagues present the homopolythioester poly(3-mercapto-2-methylpropionate) (P(3M2MP)), a new α -methylated PTE with high rubber-like elasticity (elongation at break of 2600%), and its copolyester with 3HB (P(3HB-*co*-3M2MP)). The authors investigated biosynthesis of these new materials from 3-mercapto-2-methylpropionic acid as a structurally related precursor by engineered *Escherichia coli* LSBJ, and provided in-depth characterization of the material properties. It was shown that higher 3M2MP fraction in P(3HB-*co*-3M2MP) copolyesters caused lower molecular weight, and the materials became less crystalline, softer, more flexible, and revealed lower glass transition temperature and higher elongation at break, in addition to higher light transparency. Remarkably, it was shown that the rubber-like properties of this new PTE differ from those of previously described, not branched PTEs, evidencing that material properties can be further fine-tuned by introducing α -methylated thioester monomers. For follow-up studies, the authors plan to assess an eventual biodegradability of these materials [28].

After the biotechnological conversion of PHA-rich biomass, recovery of PHA from biomass by efficient, inexpensive, and sustainable approaches constitutes a key aspect of the entire PHA production process. In principle, methods for extraction of PHA from biomass, for digestion of the non-PHA biomass, or combinations thereof are described [29]. A novel PHA isolation approach based on the use of supercritical water (SBW) was developed by Meneses and colleagues. These authors used SBW at different temperatures to extract PHA from biomass of a mixed microbial culture cultivated on fruit waste in pilot scale setups. A temperature of 150 °C was feasible for readily decomposing the non-PHA biomass without excessively damaging PHA's macromolecular structure. A polymer purity of 70% was obtained using SBW as sole PHA recovery agent; it was possible to increase purity to 80% by adding minor quantities of sodium hypochlorite solution for better solubilization of non-PHA biomass. Recovered biopolymer samples displayed some reduction in molecular mass and higher polydispersity than parallel samples extracted by

the well-established, yet health-hazardous chloroform method. However, authors suggest that PHA obtained by the novel SBW-based recovery process might be of sufficient quality for those applications where excellent mechanical properties are not needed, such as use as additives, softeners or as low-molecular mass oligomers to be used for the preparation of graft or block copolymers [30].

The restricted processability of the homopolyester P(3HB), the best described and most frequently occurring natural PHA biopolyester, originates from its high crystallinity, brittleness, and low difference between the temperature of melting and onset of thermal degradation (too narrow “window of processability”). Addition of plasticizers is known a remedy to improve the mechanical properties of P(3HB) [31]. Such novel additives with antioxidative properties were developed and tested by Longé et al.; these authors esterified ferulic acid with butanediol, pentanediol, or glycerol, and used obtained esters for preparation of P(3HB)-based biocomposites by extrusion. Three hours after extrusion of pristine P(3HB) and the composites, respectively, it was shown that addition of ferulic acid esterified with butanediol to P(3HB) resulted in a strongly enhanced elongation at break from 11% (P(3HB)) to 270% for the composite consisting of 30% P(3HB) and 70% ester, reduced stress at break and Young’s modulus, and a ten-fold increase of the window of processability. Interestingly, this material improvement was not stable over time, but could be recovered by simple thermal treatment of the composite at a temperature below P(3HB)’s melting point, but just above the melting point of the butanediol ester of ferulic acid. Moreover, the high thermal stability of the additive further resulted in an increase in the fire retardancy property of the P(3HB)/ferulic ester composite material, while ferulic acid’s phenolic structure induced antioxidative properties as shown by radical scavenging tests. The authors suggest the need to study the suitability of prepared P(3HB)/additive composites, which are less hydrophobic than native P(3HB), for different packaging purposes [32].

Post-synthetic modification of microbial PHA to generate novel, functional materials becomes of increasing significance for improvement of performance of these bioproducts [33]. Brelle and colleagues prepared a novel class of *mcl*-PHA-based gels by using ionic interactions. First, highly hydrophilic sulfonated *mcl*-PHA derivatives were prepared from *mcl*-PHA samples with pending unsaturated side chains (poly(3-hydroxyoctanoate-*co*-33%-3-hydroxyundecenoate)); this was accomplished by thiol-ene reaction in presence of sodium-3-mercapto-1-ethanesulfonate. Such sulfonated *mcl*-PHA derivatives were crosslinked by bivalent inorganic cations or by ammonium derivatives of gallic acid or tannic acid. The nature of the cations highly determined the formation of the crosslinked networks. Using Ca^{2+} as bivalent cation, a network of low viscoelasticity was formed. With gallic acid derivatives, no network formation was possible, while the mechanical properties strongly increased in the presence of tannic acid derivatives. Due to the presence of tannic acid, gels prepared this way displayed high antioxidant activity and remained stable for several months. The authors suggest these novel *mcl*-PHA-based networks for future use as active soft biomaterials in biomedical applications [34].

The final contribution to this Special Issue reviews current activities aiming at commercialization of PHA biopolyesters. Indeed, several companies have already started to produce and use PHA for a variety of applications. Currently, at least 25 companies and start-ups and more than 30 brand owners are declaring interest in PHA production and application. However, the combined product portfolio of currently active PHA manufacturing companies is still limited to five major types of PHA, namely the homopolyesters P(3HB) and poly(4-hydroxybutyrate) (P(4HB)), and the copolyesters poly(3-hydroxybutyrate-*co*-3-hydroxyvalerate) (P(3HB-*co*-3HV)), poly(3-hydroxybutyrate-*co*-4-hydroxybutyrate) (P(3HB-*co*-4HB)), and poly(3HB-*co*-3HHx), while only one company produces *mcl*-PHA of different composition on a reasonable scale as contract work. Optimistic capacity enlargements from currently estimated 1.5 million t over the next five years have been announced by different companies [35]. It will be fascinating to see the de facto developments on the PHA market during the next few years, in particular whether these enthusiastic industrial announcements can keep up with the actual increases in production and capacity!

3. Conclusions

The contributions to this Special Issue take readers on a journey into topical research activities in the realm of PHA biopolyesters. Aspects as manifold as microbiology, strain isolation, genetic engineering, process design and feeding regimes, in situ PHA quantification, inexpensive feedstocks, hetero- and autotrophic cultivation, novel downstream process strategies, *post synthesis* PHA modification, and preparation of compatible composites and blends are covered. As guest editor, I am optimistic that this third PHA-related *Bioengineering* Special Issue at hand will again spark inspiration and ideas for further research and development activities in the field of these fascinating biomaterials.

Funding: This research received no external funding.

Acknowledgments: Guest editor M.K. would like to express his deep gratitude to all involved contributors for their submissions to this Special Issue of *Bioengineering*.

Conflicts of Interest: The authors declare no conflict of interest.

References

- MacLeod, M.; Arp, H.P.H.; Tekman, M.B.; Jahnke, A. The global threat from plastic pollution. *Science* **2021**, *373*, 61–65. [CrossRef] [PubMed]
- Geyer, R. Production, use, and fate of synthetic polymers. In *Plastic Waste and Recycling*; Letcher, T.M., Ed.; Academic Press: Cambridge, MA, USA, 2020; pp. 13–32. ISBN 978-012-817-880-5.
- Bioplastics Market Data. Available online: <https://www.european-bioplastics.org/market/#> (accessed on 8 July 2022).
- Mukherjee, A.; Koller, M. Polyhydroxyalkanoate (PHA) biopolyesters—Emerging and major products of Industrial Biotechnology. *EuroBiotech J.* **2022**, *6*, 49–60. [CrossRef]
- Guleria, S.; Singh, H.; Sharma, V.; Bhardwaj, N.; Arya, S.K.; Puri, S.; Khatri, M. Polyhydroxyalkanoates production from domestic waste feedstock: A sustainable approach towards bio-economy. *J. Clean. Prod.* **2022**, *340*, 130661. [CrossRef]
- Sen, K.Y.; Baidurah, S. Renewable biomass feedstocks for production of sustainable biodegradable polymer. *Curr. Opin. Green Sustain. Chem.* **2021**, *27*, 100412. [CrossRef]
- Kiselev, E.G.; Demidenko, A.V.; Zhila, N.O.; Shishatskaya, E.I.; Volova, T.G. Sugar beet molasses as a potential C-substrate for PHA production by *Cupriavidus necator*. *Bioengineering* **2022**, *9*, 154. [CrossRef]
- Chang, Y.C.; Reddy, M.V.; Imura, K.; Onodera, R.; Kamada, N.; Sano, Y. Two-stage polyhydroxyalkanoates (PHA) production from cheese whey using *Acetobacter pasteurianus* C1 and *Bacillus* sp. CYR1. *Bioengineering* **2021**, *8*, 157. [CrossRef]
- Obulisamy, P.K.; Mehariya, S. Polyhydroxyalkanoates from extremophiles: A review. *Bioresour. Technol.* **2021**, *325*, 124653. [CrossRef]
- Yu, L.P.; Wu, F.Q.; Chen, G.Q. Next-generation industrial biotechnology—Transforming the current industrial biotechnology into competitive processes. *Biotechnol. J.* **2019**, *14*, 1800437. [CrossRef]
- Wu, F.; Chen, G.Q. Next Generation Industrial Biotechnology (NGIB) for PHA Production. In *The Handbook of Polyhydroxyalkanoates, Kinetics, Bioengineering, and Industrial Aspects*, 1st ed.; Koller, M., Ed.; CRC Press: Boca Raton, FL, USA; Taylor & Francis: Boca Raton, FL, USA, 2020; pp. 405–416. ISBN 978-042-929-663-5.
- Kourilova, X.; Pernicova, I.; Vidlakova, M.; Krejcirik, R.; Mrazova, K.; Hrubanova, K.; Krzyzanek, V.; Nebesarova, J.; Obruca, S. Biotechnological conversion of grape pomace to poly(3-hydroxybutyrate) by moderately thermophilic bacterium *Tepidimonas taiwanensis*. *Bioengineering* **2021**, *8*, 141. [CrossRef]
- Lambauer, V.; Kratzer, R. Lab-scale cultivation of *Cupriavidus necator* on explosive gas mixtures: Carbon dioxide fixation into polyhydroxybutyrate. *Bioengineering* **2022**, *9*, 204. [CrossRef]
- Tanaka, K.; Yoshida, K.; Orita, I.; Fukui, T. Biosynthesis of poly(3-hydroxybutyrate-co-3-hydroxyhexanoate) from CO₂ by a recombinant *Cupriavidus necator*. *Bioengineering* **2021**, *8*, 179. [CrossRef] [PubMed]
- Koller, M. “Bioplastics from microalgae”—Polyhydroxyalkanoate production by cyanobacteria. In *Handbook of Microalgae-Based Processes and Products*, 1st ed.; Jacob-Lopes, E., Manzoni Maroneze, M., Queiroz, M.I., Queiroz Zepka, L., Eds.; Academic Press: Cambridge, MA, USA; Elsevier: Amsterdam, The Netherlands, 2020; pp. 597–645. ISBN 978-012-818-536-0.
- Meixner, K.; Daffert, C.; Bauer, L.; Drosig, B.; Fritz, I. PHB producing cyanobacteria found in the neighborhood—their isolation, purification and performance testing. *Bioengineering* **2022**, *9*, 178. [CrossRef] [PubMed]
- Doppler, P.; Gasser, C.; Kriechbaum, R.; Ferizi, A.; Spadiut, O. In Situ Quantification of polyhydroxybutyrate in photobioreactor cultivations of *Synechocystis* sp. using an ultrasound-enhanced ATR-FTIR spectroscopy probe. *Bioengineering* **2021**, *8*, 129. [CrossRef] [PubMed]
- Morgan-Sagastume, F.; Bengtsson, S.; De Grazia, G.; Alexandersson, T.; Quadri, L.; Johansson, P.; Magnusson, P.; Werker, A. Mixed-culture polyhydroxyalkanoate (PHA) production integrated into a food-industry effluent biological treatment: A pilot-scale evaluation. *J. Environ. Chem. Eng.* **2020**, *8*, 104469. [CrossRef]

19. Werker, A.; Lorini, L.; Villano, M.; Valentino, F.; Majone, M. Modelling mixed microbial culture polyhydroxyalkanoate accumulation bioprocess towards novel methods for polymer production using dilute volatile fatty acid rich feedstocks. *Bioengineering* **2022**, *9*, 125. [[CrossRef](#)]
20. Kacanski, M.; Pucher, L.; Peral, C.; Dietrich, T.; Neureiter, M. Cell retention as a viable strategy for PHA production from diluted VFAs with *Bacillus megaterium*. *Bioengineering* **2022**, *9*, 122. [[CrossRef](#)]
21. Ienczak, J.L.; Schmidell, W.; de Aragão, G.M.F. High-cell-density culture strategies for polyhydroxyalkanoate production: A review. *J. Ind. Microbiol. Biotechnol.* **2013**, *40*, 275–286. [[CrossRef](#)]
22. Blunt, W.; Levin, D.B.; Cicek, N. Bioreactor operating strategies for improved polyhydroxyalkanoate (PHA) productivity. *Polymers* **2018**, *10*, 1197. [[CrossRef](#)]
23. Koller, M. A review on established and emerging fermentation schemes for microbial production of polyhydroxyalkanoate (PHA) biopolyesters. *Fermentation* **2018**, *4*, 30. [[CrossRef](#)]
24. Haas, C.; El-Najjar, T.; Virgolini, N.; Smerilli, M.; Neureiter, M. High cell-density production of poly(3-hydroxybutyrate) in a membrane bioreactor. *New Biotechnol.* **2017**, *37*, 117–122. [[CrossRef](#)]
25. Reddy, V.; Ramanaiah, S.V.; Reddy, M.V.; Chang, Y.C. Review of the developments of bacterial medium-chain-length polyhydroxyalkanoates (mcl-PHAs). *Bioengineering* **2022**, *9*, 225. [[CrossRef](#)] [[PubMed](#)]
26. Wübbeler, J.H.; Steinbüchel, A. New pathways for bacterial polythioesters. *Curr. Opin. Biotechnol.* **2014**, *29*, 85–92. [[CrossRef](#)] [[PubMed](#)]
27. Elbanna, K.; Lütke-Eversloh, T.; Jendrossek, D.; Luftmann, H.; Steinbüchel, A. Studies on the biodegradability of polythioester copolymers and homopolymers by polyhydroxyalkanoate (PHA)-degrading bacteria and PHA depolymerases. *Arch. Microbiol.* **2004**, *182*, 212–225. [[CrossRef](#)]
28. Ceneviva, L.V.S.; Mierzati, M.; Miyahara, Y.; Nomura, C.T.; Taguchi, S.; Abe, H.; Tsuge, T. Poly(3-mercapto-2-methylpropionate), a novel α -methylated bio-polythioester with rubber-like elasticity, and its copolymer with 3-hydroxybutyrate: Biosynthesis and characterization. *Bioengineering* **2022**, *9*, 228. [[CrossRef](#)]
29. Koller, M. Established and advanced approaches for recovery of microbial polyhydroxyalkanoate (PHA) biopolyesters from surrounding microbial biomass. *EuroBiotech J.* **2020**, *4*, 113–126. [[CrossRef](#)]
30. Meneses, L.; Esmail, A.; Matos, M.; Sevrin, C.; Grandfils, C.; Barreiros, S.; Reis, M.A.M.; Freitas, F.; Paiva, A. Subcritical water as a pre-treatment of mixed microbial biomass for the extraction of polyhydroxyalkanoates. *Bioengineering* **2022**, *9*, 302. [[CrossRef](#)]
31. Turco, R.; Santagata, G.; Corrado, I.; Pezzella, C.; Di Serio, M. In vivo and *post-synthesis* strategies to enhance the properties of PHB-based materials: A review. *Front. Bioeng. Biotechnol.* **2021**, *8*, 619266. [[CrossRef](#)] [[PubMed](#)]
32. Longé, L.F.; Michely, L.; Gallos, A.; Rios De Anda, A.; Vahabi, H.; Renard, E.; Latroche, M.; Allais, F.; Langlois, V. Improved processability and antioxidant behavior of poly(3-hydroxybutyrate) in presence of ferulic acid-based additives. *Bioengineering* **2022**, *9*, 100. [[CrossRef](#)]
33. Abd El-malek, F.; Steinbüchel, A. Post-synthetic enzymatic and chemical modifications for novel sustainable polyesters. *Front. Bioeng. Biotechnol.* **2021**, *9*, 817023. [[CrossRef](#)]
34. Brelle, L.; Renard, E.; Langlois, V. Antioxidant network based on sulfonated polyhydroxyalkanoate and tannic acid derivative. *Bioengineering* **2021**, *8*, 9. [[CrossRef](#)]
35. Koller, M.; Mukherjee, A. A new wave of industrialization of PHA biopolyesters. *Bioengineering* **2022**, *9*, 74. [[CrossRef](#)] [[PubMed](#)]

Article

Sugar Beet Molasses as a Potential C-Substrate for PHA Production by *Cupriavidus necator*

Evgeniy G. Kiselev ^{1,2}, Aleksey V. Demidenko ^{1,2}, Natalia O. Zhila ^{1,2,*}, Ekaterina I. Shishatskaya ^{1,2} and Tatiana G. Volova ^{1,2}

¹ Basic Department of Biotechnology, School of Fundamental Biology and Biotechnology, Siberian Federal University, 79 Svobodnyi Av., 660041 Krasnoyarsk, Russia; evgeniygek@gmail.com (E.G.K.); kraysoInca@mail.ru (A.V.D.); shishatskaya@inbox.ru (E.I.S.); volova45@mail.ru (T.G.V.)

² Institute of Biophysics SB RAS, Federal Research Center "Krasnoyarsk Science Center SB RAS", 50/50 Akademgorodok, 660036 Krasnoyarsk, Russia

* Correspondence: nzhila@mail.ru; Tel.: +7-391-290-54-91; Fax: +7-391-243-34-00

Abstract: To increase the availability and expand the raw material base, the production of polyhydroxyalkanoates (PHA) by the wild strain *Cupriavidus necator* B-10646 on hydrolysates of sugar beet molasses was studied. The hydrolysis of molasses was carried out using β -fructofuranosidase, which provides a high conversion of sucrose (88.9%) to hexoses. We showed the necessity to adjust the chemical composition of molasses hydrolysate to balance with the physiological needs of *C. necator* B-10646 and reduce excess sugars and nitrogen and eliminate phosphorus deficiency. The modes of cultivation of bacteria on diluted hydrolyzed molasses with the controlled feeding of phosphorus and glucose were implemented. Depending on the ratio of sugars introduced into the bacterial culture due to the molasses hydrolysate and glucose additions, the bacterial biomass concentration was obtained from 20–25 to 80–85 g/L with a polymer content up to 80%. The hydrolysates of molasses containing trace amounts of propionate and valerate were used to synthesize a P(3HB-co-3HV) copolymer with minor inclusions of 3-hydroxyvalerate monomers. The introduction of precursors into the medium ensured the synthesis of copolymers with reduced values of the degree of crystallinity, containing, in addition to 3HB, monomers 3HB, 4HB, or 3HHx in an amount of 12–16 mol.%.

Keywords: sugar beet molasses; hydrolysis; *Cupriavidus necator*; synthesis; properties of PHA

Citation: Kiselev, E.G.; Demidenko, A.V.; Zhila, N.O.; Shishatskaya, E.I.; Volova, T.G. Sugar Beet Molasses as a Potential C-Substrate for PHA Production by *Cupriavidus necator*. *Bioengineering* **2022**, *9*, 154. <https://doi.org/10.3390/bioengineering9040154>

Academic Editor: Martin Koller

Received: 2 March 2022

Accepted: 1 April 2022

Published: 4 April 2022

Publisher's Note: MDPI stays neutral with regard to jurisdictional claims in published maps and institutional affiliations.



Copyright: © 2022 by the authors. Licensee MDPI, Basel, Switzerland. This article is an open access article distributed under the terms and conditions of the Creative Commons Attribution (CC BY) license (<https://creativecommons.org/licenses/by/4.0/>).

1. Introduction

The output of indestructible synthetic plastics, which are widely used in all spheres of human activity and obtained from non-renewable resources, has exceeded 380 million tons per year—and their production volumes are constantly growing. The bulk of plastic waste accumulates in landfills, creating a global environmental problem [1–3], and causing large-scale environmental pollution, structural damage, and instability in natural ecosystems and threatens beneficial biota and human health [4,5]. Currently, the global average for recycling of plastic waste is about 15%. In case the increase in plastic production and the low level of plastic recycling continues at its current levels, then, by 2050, approximately 12,000 Mt of plastic waste are believed to be in landfills or the natural environment [4]. Studies of the microbiological transformation of synthetic plastics in the natural environment under anaerobic soil conditions and in the waters of the World Ocean [6] have shown that these are extremely long processes. The low efficiency of biodegradation of plastics and the resulting microplastics represent a new and more dangerous environmental threat.

In addition to the prohibitive measures currently in force in more than 60 countries and aimed at reducing the consumption of plastics, the way out is seen in a gradual transition/conversion to new materials that can degrade in the environment without the formation of toxic products. Today, the development of new polymeric materials that can be included in biospheric cycles is one of the high-ranking areas of critical technologies of

the 21st century and actualizes research aimed at finding and developing biodegradable “green” plastics as an alternative to synthetic materials [7,8].

Polymers of hydroxyalkanoic acids, polyhydroxyalkanoates (PHAs), are the true products of biotechnology—the so-called “green” plastics. This is a family of polymers with different chemical compositions, different basic properties, and are obtained from various carbon substrates, including waste [9–16]. Such properties as resistance to UV rays, absence of hydrolysis in liquid media, and thermoplasticity make it possible to process PHA into specialized products using available methods from various phase states (solutions, emulsions, powders, and melts) [17,18]. These useful properties, combined with biodegradability and high biocompatibility, put PHA into the category of promising materials for the 21st century and allow them to be considered as a competitor to well-known biodegradable plastics (polylactide, polyethylene terephthalate, polyamides, etc.) for use in various fields from a municipal and agricultural economy to pharmacology and biomedicine [15,16,19–22].

Potentially, substrates with different degrees of reduction, energy content, and cost can serve as raw materials for PHA production. Among them are individual compounds, as well as complex substrates, including waste [23,24]. The list of microorganisms capable of accumulating PHA includes over 300 bacteria. These are both wild and genetically modified strains.

Promising PHA producers include hydrogen-oxidizing bacteria of the genus *Cupriavidus* (former systematic names: *Wautersia*, *Ralstonia*, *Alcaligenes*, *Hydrogenomonas*) [25], which, in addition to autotrophy and PHA synthesis on mixtures of carbon dioxide and hydrogen [26–31], are characterized by a wide organotrophic potential and the ability to synthesize PHA of various chemical structures using various substrates [32–34]. However, from the spectrum of sugars, the utilization of which in these microorganisms is realized by the Entner–Doudoroff pathway, they are capable of growing only on fructose, and they are easily susceptible to mutations with the formation of glucose-assimilating mutant strains [35]. Representatives of the *Cupriavidus* taxon are characterized by a high PHA content, which is associated with a powerful intracellular system for the synthesis of reserve polyhydroxyalkanoates and features of growth physiology. In cultures of these microorganisms, even on a complete medium in the middle of the linear growth phase, protein synthesis is inhibited and the formation of poly-3-hydroxybutyrate [P(3HB)] is activated [26,27].

Despite the urgent need for degradable polymeric materials in practice and the high attractiveness of PHA, the increase in their production volumes and the expansion of their applications are constrained by high costs and technical difficulties. Professor G. Chen, the scientific director of one of the world’s leading teams in the field of PHA biotechnology, identifies the following ones:

- the energy intensity of the fermentation process implemented in a strictly sterile batch culture;
- complexity and cost of extraction processes;
- the high crystallinity of the most available PHA poly(3-hydroxybutyrate);
- the difficulty of obtaining more technologically advanced copolymeric PHAs;
- the high cost (up to 40–45%) of the carbon substrate [36].

The key problem of PHA biotechnology is the optimization of the processes of biotechnological synthesis in general, primarily through using new productive strains capable of growing on available substrates and synthesizing PHA of various chemical compositions.

Sugars are the most widely used substrate in biotechnology. Sugar-containing industrial and agricultural wastes, as well as hydrolysates of plant raw materials of various origins, are an inexhaustible renewable substrate resource for the production of target biotechnology products, including PHA [37,38]. The research aimed at the more efficient use of agro-industrial waste for the production of a number of valuable products is being updated. Hydrolysates of various origins have been studied as potential sugar-containing substrates for PHA production: wood [39], sunflower stems [40], miscanthus biomass [41],

palm oil [42], cereal straw and husks [43–45], sugar beet and sugar cane cakes and peels [46], and others. The research results indicate the promise of plant hydrolysates for productive processes of PHA biosynthesis. However, as a rule, hydrolysates, in addition to hexoses (glucose and fructose) available for PHA producers, also include difficult-to-metabolize sugars, such as galactose and mannose (hexose hydrolysis products), arabinose, and xylose (pentose hydrolysis products). Therefore, to increase the completeness of sugar utilization by microbial cultures during growth on hydrolysates, genetically modified strains with an extended metabolic potential are constructed. For example, in [40], a recombinant *R. eutropha* strain NCIMB11599 (pKM212-XylAB) is described to be capable of utilizing xylose; the *C. necator* W50 strain, which expresses genes from *E. coli*, metabolizes arabinose [47].

Sugar production wastes (cane and beet molasses) are of great importance for biotechnology as a C-substrate [48]. It is an inexpensive carbon source containing, in addition to sugars, vitamins and a spectrum of mineral elements. The main sugar in molasses is disaccharide sucrose, and not all PHA producers have glycosyl hydrolases for the metabolism of sucrose and its transformation into compounds available to cells. Therefore, molasses must be further processed before use. As a result of processing, sucrose hydrolysis occurs and the content of the components that make up the original molasses changes [49]. In addition to glucose and fructose, depending on the hydrolysis method (acidic, alkaline, enzymatic) and conditions (hard or soft), toxic impurities can form in molasses, which negatively affects the biosynthesis process [50]. As a result of the very high content of nitrogen compounds in molasses, which negatively affects its accumulation in PHA cells, it is necessary to adjust the nitrogen concentration as well as the number of mineral elements [51,52].

For the synthesis of PHA using molasses as a C-substrate, two approaches are applicable. The first one is the preliminary hydrolysis of molasses and the sucrose contained in it, and/or the second one is the genetic engineering of recombinant strains capable of metabolizing sucrose. For example, it was shown that molasses can be used as the sole carbon source for the *Klebsiella aerogenes* strain carrying genes for PHB synthesis from *Alcaligenes eutrophus* [53]. In another paper, a recombinant strain of *C. necator* was obtained containing sucrose utilization (csc) genes from *Escherichia coli* W, capable of producing high concentrations of bacterial biomass (up to 113 g/L) with a content of the copolymer P(3HB-co-3HHx) up to 70–80% [54]. Additionally, the growth on untreated molasses of another genetically engineered producer, the *Cupriavidus necator* 2058/pCB113 of P(3HB-co-3HHx) copolymers, was described [55]. A recombinant strain of *Ralstonia eutropha* is known to contain the sacC gene from *Mannheimia ucciniciproducens*, encoding β -fructofuranosidase, which is capable of hydrolyzing sucrose into glucose and fructose and synthesizing a copolymer of poly(3-hydroxybutyrate-co-lactate) [P(3HB-co-LA)] [56].

Another solution to the problem is to pretreat molasses to hydrolyze sucrose to its glucose and fructose monomers. Sucrose hydrolysis can be carried out using chemical (acid, alkali) or enzymatic (sucrose, invertase) methods [57,58]. It has been shown that the mode of molasses hydrolysis affects the ratio of formed glucose and fructose [57].

The available literature contains a limited number of publications on the study of PHA production on molasses derivatives by representatives of *Cupriavidus* (*Ralstonia*). In one of the first works of this plan, in a culture of *Cupriavidus necator* DSM 545 (formerly known as *Ralstonia eutropha* or *Alcaligenes eutrophus*), it was shown that a small addition of non-hydrolyzed sugar cane molasses (3 g/L) to a medium containing glucose as the main carbon source provides a biomass concentration and polymer content of up to 23 g/L and 39%, respectively [59]. The growth processes of the *Ralstonia eutropha* PTCC1615 bacterium on acid hydrolysates of sugar cane, beet, and soybean molasses were studied [60]. The hydrolysates of sugar cane molasses obtained by various methods, including alkaline or acid hydrolysis—or acid hydrolysis with the preliminary hydrothermal treatment of molasses with oven or oil bath—ensured a polymer accumulation of up to 27% in a *C. necator* culture [57]. In the *C. necator* DSM culture, using pre-hydrolyzed sugar cane molasses with sulfuric acid at high temperatures, the polymer content did not exceed 13% [61]. Vinasse

and sugar cane molasses hydrolyzed with acids (HCl or H₂SO₄) or with the enzyme invertase provided biomass concentration and polymer content of up to 23 g/L and 56%, respectively, was observed in a culture of the natural strain *Cupriavidus necator* [50]. In the culture of the natural strain *Cupriavidus necator* ATCC 25207, the applicability of untreated sugar beet molasses and molasses hydrolyzed with acid or invertase for PHB production in various cultivation modes was evaluated [58]. During cultivation in flasks on untreated molasses, the biomass concentration was 2.1–3.9 g/L and the polymer content was 4.4–4.9%. The values for hydrolyzed molasses were higher, 5.5 g/L and 43.2%, respectively. When cultivating bacteria in a fermenter, the concentration of biomass and polymer was 29 g/L and 53%.

In general, given the promise of molasses as a potential source of carbon in PHA production and the ambiguity and wide scatter of available data, it is necessary to study the processes of PHA biosynthesis in conjunction with methods for pretreatment of molasses. The purpose of this work is to study PHA production by a natural strain of *Cupriavidus necator* using sugar beet molasses as the main growth substrate

2. Materials and Methods

2.1. Microorganisms

The polymers were synthesized using the *Cupriavidus necator* B-10646 wild strain, which is registered in the Russian National Collection of Industrial Microorganisms (NCIM) [62]. The strain is capable of synthesizing valuable PHA copolymers at high contents and is tolerant to precursor substrates. The strain has a broad organotrophic potential and can utilize such carbon sources as sugars, amino acids, organic acids, alcohols, CO₂, and CO. The strain synthesizes PHA copolymers composed of short- and medium-chain-length monomers [63].

2.2. Nutrient Medium

The Schlegel medium with CO(NH₂)₂ as a source of nitrogen with 1.0 g/L [26] was taken as the basis. The medium had the following composition: Na₂HPO₄·12H₂O–9.1; KH₂PO₄–1.5; MgSO₄·7H₂O–0.2; C₆H₅O₇Fe·nH₂O–0.025 (g/L), and the trace element solution (3 mL of standard solution per 1 L of the medium). The solution contained H₃BO₃–0.288; CoCl₂·6H₂O–0.030; CuSO₄·5H₂O–0.08; MnCl₂·4H₂O–0.008; ZnSO₄·7H₂O–0.176; and NaMoO₄·2H₂O–0.050; NiCl₂–0.008 (g/L). A nitrogen concentration of 0.4–0.6 g/L, limiting the growth of bacteria, and was adopted at the first stage of the two-stage mode of PHA synthesis. The main carbon source was glucose (China, purity 98%). A complex sugar-containing substrate was represented by sugar beet molasses and its derivatives. The initial molasses (manufactured by Ertilsky Sakhar Ltd., Ertil, Russia) contained 79.6 and 46.8 solids, 1.5–2.0 total nitrogen, 4.0–7.0 betaine, and 6.0–11.0 conductometric ash (% by weight). To synthesize PHA copolymers, the cell culture was supplemented with precursors of different monomers: potassium propionate and valerate, hexanoate, or ε-caprolactone (Sigma-Aldrich, Saint Louis, MO, USA) at concentrations of 1–2 g/L.

2.3. Hydrolysis of Sucrose to Molasses

Molasses was subjected to hydrolysis to transform sucrose into hexoses that are accessible to bacteria. For this, acid and enzymatic hydrolysis was carried out. The molasses was preliminarily twice diluted with water, to a solid concentration of 40%. The degree of hydrolysis (D) was determined by the formula:

$$D (\%) = S_v / C_0 \times 100\%,$$

where S_v—the total amount of reducing sugar (glucose + fructose) in g/L, C₀—initial concentration of sucrose.

The acid hydrolysis of sucrose in molasses was carried out with a solution of 1.5 N hydrochloric acid (HCl): 5 mL of HCl was added to 100 mL of a 500 g/L sucrose solution and kept at 90 °C in a water bath for 60 min. Then, the solution was cooled to room

temperature for 30 min and the pH was adjusted to 7 with 1M KOH solution [57]. The enzymatic hydrolysis of sucrose in molasses was carried out with the extracellular enzyme β -fructofuranosidase, which obtained by the autolysis of *Saccharomyces cerevisiae* yeast cells [64]. To do this, 31.5 g of pressed baker's yeast was mixed in 50 mL of water (or 6.3 g of dry, previously aged yeast in 100 mL of warm water for 15 min) and the baker's yeast was kept at 50 °C for 20 h on a magnetic stirrer. The resulting autolysate was centrifuged at 6000 rpm, and the precipitate was suspended in 100 mL of an aqueous solution of 0.15 KCl and centrifuged again at 6000 rpm. The suspension and centrifugation of the precipitate were repeated two more times until a clear, colourless centrifuge was obtained. The precipitate obtained, consisting mainly of yeast cell walls, was suspended in 200 mL of distilled water and centrifuged at $6000 \times g$ for 10 min. Next, the precipitate was added to 250 mL of molasses solution, which was previously diluted 1:1 with distilled water, and the pH was adjusted to 4.5 by adding concentrated sulfuric acid and was kept at 55 °C for 24 h on a magnetic stirrer. The resulting hydrolyzed molasses was neutralized with a KOH solution. The clarification and removal of components other than sugars in molasses were carried out after sucrose hydrolysis according to the method [65]. Molasses with hydrolyzed sucrose were heated to 55 °C on a stove with a stirrer and 33% hydrogen peroxide was added in an amount of 7% by volume and was kept for 24 h. Then, the molasses was cooled and centrifuged at 6000 rpm for 5 min. The supernatant was decanted, the weight of the dry residue was determined, and the optical density was measured at 600 nm.

2.4. Study of the Composition of Molasses

The concentration of fructose was determined using the resorcinol method [66]. The concentration of glucose was determined spectrophotometrically at 490 nm by the glucose oxidase method using a Fotoglucoza kit (Impact Ltd., Moscow, Russia). The nitrogen concentration in the culture medium was analyzed at different time points using a photometric method with Nessler's reagent. To measure the concentrations of major elements (S, K, Mg, P, Na, Ca) and trace elements, samples of the culture medium were taken periodically and measured using inductively coupled plasma atomic emission spectroscopy in an ICAP-6000 Thermosystem (Thermo Electron Corporation, Waltham, MA, USA).

2.5. Technique and Methods of Cultivation of Microorganisms

For the cultivation of bacteria, various types of laboratory fermentation equipment were used. Cultivation was carried out in 1 L and 2 L glass flasks, with a filling of 50% on a thermostatically controlled Incubator Shaker Innova[®] series 44 (New Brunswick Scientific, Edison, NJ, USA). Process scaling is implemented in fermenters. We used an 8 L BioFlo 110 (New Brunswick Scientific, Edison, NJ, USA). We cultivated bacteria in a batch mode, observing the conditions developed earlier for PHA biosynthesis. The inoculum was obtained from the museum culture under strictly sterile conditions in glass flasks and used for the inoculation of fermentation apparatuses. The starting concentration of cells in the medium when using flasks was not less than 0.1–0.2 g/L, and it was not less than 1.0–2.0 g/L when using fermenters. Bacteria were cultivated on a saline Schlegel medium at an initial concentration of C-substrate of 10–15 g/L and a medium temperature of 30 °C. A periodic two-stage process was used with cells grown under limited nitrogen supply in the first stage and no nitrogen in the second. In high-density fermentation cultures, as the cell concentration increased, the medium was periodically replenished with concentrated solutions of C-substrate and mineral elements using peristaltic dosing pumps.

2.6. Methods for Controlling the Parameters of the Bacteria Cultivation Process in the PHA Synthesis Mode

The culture samples were periodically taken for analysis during cultivation. The dynamics of cell growth in culture was detected by the optical density of the bacterial suspension at a wavelength of $\lambda = 440$ nm (UNICO 2100 photoelectric calorimeter, Dayton,

NJ, USA). The bacterial biomass concentration (X , g/L) was estimated by weight drying at 105 °C for 24 h for washed cells and preliminarily centrifuged at 6000 rpm.

The intracellular PHA content in bacterial cells and its composition were determined by chromatography of fatty acid methyl esters after methanolysis of biomass samples on an Agilent Technologies 7890A chromatography-mass spectrometer with a 5975C mass detector (Agilent Technologies, Santa Clara, CA, USA). Methanolysis of the samples was conducted as follows: 1 mL chloroform, 0.85 mL methanol, and 0.15 mL concentrated sulfuric acid were added to a 4.0–4.5 mg polymer sample and boiled under reflux condensers for 160 min. At the end of the methanolysis reaction, 1 mL distilled water was added to the flask. After phase separation, the lower organic phase containing hydroxyalkanoic acid methyl esters was analyzed. Benzoic acid was used as an internal standard to determine total intracellular PHA [67].

The concentration of cell biomass in culture (X , g/L), the concentration and content of PHA (g/L and in % of the weight of dry matter content), the specific rates of bacterial growth and PHA synthesis (μ , h⁻¹), the productivity of the biosynthesis process in terms of biomass and polymers (P , g/L × h), and the economic coefficient in terms of biomass and polymers ($Y_{g/g}$) were recorded using conventional methods. Microorganism cultivation techniques and microbial culture control methods had been previously described in detail [68].

2.7. Physicochemical Properties of PHAs

PHA was extracted from the cell biomass, which was previously separated from the culture fluid by centrifugation in an AvantiJ-HC centrifuge (BeckmanCoulter, Indianapolis, IN, USA). Then, the biomass was dried in an LP10R freeze dryer (ilShinBioBase, Dongducheon-si, Korea) to a residual moisture content of 5%. The extraction was carried out in two stages: at the first stage, the biomass was degreased with ethyl alcohol; at the second stage the polymer was extracted with methylene chloride. Thereafter, the polymer solution was filtered, and the polymer was precipitated with ethanol.

The physicochemical properties of PHAs were examined by using high performance liquid chromatography, X-Ray structure analysis, and differential scanning calorimetry. The methods and instruments had been described in detail before. The molecular-weight properties of PHAs were examined with gel permeation chromatography and a DB-35MS column (Agilent Technologies 1260 Infinity, Santa Clara, CA). The weight average molecular weight (M_w), number average molecular weight (M_n), and polydispersity (\mathcal{D}) were measured using polystyrene standards (PS) (Agilent Technologies, Santa Clara, CA, USA). The melting point (T_{melt}) and thermal degradation temperature (T_{degr}) were measured using a DSC-1 differential scanning calorimeter (Mettler Toledo, Schwerzenbac, Switzerland) and TGA (Mettler Toledo, Schwerzenbac, Switzerland), respectively. The melting point and thermal degradation temperature were determined from endothermic peaks in thermograms. The thermograms were analyzed using the STArE v11.0. software (Mettler Toledo, Schwerzenbac, Switzerland). The X-Ray structure analysis was performed to determine the crystallinity of copolymers employing a D8 ADVANCE X-Ray powder diffractometer equipped with a VANTEC fast linear detector (Bruker AXS, Karlsruhe, Germany). The degree of crystallinity (C_x) was calculated as a ratio of the total area of crystalline peaks to the total area of the radiogram (the crystalline + amorphous components). The calculations were done by using the Eva program of the diffractometer software.

2.8. Statistics

The statistic processing of the experimental data was carried out by conventional methods using the standard Microsoft Excel software package. The average values of the results were determined. The deviations from the mean for each result variance, the standard deviation of an individual result, and the standard deviation of a mean result were calculated.

3. Results and Discussion

In the studied sample of molasses, the content of dry substances was 79.6% and the content of sugars was 52.3%. Based on the initial composition of molasses, which contains sucrose and is not available for growing strains of *Cupriavidus necator*, an attempt was made to adapt the strain to this substrate. The original molasses was diluted with tap water to a physiologically acceptable concentration of sucrose for bacteria (10–20 g/L). In the original molasses, the content of glucose and fructose (C-substrates utilized by this strain for the growth and synthesis of PHA) is extremely low (1.6 and 1.7 g/L, respectively). After sterilization in an autoclave, as a result of the partial hydrolysis of sucrose, the content of glucose and fructose in molasses increased to 7.5 and 7.6 g/L, respectively. Based on the previously determined limits of physiological action for this strain of fructose (not higher than 15 g/L) and glucose (up to 30 g/L), as well as the known data on high minerals and other components of molasses that inhibit the growth of many microorganisms [58], molasses was diluted 20 times with water (50 mL per 1 L of medium). However, an attempt to adapt the strain to native molasses as the only C-substrate did not give positive results, despite the fact that dozens of bacteria passages were carried out. An extremely low concentration of bacterial biomass, below 0.5–0.7 g/L, was obtained due to the utilization of hexoses, which are included in the molasses. This is consistent with published results [58,60] that showed an extremely low biomass concentration and polymer production in *Ralstonia eutropha* PTCC1615 and *Cupriavidus necator* ATCC 25207 strains using raw sugar cane molasses or beets.

Therefore, we decided to subject the molasses to preliminary hydrolysis to transform sucrose into glucose and fructose, which are utilized by the studied bacterial strain *C. necator* B-10646.

3.1. Characteristics of the Hydrolysates of Sugar Beet Molasses

The characteristics of the hydrolysates of sugar beet molasses are given in Table 1. The most complete conversion of sucrose to hexoses (88.9%), and with the almost equal formation of glucose and fructose, was obtained with enzymatic hydrolysis at a significantly longer time (24 h) compared to chemical hydrolysis (3 h) (Table 1).

Table 1. Indicators of sucrose hydrolysis and the composition of hexoses formed.

Molasses Hydrolysis Method	Glucose, g/L	Fructose, g/L	Hydrolysis Time, h	Degree of Hydrolysis, %
Acid	224.7	73.7	3	51.0
Enzymatic	258.9	261.4	24	88.9

During acid hydrolysis, only half of the sucrose was hydrolyzed into hexoses, with an uneven 3:1 ratio of glucose and fructose. The acid hydrolysis of sucrose is known to be accompanied by the formation of undesirable side products, such as formic and acetic acids, hydroxymethylfurfural (HMF), monosaccharide anhydrides, and humic substances, which can inhibit the growth of microorganisms [57,69]. Enzymatic hydrolysis avoids the oxidation of fructose, and the resulting molasses contains almost equal amounts of glucose and fructose. Based on the results obtained, an enzymatic method for the hydrolysis of molasses was used.

Further, the resulting molasses hydrolysate was subjected to clarification using H_2O_2 to precipitate an excess amount of mineral substances [65]. The results of the analysis of the chemical composition of the initial molasses and the resulting hydrolysate are presented in Table 2. The concentration was selected (7 mL H_2O_2 /100 mL hydrolysate), at which point a part of the element's precipitates, which are not biogenic for bacteria—including 95% Ca, 78% Cr, 75% Sr—were used. There was also a slight decrease in the concentration of a number of trace elements: B, Co, Mn, Mo, and Ni (Table 2). The results of the mineral composition analysis of the initial molasses and molasses after clarification are presented in Table 2. A similar treatment of molasses was carried out using activated carbon [56]. This

treatment made it possible to reduce the content of calcium, iron, silicon, phosphorus, and titanium without changing the sugar content.

Table 2. Chemical composition of sugar beet molasses and the resulting hydrolysate.

Type of Molasses	Macroelements, g/L						N Total
	Na	K	P	Fe	Mg	S	
Molasses initial	17.295	44.324	0.107	0.077	0.216	1.563	25.825
Molasses hydrolysate clarified	17.126	44.324	0.107	0.046	0.216	1.563	25.825
Type of Molasses	Trace Elements, mg/L						Ni
	B	Co	Cu	Mn	Zn	Mo	
Molasses initial	6.118	1.050	0.518	15.862	11.424	0.420	4.074
Molasses hydrolysate clarified	2.856	0.756	0.518	11.704	11.424	0.252	2.758

We performed an analysis of the balance in chemical composition of the obtained molasses hydrolysate with the physiological needs of bacteria based on the data obtained earlier in the study of the mineral nutrition of hydrogen-oxidizing bacteria [70]. The specific needs of the culture of hydrogen-oxidizing bacterium *A. eutrophus* Z1 in nitrogen and mineral elements are $N = 125 \pm 5$; $P = 18 \pm 0.5$; $S = 6.5 \pm 0.5$; and K and Mg at 5.0 ± 0.5 mg/g, which was calculated for the synthesis of 1.0 g of CDW. It is important to note that the physiological requirements of mineral elements for bacteria are very wide, and inhibition of cell growth by an excess of macro- and microelements occurs when their concentration in the culture medium increases above 500–700 mg/L. Therefore, the excess content of some macro-elements in molasses did not cause concern.

Based on the results of comparing the content of C-substrate (glucose + fructose) and mineral macro- and microelements in the standard Schlegel medium—and the obtained sugar beet molasses hydrolysate—we concluded that the sugar content is excessive (by more than an order of magnitude), and the composition of the molasses hydrolysate is balanced for most mineral elements to provide the physiological needs and unlimited growth of bacteria. The exceptions were nitrogen and phosphorus. The amount of nitrogen is excessive, which stimulates cell growth and the synthesis of the main intracellular components (protein and nucleic acids). Obtaining the highest content of PHA (up to 80–85% and higher) in the culture of *C. necator* B-10646 and the closely related strains is possible only with unbalanced growth and by limiting the growth of bacteria for this element [12]. At the same time, the phosphorus content in the molasses hydrolysate is low (about 100 mg/L), which can provide no more than 6.0 g of cell biomass. Given the need to dilute the hydrolyzed molasses to reduce the excess concentration of sugars and nitrogen, a deficiency of this element will limit cell growth. Therefore, a source of phosphorus must be added to the molasses hydrolysate when it is used as the basis of a nutrient medium for bacteria. The total content of elements in molasses after the hydrolysis procedure did not show in what forms they are present and how accessible they are for assimilation by bacteria.

3.2. Production Characteristics of *Cupriavidus necator* B-10646 Culture When Grown on Molasses Hydrolysate

Preliminary testing of the balance and availability of hydrolyzed molasses components for the studied bacterial strain was carried out by varying the composition of the nutrient medium. The results of cultivating bacteria in 1.0 L flasks using various options for diluting molasses hydrolysate in comparison with the Schlegel medium are given in Figure 1. Phosphorus was introduced into hydrolyzed molasses in the form of magnesium phosphate.

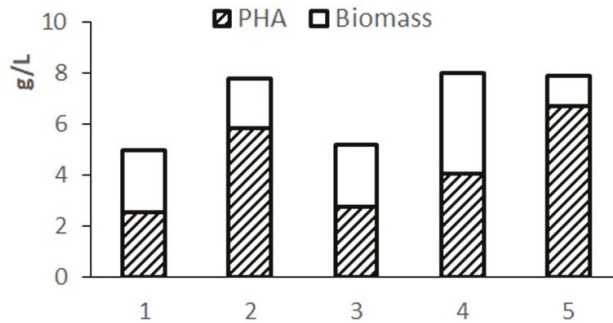


Figure 1. Indicators of the culture of *Cupriavidus necator* B-10646 when grown on molasses hydrolysate and Schlegel's medium: 1-; 2-, 3-, 10-, 20-, 30-fold dilution of molasses hydrolysate, respectively; 4-complete Schlegel medium; 5-with 50% nitrogen content. Biomass concentration (X, g/L), polymer (% of CDW).

The complete Schlegel medium provides a concentration of cell biomass up to 7–8 g/L but limits the accumulation of the polymer due to excess nitrogen in the medium. The highest biomass concentration and polymer content were obtained on Schlegel's medium with a halved nitrogen content. A close result is provided by using a 20-fold dilution of molasses hydrolysate. When using a less diluted hydrolysate, cell growth and polymer synthesis are inhibited due to excess sugars. A highly diluted hydrolysate (30-fold dilution) limits cell growth with less of an effect on polymer production due to reduced sugar content. The results showed the need to adjust the composition of the nutrient medium based on molasses hydrolysates in terms of sugars and nitrogen.

Figure 2 illustrates the need and result of adjusting the composition of the medium based on molasses hydrolysate. As follows from Figure 2a, when using a 20-fold dilution of molasses hydrolysate, the initial concentrations of sugars (fructose + glucose) and nitrogen were 26.0 and 1.2 g/L, respectively. The concentration of phosphorus was 5.4 mg/L, therefore, it was introduced into the culture in the first hours of the bacterial cultivation process. The nitrogen concentration in the culture medium decreased. However, even during the entire second stage, nitrogen was determined in culture, which indicated an excess of this element and a negative effect on the accumulation of the polymer in cells. The intracellular content of the polymer increased by the end of the first stage to 45% and remained practically unchanged (at the level of 50%) until the end of the cultivation process (68–70 h). The bacterial biomass concentration was about 8.0 g/L.

To increase the production indicators of the culture and eliminate the excess nitrogen content in the bacterial culture, a process for growing bacteria with an adjustment to the composition of the medium during culture development is proposed (Figure 2b). In this variant, a 30-fold dilution of molasses hydrolysate was used. Therefore, the initial concentrations of sugars and nitrogen in it were reduced to 18.0 and 0.8 g/L, respectively. The phosphorus concentration did not exceed 3.5 mg/L (it was added to the culture in the first hour of the process). The nitrogen concentration dropped during the first stage, but it was preserved in the culture at the second stage. At the beginning of the second stage (34–35 h), the culture was supplemented with glucose. Glucose was added because the initial sugar content was reduced, and molasses additives were not used to eliminate excess nitrogen. The bacterial biomass concentration was 8.0 g/L by the end of the experiment and the intracellular polymer content was 75%. It should be noted that hexoses (fructose and glucose) were utilized from the medium by the cells simultaneously; no diauxia was observed. The proposed mode provided a productive process under the conditions of a low-diluted flask culture with indicators in terms of X and g/L comparable to the studied strain on pure sugars, however, with a slight decrease in the polymer content (up to 70–75%).

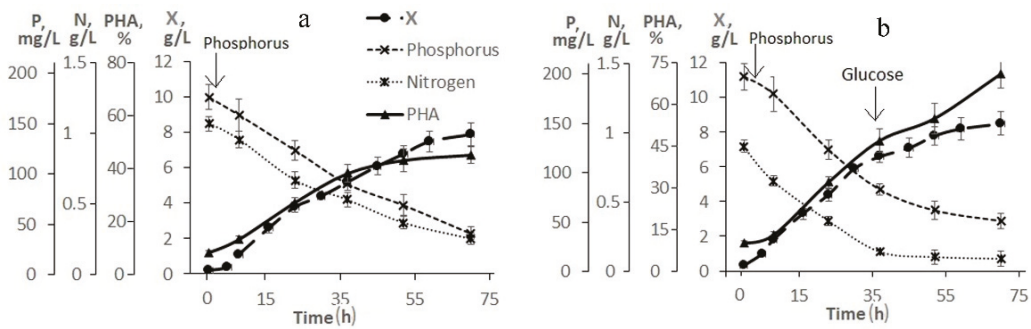


Figure 2. Production parameters of bacterium *Cupriavidus necator* B-10646 when grown on hydrolyzed sugar beet molasses in 2 L glass flasks under different scenarios of its use: (a)—20-fold dilution of molasses hydrolysate; (b)—30-fold dilution of molasses hydrolysate with the addition of phosphorus and glucose to the culture (indicated by arrows).

A comparison of the obtained results with published ones showed the following. Natural strains, representatives of the taxon *Cupriavidus* (formerly *Ralstonia*), when grown on hydrolyzed sugar cane molasses obtained by various methods and can provide different indicators of PHA production when growing bacteria in flasks. For example, the indicators were low, and the polymer content was at the level of 27% at a bacterial biomass concentration of 2.9 g/L [57]. Similarly, in [60], *Ralstonia eutropha* PTCC1615 bacterium, when grown in flasks, accumulated no more than 30% polymer on the cane and sugar beet hydrolysates at a biomass concentration of about 3.0 g/L. When grown on treated molasses, the natural strain *Cupriavidus necator* ATCC 25207 synthesized up to 43.2% polymer at a low biomass concentration of 5.5 g/L [58]. A higher biomass concentration of *C. necator* DSM 545 (about 10 g/L) was obtained in [61], while the polymer content did not exceed 13%.

A similar spread of indicators is typical for genetically engineered strains, which can accumulate PHA on raw molasses with different biomass concentrations—from a relatively low polymer content, about 24–32%, at X values below 5.0 g/L [55] and 46.9% and X = 4.4 g/L [56] for higher values. For example, up to 40% PHA was synthesized in 36 h at a bacterial biomass concentration of 8.0 g/L [54] and 65% of the polymer was synthesized in 72 h at X = 7.0 g/L [55].

The subsequent modification of the proposed mode of cultivating bacteria (Figure 2b) and scaling the process using fermenters ensured the implementation of a productive process in terms of the biomass concentration and PHA content. However, due to obtaining a significantly higher biomass concentration when growing bacteria in a fermenter compared to flask cultures, the medium composition must be adjusted for the mode of controlled feeding of the culture with all nutrients. At the same time, current concentrations in the culture of sugars, nitrogen, and phosphorus, which is sharply deficient, should be under special control. Preliminary experiments in the 8 L BioFlo fermentation complex with a fill factor of 0.5 and a mass transfer coefficient of KLa 200–800 h^{-1} showed the possibility of obtaining a biomass concentration on diluted molasses hydrolysates of up to 10–15 g/L.

When using 20-fold molasses hydrolysate and adding only phosphorus to the culture at the first stage of the process, the biomass concentration by the end of the first stage was about 10–15 g/L with a polymer content of about 40–45%. The maximum specific growth rate was reached at 20 h of cultivation and was 0.05 h^{-1} ; the specific rate of polymer synthesis reached its maximum at the end of the first stage and the beginning of the second stage of cultivation and was 0.07 h^{-1} . The culture was also supplied with glucose, the consumption of which sharply decreased as the growth and division of cells stopped and the polymer accumulated in them. With this background, the specific growth rate of bacteria decreased to 0.01 h^{-1} . Glucose supplementation was used instead of molasses to avoid excess nitrogen in the culture, which limited polymer accumulation (Figure 3a). By

the end of the second stage, the bacterial biomass concentration was 20 g/L; the polymer content was about 75%.

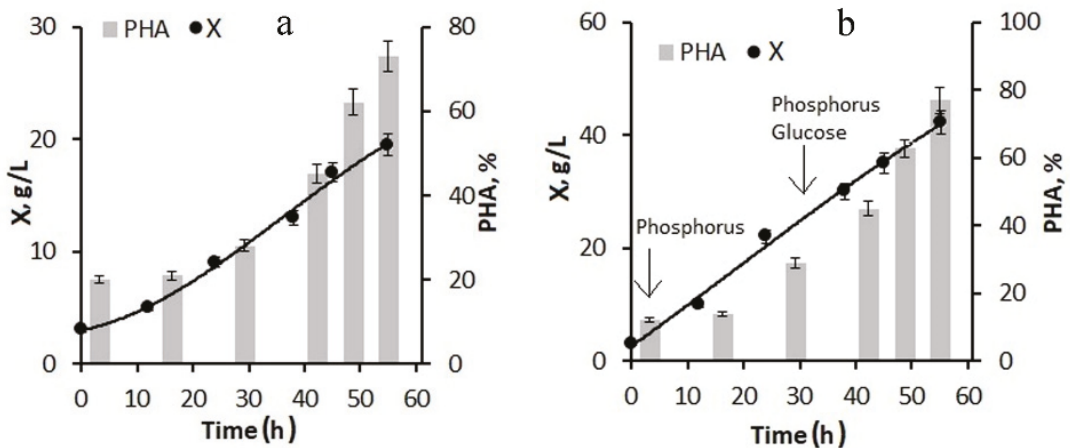


Figure 3. Production parameters of the bacterial culture *Cupriavidus necator* B-10646 when grown on hydrolyzed sugar beet molasses in the 8 L fermenter under different versions of feeding the culture with nutritive elements: (a)—20-fold dilution of molasses hydrolysate; culture feeding with phosphorus at the first stage, and feeding with phosphorus + glucose at the second stage; (b)—20-fold dilution of molasses hydrolysate with feeding the culture with phosphorus and glucose at the first and second stages (indicated by arrows).

The next version of the process for increasing the concentration of the bacterial biomass included feeding the bacterial culture with glucose in addition to phosphorus at the first stage (Figure 3b). The phosphorus supply to the culture began from the first hours of the bacterial cultivation process; the glucose supply began in the middle of the first stage. As a result, by the end of the first stage, the bacterial biomass concentration was 25–30 g/L, the specific growth rate of bacteria was 0.08 h^{-1} , and the specific rate of polymer synthesis was 0.13 h^{-1} . At the end of the experiment, the biomass concentration reached 42 g/L at a polymer content of about 77–80%. Thus, the combination of molasses hydrolysate with glucose feeding of the culture can significantly increase the biomass concentration while maintaining a high polymer content.

Thus, using diluted hydrolyzed molasses, due to excess nitrogen, does not allow for high concentrations of biomass to be obtained due to the low sugar content. The addition of glucose at the first stage of the process has a positive effect. Figure 4 shows the results of using a larger amount of glucose and phosphorus additions and a 5 g/L inoculum concentration for the fermenter inoculation. By the end of the first stage, it was possible to increase the bacterial biomass concentration to 45–50 g/L, and the total biomass concentration for the entire process increased to 75–80 g/L. At the same time, the specific rate of bacterial synthesis increased to 0.12 h^{-1} from the beginning of the process and decreased to 0.01 h^{-1} by the end of cultivation.

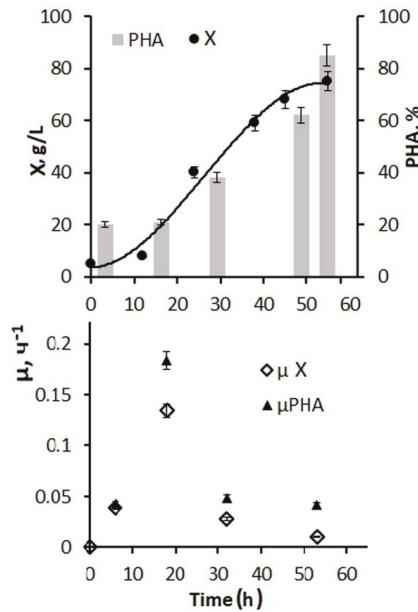


Figure 4. Production parameters of *Cupriavidus necator* B-10646 culture when cultivated in the 8 L fermenter using 20-fold dilution of molasses hydrolysate, concentrated inoculum (5 g/L), and a larger amount of glucose and phosphorus supplementation as a source of carbon, nitrogen, and mineral elements at the first stage with feeding with phosphorus and glucose; at the second stage—in a nitrogen-free medium with culture fed with glucose and phosphorus (feeds are shown by arrows): the concentration of the total cell biomass in the culture (X, g/L) and the polymer in the cells (PHA% of CDW); specific cell growth rate (μX h⁻¹) and specific polymer synthesis rate (μ PHA, h⁻¹).

Active cell and biomass growth in the exponential phase were accompanied by active consumption of both hexoses, and the average value for this stage of the process was 2.7–2.9 g/g·h. Further, at the second stage, in the presence of a decrease in growth characteristics, the consumption of supplied glucose decreased and by the end of the process amounted to 0.05–0.08 g/g h. The productivity of the process for biomass was 1.48 g/L·h. For the polymer, it was 1.23 g/L·h. The values of the effectiveness for using the C-substrate, which were estimated by the economic coefficient, are somewhat inferior to those obtained in this culture on individual sugars. This is a consequence of the presence of inhibitory components in the composition of molasses, which did not affect the concentration of the bacterial biomass under nitrogen-limited cell growth, but compensatory increased substrate consumption was performed to reduce the inhibitory effect. Therefore, the economic coefficient for C-substrate (Y g/g) for biomass was 0.29 and for PHA it was 0.23.

Thus, the developed mode of cultivating bacteria in a fermenter using molasses hydrolysates in combination with glucose and phosphorus additives ensured the implementation of a productive process of PHA synthesis. Depending on the number of glucose additions to molasses hydrolysates and the sugar ratio of these two sources (from 1:1 to 1:10), it is possible to obtain a bacterial biomass concentration from 20 to 80–85 g/L with a polymer content of about 80%.

Comparing the results obtained with publications showed that they are superior to the data of some works but also inferior to individual data. The spread of data on the production parameters of the PHA synthesis process is mainly related to the type of producer strain used. In cultures of natural strains of the taxon *Cupriavidus* (*Ralstonia*), as a rule, the results are inferior to those obtained in this work. Thus, when growing the natural strain *Ralstonia eutropha* ATCC 17699 and using untreated molasses and vinasse

as a carbon substrate for 50 h of cultivation in a 5 L fermenter at a ratio of molasses and vinasse such as 25:75, the biomass and polymer concentrations were low and amounted to 3.9 and 2.7 g/L, respectively. In the original molasses, sucrose was the main sugar (60–63%); in vinasse, the content of sucrose, glucose, and fructose was 3.7, 2.4, and 5.5 g/L, respectively [71]. When cultivating the natural strain *Cupriavidus necator* ATCC 25207 in a 5 L fermenter for 52 h, the maximum biomass concentration (29 g/L) and polymer content (53%) were obtained on a medium containing molasses hydrolyzed with sulfuric acid. The initial concentration of the hydrolyzed molasses solution was 55 g/L and the total concentration of the added molasses solution was 112 g/L [58]. In the culture of the natural strain *Cupriavidus necator* grown on molasses hydrolysate in a 7.5 L fermenter for 50 h, the biomass concentration was 23 g/L with a low polymer content of 56% [50]. Higher rates are typical for processes using recombinant strains capable of metabolizing molasses sucrose. In the culture of the recombinant strains of *Ralstonia eutropha* containing the sacC gene from *Mannheimiasuc ciniciproducens*, encoding β -fructofuranosidase, which can hydrolyze sucrose into glucose and fructose in a nutrient medium in a 2.5 L fermenter, led to the following indicators being achieved in 36 h: biomass of about 30 g/L, polymer content 82.5% [56]. A recombinant strain of *Klebsiella aerogenes* carrying genes for PHB synthesis from *Alcaligenes eutroplus* was grown on molasses as the only carbon source in a 10 L fermenter for 32 h. The concentration of the bacterial biomass was 37 g/L and the polymer content was 70% [53]. The highest result was obtained by Arikawa et al. 2017 [54]. A recombinant strain of *C. necator* containing genes for utilizing sucrose from *E. coli* in a 5 L fermenter provided a bacterial biomass concentration of 113 g/L in 65 h with a polymer content of 70–80%.

The obtained results and published data allow us to conclude that molasses is a promising substrate for PHA production, including highly productive representatives of the *Cupriavidus* taxon.

3.3. Properties of PHA Synthesized from Sugar Beet Molasses

Properties of PHAs are determined, primarily, by the structure of side chains in the polymer carbon chain and the distance between the ester groups in a molecule. The valuable properties of PHA producers include the ability to synthesize more technologically advanced copolymers ((P(3HB-co-3HV), P(3HB-co-3HHx), and P(3HB-co-4HB), etc.) in addition to the highly crystalline homopolymer of 3-hydroxybutyric acid [P(3HB)]. The synthesis of PHA copolymers is usually achieved by supplementing the culture medium with different additional precursor carbon sources (valerate, hexanoate, ϵ -caprolactone, etc.), which are toxic to bacteria and, thus, impair the total productivity of the biosynthesis and reduce polymer yields. Therefore, it is important to find and/or engineer strains that would be tolerant to these compounds. Depending on the structure of the C-chain, the known types of PHA are divided into three groups: short-chain, formed by monomers with a C-chain length from C3 to C5, medium-chain (C6–C16), and long-chain (C17 and above) [72]. A carbon source is one of the cultivation conditions considerably influencing the chemical composition and properties of PHAs. As a rule, the synthesis of copolymeric PHAs is realized using genetically engineered strains. The ability of individual natural strains to synthesize copolymeric PHA, including those containing short- and medium-chain monomers, was first shown in cultures of natural strains *R. eutropha* B5786 and *R. eutropha* H-16 [32,73,74].

The authors of these works added valerate, hexanoate, and octanoate as precursors for the monomers other than 3-hydroxybutyrate to bacterial cultures in the PHA synthesis mode and obtained some copolymers.

In the composition of hydrolysates of sugar beet molasses obtained by the enzymatic method, the presence of propionic (up to 0.3%) and n-valeric (up to 0.2%) acids, which are precursors for the synthesis of the monomer 3-hydroxyvalerate (3HV), were found in small concentrations. It prompted us to analyze the chemical composition of the polymer synthesized by *C. necator* B-10646 on this substrate. It was shown that regardless of the cultivation

technique and intensity of mass transfer (glass flasks installed in a shaker-incubator or fermentation complexes), the synthesized polymer is a P(3HB-co-3HV) copolymer with minor (0.3–0.5 mol.%) inclusions of 3HV monomers (Table 3).

Table 3. Properties of PHAs synthesized *Cupriavidus necator* B-10646 from sugar beet molasses hydrolysate.

PHAs Composition, mol. %	Number Average Molecular Weight, M_n , kDa	Weight Average Molecular Weight, M_w , kDa	Polydispersity, \bar{D}	Degree of Crystallinity, C_x , %	Melting Point, T_{melt} , °C	Thermal Degradation Temperature, T_{degr} , °C
C-substrate–molasses hydrolysate						
2 L Flask P(3HB-co-0.4mol.%3HV)	410	820	2.6	82	173.2	287.4
8 L Fermenter P(3HB-co-0.5mol.%3HV)	356	996	2.8	78	169.0 176.1	276.2
8 L Fermenter P(3HB-co-0.3mol.%3HV)	506	1214	2.4	76	169.4 179.7	276.0
C-substrate–molasses hydrolysate + precursors						
P(3HB-co-4HB) *						
P(3HB-co-6.5mol.%4HB)	144	461	3.2	45	152.0 163.8	286.3
P(3HB-co-12.0mol.%4HB)	200	600	3.0	38	153.2 167.8	288.0
P(3HB-co-3HV)						
P(3HB-co-8.0mol.%3HV)	212	678	3.2	67	163.5 172.2	283.5
P(3HB-co-16.5mol.%3HV)	200	740	3.7	55	167.4 169.0	287.0
P(3HB-co-3HHx) **						
P(3HB-co-5.6mol.%3HHx)	210	756	3.6	70	161.1 169.4	283.2
P(3HB-co-10.3mol.%3HHx)	180	738	4.1	68	165.4 167.8	270.0

Note: Minor inclusions of 3HV monomers are not shown, less than 0.5 mol.% in copolymers. * P(3HB-co-4HB) and ** P(3HB-co-3HHx).

The literature analysis has shown that the vast majority of data described the synthesis of the P(3HB) homopolymer on the growth of natural and recombinant strains on molasses or its hydrolysates. The synthesis of P(3HB-co-3HV) copolymers was recorded in [75] when the bacteria *Bacillus cereus* RCL 02 (MCC 3436) was grown on sugar cane molasses; the copolymer content was high (up to 83.5%) and the content of 3HB monomers varied from 1.2 to 12.4 mol.% depending on the concentration of molasses in the medium. There are also examples of the synthesis of P(3HB-co-3HHx) copolymers on molasses in cultures of genetically engineered producers, *C. necator*, which contain genes for the metabolism of sucrose from *E. coli* [54], and *C. necator* 2058/pCB113 [55]. The ability to synthesize a poly(3-hydroxybutyrate-co-lactate) [P(3HB-co-LA)] copolymer was found by a recombinant *Ralstonia eutropha* strain containing the sacC gene from *Mannheimia succiniciproducens* encoding β -fructofuranosidase [56].

It was shown that the addition of precursor substrates (potassium propionate or valerate, ϵ -caprolactone, or hexanoate at a concentration of 1.0–2.0 g/L) to the culture of *C. necator* B-10646 grown on the hydrolysates of sugar beet molasses was accompanied by the synthesis of copolymers of various compositions P(3HB-co-4HB), P(3HB-co-3HV) and P(3HB-co-3HHx) with more significant inclusions of second monomers other than 3HB. The additions were made during the period of active polymer synthesis. This is 10–12 h from the beginning of the cultivation process. The highest level of incorporation of 4HB, 3HV, or 3HHx monomers into the 3-hydroxybutyrate chain occurred 10–15 h after adding the precursor at the end of the first stage of bacterial cultivation. Further, the content of monomers other than 3HB decreased, which is due to the activity of enzymes of intracellular degradation of the polymer, primarily PHA-depolymerase.

Properties of PHA with different composition are presented in Table 3.

The properties of P(3HB-co-3HV) with a minor content of 3HV monomers grown on molasses hydrolysate (without the addition of precursors) corresponded to the values characteristic of the P(3HB) homopolymer. It includes a high degree of crystallinity (76–80%), the melting temperature, and thermal degradation values (173–180 and 276–287 °C, respectively), with a gap between the values of T_{melt} and T_{degr} of at least 100 °C. The samples are also characterized by a variability in the molecular weight characteristics and relatively low polydispersity values (less than 3.0).

All PHA samples synthesized on molasses hydrolysate with the addition of precursors and having significant inclusions of second monomers (from 5–6 to 10–16 mol.%) are characterized by a slight decrease in molecular weight and an increase in polydispersity. The most important parameter of polymer materials is the degree of crystallinity: the ratio of the crystalline to amorphous phase. The percentage of the monomers other than 3HB affected the degree of crystallinity of the polymers, which decreased as the fraction of the second monomer increased. That was more noticeable in the P(3HB-co-4HB) specimens, whose C_x decreased to 45 and 38% at 4HB 6.5 mol.% and 12.0 mol.%, respectively. The P(3HB-co-3HV) and P(3HB-co-3HHx) copolymers exhibited a similar, although less obvious, trend. The degree of crystallinity of P(3HB-co-3HV) containing 3HV 8.0 and 16.5 mol.% was 67 and 55%, respectively; the degree of crystallinity of P(3HB-co-3HHx) containing 3HHx 5.6 and 10.3 mol.% was 70 and 68%, respectively. Thus, in all PHA copolymers, the crystalline phase decreased while the amorphous, disordered regions increased, indicating better processability of these polymers.

Double peaks are present on the thermograms of the copolymers (Figure S1), which indicate the presence of crystals of various shapes or sizes in the polymer mixture. This confirms the presence of a mixture of homopolymers and copolymers. In general, the properties of the studied samples correspond to the large array of published data characterizing the relationship between the set and ratio of monomers in copolymer PHA and their basic physicochemical properties and are consistent with the results of many other studies [9–11,14,15].

Other authors made a similar conclusion while studying the PHA properties, which were synthesized by various strains on molasses and its derivatives. Thus, analyzing the properties of the P(3HB) homopolymer synthesized when grown on molasses of various origins or its derivatives, the authors [55,58] concluded that the properties of the samples were similar to commercial analogues of poly(3-hydroxybutyrate). Thus, M_w was determined, levelling from 384 to 670 kDa and polydispersity was determined, levelling from 1.8 to 3.81. One of the polymer samples had two melting peaks: 142.08 and 159.43 °C. In others, for T_{melt} it was 172.43 °C and the beginning of T_{degr} was 262.0 °C. At the same time, P(3HB) samples synthesized on molasses by strains of other taxa showed some differences in the properties of P(3HB). Thus, P(3HB) synthesized by *Pseudomonas fluorescens* on molasses had low values of the degree of crystallinity (9.5%), which was determined based on enthalpy measurements; at the same time, in a commercial sample, the C_x value was also significantly lower than the generally accepted values [76]. The P(3HB) sample synthesized by the *Bacillus megaterium* JHA strain on molasses had two melting peaks: 136.41 °C and 158.04 °C.

While measuring the molecular weight characteristics of the polymer, the presence of two peaks in the chromatogram was shown. The first one was in the region of $M_n = 47.84$ kDa and $M_w = 71.65$ kDa with a polydispersity of 1.49; the second peak was $M_n = 0.08$ kDa and $M_w = 0.55$ kDa with a polydispersity of 6.85. The presence of both peaks confirms that the resulting polymer P(3HB) is a mixture [77].

There is little information about the synthesis of molasses and the study of copolymer PHA. Thus, the P(3HB-co-3HV) copolymer synthesized by *B. cereus* RCL 02 on sugar cane molasses was studied and the content of 3HV monomers varied from 1.2 to 12.4 mol.% depending on the concentration of molasses [75]. The maximum inclusion (12.4 mol.%) was obtained using 4% molasses. T_{degr} of the copolymer (in terms of 50% weight loss) was fixed at 263.14 °C. The melting point of the polymer was 169.72 °C. The P(3HB-co-3HHx) copolymer characterized by Purama et al. 2018 had M_w values in the range of 580–830 kDa; the highest M_w was determined for the sample containing 5 mol.% of 3HHx [55]. Two peaks of T_{melt} (142.08 and 159.43 °C) and slightly lower temperature characteristics were found.

The published data and the results of the presented work allow us to summarize the important possibility of synthesizing more technologically advanced PHA copolymers using molasses and precursors of 3HV, 3HHx, and 4HB monomers as C-substrates.

4. Conclusions

We studied beet molasses as the main growth substrate for the PHA synthesis. Acid and enzymatic hydrolysis were carried out to transform molasses sucrose into hexoses that were accessible to the studied strain-producer. Enzymatic hydrolysis using β -fructofuranosidase provided the complete conversion of sucrose (88.9%) to hexoses with an almost equal ratio of glucose and fructose, in the level of about 35–45% of the obtained monosaccharides. The chemical composition analysis of the hydrolysate of beet molasses showed the need to adjust some elements to balance with the physiological needs of the studied bacterial strain *C. necator* B-10646. To reduce the excess content of sugars and nitrogen, and remove the deficiency of phosphorus, which negatively affects the biomass concentration and PHA content, controlled modes of replenishment of the batch culture of bacteria with phosphorus and glucose were proposed and implemented, thereby providing high production rates for the process. Depending on the ratio of sugars introduced into the bacterial culture due to molasses hydrolysate and glucose additives, bacterial biomass concentrations were obtained from 20–25 to 80–85 g/L with a polymer content of up to 80%. A P(3HB-co-3HV) copolymer with minor inclusions of 3-hydroxyvalerate monomers was the polymer synthesized on hydrolysates of molasses containing trace amounts of propionate and valerate. The introduction of precursor substrates into the culture of bacteria ensures the synthesis of copolymers of various compositions with reduced values of the degree of crystallinity, containing monomers of 3HV, 4HB, or 3HHx from 5–8 to 12–16 mol.%.

The studies have shown the possibility of productively synthesizing degradable polyhydroxyalkanoates from sugar beet molasses, a complex sugar-containing substrate, which is a large-tonnage waste of the sugar industry.

Supplementary Materials: The following supporting information can be downloaded at: <https://www.mdpi.com/article/10.3390/bioengineering9040154/s1>, Figure S1: Results of thermal analysis of PHAs synthesized by *Cupriavidus necator* B-10646 from molasses hydrolysate.

Author Contributions: T.G.V.; conceptualization, methodology, analysis; A.V.D., molasses hydrolysis; E.G.K., production polymers in fermenters; N.O.Z., production copolymers; E.I.S., polymers properties. All authors have read and agreed to the published version of the manuscript.

Funding: This study was financially supported by Project “Agropreparations of the new generation: a strategy of construction and realization” (Agreement No. 075-15-2021-626) in accordance with Resolution No. 220 of the Government of the Russian Federation of 9 April 2010, “On measures designed to attract leading scientists to the Russian institutions of higher learning” (polymer synthesis), and by the State Assignment of the Ministry of Science and Higher Education of the Russian Federation No. FSRZ-2020-0006 (copolymers properties).

Institutional Review Board Statement: Not applicable.

Informed Consent Statement: Not applicable.

Data Availability Statement: All data is available in the paper.

Acknowledgments: The authors would like to express their special thanks to the Krasnoyarsk Regional Center of Research Equipment of Federal Research Center “Krasnoyarsk Science Center SB RAS” for providing equipment to ensure the accomplishment of this project.

Conflicts of Interest: The authors declare that they have no conflict of interest in the publication of this article. The manuscript was written through contributions of all authors. All authors have given approval to the final version of the manuscript.

References

- Lebreton, L.; Andrady, A. Future scenarios of global plastic waste generation and disposal. *Palgrave Commun.* **2019**, *5*, 6. [CrossRef]
- Quecholac-Piña, X.; Hernández-Berriel, M.; Mañón-Salas, M.; Espinosa-Valdemar, R.M.; Vázquez-Morillas, A. Degradation of plastics under anaerobic conditions: A short review. *Polymers* **2020**, *12*, 109. [CrossRef] [PubMed]
- Sohn, Y.J.; Kim, H.T.; Baritugo, K.A.; Jo, S.Y.; Song, N.M.; Park, S.Y.; Park, S.K.; Pyo, J.; Cha, H.G.; Kim, H.; et al. Recent advances in sustainable plastic upcycling and biopolymers. *Biotechnol. J.* **2020**, *15*, 1900489. [CrossRef] [PubMed]
- Geyer, R.; Jambeck, J.R.; Law, K.L. Production, use, and fate of all plastics ever made. *Sci. Adv.* **2017**, *3*, e1700782. [CrossRef] [PubMed]
- Katyal, D.; Kong, E.; Villanueva, J. Microplastics in the environment: Impact on human health and future mitigation strategies. *Environ. Health Rev.* **2020**, *63*, 27–31. [CrossRef]
- Urbanek, A.K.; Rymowicz, W.; Mirończuk, A.M. Degradation of plastics and plastic-degrading bacteria in cold marine habitats. *Appl. Microbiol. Biotechnol.* **2018**, *102*, 7669–7678. [CrossRef] [PubMed]
- Mannina, G.; Presti, D.; Montiel-Jarillo, G.; Suárez-Ojeda, M.E. Bioplastic recovery from wastewater: A new protocol for polyhydroxyalkanoates (PHA) extraction from mixed microbial cultures. *Bioresour. Technol.* **2019**, *282*, 361–369. [CrossRef]
- Huang, L.; Chen, Z.; Wen, Q.; Ji, Y.; Wu, Z.; Lee, D.J. Toward flexible regulation of polyhydroxyalkanoate composition based on substrate feeding strategy: Insights into microbial community and metabolic features. *Bioresour. Technol.* **2020**, *296*, 122369. [CrossRef]
- Chen, G.Q. Plastics completely synthesized by bacteria: Polyhydroxyalkanoates. In *Plastics from Bacteria. Natural Functions and Applications*; Springer: Berlin/Heidelberg, Germany, 2010; pp. 17–37.
- Sudesh, K.; Abe, H. *Practical Guide to Microbial Polyhydroxyalkanoates*, 1st ed.; iSmithers Rapra Publishing: Shrewsbury, UK, 2010; 160p.
- Laycock, B.; Halley, P.; Pratt, S.; Werker, A.; Lant, P. The chemomechanical properties of microbial polyhydroxyalkanoate. *Prog. Polym. Sci.* **2013**, *38*, 536–583. [CrossRef]
- Volova, T.G.; Shishatskaya, E.L.; Sinskey, A.J. *Degradable Polymers: Production, Properties, Applications*; Nova Science Pub Inc.: Hauppauge, NY, USA, 2013; 380p.
- Zheng, J.; Suh, S. Strategies to reduce the global carbon footprint of plastics. *Nat. Clim. Change* **2019**, *9*, 374–378. [CrossRef]
- Chen, G.Q.; Jiang, X.R.; Guo, Y. Synthetic biology of microbes synthesizing polyhydroxyalkanoates (PHA). *Synth. Syst. Biotechnol.* **2016**, *1*, 236–242. [CrossRef] [PubMed]
- Koller, M.; Mukherjee, A. Polyhydroxyalkanoates—Linking properties, applications, and end-of-life options. *Chem. Biochem. Eng. Q.* **2020**, *34*, 115–129. [CrossRef]
- Kalia, V.C.; Ray, S.; Patel, S.K.S.; Singh, M.; Singh, G.P.; Kalia, P. The dawn of novel biotechnological applications of polyhydroxyalkanoates. In *Biotechnological Applications of Polyhydroxyalkanoates*; Kalia, V.C., Ed.; Springer: Singapore, 2019; pp. 1–11.
- Tarrahi, R.; Fathi, Z.; Özgür, M.; Seydibeyoğlu, K.; Doustkhah, E.; Khataee, A. Polyhydroxyalkanoates (PHA): From production to nanoarchitecture. *Int. J. Biol. Macromol.* **2020**, *146*, 596–619. [CrossRef] [PubMed]
- Gogante, P.; Cinelli, P.; Seggiani, V.A.; Alaverex, A.; Lazzeri, A. Processing and thermomechanical properties of PHA. In *The Handbook of Polyhydroxyalkanoates. Kinetics, Bioengineering, and Industrial Aspects*, 1st ed.; Koller, M., Ed.; CRC Press: Boca Raton, FL, USA, 2020; Volume 3, pp. 91–118.
- Mitra, R.; Xu, T.; Chen, G.-Q.; Xiang, H.; Han, J. An updated overview on the regulatory circuits of polyhydroxyalkanoates synthesis. *Microb. Biotechnol.* **2022**. [CrossRef] [PubMed]
- Adeleye, A.T.; Odoh, C.K.; Enudi, O.C.; Banjoko, O.O.; Osiboye, O.O.; Odediran, E.T.; Louis, H. Sustainable synthesis and applications of polyhydroxyalkanoates (PHAs) from biomass. *Process Biochem.* **2020**, *96*, 174–193. [CrossRef]
- Ansari, S.; Sami, N.; Yasin, D.; Ahmad, N.; Fatma, T. Biomedical applications of environmental friendly poly-hydroxyalkanoates. *Int. J. Biol. Macromol.* **2021**, *183*, 549–563. [CrossRef] [PubMed]
- Hinchliffe, J.D.; Madappura, A.P.; Mohamed, S.M.D.S.; Roy, I. Biomedical applications of bacteria-derived polymers. *Polymers* **2021**, *13*, 1081. [CrossRef]
- Khosravi-Darani, K.; Mokhtari, Z.B.; Amai, T.; Tanaka, K. Microbial production of poly (hydroxybutyrate) from C1 carbon sources. *Appl. Microbiol. Biotechnol.* **2013**, *97*, 1407–1424. [CrossRef] [PubMed]

24. Riedel, S.L.; Brigham, C.J. Inexpensive and waste raw materials for PHA Production. In *The Handbook of Polyhydroxyalkanoates. Kinetics, Bioengineering, and Industrial Aspects*, 1st ed.; Koller, M., Ed.; CRC Press: Boca Raton, FL, USA, 2020; Volume 1, pp. 203–220.
25. Vandamme, P.; Coenye, T. Taxonomy of the genus *Cupriavidus*: A tale of lost and found. *Int. J. Syst. Evol. Microbiol.* **2004**, *54*, 2285–2289. [[CrossRef](#)] [[PubMed](#)]
26. Schlegel, H.G.; Kaltwasser, H.; Gottschalk, G. A submersion method for culture of hydrogen-oxidizing bacteria: Growth physiological studies. *Arch. Fur Mikrobiol.* **1961**, *38*, 209–222. [[CrossRef](#)]
27. Zavarzin, G.A. *Hydrogen Bacteria and Carboxydobacteria (Vodorodnyye Bakterii i Karboksidobakterii)*; Nauka: Moscow, Russia, 1978; 203p. (In Russian)
28. Tanaka, K.; Ishizaki, A.; Kanamaru, T.; Kawano, T. Production of poly (D-3-hydroxybutyrate) from CO₂, H₂, and O₂ by high cell density autotrophic cultivation of *Alcaligenes eutrophus*. *Biotechnol. Bioeng.* **1995**, *45*, 268–275. [[CrossRef](#)] [[PubMed](#)]
29. Tanaka, K.; Miyawaki, K.; Yamaguchi, A.; Khosravi-Darani, K.; Matsusaki, H. Cell growth and P(3HB) accumulation from CO₂ of a carbon monoxide-tolerant hydrogen-oxidizing bacterium, *Ideonella* sp. O-1. *Appl. Microbiol. Biotechnol.* **2011**, *92*, 1161–1169. [[CrossRef](#)] [[PubMed](#)]
30. Volova, T.G. *Hydrogen-Based Biosynthesis*; Nova Science Pub Inc.: Hauppauge, NY, USA, 2009; 287p.
31. Volova, T.; Kiselev, E.; Shishatskaya, E.; Zhila, N.; Boyandin, A.; Syrvacheva, D.; Vinogradova, O.; Kalacheva, G.; Vasiliev, A.; Peterson, I. Cell growth and PHA accumulation from CO₂ and H₂ of a hydrogen-oxidizing bacterium, *Cupriavidus eutrophus* B-10646. *Bioresour. Technol.* **2013**, *146*, 215–222. [[CrossRef](#)] [[PubMed](#)]
32. Green, P.R.; Kemper, J.; Schechtman, L.; Guo, L.; Satkowski, M.; Fiedler, S.; Steinbüchel, A.; Rehm, B.H.A. Formation of short chain length/medium chain length polyhydroxyalkanoate copolymers by fatty acid β -oxidation inhibited *Ralstonia eutropha*. *Biomacromolecules* **2002**, *3*, 208–213. [[CrossRef](#)] [[PubMed](#)]
33. Chanprateep, S.; Kulpreecha, S. Production and characterization of biodegradable terpolymer poly(3-hydroxybutyrate-co-3-hydroxyvalerate-co-4-hydroxybutyrate) by *Alcaligenes* sp. A-04. *J. Biosci. Bioeng.* **2006**, *101*, 51–56. [[CrossRef](#)]
34. Cavalheiro, J.M.B.T.; Raposo, R.S.; de Almeida, M.C.M.D.; Cesario, M.T.; Sevrin, C.; Grandfils, C.; da Fonseca, M.M.R. Effect of cultivation parameters on the production of poly (3-hydroxybutyrate-co-4-hydroxybutyrate) and poly (3-hydroxybutyrate-4-hydroxybutyrate-3-hydroxyvalerate) by *Cupriavidus necator* using waste glycerol. *Bioresour. Technol.* **2012**, *111*, 391–397. [[CrossRef](#)] [[PubMed](#)]
35. Collins, S.H. Choice of substrate in polyhydroxybutyrate synthesis. *Spec. Publ. Soc. General Microbiol.* **1987**, *21*, 161–168.
36. Chen, G.Q.; Chen, X.Y.; Wu, F.Q.; Chen, J.C. Polyhydroxyalkanoates (PHA) toward cost competitiveness and functionality. *Adv. Ind. Eng. Polym. Res.* **2020**, *3*, 1–7. [[CrossRef](#)]
37. da Silva, L.F.; Oliveira-Filho, E.R.; Piccoli, R.A.M.; Taciro, M.K.; Gomez, J.G.C. PHA biosynthesis starting from sucrose and materials from the sugar industry. In *The Handbook of Polyhydroxyalkanoates. Kinetics, Bioengineering, and Industrial Aspects*, 1st ed.; Koller, M., Ed.; CRC Press: Boca Raton, FL, USA, 2020; Volume 2, pp. 417–454.
38. Saratale, R.G.; Cho, S.K.; Saratale, G.D.; Kadam, A.A.; Ghodake, G.S.; Kumar, M.; Bharagava, R.N.; Kumar, G.; Kim, D.S.; Mulla, S.I.; et al. A comprehensive overview and recent advances on polyhydroxyalkanoates (PHA) production using various organic waste streams. *Bioresour. Technol.* **2021**, *325*, 124685. [[CrossRef](#)] [[PubMed](#)]
39. Dietrich, D.; Illman, B.; Crooks, C. Differential sensitivity of polyhydroxyalkanoate producing bacteria to fermentation inhibitors and comparison of polyhydroxybutyrate production from *Burkholderia cepacia* and *Pseudomonas pseudoflava*. *BMC Res. Notes* **2013**, *6*, 219. [[CrossRef](#)]
40. Kim, H.S.; Oh, Y.H.; Jang, Y.A.; Kang, K.H.; David, Y.; Yu, J.H.; Song, B.K.; Choi, J.; Chang, Y.K.; Joo, J.C.; et al. Recombinant *Ralstonia eutropha* engineered to utilize xylose and its use for the production of poly (3-hydroxybutyrate) from sunflower stalk hydrolysate solution. *Microb. Cell Fact.* **2016**, *15*, 95. [[CrossRef](#)] [[PubMed](#)]
41. Bhatia, S.K.; Gurav, R.; Choi, T.R.; Jung, H.R.; Yang, S.Y.; Moon, Y.M.; Song, H.S.; Jeon, J.M.; Choi, K.Y.; Yang, Y.H. Bioconversion of plant biomass hydrolysate into bioplastic (polyhydroxyalkanoates) using *Ralstonia eutropha* 5119. *Bioresour. Technol.* **2019**, *271*, 306–315. [[CrossRef](#)]
42. Hidayat, N.; Alamsyah, R.; Roslan, A.M.; Hermansyah, H.; Gozan, M. Production of polyhydroxybutyrate from oil palm empty fruit bunch (OPEFB) hydrolysates by *Bacillus cereus suaeda* B-001. *Biocatal. Agric. Biotechnol.* **2019**, *18*, 101019.
43. Ahn, J.; Jho, E.H.; Nam, K. Effect of acid-digested rice straw waste feeding methods on the 3HV fraction of bacterial poly(3-hydroxybutyrate-co-3-hydroxyvalerate) production. *Process Biochem.* **2016**, *51*, 2119–2126. [[CrossRef](#)]
44. Tanamool, V.; Soemphol, W. Polyhydroxyalkanoate (PHA) synthesis by newly bacterial isolates using non-detoxified rice husk hydrolysate. *Asia-Pacific J. Sci. Technol.* **2016**, *21*, 404–410.
45. Soto, L.R.; Byrne, E.; van Niel, E.W.J.; Sayed, M.; Villanueva, C.C.; Hatti-Kaul, R. Hydrogen and polyhydroxybutyrate production from wheat straw hydrolysate using *Caldicellulosus irruptor* species and *Ralstonia eutropha* in a coupled process. *Bioresour. Technol.* **2019**, *272*, 259–266. [[CrossRef](#)]
46. Kulkarni, S.O.; Kanekar, P.P.; Jog, J.P.; Sarnaik, S.S.; Nilegaonkar, S.S. Production of copolymer, poly(hydroxybutyrate-co-hydroxyvalerate) by *Halomonas campisalis* MCM B-1027 using agro-wastes. *Int. J. Biol. Macromol.* **2015**, *72*, 784–789. [[CrossRef](#)] [[PubMed](#)]
47. Lu, X.G.; Wang, Y.; Ding, J.; Weng, W. Engineering of an L-arabinose metabolic pathway in *Ralstonia eutropha* W50. *Wei Sheng Wu Xue Bao* **2013**, *53*, 1267–1275. (In Chinese) [[PubMed](#)]

48. Albuquerque, M.G.E.; Eiroa, M.; Torres, C.; Nunes, B.R.; Reis, M.A.M. Strategies for the development of a side stream process for polyhydroxyalkanoate (PHA) production from sugar cane molasses. *J. Biotechnol.* **2007**, *130*, 411–421. [[CrossRef](#)] [[PubMed](#)]
49. Park, S.J.; Jang, Y.A.; Noh, W.; Oh, Y.H.; Lee, H.; David, Y.; Baylon, M.G.; Shin, J.; Yang, J.E.; Choi, S.Y.; et al. Metabolic engineering of *Ralstonia eutropha* for the production of polyhydroxyalkanoates from sucrose. *Biotechnol. Bioeng.* **2015**, *112*, 638–643. [[CrossRef](#)] [[PubMed](#)]
50. Dalsasso, R.R.; Pavan, F.A.; Bordignon, S.E.; de Aragão, G.M.F.; Poletto, P. Polyhydroxybutyrate (PHB) production by *Cupriavidus necator* from sugarcane vinasse and molasses as mixed substrate. *Process Biochem.* **2019**, *85*, 12–18. [[CrossRef](#)]
51. Taher, I.B.; Fickers, P.; Chniti, S.; Hassouna, M. Optimization of enzymatic hydrolysis and fermentation conditions for improved bioethanol production from potato peel residues. *Biotechnol. Prog.* **2017**, *33*, 397–406. [[CrossRef](#)]
52. Naheed, N.; Jamil, N. Optimization of biodegradable plastic production on sugar cane molasses in *Enterobacter* sp. SEL2. *Braz. J. Microbiol.* **2014**, *45*, 417–426. [[CrossRef](#)] [[PubMed](#)]
53. Zhang, H.; Obias, V.; Gonyer, K.; Dennis, D. Production of polyhydroxyalkanoates in sucrose-utilizing recombinant *Escherichia coli* and *Klebsiella* strains. *Appl. Environ. Microbiol.* **1994**, *60*, 1198–1205. [[CrossRef](#)] [[PubMed](#)]
54. Arikawa, H.; Matsumoto, K.; Fujiki, T. Polyhydroxyalkanoates production from sucrose by *Cupriavidus necator* strains harboring csc genes from *Escherichia coli* W. *Appl. Microbiol. Biotechnol.* **2017**, *101*, 7497–7507. [[CrossRef](#)] [[PubMed](#)]
55. Purama, R.K.; Al-Sabahi, J.N.; Sudesh, K. Evaluation of date seed oil and date molasses as novel carbon sources for the production of poly (3-hydroxybutyrate-co-3-hydroxyhexanoate) by *Cupriavidus necator* H16 Re 2058/pCB113. *Ind. Crops Prod.* **2018**, *119*, 83–92. [[CrossRef](#)]
56. Jo, S.Y.; Sohn, Y.J.; Park, S.Y.; Son, J.; Yoo, J.I.; Baritugo, K.A.; David, Y.; Kang, K.H.; Kim, H.; Choi, J.; et al. Biosynthesis of polyhydroxyalkanoates from sugarcane molasses by recombinant *Ralstonia eutropha* strains. *Korean J. Chem. Eng.* **2021**, *38*, 1452–1459. [[CrossRef](#)]
57. Sen, K.Y.; Hussin, M.H.; Baidurah, S. Biosynthesis of poly (3-hydroxybutyrate) (PHB) by *Cupriavidus necator* from various pretreated molasses as carbon source. *Biocatal. Agric. Biotechnol.* **2019**, *17*, 51–59. [[CrossRef](#)]
58. Ertan, F.; Keskinler, B.; Tanniseven, A. Exploration of *Cupriavidus necator* ATCC 25207 for the production of poly(3-hydroxybutyrate) using acid treated beet molasses. *J. Polym. Environ.* **2021**, *29*, 2111–2125. [[CrossRef](#)]
59. Beaulieu, M.; Beaulieu, Y.; Mélinard, J.; Pandian, S.; Goulet, J. Influence of ammonium salts and cane molasses on growth of *Alcaligenes eutrophus* and production of polyhydroxybutyrate. *Appl. Environ. Microbiol.* **1995**, *61*, 165–169. [[CrossRef](#)]
60. Bozorg, A.; Vossoughi, M.; Kazemi, A.; Alemzadeh, I. Optimal medium composition to enhance poly-β-hydroxybutyrate production by *Ralstonia eutropha* using cane molasses as sole carbon source. *Appl. Food Biotechnol.* **2015**, *2*, 39–47.
61. Baei, M.S.; Najafpour, G.D.; Younesi, H.; Tabandeh, F.; Issazadeh, H.; Khodabandeh, M. Growth kinetic parameters and biosynthesis of polyhydroxybutyrate in *Cupriavidus necator* DSNZ 545 on selected substrates. *Chem. Ind. Chem. Eng. Q.* **2011**, *17*, 1–8. [[CrossRef](#)]
62. Volova, T.G.; Shishatskaya, E.I. *Cupriavidus eutrophus* Bacterial Strain VKPM B-10646-A Producer of Polyhydroxyalkanoates and a Method of Their Production (Cupriavidus eutrophus Shtamm Bakterii VKPM B-10646-Producent Poligidroksialkanoatov i Sposob Ikh Polucheniya. RF Patent No. 2439143, 10 January 2012. (In Russian).
63. Volova, T.; Kiselev, E.; Nemtsev, I.; Lukyanenko, A.; Sukovatyi, A.; Kuzmin, A.; Ryltseva, G.; Shishatskaya, E. Properties of degradable PHAs with different monomer compositions. *Int. Biol. Macromol.* **2021**, *182*, 98–114. [[CrossRef](#)]
64. Ryazanov, E.M.; Ostrovsky, D.I.; Bubnov, A.V. A Method for Obtaining Immobilized Invertase for the Hydrolysis of Sucrose (Metod Dlya Polucheniya Immobilizovannoi Invertazi Dlya Gidroliza Sakharozii). RF Patent No. 2158761C1, 10 November 2000. (In Russian).
65. Slavyanskiy, A.A.; Moiseyak, M.B.; Orekhova, I.S. Patent RU. Method for Purifying Molasses (Sposob Ochistki Melassi). RF Patent No. 230126, 20 June 2007.
66. Ermakov, A.I.; Arasimovich, V.V.; Smirnova-Ikonnikova, M.I.; Yarosh, N.P.; Lukovnikova, G.A. *Methods of Biochemical Plant Research (Metody Biokhimicheskogo Issledovaniya Rastenii)*; Kolos: Leningrad, Russia, 1972; 456p. (In Russian)
67. Braunnegg, G.; Sonnleitner, B.; Lafferty, R.M. A rapid gas chromatographic method for the determination of poly-β-hydroxybutyric acid in microbial biomass. *Eur. J. Appl. Microbiol. Biotechnol.* **1978**, *6*, 29–37. [[CrossRef](#)]
68. Volova, T.G.; Kiselev, E.G.; Vinogradova, O.N.; Nikolaeva, E.D.; Chistyakov, A.A.; Sukovatyi, A.G.; Shishatskaya, E.I. A glucose-utilizing strain, *Cupriavidus eutrophus* B-10646: Growth kinetics, characterization and synthesis of multicomponent PHAs. *PLoS ONE* **2014**, *9*, e87551. [[CrossRef](#)]
69. Chesnokov, N.V.; Yatsenkova, O.V.; Chudina, A.I.; Skripnikov, A.M.; Kuznetsov, B.N. The study of the sucrose hydrolysis with acid catalysts (Izuchenie reaktsii kislotno-kataliticheskogo gidroliza sakharozii). *J. Sib. Fed. Univ. Chem.* **2012**, *5*, 311–319. (In Russian)
70. Volova, T.G. Mineral nutrition of hydrogen and carboxydobacteria. In *Hydrogen-Based Biosynthesis*; Nova Science Publishers Inc.: New York, NY, USA, 2009; pp. 75–92.
71. Acosta-Cárdenas, A.; Alcaraz-Zapata, W.; Cardona-Betancur, M. Sugarcane molasses and vinasse as a substrate for polyhydroxyalkanoates (PHA) production. *Dyna* **2018**, *85*, 220–225. [[CrossRef](#)]
72. Steinbüchel, A.; Valentin, H.E. Diversity of bacterial polyhydroxyalkanoic acids. *FEMS Microbiol. Lett.* **1995**, *128*, 219–228. [[CrossRef](#)]

73. Volova, T.G.; Belyaeva, O.G.; Gitelzon, I.I.; Kalacheva, G.S.; Plotnikov, V.F.; Lukovenko, S.G. Preparation and study of microbial heteropolymer polyhydroxyalkanoates (Poluchenie i issledovanie mikrobnikh geteropolimernikh polioksialkanoatov). *Rep. Russ. Acad. Sci.* **1996**, *347*, 256–258. (In Russian)
74. Volova, T.G.; Kalacheva, G.S.; Steinbüchel, A. Biosynthesis of multi-component polyhydroxyalkanoates by the bacterium *Wautersia eutropha*. *Macromol. Symp.* **2008**, *269*, 1–7. [[CrossRef](#)]
75. Das, R.; Pal, A.; Paul, A.K. Bioconversion of sugarcane molasses to poly(3-hydroxybutyrate-co-3-hydroxyvalerate) by endophytic *Bacillus cereus* RCL 02. *J. Appl. Biol. Biotechnol.* **2019**, *7*, 20–24.
76. Hendrawan, Y.; Alvianto, D.; Sumarlan, S.H.; Wibisono, Y. Characterization of *Pseudomonas fluorescens* polyhydroxyalkanoates produced from molasses as a carbon source. *Adv. Food Sci. Sustain. Agric. Agroind. Eng.* **2020**, *3*, 1–10. [[CrossRef](#)]
77. Mascarenhas, J.; Aruna, K. Production and characterization of polyhydroxyalkanoates (PHA) by *Bacillus megaterium* strain JHA using inexpensive agro-industrial wastes. *Int. J. Rec. Sci. Res.* **2019**, *10*, 33359–33374.

Article

Two-Stage Polyhydroxyalkanoates (PHA) Production from Cheese Whey Using *Acetobacter pasteurianus* C1 and *Bacillus* sp. CYR1

Young-Cheol Chang^{1,2,*}, Motakatla Venkateswar Reddy³, Kazuma Imura¹, Rui Onodera¹, Natsumi Kamada² and Yuki Sano¹

¹ Course of Chemical and Biological Engineering, Division of Sustainable and Environmental Engineering, Muroran Institute of Technology, Hokkaido 050-8585, Japan; 21041006@mmm.muroran-it.ac.jp (K.I.); rui.onodera08@gmail.com (R.O.); 21041034@mmm.muroran-it.ac.jp (Y.S.)

² Course of Biosystem, Department of Applied Sciences, Muroran Institute of Technology, Hokkaido 050-8585, Japan; 18023034@mmm.muroran-it.ac.jp

³ Center for Biotechnology and Interdisciplinary Studies, Rensselaer Polytechnic Institute, Troy, NY 12180, USA; mvr_234@yahoo.co.in or motakv@rpi.edu

* Correspondence: ychang@mmm.muroran-it.ac.jp; Tel.: +81-143-46-5757

Abstract: Cheese whey (CW) can be an excellent carbon source for polyhydroxyalkanoates (PHA)-producing bacteria. Most studies have used CW, which contains high amounts of lactose, however, there are no reports using raw CW, which has a relatively low amount of lactose. Therefore, in the present study, PHA production was evaluated in a two-stage process using the CW that contains low amounts of lactose. In first stage, the carbon source existing in CW was converted into acetic acid using the bacteria, *Acetobacter pasteurianus* C1, which was isolated from food waste. In the second stage, acetic acid produced in the first stage was converted into PHA using the bacteria, *Bacillus* sp. CYR-1. Under the condition of without the pretreatment of CW, acetic acid produced from CW was diluted at different folds and used for the production of PHA. Strain CYR-1 incubated with 10-fold diluted CW containing 5.7 g/L of acetic acid showed the higher PHA production (240.6 mg/L), whereas strain CYR-1 incubated with four-fold diluted CW containing 12.3 g/L of acetic acid showed 126 mg/L of PHA. After removing the excess protein present in CW, PHA production was further enhanced by 3.26 times (411 mg/L) at a four-fold dilution containing 11.3 g/L of acetic acid. Based on Fourier transform infrared spectroscopy (FT-IR), and ¹H and ¹³C nuclear magnetic resonance (NMR) analyses, it was confirmed that the PHA produced from the two-stage process is poly-β-hydroxybutyrate (PHB). All bands appearing in the FT-IR spectrum and the chemical shifts of NMR nearly matched with those of standard PHB. Based on these studies, we concluded that a two-stage process using *Acetobacter pasteurianus* C1 and *Bacillus* sp. CYR-1 would be applicable for the production of PHB using CW containing a low amount of lactose.

Keywords: cheese whey; acetic acid; *Acetobacter pasteurianus* C1; *Bacillus* sp. CYR-1; PHA; PHB

Citation: Chang, Y.-C.; Reddy, M.V.; Imura, K.; Onodera, R.; Kamada, N.; Sano, Y. Two-Stage Polyhydroxyalkanoates (PHA) Production from Cheese Whey Using *Acetobacter pasteurianus* C1 and *Bacillus* sp. CYR1. *Bioengineering* **2021**, *8*, 157. <https://doi.org/10.3390/bioengineering8110157>

Academic Editor: Martin Koller

Received: 14 September 2021

Accepted: 21 October 2021

Published: 24 October 2021

Publisher's Note: MDPI stays neutral with regard to jurisdictional claims in published maps and institutional affiliations.



Copyright: © 2021 by the authors. Licensee MDPI, Basel, Switzerland. This article is an open access article distributed under the terms and conditions of the Creative Commons Attribution (CC BY) license (<https://creativecommons.org/licenses/by/4.0/>).

1. Introduction

The replacement of traditional plastics by bioplastics is gaining interest in the increasing of the sustainability of the polymer industry. One of the most promising groups of bioplastics are polyhydroxyalkanoates (PHA) [1]. However, the popularization of PHA has been limited by their production cost, which remains rather high, with raw materials responsible for most of the cost [2]. Therefore, in order to make PHA production more feasible for industrial application, different inexpensive substrates, such as molasses, sugars, oils, fatty acids, glycerol, organic matter from waste, starch-based materials, cellulosic materials, and hemi-cellulosic materials have been tested [3]. Reports are also available for the valorization of cheese whey (CW) into PHA [4]. CW is the liquid part of milk that is separated from the curd at the beginning of cheese manufacture, is available in large

amounts as a by-product, and contains fermentable nutrients, such as lactose, lipids, and soluble proteins [4]. CW separated in cheese production corresponds to about 90% in raw milk; therefore, its disposal as waste causes serious pollution problems in the surrounding environment [5,6]. In Japan, the number of cheese-producing factories is steadily increasing. Compared to 2006, the number of factories was tripled (319 factories, excluding major dairy companies) in 2018 (Japan Agriculture & Livestock Industries Corporation). However, the majority of CW is discarded into the environment, owing to expensive treatment processes. Therefore, the conversion of CW into a useful product, PHA, is a good option to reduce the environmental burden.

Reports are available for PHA production using CW and various microorganisms, such as *Methylobacterium* sp. ZP24, *Bacillus megaterium* CCM2037, *Azohydromonas lata* DSM1123, *Hydrogenophaga pseudoflava* DSM1034, and *Haloferax mediterranei* DSM1411 [5]. Most of the studies used CW, which contains high amounts of lactose. Lactose present in CW converts into glucose-galactose by the action of β -galactosidase enzymes, and then converts further into PHA [5]. For achieving an economically competitive production of PHA from CW, there is a need to discover the wild-type bacterial species that can directly produce high levels of PHA. However, currently, only a few wild-type bacteria are available that can directly produce PHA from whey lactose [7]. Recombinant *E. coli* is widely used for PHA production, because many wild-type bacteria cannot directly metabolize the CW, due to the absence of β -galactosidase enzymes [8].

While the genetic engineering method is a versatile tool for PHA production, it requires more controlled production plants, which increases the cost [9]. Amaro et al. suggested that using CW and wild-type strains will reduce the production cost [9]. Hence, the present studies were carried out using CW and wild-type bacterial strains for the production of PHA.

PHA has been extensively studied as an alternative to petroleum-based plastics [10]. However, it has not yet been in practical use because of its high production cost, primarily owing to the high cost of substrates (11% of the total production cost) that are used for the growth of microorganisms [10]. For this reason, in our previous study, we examined the capability of strain CYR1 in producing PHA using raw CW as a feed stock. However, the production yield was not as high as we expected, at 0.15 g/L PHB of the dry cell weight (DCW) [10]. On the other hand, various fatty acids (short and medium chain fatty acids) and their subsequent conversion into PHA were evaluated in order to investigate the possibility of using wastewater containing fatty acids. As a result, acetic acid was the most efficient carbon source for PHA production among the tested fatty acids [11]. Obviously, CW is still a very attractive feedstock for the production of PHA. Thus, to improve the capability of PHA production, we designed a two-stage process: CW was converted to acetic acid using *Acetobacter pasteurianus* C1 in the first stage, and, in the second stage, acetic acid produced from CW was converted to PHA using *Bacillus* sp. CYR-1. Firstly, acetic-acid-producing bacteria (*Acetobacter pasteurianus* C1) was isolated, and the culture conditions for acetic acid production from CW were determined. In the previous study, we did not know whether strain CYR1 utilizes the lactose that is in CW. Therefore, a utilization test of lactose using strain CYR1 and *Acetobacter pasteurianus* C1 was performed. Further experiments were conducted for PHA production with acetic acid produced from CW. Furthermore, the PHA production was also evaluated with pretreated CW (after removing excess protein). The consumption of acetic acid and the concentration of the PHA produced were analyzed with high-performance liquid chromatography (HPLC). Finally, the functional groups, primary structure, higher-order structure, and thermal properties of the produced poly- β -hydroxybutyrate (PHB) from the two-stage process were analyzed using Fourier transform infrared spectroscopy (FT-IR), ^1H ^{13}C nuclear magnetic resonance (NMR), and thermogravimetric analysis (TGA), respectively.

2. Materials and Methods

2.1. Biocatalyst

Bacteria *Acetobacter pasteurianus* C1 isolated in the present study and *Bacillus* sp. CYR1 were used to produce acetic acid and PHA, respectively. Our previous studies have proven that CYR1 strain can utilize diverse types of fatty acids, such as C2–C6, for its growth [10].

2.2. Isolation of Acetic-Acid-Producing Bacteria and Optimum Conditions for Acetic Acid Production

Fermented food waste was used for the isolation of acetic-acid-producing bacteria. The liquid (leachate) obtained from the food waste was diluted at 10 folds with saline solution (NaCl, 0.9%), spread on agar plates, and incubated under aerobic conditions at 30 °C for several days. Obtained bacterial colonies were separated based on the color, shape, and size, and each individual colony was grown on new agar plates until a pure culture was obtained. Morphological characterization of pure bacterial colonies was carried out by staining with a Gram stain kit (Becton Dickinson Company, Tokyo, Japan). A total of 40 pure bacterial colonies were obtained, and the purity of each isolate was determined using an optical microscope (DA1-180M, AS ONE, Osaka, Japan).

Isolated bacteria (40 pure colonies) were separately pre-grown for 72 h on mineral salt medium (MS medium) containing yeast extract (10 g/L) as a sole nutrient source. The medium pH was adjusted to 5.8 and sterilized in an autoclave for 15 min at 121 °C. Pre-cultures were harvested by centrifugation (8000× g, 4 °C, 10 min), and obtained pellet was washed two times to remove the remaining carbon sources and suspended in MS medium, which contains 36 g/L of glucose, 10 g/L of yeast extract, and ethanol (7.76 g/L) in serum bottles capped with autoclave-sterilized air-permeable silicone plugs, which were then incubated aerobically with orbital shaking at 120 rpm for 5 days at 30 °C for acetic acid production. The optimum conditions, i.e., initial cell concentration, pH (3 to 8), temperature (25 to 42 °C), ethanol concentration (0 to 77.63 g/L), and rotation speed, were also determined to produce acetic acid using the MS medium. Experiments were conducted for 4 days under shaking at 100 rpm and pH 7.0 in 50 mL serum bottles. Ethanol concentration experiments were conducted for 10 days. Agar plates were prepared by dissolving polypeptone (5 g), yeast extract (5 g), glucose (5 g), MgSO₄·7H₂O (1 g), and agar (20 g) in one liter of distilled water. One liter of MS medium contained the following composition: 1.0 g K₂HPO₄, 0.05 g NaCl, 0.2 g MgSO₄·7H₂O, 0.05 g CaCl₂, 0.0083 g FeCl₃·6H₂O, 0.014 g MnCl₂·4H₂O, 0.017 g NaMoO₄·2H₂O, and 0.001 g ZnCl₂.

Among 40 pure colonies, the highest acetic-acid-producing bacteria were identified by 16S rDNA analysis. The isolate was grown on a yeast extract medium, and total genomic DNA was extracted using the achromopeptidase (Fujifilm Wako Pure Chemical, Japan) in accordance with the protocol provided by the manufacturer. Extracted bacterial genomic DNA was amplified by polymerase chain reaction (PCR) with a pair of universal primers: 10f (5'-GAGTTTGATYCTGGCTCAG-3') and 1510r (5'-GGTTACCTTGTTACGACTT-3'), under standard conditions. PCR was performed for 2 min at 94 °C, followed by 30 amplification cycles of 45 s at 94 °C, 30 s at 52 °C, and 90 s at 72 °C, with a final cycle for 20 min at 72 °C. Amplified PCR products were purified with a QIAquick PCR purification kit (Qiagen, Hilden, Germany). Sequences were determined using an ABI prism 3130 Sequencer (Applied Biosystems, CA, USA), and the sequence products were assembled with ChromasPro 2.1 (Technelysium, Tewantin, Australia). Obtained DNA sequences were compared using Basic Local Alignment Search Tool (BLAST) search program with the National Center for Biotechnology Information (NCBI) gene bank database (www.ncbi.nlm.nih.gov, accessed on 28 September 2021). DNA sequencing was performed according to the previously reported method [12,13].

2.3. Acetic Acid Production with CW

CW was collected from a cheese-producing factory in Hokkaido, Japan, and stored in a darkroom at 4 °C. Even though it had high chemical oxygen demand (COD, 107,000 mg/L) and total nitrogen (TN, 1380 mg/L), it contained low lactose (approximately 4.0 g/L) concentration. The addition of ethanol is indispensable for the current acetic acid fermentation [14]. The CW was diluted 2-fold with deionized water, and pH was adjusted to 5.5 or 6.6 with 1 N HCl or 1 N NaOH, which was added (200 mL) into 500 mL Erlenmeyer flask, and autoclaved (121 °C, 15 min). After cooling, 2 mL of pre-cultivated cells and 2 mL of 99.5% ethanol were added, and the flasks were capped with autoclave-sterilized air-permeable silicone plugs and maintained under shaking (100 rpm) at 30 °C in an incubator. Control experiments were carried out without adding C1 strain. Samples were collected at different time intervals aseptically on a clean bench to measure the pH, acetic acid concentration, and ethanol concentration. Experiments were stopped when ethanol concentration reached below 0.3 g/L, because acetic acid production is dependent on ethanol consumption, as confirmed in our preliminary experiments.

2.4. Lactose Utilization Experiments

PHA-producing bacteria (*Bacillus* sp. CYR1) and acetic-acid-producing bacteria (C1 strain) were examined regarding whether these bacteria can utilize lactose or not. Acetic acid, glucose, yeast extract, lactose, and poly peptone, each at 5 g/L concentration, as well as 0.2 mL of ethanol, were added in MS medium. Medium pH was adjusted to 7.0, and 20 mL of medium was dispensed into a 50 mL serum bottle and autoclaved. Ethanol was added after autoclave. Bacteria were added in each serum bottle except blank, and the serum bottles were incubated aerobically at 30 °C with orbital shaking at 120 rpm for 7 days and 11 days for CYR1 and C1 strains, respectively. All of the conditions were tested as biological triplicates (three serum bottles, $n = 3$) within a single experiment.

2.5. PHA Production without Pre-Treatment of CW and Quantification

Two-stage PHA production experiments were performed with *Acetobacter pasteurianus* C1 and *Bacillus* sp. CYR-1 using acetic acid obtained from CW. The initial concentration of acetic acid and total nitrogen from the CW fermentation step was 24.6 g/L and 0.853 g/L, respectively. To lower the concentration of total nitrogen, dilutions were made (4-fold, 10-fold, and 20-fold) and used for the PHA production. The two-stage process was carried out in different Erlenmeyer flasks. Experiments were also carried out using the CW without dilution. PHA production experiments were conducted in 1 L Erlenmeyer flasks that contain 500 mL of diluted CW containing acetic acid after adjusting the pH to 7.0. Pre-grown CYR1 cultures were added to each flask and incubated for 60 h under shaking (100 rpm) at 30 °C. For diluted CW, the growth curve was measured using a spectrophotometer (UV-1800, Shimadzu, Kyoto, Japan) at OD₆₀₀. Each diluted CW without addition of bacteria (1 mL) was used as a blank [10]. We did not adopt the dry weight method because the variation of each sample was significant due to the amount of whey being much higher than that of the cells.

PHA separation from culture was performed as mentioned by Law and Slepecky [15], as well as by the Soxhlet extraction method. Centrifugation (8000 × g for 10 min at 4 °C) was used to separate the cells, and cell disruption was carried out using a Branson ultrasonic disrupter (Sonifer 250, Danbury, CT, USA) at three-minute flash for 30 min at output—3 and duty cycle—50%. Cell debris was removed by centrifugation at 3000 × g for 20 min. Sodium hypochlorite (4%) was used for suspension of biomass pellet, and the solution was incubated for 4 h at room temperature. The resulting solution (the pellet with lysed cells) was centrifuged, and the supernatant was discarded. The lysed cells were washed with acetone and ethanol, and they were liquefied in hot CHCl₃ and filtered. The filtrate was concentrated using a rotary evaporator (EYELA N-1000, Tokyo Rikakikai, Japan), followed by drying until obtaining a persistent weight. This procedure was adopted for the evaluation of dry cell mass. To enhance the PHA extraction effect, the Soxhlet

extraction method was adopted. After centrifugation, the biomass pellet was disrupted with a Branson ultrasonic disrupter. Cell debris was removed by centrifugation at $8000\times g$ for 10 min, and the pellet was placed in an extraction thimble. CHCl_3 was added to the round-bottom flask, and Soxhlet extraction was carried out for 24 h.

2.6. Effect of Pre-Treatment of CW for the Production of PHA

After finishing the above-mentioned two-stage PHA production experiments, we realized that many studies removed excess protein present in CW for the PHA production experiments [9,16,17]. To remove excess protein present, CW was acidified at pH 4.0 with 1.0 M H_2SO_4 [16]. The solution was autoclaved at 121 °C for 15 min and centrifuged at $8000\times g$ in sterilized tubes for 10 min to remove aggregates [17]. The supernatant (whey supernatant) was passed through ADVANTEC No. 2 filters (ADVANTEC, City, Japan). PHA production was performed in a two-stage process with *Acetobacter pasteurianus* C1 and *Bacillus* sp. CYR1.

2.7. PHB Identification

The FT-IR spectrum of PHB produced by CYR-1 was measured by attenuated total reflection using a Nicolet 6700 FT-IR spectrometer (Thermo Fisher Scientific, Waltham, MA, USA). ^1H (300 MHz) and ^{13}C (75 MHz) NMR spectra were recorded on an Oxford YH300 NMR spectrometer (Oxford instrument, Oxford, UK) at 20 °C. The NMR sample was dissolved in deuterated chloroform (CDCl_3 , Sigma-Aldrich), and impurities were removed by filtration with cotton. TGA (TGA 2050, TA Instruments, New Castle, DE, USA) was used to determine the decomposition temperature (Td) of PHB.

2.8. Analysis

COD_{Mn} was measured using the permanganate method with a COD-60A meter (DKK-TOA Corp., Shinjuku-ku, Japan). Total nitrogen (TN) was measured using a DRB 200 dual block (Hach, Loveland, CO, USA) and DR 900 multiparameter portable colorimeter (Hach, Loveland, CO, USA). Spectrometric analysis was conducted to determine the PHB concentration. The extracted PHB by using the Soxhlet method was dissolved in 1 mL of sulfuric acid (36 N), and the resultant solution was heated at 100 °C in a dry thermost bath for 60 min. The addition of sulfuric acid converted PHB into crotonic acid. The solution was cooled and diluted 50 times using sulfuric acid (0.01 N). The solution was filtrated and analyzed by HPLC (Shimadzu, Kyoto, Japan) with an SPD-10AV UV/Vis detector and a Shim-pack SCR-102 (H) column (Shimadzu, Kyoto, Japan). Filtered and degassed 5 mmol/L perchloric acid was used as mobile phase at a flow rate of 1.5 mL/min. The column was maintained at a temperature of 40 °C in a thermostat chamber. The absorbance was measured at 210 nm for determining the PHB concentration. A standard curve was prepared using pure PHB (Sigma-Aldrich). The concentrations of acetic acid and lactose at different time intervals were analyzed on HPLC (Shimadzu) with an RI detector and Shim-pack SCR-102 (H) column (Shimadzu, Kyoto, Japan). Samples collected for HPLC analysis were acidified with phosphoric acid (10%, w/v) to stop the biological reaction and centrifuged at $8000\times g$ for 10 min. The resulting supernatant was filtered and analyzed directly by HPLC. Filtered and degassed 5 mmol/L perchloric acid was used as mobile phase at a flow rate of 1.5 mL/min. The column was maintained at a temperature of 40 °C in a thermostat chamber.

3. Results and Discussion

3.1. *Acetobacter Pasteurianus* C1 Strain

Acetic acid production studies were conducted using the 40 isolated bacterial strains; among them, three colonies produced good amounts of acetic acid, but colony #36 produced the highest amount of acetic acid. Hence, genomic DNA was isolated from this strain and 16S rDNA sequence analysis was carried out. The gene sequence analysis showed that the strain has a 100% identity with *Acetobacter pasteurianus* LMG 1262^T (Figure 1), so strain #36

was named as *Acetobacter pasteurianus* C1, and its 16S rDNA sequence was deposited in the DNA Data Bank of Japan (DDBJ, Accession number LC646164). Below is the phylogenetic tree constructed based on the BLAST homology search for the International Nucleotide Sequence Databases.

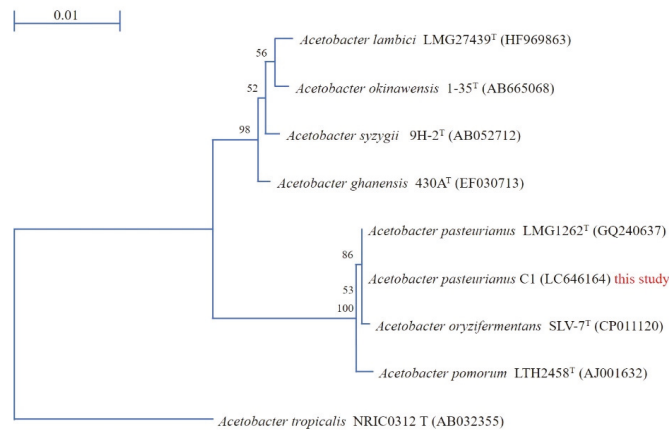


Figure 1. A neighbor-joining tree showing the phylogenetic relationship of the 16S rDNA sequence of C1 strain with related organisms. Bootstrap values of 100 analyses are shown at the branch point.

It is a Gram-negative, rod-shaped bacteria, commonly associated with plants and plant products, and is widely used in the production of fermented foods, such as kefir and vinegar [18,19]. Acetic acid production using wild and engineered *Acetobacter pasteurianus* strains (*A. pasteurianus* SKU1108, *A. pasteurianus* TI and TH-3 (thermo-adapted strain SKU1108), *A. pasteurianus* CICIM B7003-2, *A. pasteurianus* CWBI-B419, *A. aceti* subs. *Xylinum* NBI1002, *A. aceti* subs. *aceti* 1023, *A. aceti* M23) and *Gluconacetobacter* bacterial strains (*G. europaeus* DES11-DSM 6160, *G. europaeus* V3 and JK2, *G. intermedius* JK3, *G. entanii* LTH 4560T) have been well-documented by Gullo et al. [20].

3.2. Optimum Conditions for the Production of Acetic Acid

Optimum conditions (pH, temperature, ethanol concentration, rotation speed) for the production of acetic acid were determined using the C1 strain. A high amount of acetic acid production (10.05 g/L) was observed at pH 4.0 and 5.0 (Figure 2). Strain C1 produced acetic acid between pH 4.0 and 7.0, but it was unable to produce at pH 3.0 and 8.0 (Figure 2). At pH 3 and 8 lower growth was observed, (Figure 3), but, slight decrease in ethanol concentration at pH 3 and 8 (Figure 4) was observed it might be due to the evaporation of ethanol. A relatively similar cell growth of strain C1 was observed between pH 4 and pH 7. A rapid initial cell growth was observed at pH 4, 5 and 7 (Figure 3). Decrements in the ethanol concentration under different pH conditions were determined (Figure 4). Ethanol was completely utilized within 3 days at pH 4, 5, 6, and 7. The effect of the optimum ethanol concentration on acetic acid production was also examined. Acetic acid production was not observed without the addition of ethanol, and also at higher (77.63 g/L) ethanol concentrations (data not shown), whereas a higher acetic acid production (37.02 g/L) was observed at 54.34 g/L of ethanol (Figure 5). Regarding temperature, the C1 strain showed a higher acetic acid production (9.61 g/L) at 30 °C (Figure 6), and no production at above 40 °C (data not shown). The acetic acid production (Figure 7A) and growth curve of strain C1 (Figure 7B) at different rotation speeds were determined. The highest acetic acid production and cell growth were obtained at the rotation speed of 180 rpm. After the optimization of all of the conditions, the C1 strain showed a higher acetic acid production (37.02 g/L), with an initial cell concentration of 0.45 g/L, ethanol concentration of 54.34 g/L,

and at the rotation speed of 180 rpm (data not shown). The acetic-acid-producing ability of the C1 strain was comparable to other wild-type strains (Table 1).

Ndoye et al. reported that *A. pasteurianus* CWBI-B419 produced 16 g/L of acetic acid under the optimum conditions (38 °C, ethanol concentration of 19.4 g/L, and the rotation speed of 130 rpm) [21]. Kanchanarach et al. reported that *A. pasteurianus* MSU10 and SKU1108 produced 25 g/L and 35 g/L of acetic acid at 37 °C, with an ethanol concentration of 38.82–46.58 g/L and a rotation speed of 200 rpm [22]. Perumpuli et al. reported that *A. pasteurianus* SL13E-2, SL13E-3, and SL13E-4 produced more than 40 g/L of acetic acid at 37 °C, an ethanol concentration of 46.58 g/L, and at 200 rpm [23]. Es-sbata et al. reported that *A. malorum* strains produced more than 40 g/L of acetic acid at 37 °C [24]. Kadere et al. isolated several *Acetobacter* and *Gluconobacter* strains. The isolated *Acetobacter* and *Gluconobacter* strains both showed growth at 25, 30, and 40 °C and at pH 7.0 and 4.5, whereas there was no growth at 45 °C, and pH 2.5 and 8.5 [25]. Iino et al. reported that *G. kakaiceti* sp. I5-1^T and G5-1 showed growth at pH 3.5–8.0, whereas there was no growth at pH 3.0 and 8.5 [26]. Saeki et al. reported that *A. rancens* SKU 1102 produced approximately 43.0 g/L of acetic acid at 38 °C, with an ethanol concentration of 31.05 g/L and at 220 rpm, and with a supplement of acetic acid (10 g/L) [27]. Vashisht et al. reported that *A. pasteurianus* SKYAA25 produced 52.4 g of acetic acid using 100 g of dry matter of apple pomace at pH 5.5, temp 37 °C, ethanol concentration of 62.10 g/L, and at 180 rpm [28]. Chen et al. reported that *A. pasteurianus* AAB4 produced 42 g/L of acetic acid at 37 °C, an ethanol concentration of 77.63 g/L, and at 180 rpm [29]. Wu et al. reported that *A. pasteurianus* CICC 20001 produced 48.24 g/L of acetic acid in a 15 L stir tank reactor at 32 °C, an ethanol concentration of 35.70 g/L, and at 180 rpm, and with a supplement of acetic acid (12 g/L) [30]. Engineered strains *A. aceti* subsp. *Xylinum* NBI2099 (pAL25) and *A. pasteurianus* CICIM B7003-2 produced higher amounts of acetic acid, at 96.6 g/L and 90 g/L of acetic acid, respectively, than wild-type strains [31,32]. In order to compare the acetic acid production ability with other *Acetobacter*, *Acetobacter pasteurianus* (NBRC105185) was purchased from National Institute of Technology and Evaluation, Japan, and experiments were conducted for 10 days under similar conditions using both the strains in separate flasks. *Acetobacter pasteurianus* produced 33.9 g/L, whereas our strain C1 produced 37.02 g/L of acetic acid. Therefore, it can be concluded that the acetic acid production ability of the C1 strain is greater than that of *Acetobacter pasteurianus* (NBRC105185).

Table 1. Overview of optimum conditions reporting acetic acid production using pure microbial cultures.

Strain	Acetic Acid (g/L)	pH	Temperature (°C)	Ethanol (g/L)	Rotation Speed (rpm)	References
<i>Acetobacter pasteurianus</i> CWBI-B419	16	n.a	38	19.4	130	[21]
<i>Acetobacter pasteurianus</i> MSU10	25	n.a	37	38.82–46.58	200	[22]
<i>Acetobacter pasteurianus</i> SKU1108	35	n.a	37	38.82–46.58	200	[22]
<i>Acetobacter pasteurianus</i> SL13E-2	40	n.a	37	46.58	200	[23]
<i>Acetobacter pasteurianus</i> SL13E-3	40	n.a	37	46.58	200	[23]
<i>Acetobacter pasteurianus</i> SL13E-4	40	n.a	37	46.58	200	[23]
<i>Acetobacter malorum</i>	40	n.a	37	n.a	n.a	[24]
<i>Acetobacter rancens</i> SKU 1102	43.0	n.a	38	31.05	220	[27]

Table 1. Cont.

Strain	Acetic Acid (g/L)	pH	Temperature (°C)	Ethanol (g/L)	Rotation Speed (rpm)	References
<i>Acetobacter pasteurianus</i> SKYAA25	52.5 g/100 g of dry substrate	5.5	37	62.10	180	[28]
<i>Acetobacter pasteurianus</i> AAB4	42	n.a	37	77.63	180	[29]
<i>Acetobacter pasteurianus</i> CICC 20001	48.24	n.a	32	35.70	180	[30]
<i>Acetobacter pasteurianus</i> C1	37.02	4–5	30	54.34	180	This study

n.a.: not available.

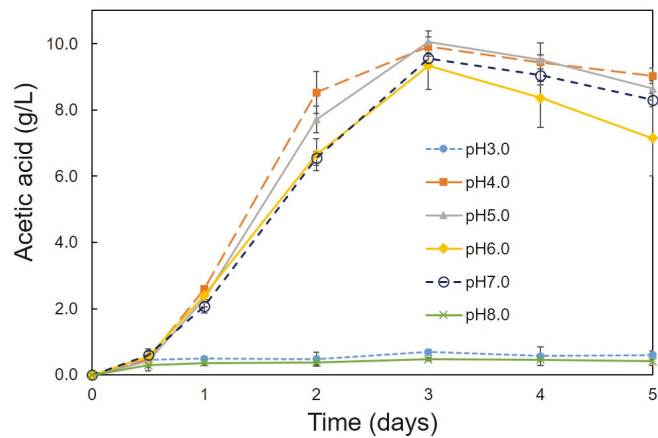


Figure 2. Evaluation of pH values for acetic acid production. Cultivation was conducted at 30 °C with initial cell concentration of 0.45 g/L, ethanol concentration of 7.76 g/L, and at the rotation speed of 100 rpm.

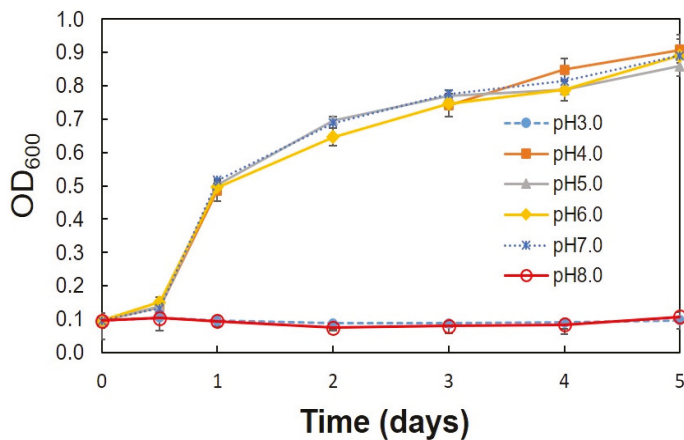


Figure 3. Growth curve of strain C1 at different initial pH values. Cultivation was conducted at 30 °C with initial cell concentration of 0.45 g/L, ethanol concentration of 7.76 g/L, and at the rotation speed of 100 rpm.

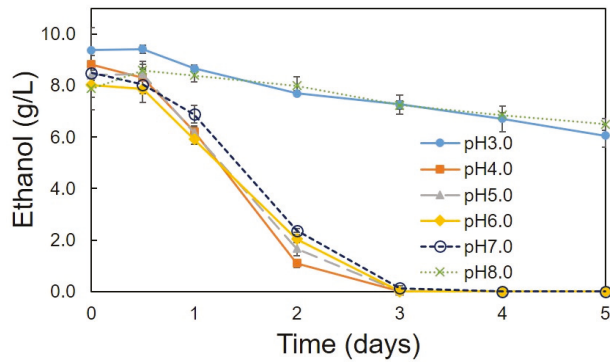


Figure 4. Evaluation of pH values for ethanol utilization. Cultivation was conducted at 30 °C with initial cell concentration of 0.45 g/L and at the rotation speed of 100 rpm. Ethanol (7.76 g/L) was added to the cultures at different pH values.

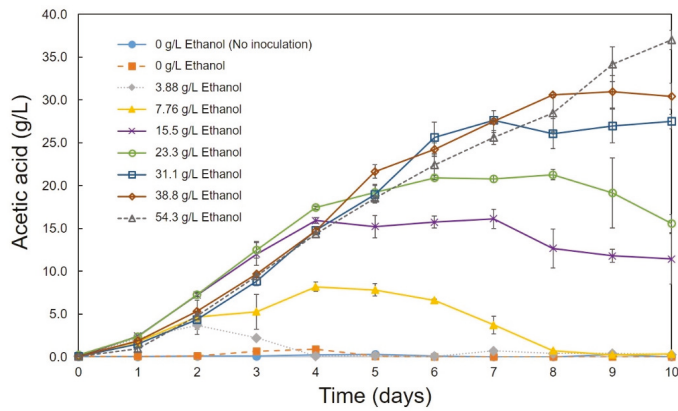


Figure 5. Acetic acid production at different initial ethanol concentrations. Cultivation was conducted at 30 °C with initial cell concentration of 0.45 g/L and at the rotation speed of 100 rpm.

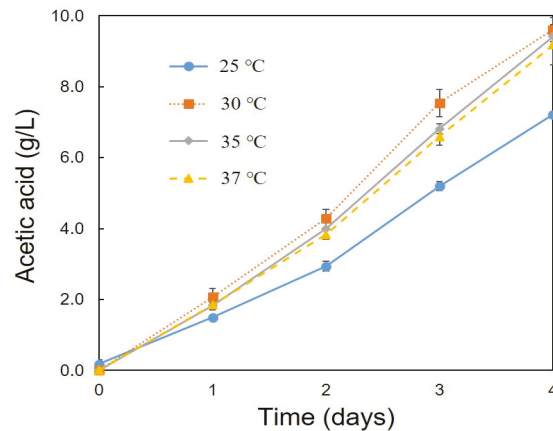


Figure 6. Optimal temperature conditions for acetic acid production. Cultivation was conducted with initial cell concentration of 0.45 g/L, ethanol concentration of 7.76 g/L, and at the rotation speed of 100 rpm.

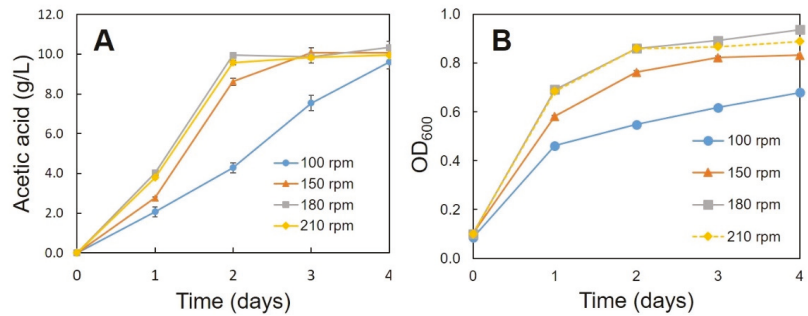


Figure 7. Acetic acid production (A) and growth curve of strain C1 (B) at different rotation speeds. Cultivation was conducted at 30 °C with initial cell concentration of 0.45 g/L and ethanol concentration of 7.76 g/L.

All of the conditions were tested as biological triplicates (three serum bottles, $n = 3$) within a single experiment. The data were presented as mean \pm standard deviation.

3.3. Lactose Utilization

Various carbon sources (acetic acid, glucose, lactose) and nutrient sources (peptone, yeast extract) at different combinations were used for the growth of CYR1, and the growth was measured with a spectrophotometer by taking the culture absorbance at OD₆₀₀, as shown in Figure 8. OD₆₀₀ increased with all of the conditions except the control. Control experiments were conducted without adding the CYR1 strain. Bacteria grown with the medium, which contained glucose and acetic acid as carbon sources, showed the highest growth (OD₆₀₀ 2.05). There was no difference in the growth of bacteria when they were grown with a medium that contained only acetic acid, or with the combination of acetic acid and lactose. Lactose utilization was examined also using the *Acetobacter pasteurianus* C1 strain. However, as shown in Figure 9, a decrement in the lactose concentration was not observed in all experiments regardless of the presence or absence of a co-substrate. Thus, it can be understood that the CYR1 and C1 strains are unable to utilize lactose as a carbon source for their growth. The HPLC analysis results also supported this statement: no decrement in the lactose concentration was observed until the end of the experiment (data not shown).

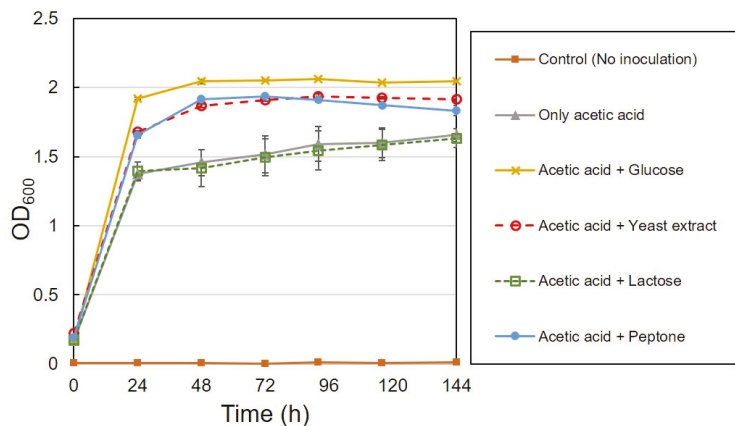


Figure 8. Bacterial growth curve using strain CYR1 with different carbon and nutrient sources. Cultivation was conducted at 30 °C, pH 7.0, ethanol concentration of 7.76 g/L, and at the rotation speed of 120 rpm.

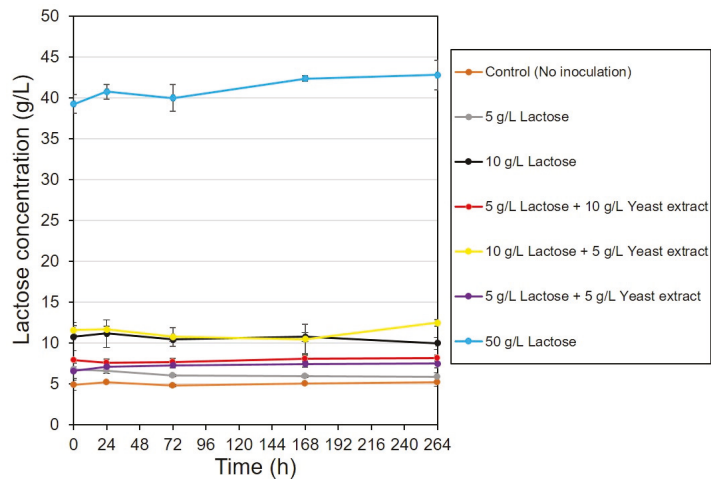


Figure 9. Lactose utilization experiments by strain C1 using various carbon sources. Cultivation was conducted at 30 °C, pH 7.0, ethanol concentration of 7.76 g/L, and at the rotation speed of 120 rpm.

3.4. PHA Production with Two-Stage Methodology

3.4.1. First Stage—Acetic Acid Production

Acetic acid production using the C1 strain with diluted CW was performed. As shown in Figure 10A, the acetic acid concentration (24.4 g/L) gradually increased until 96 h of incubation time. Up to the present day, several reports about acetic acid production with CW have been reported. Lustrato et al. used a yeast (*Kluyveromyces marxianus* Y102) and *Acetobacter aceti* DSM-G3508 co-culture in a bioreactor and produced 4.35 g/L of acetic acid per day under anaerobic conditions [33]. Veeravalli and Mathews produced 24 g/L of acetate under anaerobic conditions using *Lactobacillus buchmeri* and CW [34]. *Enterobacter aerogenes* MTCC 2822 immobilized on a column reactor produced 2.1 g/L of acetic acid under anaerobic conditions [35]. Pandey et al. reported that 7 g/L of acetic acid was produced under anaerobic condition by *Lactobacillus acidophilus* in a bioreactor using CW [36]. Ricciardi et al. reported that 1.23 g/L of acetic acid was produced under aerobic conditions by *Lactobacillus casei* in a bioreactor using CW [37]. Gullo et al. reported that acetic acid bacteria can produce acetic acid in fermenting liquids, in which, the ethanol content ranges from 2–3% to 15–18%, depending on the fermentation system and the microbial strains used [20]. As shown in Figure 10B, the ethanol concentration decreased as the acetic acid concentration increased. After 108 h, cultivation was terminated, as the ethanol concentration was 0.27 ± 0.26 g/L, and, in addition, no increment in the acetic acid concentration was observed after 96 h.

The acetic acid concentration at the initial and final stages was calculated, and a decrement was observed under all of the conditions because of its utilization by bacteria (Table 2). The highest acetic acid consumption of 49.1% was observed at a 10-fold dilution, followed by 31.6%, 14%, and 9% at 20-fold, 4-fold, and 2-fold dilutions, respectively. No decrement was observed with the control (without bacteria), indicating that the CYR1 strain utilizes the acetic acid as a carbon source for its growth.

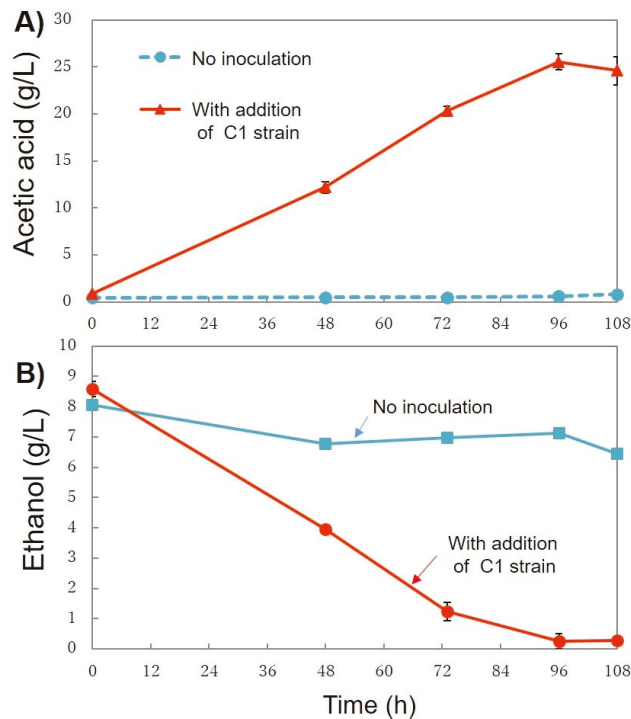


Figure 10. Acetic acid production (A) and utilization of ethanol (B) by strain C1 using CW (2-fold diluted). CW was used without pre-treatment. All of the conditions were tested as biological triplicates (three Erlenmeyer flasks, $n = 3$) within a single experiment. The data were presented as mean \pm standard deviation.

Table 2. Acetic acid consumption by CYR1 strain using acetic-acid-fermented CW. CW was used without pre-treatment at different dilutions.

Culture Condition	20-Fold	10-Fold	4-Fold	2-Fold
Initial concentration of acetic acid (g/L)	3.8	5.7	12.3	24.4
Final concentration of acetic acid (g/L)	2.6	2.9	10.6	22.2
The utilized acetic acid (g/L)	1.2	2.8	1.7	2.2
The utilized acetic acid (%)	31.6	49.1	13.8	9.0

All of the conditions were tested as biological duplicates (two Erlenmeyer flasks, $n = 2$) within a single experiment. Data are the mean values of two Erlenmeyer samples.

3.4.2. Second Stage—PHA Production

For PHA production, acetic acid produced from acetic-acid-fermented CW at four dilutions (20-fold, 10-fold, 4-fold, 2-fold) was used. Experiments were also conducted with undiluted CW. The initial acetic acid concentration is 3.8 g/L (20-fold), 5.7 g/L (10-fold), 12.3 g/L (4-fold), and 24.4 g/L (2-fold), and the initial TN concentration is 108 mg/L (20-fold), 234 mg/L (10-fold), 509 mg/L (4-fold), and 1077 mg/L (2-fold). Table 3 shows the results of PHA production at each dilution ratio. The highest PHA production of 240.6 mg/L was obtained with CW at the 10-fold dilution (5.7 g/L, acetic acid).

Figure 11 shows the growth of CYR1 with acetic-acid-fermented CW at different dilution rates. The strain CYR1 with undiluted acetic-acid-fermented CW did not show any growth. The strain CYR1 grown with acetic-acid-fermented CW at 4-fold dilution (12.3 g/L,

acetic acid) showed growth until 36 h, reached the maximum OD value of 1.66, and then decreased. The strain CYR1 grown with acetic-acid-fermented CW at 10-fold dilution (5.7 g/L, acetic acid) showed growth until 48 h, reached the maximum OD value of 1.33, and then decreased; therefore, the culture was collected at 60 h for PHA extraction. With the 20-fold dilution (3.8 g/L, acetic acid) of CW, the maximum OD value (1.24) was reached at 24 h, which then decreased, so the PHA was extracted at 36 h. The difference in the increase in OD₆₀₀ (final OD–initial OD) was 0.93, 0.91, and 0.79 at 10-fold (5.7 g/L, acetic acid), 20-fold (3.8 g/L, acetic acid), and 4-fold dilutions (12.3 g/L, acetic acid), respectively.

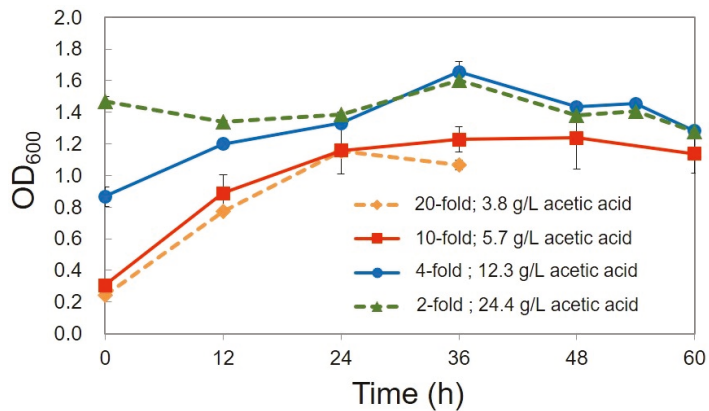


Figure 11. Growth curve of strain CYR1 using acetic-acid-fermented CW without pre-treatment at different dilution rates. All of the conditions were tested as biological triplicates (three Erlenmeyer flasks, *n* = 3) within a single experiment. The data were presented as mean ± standard deviation.

Table 3. PHA production after the two-stage process using acetic-acid-fermented CW without pre-treatment.

Culture Condition	20-Fold (Acetic Acid; 3.8 g/L)	10-Fold (Acetic Acid; 5.7 g/L)	4-Fold (Acetic Acid; 12.3 g/L)	2-Fold (Acetic Acid; 24.4 g/L)
CDW (mg)	151.6	319.4	638.2	831.7
PHA production (mg/L)	43.6	240.6	126.2	77.2
PHA production (%CDW)	28.8	75.4	19.8	9.2
Yield of PHA from acetic acid (%)	3.6	8.6	7.4	3.5
PHA volumetric productivity (mg PHA/ L/hour)	1.21	4	2.1	1.28

CDW: cell dry weight; All of the conditions were tested as biological duplicates (two Erlenmeyer flasks, *n* = 2) within a single experiment. Data are the means values of two samples.

PHA production was carried out with sterilized raw CW and acetic-acid-fermented CW without pre-treatment (Table 4). Koller et al. [38] reported that the sterilization of CW is crucial for PHA production using pure cultures. CYR1 incubated with sterilized CW without acidification at 30-fold dilution produced 46.6 mg of PHA (Table 4). Commercially available acetic acid at various concentrations (5–30 g/L) was also used to produce PHA, where the results showed that the bacteria produced similar amounts of PHA with commercial acetic acid and acetic acid produced from CW (Table 4). Bacteria incubated at a 10 g/L concentration showed a higher PHA production (287 mg/L) than other concentrations. Interestingly, bacteria incubated with acetic acid produced from CW showed a higher PHA production (240.6 mg/L) at 5.7 g/L of the initial acetic acid concentration.

Table 4. PHA production under each condition using acetic-acid-fermented CW without pretreatment, raw CW, and pure acetic acid.

Media (Substrates)		Initial Acetic Acid Concentration (g/L)	Extracted PHA (mg/L)
Acetic acid fermented from CW	2-fold	24.4	77.2
	4-fold	12.3	126.1
	10-fold	5.7	240.6
	20-fold	3.8	43.6
One step production of PHA using raw CW	30-fold	not detected	46.6
One step production of PHA using mineral medium containing pure acetic acid	30 g/L	30.0	8.6
	20 g/L	20.0	231.0
	10 g/L	10.0	287.0
	5 g/L	5.0	146.6

All media were sterilized. All of the conditions were tested as biological duplicates (two Erlenmeyer flasks, $n = 2$) within a single experiment. Data are the means values of two samples.

Effect of Nitrogen Concentration on PHA Production

An effective PHA production was observed under the low nitrogen concentrations (100 mg/L and 500 mg/L, data not shown); if the nitrogen concentration increased beyond 500 mg/L, the PHA production decreased. This phenomenon was also observed in our previous experiments [39,40]. Our previous studies demonstrated that the gene *PhaC* expression in *Cupriavidus* sp. CY-1 under nitrogen stress was up-and down-regulated with varying nitrogen concentrations [41]. Our previous studies also demonstrated that the strain CYR1 contains four genes, *phaA*, *phaB*, *phaC*, and *phaJ*, which encode the enzymes β -ketothiolase, acetoacetyl-CoA reductase, PHA synthase, and enoyl-CoA hydratase, respectively, which are involved in PHA production [11]. Nitrogen limitation enhances the PHA production in some bacteria because cells cannot grow under the low nitrogen concentration, and try to retain by accumulating PHA, a storage substance of carbon source, for their survival [42,43]. This is why a high PHA production was observed at a 200-500 mg/L nitrogen concentration in our experiments. Apart from the nitrogen concentration, the phosphorus concentration and osmotic pressure of the culture solution might also affect the growth of cells and PHA production [44–50].

PHA Production with Pretreated CW

A COD and TN removal of 24.6% and 28.2% was observed after the pretreatment of raw CW. PHA production experiments were performed using the two-stage process using pretreated CW. As a result, the PHA production was enhanced by 3.26 times (411 mg/L) after pretreatment with the four-fold dilution of fermented CW (Table 5).

Table 5. PHA production of the two-stage process using pre-treated CW at different dilutions.

Culture Condition	20-Fold (Acetic Acid; 2.3 g/L)	10-Fold (Acetic Acid; 4.5 g/L)	4-Fold (Acetic Acid; 11.3 g/L)
CDW (mg)	155.2	261.4	1227.2
PHA production (mg/L)	58.0	96.6	411.2
PHA production (%CDW)	37.4	37.0	33.5

All of the conditions were tested as biological duplicates (two Erlenmeyer flasks, $n = 2$) within a single experiment. Data are the means values of two samples.

The PHA production (%CDW) was increased by approximately two times after the pretreatment of CW at all of the dilution rates. It is easy to work with whey supernatants because they are sterile, homogeneous, and straightforward solutions, and produce more PHA than whey powder and whey permeates [6].

The disposal of CW is a major problem that all of the dairy industries are facing, and the large amounts of CW are disposed of as a waste material [51–53]. Hence, our studies focused on the utilization of whey as an inexpensive carbon source for acetic acid production and the usage of this acetic acid as a potential carbon source for PHA production. As mentioned above, a higher amount of PHA was obtained from acetic-acid-fermented CW rather than whey itself as a raw carbon source. On the other hand, several issues need to be resolved for the commercialization of PHA. The first issue is higher costs, which are associated with the multi-stage production process and the maintenance of the reactors; however, this can be overcome by improving the production efficiency. The second issue is the improvement of PHA yields from CW, which contains lactose. In order to solve this problem, the hydrolysis of lactose into monosaccharides should be considered. If lactose can be efficiently used as a carbon source for bacterial growth, PHA production will be improved. However, our experimental results in this study suggested that the CYR1 strain cannot utilize lactose as a carbon source for its growth.

The use of enzymatic hydrolysis significantly increases the PHA production cost, and so should be avoided from an industrial point of view. These problems can be avoided by deploying genetic engineering techniques. Therefore, *E. coli* cells that are capable of consuming lactose were modified to express PHA biosynthesis genes from high PHA-producing microorganisms [54–56]. Alternatively, high PHA-producing strains were engineered to express lactose degradation genes [57]. Recombinant *E. coli* has commonly been employed for PHA production due to its convenience for genetic manipulation, fast growth, high cell density cultivation, and its ability to utilize inexpensive carbon sources [58]. Therefore, the development of recombinant *E. coli* will be one of the applicable methods to improve PHA production. The third issue is to improve the efficiency of acetic acid utilization. As shown in Table 2, the concentration of acetic acid consumed by the CYR1 strain is 1.0 to 3.0 g/L, regardless of its initial concentration. A large amount of acetic acid remained unused by bacteria; at the moment, we do not know the exact reason. If bacteria can utilize more acetic acid for their growth, the PHA production will improve. Recently, Chen et al. reported the metabolic engineering of *E. coli* for the synthesis of PHA using acetate as the primary carbon source [59]. The overexpression of the phosphotransacetylase/acetate kinase pathway was shown to be an effective strategy for improving acetate assimilation and biopolymer production. The recombinant strain overexpressing the phosphotransacetylase/acetate kinase and PHB synthesis operon produced 1.27 g/L PHB when grown on a minimal medium supplemented with 10 g/L yeast extract and 5 g/L acetate in shake flask cultures. Thus, the metabolic engineering of *E. coli* will be one of the applicable methods to improve PHA production. The fourth issue is that the production cost of plastics from petrochemical products is still more competitive, and chemical synthesis is preferred by companies [60]. To overcome these problems, research must focus on the production of PHA from CW.

3.5. Identification of PHB Produced from the Two-Stage Process

The band appearing in the FT-IR spectrum at 1453 cm^{-1} matches the asymmetrical deformation of the C–H bond within CH_2 groups, and CH_3 groups at 1379 cm^{-1} (Figure 12). The band at 1724 cm^{-1} corresponds to the stretching of the C=O bond, whereas a series of intense bands located at $1000\text{--}1300\text{ cm}^{-1}$ corresponds to the stretching of the C–O bond of the ester group. All bands in the sample are identical to those of standard PHB. The methylene C–H vibration near 2933 cm^{-1} is also observed. The presence of absorption bands at 1724 cm^{-1} and 1280 cm^{-1} in the extracted PHB sample are characteristic of C=O and C–O, respectively.

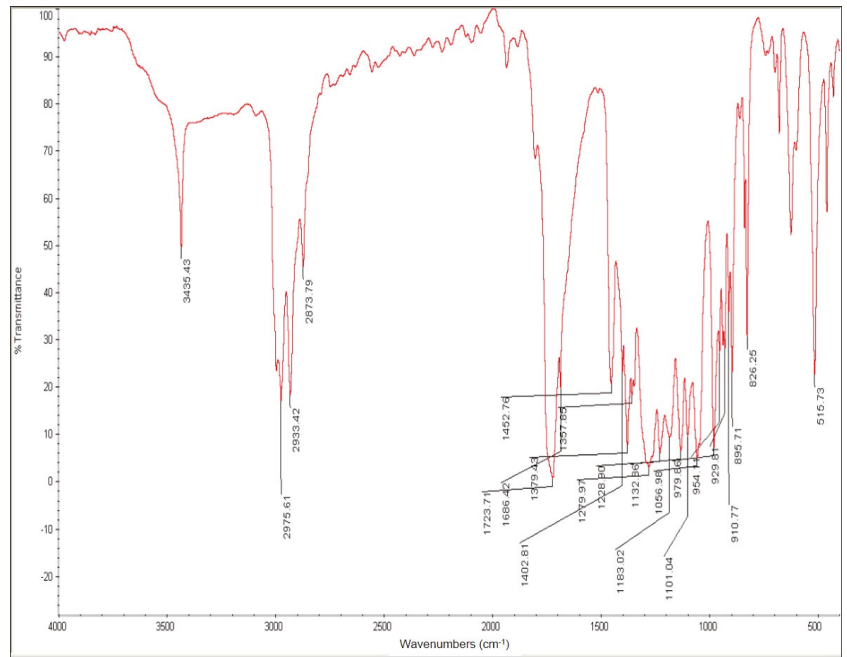


Figure 12. FT-IR spectra of PHB extracted from fermented CW containing 5.7 g/L of acetic acid. The fermented CW is obtained without pre-treatment of CW.

The ^1H NMR and ^{13}C NMR spectra of the CDCl_3 -soluble part of PHB, extracted from CYR-1 grown with fermented CW containing acetic acid (5.7 g/L), were measured at 20 °C. Based on their peak positions, each peak was assigned to the protons on methine (5.25 ppm), methylene (2.64–2.43 ppm), and methyl (1.25 ppm) groups in the ^1H NMR spectrum (Figure 13A). The peaks in the ^{13}C NMR spectrum (Figure 13B) were assigned to the carbon of the carbonyl (169.36 ppm), methine (67.82), methylene (41.88 ppm), and methyl (20.92 ppm) groups. The chemical shifts of these peaks were nearly identical to those of standard PHB previously reported by Reddy et al. [10] and Chang et al. [61].

In the TGA thermogram, the initial weight loss temperature of the PHB produced by strain CYR1 is at ~170 °C, and its Td is at 200 °C, with its decomposition incomplete until 800 °C (Figure 14). The characteristics of the PHB produced from the two-stage process were comparable to standard PHB.

PHB is synthesized and stored by a wide variety of bacteria, such as *Bacillus* sp. and *Pseudomonas* sp., through the fermentation of various substrates [62]. Among the pure cultures, the bacteria *Bacillus* strains have been widely studied because of their potential in producing significant amounts of PHB from organic carbon substrates, such as glycerol, dairy wastes, agro-industrial wastes, food industry waste, fatty acids, toxic chemical compounds, and sugars [11,63–68].

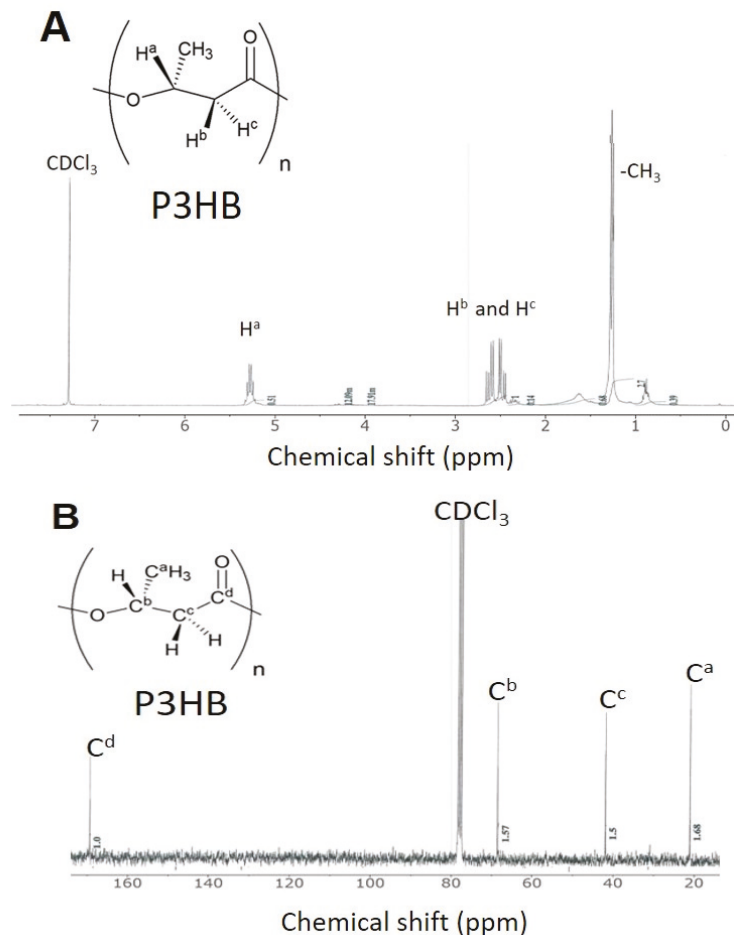


Figure 13. (A) ^1H and (B) ^{13}C NMR spectra of PHB extracted from fermented CW containing 5.7 g/L of acetic acid. The fermented CW is obtained without pre-treatment of CW.

As shown in Table 6, the amount of PHB accumulation from *Bacillus* strains can wildly vary from 17% to 89% of its dry cell weight, depending on the type and concentration of the substrate [5,64–67]. *Bacillus aryabhattai* T34-N4 hydrolyzed the cassava pulp and oil palm trunk starch and accumulated up to 17% PHB of the dry cell weight [69]. Moreover, *Bacillus cereus* EGU3 was reported to yield up to 66.6% (0.5 g/L) of PHB content when using contaminated food as a carbon source [70]. Hassan et al. reported that *Bacillus subtilis* yielded up to 62.6% (0.81 g/L) of PHB using rice bran [71]. *Bacillus* sp. N-2 was reported to yield up to 20% (0.17 g/L) of PHB content when using glucose as a carbon source [64]. *Bacillus megaterium* VB89 produced 36.17% (0.67 g/L) of PHB using slurry from the Nisargruna biogas plant [63]. *Bacillus drentensis* BP17 hydrolyzed pineapple peel and accumulated 5.55 g/L of PHB dry cell weight [72]. *Bacillus megaterium* strain A1 isolated from hydrocarbon-contaminated soil produced 48.7% of PHB using molasses [73]. *Bacillus megaterium* S29 and *Bacillus* sp. IPCB-403 accumulated over 70% PHB content per dry cell weight in optimal conditions and using glucose and activated sludges, respectively [74,75]. On the other hand, the strain *Bacillus* sp. CYR1 used in this study produced the highest PHB production with phenol (51%; 0.51 g/L), naphthalene (42%; 0.42 g/L), 4-chlorophenol (32%; 0.32 g/L), and 4-nonylphenol (29%; 0.29 g/L) [67]. *Bacillus firmus* NII 0830 yielded

up to 89% (1.9 g/L) of PHB using rice straw [76,77]. *Bacillus cereus* CFR06 produced up to 48% (0.48 g/L) of PHB using starch-based materials [78]. *Bacillus megaterium* produced 26% (0.47 g/L) of PHB using lactose [5]. *Bacillus cereus suaeda* B-001 produced 55.4% (0.47 g/L) of PHB using oil palm empty fruit bunch hydrolysates [79]. *Bacillus flexus* Azu-A2 produced 20.96% (0.95 g/L) of PHB using CW [80]. *Bacillus megaterium* B-10 produced 32.56% (1.496 g/L) of PHB using dilute acid pretreatment liquor of lignocellulose containing abundant waste sugar resource from rice straw [81]. *Bacillus megaterium* strain CAM12 produced 51% (8.31 g/L) of PHB using finger millet straw hydrolysates [82]. *Bacillus tequilensis* PSR-2 produced 49.12% (2.8 g/L) of PHB using glucose (1%) [83]. In addition, the strain PSR-2 could produce a maximum of 12.4 g/L of PHB using an alkali-pretreated spent mushroom substrate of sugarcane bagasse [83]. *B. cereus* 2156 produced 2.2 g/L of PHB using sugarcane molasses [84]. *Bacillus* sp. produced 56% (5.0 g/L) of PHB using sugarcane bagasse hydrolysates [85]. *Bacillus flexus* ME-77 produced 15% (4.5 g/L) of PHB using sugarcane molasses [86]. *B. thuringiensis* SBC4 produced 43.95% (0.4 g/L) of PHB using glucose and corn cob [87]. Recently, Werlang et al. reported that *Bacillus pumilus* could produce PHB using the hydrolysate of the *Arthrospira platensis* biomass as carbon sources, in addition to glucose [88]. The average production during the experiments was 1.2 mg of PHB from 0.4 g of bacterial biomass [88]. In this study, *Bacillus* sp. CYR1 yielded 33.5% (0.41 g/L) of PHB through the two-stage process. Therefore, it can be said the productivity of PHB is similar to *Bacillus cereus* CFR06, *Bacillus cereus suaeda* B-001, *Bacillus megaterium*, and *B. thuringiensis* SBC4 [5,78,79,87]. According to Sirohi et al. [68], which was recently reviewed, PHB synthesis can be done from several substrates in aerobic/anaerobic conditions and at different temperatures, pH, and states of fermentation, using starch, cellulose, sucrose, molasses, whey, glycerol, and others, which can be present in wastes. In future, we will conduct a study to determine the optimal condition (agitation speed, pH, and temperature) for the production of PHB through the development of the second stage of the process using strain CYR1. In addition to the development of optimal culture conditions, the utilization ability of lactose and acetic acid through molecular engineering methods can be improved; the two-stage process will be adoptable for the industrial process for the production of PHB.

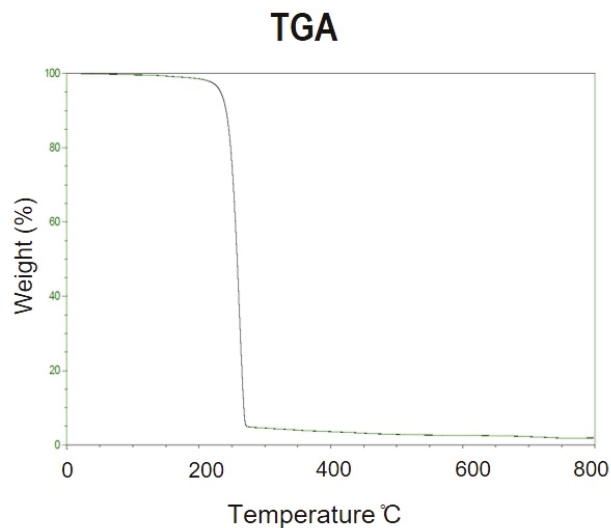


Figure 14. TGA thermograms of PHB extracted from fermented CW containing 5.7 g/L of acetic acid. The fermented CW is obtained without pre-treatment of CW.

Table 6. Overview of PHB production of genus *Bacillus* using various carbon sources.

Strain	Carbon Source	PHAs Monomer	PHB Conc. (g/L)	PHB Content. (wt%)	References
<i>Bacillus megaterium</i>	lactose	PHB	0.47	26.0	[5]
<i>Bacillus megaterium</i> VB89	slurry from Nisargruna biogas plant	PHB	0.67	36.17	[63]
<i>Bacillus</i> sp. N-2	glucose	PHB	0.17	20.0	[64]
<i>Bacillus</i> sp. CYR1	phenol	PHB	0.51	51.0	[67]
<i>Bacillus</i> sp. CYR1	naphthalene	PHB	0.42	42.0	[67]
<i>Bacillus</i> sp. CYR1	4-chlorophenol	PHB	0.32	32.0	[67]
<i>Bacillus</i> sp. CYR1	4-nonylphenol	PHB	0.29	29.0	[67]
<i>Bacillus aryabhatai</i> T34-N4	oil palm trunk starch	PHB	0.33	17.0	[69]
<i>Bacillus cereus</i> EGU3	contaminated food	PHB	0.5	66.6	[70]
<i>Bacillus subtilis</i>	rice bran	PHB	0.81	62.6	[71]
<i>Bacillus drentensis</i> BP17	pineapple peel	PHB	5.55	n.a	[72]
<i>Bacillus megaterium</i> strain A1	molasses	PHB	14.6	48.7	[73]
<i>Bacillus megaterium</i> S29	glucose	PHB	n.a	≥70	[74]
<i>Bacillus</i> sp. IPCB-403	activated sludges	PHB	n.a	≥70	[75]
<i>Bacillus firmus</i> NII 0830	rice straw	PHB	1.9	89.0	[76,77]
<i>Bacillus cereus</i> CFR06	starch-based materials	PHB	0.48	48.0	[78]
<i>Bacillus cereus suaeda</i> B-001	oil palm empty fruit bunch hydrolysates	PHB	0.47	55.4	[79]
<i>Bacillus flexus</i> Azu-A2	cheese whey	PHB	0.95	20.96	[80]
<i>Bacillus megaterium</i> B-10	dilute acid pretreatment liquor of lignocellulose from rice straw	PHB	1.496	32.56	[81]
<i>Bacillus megaterium</i> strain CAM12	finger millet straw hydrolysates	PHB	8.31	51.0	[82]
<i>Bacillus tequilensis</i> PSR-2	glucose	PHB	2.8	49.12	[83]
<i>Bacillus tequilensis</i> PSR-2	an alkali-pretreated spent mushroom substrate of sugarcane bagasse	PHB	12.4	n.a	[83]
<i>B. cereus</i> 2156	sugarcane molasses	PHB	2.2	n.a	[84]
<i>Bacillus</i> sp.	sugarcane bagasse hydrolysates	PHB	5.0	56.0	[85]
<i>Bacillus flexus</i> ME-77	sugarcane molasses	PHB	4.5	15.0	[86]
<i>Bacillus thuringiensis</i> SBC4	glucose and corn cob	PHB	0.4	43.95	[87]
<i>Bacillus pumilus</i>	hydrolysate of the <i>Arthrospira platensis</i> biomass	PHB	n.a	0.3	[88]
<i>Bacillus</i> sp. CYR1	cheese whey	PHB	0.41	33.5	This study

n.a.: not available.

4. Conclusions

A two-stage process was applied to produce PHA from CW containing a low level of lactose using *Acetobacter pasteurianus* C1 and *Bacillus* sp. CYR1. Acetic acid fermentation was effectively conducted using CW by a newly isolated C1 strain. The dilution of acetic acid-fermented liquid is essential to lower the nitrogen concentration and to improve the PHA production. In addition, the pretreatment of raw CW also enhanced the PHA production. The PHA produced from the two-stage process using CW was PHB. Results

discovered that, instead of the hydrolysis of lactose (which enhances the production cost), a two-stage treatment would be applicable for PHA production from CW, which contains a low level of lactose.

Author Contributions: Conceptualization, Y.-C.C.; methodology, Y.-C.C.; funding acquisition, Y.-C.C.; investigation, K.I., N.K., R.O., Y.S., and Y.-C.C.; data curation, Y.-C.C., R.O., and K.I.; writing—draft preparation, Y.-C.C.; writing—review and editing, M.V.R. and Y.-C.C. All authors have read and agreed to the published version of the manuscript.

Funding: This research was funded by Japan Science and Technology Agency, grant number VP29117937927.

Institutional Review Board Statement: Not applicable.

Informed Consent Statement: Not applicable.

Data Availability Statement: Not applicable.

Acknowledgments: We want to thank Yasuteru Mawatari of Muroran Institute of Technology for the Soxhlet extraction. We also would like to thank D.B. Choi of Chosun University for FT-IR and NMR analyses.

Conflicts of Interest: The authors declare no conflict of interest.

References

1. Khanna, S.; Srivastava, A.K. Recent advances in microbial polyhydroxyalkanoates. *Process. Biochem.* **2005**, *40*, 607–619. [[CrossRef](#)]
2. Berezina, N.; Yada, B.; Lefebvre, R. From organic pollutants to bioplastics: Insights into the bioremediation of aromatic compounds by *Cupriavidus necator*. *New Biotechnol.* **2015**, *32*, 47–53. [[CrossRef](#)]
3. Castilho, L.R.; Mitchell, D.A.; Freire, D.M.G. Production of polyhydroxyalkanoates (PHAs) from waste materials and by-products by submerged and solid-state fermentation. *Bioresour. Technol.* **2009**, *100*, 5996–6009. [[CrossRef](#)] [[PubMed](#)]
4. Valta, K.; Damala, P.; Angeli, E.; Antonopoulou, G.; Malamis, D.; Haralambous, K.J. Current treatment technologies of cheese whey and wastewater by Greek cheese manufacturing units and potential valorization opportunities. *Waste Biomass Valoriz.* **2017**, *8*, 1649–1663. [[CrossRef](#)]
5. Koller, M.; Salerno, A.; Muhr, A.; Reiterer, A.; Chiellini, E.; Casella, S.; Horvat, P.; Braunegg, P.H.A.G. Whey Lactose as a Raw Material for Microbial Production of Biodegradable Polyesters. In *Poliester*; Saleh, H.E.-D.M., Ed.; IntechOpen: London, UK, 2013. [[CrossRef](#)]
6. Pescuma, M.; de Valdez, G.F.; Mozzi, F. Whey-derived valuable products obtained by microbial fermentation. *Appl. Microbiol. Biotechnol.* **2015**, *99*, 6183–6196. [[CrossRef](#)] [[PubMed](#)]
7. Berwig, K.H.; Baldasso, C.; Dettmer, A. Production and characterization of poly(3-hydroxybutyrate) generated by *Alcaligenes latus* using lactose and whey after acid protein precipitation process. *Bioresour. Technol.* **2016**, *218*, 31–37. [[CrossRef](#)] [[PubMed](#)]
8. Khatami, K.; Perez-Zabaleta, M.; Owusu-Agyeman, I.; Cetecioglu, Z. Waste to bioplastics: How close are we to sustainable polyhydroxyalkanoates production? *Waste Manag.* **2021**, *119*, 374–388. [[CrossRef](#)] [[PubMed](#)]
9. Amaro, T.M.M.M.; Rosa, D.; Comi, G.; Iacumin, L. Prospects for the Use of Whey for Polyhydroxyalkanoate (PHA) Production. *Front. Microbiol.* **2019**, *10*, 992. [[CrossRef](#)]
10. Reddy, M.V.; Mawatari, Y.; Onodera, R.; Nakamura, Y.; Yajima, Y.; Chang, Y.-C. Bacterial conversion of waste into polyhydroxybutyrate (PHB): A new approach of bio-circular economy for treating waste and energy generation. *Bioresour. Technol. Rep.* **2019**, *7*, 100246. [[CrossRef](#)]
11. Reddy, M.V.; Watanabe, A.; Onodera, R.; Mawatari, Y.; Tsukiori, Y.; Watanabe, A.; Kudou, M.; Chang, Y.-C. Polyhydroxyalkanoates (PHA) production using single or mixture of fatty acids with *Bacillus* sp. CYR1: Identification of PHA synthesis genes. *Bioresour. Technol. Rep.* **2020**, *11*, 100483. [[CrossRef](#)]
12. Chang, Y.-C.; Ikeutsu, K.; Toyama, T.; Choi, D.; Kikuchi, S. Isolation and characterization of tetrachloroethylene- and cis-1,2-dichloroethylene-dechlorinating propionibacteria. *J. Ind. Microbiol. Biotechnol.* **2011**, *38*, 1667–1677. [[CrossRef](#)]
13. Chang, Y.C.; Takada, K.; Choi, D.B.; Toyama, T.; Sawada, K.; Kikuchi, S. Isolation of biphenyl and polychlorinated bi-phenyl-degrading bacteria and their degradation pathway. *Appl. Biochem. Biotechnol.* **2013**, *170*, 381–398. [[CrossRef](#)]
14. Saichana, N.; Matsushita, K.; Adachi, O.; Frébort, I.; Frébortova, J. Acetic acid bacteria: A group of bacteria with versatile biotechnological applications. *Biotechnol. Adv.* **2015**, *33*, 1260–1271. [[CrossRef](#)]
15. Law, J.H.; Slepceky, A.S. Assay of poly- β -hydroxybutyric acid. *J. Bacteriol.* **1961**, *82*, 33–36. [[CrossRef](#)]
16. Obruca, S.; Marova, I.; Melusova, S.; Mravcova, L. Production of polyhydroxyalkanoates from cheese whey employing *Bacillus megaterium* CCM 2037. *Ann. Microbiol.* **2011**, *61*, 947–953. [[CrossRef](#)]
17. Yellore, V.; Desai, A. Production of poly-3-hydroxybutyrate from lactose and whey by *Methylobacterium* sp. ZP24. *Let. Appl. Microbiol.* **1998**, *26*, 391–394. [[CrossRef](#)]
18. Sengun, I.Y.; Karabiyikli, S. Importance of acetic acid bacteria in food industry. *Food Control.* **2011**, *22*, 647–656. [[CrossRef](#)]

19. Pallach, M.; di Lorenzo, F.; Facchini, F.A.; Gully, D.; Giraud, E.; Peri, F.; Duda, K.A.; Molinaro, A.; Silipo, A. Structure and inflammatory activity of the LPS isolated from *Acetobacter pasteurianus* CIP103108. *Int. J. Biol. Macromol.* **2018**, *119*, 1027–1035. [[CrossRef](#)] [[PubMed](#)]
20. Gullo, M.; Verzelloni, E.; Canonico, M. Aerobic submerged fermentation by acetic acid bacteria for vinegar production: Process and biotechnological aspects. *Process. Biochem.* **2014**, *49*, 1571–1579. [[CrossRef](#)]
21. Ndoye, B.; Lebecque, S.; Dubois-Dauphin, R.; Toukara, L.; Guiro, A.-T.; Kere, C.; Diawara, B.; Thonart, P. Thermoresistant properties of acetic acids bacteria isolated from tropical products of Sub-Saharan Africa and destined to industrial vinegar. *Enzym. Microb. Technol.* **2006**, *39*, 916–923. [[CrossRef](#)]
22. Kanchanarach, W.; Theeragool, G.; Yakushi, T.; Toyama, H.; Osao Adachi, O.; Matsushita, K. Characterization of thermotolerant *Acetobacter pasteurianus* strains and their quinoprotein alcohol dehydrogenases. *Appl. Microbiol. Biotechnol.* **2010**, *85*, 741–751. [[CrossRef](#)]
23. Perumpuli, P.A.B.N.; Watanabe, T.; Toyama, H. Identification and characterization of thermotolerant acetic acid bacteria strains isolated from coconut water vinegar in Sri Lanka. *Biosci. Biotechnol. Biochem.* **2014**, *78*, 533–541. [[CrossRef](#)] [[PubMed](#)]
24. Es-Sbata, I.; Lakhfli, T.; Yatim, M.; El-Abid, H.; Belhaj, A.; Hafidi, M.; Zouhair, R. Screening and molecular characterization of new thermo- and ethanol-tolerant *Acetobacter malorum* strains isolated from two biomes Moroccan cactus fruits. *Biotechnol. Appl. Biochem.* **2021**, *68*, 476–485. [[CrossRef](#)] [[PubMed](#)]
25. Kadere, T.T.; Miyamoto, T.; Oniang'o, R.K.; Kutima, P.M.; Njoroge, S.M. Isolation and identification of the genera *Acetobacter* and *Gluconobacter* in coconut toddy (mnazi). *Afr. J. Biotechnol.* **2008**, *7*, 2963–2971.
26. Iino, T.; Suzuki, R.; Tanaka, N.; Kosako, Y.; Ohkuma, M.; Komagata, K.; Uchimura, T. *Gluconacetobacter kakiaceti* sp. nov., an acetic acid bacterium isolated from a traditional Japanese fruit vinegar. *Int. J. Syst. Evol. Microbiol.* **2012**, *62*, 1465–1469. [[CrossRef](#)] [[PubMed](#)]
27. Saeki, A.; Theeragool, G.; Matsushita, K.; Toyama, H.; Lotong, N.; Adachi, O. Development of thermotolerant acetic acid bacteria useful for vinegar fermentation at higher temperature. *Biosci. Biotechnol. Biochem.* **1997**, *61*, 138–145. [[CrossRef](#)]
28. Vashisht, A.; Thakur, K.; Kauldhar, B.S.; Kumar, V.; Yadav, S.K. Waste valorization: Identification of an ethanol tolerant bacterium *Acetobacter pasteurianus* SKYAA25 for acetic acid production from apple pomace. *Sci. Total. Environ.* **2019**, *690*, 956–964. [[CrossRef](#)]
29. Chen, Y.; Bai, Y.; Li, D.; Wang, C.; Xu, N.; Hu, Y. Screening and characterization of ethanol-tolerant and thermotolerant acetic acid bacteria from Chinese vinegar Pei. *World J. Microbiol. Biotechnol.* **2016**, *32*, 14. [[CrossRef](#)]
30. Wu, X.; Yao, H.; Liu, Q.; Zheng, Z.; Cao, L.; Mu, D.; Wang, H.; Jiang, S.; Li, X. Producing acetic acid of *Acetobacter pasteurianus* by fermentation characteristics and metabolic flux analysis. *Appl. Biochem. Biotechnol.* **2018**, *186*, 217–232. [[CrossRef](#)]
31. Fukaya, M.; Tayama, K.; Tamaki, T.; Tagami, H.; Okumura, H.; Kawamura, Y.; Beppu, T. Cloning of the membrane-bound aldehyde dehydrogenase gene of *Acetobacter polyoxogenes* and improvement of acetic acid production by use of the cloned gene. *Appl. Environ. Microbiol.* **1989**, *55*, 171–176. [[CrossRef](#)]
32. Qi, Z.; Wang, W.; Yang, H.; Xia, X.; Yu, X. Mutation of *Acetobacter pasteurianus* by UV irradiation under acidic stress for high-acidity vinegar fermentation. *Int. J. Food Sci. Technol.* **2013**, *49*, 468–476. [[CrossRef](#)]
33. Lustrato, G.; Salimei, E.; Alfano, G.; Belli, C.; Fantuz, F.; Grazia, L.; Ranalli, G. Cheese whey recycling in traditional dairy food chain: Effects of vinegar from whey in dairy cow nutrition. *Acetic Acid Bact.* **2013**, *2*, e8. [[CrossRef](#)]
34. Veeravalli, S.S.; Mathews, A.P. Exploitation of acid-tolerant microbial species for the utilization of low-cost whey in the production of acetic acid and propylene glycol. *Appl. Microbiol. Biotechnol.* **2018**, *102*, 8023–8033. [[CrossRef](#)] [[PubMed](#)]
35. Rai, P.; Singh, S.P.; Asthana, R.K. Biohydrogen Production from Cheese Whey Wastewater in a Two-Step Anaerobic Process. *Appl. Biochem. Biotechnol.* **2012**, *167*, 1540–1549. [[CrossRef](#)]
36. Pandey, A.; Srivastava, S.; Rai, P.; Duke, M. Cheese whey to biohydrogen and useful organic acids: A non-pathogenic microbial treatment by *L. acidophilus*. *Sci. Rep.* **2019**, *9*, 1–9. [[CrossRef](#)]
37. Ricciardi, A.; Zotta, T.; Ianniello, R.G.; Boscaino, F.; Matera, A.; Parente, E. Effect of Respiratory Growth on the Metabolite Production and Stress Robustness of *Lactobacillus casei* N87 Cultivated in Cheese Whey Permeate Medium. *Front. Microbiol.* **2019**, *10*, 851. [[CrossRef](#)]
38. Koller, M.; Hesse, P.; Salerno, A.; Reiterer, A.; Braunnegg, G. A viable antibiotic strategy against microbial contamination in biotechnological production of polyhydroxyalkanoates from surplus whey. *Biomass- Bioenergy* **2011**, *35*, 748–753. [[CrossRef](#)]
39. Wong, T.Y.; Pei, H.; Bancroft, K.; Wang, F.; Lee, S.Y. Poly(3-hydroxybutyrate) production with high polymer content by fed-batch culture of *Alcaligenes latus* under nitrogen limitation. *Appl. Environ. Microbiol.* **1997**, *63*, 3703–3706. [[CrossRef](#)]
40. Kessler, B.; Witholt, B. Factors involved in the regulatory network of polyhydroxyalkanoate metabolism. *J. Biotechnol.* **2001**, *86*, 97–104. [[CrossRef](#)]
41. Reddy, M.V.; Yajima, Y.; Mawatari, Y.; Hoshino, T.; Chang, Y.-C. Degradation and conversion of toxic compounds into useful bioplastics by *Cupriavidus* sp. CY-1: Relative expression of the PhnC gene under phenol and nitrogen stress. *Green Chem.* **2015**, *17*, 4560–4569. [[CrossRef](#)]
42. Nath, A.; Dixit, M.; Bandiya, A.; Chavda, S.; Desai, A.J. Enhanced PHB production and scale up studies using cheese whey in fed batch culture of *Methylobacterium* sp. ZP24. *Bioresour. Technol.* **2008**, *99*, 5749–5755. [[CrossRef](#)]
43. Verlinden, R.A.J.; Hill, D.J.; Kenward, M.A.; Williams, C.D.; Radecka, I. Bacterial synthesis of biodegradable polyhydroxyalkanoates. *J. Appl. Microbiol.* **2007**, *102*, 1437–1449. [[CrossRef](#)]

44. Chinwetkitvanich, S.; Randall, C.W.; Panswad, T. Effects of phosphorus limitation and temperature on PHA production in activated sludge. *Water Sci. Technol.* **2004**, *50*, 135–143. [[CrossRef](#)]
45. Shi, H.P.; Lee, C.M.; Ma, W.H. Influence of electron acceptor, carbon, nitrogen, and phosphorus on polyhydroxyalkanoate (PHA) production by *Brachymonas* sp. P12. *World J. Microbiol. Biotechnol.* **2007**, *23*, 625–632. [[CrossRef](#)]
46. Oliveira-Filho, E.; Silva, J.G.P.; de Macedo, M.A.; Taciro, M.K.; Gomez, J.G.C.; Silva, L.F. Investigating Nutrient Limitation Role on Improvement of Growth and Poly(3-Hydroxybutyrate) Accumulation by *Burkholderia sacchari* LMG 19450 From Xylose as the Sole Carbon Source. *Front. Bioeng. Biotechnol.* **2020**, *7*, 416. [[CrossRef](#)]
47. Montiel-Jarillo, G.; Carrera, J.; Suárez-Ojeda, M.E. Enrichment of a mixed microbial culture for polyhydroxyalkanoates production: Effect of pH and N and P concentrations. *Sci. Total. Environ.* **2017**, *583*, 300–307. [[CrossRef](#)] [[PubMed](#)]
48. Sedlacek, P.; Slaninova, E.; Koller, M.; Nebesarova, J.; Marova, I.; Krzyzanek, V.; Obruca, S. PHA granules help bacterial cells to preserve cell integrity when exposed to sudden osmotic imbalances. *New Biotechnol.* **2019**, *49*, 129–136. [[CrossRef](#)] [[PubMed](#)]
49. Pernicova, I.; Novackova, I.; Sedlacek, P.; Kourilova, X.; Koller, M.; Obruca, S. Application of osmotic challenge for enrichment of microbial consortia in polyhydroxyalkanoates producing thermophilic and thermotolerant bacteria and their subsequent isolation. *Int. J. Biol. Macromol.* **2020**, *144*, 698–704. [[CrossRef](#)]
50. Taieb, H.M.; Garske, D.S.; Contzen, J.; Gossen, M.; Bertinetti, L.; Robinson, T.; Cipitria, A. Osmotic pressure modulates single cell cycle dynamics inducing reversible growth arrest and reactivation of human metastatic cells. *Sci. Rep.* **2021**, *11*, 1–13. [[CrossRef](#)]
51. Colombo, B.; Sciarria, T.P.; Reis, M.A.; Scaglia, B.; Adani, F. Polyhydroxyalkanoates (PHAs) production from fermented cheese whey by using a mixed microbial culture. *Bioresour. Technol.* **2016**, *218*, 692–699. [[CrossRef](#)]
52. Ryan, M.P.; Walsh, G. The biotechnological potential of whey. *Rev. Environ. Sci. Bio/Technol.* **2016**, *15*, 479–498. [[CrossRef](#)]
53. Chandrapala, J.; Duke, M.C.; Gray, S.R.; Zisu, B.; Weeks, M.; Palmer, M.; Vasiljevic, T. Properties of acid whey as a function of pH and temperature. *J. Dairy Sci.* **2015**, *98*, 4352–4363. [[CrossRef](#)] [[PubMed](#)]
54. Ahn, W.S.; Park, S.J.; Lee, S.Y. Production of Poly(3-Hydroxybutyrate) by Fed-Batch Culture of Recombinant *Escherichia coli* with a Highly Concentrated Whey Solution. *Appl. Environ. Microbiol.* **2000**, *66*, 3624–3627. [[CrossRef](#)] [[PubMed](#)]
55. Ahn, W.S.; Park, S.J.; Lee, S.Y. Production of poly(3-hydroxybutyrate) from whey by cell recycle fed-batch culture of re-combinant *Escherichia coli*. *Biotechnol. Lett.* **2001**, *23*, 235–240. [[CrossRef](#)]
56. Koller, M. Recycling of Waste Streams of the Biotechnological Poly(hydroxyalkanoate) Production by *Haloferax mediterranea* Whey. *Int. J. Polym. Sci.* **2015**, *2015*, 1–8. [[CrossRef](#)]
57. Povoio, S.; Toffano, P.; Basaglia, M.; Casella, S. Polyhydroxyalkanoates production by engineered *Cupriavidus necator* from waste material containing lactose. *Bioresour. Technol.* **2010**, *101*, 7902–7907. [[CrossRef](#)]
58. Yee, L.-N.; Mumtaz, T.; Mohammadi, M.; Phang, L.-Y.; Ando, Y.; Raha, A.R.; Sudesh, K.; Ariffin, H.; Hassan, M.A.; Zakaria, M.R. Polyhydroxyalkanoate Synthesis by Recombinant *Escherichia coli* JM109 Expressing PHA Biosynthesis Genes from *Comamonas* sp. EB172. *J. Microb. Biochem. Technol.* **2012**, *4*, 103–110. [[CrossRef](#)]
59. Chen, J.; Li, W.; Zhang, Z.-Z.; Tan, T.-W.; Li, Z.-J. Metabolic engineering of *Escherichia coli* for the synthesis of polyhydroxyalkanoates using acetate as a main carbon source. *Microb. Cell Factories* **2018**, *17*, 1–12. [[CrossRef](#)]
60. Zotta, T.; Solieri, L.; Iacumin, L.; Picozzi, C.; Gullo, M. Valorization of cheese whey using microbial fermentations. *Appl. Microbiol. Biotechnol.* **2020**, *104*, 2749–2764. [[CrossRef](#)]
61. Chang, Y.-C.; Reddy, M.V.; Choi, D. Cometabolic degradation of toxic trichloroethene or cis-1,2-dichloroethene with phenol and production of poly- β -hydroxybutyrate (PHB). *Green Chem.* **2021**, *23*, 2729–2737. [[CrossRef](#)]
62. Reddy, M.V.; Onodera, R.; Chang, Y.-C. Degradation of aromatic compounds and their conversion into useful energy by bacteria. In *Microbial Biodegradation of Xenobiotic Compounds*; Chang, Y.-C., Ed.; CRC Press: Boca Raton, FL, USA, 2020; pp. 1–23.
63. Baikar, V.; Rane, A.; Deopurkar, R. Characterization of Polyhydroxyalkanoate Produced by *Bacillus megaterium* VB89 Isolated from Nisargruna Biogas Plant. *Appl. Biochem. Biotechnol.* **2017**, *183*, 241–253. [[CrossRef](#)]
64. Hassan, M.; Bakhiet, E.; Ali, S.; Hussien, H. Production and characterization of polyhydroxybutyrate (PHB) produced by *Bacillus* sp. isolated from Egypt. *J. Appl. Pharm. Sci.* **2016**, *6*, 46–51. [[CrossRef](#)]
65. Koller, M.; Brauneegg, G. Potential and Prospects of Continuous Polyhydroxyalkanoate (PHA) Production. *Bioengineering* **2015**, *2*, 94–121. [[CrossRef](#)] [[PubMed](#)]
66. Koller, M.; Hesse, P.; Bona, R.; Kutschera, C.; Atlić, A.; Brauneegg, G. Potential of Various Archae- and Eubacterial Strains as Industrial Polyhydroxyalkanoate Producers from Whey. *Macromol. Biosci.* **2007**, *7*, 218–226. [[CrossRef](#)]
67. Reddy, M.V.; Mawatari, Y.; Yajima, Y.; Seki, C.; Hoshino, T.; Chang, Y.C. Poly-3-hydroxybutyrate (PHB) production from alkylphenols, mono and poly-aromatic hydrocarbons using *Bacillus* sp. CYR1: A new strategy for wealth from waste. *Bioresour. Technol.* **2015**, *192*, 711–717. [[CrossRef](#)]
68. Sirohi, R.; Pandey, J.P.; Gaur, V.K.; Gnansounou, E.; Sindhu, R. Critical overview of biomass feedstocks as sustainable substrates for the production of polyhydroxybutyrate (PHB). *Bioresour. Technol.* **2020**, *311*, 123536. [[CrossRef](#)]
69. Bomrungnok, W.; Arai, T.; Yoshihashi, T.; Sudesh, K.; Hatta, T.; Kosugi, A. Direct production of polyhydroxybutyrate from waste starch by newly-isolated *Bacillus aryabhattai* T34-N4. *Environ. Technol.* **2020**, *41*, 3318–3328. [[CrossRef](#)]
70. Porwal, S.; Kumar, T.; Lal, S.; Rani, A.; Kumar, S.; Cheema, S.; Purohit, H.J.; Sharma, R.; Patel, S.K.S.; Kalia, V.C. Hydrogen and polyhydroxybutyrate producing abilities of microbes from diverse habitats by dark fermentative process. *Bioresour. Technol.* **2008**, *99*, 5444–5451. [[CrossRef](#)]

71. Hassan, M.A.; Bakhiet, E.K.; Hussein, H.R.; Ali, S.G. Statistical optimization studies for polyhydroxybutyrate (PHB) production by novel *Bacillus subtilis* using agricultural and industrial wastes. *Int. J. Environ. Sci. Technol.* **2019**, *16*, 3497–3512. [[CrossRef](#)]
72. Penkhrue, W.; Jendrossek, D.; Khanongnuch, C.; Pathom-Aree, W.; Aizawa, T.; Behrens, R.L.; Lumyong, S. Response surface method for polyhydroxybutyrate (PHB) bioplastic accumulation in *Bacillus drentensis* BP17 using pineapple peel. *PLoS ONE* **2020**, *15*, e0230443. [[CrossRef](#)]
73. Güngörmedi, G.; Demirbilek, M.; Mutlu, M.B.; Denkbaş, E.B.; Çabuk, A. Polyhydroxybutyrate and hydroxyvalerate production by *Bacillus megaterium* strain A1 isolated from hydrocarbon-contaminated soil. *J. Appl. Polym. Sci.* **2014**, *131*, 1–8. [[CrossRef](#)]
74. Dave, H.; Ramakrishna, C.; Desai, J. Production of polyhydroxybutyrate by petrochemical activated sludge and *Bacillus* sp. IPCB-403. *Indian J. Exp. Biol.* **1996**, *34*, 216–219.
75. Rodriguez-Contreras, A.; Koller, M.; de Sousa Dias, M.M.; Calafell, M.; Brauneegg, G.; Marqués-Calvo, M.S. Novel poly [(R)-3-hydroxybutyrate]-producing bacterium isolated from a Bolivian hypersaline lake. *Food Technol. Biotechnol.* **2013**, *51*, 123–130.
76. Sindhu, R.; Silviya, N.; Binod, P.; Pandey, A. Pentose-rich hydrolysate from acid pretreated rice straw as a carbon source for the production of poly-3-hydroxybutyrate. *Biochem. Eng. J.* **2013**, *78*, 67–72. [[CrossRef](#)]
77. Sindhu, R.; Gnansounou, E.; Binod, P.; Pandey, A. Bioconversion of sugarcane crop residue for value added products—An overview. *Renew. Energy* **2016**, *98*, 203–215. [[CrossRef](#)]
78. Halami, P.M. Production of polyhydroxyalkanoate from starch by the native isolate *Bacillus cereus* CFR06. *World J. Microbiol. Biotechnol.* **2008**, *24*, 805–812. [[CrossRef](#)]
79. Yustinah; Hidayat, N.; Alamsyah, R.; Roslan, A.M.; Hermansyah, H.; Gozan, M. Production of polyhydroxybutyrate from oil palm empty fruit bunch (OPEFB) hydrolysates by *Bacillus cereus* suaeda B-001. *Biocatal. Agric. Biotechnol.* **2019**, *18*, 101019. [[CrossRef](#)]
80. Khattab, A.M.; Esmael, M.E.; Farrag, A.A.; Ibrahim, M.I. Structural assessment of the bioplastic (poly-3-hydroxybutyrate) produced by *Bacillus flexus* Azu-A2 through cheese whey valorization. *Int. J. Biol. Macromol.* **2021**, *190*, 319–332. [[CrossRef](#)]
81. Li, J.; Yang, Z.; Zhang, K.; Liu, M.; Liu, D.; Yan, X.; Si, M.; Shi, Y. Valorizing waste liquor from dilute acid pretreatment of lignocellulosic biomass by *Bacillus megaterium* B-10. *Ind. Crop. Prod.* **2021**, *161*, 113160. [[CrossRef](#)]
82. Silambarasan, S.; Logeswari, P.; Sivaramakrishnan, R.; Pugazhendhi, A.; Kamaraj, B.; Ruiz, A.; Ramadoss, G.; Cornejo, P. Polyhydroxybutyrate production from ultrasound-aided alkaline pretreated finger millet straw using *Bacillus megaterium* strain CAM12. *Bioresour. Technol.* **2021**, *325*, 124632. [[CrossRef](#)]
83. Susithra, K.; Narayanan, K.B.; Ramesh, U.; Raja, C.E.; Premkumar, G.; Varatharaju, G.; Vijayakumar, A.; Kannan, M.; Rajarathinam, K. Statistical Optimization of Poly-β-Hydroxybutyrate Biosynthesis Using the Spent Mushroom Substrate by *Bacillus tequilensis* PSR-2. *Waste Biomass Valoriz.* **2021**, 1–17. [[CrossRef](#)]
84. Suryawanshi, S.S.; Sarje, S.S.; Loni, P.C.; Bhujbal, S.; Kamble, P.P. Bioconversion of Sugarcane Molasses into Bioplastic (Polyhydroxybutyrate) using *Bacillus cereus* 2156 under Statistically Optimized Culture Conditions. *Anal. Chem. Lett.* **2020**, *10*, 80–92. [[CrossRef](#)]
85. Getachew, A.; Woldesenbet, F. Production of biodegradable plastic by polyhydroxybutyrate (PHB) accumulating bacteria using low cost agricultural waste material. *BMC Res. Notes* **2016**, *9*, 1–9. [[CrossRef](#)] [[PubMed](#)]
86. El-Sheekh, M.M.; el-Abd, M.A.; el-Diwany, A.I.; Ismail, A.M.S.; Mohsen, S.; Omar, T.H. Poly-3-hydroxybutyrate (PHB) production by *Bacillus flexus* ME-77 using some industrial wastes. *Rend. Fis. Acc. Lincei* **2015**, *26*, 109–119. [[CrossRef](#)]
87. Odeniyi, O.A.; Adeola, O.J. Production and characterization of polyhydroxyalkanoic acid from *Bacillus thuringiensis* using different carbon substrates. *Int. J. Biol. Macromol.* **2017**, *104*, 407–413. [[CrossRef](#)] [[PubMed](#)]
88. Werlang, E.B.; Moraes, L.B.; Muller, M.V.G.; Julich, J.; Corbellini, V.A.; Neves, F.D.F.; de Souza, D.; Benitez, L.B.; de Cassia de Souza Schneider, R. Polyhydroxybutyrate (PHB) Production via bioconversion using *Bacillus pumilus* in liquid phase cultivation of the biomass of *Arthrospira platensis* hydrolysate as a carbon source. *Waste Biomass Valoriz.* **2021**, *12*, 3245–3255. [[CrossRef](#)]

Article

Biotechnological Conversion of Grape Pomace to Poly(3-hydroxybutyrate) by Moderately Thermophilic Bacterium *Tepidimonas taiwanensis*

Xenie Kourilova ^{1,†}, Iva Pernicova ^{1,†}, Michaela Vidlakova ¹, Roman Krejcirik ¹, Katerina Mrazova ², Kamila Hrubanova ², Vladislav Krzyzanek ², Jana Nebesarova ^{3,4} and Stanislav Obruca ^{1,*}

- ¹ Department of Food Chemistry and Biotechnology, Faculty of Chemistry, Brno University of Technology, Purkynova 118, 612 00 Brno, Czech Republic; xckourilovax@fch.vut.cz (X.K.); xcpernicovai@fch.vut.cz (I.P.); Michaela.Vidlakova@vut.cz (M.V.); xckrejcirik@fch.vut.cz (R.K.)
- ² Institute of Scientific Instruments of the Czech Academy of Sciences, v.v.i., Kralovopolska 147, 612 64 Brno, Czech Republic; Katerina.Mrazova@vut.cz (K.M.); hrubanova@isibrno.cz (K.H.); krzyzanek@ISIBrno.Cz (V.K.)
- ³ Biology Centre, The Czech Academy of Sciences, v.v.i., Branisovska 31, 370 05 Ceske Budejovice, Czech Republic; nebe@paru.cas.cz
- ⁴ Faculty of Science, Charles University, Vinicna 7, 128 43 Prague 2, Czech Republic
- * Correspondence: obruca@fch.vut.cz
- † Xenie Kourilova and Iva Pernicova contributed equally.

Citation: Kourilova, X.; Pernicova, I.; Vidlakova, M.; Krejcirik, R.; Mrazova, K.; Hrubanova, K.; Krzyzanek, V.; Nebesarova, J.; Obruca, S. Biotechnological Conversion of Grape Pomace to Poly(3-hydroxybutyrate) by Moderately Thermophilic Bacterium *Tepidimonas taiwanensis*. *Bioengineering* **2021**, *8*, 141. <https://doi.org/10.3390/bioengineering8100141>

Academic Editors: Martin Koller and Ilaria Fratoddi

Received: 24 September 2021
Accepted: 12 October 2021
Published: 14 October 2021

Publisher's Note: MDPI stays neutral with regard to jurisdictional claims in published maps and institutional affiliations.



Copyright: © 2021 by the authors. Licensee MDPI, Basel, Switzerland. This article is an open access article distributed under the terms and conditions of the Creative Commons Attribution (CC BY) license (<https://creativecommons.org/licenses/by/4.0/>).

Abstract: Polyhydroxyalkanoates (PHA) are microbial polyesters that have recently come to the forefront of interest due to their biodegradability and production from renewable sources. A potential increase in competitiveness of PHA production process comes with a combination of the use of thermophilic bacteria with the mutual use of waste substrates. In this work, the thermophilic bacterium *Tepidimonas taiwanensis* LMG 22826 was identified as a promising PHA producer. The ability to produce PHA in *T. taiwanensis* was studied both on genotype and phenotype levels. The gene encoding the Class I PHA synthase, a crucial enzyme in PHA synthesis, was detected both by genome database search and by PCR. The microbial culture of *T. taiwanensis* was capable of efficient utilization of glucose and fructose. When cultivated on glucose as the only carbon source at 50 °C, the PHA titers reached up to 3.55 g/L, and PHA content in cell dry mass was 65%. The preference of fructose and glucose opens the possibility to employ *T. taiwanensis* for PHA production on various food wastes rich in these abundant sugars. In this work, PHA production on grape pomace extracts was successfully tested.

Keywords: polyhydroxyalkanoates; *Tepidimonas taiwanensis*; grape pomace; thermophiles

1. Introduction

Pollution of the environment by solid resistant petrochemical polymers represents one of the most important ecological problems. Every year, several million tons of plastic are produced, which has a wide range of uses, but a large part of them end up being thrown away and accumulating in nature. A potential solution of this problem might be, at least in part, the substitution of petrochemical polymers with biodegradable and renewable materials. One of the alternatives is polyhydroxyalkanoates (PHA). PHA are microbial polyesters that are produced by numerous prokaryotes in the form of intracellular granules to store energy and carbon, but in addition, PHA reveal a protective function concerning the adverse effects of the environment [1]. PHA can be divided based on chain length into scl-PHA (short-chain length), which contains three to five carbons in the monomer, and mcl-PHA (medium-chain length), which contains 6 to 14 carbons in the monomer. A homopolymer of 3-hydroxybutyrate, poly(3-hydroxybutyrate)(PHB) is accumulated by numerous prokaryotes; it can be stated to be the most common and the best-studied

member of the PHA family [2,3]. Generally, PHA are a great alternative to petrochemical plastics. They are fully biodegradable and biocompatible; therefore, PHA demonstrate broad application potential [4] in medicine [5] or cosmetics [6], but also in numerous fields of industry, such as the food industry, packaging industry, or agriculture [7]. However, their disadvantage is still the high cost of production as compared to petrochemical polymers. The price of a commercially produced PHA can range from USD 2 to 5 per kilogram, but the price of, for example, polypropylene is about USD 1 per kilogram [8]. The use of waste substrates, stemming especially from the food industry or agriculture, as input carbon sources can reduce the costs. Furthermore, the price of the material can also be influenced by selecting a suitable microbial producer of PHA, for example, from the ranks of extremophilic microorganisms.

Extremophiles are organisms that live and prosper under extreme conditions relative to human life. These are environments with high or very low pH, temperature, pressure, or salinity values [9]. Previously, it was thought that these sites, such as salt lakes, black smokers, or geothermal springs, were dead, but in fact, they are abundantly inhabited by extremophile microorganisms [10]. In recent years, extremophiles have been at the forefront of science and industry. By adapting them to extreme environments, they offer great potential for applications [11]. Their enzymes, also called extremozymes, have wide use in applications where the conditions are unfavorable for “common” enzymes [12]. However, that is not the only advantage of extremophiles in biotechnology. Their unusual cultivation conditions also offer new possibilities for the biotechnology process. As a result, the sterility requirements of the entire production process may be reduced, thereby lowering the cost of biotechnological production and enhancing the competitiveness of the entire biotechnology application. The introduction of extremophiles into the industry is the main idea of the new generation of industrial biotechnology [13].

There are several producers of PHA among extremophiles. Generally, the most studied extremophilic producers of PHA are halophiles [14]. These are microorganisms that thrive in the presence of salt. PHA is not only used to store carbon and energy, but PHA also helps halophiles survive fluctuations in osmotic pressure [15]. Halophilic PHA producers include not only bacteria but also archaea. One of the most famous producers belonging to the Archaea domain is *Haloflex mediterranei* [16]. It is also able to use various waste substrates from the food industry. Another well-studied genus is *Halomonas* [17]. There are many producers such as *Halomonas halophila* [18], *Halomonas boliviensis* [19] *Halomonas campisalis* [20], or *Halomonas hydrothermalis*, which is capable of producing PHA from waste frying oil [21]. However, high salt loads required by halophilic PHA producers bring numerous complications, such as heavy corrosion of equipment, increased medium costs, and demanding waste-water management.

Therefore, a group of thermophilic microorganisms is also of interest with respect to PHA production. These microorganisms thrive at temperatures of 45 °C and above. There are also some described PHA producers in this group, including *Chelatococcus themostellatus* [22], *Caldimonas taiwanensis* [23], or new isolate bacteria *Aneurinibacillus* sp. H1 [24]. PHA production has also recently been described in the bacterium *Scheeleella thermodepolymerans* using xylose as the most preferred substrate [25].

Grape wine is one of the most popular alcoholic beverages, and its consumption is increasing every year. The annual production of grapes is approximately 78 million tonnes (2018), almost 60% of which are intended for the production of alcoholic beverages [26]. Wine production produces waste in several steps; the most important waste is grape pomace—solid residues after the preparation of grape juice. Grape pomace comprises 10 to 30% of the weight of processed wine and consists mainly of husks, seeds, and any other solids remaining after pressing [27]. It is a complex material; its composition is determined by grape variety, season, weather conditions, etc., but generally, its composition is approximately 30% neutral polysaccharides, 20% acidic pectic substances, 15% insoluble proanthocyanins, lignin, and structural proteins [28]. The profile and quantity of sugars are based on the variety used. Red wines have a lower proportion of soluble sugars that

have already been used in fermentation by yeast. White varieties, on the other hand, have a higher proportion of soluble sugars, with a fructose content of almost 9% and glucose of up to 27% per dry mass [29]. Grape pomace has several uses; it can be used as a food supplement [30], fertilizer [31], or feed [32–34]. However, it can also be used as a carbon waste source for biotechnology purposes [35,36]. Therefore, this material can be a suitable resource to produce PHA. The use of grape pomace to produce PHA has already been tested by mesophilic producers to reduce the cost of the biotechnology process. For example, *Pseudomonas putida* KT2440 was used to produce mcl-PHA on grape pomace in a two-stage process. The process involved a growth phase on grape pomace extract of the Gewürztraminer variety, and then a mixture of octanoic acid and 10-undecenoic acid was added in the production phase. With this bioengineering approach, the dry biomass mass was about 14 g/L, and the copolymer poly(3-hydroxyoctanoate-co-3-hydroxy-10-undecenoate) represented 41% of cell dry mass. The experiment was carried out in a laboratory fermenter and is a promising option to increase the competitiveness of mcl-PHA [36].

Grape pomace extract was also used to produce PHA using *Cupriavidus necator* H16 or halophiles such as *Halomonas halophila* or *Halomonas organivorans*. The prepared lyophilized grape extract contained 33% fructose and 28% glucose. Using 20 g/L of grape sugar extract in the flask test, the cell dry mass of *Cupriavidus necator* H16 reached 4 g/L, and PHA production was almost 2 g/L. Furthermore, PHA production using halophilic strains produced comparable results of 1.8 g/L for *Halomonas halophila*, and the highest production was recorded in *Halomonas organivorans* 2.1 g/L [35]. Extremophiles may be a suitable alternative to mesophiles regarding PHA production. Combined with extremophilic producers, costs may fall, thanks to the use of waste substrates and the reduction in sterility claims, thus causing a decrease in the price of PHA production and an increase in their competitiveness.

The genus *Tepidimonas* accommodates moderately thermophilic Gram-negative, rod-shaped, chemoorganoheterotrophic, motile bacteria with a single polar flagellum. Although these bacteria are not described as PHA producers, they harbor gene machinery for PHA synthesis. However, their biotechnological potential is limited by their relatively low catabolic flexibility. Members of the *Tepidimonas* genus are capable of the utilization of organic acids and amino acids, but usually, carbohydrates are not assimilated. The unique exception is *Tepidimonas taiwanensis*, which should be capable of the utilization of glucose and fructose [37], the main monosaccharides present in grape pomace. Therefore, in this work, *T. taiwanensis* LMG 22826 was evaluated for the first time regarding its PHA synthetic potential. Special attention was paid to its capability to synthesize PHA from inexpensive grape pomace, which could be a route toward sustainable and feasible PHA production.

2. Materials and Methods

2.1. Microorganisms and Cultivation

The bacterium *Tepidimonas taiwanensis* LMG 22826 was purchased from Belgian coordinate collections of microorganisms, Ghent University. This bacterial strain was cultivated usually for 24 h in complex medium (Nutrient Broth with peptone 1 wt.%) and then for 72 h in mineral medium ($\text{Na}_2\text{HPO}_4 \cdot 12 \text{H}_2\text{O}$ (9.0 g/L), KH_2PO_4 (1.5 g/L), NH_4Cl (1.0 g/L), $\text{MgSO}_4 \cdot 7 \text{H}_2\text{O}$ (0.2 g/L), $\text{CaCl}_2 \cdot 2 \text{H}_2\text{O}$ (0.02 g/L), $\text{Fe}^{(\text{III})}\text{NH}_4\text{citrate}$ (0.0012 g/L), yeast extract (0.5 g/L), 1 mL/L of microelements solution (EDTA (50.0 g/L), $\text{FeCl}_3 \cdot 6 \text{H}_2\text{O}$ (13.8 g/L), ZnCl_2 (0.84 g/L), $\text{CuCl}_2 \cdot 2 \text{H}_2\text{O}$ (0.13 g/L), $\text{CoCl}_2 \cdot 6 \text{H}_2\text{O}$ (0.1 g/L), $\text{MnCl}_2 \cdot 6 \text{H}_2\text{O}$ (0.016 g/L), H_3BO_3 (0.1 g/L), dissolved in distilled water), with a carbon source (mainly glucose, 20 g/L) to promote PHA synthesis. In the case of the inoculation phase, the bacteria were cultivated in 100 mL Erlenmeyer flasks with a medium volume of 50 mL. The production part of the cultivation was performed in 250 mL Erlenmeyer flasks with a total volume of 100 mL of medium, including 10 vol.% of inoculum. In both parts of cultivation, Erlenmeyer flasks were constantly shaken at 50 °C unless otherwise noted.

Screening of the optimal carbon source was performed in 96-well microtiter plates. Tested carbon sources were fructose, galactose, glucose, glycerol, lactose, mannose, soluble starch, sucrose, and xylose. Each well was inoculated by 20 μ L of inoculum, 75 μ L 2 \times concentrated mineral medium, and 75 μ L relevant carbon source (40 g/L). Optical density was measured using ELISA reader at 630 nm, (ELx808, Biotek, Winooski, VA, USA) at the beginning of cultivation and after 48 h. From the difference of the measured values, it was possible to compare the increase in the bacterial culture.

The optimal cultivation temperature was tested under the conditions described at the beginning of Section 2.1. The selected temperatures were 45, 50, 55, and 60 °C.

Based on the optimized carbon sources and temperature, the ability to produce copolymers was also investigated. Precursors for accumulation of copolymers poly(3-hydroxybutyrate-co-3-hydroxyvalerate) (P{3HB-co-3HV}) and P(3-hydroxybutyrate-co-4-hydroxybutyrate) (P{3HB-co-4HB}) were chosen; specifically for 3HV introduction, valeric acid and sodium propionate were applied at a concentration of 2 g/L along with 20 g/L of glucose; for 4HB, 1,4-butanediol and γ -butyrolactone were tested as precursors at a concentration of 8 g/L as the sole carbon source. Medium with 20 g/L of glucose was used as a control.

Based on the obtained data, a suitable waste substrate—grape pomace—was selected. The individual components of the mineral medium were dissolved directly in the grape pomace extract, not in distilled water. Subsequently, cultivations were performed under optimal conditions (50 °C, 180 rpm). In the case of cultivation with diluted extracts, the extracts were diluted with distilled water in a ratio 1:1.

2.2. Verification of PHA Production at Genotype and Phenotype Level

Multiplex Polymerase Chain Reaction (PCR) was performed to confirm the ability to produce PHA at the genotype level. The procedure was the same as reported previously [18]. Bacterial DNA (*16SrRNA* gene) and PHA class I synthase (*phaC* gene) were detected.

PHA content in bacterial biomass was determined in dry bacterial biomass. Gas chromatography with flame ionization detection was used for the analysis. The conditions were set as previously described [38]. Product yield coefficient ($Y_{P/S}$) was calculated, which is determined as a ratio of the amount of product to substrate consumed by microbial culture.

The cell morphology was investigated employing transmission electron microscopy (TEM) analysis, using the microscope JEOL 1010 (JEOL, Tokyo, Japan) as described previously [39]. The cells were centrifuged, and a concentrated pellet was pipetted on 3 mm aluminum carriers pretreated with 1% solution of lecithin in chloroform and fixed using the high-pressure freezer EM ICE (Leica Microsystems, Vienna, Austria). Frozen samples were transferred into freeze substitution unit AFS2 (Leica Microsystems, Vienna, Austria). The substitution solution contained 1.5% OsO₄ in acetone, and the substitution protocol was set as previously described [40]. Following freeze-substitution, samples were washed with acetone for 15 min 3 times and were gradually infiltrated with mixtures of epoxy resin (Epoxy Embedding Medium kit, Sigma-Aldrich, St. Louis, MO, USA) and acetone in ratios 1:2, 1:1, and 2:1 and pure resin (1 h each). Samples were then left in fresh pure resin overnight under vacuum and finally embedded in fresh pure resin using 62 °C heat for 48 h. Embedded samples were then cut to ultrathin sections using a diamond knife with cutting angle 45 (Diatome, Nidau, Switzerland) and ultramicrotome UTC Ultracut (Leica Microsystems, Vienna, Austria). Sections were stained with uranyl acetate and lead citrate. Additionally, the elastic behavior of the PHA granules, which was previously described [41], was confirmed by cryogenic scanning electron microscopy (cryo-SEM) using the microscope equipped with a cryo stage (Magellan 400/L, FEI). The concentrated pellet of cells was pipetted on 6 mm aluminum carrier and fixed using high-pressure freezing (EM ICE, Leica Microsystems, Vienna, Austria). Frozen samples were transferred into cryo-vacuum preparation chamber (ACE600, Leica Microsystems) where the samples underwent

freeze fracturing and sublimation at $-95\text{ }^{\circ}\text{C}$ for 7 min. Following sublimation, cells were observed in a scanning electron microscope at $-120\text{ }^{\circ}\text{C}$ using 1–2 keV electron beam.

2.3. Grape Pomace Extract

The grape pomace used was obtained from Rathouzsky winery from the Moravské Bránice. The extracts were prepared from the following varieties: Muller Thurgau weiss, Veltliner fruehrot, Palava, Sauvignon, Pinot blanc, and Blaufraenkisch. Extracts were obtained by mixing grape pomace with water (5% *w/v*). Subsequently, the pH was corrected to 4 with 1 M H_2SO_4 and 0.2% (*v/v*) of Viscozyme was added. The incubation occurred for 24 h at $50\text{ }^{\circ}\text{C}$ and 100 rpm. Subsequently, the contents were filtered and pH neutralized with 30% (*w/v*) NaOH.

The content of monosaccharides, organic acids, and total phenolic substances was determined in the grape pomes extract. In the case of monosaccharides, high-performance liquid chromatography Shimadzu 10AD with a refractive index detector was used for analysis (Shimadzu Corporation, Kyoto, Japan). The separation conditions were as follows: a Waters Carbohydrate Analysis 3.9×300 mm column, isocratic elution, mobile phase (acetonitrile: water (80:20)), and flow rate 1.2 mL/min.

Organic acids were determined by ion chromatography 850 Professional, Metrohm with conductivity detector (column—Metrosep Organic Acids, 250/7.8, Metrohm; mobile phase—0.5 mM sulphuric acid and 15% acetone in water, 0.5 mL/min; suppressor—10 mM LiCl).

A slightly modified Folin–Ciocalteu method [42] was used to determine the total phenolic content. First, 1 mL Folin–Ciocalteu reagent diluted 10 \times was mixed with 1 mL distilled water and 50 μL sample diluted as needed. All components were mixed and incubated for 5 min at room temperature. Subsequently, 1 mL of a saturated sodium carbonate solution was added, mixed, and incubated for 15 min. The absorbance of the mixture was measured at 750 nm using a UV-VIS spectrophotometer (Nanophotometer, Implen P300, Implen GmbH, Munchen, Germany).

3. Results and Discussion

3.1. PHA-Related Genes of Strain *T. taiwanensis* LMG 22826

PHA are produced by numerous prokaryotic microorganisms. An important predisposition of PHA production by prokaryotes is the presence of genes encoding a crucial enzyme required for PHA synthesis—PHA synthase (PhaC). These enzymes are divided into four classes based on substrate specificity and subunit composition [43]. The thermophilic bacterium *Tepidimonas taiwanensis* LMG 22826 can be a suitable candidate for PHA production [37]. However, in general, the *Tepidimonas* species are scarcely studied in terms of PHA production. Several genome assemblies of various *T. taiwanensis* strains are available including that of LMG 22826 (also marked as I1-1strain), accession number of this genome assembly in GeneBank is ASM755667v1. Our basic bioinformatics analysis demonstrated that *T. taiwanensis* LMG 22826 harbors enzyme machinery necessary for PHA synthesis; it was found that the bacterium contains the gene encoding for the Class I PHA synthase (Uniprot accession number A0A554X3G4). The encoded protein exhibits some homology with other Class I PHA synthases, primarily with those from other *Proteobacteria* strains, including the genus *Burkholderia*, for which PHA production is already described [44,45]. The genus *Tepidimonas* also belongs to the order *Burkholderiales*. In addition to PHA synthase, the sequence of a protein called a polyhydroxyalkanoate synthesis repressor (PhaR) was also identified (Uniprot accession number A0A554X7W2). The presence of PHA depolymerase (PhaZ), the enzyme responsible for the mobilization of PHA granules is also known from the available genome assemblies (Uniprot accession number A0A554X7W2).

However, in addition to public database screening of genes involved in PHA metabolism, PHA synthase was also verified using the conventional PCR method. When multiplex PCR was used to confirm both bacterial DNA, gene *16S rRNA*, and confirmation of PHA synthase class I. Figure 1 shows confirmation of the presence of Class I PHA synthase gene.

T. taiwanensis LMG 22826 is therefore well equipped to be a producer of PHA. However, this still needs to be verified on the phenotype level.

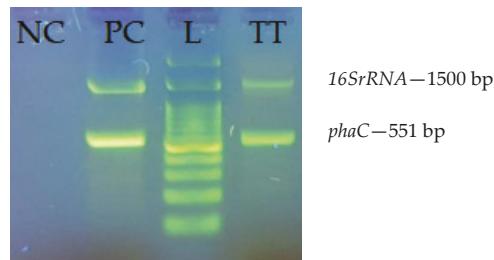


Figure 1. Detection of Class I PHA synthase by conventional PCR. NC—negative control; PC—positive control (*Cupriavidus necator* H16); L—DNA ladder; TT—*Tepidimonas taiwanensis* LMG 22826.

3.2. Screening of PHA Production and the Influence of Culture Parameters on PHA Production

After confirmation of the predisposition to produce PHA on the genotype level, the ability to produce PHA using *T. taiwanensis* LMG 22826 was also verified on the phenotype level. To detect PHA in dry biomass, it was first necessary to ensure sufficient growth of the strain. Therefore, various substances such as glycerol, glucose, fructose, galactose, mannose, xylose, sucrose, lactose, and starch were screened as carbon substrates at 20 g/L (Figure 2). The screening was performed only in a microtitration plate where absorbance was measured. Glucose and fructose proved to be the most suitable substrates, which is in accordance with Chen et al., who also stated that *T. taiwanensis* is capable of the utilization of these sugars as the only carbohydrates [37].

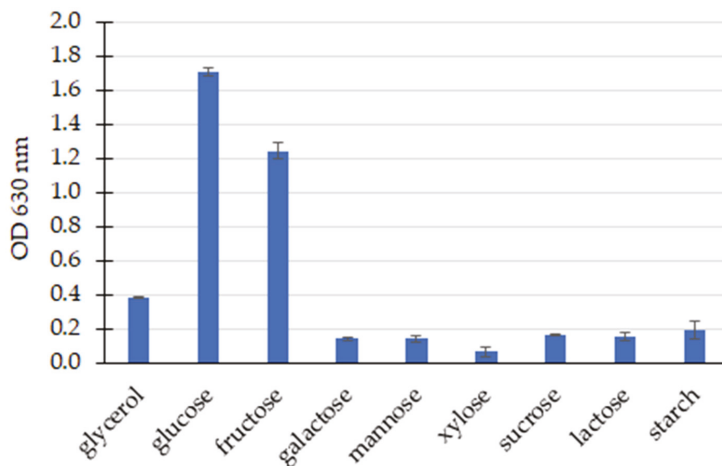


Figure 2. Measured turbidity at OD 630 nm for growth of *T. taiwanensis* biomass for various substrates.

PHA production was further tested in flasks with glucose and fructose as the carbon sources, the presence of PHA was detected by gas chromatography. The biomass and PHA titers reached 5.23 g/L and 3.55 g/L on glucose, respectively. The yields on fructose were slightly lower—about 3.6 g/L of cell dry mass and 2.12 g/L of PHA. According to expectation, the bacterial culture accumulated PHB homopolymer.

In addition, the morphology of *Tepidimonas taiwanensis* LMG 22826 cells grown on glucose was inspected by TEM analysis. As can be seen in Figure 3, the cells are filled with PHA granules. The number of granules in the cell is rather high, over 10 smaller granules

per cell. Generally, the morphology of granules in cells is different and depends on the species of bacteria. For example, *Cupriavidus necator* H16 contains three to seven larger granules in the cell [39], whereas the halophilic bacterium *Halomonas hydrothermalis* contains a large number of small PHA granules in the cell [21]. Additionally, as was previously described for *Cupriavidus necator* H16, PHA granules stay elastic at temperatures of liquid nitrogen and can be observed using freeze fracturing method followed by cryo-SEM [41]. Figure 4 shows cryo-SEM microphotograph of fractured cells of *Tepidimonas taiwanensis* LMG 22826. Needle type of deformation of the PHA granules can be observed, together with concave deformation-holes where the PHA granules were placed before being pulled out of the cell during fracturing.

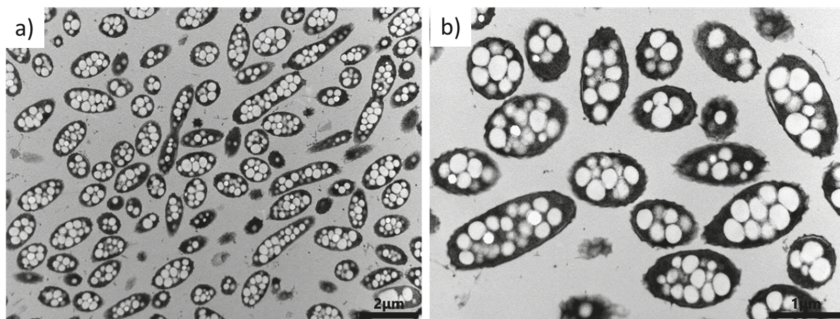


Figure 3. Morphology of PHA and bacterial strain *T. taiwanensis* as seen by TEM. (a) lower magnification; (b) higher magnification.

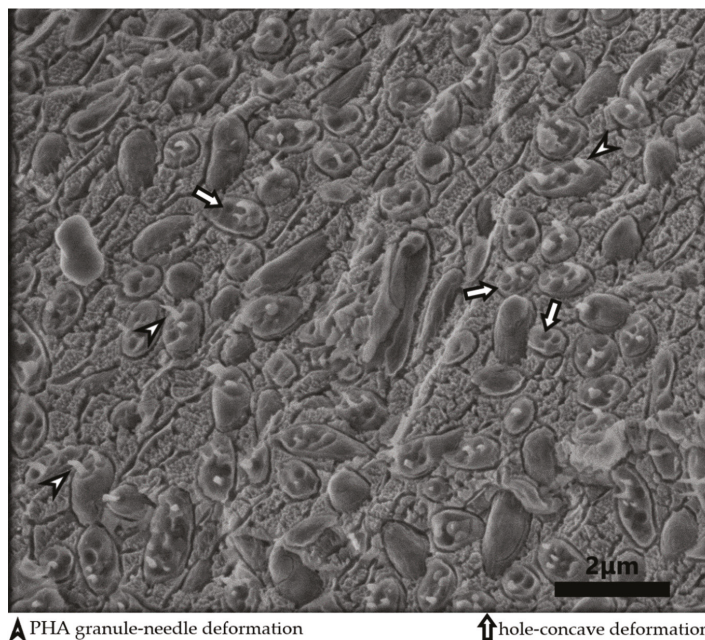


Figure 4. Deformation of PHA granules in the cells of *T. taiwanensis* was caused by freeze fracturing observed using cryo-SEM.

In order to increase the production of PHA, it is necessary to optimize culture conditions; therefore, the ability to grow and produce PHA in the range of cultivation temperatures 45 to 60 °C (with a step-up of 5 °C) was also tested. The obtained data (Table 1) indicate that the bacterium can grow throughout the range of temperatures tested. However, the highest biomass and PHA productions were obtained at temperatures of 50 and 55 °C. The temperature of 50 °C was selected for further experiments when the cell dry mass (CDM) concentration was 5.45 g/L and the PHB concentration was 3.6 g/L. Ibrahim and Steinbuchel proved that even a temperature of 50 °C is high enough to prevent fermentation from contamination and that the process of PHA production can be operated for long periods in semi-sterile mode [46].

Table 1. Effect of culture temperature on PHA production using glucose as the sole source of carbon.

Temperature (°C)	CDM (g/L)	P(3HB) (%)	PHB (g/L)
45	5.08 ± 0.11	67.3 ± 2.1	3.417 ± 0.076
50	5.45 ± 0.22	65.5 ± 5.7	3.559 ± 0.169
55	5.36 ± 0.16	63.9 ± 2.9	3.421 ± 0.056
60	1.60 ± 0.08	49.8 ± 8.5	0.801 ± 0.178

T. taiwanensis proved to be a suitable producer of PHA, especially PHB homopolymer. Therefore, we also tested its ability to synthesize various copolymers using precursors of 3-hydroxyvalerate or 4-hydroxybutyrate. Generally, the copolymers reveal superior mechanical and technological properties as compared to PHB homopolymer. PHB itself is relatively crystalline and therefore brittle and inflexible, but copolymers containing 3HV have a lower crystalline content [47]. Moreover, copolymers with 4HB are even more elastic and have wider applications in medical applications [48]. Nevertheless, *T. taiwanensis* was unable to produce a copolymer with 4HB (see Table 2). However, it was able to form a P(3HB-co-3HV) copolymer using the sodium propionate precursor. When the total PHA content was 44% by weight of dry biomass, resulting in PHA titers of 1.8 g/L, the 3HV content in the copolymer was 6.6 mol. %.

Table 2. Ability to produce copolymers containing 3HV or 4HB from different types of precursors.

Precursors	CDM (g/L)	P(3HB) (%)	PHA (g/L)	3HV (mol. %)	4HB (mol. %)
control	4.21 ± 0.19	49.2 ± 4.1	2.069 ± 0.041	n.d.	n.d.
1,4-butanediol	0.32 ± 0.12	14.2 ± 2.5	0.091 ± 0.022	n.d.	n.d.
γ-butyrolactone	0.08 ± 0.01	n.d.	n.d.	n.d.	n.d.
valeric acid	0.03 ± 0.01	n.d.	n.d.	n.d.	n.d.
sodium propionate	4.16 ± 0.17	44.8 ± 3.8	1.860 ± 0.130	6.6	n.d.

n.d.—not detected.

3.3. Use of Grape Pomace to Produce PHA

3.3.1. Characterization of Extract of Grape Pomace

Grapes are generally one of the most cultivated crops in the world. They are not only intended for direct consumption but also the production of other foods (jam, wine vinegar, grape oil, dried kernel extracts, etc.) [49]. One of the most popular products is wine. The processing of grapes into wine produces a variety of wastes, including grape pomace. Thus, grape pomace represents a significant part of the waste from the winery. They have some other uses, especially recently developing their use as potential resources for added value [50]. Their composition depends on the variety used and the procedure of wine preparation. Grape pomace can also be made into a sugar-rich extract, which can be used by microbiological conversion to PHA, for example.

Grape pomace extracts were prepared as described in Section 2.3, and they were analyzed before being utilized as substrates for PHA production employing *T. taiwanensis*. Organic acids (citric acid, malic acid, lactic acid, acetic acid, formic acid, propionic acid), total polyphenols, sugars, mainly glucose and fructose, were analyzed in the extracts. As

can be seen in Table 3, the parameters monitored vary among the varieties used. The highest content of organic acids was determined in Veltliner fruehrot extract, and the highest concentrations of total polyphenols were determined in Blaufraenkisch extract (red), where the highest sugar content was also determined.

Generally, grape pomace extracts have a wide application, depending on the wine variety and the preparation of the extract. For example, red wine extracts were found to contain higher levels of flavonoid and phenolic compounds and exhibit stronger oxygen radical absorption capabilities than apple pomace. Grape pomace extracts also indicate potential medical use in the treatment of diabetes [51], and they are also used in natural cosmetic products [52].

Table 3. Characterization of grape pomace.

Composition of Grape Pomace Extracts		Muller Thurgau weiss	Veltliner Fruehrot	Palava	Sauvignon	Pinot Blanc	Blaufraenkisch (Red)	Blaufraenkisch (Rose)
Organic acid (g/L)	Citric acid	0.009	0.096	0.027	0.147	0.137	0.017	0.104
	Malic acid	0.620	0.939	0.956	0.979	0.0849	0.319	0.877
	Succinic acid	0.093	0.054	0.045	0.101	0.115	0.107	0.012
	Lactic acid	n.d.	0.006	0.006	0.009	0.014	0.022	0.001
	Acetic acid	0.131	0.156	0.059	0.100	0.119	0.071	0.054
	Formic acid	n.d.	0.004	0.005	0.004	0.006	0.004	n.d.
	Propionic acid	0.062	0.067	0.064	0.064	0.066	0.061	0.052
Total polyphenols (g/L)		0.453	0.301	0.520	0.160	0.231	0.821	0.548
Sugars (g/L)	Fructose	5.49	4.73	6.68	2.84	2.97	11.65	9.04
	Glucose	5.71	6.61	6.66	4.13	4.31	11.09	8.22
Total sugars (g/L)		11.20	11.35	13.34	6.97	7.28	22.73	17.26

n.d.—not detected.

3.3.2. Grape Pomace Extracts as a Carbon Source for PHA Production

The ability to produce PHA has been confirmed in *Tepidimonas taiwanensis*, and it was also confirmed that the bacterium is capable of using both glucose and fructose. Since glucose and fructose comprise the dominant portion of sugars in the prepared extracts of wine pomace, these extracts were used to produce PHA. Extracts without dilution supplemented by the components of the cultivation media were tested first; the results are demonstrated in Table 4. The grape pomace extract of the variety of Veltliner fruehrot demonstrated the highest potential since CDM of the bacterial culture reached 4.36 g/L and PHA titer was 2.09 g/L. High PHA yields were also achieved on grape pomace extracts of Sauvignon (1.498 g/L PHA) and Pinot blanc (1.585 g/L). It is important to note that, for these extracts, the yield coefficient $Y_{P/S}$ was almost identical (0.22), but the highest yield coefficient was obtained for Blaufraenkisch (rose), but even though the use of sugars was effective, the PHA content was low and was only around 12% by CDM.

Table 4. PHA production using grape pomace as a carbon source.

Grape Pomace From	CDM (g/L)	P(3HB) (%)	P(3HB) (g/L)	Residual Fructose (g/L)	Residual Glucose (g/L)	$Y_{P/S}$
Muller Thurgau weiss	0.35 ± 0.02	1.4 ± 0.8	0.005 ± 0.001	4.65	4.66	0.00
Veltliner fruehrot	4.36 ± 0.04	47.9 ± 2.3	2.090 ± 0.081	0.74	0.38	0.21
Palava	0.80 ± 0.04	3.7 ± 1.2	0.030 ± 0.001	6.06	6.11	0.03
Sauvignon	3.37 ± 0.13	44.5 ± 1.7	1.498 ± 0.041	0.05	n.d.	0.22
Pinot blanc	3.62 ± 0.01	43.8 ± 2.5	1.585 ± 0.046	0.12	n.d.	0.22
Blaufraenkisch (red)	0.27 ± 0.03	8.4 ± 2.6	0.022 ± 0.001	9.06	8.69	0.00
Blaufraenkisch (rose)	1.92 ± 0.35	12.3 ± 1.9	0.236 ± 0.049	8.62	8.04	0.39

n.d.—not detected.

With respect to PHA production from grape pomace extract, *T. taiwanensis* can be considered being very promising bacterium. In a similar study, Kovalcik et al. obtained comparable or lower PHB titers employing *Halomonas halophila* (1.8 g/L of PHB), *Halomonas organivorans* (2.1 g/L of PHB) and *Cupriavidus necator* (1.9 g/L PHB) [35]. Nevertheless, *T. taiwanensis* provides all the above-mentioned advantages associated with the cultivation of thermophilic bacterium.

T. taiwanensis was shown to be capable of producing PHA on grape pomace extract. Nevertheless, apart from desirable sugars, the extracts also contain phenolic substances, organic acids and also other substances that can have an inhibitory effect for microbial culture [53]. To minimize inhibition of the culture by substances naturally present in grape pomace extracts, the extracts were diluted 1:1 with distilled water, supplemented with all the constituents of the production medium and used for PHA production employing *T. taiwanensis*. This dilution resulted in the potential dilution of inhibitory substances and, unfortunately, also total sugars. Generally, PHA is overproduced by microbial cultures when carbon source is present in excess and other elements (e.g., sources of nitrogen, phosphorous, etc.) are limiting. Nevertheless, there are reports that even high excess of carbon source has a negative impact on PHA accumulation. Shang et al. reported that the highest amount of PHB was accumulated by *Ralstonia eutropha* (former designation for *Cupriavidus necator*) when cultivated on 9 g/L of glucose; when glucose concentration was increased, the PHB yields decreased significantly [54]. In Table 5, the effect of the diluted medium on the production and growth of the bacterium can be observed. It is noticeable that, for some extracts, dilution had a positive effect. For example, for the Palava extract, 2.59 g/l of biomass was achieved (in undiluted only 0.8 g/L) and PHA production also increased from the original 0.03 g/L to 0.6 g/l. However, some extracts also had a negative effect, with the production of Veltliner fruehrot extract, for example, falling from an initial 2.090 g/L to 0.883 g/L. This decrease may be due to the lack of a carbon source due to the dilution of the extracts, because, at the end of the culture, no residual sugars were detected in any use of the diluted extract. This may indicate a carbon limitation, which is not very suitable for PHA production. However, the production of PHA employing *T. taiwanensis* on waste sources such as grape pomace extracts is a suitable alternative to the production of PHA due to the extremophilic nature of the producer, and because the use of waste as an input source increases the competitiveness of the production.

Table 5. Production of PHA using diluted grape spread with water in a 1:1 ratio.

Grape Pomace From	CDM [g/L]	P(3HB) [%]	P(3HB) [g/L]	Residual Fructose [g/L]	Residual Glucose [g/L]	Y _{P/S}
Muller Thurgau weiss	1.09 ± 0.24	11.4 ± 1.2	0.115 ± 0.013	n.d.	n.d.	0.02
Veltliner fruehrot	2.39 ± 0.12	36.9 ± 2.4	0.883 ± 0.044	n.d.	n.d.	0.16
Palava	2.59 ± 0.05	31.2 ± 3.4	0.619 ± 0.070	n.d.	n.d.	0.09
Sauvignon	1.32 ± 0.08	27.2 ± 1.7	0.359 ± 0.054	n.d.	n.d.	0.10
Pinot blanc	1.97 ± 0.06	28.6 ± 5.2	0.564 ± 0.013	n.d.	n.d.	0.15
Blaufraenkisch (red)	2.87 ± 0.81	41.9 ± 3.7	1.201 ± 0.076	n.d.	n.d.	0.11
Blaufraenkisch (rose)	2.94 ± 0.09	47.7 ± 2.5	1.399 ± 0.041	n.d.	n.d.	0.16

n.d.—not detected.

4. Conclusions

Based on the obtained results, it was proved that the thermophilic bacterium *Tepidomonas taiwanensis* LMG 22826 possesses gene machinery for PHA biosynthesis, and it is a suitable candidate for PHA production, taking advantage of its thermophilic nature. The optimal cultivation temperature of this bacterium is in the range of 50–55 °C, which substantially reduces the risk of contamination by common mesophilic microflora, and hence reduces the sterility demands of the process. It was also found that this bacterium is capable of efficient utilization of glucose and fructose; therefore, it can be employed for thermophilic production of PHA on food-waste substrates rich in these abundant sugars. In this work, we utilized *T. taiwanensis* for PHA production on grape pomace—the major

waste stream of wine production, which is produced annually in extensive amounts. PHA titers on Veltliner fruehrot extract in flasks cultivation reached 2.09 g/L, which is more than comparable to PHA production reported to yields reported in the literature for mesophilic bacteria. Therefore, *T. taiwanensis* is a suitable candidate for the biotechnological production of PHA.

Author Contributions: Conceptualization, S.O.; investigation, X.K., I.P., M.V., R.K., K.M., K.H., V.K. and J.N.; writing—original draft preparation, X.K., I.P. and S.O.; writing—review and editing, K.M. and V.K.; visualization, X.K., I.P., K.M., K.H. and J.N.; supervision, S.O. All authors have read and agreed to the published version of the manuscript.

Funding: This study was funded by the project GA19-20697S of the Czech Science Foundation (GACR). TEM analysis was supported by the MEYS CR (LM2015062 Czech-Biolmaging).

Institutional Review Board Statement: Not applicable.

Informed Consent Statement: Not applicable.

Acknowledgments: We would like to thank Rathouzsky winery from Moravske Branice for providing grape pomace for experiments.

Conflicts of Interest: The authors declare no conflict of interest.

References

- Lim, H.; Chuah, J.; Chek, M.; Tan, H.; Hakoshima, T.; Sudesh, K. Identification of regions affecting enzyme activity, substrate binding, dimer stabilization and polyhydroxyalkanoate (PHA) granule morphology in the PHA synthase of *Aquitalea* sp. USM4. *Int. J. Biol. Macromol.* **2021**, *186*, 414–423. [[CrossRef](#)] [[PubMed](#)]
- Raza, Z.; Abid, S.; Banat, I. Polyhydroxyalkanoates: Characteristics, production, recent developments and applications. *Int. Biodeterior. Biodegrad.* **2018**, *126*, 45–56. [[CrossRef](#)]
- Peña, C.; Castillo, T.; García, A.; Millán, M.; Segura, D. Biotechnological strategies to improve production of microbial poly-(3-hydroxybutyrate): A review of recent research work. *Microb. Biotechnol.* **2014**, *7*, 278–293. [[CrossRef](#)] [[PubMed](#)]
- Yadav, B.; Talan, A.; Tyagi, R.; Drogui, P. Concomitant production of value-added products with polyhydroxyalkanoate (PHA) synthesis: A review. *Bioresour. Technol.* **2021**, *337*, 125419. [[CrossRef](#)] [[PubMed](#)]
- Ray, S.; Kalia, V. Biomedical Applications of Polyhydroxyalkanoates. *Indian J. Microbiol.* **2017**, *57*, 261–269. [[CrossRef](#)]
- Chen, G.; Patel, M. Plastics Derived from Biological Sources: Present and Future. *Chem. Rev.* **2012**, *112*, 2082–2099. [[CrossRef](#)]
- Poltronieri, P.; Kumar, P. Polyhydroxyalkanoates (PHAs) in Industrial Applications. In *Handbook of Ecomaterials*; Martínez, L., Kharisova, O., Kharisov, B., Eds.; Springer International Publishing: Cham, Switzerland, 2017; pp. 1–30. ISBN 978-3-319-48281-1.
- Crutchik, D.; Franchi, O.; Caminos, L.; Jeison, D.; Belmonte, M.; Pedrouso, A.; Val del Rio, A.; Mosquera-Corral, A.; Campos, J. Polyhydroxyalkanoates (PHAs) Production: A Feasible Economic Option for the Treatment of Sewage Sludge in Municipal Wastewater Treatment Plants? *Water* **2020**, *12*, 1118. [[CrossRef](#)]
- Rampelotto, P. Extremophiles and Extreme Environments. *Life* **2013**, *3*, 482–485. [[CrossRef](#)]
- Berlemont, R.; Gerday, C. Extremophiles. In *Comprehensive Biotechnology*; Elsevier: Amsterdam, The Netherlands, 2011; pp. 229–242.
- Irwin, J. Overview of extremophiles and their food and medical applications. *Physiol. Biotechnol. Asp. Extrem.* **2020**, 65–87. [[CrossRef](#)]
- Dumorne, K.; Cordova, D.; Astorga-Elo, M.; Renganathan, P. Extremozymes: A Potential Source for Industrial Applications. *J. Microbiol. Biotechnol.* **2017**, *27*, 649–659. [[CrossRef](#)] [[PubMed](#)]
- Chen, G.; Jiang, X. Next generation industrial biotechnology based on extremophilic bacteria. *Curr. Opin. Biotechnol.* **2018**, *50*, 94–100. [[CrossRef](#)]
- Quillaguamán, J.; Guzmán, H.; Van-Thuoc, D.; Hatti-Kaul, R. Synthesis and production of polyhydroxyalkanoates by halophiles: Current potential and future prospects. *Appl. Microbiol. Biotechnol.* **2010**, *85*, 1687–1696. [[CrossRef](#)]
- Sedlacek, P.; Slaninova, E.; Koller, M.; Nebesarova, J.; Marova, I.; Krzyzanek, V.; Obruca, S. PHA granules help bacterial cells to preserve cell integrity when exposed to sudden osmotic imbalances. *New Biotechnol.* **2019**, *49*, 129–136. [[CrossRef](#)] [[PubMed](#)]
- Alsafadi, D.; Al-Mashaqbeh, O. A one-stage cultivation process for the production of poly-3-(hydroxybutyrate-co-hydroxyvalerate) from olive mill wastewater by *Haloferax mediterranei*. *New Biotechnol.* **2017**, *34*, 47–53. [[CrossRef](#)]
- Tan, D.; Wu, Q.; Chen, J.; Chen, G. Engineering *Halomonas* TD01 for the low-cost production of polyhydroxyalkanoates. *Metab. Eng.* **2014**, *26*, 34–47. [[CrossRef](#)]
- Kucera, D.; Pernicová, I.; Kovalčík, A.; Koller, M.; Mullerova, L.; Sedlacek, P.; Mravec, F.; Nebesarova, J.; Kalina, M.; Marova, I.; et al. Characterization of the promising poly(3-hydroxybutyrate) producing halophilic bacterium *Halomonas halophila*. *Bioresour. Technol.* **2018**, *256*, 552–556. [[CrossRef](#)]

19. Rivera-Terceros, P.; Tito-Claros, E.; Torrico, S.; Carballo, S.; Van-Thuoc, D.; Quillaguamán, J. Production of poly(3-hydroxybutyrate) by *Halomonas boliviensis* in an air-lift reactor. *J. Biol. Res.-Thessalon.* **2015**, *22*, 8. [CrossRef]
20. Kulkarni, S.; Kanekar, P.; Nilegaonkar, S.; Sarnaik, S.; Jog, J. Production and characterization of a biodegradable poly (hydroxybutyrate-co-hydroxyvalerate) (PHB-co-PHV) copolymer by moderately haloalkalitolerant *Halomonas campisalis* MCM B-1027 isolated from Lonar Lake, India. *Bioresour. Technol.* **2010**, *101*, 9765–9771. [CrossRef] [PubMed]
21. Pernicova, I.; Kucera, D.; Nebesarova, J.; Kalina, M.; Novackova, I.; Koller, M.; Obruca, S. Production of polyhydroxyalkanoates on waste frying oil employing selected *Halomonas* strains. *Bioresour. Technol.* **2019**, *292*, 122028. [CrossRef] [PubMed]
22. Ibrahim, M.; Willems, A.; Steinbüchel, A. Isolation and characterization of new poly(3HB)-accumulating star-shaped cell-aggregates-forming thermophilic bacteria. *J. Appl. Microbiol.* **2010**, *109*, 1579–1590. [CrossRef]
23. Sheu, D.; Chen, W.; Yang, J.; Chang, R. Thermophilic bacterium *Caldimonas taiwanensis* produces poly(3-hydroxybutyrate-co-3-hydroxyvalerate) from starch and valerate as carbon sources. *Enzym. Microb. Technol.* **2009**, *44*, 289–294. [CrossRef]
24. Pernicova, I.; Novackova, I.; Sedlacek, P.; Kourilova, X.; Kalina, M.; Kovalcik, A.; Koller, M.; Nebesarova, J.; Krzyzaneck, V.; Hrubanova, K.; et al. Introducing the Newly Isolated Bacterium *Aneurinibacillus* sp. H1 as an Auspicious Thermophilic Producer of Various Polyhydroxyalkanoates (PHA) Copolymers—1. Isolation and Characterization of the Bacterium. *Polymers* **2020**, *12*, 1235. [CrossRef]
25. Kourilova, X.; Pernicova, I.; Sedlar, K.; Musilova, J.; Sedlacek, P.; Kalina, M.; Koller, M.; Obruca, S. Production of polyhydroxyalkanoates (PHA) by a thermophilic strain of *Schlegelella thermodepolymerans* from xylose rich substrates. *Bioresour. Technol.* **2020**, *315*, 123885. [CrossRef] [PubMed]
26. 2019 Statistical Report on World Vitiviniculture, 1st ed.; International Organisation of Vine and Wine Intergovernmental Organisation: International Organisation of Vine and Wine Intergovernmental Organisation. 2020. Available online: <http://oiv.int/public/medias/6782/oiv-2019-statistical-report-on-world-vitiviniculture.pdf> (accessed on 9 September 2021).
27. Moreno, A.; Ballesteros, M.; Negro, M. Biorefineries for the valorization of food processing waste. In *The Interaction of Food Industry and Environment*; Academic Press: Cambridge, MA, USA, 2020; pp. 155–190.
28. Dávila, I.; Robles, E.; Egúés, I.; Labidi, J.; Gullón, P. The Biorefinery Concept for the Industrial Valorization of Grape Processing By-Products. In *Handbook of Grape Processing By-Products*; Academic Press: Cambridge, MA, USA, 2017; pp. 29–53.
29. Antonić, B.; Jančíková, S.; Dordević, D.; Tremlová, B. Grape Pomace Valorization: A Systematic Review and Meta-Analysis. *Foods* **2020**, *9*, 1627. [CrossRef]
30. González-Paramás, A.; Esteban-Ruano, S.; Santos-Buelga, C.; de Pascual-Teresa, S.; Rivas-Gonzalo, J. Flavanol Content and Antioxidant Activity in Winery Byproducts. *J. Agric. Food Chem.* **2004**, *52*, 234–238. [CrossRef]
31. Manios, T. The composting potential of different organic solid wastes: Experience from the island of Crete. *Environ. Int.* **2004**, *29*, 1079–1089. [CrossRef]
32. Sánchez, A.; Ysunza, F.; Beltrán-García, M.; Esqueda, M. Biodegradation of Viticulture Wastes by *Pleurotus*: A Source of Microbial and Human Food and Its Potential Use in Animal Feeding. *J. Agric. Food Chem.* **2002**, *50*, 2537–2542. [CrossRef]
33. Zacharof, M. Grape Winery Waste as Feedstock for Bioconversions: Applying the Biorefinery Concept. *Waste Biomass Valorization* **2017**, *8*, 1011–1025. [CrossRef]
34. Taurino, R.; Ferretti, D.; Cattani, L.; Bozzoli, F.; Bondioli, F. Lightweight clay bricks manufactured by using locally available wine industry waste. *J. Build. Eng.* **2019**, *26*, 100892. [CrossRef]
35. Kovalcik, A.; Pernicova, I.; Obruca, S.; Sztokowski, M.; Enev, V.; Kalina, M.; Marova, I. Grape winery waste as a promising feedstock for the production of polyhydroxyalkanoates and other value-added products. *Food Bioprod. Process.* **2020**, *124*, 1–10. [CrossRef]
36. Follonier, S. Pilot-scale Production of Functionalized mcl-PHA from Grape Pomace Supplemented with Fatty Acids. *Chem. Biochem. Eng. Q.* **2015**, *29*, 113–121. [CrossRef]
37. Chen, T.; Chou, Y.; Chen, W.; Arun, B.; Young, C. *Tepidimonas taiwanensis* sp. nov., a novel alkaline-protease-producing bacterium isolated from a hot spring. *Extremophiles* **2006**, *10*, 35–40. [CrossRef]
38. Obruca, S.; Petrik, S.; Benesova, P.; Svoboda, Z.; Eremka, L.; Marova, I. Utilization of oil extracted from spent coffee grounds for sustainable production of polyhydroxyalkanoates. *Appl. Microbiol. Biotechnol.* **2014**, *98*, 5883–5890. [CrossRef]
39. Mravec, F.; Obruca, S.; Krzyzaneck, V.; Sedlacek, P.; Hrubanova, K.; Samek, O.; Kucera, D.; Benesova, P.; Nebesarova, J.; Steinbüchel, A. Accumulation of PHA granules in *Cupriavidus necator* as seen by confocal fluorescence microscopy. *FEMS Microbiol. Lett.* **2016**, *363*, fnw094. [CrossRef]
40. Kouřilová, X.; Schwarzerová, J.; Pernicová, I.; Sedlár, K.; Mrázová, K.; Krzyžánek, V.; Nebesářová, J.; Obruča, S. The First Insight into Polyhydroxyalkanoates Accumulation in Multi-Extremophilic *Rubrobacter xylanophilus* and *Rubrobacter spartanus*. *Microorganisms* **2021**, *9*, 909. [CrossRef]
41. Obruca, S.; Sedlacek, P.; Krzyzaneck, V.; Mravec, F.; Hrubanova, K.; Samek, O.; Kucera, D.; Benesova, P.; Marova, I.; Chen, G.-Q. Accumulation of Poly(3-hydroxybutyrate) Helps Bacterial Cells to Survive Freezing. *PLoS ONE* **2016**, *11*, e0157778. [CrossRef]
42. Singleton, V.; Rossi, J. Colorimetry of Total Phenolics with Phosphomolybdic-Phosphotungstic Acid Reagents. *Am. J. Enol. Viticulture* **1965**, *16*, 144–158.
43. Tan, I.; Foong, C.; Tan, H.; Lim, H.; Zain, N.; Tan, Y.; Hoh, C.; Sudesh, K. Polyhydroxyalkanoate (PHA) synthase genes and PHA-associated gene clusters in *Pseudomonas* spp. and *Janthinobacterium* spp. isolated from Antarctica. *J. Biotechnol.* **2020**, *313*, 18–28. [CrossRef]

44. Pan, W.; Perrotta, J.; Stipanovic, A.; Nomura, C.; Nakas, J. Production of polyhydroxyalkanoates by *Burkholderia cepacia* ATCC 17759 using a detoxified sugar maple hemicellulosic hydrolysate. *J. Ind. Microbiol. Biotechnol.* **2012**, *39*, 459–469. [[CrossRef](#)]
45. Kourmentza, C.; Costa, J.; Azevedo, Z.; Servin, C.; Grandfils, C.; De Freitas, V.; Reis, M. *Burkholderia thailandensis* as a microbial cell factory for the bioconversion of used cooking oil to polyhydroxyalkanoates and rhamnolipids. *Bioresour. Technol.* **2018**, *247*, 829–837. [[CrossRef](#)]
46. Ibrahim, M.; Steinbüchel, A. High-Cell-Density Cyclic Fed-Batch Fermentation of a Poly(3-Hydroxybutyrate)-Accumulating Thermophile, *Chelatococcus* sp. Strain MW10. *Appl. Environ. Microbiol.* **2010**, *76*, 7890–7895. [[CrossRef](#)]
47. Keenan, T.; Nakas, J.; Tanenbaum, S. Polyhydroxyalkanoate copolymers from forest biomass. *J. Ind. Microbiol. Biotechnol.* **2006**, *33*, 616–626. [[CrossRef](#)]
48. Norhafini, H.; Huong, K.; Amirul, A. High PHA density fed-batch cultivation strategies for 4HB-rich P(3HB-co-4HB) copolymer production by transformant *Cupriavidus malaysiensis* USMAA1020. *Int. J. Biol. Macromol.* **2019**, *125*, 1024–1032. [[CrossRef](#)]
49. Venkitasamy, C.; Zhao, L.; Zhang, R.; Pan, Z. Grapes. In *Integrated Processing Technologies for Food and Agricultural By-Products*; Elsevier: Amsterdam, The Netherlands, 2019; pp. 133–163, ISBN 9780128141380.
50. Chowdhary, P.; Gupta, A.; Gnansounou, E.; Pandey, A.; Chaturvedi, P. Current trends and possibilities for exploitation of Grape pomace as a potential source for value addition. *Environ. Pollut.* **2021**, *278*, 116796. [[CrossRef](#)]
51. Hogan, S.; Zhang, L.; Li, J.; Sun, S.; Canning, C.; Zhou, K. Antioxidant rich grape pomace extract suppresses postprandial hyperglycemia in diabetic mice by specifically inhibiting alpha-glucosidase. *Nutr. Metab.* **2010**, *7*, 71. [[CrossRef](#)]
52. Pinto, D.; Cádiz-Gurrea, M.; Silva, A.; Delerue-Matos, C.; Rodrigues, F. Cosmetics—food waste recovery. In *Food Waste Recovery*; Elsevier: Amsterdam, The Netherlands, 2021; pp. 503–528, ISBN 9780128205631.
53. Luchian, C.; Cotea, V.; Vlase, L.; Toiu, A.; Colibaba, L.; Răschip, I.; Nadăș, G.; Gheldiu, A.; Tuchiluş, C.; Rotaru, L.; et al. Antioxidant and antimicrobial effects of grape pomace extracts. *BIO Web Conf.* **2019**, *15*, 04006. [[CrossRef](#)]
54. Shang, L.; Jiang, M.; Chang, H.N. P oly(3-hydroxybutyrate) synthesis in fed-batch culture of *Ralstonia eutropha* with phosphate limitation under different glucose concentrations. *Biotechnol. Lett.* **2003**, *25*, 1415–1419. [[CrossRef](#)]

Article

Lab-Scale Cultivation of *Cupriavidus necator* on Explosive Gas Mixtures: Carbon Dioxide Fixation into Polyhydroxybutyrate

Vera Lambauer^{1,2} and Regina Kratzer^{1,2,*}

¹ Austrian Centre of Industrial Biotechnology (ACIB), Krenngasse 37, A-8010 Graz, Austria; veralambauer@acib.at

² Institute of Biotechnology and Biochemical Engineering, Graz University of Technology, NAWI Graz, Petersgasse 12/II, A-8010 Graz, Austria

* Correspondence: regina.kratzer@tugraz.at

Abstract: Aerobic, hydrogen oxidizing bacteria are capable of efficient, non-phototrophic CO₂ assimilation, using H₂ as a reducing agent. The presence of explosive gas mixtures requires strict safety measures for bioreactor and process design. Here, we report a simplified, reproducible, and safe cultivation method to produce *Cupriavidus necator* H16 on a gram scale. Conditions for long-term strain maintenance and mineral media composition were optimized. Cultivations on the gaseous substrates H₂, O₂, and CO₂ were accomplished in an explosion-proof bioreactor situated in a strong, grounded fume hood. Cells grew under O₂ control and H₂ and CO₂ excess. The starting gas mixture was H₂:CO₂:O₂ in a ratio of 85:10:2 (partial pressure of O₂ 0.02 atm). Dissolved oxygen was measured online and was kept below 1.6 mg/L by a stepwise increase of the O₂ supply. Use of gas compositions within the explosion limits of oxyhydrogen facilitated production of 13.1 ± 0.4 g/L total biomass (gram cell dry mass) with a content of 79 ± 2% poly-(R)-3-hydroxybutyrate in a simple cultivation set-up with dissolved oxygen as the single controlled parameter. Approximately 98% of the obtained PHB was formed from CO₂.

Keywords: non-phototrophic CO₂ assimilation; *Knallgas* cultivation; *Chemolithotrophs*; ATEX compliant bioreactor; dissolved oxygen control

Citation: Lambauer, V.; Kratzer, R. Lab-Scale Cultivation of *Cupriavidus necator* on Explosive Gas Mixtures: Carbon Dioxide Fixation into Polyhydroxybutyrate. *Bioengineering* **2022**, *9*, 204. <https://doi.org/10.3390/bioengineering9050204>

Academic Editor: Martin Koller

Received: 30 March 2022

Accepted: 5 May 2022

Published: 10 May 2022

Publisher's Note: MDPI stays neutral with regard to jurisdictional claims in published maps and institutional affiliations.



Copyright: © 2022 by the authors. Licensee MDPI, Basel, Switzerland. This article is an open access article distributed under the terms and conditions of the Creative Commons Attribution (CC BY) license (<https://creativecommons.org/licenses/by/4.0/>).

1. Introduction

CO₂ emissions from fossil fuel combustion and further anthropogenic activities are the largest driver of global warming. Stripping the CO₂ back out of waste streams and using it as carbon feedstock would close the carbon loop and spare fossil fuels. Therefore, CO₂ emissions would be limited and climate change impacts mitigated. One major obstacle in CO₂ reuse is the high stability of the molecule. Considerable energy input is needed to activate CO₂ for further use and large-volume CO₂ conversion processes are currently limited to a few industrial processes (e.g., urea, methanol, carbonate, and formic acid production) [1,2]. Nature has evolved highly sophisticated mechanisms for carbon fixation and utilization. The reducing energy for CO₂ reduction is either obtained from light-dependent reactions or from oxidation of inorganic compounds. Aerobic hydrogen-oxidizing bacteria (HOBs or *Knallgas* bacteria) assimilate CO₂ by H₂ oxidation. Provision of the reducing power by H₂ oxidation is an efficient route in non-phototrophic CO₂ assimilation and promises higher growth rates while promoting drastically less land, fresh water, and mineral requirements as compared to photosynthetic organisms [3,4]. The HOB *Cupriavidus necator* was compared to the green microalga *Neochloris oleoabundans* in microbial CO₂ fixation. *C. necator* has been reported to exhibit 3–6 times higher energy efficiencies and higher biomass yields in comparison to *N. oleoabundans* in microbial CO₂ fixation [5]. *C. necator* can accumulate polyhydroxyalkanoate as carbon storage to levels of up to 82% of the cell's dry weight (on CO₂ under chemolithotrophic conditions) [6,7]. The metabolism is tractable by genetic engineering, and alternative products from CO₂ such as tailor-made polyhydroxyalkanoates or

versatile organic solvents become available [8–11]. However, applications of *C. necator* and other HOBs for CO₂ fixation are still hesitant despite the increasing demand for cheap feedstocks. The largest published HOB cultivation of 23 L was reported in 1976 [12]. The main reason for slow implementation of chemolithotrophic cultivations is technical hurdles, and thus high implementation costs due to the explosiveness of H₂ and O₂ mixtures (low ignition energy ≥ 0.016 mJ). Gases must be mixed on-site (requiring several gas lines), labs need safety measures (gas sensors, check-valves, ventilated hoods, explosion doors, antistatic workwear, etc.), and equipment must be explosion-proof (avoidance of ignition sparks and electrostatic discharges). Construction measures are time-consuming and explosion-proof equipment is, as a rule of thumb, at least 10 times more expensive than standard equipment (magnetic stirrers, bioreactors etc.). Finally, some residual uncertainty regarding lab safety remains despite all safety measures. In the last several years, a restricted number of labs equipped for fermentations of explosive gas mixtures were reported (with no claim to completeness [10,13–17]). In parallel, several groups engineered HOB strains (first and foremost *C. necator*). However, labs focusing on molecular biotechnology are generally not equipped for oxyhydrogen cultivations (exceptions e.g., [10,11,13,18]). Therefore, newly developed strains were often grown in closed jars or bottles flushed with gases once or twice a day (e.g., [8,9,16,19]). Obviously, fast-growing HOB strains are nutrient-limited under these conditions and strain characterization is affected (difficulties in measuring growth and nutrient levels).

In the present study, we report on reproducible, safe, and easy-to-perform chemolithotrophic cultivations of HOBs. Conditions for long-term strain maintenance of *C. necator* H16 were optimized and mineral media composition for chemolithotrophic cultivation was studied. An ATEX compliant cultivation system was developed and used to cultivate *C. necator* on a gram scale. We note that ATEX directives are EU directives describing the minimum safety requirements for workplaces and equipment used in explosive atmospheres. Dissolved oxygen concentration (DO) is generally considered the most critical parameter in the autotrophic cultivation of HOBs [6,20]. Here, we compared different oxygen supply strategies: a constant oxygen supply adjusted to the oxygen need of the inoculum, a stepwise increased oxygen supply guided by the biomass formation over time, and a finely tuned oxygen supply guided by an implemented O₂ dipping probe measuring the DO concentration. Our results pave the way towards a broader use of efficient, microbial CO₂ assimilation.

2. Materials and Methods

2.1. Chemicals, Enzymatic Assays and Strains

The tryptic soy broth (TSB, CASO Buillon, X938.2) was from Carl Roth (Karlsruhe, Germany). The kanamycin sulfate (≥ 750 I.U./mg, T832.1), ampicillin sodium salt ($\geq 97\%$, K029.5), chloramphenicol ($\geq 98.5\%$, 3886.1), geneticin disulfate (Bio-Science grade, 2039.2), and erythromycin ($\geq 98.0\%$, 4166.1) were from Carl Roth. The tetracycline ($\geq 98.0\%$, 87128) was from Fluka (Vienna, Austria) and poly-(*R*)-3-hydroxybuttersäure (quality level 200, 363502) from Sigma-Aldrich (Vienna, Austria). Other chemicals were from Sigma-Aldrich/Fluka or Carl Roth and were of the highest purity available. An enzymatic assay for ammonium (K-AMIAR) was obtained from Megazyme International (Wicklow, Ireland). The strain *C. necator* H16 DSM 428 (aka ATCC 17699, NCIB 10442) was from DSMZ, Deutsche Sammlung für Mikroorganismen und Zellkulturen.

2.2. Growth Media

The TSB media was prepared with 30 g/L TSB supplemented and 50 mg/L kanamycin sulfate, if not mentioned otherwise (note that no additional C-source was added to TSB media). The mineral media (MM) was prepared as described by Atlić et al. [21] (Table 1) with small modifications. Kanamycin sulfate (end concentration 50 mg/L) was added to part 1 prior to autoclaving. Parts 1 to 5 were autoclaved separately, and part 6 was sterile filtered (0.2 μ m). Parts were combined prior to cultivation. For media with B12, 0.01 to

10 mg/L B12 (sterile filtered) was added to the media. In chemolithotrophic cultivations, 2 g/L fructose were added. For agar plates, mineral media with 20 g/L agar-agar and 10 g/L fructose was used.

Table 1. Mineral media (MM) component list.

Substance	g/L	Part
KH ₂ PO ₄	1.5	1
Na ₂ HPO ₄ ·2H ₂ O	4.5	
(NH ₄) ₂ SO ₄	1.5	2
MgSO ₄ ·7H ₂ O	0.2	
NH ₄ Fe(III) citrate	0.05	3
CaCl ₂ ·2H ₂ O	0.02	
Tungsten solution	1 mL	4
Fructose	20	5
Trace element solution	1 mL	6
Tungsten solution		
Na ₂ WO ₄ ·2H ₂ O	0.06	
Trace element solution		
H ₃ BO ₃	0.6	
CoCl ₂ ·6H ₂ O	0.4	
ZnSO ₄ ·7H ₂ O	0.2	
MnCl ₂ ·4H ₂ O	0.06	
NaMoO ₄ ·2H ₂ O	0.06	
NiCl ₂ ·6H ₂ O	0.4	
CuSO ₄ ·7H ₂ O	0.02	

2.3. Heterotrophic Cultivations

For precultures, 300 mL baffled flasks (50 mL TSB or MM with fructose) were inoculated from agar plates and incubated at 30 °C and 110 rpm (Rotary shaker CERTOMAT BS-1) for 24 h. Main cultures (300 mL baffled flasks, 50 mL TSB media, or MM with fructose) were inoculated with 1 mL of preculture to start optical densities 600 nm (OD₆₀₀) of ~0.2 and incubated at 30 °C and 110 rpm for 2 days, unless otherwise stated.

2.3.1. Antibiotic Resistances

TSB main cultures (300 mL baffled flasks) were used to study antibiotic resistances. The media was supplemented with six antibiotics, each applied at three different concentrations: kanamycin (50; 25; 10 mg/L), ampicillin (115; 58; 23 mg/L), chloramphenicol (34; 17; 6.8 mg/L), gentamicin (50; 25; 10 mg/L), tetracycline (50; 25; 10 mg/L), and erythromycin (30; 15; 6 mg/L). All antibiotics were sterile filtered (0.2 µm) and added to the autoclaved media. Cultures without antibiotics served as reference. The OD₆₀₀ was measured after 48 h. Experiments were done in duplicates.

2.3.2. Comparison of TSB and MM

Precultures and main cultures were prepared with the respective media in 300 mL baffled flasks (50 mL TSB or MM with fructose). Experiments were done in duplicates.

2.3.3. Effect of Cultivation Temperature on Growth

Precultures were cultivated in 300 mL baffled flasks with 50 mL MM and incubated at 30 °C and 110 rpm for 24 h. Main cultures were either cultivated in 1 L baffled shaken flasks

(with a magnetic bar of 70 × 10 mm, 250 mL of MM) or in a 1 L DURAN® GLS 80 wide-neck threaded glass bottle with a magnetic anchor stirrer (from DWK Life Sciences purchased at Roth, Germany) (950 mL MM). Mixing was accomplished by stirring at 400 rpm on magnetic stirrers. Main cultures were inoculated to OD₆₀₀ of ~0.2. Cultures in 1 L baffled flasks were stirred at room temperature (22–24 °C) and 30 °C. The DURAN® GLS 80 bottle was stirred at room temperature. The OD₆₀₀ was measured over time. Experiments were done in duplicates.

2.3.4. Determination of Optical Density (OD₆₀₀) and Cell Dry Mass (CDM)

The wavelength for optical cell density measurements was set to 600 nm according to wavelength scans of pure TSB and MM media (Figure S1 in the Supplementary Information). Cell dry mass (CDM) was determined gravimetrically. Note that there was no differentiation between microbial biomass and stored polyhydroxybutyrate. The correlation factor of g_{CDM}/OD_{600} was 0.246 with a R² of 0.965 (Figure S2 in the Supplementary Information).

2.4. Preservation of *C. necator* H16

For short-term storage of up to 1 month, cells were maintained on TSB or minimal medium agar plates at 4 °C. For long-term storage, cryoservation solutions containing glycerol, trehalose, and DMSO were tested. Stock solutions of glycerol, trehalose, and DMSO were mixed with the cell suspension (overnight cultures in TSB media) to end concentrations of 17%, 25%, and 33% glycerol, 0.8 M trehalose, 17% glycerol + 0.6 M trehalose, or 50% DMSO. Cryoservation stocks (2 mL free-standing cryogenic vials, with outer thread from Carl Roth) were frozen in liquid N₂ and stored at –80 °C. Every second month, 300 mL baffled flasks with 50 mL TSB media were inoculated with 75 µL cells from cryoservation stocks. After 24 h of cultivation, the OD₆₀₀ was measured.

2.5. Chemolithotrophic Cultivation (*Oxyhydrogen Cultivation*)

Explosion safety to ensure personal and technical safety was considered according to Austrian and European standards (ATEX directive RL 1999/92/EG and RL 2014/34/EU). In Figure 1, a detailed scheme of the ex-safe cultivation set-up is displayed. Gas lines for the mixed substrate gas, the interior of the bioreactor, and the off-gas line were defined as ex-zone 0 (the area in which an explosive atmosphere is present continuously or for long periods). The remaining interior of the room and fume hood was defined as ex-zone 2 (no ex-zone 1 was defined due to strong ventilation by the fume hood, see below).

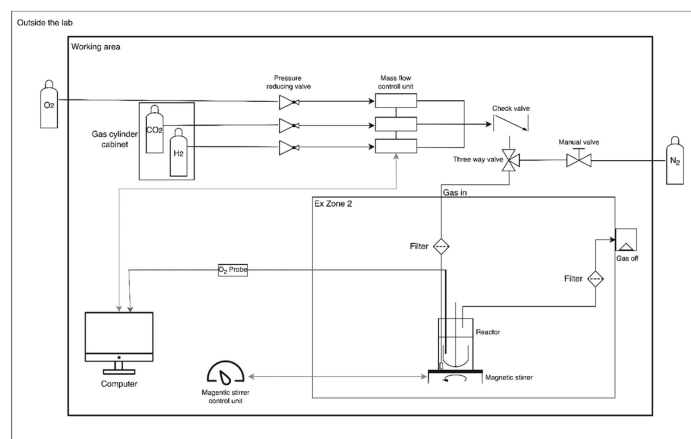


Figure 1. Scheme of gas cultivation setup. Flow diagram of installations and cultivation equipment. (Open-source program diagrams.net © 2005–2021 JGraph Ltd. was used for figure preparation).

2.5.1. Installations and Equipment

The room had an antistatic floor and a pressure relief flap (40 × 40 cm). The room was equipped with two gas cylinder cabinets with pressure-reducing valves (O₂ and H₂ separated, cylinder cabinet for H₂ ventilated with 60 m³/h), gas lines and gas mass flow controllers for CO₂, H₂, O₂ (MFCs; red-y smart controller from Vögtling Instruments GmbH, Switzerland), and an additional gas line for the inert gas N₂. Gas flow rates of CO₂, H₂, and O₂ were adjusted online by the respective MFCs using the get red-y software (from BURDE•CO GmbH, Vienna, Austria). A RF 53 series check valve (Wittgas Gastechnik GmbH & Co KG, Witten, Germany) was installed directly after the gas mixer. The N₂ was connected to the substrate gas line by a three-way valve to enable purging of the bioreactor prior to sampling. All gas cultivations were done under explosion-safe conditions in an ex-safe fume hood (559 m³/h; Secuflow from Waldner, Germany, Wangen, for use in zone 1 II2G/Gb according to ATEX directive RL 1999/92/EG). The fume hood had an H₂ sensor coupled to an automatic 2/2-way magnetic valve (Tescom Europe Selnsdorf, Germany). Experimenters wore safety glasses, antistatic lab coats, antistatic shoes, and a portable gas detector (MSA Multi-Gaswarngerät Altair 4XR, Schloffer Arbeitsschutz GmbH, Hart bei Graz, Austria).

The gas cultivation setup is displayed in Figure 2. The substrate gas passed H₂-tight, autoclavable, polyvinylidene fluoride filters (filter #12.32.5K 99.99% removal of 0.1 micron particles, stainless steel housing #SS117.201 purchased at BURDE•CO) prior and subsequent to the cultivation vessel. Off-gas was drained into the fume hood exhaust air. As the cultivation vessel, a stirred 1000 mL DURAN[®] GLS 80 wide-neck threaded glass bottle was used. A stirrer reactor cap GLS 80 with a magnetic anchor stirrer was attached (from DWK Life Sciences purchased at Roth, Germany). A magnetic stirrer atexMIXdrive (2 mag AG, Munich, Germany) ensured explosion-proof stirring. The substrate gas mixture was supplied through a 6 mm steel tube connected to a 5 mm silicon tube ending in a PTFE frit (product code 01018-22707, Agilent Technologies Österreich GmbH, Vienna, Austria). Online monitoring of dissolved oxygen (DO) was established using an oxygen-dipping probe DP-PSt3 from PreSens GmbH, Regensburg, Germany. The oxygen-dipping probe consisted of a polymer optical fiber (coated with an oxygen-sensitive foil at the end), covered in a high-grade steel tube (35 cm) to facilitate fitting of the probe into the reactor. The steel tube was connected to an equipotential socket in the hood. Read-out electronics were outside of the ventilated hood (facilitated by the 2.8 m fiber-optical cable). No ignition sources were in the ventilated hood. The outlet for the off-gas was a steel pipe connected to a gas-tight, flexible tube.

2.5.2. Determination of the Volumetric Oxygen Transfer Coefficient (k_{La})

The k_{La} of the bioreactor was determined with the “static gassing-out” method [22]. The DO concentration was measured with the O₂-dipping probe in MM without cells (see also Figures S3 and S4 in the Supplementary Information). First, the media was gassed with O₂ for 30 min. The subsequently measured DO value represented the maximum amount of O₂, referred to as O* and 100% oxygen saturation. (The read-out of the dipping probe was % oxygen saturation.) Next, the media was degassed with N₂ for 30 min. Then, the O₂ gas flow was set to 100, 200, and 400 mL/min at 340 rpm stirrer speed. The increasing DO concentration was measured over time and recorded (as % oxygen saturation).

The k_{La} was determined using the integrated form of Equation (1).

$$\frac{dDO}{dt} = k_{La}(O^* - DO) \text{ integration} \rightarrow \ln(O^* - DO) = -k_{La} t \quad (1)$$

The response time of the O₂-dipping probe (t_{90}) was <40 s as specified by the manufacturer.



Figure 2. Explosion-proof bioreactor setup consisting of a 1 L DURAN® bottle with a magnetic anchor stirrer on a magnetic stirrer plate. Gas substrate is supplied by a steel tube with a PTFE frit at the end.

2.5.3. Calculation of Henry’s Law Constant H^{CP} and Oxygen Transfer Theory

O^* is proportional to the partial pressure p_{O_2} of O_2 in the gas mixture and the Henry’s law constant H^{CP} ($1.3 \cdot 10^{-3}$ M/atm at 25 °C in pure water) as a proportionality factor (Equation (2)).

$$O^* = H^{\text{CP}} p_{\text{O}_2} \quad (2)$$

In a typical cultivation medium, O_2 solubility is considered 5 to 25% lower than in water. Here, we calculated a H^{CP} of 1.18 mM/atm (according to Schumpe et al. [23]).

The actual concentration of the DO in the bioreactor is a dynamic value constituted by the oxygen transfer rate (OTR) and the oxygen uptake rate (OUR). The OTR depends on O^* (equilibrium O_2 concentration), the liquid phase mass transfer coefficient k_L and the specific exchange area a (gas–liquid interfacial area per unit of fluid) (Equation (1)).

The OUR depends on the biomass concentration X and the specific O_2 consumption rate q_{O_2} (Equation (3)).

$$\frac{dn}{dt} = q_{\text{O}_2} X = \text{OUR} \quad (3)$$

In a quasi-steady state, the OTR equals the OUR (Equation (4)).

$$\text{OTR} = \text{OUR} \quad (4)$$

2.5.4. Gas Cultivations

Gas cultivations were done either with constant gas flow rates (low and high p_{O_2}), with manually increased oxygen supply guided by the biomass concentration (biomass concentrations measured from samples taken over time) or with manually increased oxygen supply guided by the DO concentration (in situ measurement of DO concentration using the O_2 -dipping probe, referred to cultivations 1 to 4 in the text).

For all chemolithotrophic experiments, precultures were cultivated heterotrophically in MM with fructose overnight (end $\text{OD}_{600} \sim 9$). For the main culture, the autoclaved 1 L DURAN® bottle was filled with 950 mL MM and 50 mL preculture under sterile conditions (start $\text{OD}_{600} < 1.4$). If used, the O_2 -dipping probe was chemically sterilized with ethanol 70% (v/v) and fit into the reactor. The filled bioreactor was connected to the substrate gas and off-gas lines. Tightness of connections was checked with the purge gas N_2 and a

leak detector spray. H₂, CO₂, and O₂ gas flows (NmL/min) were adjusted online. Total flow rates of 100 to 400 NmL/min were used. Two to three samples were taken per day. Prior (and subsequent) to opening the cultivation vessel, the substrate gas was switched off and the whole system was purged with N₂ for 5 min. Samples were taken with a syringe with a 120 mm needle. Gas supply was summarized in Table 2. Note that individual partial pressures (and hence dissolved gas concentrations) do not depend on total gas flows according to Dalton’s law.

Table 2. Partial pressures of H₂, CO₂, O₂, and total gas flows in individual gas cultivations.

Cultivation	PH ₂ :PCO ₂ :PO ₂	Total Flow Rate (NmL/min)	Comment
Constant low O ₂ supply	Constant 90:8:2	400	-
Constant high O ₂ supply	Constant 85:10:5	100	-
Stepwise increase of O ₂ guided by the biomass	start 90:8:2 end 80:8:12	400	Intermittent gas compositions are in the Supplementary Data file.
Stepwise increase of O ₂ guided by the DO probe			
Cultivation 1	start 85:10:2 end 71:7:21	start 97 end 140	All intermittent gas compositions are in the Supplementary Data file.
Cultivation 2	start 85:10:2 end 80:8:12	start 97 end 250	
Cultivation 3	start 85:10:2 end 81:8:11	start 97 end 250	
Cultivation 4	start 85:10:2 end 81:8:11	start 97 end 250	

In experiments with increased oxygen supply, the O₂ flow rate was manually adjusted using the get red-y software of gas mass flow controllers.

2.5.5. Sample Analysis with PHB Quantification

All samples were taken in duplicates. OD₆₀₀ of samples was measured in quadruplicates. 5 mL of cell culture was transferred into 15 mL Sarstedt tubes and centrifuged for 30 min. The supernatants and pellets were stored at −20 °C for further analysis. The ammonium concentrations were determined in the supernatant with the Megazyme assay kit K-AMIAR according to the supplier’s manual. PHB content was analysed on GC. Samples were prepared according to Atlič et al. [21] with small modifications. Pellets were lyophilized and suspended in at least 10-fold pure EtOH (96%) (for small pellets, more EtOH was used to achieve sufficient mixing). Samples were stirred on a magnetic stirrer for 1 day at room temperature. After centrifugation for 30 min at 5000 rpm, the supernatant was discarded. Samples were dried at 70 °C for 2 h, transferred into glass vials with 30-fold chloroform (*w/w*) and stirred for 1 day at room temperature. PHB was precipitated by the addition of ice cold EtOH (96%) and filtered through a Whatman filter paper (HK26.1, Carl Roth). The filter cake was dried overnight at room temperature under the fume hood. Dry PHB was scratched from the weighted filter paper and transferred into new glass tubes. At this step, 11 ± 2% of purified PHB was lost. 2 mL of esterification mixture (94.9 mL MeOH, 5 mL H₂SO₄, 0.108 mL hexanoic acid, and 2 mL of chloroform) were added, and the glass tubes were tightly closed. For transesterification, the samples were shaken at 95 °C in a water bath for 3.5 h. Tubes were cooled down to room temperature and 1 mL of NaHCO₃ (10% *w/v*) was added. Samples were vortexed for 5 min. After 15 to 30 min, the organic phase was transferred into a GC vial using a glass Pasteur pipette and closed tightly. PHB content was analysed on GC using a ZB-5 column (Phenomenex, 30 m length, 0.32 mm inner

diameter and 0.25 μm film thickness) and an FID detector according to Juengert et al. [24]. As reference, a standard curve with pure PHB was prepared (R^2 0.9999). Standards were treated like the isolated PHB. PHB content in percent per CDM was calculated. The $11 \pm 2\%$ weight loss of PHB during transfer from the filter paper into the glass vial was considered. During the transfer from the Sarsted tube into the glass vial, less than 1% of cell dry matter was lost and not considered for PHB calculations.

3. Results

3.1. Heterotrophic cultivation

3.1.1. Antibiotic Resistances of *C. necator* H16

Addition of antibiotics is the most common strategy in the cultivation of microorganisms to prevent growth of contaminating microbes. Here, we decided to add an antibiotic as the bioreactor had to be opened for sampling. A range of strain-dependent resistances to antibiotics have been reported for native *C. necator* strains [25–27]. Fast adaptivity of *C. necator* might also lead to altered antibiotic resistances [28,29]. Therefore, resistances of the used *C. necator* H16 strain against six antibiotics generally used in the cultivation of microorganisms were probed, and the effect on culture density quantified after 2 days of cultivation (Figure 3). The addition of 115, 57.5, or 23 mg/L ampicillin and 50, 25, or 10 mg/L kanamycin or geneticin did not significantly affect growth. The presence of 34, 17, or 6.8 mg/L chloramphenicol slightly reduced OD_{600} after 2 days. OD_{600} of ~70% compared to the reference culture was obtained at the highest chloramphenicol concentration. The addition of 30, 15, or 6 mg/L erythromycin diminished culture densities to between 8 and 32% as compared to the reference. The presence of 50, 25, or 10 mg/L tetracycline totally inhibited growth. Kanamycin was chosen as the most suitable antibiotic in all further experiments for the following reasons: it does not inhibit the growth of *C. necator* at a concentration of 50 mg/L, it can be added to the medium prior to autoclaving, and it is used as a standard antibiotic in biotechnological labs.

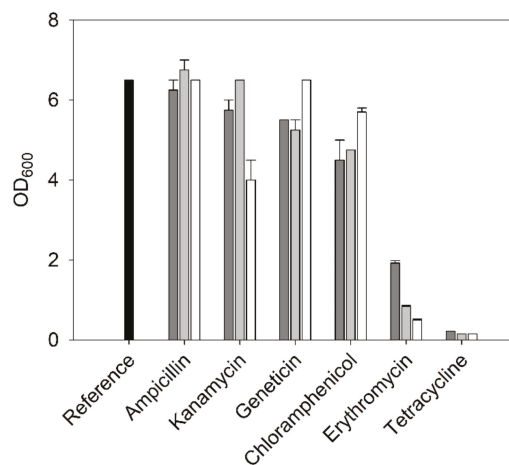


Figure 3. OD_{600} values of *C. necator* cultures in the presence of six antibiotics. Dark gray bars illustrate lowest, light gray bars medium, and white bars highest antibiotics concentrations. Black bar refers to reference cultures without antibiotics. (2 days of cultivation in TSB at 30°C).

3.1.2. Heterotrophic Cultivations Using Mineral Media (MM)

Chemolithotrophic growth facilitates formation of biomass from CO_2 , H_2 , O_2 , and ammonium salts without a further carbon source. Here, we used a mineral medium reported for heterotrophic cultivations of *C. necator* described by Atlić et al. [21] supplemented with tungsten (recommended by Cramm, [30]) (Table 1). As a C-source, 20 g/L fructose was

added to the mineral medium. After 2 days of cultivation, OD_{600} values reached 19 and 11 with MM and TSB media, respectively. Motivated by a notion in Pohlmann et al. [31] that *C. necator* H16 is not able to produce vitamin B₁₂ (though it can bypass vitamin B₁₂-dependent reactions), we added 0.01 to 10 mg/L of vitamin B₁₂ to the MM with fructose. No effect of B₁₂ supplementation was seen (Figure 4).

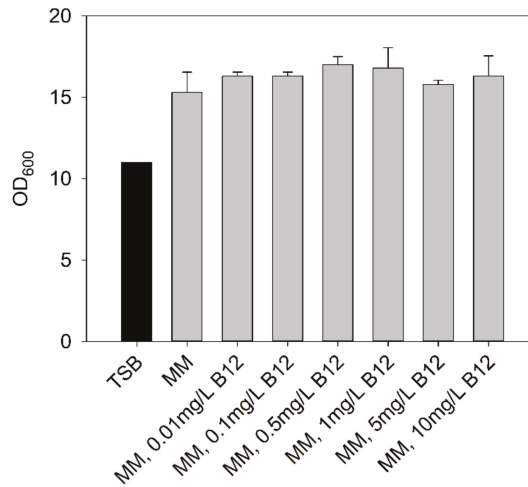


Figure 4. OD_{600} values of *C. necator* cultures in MM supplemented with B₁₂. Black bar refers to cultures in TSB. (2 days of cultivation at 30 °C.)

3.1.3. Effect of Temperature on Growth Rate

Temperature control in an explosive atmosphere adds complexity to the cultivation system. Autotrophic cultivation at room temperature without temperature control was hence aimed at. Comparison of microbial growth in heterotrophic cultivations performed at room temperature (22–24 °C) and at 30 °C was used to study the effect of lower temperature on microbial growth. The maximum growth rate in MM was 1.4 times higher at 30 °C as compared to room temperature ($\mu_{\max,30^\circ\text{C}} 0.17 \pm 0.01$ versus $\mu_{\max,RT} 0.13 \pm 0.01 \text{ h}^{-1}$). After 3 days, all cultures had reached optical densities (OD_{600}) of 37 (for growth curves and rates, see Supplementary Information Table S1 and Figure S5).

3.1.4. Strain Maintenance

Setup of a reproducible oxyhydrogen cultivation system for *C. necator* requires stable short-term and long-term strain maintenance. Cultures grown on agar plates were storable at 4 °C for at least 4 weeks. Low recultivability from cryostocks kept at –80 °C with glycerol as cryoprotectant was observed. Therefore, recultivability of cells from cryostocks containing different cryoprotectants was tested. Recultivability after 1 to 11 months of cells stored in glycerol (33%, 25%, 17%), trehalose (0.8 M), DMSO (50% *v/v*), and glycerol and trehalose (17% glycerol, 0.6 M trehalose) is displayed in Figure 5. After 11 months, the highest recultivability in 0.8 M trehalose and 0.6 M trehalose with 17% glycerol was experienced.

3.2. Chemolithotrophic Cultivation

C. necator, as a HOB, forms biomass from CO₂ as a carbon source using H₂ as an electron donor and O₂ as an electron acceptor. Reported substrate gas mixtures indicate ratios of 7:1:1, 7:2:1, or 65:25:10 (reviewed in 10). The two most evident problems connected with substrate gas mixtures containing H₂ and O₂ are their high explosion capability and low water solubility. Gases must be dissolved in the aqueous medium to be available for the cells, and the parameters of interest are therefore the dissolved gas concentrations [32].

The O_2 concentration is of particular importance as growth of *C. necator* is reported to be inhibited at $DO > 11.5$ mg/L [33]. Previous results have indicated an extended lag phase when the DO was > 3 mg/L. The highest values for μ (and q_{O_2}) were observed with DO concentrations of ~ 2.6 mg/L [20].

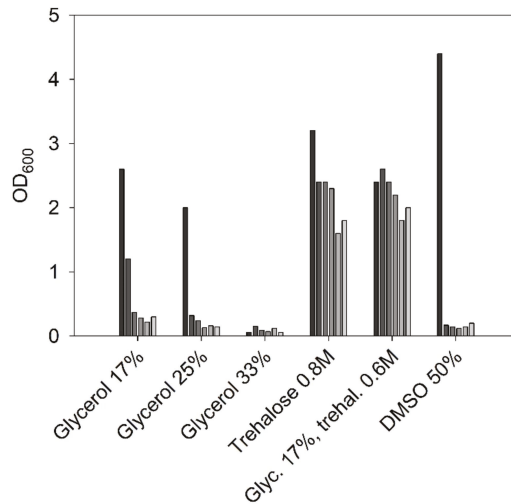


Figure 5. OD_{600} values of *C. necator* cultures inoculated directly with cells from cryoservation stocks. Bars indicate recultivability after 1, 3, 5, 7, 9, 11 months (starting with black bars, descending grey intensities). (1 day of cultivation in TSB at $30^\circ C$).

The actual concentration of DO in the bioreactor is a dynamic value constituted by the oxygen transfer rate (OTR) and the oxygen uptake rate (OUR). An increasing biomass concentration at constant O_2 supply leads to a decrease in the dissolved O_2 concentration over time. For optimal growth, the O_2 supply (OTR) needs to be increased to compensate for the increased biomass concentration and increased OUR.

3.2.1. Chemolithotrophic Cultivations with Constant Gas Flow

The substrate gas mixture was composed of $H_2:CO_2:O_2$ in a ratio of 90:8:2 (total flow rate 400 NmL/min) and kept constant over the entire cultivation time. Gas supply was switched on after transfer of media (MM with 2 g/L fructose) and heterotrophically grown inoculum into the stirred bioreactor. A μ_{max} of 0.008 h⁻¹ and a final OD_{600} of 5 (1.2 g_{CDM}/L) were obtained after 158 h (Figure 6) (μ_{max} determination Supplementary Information Figure S6). The applied gas composition resulted in a p_{O_2} of 0.0175 atm. According to Equation (2), with a H^c_p of 1.18 mM/atm, the O^* was calculated to be 0.7 mg/L. The linear shape of the growth curve indicated O_2 limitation. However, gas cultivations starting with a relatively high O^* of ~ 1.6 mg/L did not lead to chemolithotrophic growth of *C. necator* after 50 h (Supplementary Information Figure S7).

3.2.2. Chemolithotrophic Cultivations with Stepwise Increased Gas Flow Guided by the Biomass Concentration

Samples were taken over time, OD_{600} values were measured, and the biomass concentrations were calculated. An average q_{O_2} of 1.4 mmol g_{CDM}⁻¹h⁻¹ was anticipated because this value was at the lower end of q_{O_2} values reported by Lu and Yu (2019) [15] and ensured low DO concentrations (below toxic levels) in autotrophic cultivations. OURs were calculated by multiplying current biomass concentrations (obtained from samples) with the average q_{O_2} (Equation (3)). Assuming a quasi-steady state, the OTR equalled OUR (Equation (4)). The DO was set to zero which simplifies OTR to the product of $k_L a$ and

O^* (Equation (1)). The required O^* was adjusted by the partial pressure of O_2 mass flow (Equation (2); note that the O_2 gas flow was reduced at 150 h as biomass formation rate decreased.) After 163 h, a final biomass concentration of $6.5 \text{ g}_{\text{CDM}}/\text{L}$ (OD_{600} 26.5) and a μ_{max} of 0.055 h^{-1} were obtained (Figure 6, μ_{max} determination Supplementary Information Figure S6).

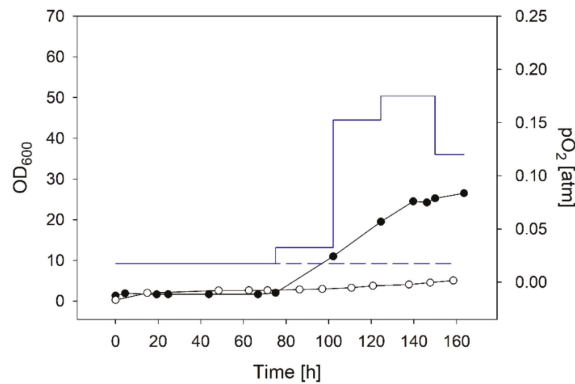


Figure 6. Time curves of gas cultivations with constant gas flow and stepwise increased p_{O_2} . Circles indicate OD_{600} values, blue lines p_{O_2} (constant gas flow white circles and dashed line; stepwise increased p_{O_2} black circles and full line).

3.2.3. O_2 Supply Guided by an O_2 Sensor

Four gas cultivations with manually stepwise increased O_2 mass flows guided by the DO concentration were performed (Figure 7A; all data of gas cultivations are summarized in the Supplementary Data). The starting substrate gas mixture in all four cultivations was composed of $H_2:CO_2:O_2$ in a ratio of 85:10:2 (total flow rate $97 \text{ NmL}/\text{min}$, p_{O_2} of 0.02 atm). The O_2 consumption (seen as a drop in DO concentration) gave information about the consumption of C sources. The fructose was used up in the first $\sim 20 \text{ h}$ (e.g., in cultivation 4, the fructose was used up after 19 h at a cell dry mass of $0.76 \text{ g}_{\text{CDM}}/\text{L}$; data not displayed). During a lag phase in O_2 consumption of $\sim 24 \text{ h}$, the cellular metabolism switched from heterotrophy to lithotrophy. CO_2 assimilation was marked by a drop in the DO. From then, the O_2 supply was manually increased over time but kept below $\sim 1.1 \text{ mg}/\text{L}$. The p_{O_2} was 0.12 to 0.15 atm after 50 to 60 h in all four cultivations at constant H_2 and CO_2 flow rates. After $\sim 60 \text{ h}$ of cultivation, biomass concentrations were $\sim 2 \text{ g}_{\text{CDM}}/\text{L}$ and the ammonium was depleted (Figure 7B,C, Supplementary Information Figure S8). Growth curves indicated remarkable reproducibility and a mean maximal growth rate of $0.088 \pm 0.010 \text{ h}^{-1}$ (Figure 7A; determination of μ_{max} Supplementary Information Figure S6). After 60 to 70 h of fermentation, growth rates decelerated. In cultivation 1, the H_2 and CO_2 flow rates were kept constant (Figure 7A and Supplementary Information Figure S8). In cultivations 2 (Supplementary Information Figure S8), 3 (Figure 7B), and 4 (Figure 7C), H_2 and CO_2 were increased to 200 and $20 \text{ NmL}/\text{min}$ after 60 h to avoid H_2 limitations. In all cultivations, the O_2 flow rates were further increased after 60 h , but due to increasing DO concentrations, the O_2 flow rates were back regulated again. Increases of H_2 and CO_2 gas flow rates to 200 and $20 \text{ NmL}/\text{min}$, respectively, had no significant effect on final cell dry mass (cultivations 3 and 4 in Figure 7B,C, cultivation 2 in Supplementary Information Figure S8). Final OD_{600} values of 53.5 ± 1.5 were obtained after $\sim 150 \text{ h}$. The OD_{600} correlated to a mean cell dry mass of $13.1 \pm 0.4 \text{ g}_{\text{CDM}}/\text{L}$ (mean value and deviation from the mean for gas cultivations 3 and 4). The PHB content in biomass samples was determined for cultivation 4. The PHB content started at 9% and steadily increased after the ammonium was depleted to 80% after 90 h (Figure 7C). The PHB content was constant ($\pm 1.6\%$) until the end of the gas cultivation.

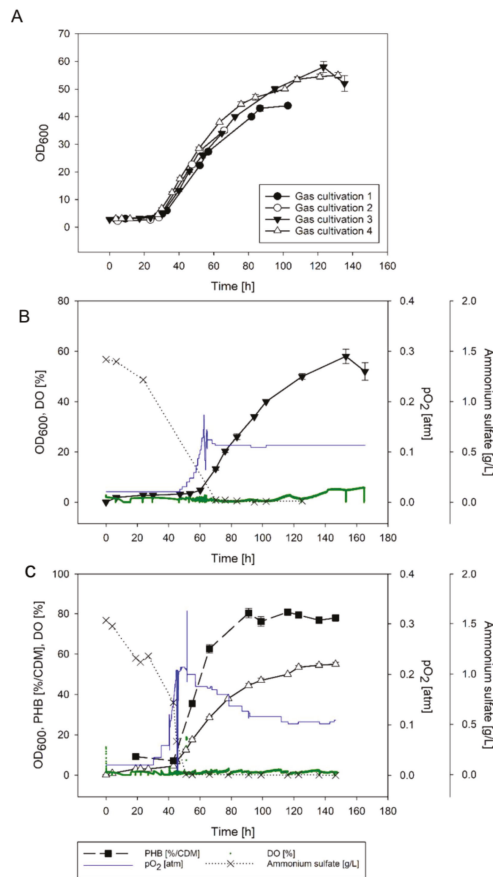


Figure 7. Time curves of gas cultivations with manual DO control using a dipping probe. Panel (A) indicates OD₆₀₀ values over time of all four gas cultivations (starting points of gas cultivations in panel A were normalized to the start of CO₂ assimilation). Panels (B,C) indicate gas cultivations 3 and 4, respectively (triangles indicate OD₆₀₀ values from Figure 7A, pO₂ blue line, DO in % (100% corresponds to full saturation with pure oxygen) illustrated as green dots, ammonium sulfate [g/L] black crosses, PHB in % per CDM black squares). All data of gas cultivations are summarized in the Supplementary Data and the Supporting Information Figure S8.

3.2.4. pH Development in Chemolithotrophic Cultivations

In classic bioreactor systems, pH is monitored and computer-controlled by the addition of acid and base. pH-stat systems are equipped with a pH-probe and two peristaltic pumps for the correcting liquids. A value of 6.8 was previously used in heterotrophic and chemolithotrophic cultivations of *C. necator* (e.g., [21,34]). In the present chemolithotrophic cultivations, no correction of pH was required. The used MM media with fructose had a starting pH value of 6.8. pH values between 6.8 and 7.0 were measured in all samples taken from chemolithotrophic cultures.

4. Discussion

4.1. Chemolithotrophic Cultivation

Gas compositions vary widely in reported gas cultivations [12,15,35–38]. The decisive parameters are, however, the concentrations of gases that are dissolved in the aqueous phase and available for the cells [32]. CO₂ dissolves easily in water (~1.4 g/L) but H₂ and

O₂ have low solubilities of 1.6 and 40 mg/L, respectively (data for pure water at 25 °C and p_i of 1). In the presented experiments, we used excesses of H₂ and CO₂ under O₂-limiting conditions. The DO concentration is one of the most crucial parameters in the cultivation of *C. necator* [6,20,33,34]. The window of operation for DO concentrations in gas cultivations is relatively small. Due to the rapid growth of HOBs, their oxygen consumption increases rapidly over time. A constant oxygen supply adjusted to the oxygen need of the inoculum lead to fast oxygen limitation and a final OD₆₀₀ of 5 (Figure 6). A stepwise increase guided by the biomass concentration (sampling offline) resulted in a final OD₆₀₀ of 26.5, and a stepwise increase guided by the in situ measured DO resulted in a doubled OD₆₀₀ of 56.5. Our findings are briefly summarized in Table 3.

Table 3. Comparison of different O₂ supply strategies. Effect of starting pO₂ and pCO₂ supply method.

Cultivation	pO ₂ (atm)	μ _{max} (h ⁻¹)	Final OD ₆₀₀	Comment
Constant low O ₂ supply	constant at 0.02	0.008	5.0	Figure 6
Constant high O ₂ supply	constant at 0.05	not determined	1.3	Figure S7
Stepwise increase of O ₂ guided by the biomass	start 0.02 end 0.12	0.055	26.5	Figure 6; biomass conc. measured offline, O ₂ supply increased manually
Stepwise increase of O ₂ guided by the DO probe (cultivations 3, 4) *	start 0.02 ± 0.00 highest 0.19 ± 0.02 end 0.11 ± 0.00	0.095 ± 0.01	53.5 ± 1.5	Figure 7; DO measured online, O ₂ supply increased manually

* Note that cultivations 1 and 2 stopped at earlier timepoints and were hence not used for the summary. O₂ supply is critical from a biological and technological point of view.

4.1.1. Biological Limitations of DO Concentration

The organism *C. necator* displays an upper limit of 30 kPa (DO < ~11.5 mg/L) for O₂ when grown under chemolithotrophic conditions [33]. Previous results have indicated an extended lag phase when the DO was >3 mg/L. The highest values for μ (and q_{O₂}) were observed with DO concentrations of ~2.6 mg/L. At DO concentrations of <1.9 and ≥7 mg/L, significantly lower values for μ (and q_{O₂}) were reported [20]. Under an O₂ concentration of 3.2 kPa (DO < ~1.1 mg/L) *C. necator* grows under O₂ limitation [33]. From a Monod model of an O₂-limited chemolithotrophic growth curve, an affinity constant for O₂ (K_{O₂}) of 0.12 mg/L was determined at the cellular level (at 31 °C, [39]). Under autotrophic conditions and O₂ limitation, *C. necator* was reported to efficiently accumulate PHB while the formation of protein almost ceased [37]. O₂ sensitivity of *C. necator* was attributed back to O₂ inhibition of the involved [NiFe]-hydrogenases. Most [NiFe]-hydrogenases indicates inhibition by O₂. The β-proteobacterium *C. necator* H16, however, hosts three relatively O₂-tolerant [NiFe]-hydrogenases involved in energy conversion and H₂ sensing under aerobic conditions [40].

4.1.2. Technological Limitations in Oxyhydrogen Cultivations

O₂ transfer from gas into aqueous media is a well-known limitation in cultivation technology due to the low solubility of O₂. In the cultivation of HOBs, the presence of H₂ massively complicates processing. O₂ and H₂ form explosive gas mixtures with lower and upper explosion limits of 4 and 95.2% H₂, respectively. The situation is aggravated by the very low ignition energy of 0.016 mJ and is therefore considered to be extremely ignitable. O₂ concentrations of <6.9 or 5% were previously used as a strategy to maintain the O₂ concentration below the lower explosion limit (6.9% v/v in the gas mixture) [10,35]. To promote a sufficiently high DO concentration, extremely high k_{1a}-values [35] or increased pressure were used [10]. Alternatively, electrodes were introduced into the cultivation medium and, by applying sufficient potentials, water was in situ split into O₂ and H₂. In non-separated systems, both gaseous substrates were produced in situ and were constantly available [41–44]. The complete replacement of the terminal acceptor O₂ by nitrate in autohydrogenotrophic growth of *C. necator* led to low μ of 0.02 h⁻¹ [45].

In the present study, an alternative strategy was used: A simplified bioreactor without ignition sources facilitated the safe usage of gas mixtures that were within the explosion range of H₂ and O₂. The reactor was driven by an explosion-proof magnetic stirrer, the fume hood was grounded, the lab had an antistatic floor, and scientists were equipped during the gas cultivation with antistatic lab coats and shoes. With the chosen equipment, biomass concentrations of ~13.1 g_{CDM}/L were reproducibly obtained despite low k_{La} -values of 20 to 33 h⁻¹. The high biomass concentrations were achieved through tight regulation of the DO. While the DO was kept largely below 1.1 mg/L (Figure 7B,C and Supplementary Information Figure S8), the actual p_i of O₂ was stepwise increased from 0.02 to 0.14 in chemolithotrophic cultivations. Specific growth rates of maximally 0.09 h⁻¹ were obtained. The very high μ_{max} of 0.42 h⁻¹ (and final biomass concentration of 91 g_{CDM}/L) reported by Tanaka et al. [35] is explicable by the high k_{La} value of 2970 h⁻¹. The study by Tanaka et al. from 1995 is considered the gold standard in autotrophic cultivation. However, complying with modern safety regulations, an oxygen concentration in the gas mixture of <6.9% O₂ is not considered safe in the published setup for two main reasons: First, back then, a lower explosion limit of 6.9% O₂ in oxyhydrogen mixtures was stated, whereas currently, a lower explosion limit of 4.8% O₂ is stated [35,46]. Second, Tanaka et al. used either a bioreactor described as mini-jar fermenter (200 mL) from Able Co., Ltd., Tokyo, Japan [38] or a glass jar fermenter (2 L). From the description and schemes given by them, we assume that both bioreactors had a brush motor on top. Brush motors are considered possible ignition sources, and thus the oxygen concentration in the gas mixture would need to be lower than 4.8% (in the best case several fold lower) to comply with current safety regulations.

4.1.3. Online Analytics in Chemolithotrophic Cultivations

The use of sensor probes in cultivation broths that are constantly gassed by an explosive gas mixture is delicate. Dipping probes certified according to ATEX-RL 2014/34 for ex-zone 0 (Ex II 1G (Ga) IIC T3-T6 required when working with H₂ and O₂) are expensive and rare. There are several O₂ sensors certified for ex-zone 0 but, to the best of our knowledge, none for CO₂ or H₂. Here, we used an O₂-dipping probe based on an optical fiber. As safety measures, the read-out electronics were placed outside of the ventilated hood (safety distance of 2 m). The dipping probe was connected to an equipotential bonding to avoid discharges of static electricity. The dipping probe itself was completely sealed in a steal tube and directly connected to the optical fiber cable. No ignition source was inside the fermenter or the fume hood. The optical dipping probe connected to an equipotential bonding was, to the best of our knowledge, a safe method to measure the DO. High reproducibility of conditions in chemolithotrophic cultivations led to nearly superimposable growth curves illustrated in Figure 7A.

4.2. Polyhydroxyalkanoate from CO₂

Bioplastic from CO₂ has the dual advantages of CO₂ assimilation and reduction of plastic products from fossil resources. *C. necator* has been previously proven to accumulate 78 to 82% poly-D-3-hydroxybutyrate (PHB) in two-stage cultivations at cell densities between 60 and 70 g_{CDM}/L. The strategy followed a two-stage heterotrophic-chemolithotrophic cultivation using fructose as a carbon source in the heterotrophic phase [7]. The highest production rates of PHB were experienced under oxygen limitation in chemolithotrophic cultures. In heterotrophic cultures, ammonium limitation turned out as the best regime to force PHB accumulation (reviewed in [33]). Similarly, higher PHB contents (up to 82%) under oxygen limitation compared to nitrogen limitation were reported by Mozumder et al. [6]. More recently, *C. necator* was genetically engineered for the biosynthesis of copolymer polyhydroxyalkanoates from CO₂ without organic precursor molecules [8,9,47]. In the present study (data from cultivation 4), we have observed that after 19 h, the fructose was depleted at a cell dry mass of 0.76g_{CDM}/L. The cell dry mass at this timepoint had a PHB content of 9% (equal to 0.068 g_{PHB}/L). At the end of cultivation 4, 13.1 g_{CDM}/L

containing 10.2 g_{PHB}/L was obtained. We therefore assume that >98% of the obtained PHB was formed from CO₂.

4.3. Development of the Mineral Medium for Autotrophic Cultivations

TSB is usually used for fast-growing microbes and as standard media for *C. necator*. The complex media contains 20 g/L peptone as organic N- and C-source. The cells would prefer peptone over CO₂ if both were available in autotrophic cultivations. Therefore, we used TSB for heterotrophic cultivations and mineral media for all autotrophic cultivations and selected heterotrophic cultivations.

The highest biomass concentrations in chemolithotrophic cultivations of *C. necator* were previously reached by Tanaka et al. [35]. However, the use of tap water for preparation masked actual concentrations of trace elements. Repaske and Mayers [12] developed one of the first MMs for chemolithotrophic cultivation of *C. necator* and reported a final biomass concentration of 25 g_{CDM}/L. Growth limitations were attributed to depletions in ammonium and trace elements. The media was further adapted in heterotrophic cultivations [48,49] and chemolithotrophic cultivations [50,51]. However, the media used by Lu and Yu [50] led to precipitations upon pH-adjustment. Therefore, we used a medium reported for heterotrophic cultivations of *C. necator* described by Atlić et al. [21] and added tungsten solution (recommended by Cramm [30]) (Table 1). The addition of B12 was motivated by a notion in Pohlmann et al. that *C. necator* H16 is not able to produce vitamin B12. Supplementation with B12 did not improve growth, stressing that the bacteria can bypass vitamin B12-dependent reactions [31].

We decided to add an antibiotic to suppress the growth of contaminating bacteria. Antibiotic resistances of *C. necator* strains are strain-dependent and are of special interest for genetic engineering strategies. The number of antibiotic resistances found in *C. necator* previously complicated the design of plasmids. Wild-type *C. necator* H16 is known to indicate a natural resistance towards the aminoglycoside antibiotic kanamycin applied at concentrations of ≤50 mg/L. Therefore, kanamycin concentrations from 200 to 350 mg/L were previously used for the selection of kanamycin resistance plasmids in *C. necator* H16 [25,51–55]. The presence of tetracycline (tetracycline antibiotic) inhibited the growth of *C. necator* in all used concentrations, also seen for *C. necator* strains isolated from soil [25]. Lacking tetracycline resistance in *C. necator* wild-type strains was exploited for the stabilization of tetracycline-resistance plasmids [53,54].

5. Conclusions

CO₂ assimilation into biodegradable polymers is an attractive strategy to bind and recycle CO₂, reduce the production of conventional plastic products, and spare fossil resources. The most prominent HOB, *C. necator*, can accumulate polyhydroxybutyrate from CO₂ to levels of up to 82% of the cell's dry weight ([6,7] this work). The metabolism of *C. necator* is tractable by genetic engineering, and alternative products (including polyhydroxyalkanoates with altered properties) made from CO₂ become available [8,10,26,34,56]. One serious bottleneck in the development of new processes based on HOBs is the complexity of oxyhydrogen cultivations with respect to safety aspects, gas mass transfer, and analytics of gaseous substrates dissolved in the aqueous phase. An easy method to test, optimize, and compare growth conditions and strains (engineered and native) was presented. The method built upon an explosion-proof setup for the continuous supply of H₂, CO₂, and O₂. Biomasses of 13.1 g_{CDM}/L with 79% PHB (with approximately 98% of the obtained PHB formed from CO₂) were easily obtainable with DO as a single controlled parameter. No feeding of salts and no pH and temperature control was required.

Supplementary Materials: The following supporting information can be downloaded at: <https://www.mdpi.com/article/10.3390/bioengineering9050204/s1>, Figure S1: Wavelength scan of water, TSB and mineral media; Figure S2: Correlation of OD₆₀₀ to CDM in *C. necator* cultures; Figure S3: Gassing and bubble formation in the stirred 1000 mL DURAN®GLS 80 bioreactor; Figure S4: *k_La* values for the 1 L DURAN®GLS 80 bioreactor at gas flows of 100, 200 and 400 mL at 340 rpm;

Figure S5: Heterotrophic cultivations at room temperature (22–24 °C, orange dots) and at 30 °C (grey dots) in 1 L baffled flasks (magnetic bar, stirring at 400 rpm); Figure S6: Determination of maximal growth rates from chemoautotrophic cultivations depicted in Figures 6 and 7 (main part); Figure S7: Time curve of a gas fermentation with constant high O₂ supply. OD₆₀₀ values (black circles) and pO₂ (blue line); Figure S8: Time curves of gas cultivations 1 (panel A) and 2 (panel B) with manual DO control using a dipping probe (supplementing Figure 7A main part); Table S1: Maximal growth rates (μ_{\max} h⁻¹) obtained at room temperature or 30 °C.

Author Contributions: V.L. designed, performed, and analyzed chemolithotrophic cultivations, interpreted the data, and was involved in manuscript preparation. R.K. conceptualized the study, contributed to the design of experiments, interpreted the data, and drafted the manuscript. All authors have read and agreed to the published version of the manuscript.

Funding: The COMET center ACIB: Next Generation Bioproduction was funded by BMK, BMDW, SFG, Standortagentur Tirol, Government of Lower Austria und Vienna Business Agency in the framework of COMET—Competence Centers for Excellent Technologies. The COMET-Funding Program was managed by the Austrian Research Promotion Agency FFG (funding number 872161). Role of funding: employment of VL, financing cultivation equipment (portable).

Institutional Review Board Statement: Not applicable.

Informed Consent Statement: Not applicable.

Data Availability Statement: The data presented in this study is available in [Supplementary data.xls] file.

Acknowledgments: We thank the Faculty of Technical Chemistry, Chemical and Process Engineering, Biotechnology, Graz University of Technology for providing gas cultivation equipment (non-portable). We thank Vanja Subotic, Markus Raiber, Markus Sackl, and Heinz Strauß from the Institute of Thermal Engineering, Graz University of Technology for discussions and practical support in H₂ handling and bioreactor setup. We thank Zdenek Petrasek for help with the oxygen-dipping probe.

Conflicts of Interest: The authors declare no conflict of interest.

References

- Jajesniak, P.; Ali, H.E.M.O.; Wong, T.S. Carbon dioxide capture and utilization using biological systems: Opportunities and challenges. *J. Bioprocess. Biotech.* **2014**, *4*, 155. [[CrossRef](#)]
- Olajire, A.A. Valorization of greenhouse carbon dioxide emissions into value-added products by catalytic processes. *J. CO₂ Util.* **2013**, *3–4*, 74–92. [[CrossRef](#)]
- Pander, B.; Mortimer, Z.; Woods, C.; McGregor, C.; Dempster, A.; Thomas, L.; Maliepaard, J.; Mansfield, R.; Rowe, P.; Krabben, P. Hydrogen oxidising bacteria for production of single-cell protein and other food and feed ingredients. *Eng. Biol.* **2020**, *4*, 21–24. [[CrossRef](#)]
- Sillman, J.; Nygren, L.; Kahiluoto, H.; Ruuskanen, V.; Tamminen, A.; Bajamundi, C.; Nappa, M.; Wuokko, M.; Lindh, T.; Vainikka, P.; et al. Bacterial protein for food and feed generated via renewable energy and direct air capture of CO₂: Can it reduce land and water use? *Glob. Food Sec.* **2019**, *22*, 25–32. [[CrossRef](#)]
- Lu, Y.; Yu, J. Comparison analysis on the energy efficiencies and biomass yields in microbial CO₂ fixation. *Proc. Biochem.* **2017**, *62*, 151–160. [[CrossRef](#)]
- Mozumder, S.I.; Garcia-Gonzalez, L.; DeWever, H.; Volcke, E.I.P. Poly(3-hydroxybutyrate) (PHB) production from CO₂: Model development and process optimization. *Biochem. Eng. J.* **2015**, *98*, 107–116. [[CrossRef](#)]
- Taga, N.; Tanaka, K.; Ishizaki, A. Effects of rheological change by addition of carboxymethylcellulose in culture media of an air-lift fermentor on poly-D-3-hydroxybutyric acid productivity in autotrophic culture of hydrogen-oxidizing bacterium, *Alcaligenes eutrophus*. *Biotechnol. Bioeng.* **1997**, *53*, 529–533. [[CrossRef](#)]
- Nangle, S.N.; Ziesack, M.; Buckley, S.; Trivedi, D.; Lohe, D.M.; Nocera, D.G.; Silver, P.A. Valorization of CO₂ through lithoautotrophic production of sustainable chemicals in *Cupriavidus necator*. *Metab. Eng.* **2020**, *62*, 207–220. [[CrossRef](#)]
- Tanaka, K.; Yoshida, K.; Orita, I.; Fukui, T. Biosynthesis of poly(3-hydroxybutyrate-co-3-hydroxyhexanoate) from CO₂ by a recombinant *Cupriavidus necator*. *Bioengineering* **2021**, *8*, 179. [[CrossRef](#)]
- Garrigues, L.; Maignien, L.; Lombard, E.; Singh, J.; Guillouet, S.E. Isopropanol production from carbon dioxide in *Cupriavidus necator* in a pressurized bioreactor. *N. Biotechnol.* **2020**, *56*, 16–20. [[CrossRef](#)]
- Müller, J.; MacEachran, D.; Burd, H.; Sathitsuksanoh, N.; Bi, C.; Yeh, Y.-C.; Lee, T.S.; Hillson, N.J.; Chhabra, S.R.; Singer, S.W.; et al. Engineering of *Ralstonia eutropha* H16 for autotrophic and heterotrophic production of methyl ketones. *Appl. Environ. Microbiol.* **2013**, *79*, 4433–4439. [[CrossRef](#)] [[PubMed](#)]

12. Repaske, R.; Mayer, R. Dense autotrophic cultures of *Alcaligenes eutrophus*. *Appl. Environ. Microbiol.* **1976**, *32*, 592–597. [[CrossRef](#)] [[PubMed](#)]
13. Bommareddy, R.R.; Wang, Y.; Pearcy, N.; Hayes, M.; Lester, E.; Minton, N.P.; Conradie, A.V. A sustainable chemicals manufacturing paradigm using CO₂ and renewable H₂. *iScience* **2020**, *23*, 101218. [[CrossRef](#)] [[PubMed](#)]
14. Lai, Y.H.; Lan, C.-W. Enhanced polyhydroxybutyrate production through incorporation of a hydrogen fuel cell and electro-fermentation system. *Int. J. Hydrog. Energy* **2021**, *46*, 16787–16800. [[CrossRef](#)]
15. Lu, Y.; Yu, J. Biomass yield, reversal respiratory quotient, stoichiometric equations and bioenergetics. *Biochem. Eng. J.* **2019**, *152*, 107369. [[CrossRef](#)]
16. Milker, S.; Sydow, A.; Torres-Monroy, I.; Jach, G.; Faust, F.; Kranz, L.; Tkatschuk, L.; Holtmann, D. Gram-scale production of the sesquiterpene α -humulene with *Cupriavidus necator*. *Biotechnol. Bioeng.* **2021**, *118*, 2694–2702. [[CrossRef](#)]
17. Nyyssölä, A.; Ojala, L.S.; Wuokko, M.; Peddinti, G.; Tamminen, A.; Tsitko, I.; Nordlund, E.; Lienemann, M. Production of endotoxin-free microbial biomass for food applications by gas fermentation of gram-positive H₂-oxidizing bacteria. *ACS Food Sci. Technol.* **2021**, *1*, 470–479. [[CrossRef](#)]
18. Lütte, S.; Pohlmann, A.; Zaychikov, E.; Schwartz, E.; Becher, J.R.; Heumann, H.; Friedrich, B. Autotrophic production of stable-isotope-labeled arginine in *Ralstonia eutropha* strain H16. *Appl. Environ. Microbiol.* **2012**, *78*, 7884–7890. [[CrossRef](#)]
19. Assil-Companioni, L.; Schmidt, S.; Heidinger, P.; Schwab, H.; Kourist, R. Hydrogen-driven cofactor regeneration for stereoselective whole-cell C=C bond reduction in *Cupriavidus necator*. *ChemSusChem* **2019**, *12*, 2361–2365. [[CrossRef](#)]
20. Sonnleitner, B.; Heinze, E.; Brauneck, G.; Lafferty, R.M. Formal kinetics of poly- β -hydroxybutyric acid (PHB) production in *Alcaligenes eutrophus* H 16 and *Mycoplana rubra* R 14 with respect to the dissolved oxygen tension in ammonium-limited batch cultures. *Eur. J. Appl. Microbiol. Biotechnol.* **1979**, *7*, 1–10. [[CrossRef](#)]
21. Atlić, A.; Koller, M.; Scherzer, D.; Kutschera, C.; Grillo-Fernandes, E.; Horvat, P.; Chiellini, E.; Brauneck, G. Continuous production of poly([R]-3-hydroxybutyrate) by *Cupriavidus necator* in a multistage bioreactor cascade. *Appl. Microbiol. Biotechnol.* **2011**, *91*, 295–304. [[CrossRef](#)] [[PubMed](#)]
22. Riet, K.V. Review of measuring methods and results in nonviscous gas-liquid mass transfer in stirred vessel. *Ind. Eng. Chem. Process Des. Dev.* **1979**, *18*, 357–364. [[CrossRef](#)]
23. Schumpe, A.; Adler, I.; Deckwer, W.D. Solubility of oxygen in electrolyte solutions. *Biotechnol. Bioeng.* **1978**, *20*, 145–150. [[CrossRef](#)]
24. Juengert, J.R.; Bresan, S.; Jendrossek, D. Determination of polyhydroxybutyrate content in *Ralstonia eutropha* using gas chromatography and Nile red staining. *Bio Protoc.* **2018**, *8*, e2748. [[CrossRef](#)] [[PubMed](#)]
25. Florentino, L.A.; Jaramillo, P.M.D.; Silva, K.; da Silva, J.S.; de Oliveira, S.M.; de Souza Moreira, F.M. Physiological and symbiotic diversity of *Cupriavidus necator* strains isolated from nodules of Leguminosae species. *Sci. Agric.* **2012**, *69*, 247–258. [[CrossRef](#)]
26. Gruber, S.; Schwendenwein, D.; Magomedov, Z.; Thaler, E.; Hagen, J.; Schwab, H.; Heidinger, P. Design of inducible expression vectors for improved protein production in *Ralstonia eutropha* H16 derived host strains. *J. Biotechnol.* **2016**, *235*, 92–99. [[CrossRef](#)]
27. Massip, C.; Coullaud-Gamel, M.; Gaudru, C.; Amoureux, L.; Doleans-Jordheim, A.; Hery-Arnaud, G.; Marchandin, H.; Oswald, E.; Segonds, C.; Guet-Revillet, H. In vitro activity of 20 antibiotics against *Cupriavidus* clinical strains. *J. Antimicrob. Chemother.* **2020**, *75*, 1654–1658. [[CrossRef](#)]
28. González-Villanueva, M.; Galaiya, H.; Staniland, P.; Staniland, J.; Savilli, I.; Wong, T.S.; Tee, K.L. Adaptive laboratory evolution of *Cupriavidus necator* H16 for carbon co-utilization with glycerol. *Int. J. Mol. Sci.* **2019**, *20*, 5737. [[CrossRef](#)]
29. Novackova, I.; Kucera, D.; Porizka, J.; Pernicova, I.; Sedlacek, P.; Koller, M.; Kovalcik, A.; Obruca, S. Adaptation of *Cupriavidus necator* to levulinic acid for enhanced production of P(3HB-co-3HV) copolyesters. *Biochem. Eng. J.* **2019**, *151*, 107350. [[CrossRef](#)]
30. Cramm, R. Genomic view of energy metabolism in *Ralstonia eutropha* H16. *J. Mol. Microbiol. Biotechnol.* **2009**, *16*, 38–52. [[CrossRef](#)]
31. Pohlmann, A.; Fricke, W.; Reinecke, F.; Kusian, B.; Liesegang, H.; Cramm, R.; Eitinger, T.; Ewering, C.; Pötter, M.; Schwartz, E.; et al. Genome sequence of the bioplastic-producing “Knallgas” bacterium *Ralstonia eutropha* H16. *Nat. Biotechnol.* **2006**, *24*, 1257–1262. [[CrossRef](#)] [[PubMed](#)]
32. Foster, J.F.; Litchfield, J.H. A continuous culture apparatus for the microbial utilization of hydrogen produced by electrolysis of water in closed-cycle space systems. *Biotechnol. Bioeng.* **1964**, *6*, 441–456. [[CrossRef](#)]
33. Ishizaki, A.; Tanaka, K.; Taga, N. Microbial production of poly-D-3-hydroxybutyrate from CO₂. *Appl. Microbiol. Biotechnol.* **2001**, *57*, 6–12. [[CrossRef](#)] [[PubMed](#)]
34. Garcia-Gonzalez, L.; Mozumder, S.I.; Dubreuil, M.; Volcke, E.I.P.; DeWever, H. Sustainable autotrophic production of polyhydroxybutyrate (PHB) from CO₂ using a two-stage cultivation system. *Catal. Today* **2015**, *257*, 237–245. [[CrossRef](#)]
35. Tanaka, K.; Ishizaki, A.; Kanamaru, T.; Kawano, T. Production of poly(D-3-hydroxybutyrate) from CO₂, H₂, and O₂ by high cell density autotrophic cultivation of *Alcaligenes eutrophus*. *Biotechnol. Bioeng.* **1995**, *45*, 268–275. [[CrossRef](#)]
36. Crépin, L.; Lombard, E.; Guillouet, S.E. Metabolic engineering of *Cupriavidus necator* for heterotrophic and autotrophic alka(e)ne production. *Metab. Eng.* **2016**, *37*, 92–101. [[CrossRef](#)]
37. Ishizaki, A.; Tanaka, K. Production of poly- β -hydroxybutyric acid from carbon dioxide by *Alcaligenes eutrophus* ATCC 17697^T. *J. Ferment. Bioeng.* **1991**, *71*, 254–257. [[CrossRef](#)]
38. Ishizaki, A.; Tanaka, K. Batch culture of *Alcaligenes eutrophus* ATCC 17697 T using recycled gas closed circuit culture system. *J. Ferment. Bioeng.* **1990**, *69*, 170–174. [[CrossRef](#)]
39. Siegel, R.S.; Ollis, D.F. Kinetics of growth of the hydrogen-oxidizing bacterium *Alcaligenes eutrophus* (ATCC 17707) in chemostat culture. *Biotechnol. Bioeng.* **1984**, *26*, 764–770. [[CrossRef](#)]

40. Burgdorf, T.; Lenz, O.; Buhrke, T.; van der Linden, E.; Jones, A.K.; Albracht, S.P.J.; Friedrich, B. [NiFe]-Hydrogenases of *Ralstonia eutropha* H16: Modular enzymes for oxygen-tolerant biological hydrogen oxidation. *J. Mol. Microbiol.* **2005**, *10*, 181–196. [[CrossRef](#)]
41. Li, Z.; Li, G.; Chen, X.; Xia, Z.; Yao, J.; Yang, B.; Lei, L.; Hou, Y. Water splitting–biosynthetic hybrid system for CO₂ conversion using nickel nanoparticles embedded in N-doped carbon nanotubes. *ChemSuschem* **2018**, *11*, 2382–2387. [[CrossRef](#)] [[PubMed](#)]
42. Krieg, T.; Sydow, A.; Faust, S.; Huth, I.; Holtmann, D. CO₂ to terpenes: Autotrophic and electroautotrophic α -humulene production with *Cupriavidus necator*. *Angew. Chem. Int. Ed.* **2017**, *57*, 1879–1882. [[CrossRef](#)] [[PubMed](#)]
43. Schuster, E.; Schlegel, H.G. Chemolithotrophic growth of *Hydrogenomonas* H16 using electrolytic production of hydrogen and oxygen in a chemostat. *Arch. Mikrobiol.* **1967**, *58*, 380–409. [[CrossRef](#)] [[PubMed](#)]
44. Torella, J.P.; Gagliardi, C.J.; Chen, J.S.; Bediako, D.K.; Colon, B.; Way, J.C.; Silver, P.A.; Nocera, D.G. Efficient solar-to-fuels production from a hybrid microbial–water-splitting catalyst system. *Proc. Natl. Acad. Sci. USA* **2015**, *112*, 2337–2342. [[CrossRef](#)] [[PubMed](#)]
45. Tiemeyer, A.; Link, H.; Weuster-Botz, D. Kinetic studies on autohydrogenotrophic growth of *Ralstonia eutropha* with nitrate as terminal electron acceptor. *Appl. Microbiol. Biotechnol.* **2007**, *76*, 75–81. [[CrossRef](#)]
46. Schröder, V. Explosionsgrenzen von Wasserstoff und Wasserstoff/Methan-Gemischen. In *Forschungsbericht Nr. 253*; Bundesanstalt für Materialforschung und -prüfung: Berlin, Germany, 2003; pp. 1–40. ISSN 0938-5533.
47. Miyahara, Y.; Yamamoto, M.; Thorbecke, R.; Mizuno, S.; Tsuge, T. Autotrophic biosynthesis of polyhydroxyalkanoate by *Ralstonia eutropha* from non-combustible gas mixture with low hydrogen content. *Biotechnol. Lett.* **2020**, *42*, 1655–1662. [[CrossRef](#)]
48. Aragao, G.M.F.; Lindley, N.D.; Uribealbarrea, J.L.; Pareilleux, A. Maintaining a controlled residual growth capacity increases the production of polyhydroxyalkanoate copolymers by *Alcaligenes eutrophus*. *Biotechnol. Lett.* **1996**, *18*, 937–942. [[CrossRef](#)]
49. Ramsay, B.A.; Lomaliza, K.; Chavarie, C.; Dubé, B.; Bataille, P.; Ramsay, J.A. Production of poly-(β -hydroxybutyric-co- β -hydroxyvaleric) acids. *Appl. Environ. Microbiol.* **1990**, *56*, 2093–2098. [[CrossRef](#)]
50. Lu, Y.; Yu, J. Gas mass transfer with microbial CO₂ fixation and poly(3-hydroxybutyrate) synthesis in a packed bed bioreactor. *Biochem. Eng. J.* **2017**, *122*, 13–21. [[CrossRef](#)]
51. Grousseau, E.; Lu, J.; Gorret, N.; Guillouet, S.E.; Sinskey, A.J. Isopropanol production with engineered *Cupriavidus necator* as bioproduction platform. *Appl. Microbiol. Biotechnol.* **2014**, *98*, 4277–4290. [[CrossRef](#)]
52. Boy, C.; Lesage, J.; Alfenore, S.; Gorret, N.; Guillouet, S.E. Plasmid expression level heterogeneity monitoring via heterologous eGFP production at the single-cell level in *Cupriavidus necator*. *Appl. Microbiol. Biotechnol.* **2020**, *104*, 5899–5914. [[CrossRef](#)] [[PubMed](#)]
53. Claassens, N.J.; Bordanaba-Florit, G.; Cotton, C.A.; De Maria, A.; Finger-Bou, M.; Friedeheim, L.; Giner-Laguarda, N.; Munar-Palmer, M.; Newell, W.; Scarinci, G.; et al. Replacing the Calvin cycle with the reductive glycine pathway in *Cupriavidus necator*. *Metab. Eng.* **2020**, *62*, 30–41. [[CrossRef](#)] [[PubMed](#)]
54. Sydow, A.; Pannek, A.; Krieg, T.; Huth, I.; Guillouet, S.E.; Holtmann, D. Expanding the genetic tool box for *Cupriavidus necator* by a stabilized L-rhamnose inducible plasmid system. *J. Biotechnol.* **2017**, *263*, 1–10. [[CrossRef](#)] [[PubMed](#)]
55. Wahl, A.; Schuth, N.; Pfeiffer, D.; Nussberger, S.; Jendrossek, D. PHB granules are attached to the nucleoid via PhaM in *Ralstonia eutropha*. *BMC Microbiol.* **2012**, *12*, 262. [[CrossRef](#)] [[PubMed](#)]
56. Windhorst, C.; Gescher, J. Efficient biochemical production of acetoin from carbon dioxide using *Cupriavidus necator* H16. *Biotechnol. Biofuels* **2019**, *12*, 163. [[CrossRef](#)] [[PubMed](#)]

Article

Biosynthesis of Poly(3-hydroxybutyrate-co-3-hydroxyhexanoate) from CO₂ by a Recombinant *Cupriavidus necator*

Kenji Tanaka ^{1,*}, Kazumasa Yoshida ¹, Izumi Orita ² and Toshiaki Fukui ²

¹ Department of Biological and Environmental Chemistry, Faculty of Humanity-Oriented Science and Engineering, Kindai University, Fukuoka 820-8555, Japan; 2133950002m@ed.fuk.kindai.ac.jp

² School of Life Science and Technology, Tokyo Institute of Technology, Yokohama 226-8501, Japan; iorita@bio.titech.ac.jp (I.O.); tfukui@bio.titech.ac.jp (T.F.)

* Correspondence: tanaka@fuk.kindai.ac.jp

Abstract: The copolyester of 3-hydroxybutyrate (3HB) and 3-hydroxyhexanoate (3HHx), PHBHHx, is one of the most practical kind of bacterial polyhydroxyalkanoates due to its high flexibility and marine biodegradability. PHBHHx is usually produced from vegetable oils or fatty acids through β -oxidation, whereas biosynthesis from sugars has been achieved by recombinant strains of hydrogen-oxidizing bacterium *Cupriavidus necator*. This study investigated the biosynthesis of PHBHHx from CO₂ as the sole carbon source by engineered *C. necator* strains. The recombinant strains capable of synthesizing PHBHHx from fructose were cultivated in a flask using complete mineral medium and a substrate gas mixture (H₂/O₂/CO₂ = 8:1:1). The results of GC and ¹H NMR analyses indicated that the recombinants of *C. necator* synthesized PHBHHx from CO₂ with high cellular content. When 1.0 g/L (NH₄)₂SO₄ was used as a nitrogen source, the 3HHx composition of PHBHHx in the strain MF01ΔB1/pBBP-ccr_{Me}J4a-emd was 47.7 ± 6.2 mol%. Further investigation demonstrated that the PHA composition can be regulated by using (*R*)-enoyl-CoA hydratase (PhaJ) with different substrate specificity. The composition of 3HHx in PHBHHx was controlled to about 11 mol%, suitable for practical applications, and high cellular content was kept in the strains transformed with pBBP-ccr_{Me}J_{Ac}-emd harboring short-chain-length-specific PhaJ.

Keywords: biodegradable plastic; PHBHHx; CO₂; *Cupriavidus necator*; hydrogen-oxidizing bacterium

Citation: Tanaka, K.; Yoshida, K.; Orita, I.; Fukui, T. Biosynthesis of Poly(3-hydroxybutyrate-co-3-hydroxyhexanoate) from CO₂ by a Recombinant *Cupriavidus necator*. *Bioengineering* **2021**, *8*, 179. <https://doi.org/10.3390/bioengineering8110179>

Academic Editor: Martin Koller

Received: 29 September 2021

Accepted: 4 November 2021

Published: 7 November 2021

Publisher's Note: MDPI stays neutral with regard to jurisdictional claims in published maps and institutional affiliations.



Copyright: © 2021 by the authors. Licensee MDPI, Basel, Switzerland. This article is an open access article distributed under the terms and conditions of the Creative Commons Attribution (CC BY) license (<https://creativecommons.org/licenses/by/4.0/>).

1. Introduction

Plastic wastes reaching marine environments fragmented into microplastics, but they cannot be biologically assimilated, and, unfortunately, many biodegradable plastics are also not decomposed in marine environments [1]. In contrast, bacterial polyhydroxyalkanoates (PHAs) have been shown to be biodegraded in marine environments [2]; thus, they are attracted as eco-friendly biodegradable plastics that are alternatives to petrochemical-derived plastics. More than 150 kinds of hydroxyalkanoate units have been identified as constituents of PHAs [3]. *Cupriavidus necator* H16 is the bacterium that has been used the most and studied for the biosynthesis of PHAs because it has a high ability to accumulate PHAs. *C. necator* can assimilate many types of organic compounds in heterotrophic culture conditions to accumulate PHAs within the cells.

A homopolyester of (*R*)-3-hydroxybutyric acid, P(3HB) is well known and the best studied PHA. However, P(3HB) is stiff and has relatively poor in impact strength [4]. Melting and thermal degradation temperatures of P(3HB) are 170–180 °C and 180–190 °C, respectively, resulting in very narrow processability windows caused by low resistance to thermal degradation [5]. A copolyester of 3HB and (*R*)-3-hydroxyhexanoic acid (3HHx), P(3HB-co-3HHx) [PHBHHx] is very attractive as it has high flexibility and properties that are similar to several common petroleum-based plastics. Additionally, PHBHHx shows excellent biodegradability even in seawater [6]. Since PHBHHx was firstly found in *Aeromonas caviae* FA440 in 1993, many researchers have been studied for PHBHHx and

its microbial synthesis. Kaneka Corporation (Tokyo, Japan) has constructed a PHBHx (Kaneka Biodegradable Polymer Green Planet™ (PHBH™)) plant of which its production capacity was around 5000 tons per annum in 2019 [7]. It is known that 3HHx composition is an important factor for thermal and mechanical properties of PHBHx. The melting temperature (T_m) of PHBHx decreases according to the increase in 3HHx composition [5]. For instance, T_m of P(3HB-co-10mol% 3HHx) synthesized from olive oil by *A. caviae* is 136 °C, and break elongation of the copolymer is about 400% [8]. Unfortunately, the accumulation of PHBHx in *A. caviae* is not so high, as the polymer content in the cells is within the range from 20 to 30 wt% [9]. Meanwhile, biosynthesis of many PHA copolymers usually requires the addition of a precursor compound structurally related to a second unit other than 3HB. Such precursor compounds are usually expensive and often toxic. The efficient production of useful PHA copolymers from inexpensive feedstocks is an urgent task needed for wider use in society [10]. Genetic modification of PHA-producing microbes allows us to modify or construct pathways for biosynthesis of desired PHAs from various kinds of carbon sources. There have been many reports for the biosynthesis of 3HB-based copolymers from plant oils or fatty acids, where (R)-3HA-CoAs are provided via β -oxidation of acyl-moieties. We have further constructed *C. necator* H16-based strains capable of synthesizing PHBHx from structurally unrelated sugars [11]. An artificial pathway was designed for the generation of (R)-3HHx-CoA from sugar-derived acetyl-CoA molecules and installed into *C. necator*. One of the strains, MF01 Δ B1/pBPP-ccr_{Me}J4a-emd, accumulated P(3HB-co-22mol% 3HHx) in the cells with high cellular content on fructose.

C. necator is a facultative hydrogen-oxidizing bacterium that can also grow chemolithoautotrophically by using CO₂ as the sole carbon source and H₂ and O₂ as energy sources. The former name of *C. necator* was *Alcaligenes eutropha*, *Hydrogenomonas eutrophus*, *Wautersia eutropha* and *Ralstonia eutropha*. Hydrogen-oxidizing bacteria are known to glow rapidly with high cell yields on CO₂ owing to their high CO₂-fixation ability, of which its level is the highest among all autotrophic organisms. It is, therefore, beneficial to use hydrogen-oxidizing bacteria for industrial bioprocesses in order to convert CO₂ to new cellular materials [12] as well as “single cell protein,” of which its amino acid profile is similar to high-quality animal protein [13]. *C. necator* is also one of the best suitable species for the production of the marine biodegradable plastic PHAs by using CO₂ as a carbon source. We have already succeeded in the production of P(3HB) from CO₂ by autotrophic high cell density cultivation of *C. necator* and other hydrogen-oxidizing bacteria [14–18].

In this article, we report the biosynthesis of PHBHx from CO₂ by the two engineered strains of *C. necator* H16 and by further modified strains to synthesize PHBHx with 3HHx composition suitable for practical applications, as well as the effects of the introduced genes on the synthesis and composition of the copolymer.

2. Materials and Methods

2.1. Construction of Plasmids and Strains

The bacterial strains and plasmids used in this study are listed in Table 1. The details for the construction of recombinant plasmids and strains were described in our previous report [11–20]. The genetic modifications in *C. necator* H16 (wild type) are summarized as follows. In strain MF01, the short chain length (scl)-specific β -ketothiolase gene *phaA* and PHA synthase gene *phaC* in *pha* operon on chromosome 1 were replaced with *bktB* and *pha*_{CNSDG}, respectively [20]. *bktB*, encoding medium-chain-length (mcl)-specific β -ketothiolase, is originally located at the inherent locus (h16_A1445) on the *C. necator* chromosome, and the second copy was used to replace *phaA* in the *pha* operon. *pha*_{CNSDG} encodes the N149S/D171G double mutant of PHA synthase, possessing broad substrate specificity from C₄ to C₇ derived from *A. caviae* [21]. MF01 Δ B1 was constructed by further deletion of the NADPH-dependent acetoacetyl-CoA reductase gene *phaB1* in strain MF01 [11]. *PhaB1* is the major reductase for the conversion of acetoacetyl-CosA to (R)-3HB-CoA, and *C. necator* has the minor homolog *PhaB3* that partially contributes to P(3HB) biosynthesis. In strain MF01 Δ B1, deletion of *phaB1* was supposed to change metabolic

flux distribution at acetoacetyl-CoA node, resulting in the enhanced formation of crotonyl-CoA via (S)-3HB-CoA [20]. pBPP-*ccr*_{Me}J4a-*emd* [11] has been constructed by inserting *ccr*_{Me} (crotonyl-CoA carboxylase/reductase gene from *Methylorubrum extorquens*), *pha*J4a (mcl-specific (R)-enoyl-CoA hydratase gene from *C. necator* [22]) and *emd*_{Mm} (a codon-optimized gene encoding ethylmalonyl-CoA decarboxylase derived from *Mus musculus*) at the site downstream of the *pha*P1 promoter in the broad-host-range expression vector pBPP [23]. Another plasmid pBPP-*ccr*_{Me}J_{Ac}-*emd* was constructed by replacing *pha*J4a with a scl-specific (R)-enoyl-CoA hydratase gene *pha*J_{Ac} derived from *A. caviae* [20]. Either plasmids were introduced into strains MF01 or MF01ΔB1 by transconjugation using *E. coli* S17-1. These four recombinant strains were tested for the biosynthesis of PHBHx from CO₂ in flask culture under autotrophic conditions.

Table 1. Bacterial strains and plasmids used in this study.

Bacterial Strain or Plasmids	Genotype/Characteristic	References or Sources
<i>C. necator</i>		
H16	Wild type	DSM 428
MF01	H16 derivative, Δ <i>pha</i> C:: <i>pha</i> C _{NSDG} , Δ <i>pha</i> A:: <i>bktB</i>	[19]
MF01ΔB1	MF01 derivative; Δ <i>pha</i> B1	[11]
Plasmids		
pBPP	pBBR1-MCS2 derivative, <i>P</i> _{<i>pha</i>P1} , <i>T</i> _{<i>rrn</i>B}	[23]
pBPP- <i>ccr</i> _{Me} J4a- <i>emd</i>	pBPP derivative, <i>ccr</i> _{Me} , <i>pha</i> J4a, <i>emd</i> _{Mm}	[11]
pBPP- <i>ccr</i> _{Me} J _{Ac} - <i>emd</i>	pBPP derivative, <i>ccr</i> _{Me} , <i>pha</i> J _{Ac} , <i>emd</i> _{Mm}	[20]

2.2. Culture Medium and Condition

A complete mineral salts medium was used for the autotrophic culture of the recombinant strains of *C. necator*. The basic composition of the mineral salts medium was (NH₄)₂SO₄ 0.5–2.0 g, KH₂PO₄ 4.0 g, Na₂HPO₄ 0.8 g, NaHCO₃ 1.0 g, MgSO₄·7H₂O 0.2 g and 1 L distilled water. The pH was adjusted to 7.0. After autoclaving, 1.0 mL of filter-sterilized trace elements solution [22] and 200 μg/mL of kanamycin were added to 1 L of the medium. The composition of the trace elements solution was FeCl₃ 9.7 g, CaCl₂ 7.8 g, CoCl₂·6H₂O 0.218 g, NiCl₂·6H₂O 0.118 g, CrCl₃·6H₂O 0.105 g and CuSO₄·6H₂O 0.156 g per 1 L of 0.1 M HCl. The culture was carried out by using 20 mL of mineral medium in a 300 mL Erlenmeyer flask. The air in the head space within the flask was evacuated by using a vacuum pump after the seed culture was inoculated to the medium in order to set optical density at 600 nm (OD₆₀₀) of the culture broth to 0.1. Then, the substrate gas mixture of the ratio H₂/O₂/CO₂ = 8:1:1 was introduced through a sterile filter. The flask was fitted tightly with a silicon rubber stopper and sealed with adhesive tape (Figure 1). The cells were cultivated at 30 °C, and a reciprocal shaking speed of 170 rpm was used. During the cultivation, the unconsumed substrate gas mixture within the flask was evacuated every 12 h and refilled with new gas mixtures. For each strain and condition, a culture test was carried out in triplicate.

2.3. Analyses

Zero point five milliliter of the culture broth was withdrawn from the flask at every 12 h, and the optical density at a wavelength of 600 nm (OD₆₀₀) was measured to monitor cell growth. In order to determine the concentration of dry cell mass (DCM), the cells were harvested by centrifugation after 120 h of cultivation, and the weight of the cells dried at 105 °C was measured. The PHA contents in the cells and monomer composition were determined by gas chromatography. The dry cells were heated in methanol containing 15% sulfuric acid at 100 °C for 140 min for methanolysis of PHA. Then, the methyl esters of 3HB and 3HHx were separated and quantified by gas chromatography [24].

PHA was extracted by stirring the lyophilized cells in chloroform for five days. Then, cell debris was removed by filtration. The filtrate was concentrated with rotary evaporator, and PHA in the condensed extract was precipitated by adding chilled methanol and

stirred continuously. The purified PHA was dried in a vacuum at room temperature. Ten milligram of the dried sample was dissolved in 0.7 mL of CDCl_3 containing 1% TMS, and the polymer solution was applied to 400 MHz ^1H NMR spectroscopy (Varian 400-MR).

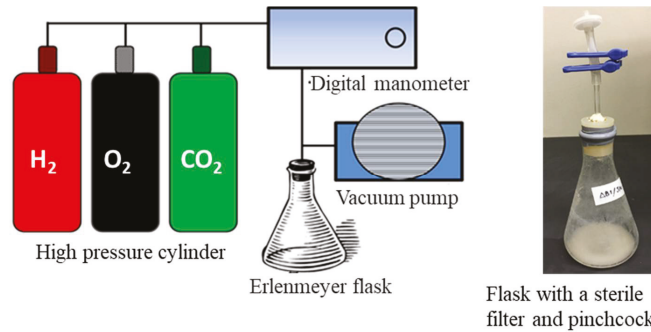


Figure 1. Apparatus for flask culture of *C. necator* in autotrophic condition and supplying substrate gas mixture.

3. Result

3.1. Autotrophic PHA Synthesis by *C. necator* MF01/pBPP-*ccr*_{Me}J4a-*emd* and MF01ΔB1/pBPP-*ccr*_{Me}J4a-*emd*

The results of flask culture of the engineered *C. necator* strains MF01/pBPP-*ccr*_{Me}J4a-*emd* and MF01ΔB1/pBPP-*ccr*_{Me}J4a-*emd* in the autotrophic condition are shown in Table 2. The concentrations of DCM, polymer content in the cells and monomer composition were determined with the samples withdrawn after 120 h of cultivation. It was observed that both recombinant strains vigorously grew and consumed the substrate gasses within the culture flask. When 1.0 g/L $(\text{NH}_4)_2\text{SO}_4$ was used as a nitrogen source in the culture medium, DCM of MF01/pBPP-*ccr*_{Me}J4a-*emd* and MF01ΔB1/pBPP-*ccr*_{Me}J4a-*emd* increased to 12.18 ± 0.40 g/L and 10.65 ± 1.35 g/L, respectively. At every concentration of $(\text{NH}_4)_2\text{SO}_4$, DCM of MF01/pBPP-*ccr*_{Me}J4a-*emd* was higher than that of MF01ΔB1/pBPP-*ccr*_{Me}J4a-*emd*. Contrary to our expectations, DCM in the culture using 2.0 g/L $(\text{NH}_4)_2\text{SO}_4$ was inferior to that using 1.0 g/L $(\text{NH}_4)_2\text{SO}_4$. In the culture using 2.0 g/L $(\text{NH}_4)_2\text{SO}_4$, pH decreased to 4.6, which would inhibit cell growth and PHA accumulation.

Table 2. PHA synthesis by autotrophic flask culture of the engineered *C. necator* strains harboring pBPP-*ccr*_{Me}J4a-*emd*.

Recombinant (Strains/Plasmid Vector)	$(\text{NH}_4)_2\text{SO}_4$ (g/L)	DCM (g/L)	PHBHHx Content (wt%)	Monomer Composition (mol%)	
				3HB	3HHx
MF01/pBPP- <i>ccr</i> _{Me} J4a- <i>emd</i>	0.5	8.52 ± 1.92	85.8 ± 13.2	96.7 ± 1.4	3.3 ± 1.4
MF01/pBPP- <i>ccr</i> _{Me} J4a- <i>emd</i>	1.0	12.18 ± 0.40	64.0 ± 3.4	94.8 ± 1.1	5.3 ± 1.1
MF01/pBPP- <i>ccr</i> _{Me} J4a- <i>emd</i>	2.0	8.01 ± 1.65	37.4 ± 2.4	97.7 ± 0.8	2.4 ± 0.8
MF01ΔB1/pBPP- <i>ccr</i> _{Me} J4a- <i>emd</i>	0.5	4.35 ± 0.78	59.0 ± 16.2	56.5 ± 1.7	43.5 ± 1.7
MF01ΔB1/pBPP- <i>ccr</i> _{Me} J4a- <i>emd</i>	1.0	10.65 ± 1.35	61.7 ± 4.6	52.3 ± 6.2	47.7 ± 6.2
MF01ΔB1/pBPP- <i>ccr</i> _{Me} J4a- <i>emd</i>	2.0	6.99 ± 1.14	21.1 ± 0.5	71.6 ± 1.9	28.5 ± 1.9

All data were obtained after 120 h of cultivation ($n = 3$). The substrate gas mixture ($\text{H}_2/\text{O}_2/\text{CO}_2 = 8:1:1$) in the flask was exchanged every 12 h.

The PHA contents in the recombinant cells and monomer composition determined by GC analysis are also shown in Table 2. It was obvious that these two recombinants synthesized the copolyester of 3HB and 3HHx from CO_2 in all the cultures tested. The 3HHx composition of PHBHHx produced by MF01ΔB1/pBPP-*ccr*_{Me}J4a-*emd* was much higher than that produced by the corresponding MF01 strain. In particular, 3HHx composition of PHBHHx in MF01ΔB1/pBPP-*ccr*_{Me}J4a-*emd* cultured with 1.0 g/L $(\text{NH}_4)_2\text{SO}_4$ medium was 47.7 ± 6.2 mol% (the highest 3HHx composition was 51.7 mol%). On

the other hand, the PHBHHx content in the cells was higher in MF01/pBBP-*ccr*_{Me}J4a-*emd* than in MF01/pBBP-*ccr*_{Me}J4a-*emd* at any concentration of (NH₄)₂SO₄. The highest PHBHHx content of 85.8 ± 13.2wt% was obtained by MF01/pBBP-*ccr*_{Me}J4a-*emd* using 0.5 g/L (NH₄)₂SO₄ medium. The lowest value was 21.1 ± 0.5wt% and was obtained by MF01ΔB1/pBBP-*ccr*_{Me}J4a-*emd* using 2.0 g/L (NH₄)₂SO₄ medium. This tendency of lower PHA content with 2.0 g/L (NH₄)₂SO₄ was also observed for MF01/pBBP-*ccr*_{Me}J4a-*emd*. It was supposed that, in the cultures using the 2.0 g/L (NH₄)₂SO₄ medium, the decrease in pH impaired cell growth as described above; thus, the concentration of unconsumed NH₄⁺ in the culture medium was too high to cause nitrogen limitation, which promotes polymer synthesis in cells, resulting in lower polymer contents.

When the same strains were subjected to heterotrophic culture by using 5.0 g/L fructose as the sole carbon source and 0.2 g/L NH₄Cl as a nitrogen source, MF01/pBBP-*ccr*_{Me}J4a-*emd* showed DCM of 1.76 ± 0.02 g/L and accumulation of P(3HB-*co*-6.4 mol% 3HHx) with cellular content of 48.5 wt%, and those by MF01ΔB1/pBBP-*ccr*_{Me}J4a-*emd* were 1.57 ± 0.02 g/L and P(3HB-*co*-22.2 mol% 3HHx) with 47.9 wt%. Cell growth and PHBHHx synthesis from CO₂ in the autotrophic condition were better and numbered than those in the heterotrophic condition on fructose.

3.2. NMR Analysis of PHBHHx Synthesized by the Autotrophic Condition

In the previous study, the structure of PHBHHx synthesized from fructose by the recombinant strains was confirmed by ¹H- and ¹³C-NMR analyses, and the distribution of 3HB and 3HHx units was statistically random [11]. The copolymer synthesized from CO₂ was also analyzed by ¹H-NMR spectroscopy in order to confirm 3HB and 3HHx units in the polymer fraction. The 400 MHz ¹H-NMR spectra of the polymer synthesized by the wild strain of *C. necator* and that by MF01ΔB1/pBBP-*ccr*_{Me}J4a-*emd* in the culture using 2.0 g/L (NH₄)₂SO₄ medium in the autotrophic condition are shown in Figure 2a,b, respectively. The signals of H4 and H6 observed in Figure 2 were assigned to be resonances of the C4-methylene groups and C6-methyl-group in the 3HHx unit, respectively, indicating actual autotrophic formation of the PHBHHx copolymer.

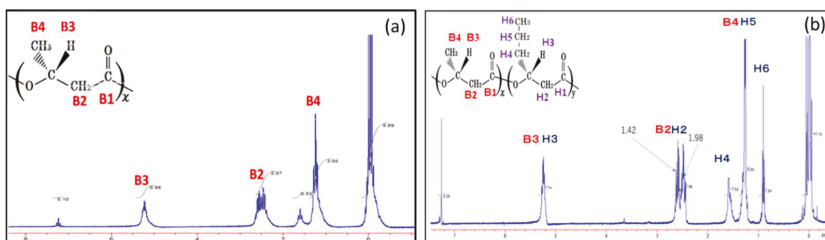


Figure 2. The 400 MHz ¹H NMR spectrum for P(3HB) synthesized by the wild strain of *C. necator* (a) and PHBHHx synthesized by MF01ΔB1/pBBP-*ccr*_{Me}J4a-*emd* (b). Each strain was cultivated in the autotrophic condition with 2.0 g/L (NH₄)₂SO₄.

3.3. Autotrophic PHA Synthesis by *C. necator* MF01/pBBP-*ccr*_{Me}J_{Ac}-*emd* and MF01ΔB1/pBBP-*ccr*_{Me}J_{Ac}-*emd*

PHBHHx synthesized from CO₂ by MF01/pBBP-*ccr*_{Me}J4a-*emd* showed remarkably high 3HHx composition. However, the thermal properties of PHBHHx composed of such very high 3HHx fractions are not good for applications. It is reported that the melting temperature of PHBHHx drastically decreases as 3HHx composition increases [5]. Therefore, we used another plasmid pBBP-*ccr*_{Me}J_{Ac}-*emd*, containing *scl*(R)-enoyl-CoA hydratase gene *pha*J_{Ac} instead of *pha*4a, to repress the excess incorporation of 3HHx unit into the polymer chain. The effects of the substrate specificity of PhaJ on the regulation of 3HHx composition has been confirmed by heterotrophic flask culture using fructose as a carbon source before the autotrophic culture test (Table 3). When MF01ΔB1 was the

host strain, the 3HHx composition in PHBHHx synthesized from fructose decreased from 22.2 mol% to 14.0 mol% by the replacement of *phaJ4a* by *phaJAc* in the plasmid. Other monomers except 3HB and 3HHx were not detected in every recombinant strain.

Table 3. PHBHHx biosynthesis from fructose by *C. necator* MF01 and MF01ΔB1 expressing different *phaJ* along with *ccrMe* and *emdMm*.

Recombinant (Strains/Plasmid)	DCM (g/L)	PHBHHx Content (wt%)	3HHx (mol%)
MF01/pBPP- <i>ccrMeJ4a</i> -emd ^a	1.76 ± 0.02	48.5 ± 0.4	6.4 ± 0.13
MF01/pBPP- <i>ccrMeJAc</i> -emd	1.81 ± 0.03	54.0 ± 3.1	10.4 ± 0.2
MF01ΔB1/pBPP- <i>ccrMeJ4a</i> -emd ^a	1.57 ± 0.02	47.9 ± 2.0	22.2 ± 1.2
MF01ΔB1/pBPP- <i>ccrMeJAc</i> -emd	1.72 ± 0.01	54.1 ± 2.1	14.0 ± 0.6

The cells were cultivated in a 100 mL MB medium containing 0.5% (w/v) fructose for 72 h at 30 °C. Standard deviation was shown with each value (*n* = 3). ^a Date from previous results [11].

The results for autotrophic flask culture of the recombinant strains MF01/pBPP-*ccrMeJAc*-emd and MF01ΔB1/pBPP-*ccrMeJAc*-emd at 120 h cultivation are shown in Table 4. The composition of 3HHx in the polymer synthesized by the new strains was successfully controlled in the range from 6.0 ± 1.3 mol% to 14.0 ± 1.3 mol%. In particular, in the culture using the 1.0 g/L (NH₄)₂SO₄ medium, these recombinants synthesized PHBHHx with 3HHx composition around 10 mol%, which is considered to produce physical properties suitable for practical applications.

Table 4. PHA synthesis by autotrophic flask culture of the engineered *C. necator* strains harboring pBPP-*ccrMeJAc*-emd.

Recombinant (Strains/Plasmid Vector)	(NH ₄) ₂ SO ₄ (g/L)	DCM (g/L)	PHBHHx Content (wt%)	Monomer (mol%)	
				3HB	3HHx
MF01/pBPP- <i>ccrMeJAc</i> -emd	0.5	7.25 ± 0.57	76.2 ± 0.0	94.0 ± 1.3	6.0 ± 1.3
MF01/pBPP- <i>ccrMeJAc</i> -emd	1.0	11.22 ± 2.67	64.6 ± 8.1	88.7 ± 6.4	11.3 ± 6.4
MF01/pBPP- <i>ccrMeJAc</i> -emd	2.0	8.46 ± 0.42	19.9 ± 1.7	88.6 ± 0.9	11.5 ± 0.9
MF01ΔB1/pBPP- <i>ccrMeJAc</i> -emd	0.5	6.93 ± 0.36	74.6 ± 2.2	86.6 ± 1.0	14.0 ± 1.3
MF01ΔB1/pBPP- <i>ccrMeJAc</i> -emd	1.0	8.52 ± 1.00	67.8 ± 1.8	87.1 ± 2.3	11.1 ± 1.3
MF01ΔB1/pBPP- <i>ccrMeJAc</i> -emd	2.0	6.03 ± 0.78	39.1 ± 1.3	90.4 ± 0.7	9.6 ± 0.7

All data were obtained after 120 h of cultivation (*n* = 3). The substrate gas mixture (H₂/O₂/CO₂ = 8:1:1) in the flask was exchanged every 12 h.

Compared to PHBHHx biosynthesis from fructose in heterotrophic culture shown in Table 3, the replacement of *phaJ4a* to *phaJAc* drastically reduced the 3HHx composition in MF01ΔB1 strains in the autotrophic culture. Contrary, in MF01 in which *phaJ4a* was replaced with *phaJAc*, the 3HHx composition increased in the autotrophic culture.

We tried to continue the flask culture for longer than 120 h with repeated exchange of the substrate gas mixture, aiming to obtain larger DCM. However, the reproducibility of the results of the prolonged culture was very low; in particular, DCM was seriously different even when the same strain was used in the medium with the same composition.

4. Discussion

There have been only a few reports on the biosynthesis of PHA copolymers from CO₂ by hydrogen-oxidizing bacteria. Volova et al. reported that *Cupriavidus necator* B-10646 produced 50 g/L of DCM with 85% of PHA content in batch culture using a recycled-gas closed-circuit culture system [25]. However, the fraction of other units in addition to 3HB was minor when CO₂ was used as sole carbon source. The higher fractions of 3HV and 4-hydroxybutyrate and 3HHx monomer units were obtained by supplementing the precursor substrates to the culture medium. According to the report by Heinrich et al., the recombinant of photosynthetic bacterium, *Rhodospirillum rubrum* pBBR1MCS-2-:*phaB_{Re}::pntAB_{Ec}*, accumulated PHAs up to 10.1 ± 1.1 wt% of the DCW with 55.5 ± 7.9 mol% of 3HV fraction when an artificial syngas atmosphere composed of 40% CO, 40% H₂, 10% CO₂ and 10% N₂ was used as the carbon and energy sources [26]. Recently, several researchers have

reported the biosynthesis of copolymer PHAs with high composition of the second or tertiary unit from CO₂ as the sole carbon source without using an organic precursor in obligate autotrophic condition (Table 5). Compared to those results, our recombinant strains showed much higher yield and productivity of copolymer PHA from CO₂.

Table 5. Comparison for biosynthesis of copolymer PHAs from CO₂ as sole carbon source by different autotrophic microorganisms.

Scheme.	Nutritional Condition	PHA Production	PHA Composition (mol%)	Ref.
<i>C. necator</i> H 16 ^a	H ₂ /CO ₂ /air = 30:15:balance	-	Various type of PHAs with C ₄ -C ₁₄ monomers	[27]
<i>C. necator</i> H 16 ^b	H ₂ /O ₂ /CO ₂ /N ₂ = 3.6: 7.6: 12.3: 76.5 (non-combustible gas)	DCM0.14 ± 0.05 g/L (PHA content 57 ± 10 wt%)	3HB-based copolymer with 1.2% 3HV ^c and 1.2% 3H4MV ^d	[28]
<i>Anabaena spiroides</i> TISTR 8075	CO ₂ + light	PHBV productivity 0.5 mg g _{dwt} ⁻¹ day ⁻¹	PHBV (3HV 43.2%)	[29]
<i>Oscillatoria okeni</i> TISTR 8549	CO ₂ + light	PHBV concentration 108 mg/L	PHBV (3HV 5.5%)	[30]

^a Recombinant expressing different thioesterases and PhaCs; ^b Recombinant harboring pBBR1/C1ABP_{ac}BktB; ^c 3HV: 3-hydroxyvalerate;

^d 3H4MV: 3-hydroxy-4-methylvalerate.

Here, we demonstrated that the engineered strains of *C. necator* capable of synthesizing PHBHHx from sugars can be applicable in copolyester production that is also from CO₂. Figure 3 shows a proposed pathway for PHBHHx biosynthesis from CO₂ in the strain MF01ΔB1/pBPP-ccr_{Me}J_{Ac}-emd. It is known that *C. necator* fixes CO₂ by the reductive pentose phosphate pathway (Calvin–Benson–Bassham (CBB) cycle) [31]. Under autotrophic conditions, two molecules of glyceraldehyde 3-phosphate (GAP) formed through the CBB cycle were converted to acetoacetyl-CoA and then reduced to (R)-3HB-CoA, a C₄-monomer unit for polymerization. The deletion of *phaB1* weakened the (R)-specific reduction of acetoacetyl-CoA, resulting in relative enforcement of competing (S)-specific reduction [20]. This was thought to cause efficient formation of crotonyl-CoA via (S)-3HB-CoA. Crotonyl-CoA is then converted to butyryl-CoA by combination of Ccr_{Me} and Emd_{Mm}, where ethylmalonyl-CoA generated by carboxylase activity of bifunctional Ccr_{Me} is converted back to butyryl-CoA by Emd_{Mm}. Alternatively, a part of crotonyl-CoA is used to form (R)-3HB-CoA by (R)-enoyl-CoA hydratase, PhaJ. Butyryl-CoA acts as a precursor of (R)-3HHx-CoA, a C₆-monomer, and the C₄-monomers and C₆-monomers are copolymerized by PhaC_{NSDG}. (R)-enoyl-CoA hydratase potentially functions in both the interconversion between (R)-3HB-CoA and crotonyl-CoA and the formation of (R)-3HHx-CoA after the elongation. When *phaJ4a* encoding mcl-specific hydratase was introduced into *C. necator*, the 3HHx composition in the copolyester produced from CO₂ by MF01ΔB1/pBPP-ccr_{Me}J_{Ac}-emd was surprisingly high (44–48 mol%). This was quite interesting since such high C₆ compositions have been not observed in heterotrophic biosynthesis, whereas the C₆-rich copolymer is too soft and, thus, is not suitable for general applications. The copolymer composition could be regulated by adopting another PhaJ in the biosynthesis pathway. It was supposed that scl-specific PhaJ_{Ac} showing high activity to crotonyl-CoA increases the additional formation of (R)-3HB-CoA from crotonyl-CoA accompanied with a relative decrease in the butyryl-CoA formation. As a result, the strain MF01ΔB1/pBPP-ccr_{Me}J_{Ac}-emd produced PHBHHx composed of 14 mol% 3HHx composition with high cellular content on CO₂.

DCM concentrations in the autotrophic culture of the engineered *C. necator* strains were much higher than those in heterotrophic conditions on fructose. In our previous study, fructose in culture media was limited to 20 g/L because higher fructose concentration was inhibitory to the growth of *C. necator* [11]. In the present autotrophic culture, the substrate gas mixture consumed within the flask was exchanged with a new gas mixture at every 12 h during the cultivation, which enabled attaining much higher DCM concentration than that in heterotrophic culture. In addition, the autotrophic culture also tended to show

higher 3HHx composition. Unfortunately, at present, we cannot explain the reason for this phenomenon. It might be that the formation of butyryl-CoA was promoted by the carboxylase activity of Ccr_{Me} increased by high concentrations of CO_2 and the activity of Emd_{Mm} , which increased 3HHx composition in autotrophic conditions. We will investigate the difference in 3HHx composition during heterotrophic culture and autotrophic culture in the future.

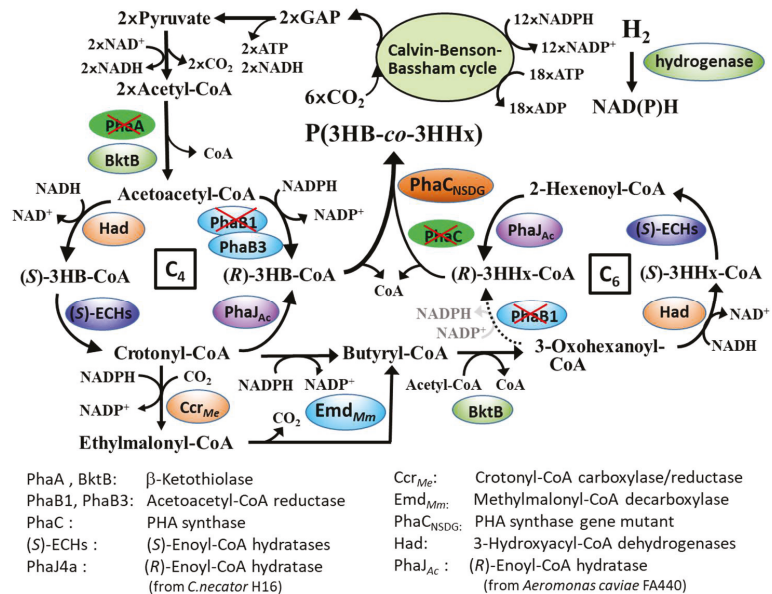


Figure 3. A proposed pathway for PHBHHx biosynthesis from CO_2 in *C. necator* MF01ΔB1/pBPP-crrMeJAc-emd.

Bktb is a medium-chain-length (mcl)-specific β -ketothiolase, which is possible to synthesize various 3-hydroxyacyl-CoAs of different carbon numbers (C_5 – C_{10}). However, only C_4 (3HB) and C_6 (3HHx) units were detected in the copolymers synthesized from CO_2 and fructose by GC and 1H NMR analyses. In our strains, several enzymes were introduced; however, the genes for synthesis of propionyl-CoA (C_5) were not introduced. Additionally, 2-hexenoyl-CoA is unlikely transformed to 3-hexanoyl-CoA (that is the precursor of C_8 -CoA) by Ccr_{Me}/Emd_{Mm} due to their substrate specificity. Pha_{CNSDG} can hardly polymerize the C_8 unit. Therefore, it may be that no other units other than 3HB and 3HHx were incorporated in the copolymer.

We already succeeded in high cell density cultivation of wild strain of *C. necator* H16 in an autotrophic culture condition using a 2 L scale jar fermenter and a recycled gas-closed circuit fermentation system. By using specially designed basket type agitation system in the jar fermenter, DCM increased to 91.3 g/L after 40 h of cultivation and homopolymer P(3HB) of 62 g/L was produced from CO_2 , while O_2 concentrations in the substrate gas mixture within the fermentation system were kept below 6.9% v/v, which is the lower limit for explosion [15]. We aim to study efficient PHBHHx production from CO_2 by the *C. necator* recombinants, and we also aim to investigate fermentation characteristics and physical properties of the polymer produced from CO_2 .

5. Conclusions

The biosynthesis of PHBHHx from CO_2 by engineered strains of a hydrogen oxidizing bacterium *C. necator* was investigated in autotrophic culture using the synthetic mineral medium and substrate gas mixture ($H_2/O_2/CO_2 = 8:1:1$). The results of GC and 1H

NMR analyses indicated that the recombinants of *C. necator* synthesized PHBHHx from CO₂ with high cellular contents in which the maximum value was 85.8 ± 13.2 wt%. The 3HHx composition of PHBHHx in the strain MF01ΔB1/pBBP-ccr_{Me}J4a-emd when using 1.0 g/L (NH₄)₂SO₄ as a nitrogen source was remarkably high (47.7 ± 6.2 mol%). Further investigation demonstrated that the PHA composition can be regulated by using (*R*)-enoyl-CoA hydratase (PhaJ) with different substrate specificities. The compositions of 3HHx in PHBHHx were controlled to about 11 mol%, which is suitable for practical applications, by keeping high cellular content in the strains transformed with pBPP-ccr_{Me}J_{Ac}-emd harboring scl-specific PhaJ derived from *A. caviae*. It is expected that the strains transformed with pBPP-ccr_{Me}J_{Ac}-emd will be useful for the industrialization of PHBHHx production from CO₂.

Author Contributions: K.T.: conceptualization; contribution to all experimental data; writing—original draft preparation; experimental contribution to autotrophic culture test of recombinant strains and GC analysis of PHBHHx. K.Y.: experimental contribution to autotrophic culture test of recombinant strains and NMR analysis of PHBHHx. I.O.: experimental contribution to gene recombination of *C. necator* H16 and GC analysis of PHBHHx. T.F.: methodology for recombination of *C. necator* H16; contribution to experimental data mainly gene recombination and GC analysis; writing—review and editing. All authors have read and agreed to the published version of the manuscript.

Funding: A part of this research was funded by the Feasibility Study Program on Energy and New Environmental Technology, NEDO (New Energy and Industrial Technology Development Organization, Japan). The foundation number is JPNP14004.

Institutional Review Board Statement: Not applicable.

Informed Consent Statement: Not applicable.

Data Availability Statement: Not applicable.

Acknowledgments: We thank Mari Nakagawa, Tokyo Institute of Technology, for her technical assistance with GC analysis.

Conflicts of Interest: The authors declare no conflict of interest.

References

- Sen, K.Y.; Baidura, S. Renewable biomass feedstocks for production of sustainable biodegradable polymer. *Curr. Opin. Green Sustain. Chem.* **2021**, *27*, 100412. [CrossRef]
- Barron, A.; Taylor, D.S. Commercial Marine-Degradable Polymers for Flexible Packaging. *Iscience* **2020**, *23*, 101353. [CrossRef] [PubMed]
- Hazer, B.; Steinbüchel, A. Increased diversification of polyhydroxyalkanoates by modification reactions for industrial and medical applications. *Appl. Microbiol. Biotechnol.* **2007**, *74*, 1–12. Available online: <https://link.springer.com/article/10.1007%2Fs00253-006-0732-8> (accessed on 12 June 2021). [CrossRef]
- Lu, J.; Tappel, R.C.; Nomura, C.T. Mini-Review: Biosynthesis of Poly(hydroxyalkanoates). *Polym. Rev.* **2009**, *49*, 226–248. [CrossRef]
- Turco, R.; Santagata, G.; Corrado, I.; Pezzella, C.; Serio, M.D. In Vivo and Post-Synthesis Strategies to Enhance the Properties of PHB-Based Materials: A Review. *Front. Bioeng. Biotechnol.* **2021**, *8*, 619266. [CrossRef] [PubMed]
- Sashiwa, H.; Fukuda, R.; Okura, T.; Sato, S.; Nakayama, A. Microbial Degradation Behavior in Seawater of Polyester Blends Containing Poly(3-hydroxybutyrate-co-3-hydroxyhexanoate) (PHBHHx). *Mar. Drugs* **2018**, *16*, 34. [CrossRef]
- Kaneka Corporation News Release. Completion of Kaneka Biodegradable Polymer PHBH™ Plant with Annual Production of 5000 Tons. 19 December 2019. Available online: <https://www.kaneka.co.jp/en/topics/news/nr20191219/> (accessed on 20 August 2021).
- Shimamura, E.; Kasuya, K.; Kobayashi, G.; Shiotani, T.; Shima, Y.; Doi, Y. Physical Properties and Biodegradability of Microbial Poly(3-hydroxybutyrate-co-3-hydroxyhexanoate). *Macromolecules* **1994**, *27*, 878–880. [CrossRef]
- Doi, Y.; Kitamura, S.; Abe, H. Microbial Synthesis and Characterization of Poly(3-hydroxybutyrate-co-3-hydroxyhexanoate). *Macromolecules* **1995**, *28*, 4822–4828. [CrossRef]
- Boey, J.Y.; Mohamad, L.; Khok, Y.S.; Tay, G.S.; Baidurah, S. A Review of the Applications and Biodegradation of Polyhydroxyalkanoates and Poly(lactic acid) and Its Composites. *Polymers* **2021**, *13*, 1544. [CrossRef]

11. Insomphun, C.; Xie, H.; Mifune, J.; Kawashima, Y.; Orita, I.; Nakamura, S.; Fukui, T. Improved artificial pathway for biosynthesis of poly(3-hydroxybutyrate-co-3-hydroxyhexanoate) with high C₆-monomer composition from fructose in *Ralstonia eutropha*. *Metab. Eng.* **2015**, *27*, 38–45. [CrossRef]
12. Matassa, S.; Boon, N.; Verstraete, W. Resource recovery from used water: The manufacturing abilities of hydrogen-oxidizing bacteria. *Water Res.* **2015**, *68*, 467–478. [CrossRef] [PubMed]
13. Volova, T.G.; Barashkov, V.A. Characteristics of proteins synthesized by hydrogen-oxidizing microorganisms. *Appl. Biochem. Microbiol.* **2010**, *46*, 574–579. Available online: <https://www.frontiersin.org/articles/10.3389/fbioe.2020.619266/full> (accessed on 12 June 2021). [CrossRef]
14. Ishizaki, A.; Tanaka, K. Production of poly-β-hydroxybutyric acid from carbon dioxide by *Alcaligenes eutrophus* ATCC 17697^T. *J. Ferment. Bioeng.* **1991**, *71*, 254–257. [CrossRef]
15. Tanaka, K.; Ishizaki, A.; Kanamaru, T.; Kawano, T. Production of poly(D-3-hydroxybutyrate) from CO₂, H₂, and CO₂ by high cell density autotrophic cultivation of *Alcaligenes eutrophus*. *Biotechnol. Bioeng.* **1995**, *45*, 268–275. Available online: <https://onlinelibrary.wiley.com/doi/10.1002/bit.260450312> (accessed on 12 June 2021). [CrossRef]
16. Taga, N.; Tanaka, K.; Ishizaki, A. Effects of rheological change by addition of carboxymethylcellulose in culture media of an air-lift fermentor on poly-D-3-hydroxybutyric acid productivity in autotrophic culture of hydrogen-oxidizing bacterium, *Alcaligenes eutrophus*. *Biotechnol. Bioeng.* **1997**, *53*, 529–533. [CrossRef]
17. Sugimoto, T.; Tsuge, T.; Tanaka, K.; Ishizaki, A. Control of acetic acid concentration by pH-stat continuous substrate feeding in heterotrophic culture phase of two-stage cultivation of *Alcaligenes eutrophus* for production of P(3HB) from CO₂, H₂ and O₂ under non-explosive condition. *Biotechnol. Bioeng.* **1999**, *62*, 625–631. Available online: [https://onlinelibrary.wiley.com/doi/10.1002/\(SICI\)1097-0290\(19990320\)62:6%3C625::AID-BIT1%3E3.0.CO;2-D](https://onlinelibrary.wiley.com/doi/10.1002/(SICI)1097-0290(19990320)62:6%3C625::AID-BIT1%3E3.0.CO;2-D) (accessed on 15 June 2021). [CrossRef]
18. Ishizaki, A.; Tanaka, K.; Taga, N. Microbial production of poly-D-3-hydroxybutyrate from CO₂. *Appl. Microbiol. Biotechnol.* **2001**, *57*, 6–12. Available online: <https://link.springer.com/article/10.1007%2Fs002530100775> (accessed on 15 June 2021). [PubMed]
19. Mifune, J.; Nakamura, S.; Fukui, T. Engineering of pha operon on *Cupriavidus necator* chromosome for efficient biosynthesis of poly(3-hydroxybutyrate-co-3-hydroxyhexanoate) from vegetable oil. *Polym. Degrad. Stab.* **2010**, *95*, 1305–1312. [CrossRef]
20. Zhang, M.; Kurita, S.; Orita, I.; Nakamura, S.; Fukui, T. Modification of acetoacetyl-CoA reduction step in *Ralstonia eutropha* for biosynthesis of poly(3-hydroxybutyrate-co-3-hydroxyhexanoate) from structurally unrelated compounds. *Microb. Cell Fact.* **2019**, *18*, 147. [CrossRef] [PubMed]
21. Tsuge, T.; Watanabe, S.; Shimada, D.; Abe, H.; Doi, Y.; Taguchi, S. Combination of N149S and D171G mutations in *Aeromonas caviae* polyhydroxyalkanoate synthase and impact on polyhydroxyalkanoate biosynthesis. *FEMS Microbiol. Lett.* **2007**, *277*, 217–222. [CrossRef] [PubMed]
22. Kawashima, Y.; Cheng, W.; Mifune, J.; Orita, I.; Nakamura, S.; Fukui, T. Characterization and functional analyses of R-specific enoyl coenzyme A hydratases in polyhydroxyalkanoate-producing *Ralstonia eutropha*. *Appl. Environ. Microbiol.* **2012**, *78*, 493–502. Available online: [http://refhub.elsevier.com/S1096-7176\(14\)00128-1/sbref20](http://refhub.elsevier.com/S1096-7176(14)00128-1/sbref20) (accessed on 15 June 2021). [CrossRef] [PubMed]
23. Fukui, T.; Ohsawa, K.; Mifune, J.; Orita, I.; Nakamura, S. Evaluation of promoters for gene expression in polyhydroxyalkanoate-producing *Cupriavidus necator* H16. *Appl. Microbiol. Biotechnol.* **2011**, *89*, 1527–1536. Available online: [http://refhub.elsevier.com/S1096-7176\(14\)00128-1/sbref13](http://refhub.elsevier.com/S1096-7176(14)00128-1/sbref13) (accessed on 15 June 2021). [CrossRef] [PubMed]
24. Kato, M.; Bao, H.J.; Kang, C.-K.; Fukui, T.; Doi, Y. Production of a novel copolyester of 3-hydroxybutyric acid and medium-chain-length 3-hydroxyalkanoic acids by *Pseudomonas* sp. 61-3 from sugars. *Appl. Microbiol. Biotechnol.* **1996**, *45*, 363–370. Available online: <https://link.springer.com/article/10.1007/s002530050697> (accessed on 10 August 2021). [CrossRef]
25. Volova, T.G.; Kiselev, E.G.; Shishatskaya, E.I.; Zhila, E.I.; Boyandin, A.N.; Syrvacheva, D.A.; Vinogradova, O.N.; Kalacheva, G.S.; Vasiliev, A.D.; Peterson, I.V. Cell growth and accumulation of polyhydroxyalkanoates from CO₂ and H₂ of a hydrogen-oxidizing bacterium, *Cupriavidus eutrophus* B-10646. *Bioresour. Technol.* **2013**, *146*, 215–222. [CrossRef]
26. Heinrich, D.; Raberg, M.; Steinbüchel, A. Synthesis of poly(3-hydroxybutyrate-co-3-hydroxyvalerate) from unrelated carbon sources in engineered *Rhodospirillum rubrum*. *FEMS Microbiol. Lett.* **2015**, *362*, fnv038. [CrossRef]
27. Nangle, S.N.; Ziesack, M.; Buckley, S.; Trivedi, D.; Loh, D.M.; Nocera, D.G.; Silvera, P.A. Valorization of CO₂ through lithoautotrophic production of sustainable chemicals in *Cupriavidus necator*. *Metab. Eng.* **2020**, *62*, 207–220. [CrossRef] [PubMed]
28. Miyahara, Y.; Yamamoto, M.; Thorbecke, R.; Mizuno, S.; Tsuge, T. Autotrophic biosynthesis of polyhydroxyalkanoate by *Ralstonia eutropha* from non-combustible gas mixture with low hydrogen content. *Biotechnol. Lett.* **2020**, *42*, 1655–1662. Available online: <https://link.springer.com/article/10.1007/s10529-020-02876-3> (accessed on 10 August 2021). [CrossRef]
29. Tarawat, S.; Incharoensakdi, A.; Monshupanee, T. Cyanobacterial production of poly(3-hydroxybutyrate-co-3-hydroxyvalerate) from carbon dioxide or a single organic substrate: Improved polymer elongation with an extremely high 3-hydroxyvalerate mole proportion. *J. Appl. Phycol.* **2020**, *32*, 1095–1102. [CrossRef]
30. Taepucharoen, K.; Tarawat, S.; Puangcharoen, M.; Incharoensakdi, A.; Monshupanee, T. Production of poly(3-hydroxybutyrate-co-3-hydroxyvalerate) under photoautotrophy and heterotrophy by non-heterocystous N₂-fixing cyanobacterium. *Bioresour. Technol.* **2017**, *239*, 523–527. [CrossRef]
31. Bowien, B.; Kusian, B. Genetics and control of CO₂ assimilation in the chemoautotroph *Ralstonia eutropha*. *Arch. Microbiol.* **2002**, *178*, 85–93. [CrossRef]

Communication

PHB Producing Cyanobacteria Found in the Neighborhood—Their Isolation, Purification and Performance Testing

Katharina Meixner ^{1,2}, Christina Daffert ¹, Lisa Bauer ², Bernhard Drosig ^{1,2} and Ines Fritz ^{1,*}

¹ Department of Agrobiotechnology IFA-Tulln, Institute of Environmental Biotechnology, University of Natural Resources and Life Sciences, Vienna, Konrad-Lorenz-Straße 20, 3430 Tulln, Austria; katharina.meixner@boku.ac.at (K.M.); christina.daffert@boku.ac.at (C.D.); bernhard.drosig@boku.ac.at (B.D.)
² BEST Bioenergy and Sustainable Technologies GmbH, Inffeldgasse 21b, 8010 Graz, Austria; lisa.bauer@best-research.eu
* Correspondence: ines.fritz@boku.ac.at; Tel.: +43-1-47654-97442

Abstract: Cyanobacteria are a large group of prokaryotic microalgae that are able to grow photo-autotrophically by utilizing sunlight and by assimilating carbon dioxide to build new biomass. One of the most interesting among many cyanobacteria cell components is the storage biopolymer polyhydroxybutyrate (PHB), a member of the group of polyhydroxyalkanoates (PHA). Cyanobacteria occur in almost all habitats, ranging from freshwater to saltwater, freely drifting or adhered to solid surfaces or growing in the porewater of soil, they appear in meltwater of glaciers as well as in hot springs and can handle even high salinities and nutrient imbalances. The broad range of habitat conditions makes them interesting for biotechnological production in facilities located in such climate zones with the expectation of using the best adapted organisms in low-tech bioreactors instead of using “universal” strains, which require high technical effort to adapt the production conditions to the organism’s need. These were the prerequisites for why and how we searched for locally adapted cyanobacteria in different habitats. Our manuscript provides insight to the sites we sampled, how we isolated and enriched, identified (morphology, 16S rDNA), tested (growth, PHB accumulation) and purified (physical and biochemical purification methods) promising PHB-producing cyanobacteria that can be used as robust production strains. Finally, we provide a guideline about how we managed to find potential production strains and prepared others for basic metabolism studies.

Keywords: cyanobacteria; habitat conditions; sampling; wild types; single species selection; purification; axenic cultures; growth; PHB

Citation: Meixner, K.; Daffert, C.; Bauer, L.; Drosig, B.; Fritz, I. PHB Producing Cyanobacteria Found in the Neighborhood—Their Isolation, Purification and Performance Testing. *Bioengineering* **2022**, *9*, 178. <https://doi.org/10.3390/bioengineering9040178>

Academic Editor: Giorgos Markou

Received: 10 March 2022

Accepted: 12 April 2022

Published: 18 April 2022

Publisher’s Note: MDPI stays neutral with regard to jurisdictional claims in published maps and institutional affiliations.



Copyright: © 2022 by the authors. Licensee MDPI, Basel, Switzerland. This article is an open access article distributed under the terms and conditions of the Creative Commons Attribution (CC BY) license (<https://creativecommons.org/licenses/by/4.0/>).

1. Introduction

The worldwide growing plastic pollution has initiated a search for plastic-like materials which are biodegradable in organic recovery facilities (well managed industrial compost) as well as in the environment. Among others, bacteria storage polymers of the type polyhydroxyalkanoate (PHA) are promising candidates [1,2]. Biotechnological production processes have already been developed that can utilize industrial waste processes (instead of agricultural raw material) as resources [3], and many of those processes have been optimized for improved productivity [4]. A production with photo-autotrophic bacteria, such as cyanobacteria, will even avoid the dependency on waste and residues, because carbon dioxide (CO₂) can be utilized as sole carbon source [5]. Cyanobacteria are known to produce the homo-polymer of hydroxybutyrate, PHB, which is only one of 150 different types of PHAs identified so far [6–8].

Well-investigated strains of cyanobacteria can be obtained from culture collections, such as DSMZ, PCC, ATCC, CCALA to name only a few. The benefit of using such strains is in the public availability of comprehensively documented properties and cellular

compositions, which makes them something like a standard—further research work does not need to start from scratch. As lucrative as those strains are for basic science studies, they are rarely suitable for biotechnological use of a bigger scale, when ambient conditions, like the influence of climate or the presence of endemic competitors and predators, cannot be controlled—at least not with justified effort.

Microorganisms that grow in significant abundance in a certain natural habitat are, most likely, well adapted to the local conditions and have developed properties that makes them superior compared to the other members of the biocenosis [9]. Temperature and average light energy emission are the most important factors in prospect of a future use in biotechnology; the ideal composition of minerals and trace elements can be adjusted in the cultivation medium.

When intending to produce PHB with photo-autotrophically grown cyanobacteria [10], production effort and production cost will decide if the process can be operated in an economical way to compete with established market prices [11–13]. Circulation of production media, mostly water and mineral nutrients will decrease the production cost [14]. Harvest and utilization of other valuable cyanobacteria cell components, such as vitamins, unsaturated fatty acids or pigments [15] can help to make a phototrophic production economically viable [16].

Temperature requirements far off from ambient conditions and the operation of closed and sterile bioreactors will increase the production effort even more and are, most likely, only viable for producing special chemicals for use in pharmaceutical or cosmetic applications. Any cyanobacteria strain that can grow at local ambient conditions as single species but in non-axenic cultivation will help to decrease costs and is worth testing and characterizing for its key properties.

Pros and cons about using wild strains:

- (+) Adapted to local climate, especially considering daily and annual temperature range and sunlight availability,
- (+) When found as abundant species in a local habitat, it will have a growth advantage over local competitors,
- (+) Resistance against local predators and pathogens,
- (+) Can be operated non-axenically (in open bioreactors),
- (+) No ecological harm from spoilage after leaks or accidents—no special admission procedure,
- (+) Free of third-party rights,
- (–) Only small chance of superior strain productivity,
- (–) High effort for strain characterization and improvement, if necessary.

Understanding the metabolic pathways and the relation between PHB synthesis and other parts of the anabolism will allow improving cyanobacterial production processes without genetic manipulation [17]. Despite increasing knowledge, expressed in a high number of publications about PHB producing cyanobacteria grown in shaking flasks in laboratory environment, comparably little is published about scale-up [18]. Growing cyanobacteria in bigger volumes in open photobioreactors under non-sterile and, probably, under not so well controlled conditions often fails and rarely succeeds [10,19].

In contrast to production goals, axenic cultures are needed for applications where the coexistence of other organisms is undesirable. Such include genome sequencing, identifying producers of bioactive compounds, or building an artificial consortium for bioremediation, as well as clarifying the relationships between microalgae and other organisms using -omics tools [20,21]. A prerequisite for applied research is knowledge about the origin or about the cause of an observed effect and, finally, to differentiate between behaviors of cyanobacteria and those of an uncontrolled heterotroph accompanying flora.

Axenic culture establishment is the process of eliminating undesirable organisms (contaminants) to obtain a viable culture of desired organisms (quarry). The strategy depends strongly on the characteristics of the quarry and on the contaminants in each microbial community [20].

The aim of this work was to isolate cyanobacteria strains that accumulate PHB and are robust enough for cultivation at outdoor conditions in an low-tech open reactor. Axenic cultures should be generated from the most promising of those isolates for subsequent characterization of their growth kinetics and for molecular analysis.

For this purpose, samples were taken at 27 locations around the world representing various climatic regions. Cyanobacteria strains were isolated, identified, screened and evaluated for growth and for PHB accumulation. Finally, we applied different methods to find the best suitable strategy to obtain axenic cultures. Therefore, physical and chemical separating and purifying methods were carried out.

2. Materials and Methods

2.1. Sampling in the Wild and Strains from Culture Collections

All samples were generally treated in the same way. Liquid samples were transferred to mineral medium [22] on site. In case of a short travel distance, the samples were brought to the lab immediately, in other cases samples were stored at windows in hotel rooms until transport to the lab. The cultures were incubated in Erlenmeyer flasks at 21 °C, in elevated CO₂ concentration (approx. 1.5 vol%), at 85–95 rpm (orbital shaker VKS 75 control, Edmund Bühler GmbH, Bodelshausen, Germany) and a day–night cycle of 16:8 h with an illumination of approx. 108 μmol photons m⁻² s⁻¹ (metal halide lamp, Philips Master HPI-T Plus, 250 W) until the first green coloration visible to the bare eye. After that, cultures were inoculated into fresh BG-11 medium approx. every three to six days to pre-select the fastest growing photo-autotrophs.

In addition to the isolated wild type strains, screening and methods for obtaining axenic cultures were also carried out with the strains *Synechocystis* sp. PCC6803 and *Synechocystis* cf. *salina* CCALA192 as reference, which were obtained from the Pasteur culture collection (FRA) and from the culture collection of autotrophic organisms (CZE), respectively, both in non-axenic form.

2.2. Growing Media

For different purposes described herein, different media were used. For selecting fast growing species, for separating into single-species cultures and for obtaining axenic cultures, a variation of BG-11 medium [22] was used, containing half of the recommended amount of sodium nitrate (code: BG-I) [23]. For PHB screening experiments as well as for evaluating growth and PHB, a nutrient limited mineral medium, also based on BG-11, was used. This nutrient limited medium (code: 220) contained following ingredients per liter: NaNO₃: 0.45 g, Fe(NO₃)₃·9H₂O: 0.025 g, MgSO₄·7H₂O: 0.10 g, CaCl₂·2H₂O: 0.60 g, Na₂CO₃: 0.20 g, K₂HPO₄: 0.08 g, trace element solution 1.50 mL. Composition of the trace element solution per liter: H₃BO₃: 0.509 g, CuSO₄·5H₂O: 0.150 g, KI: 0.181 g, FeCl₃·6H₂O: 0.293 g, MnSO₄·H₂O: 0.296 g, Na₂MoO₄·2H₂O: 0.082 g, NiSO₄·6H₂O: 0.275 g, Co(NO₃)₂·6H₂O: 0.100 g, ZnSO₄·7H₂O: 0.490 g, KAl(SO₄)₂·12H₂O: 0.395 g, KCr(SO₄)₂·12H₂O: 0.470 g [23].

Besides the liquid media, agar-plates with BG-I medium were used. For fractionated streaks, plates with BG-I containing 1.5% agar were prepared, for phototaxis experiments 0.4% or 1% agar was added to BG-I.

Depending on the approach, different active substances were added to the liquid or solid cultivation medium. Cycloheximide, which inhibits cytoplasmic protein synthesis in eukaryotes [24], was used to suppress eukaryotic microalgae in the culture. To obtain axenic cultures lysozyme, imipenem, penicillin G and streptomycin were used. Lysozyme lyses peptidoglycan of the cell wall of bacteria [25]. Imipenem, a broad-spectrum β-lactam antibiotic, inhibits the biosynthesis of bacterial peptidoglycan [26]. Penicillin G too is a β-lactam antibiotic, it inhibits the formation of the bacterial cell wall and acts on G⁺ bacterial. Streptomycin is an aminoglycoside antibiotic that inhibits protein synthesis in prokaryotic ribosome [27]. Besides that, glucose and LB medium were added to liquid and solid media in the antibiotic approaches (BG-I+ medium).

2.3. Selecting Fast Growing Species

Samples were cultivated in a mineral medium without carbon source (see Section 2.2) to get rid of the majority of heterotrophic bacteria and multicellular organisms. The cultures were transferred in short intervals (as soon as cell suspensions turned light green) into fresh media to select the fastest growing strains. Such media transfers were repeated as often as necessary, up to 12 times.

2.4. Separation into Single-Species Cultures and Identification

Once decreased numbers of morphologically different cyanobacteria were visible under the microscope, additional selection criteria were applied: (i) mixed incubation in BG-I medium with cycloheximide (100 mg L⁻¹) to suppress growth of eukaryotic microorganisms and (ii) plating on BG-I agar medium (fractionated streaks) with colonies re-inoculated in new liquid BG-I medium.

Morphological identification of non-axenic single-species strains and purity controls of the samples were carried out at bright field and phase contrast microscopy at 40-fold magnification (Olympus BX43, Austria, Vienna). Pictures were taken with a digital camera (Canon EOS 1300D).

For identification via 16S-rDNA, fragments of approx. 700 bp were used as obtained from PCR amplification using the primers 5'-CGGACGGGTGAGTAACGCGTGA-3' (CYA 106F) and 5'-GACTACTGGGGTATCTAATCCCATT-3' (CYA 781R(a)), which are specific for cyanobacteria [28,29]. The protocol of Nübel et al. [29] was followed with a higher reaction volume to gain a sufficient amount of DNA for sequencing [28].

DNA sequencing was carried out by GATC Biotech AG (European Genome and Diagnostics Center, Constance, Germany) and LGC Genomics (<http://www.lgcgroup.com/>; accessed on 24 February 2022). Subsequently, DNA sequences were compared via NCBI BLAST.

2.5. Evaluation of Growth and PHB Accumulation

Cyanobacteria strains were grown in nutrient limited mineral medium 22O, which is based on BG-I, but with reduced amounts of nitrogen and phosphorous to reach starvation at roughly 1 g dry biomass/liter. Reaching nutrient starvation, the cells started to change color from bluish-green over olive-green to orange. For a fast screening, Nile-red staining and fluorescence microscopy (Olympus AH-3 AHBT3 VANOX, RFL-T3 Transformer, Hg-burner, Leica EC3 camera) were carried out using the culture suspensions without further pretreatment.

PHB producing strains were investigated in more detail by recording growth curves and PHB accumulation kinetics. The cultures were grown about 21 days and were monitored via periodical measurement of optical density (OD), cell dry weight (CDW) and PHB content.

2.5.1. Nile-Red Staining

For PHB staining, Nile-red solution (50 µg mL⁻¹ in 98% ethanol) was directly added to the cell suspension. After 10 min reaction time, 20 µL mixture were distributed on a glass slide and heat fixed for fluorescence microscopy with 450–500 nm excitation and >550 nm emission wavelengths selected.

2.5.2. Growth Analysis

For evaluating the growth optical density (OD) was measured at 435 nm, 485 nm, 680 nm and 750 nm with an UV-VIS Spectrophotometer (Shimadzu UV-1800, Kyoto, Japan). Furthermore, the cellular dry weight (CDW) was measured from 10 mL cell suspension, which was centrifuged, washed and dried at 105 °C.

2.5.3. PHB Analysis

The PHB content of the biomass was analyzed based on the method described in [30]. Therefore, 5 to 10 mL cell suspension were washed and dried (105 °C) and subsequently digested with concentrated (98%) sulfuric acid (H₂SO₄) for 30 min at 90 °C. Afterwards, the samples were filled to 10 mL with deionized water and prepared for HPLC (high-performance liquid chromatography) analysis (Agilent 1100; column: Transgenomic COREGEL 87H3; detector: Agilent 1100 RI, Santa Clara, CA, USA).

2.6. Obtaining Axenic Cultures

Multiple approaches were tried to reduce heterotrophic accompanying flora or, in the best case, to remove it totally in order to obtain an axenic cyanobacteria culture. Those approaches were: separating methods (agar-based methods, phototaxis, micro-pipetting via cell sorter and micromanipulator), serial dilutions (MPN approach), as well as killing methods (addition of cycloheximide, lysozyme, antibiotics, incubation at elevated temperature and salinity).

2.6.1. Phototaxis

For this approach, which was tested with PCC6803, CCALA192 and *Synechocystis* sp. IFA-3 two kinds of agar-plates were prepared, one with 0.4% and one with 1% final agar concentration. On these agar plates samples (10 µL cyanobacteria culture) and glucose (5 µL, 1% solution) were applied in two small holes stuck with a glass Pasteur pipette (Figure 1). The plates were then wrapped into aluminum foil and a small hole was made (opposite the glucose spot) so that a small light beam could reach the plate. The plates were incubated for 6 days at 22 °C and light (day–night cycle: 16:8 h, light intensity: approx. 108 µmol photons m⁻² s⁻¹, metal halide lamp, Philips Master HPI-T Plus, 250 W). The experiments were carried out in triplicates.

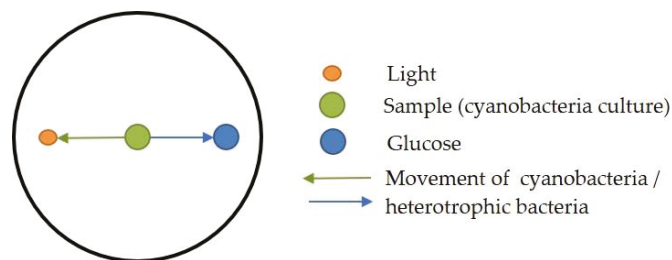


Figure 1. Agar-plate with the locations for sample (green) and glucose (blue) as well as the spot where light reaches the plate (orange) as well as the expected movement of cyanobacteria and heterotrophic bacteria (arrows).

2.6.2. Antibiotic Treatment

This approach was carried out with the *Synechocystis* strains CCALA192, *Synechocystis* sp. IFA-3 and PCC6803. The methods changed in response to first results. For the approach with PCC6803, 1 g lysozyme, 100 mg imipenem and 100 mg streptomycin per liter were added to 10 mL cell suspension, which was then incubated 4 h in the dark [31]. Subsequently, cells were washed and resuspended in mineral medium to which glucose (1 g 100 mL⁻¹) and LB-medium (10 g 100 mL⁻¹) were added before it was again incubated in the dark at 22 °C for 30 min [27]. Then, again antibiotics were added (100 mg imipenem and 100 mg streptomycin per liter) and incubated in the dark for 18 h at 22 °C.

For the approach with CCALA192 and *Synechocystis* sp. IFA-3 10 mL cell suspension were incubated for 12 to 24 h in the dark, then the cell number was counted (counting chamber Neubauer improved, Marienfeld Germany, depth: 0.01 mm, area: 0.0025 mm²). Afterwards, an organic carbon source (1.2 g glucose per 100 mL cell suspension) was added [32] and to the reference the same amount on RO water. The cultures were incubated in the dark at 22 °C and approx. 85 rpm (standard orbital shaker Model 1000, VWR®) over night. Afterwards, 100 mg imipenem per liter and 100 mg penicillin G were added [32]. Again, the cultures were incubated in the dark at 22 °C and 85–95 rpm (orbital shaker VKS 75 control, Edmund Bühler GmbH) over night.

All cultures were finally plated out the next day. Therefore, the cells were washed and re-suspended in BG-I medium before plating 50 µL on agar. The agar plates were based on BG-I and BG-I + 0.5% glucose medium, respectively. Besides that, 0.5 mL were transferred into 100 mL flasks containing 30 mL BG-I and BG-I + 0.5% glucose medium, respectively. Plates and flasks were incubated at 22 °C and a day–night cycle of 16:8 h with an illumination of approx. 108 µmol photons m⁻² s⁻¹ (metal halide lamp, Philips Master HPI-T Plus, 250 W, Philips, Amsterdam, The Netherlands) and controlled after 2 and 20 h and then 2 to 3 times per week until growth was visible. In each run, a blank was included, instead of antibiotics RO-water was added. Antibiotics were sterile filtered and glucose solutions autoclaved separately. Approaches were carried out in triplicates.

2.6.3. Elevated Temperature and Salinity

Cultures of PCC6803 as well as isolated cyanobacterial accompanying flora were inoculated in BG-I medium and in BG-I + 5 g L⁻¹ glucose. The shaking flasks were put on a shaker (standard orbital shaker Model 1000, VWR®, Radnor, PA, USA) in a climate room at 37 °C and a day–night cycle of 16:8 h (75.9 ± 9.5 µmol photons m⁻² s⁻¹, LED warm white 3000 K, 12 VDC) for 13 days. The experiments were carried out in triplicates.

An additional approach was carried out with *Synechocystis* sp. IFA-3. The aim was to evaluate how *Synechocystis* sp. and its accompanying flora can cope with salt stress and elevated temperature. For this purpose, *Synechocystis* sp. (1.2 × 10⁷ cells) was inoculated in BG-I medium and BG-I medium with 4% (684 mM) NaCl. The 100-mL Erlenmeyer flasks containing 40 mL cell suspension were incubated on a shaker (standard orbital shaker Model 1000, VWR®) in a climate room at 37 °C and a day–night cycle of 16:8 h (75.9 ± 9.5 µmol photons m⁻² s⁻¹, LED warm white 3000 K, 12 VDC) for 13 days. The experiments were carried out in triplicates.

2.6.4. Cell Sorter

Cell sorting experiments were carried out with single cellular, non-filamentous cyanobacteria using a Beckmann Coulter (LSR-System ASTRIOS, AU05037). The size of the cells in the samples was measured and those in the range of cyanobacterial cells (3 to 5 µm) were separated into small tubes and subsequently cultivated in BG-I medium. This approach was tested with the *Synechocystis* strains PCC6803, CCALA192 and IFA-3.

2.6.5. Micromanipulator

The micromanipulator consisted of a holder for a homemade glass capillary with a small disposable syringe for minimal fluid movement. The glass capillaries were produced from Pasteur pipets to accommodate about 1–5 µL of fluid, according to anticipated needs. Areas of predominantly cyanobacterial cells were sought under the inverted microscope (Nikon TMS, Nikon, Tokyo, Japan), and in each case between one and up to 20 cells were aspirated and transferred to fresh medium.

2.6.6. MPN Dilution Approach

Based on the count of cyanobacterial cells (counting chamber Neubauer improved, Marienfeld Germany, depth: 0.01 mm, area: 0.0025 mm²), dilutions were prepared to achieve a suspension of 6 cells in 2.4 mL (=2.5 mL⁻¹). In each well of a 24-well plate, 2 mL BG-I medium were put and 0.1 mL of the final dilution was added with the prospect of having distributed 6 cells over 24 wells of the plate. The plate was incubated on a shaker (New Brunswick Scientific Co G25 Controlled Environment Incubator Shaker, approx. 85 rpm; standard orbital shaker Model 1000, VWR[®], approx. 85 rpm) at 22 to 25 °C and 35 to 37 °C. After about 14 to 21 days, some wells turned slightly green. After about 28 days, cultures were microscopically controlled and putative axenic cultures were transferred into shaking flasks with BG-I medium and cultivated under the above described conditions. These approaches were carried out with the strains PCC6803, CCALA192 and *Synechocystis* sp. IFA-3.

3. Results and Discussion

3.1. Sampling

Sampling took place in different climatic regions, reaching from cold semi-arid climate (BSk), over warm-summer humid continental climate (Dfb) to tundra climate (ET) (examples in Figure 2); the classification is based on Köppen [33]. Samples from puddles, lakes, springs and rivers were directly scooped into a sterile plastic tube. When the samples could not be transported to the laboratory the same day, they were diluted with BG-I medium in equal volumes. Samples from solid surfaces were scratched off using a metal spatula and the harvested solids were suspended in sterile BG-I medium in a plastic tube on-site.

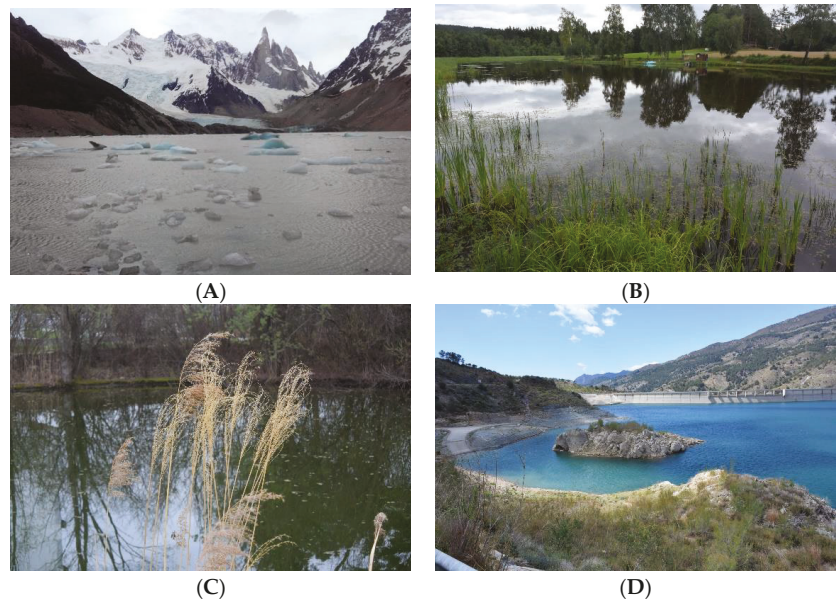


Figure 2. Example sampling locations of different climates: (A) Los Glaciares Laguna Torre ARG; (B) Heinrichs AUT (isolate: *Chlorogloeopsis fritschii*); (C) Tulln IFA-Teich AUT (isolate: *Synechocystis* sp.); and (D) Presa de Beninar ESP (isolate: *Crocospaera* sp.).

A total of 71 samples were taken from 25 locations (details in Table 1).

Table 1. Sampling locations with climate types and identified single-species strains. PHB production was tested by cultivation in a laboratory photobioreactor of ca. 5 L volume. Sequences are provided in Appendix B.

Sampling Location	Coordinates	Climate Region ¹	No. of Samples	Identification via 16S rDNA	Dry Biomass and PHB Content
Admont (AUT)	47°34'51.0" N 14°27'13.5" E	Dfc	4	<i>Pseudanabaena</i> sp. [99.6%]	n.d.
Beagle Channel (ARG)	54°50'59.7" S 68°29'37.9" W	ET	1	n.d.	n.d.
Branná (CZE)	50°09'24.6" N 17°01'17.1" E	Dfb	7	<i>Calothrix</i> sp. [99%], <i>Pseudanabaena</i> [97%]	n.d.
Chlum & Třeboně (CZE)	48°57'33.1" N 14°56'03.3" E	Cfb	6	n.d.	n.d.
Elisabethsee Amerbach (AUT)	47°10'43.4" N 12°31'44.7" E	ET	1	n.d.	n.d.
Glaciar Perito Moreno (ARG)	50°29'19.6" S 73°03'35.9" W	Cfc/ET	1	n.d.	n.d.
Gmünd, Mondteich (AUT)	48°46'40.3" N 14°59'51.5" E	Cfb	2	<i>Calothrix desertica</i> [97%]	n.d.
Greenland (GRL)	n.d.	EF/ET	5	<i>Cyanobium gracile</i> [99.8%]	n.d.
Greifenstein, Danube (AUT)	48°20'44.7" N 16°14'19.3" E	Cfb	2	<i>Pseudoanabaena biceps</i> [98.7%]	n.d.
Heidenreichstein, Hofwehrtich, (AUT)	48°52'06.1" N 15°07'44.2" E	Dfb/Cfb	1	n.d.	n.d.
Heinrichs (AUT)	48°44'56.3" N 14°50'07.9" E	Dfb/Cfb	5	<i>Calothrix</i> sp. [98%] <i>Chlorogloopsis fritschii</i> [99.8%]	n.d. 1040 mg L ⁻¹ , 4.6% PHB
Island (ISL)	64°18'45.2" N 20°18'08.3" W	Cfc/ET	1	n.d.	n.d.
Island (ISL)	63°54'53.8" N 22°41'50.9" W	Cfc/ET	1	n.d.	n.d.
Lago di San Vito (ITA)	46°28'03.8" N 12°12'06.4" E	Dfc/ET	1	n.d.	n.d.
Langenrohr, gr. Tulln (AUT)	48°19'06.8" N 16°01'00.4" E	Cfb	3	<i>Pseudoanabaena biceps</i> [99.7%] <i>Cyanobium gracile</i> [99.6%]	n.d. n.d.
National park los glaciares, Laguna Torre (ARG)	49°19'47.4" S 72°59'23.4" W	Cfc/ET	1	n.d.	n.d.
National park los glaciares, Lagunas Madre e hija (ARG)	49°18'18.8" S 72°57'03.7" W	Cfc/ET	1	n.d.	n.d.
Passo di Falzarego (ITA)	46°31'09.1" N 12°00'32.0" E	Dfc/ET	1	n.d.	n.d.
Passo della Guardia (ITA)	44°03'04.7" N 7°44'41.5" E	Csb	1	n.d.	n.d.
Presa de Beninar (ESP)	36°52'42.3" N 3°01'31.6" W	Csa	3	<i>Crocospaera</i> sp. [96%] <i>Synechococcus</i> sp. [96%]	<1% PHB n.d.
Pyhrbruck (AUT)	48°46'11.0" N 14°49'16.3" E	Cfb	3	<i>Calothrix</i> sp. [97%]	16.8 mg L ⁻¹ 1.1% PHB
Río Cacheuta (ARG)	33°02'53.5" S 69°11'47.3" W	BSk/BWk	1	n.d.	n.d.
Río De la Cascada (ARG)	49°17'37.0" S 72°54'08.6" W	Cfc/ET	1	n.d.	n.d.
Río Mendoza (ARG)	32°56'13.5" S 69°12'25.6" W	BSk/BWk	1	n.d.	n.d.
Thermal SPA Loipersdorf (AUT)	46°59'11.2" N 16°06'36.9" E	Cfb	12	<i>Anabaena Trichormus variabilis</i> [98.8%] <i>Nostoc</i> sp. [98.5%] <i>Nodosilinea nodulosa</i> [97.9%] <i>Anabaena variabilis</i> [98.8%]	n.d. n.d. n.d. n.d.
Tulln, IFA-Teich (AUT)	48°19'14.5" N 16°03'59.2" E	Cfb	5	<i>Calothrix</i> sp. [100%] <i>Synechocystis</i> sp. [98.2%] <i>Pseudanabaena biceps</i> [99.3%]	n.d. 1680 mg L ⁻¹ , 11.4% PHB n.d.

¹ According to Köppen climate classification [33]: BSk: Cold semi-arid climate, BWk: Cold desert climate, Cfb: Temperate oceanic climate, Cfc: Subpolar oceanic climate, Csa: Hot-summer Mediterranean climate, Csb: Warm-summer Mediterranean climate, Dfb: Warm-summer humid continental climate, Dfc: Subarctic climate, EF: Ice cap climate, ET: Tundra climate, n.d.: no data available.

3.2. Selecting Fast Growing Species

After transport to the lab, the samples were transferred to shaking flasks with BG-I medium and cultivated under photo-autotrophic conditions at 21 °C 16 h light/8 h dark on an orbital shaker at ca. 85–90 rpm. As soon as a culture developed a green color, a small volume was transferred into another flask with BG-I medium. Culture transfers were repeated up to 12 times or until the culture was dominated by one or two morphologically different strains (microscopic control in advance of each transfer)—or until the cultures lost all of their green color.

In total, 34 growing mixed cultures (containing eukaryotic algae and cyanobacteria) were obtained (selected examples are shown in Figure 3).

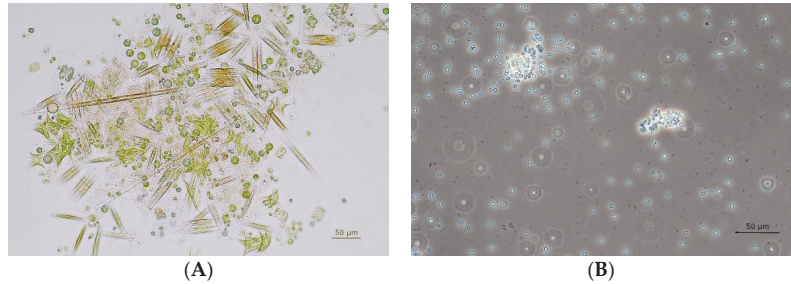


Figure 3. Microscopic control of photo-autotrophically cultivated samples from the fire-pond at IFA-Tulln (AUT); (A) original mixed culture enriched in BG-I mineral medium (bright field image) and (B) after cultivation in presence of cycloheximide (phase contrast image).

3.3. Getting Rid of Eukaryotic Microalgae

Enriched fast growing phototrophs were transferred to a BG-I medium, which contained 100 mg L^{-1} cycloheximide, and were cultivated under the same conditions as before for 5–6 days. A preliminary experiment (data in Appendix A) demonstrated the effectiveness of the antibiotics. All wild type cultures that contained vital cyanobacteria after several transfers were treated that way. Eukaryotic algae free cultures were obtained in most cases (example in Figure 3B), but in some of the cultures we lost all cyanobacteria as well.

3.4. Separation into Single-Species Cultures

Not all cyanobacteria grew well on BG-I agar, only in some cases colony-like clusters of cyanobacteria could be obtained from fractionated streaks. However, multiple differently looking colonies were obtained from some samples and were harvested separately. All of those clusters contained cyanobacteria often mixed with an even bigger amount of heterotrophic colorless bacteria. Colonies were in most cases colored blue-green, as expected, but also olive-green and red-orange colonies were obtained (see examples in Figure 4). Samples from colonies were inspected in the microscope before transfer to new shaking flasks with BG-I medium. All such isolates were numbered in ascending order per sampling site.

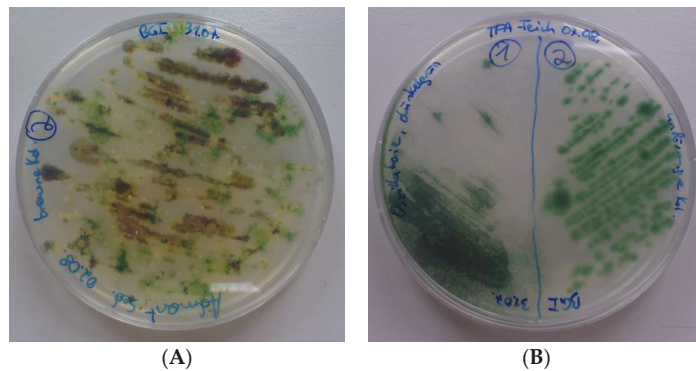


Figure 4. Fractionated streaks of mixed cyanobacteria samples after cycloheximide treatment taken from (A) Admont (AUT) and (B) Tulln, IFA-Teich (AUT).

Advantages of agar-based methods are that simple and macroscopic results are received and that axenic cultures can often be directly established without further treatment. We observed quite often long lag times until visible colonies were grown, in some cases up to four weeks. As mentioned before, no colonies were formed from some of the enriched cultures. In case the streak separates the cyanobacteria cells from essential synergists, the cyanobacteria may not grow or may even die out before they come into contact again [20].

3.5. Identification of Single-Species Cultures

All isolates and cultures had been routinely inspected microscopically, using bright field and phase contrast techniques (see Figure 3). Cyanobacteria had been characterized during all enrichment and isolation steps based on morphological characteristics. Although not axenic, DNA was extracted and cyanobacteria specific 16S rDNA [29] was amplified for sequencing. Most probable classifications and identifications are provided in Table 1, sequences are provided in Appendix C. We are aware that some of the sequences had less than 99% accordance. Therefore, we chose the most probable genera and/or species name combined from morphology and sequence accordance.

3.6. Screening of PHB Production

Single-species cyanobacteria cultures that grew in BG-I medium in shaking flasks to an optical density of at least 5 ($\lambda = 435$ nm) within 3 weeks were investigated for their ability to produce and accumulate PHB. For this purpose, inocula of the selected strains were transferred into the self-limiting mineral medium 22O and incubated at the same conditions as before. Cultures grown for four weeks were stained with Nile-red and microscopically inspected at fluorescence mode. Cultures containing at least some stained granules (see examples in Figure 5) were selected for quantitative PHB analysis and those which grew comparably fast (OD_{435} higher than 10 within two weeks) were also used for growth and PHB production experiments (results are shown in Table 1).

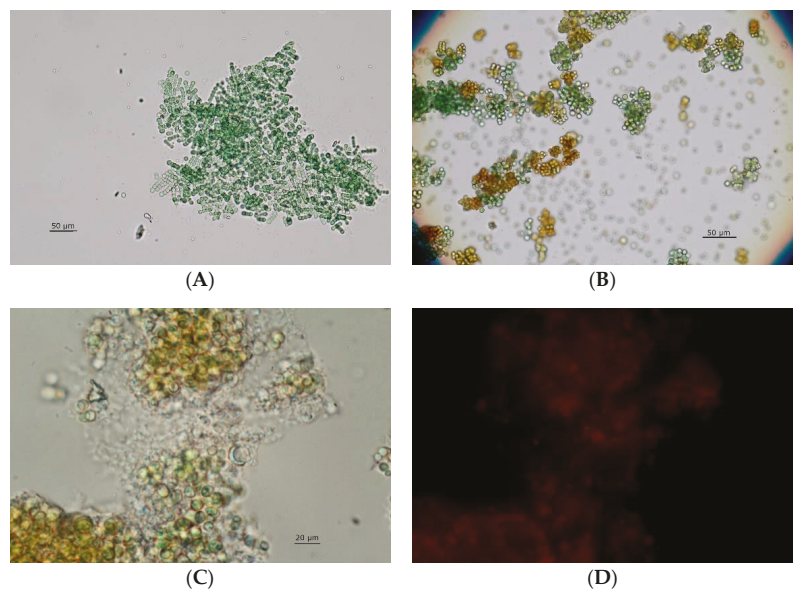


Figure 5. Microscopic imaging of *Chlorogloeopsis* sp. (Heinrichs-4, AUT) cultures; (A) blue-green cells during the growth phase and (B) in the stage of nitrogen and phosphorus limitation; (C) aged culture in stationary phase in bright field visible light and (D) the same section in fluorescence mode after staining with Nile-red.

Passing all these previous steps, we obtained four potential production strains, one from the warm Mediterranean, two from cold arid and one from temperate oceanic climate zones. Unfortunately, we were not able to isolate thermophilic or psychrophilic cyanobacteria.

3.7. Evaluation of Growth and PHB Accumulation

The four strains *Chlorogloeopsis* sp. (isolate 4 from location Heinrichs, AUT), *Crocospaera* sp. (isolate 1 from Beninar, CZE), *Calothrix* sp. (isolate 1 from Pyhrabruck, AUT) and *Synechocystis* sp. (isolate 3 from IFA-Tulln, AUT) were grown in the 5-L tubular laboratory scale photobioreactor under photo-autotrophic non-sterile conditions in self-limiting 220 medium. In addition, IFA-3 and Heinrichs-4 were also cultivated outdoors in the same tubular photobioreactor without artificial illumination and without temperature control (see Appendix C, Figure A2). Examples of harvested dried biomasses are shown in Figure 6. *Synechocystis* sp. IFA-3 produced 7.9 g and *Chlorogloeopsis* sp. Heinrichs-4 produced 5.2 g dried biomass after three weeks cultivation in the 5-L photobioreactor containing 11.4 and 4.6% PHB, respectively.



Figure 6. Dried biomasses from cultivation of *Synechocystis* sp. IFA-3 (left) and *Chlorogloeopsis* sp. Heinrichs-4 (right) in the 5-L tubular photobioreactor.

The most noticeable outcomes of the upscaling experiments were the native resistance of *Synechocystis* sp. IFA-3 against grazing ciliates to which *Synechocystis* sp. CCALA192 and *Synechocystis* PCC6803, both were highly susceptible [19] and the wide cultivation temperature range between +4 and +45 °C of *Chlorogloeopsis* sp. Heinrichs-4. These two wild type isolates will be characterized more deeply and will be investigated for maximum growth and optimized PHB production. However, *Synechocystis* IFA-3 is a superior strain for outdoor cultivation in open low-tech photobioreactors in central Europe.

3.8. Obtaining Axenic Cultures

Different methods and combinations of methods were tested to obtain axenic cyanobacteria cultures. We started with chemical and growth-related methods, such as phototaxis, salt and temperature stress and applied different antibiotics techniques. All those did not yield us axenic cultures. Thus, we successively applied different physical methods, such as cell sorting, cell picking with a micromanipulator and a serial dilution method organized like the MPN method. Not one of those procedures did yield us axenic cultures on its own, only the sequential combination of all three physical methods succeeded.

3.8.1. Phototaxis

Despite literature reports about robust positive phototaxis of *Synechocystis* sp. PCC 6803 [34], we did not observe any directed movement of cyanobacterial cells, neither on plates with 0.4% nor with 1% agar (Figure 7). In general, cyanobacteria and heterotrophic bacteria grew better on plates with 0.4% agar.

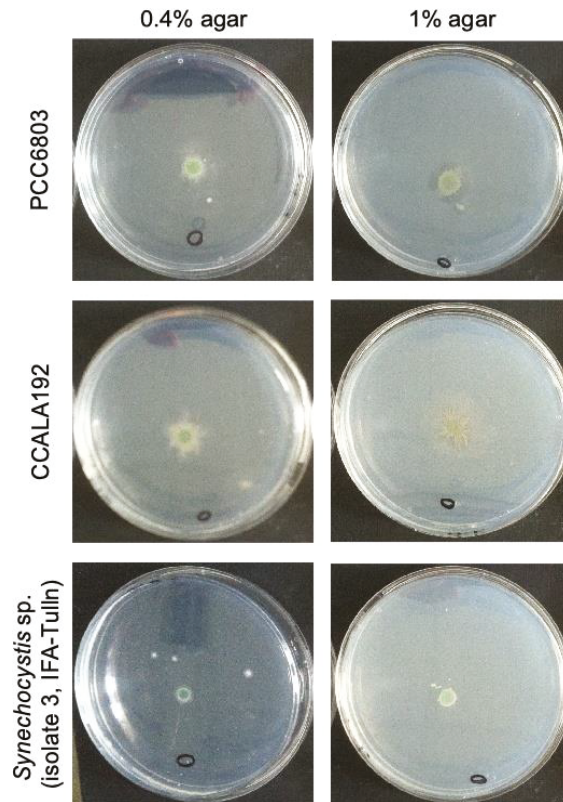


Figure 7. Results of the phototaxis experiment with cultures of PCC6803 (top), CCALA192 (middle) and *Synechocystis* sp. IFA-3 (bottom) on agar plates with 0.4% (left) and 1% agar (right). Circle: spot where glucose was applied.

The procedure is described as a simple and effective method for phototaxis-exhibiting flagellates and cyanobacteria. In contrast, it is not applicable for species with similar swimming capabilities and it is not possible to eliminate attached bacteria [20].

3.8.2. Antibiotic Treatment

In the first approach, carried out with *Synechocystis* PCC6803, neither cyanobacteria nor heterotrophic bacteria were reduced. In BG-I medium the cyanobacterial cell density increased from 1.2×10^7 to 1.6×10^8 mL^{-1} , while heterotrophs (reference) increased from 1.6×10^7 to 1.1×10^8 mL^{-1} . Even in BG-I+ medium cell densities increased—cyanobacteria from 1.2×10^7 to 3.6×10^8 mL^{-1} , heterotrophic bacteria (reference) from 1.6×10^7 to 3.3×10^8 mL^{-1} .

For the approach with the strains CCALA192 and *Synechocystis* sp. IFA-3 a similar picture was drawn. In BG-I CCALA192 increased from 4.0×10^6 to 2.2×10^8 cells mL^{-1} and heterotrophs from 3.5×10^6 to 4.1×10^7 cells mL^{-1} . *Synechocystis* sp. IFA-3 and its accompanying flora increased from 3.0×10^6 to 7.5×10^8 cells mL^{-1} and from 3.0×10^6 to 1.8×10^8 cells mL^{-1} , respectively. When glucose was added to the final medium the cell density of CCALA192 and heterotrophic bacteria increased as well—CCALA192: 1.0×10^6 to 4.6×10^7 cells mL^{-1} , accompanying flora: 6.5×10^6 to 1.7×10^7 cells mL^{-1} , the accompanying flora of *Synechocystis* sp. IFA-3: 2×10^6 to 6.1×10^9 cells mL^{-1} . *Synechocystis*

sp. IFA-3 in contrast did not grow after the antibiotic-treatment and the subsequent incubation in glucose containing medium.

3.8.3. Elevated Temperature and Salinity

At 22 °C and in BG-I medium *Synechocystis* PCC6803 reached a cell density of 6.4×10^8 cells mL⁻¹ and the heterotrophic bacteria 4.2×10^8 cells mL⁻¹. At 37 °C *Synechocystis* PCC6803 reached 6.4×10^8 cells mL⁻¹, but heterotrophs just 1.2×10^8 cells mL⁻¹. In BG-I+ medium (with glucose), heterotrophic bacteria had an advantage at 37 °C and reached 2.5×10^9 cells mL⁻¹ instead of 1.5×10^9 cells mL⁻¹ at 22 °C. It can be said that *Synechocystis* PCC6803 did not mind higher temperatures (37 °C), but the isolated cyanobacterial accompanying flora did (Figure 8).

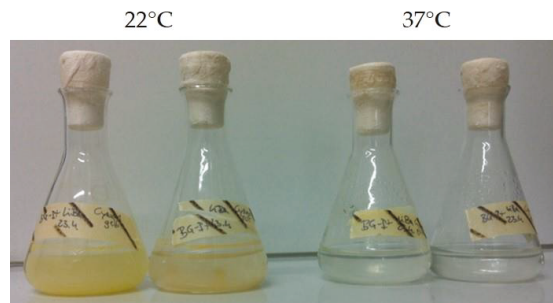


Figure 8. Growth of isolated cyanobacterial accompanying flora inoculated in BG-I medium at room temperature (22 °C) and elevated temperature (37 °C).

Synechocystis sp. IFA-3 reached a cell density of 1.3×10^8 mL⁻¹ in BG-I medium without salt at 22 °C, whereas with 4% NaCl just 1.6×10^7 cells mL⁻¹ were reached. At 37 °C 6.6×10^8 and 5.0×10^6 cells mL⁻¹ were obtained in 0% and 4% NaCl, respectively. The starting cell density was 1.2×10^7 cells mL⁻¹. A similar picture could be drawn for the heterotrophic cells which started at a cell density of 9×10^6 – 1×10^7 mL⁻¹. In the media with salt heterotrophic cells did not grow at all, in BG-I at 22 °C they grew best and reached a cell density of 5.8×10^7 mL⁻¹, at 37 °C they just reached 1.1×10^7 mL⁻¹. These results were also visible with bare eyes (Figure 9).

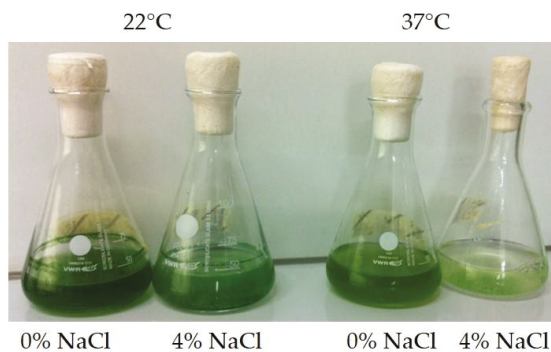


Figure 9. *Synechocystis* sp. IFA-3 inoculated in BG-I with and without NaCl at room temperature (22 °C) and elevated temperature (37 °C).

Methods using antibiotics or lysozyme are so called killing methods. According to Vu et al. (2018) advantages of these methods are that they selectively kill contaminations

over algae cells and that they can be combined with other methods to increase efficiency. Lysozyme can be used as an alternative for antibiotic-sensitive algae. Antibiotics can only be used to a limited extent for cyanobacteria, compounds are often toxic/mutagenic to algae. Additionally, beforehand the appropriate antibiotic type, concentration and treating time need to be evaluated and there is concern about the environmental impact of the spread of antibiotic-resistant microbes. In case of lysozyme, long exposure time needs to be considered since the cell membrane can be weakened [20].

3.8.4. Cell Sorter

Cultures of the three *Synechocystis* strains (PCC6803, CCALA192 and IFA-3) were counted and separated by cell size and chlorophyll fluorescence intensity into two collected and one waste fraction. The waste fraction was almost colorless and contained mostly heterotrophic bacteria and unidentified cell fragments (controlled by microscopy) while cyanobacteria of the typical spherical cell shape, but of different sizes (3–4 and 5–6 µm) were found in the other two fractions. The cyanobacteria fractions contained roughly one million cells each.

After cultivation in BG-I medium for two weeks, the cultures were inspected and turned out to be still not axenic. Furthermore, cell sizes were distributed in the same ranges as before, independent from the cultivated fraction. A second cell sorting with each of those cultures gave a similar, almost identical separation into one waste and two fractions of *Synechocystis* sp. in two cell size classes.

While cell sorting appeared to be not suitable for obtaining axenic cultures, the meaning of parallel existence of two cell sizes in a culture of a single-species *Synechocystis* strain remains unclear.

3.8.5. Micromanipulator

Several attempts were made to pick a small number of cyanobacteria cells from a single-species non axenic culture of each of the three *Synechocystis* strains (PCC6803, CCALA 192 and IFA-3). The number of picked cells was always in the range of 5 to 20.

As described by Vu et al., 2018 [20], it was hard to catch the tiny *Synechocystis* cells but avoid catching heterotrophic bacteria. Therefore, only the cultures obtained from the commercial culture collections and those which had comparably low numbers of heterotrophic bacteria from the selection cultures (as described in Sections 3.2–3.4) were used.

We achieved new cultures of all three strains that contained a lower variety of heterotrophic bacteria (compared by cell sizes and shapes from microscopic inspection), but we were not able to obtain axenic cultures with this method.

3.8.6. MPN Dilution Approach

Serial dilutions have the advantage of being simple and suitable to isolate new algal species from environmental samples. According to Vu et al. (2018), only monoculture levels can be achieved and this method is only suitable for organisms that are abundant in the sample and is largely ineffective for rare organisms [20].

We used the previously enriched cyanobacteria cultures of the three *Synechocystis* strains PCC6803, CCALA192 and IFA-3, which we obtained after the micromanipulator process. This increased the chance to get single cyanobacteria cells separated from the, meanwhile, lower number of heterotrophic bacteria distributed over the 24 wells of the plate. Cultivation times were four to six weeks for each trial until enough cells were grown in the wells to allow microscopic control. Putative axenic cultures were transfer into shaking flasks with BG-I medium and were controlled weekly.

After several separation cycles we obtained axenic cultures from PCC6803 and CCALA192 and one culture from *Synechocystis* sp. IFA-3 which contained a low number of only one coccoid heterotrophic bacteria type of ca. 1–1.5 µm diameter. We have strong evidence that these bacteria are obligate synergists to *Synechocystis* sp. IFA-3, as all further trials to separate

them resulted either in a culture with the heterotrophic bacteria present or in no growth at all.

3.9. All Efforts from Isolation to Axenic Cultures in Summary

The choice of sampling sites is always determined by the goal to be achieved. In our case, we hoped to find strains which were adapted to warm (Mediterranean) and other adapted to cool or cold (alpine) climate.

A selection for fastest growing strains by frequent transfer of mixed cultures into new mineral medium was the most obvious procedure to search for potential production strains suitable for biotechnological processes and was comparably easy to achieve. The frequent transfers reduced heterotrophs, as accumulation of dead cells (and of potential organic substrate) was held at a minimum.

Getting rid of eukaryotic microorganisms succeeded in the majority of cases at the first attempt by cycloheximide addition. However, we lost about one third of the isolates which previously contained fast growing cyanobacteria due to the application of antibiotics. Especially all of the samples deriving from habitats in cold environments showed increased susceptibility.

The highest effort of all was the purification to axenic cultures. Especially all of the chemical (media composition, salinity), the temperature and the phototaxis approaches failed completely. By empirical trial and error attempts, we were able to reduce the amount and diversity (checked by morphological criteria via light microscopy) of the accompanying flora. The steps were a twofold sequential separation of cells by size and optical properties in the cell sorter, followed by multiple sequential cell picks with the micromanipulator. This resulted in cultures that showed a significantly reduced number of cell shapes in comparably low abundances as remaining accompanying flora and which were dominated by the cyanobacteria cells. The dilution method was the final necessary step to obtain axenic cultures from those pre-purified cultures, and even this method had a high failure rate.

We succeeded in getting axenic *Synechocystis* cultures from the non-axenic products obtained from commercial culture collection strains PCC6803 and CCALA192. The wild type IFA-3 refused to grow as axenic culture, its accompanying coccoidal bacteria are, most probably, obligate synergists.

4. Conclusions

Sampling 25 locations from so different sites as a geyser in Iceland, a wet rock in the Dolomite Alps, a dammed lake in southern Spain, a glacier lake in Argentina and a snow field in Greenland resulted in 71 primary cultures of which 34 were growing stable over multiple medium transfers. 19 among those were purified into single-species cyanobacteria strains and identified. Only four of them were producing and accumulating PHA or PHB and were tested in a tubular laboratory photobioreactor, and only two are promising production strains that can be cultivated in open non-axenic photobioreactors without artificial illumination and without temperature control.

The lessons learned from three years of collecting, cultivating and characterizing wild type cyanobacteria strains and two additional years of preparing axenic cultures are (1) to be patient and (2) to purify only those isolates into axenic cultures that are intended for advanced molecular analysis, such as transcriptomics or genetic manipulations. We achieved production of biomass and PHA or PHB under rough outdoor conditions from non-axenic strains with acceptable biomass growth and with promising PHA or PHB production rates. For the purpose of this work, it was of primary importance to find strains that are adapted to the local climate and can be grown outdoors with the lowest effort for process control. Sure, we would have been happy to find a strain that would have outgrown all others while accumulating the highest PHA or PHB amounts. However, that did not happen.

It is not without a certain irony that among the samples collected from almost all over the world, a strain isolated from the fire pond in front of the institute building showed the most rapid growth and the best PHB production characteristics.

Axenic cultures and *Synechocystis* sp. IFA-3 will be deposited at Culture collection of Autotrophic Organisms (CCALA). Investigations on the putative obligate synergism of the IFA-3 culture is already in work, and the upscaling and growth optimization of the *Chlorogloeopsis* Heinrichs-4 isolate will be the topic of upcoming research.

Author Contributions: Conceptualization, K.M. and I.F.; methodology, K.M., C.D., L.B. and I.F.; investigation, K.M., C.D., L.B.; resources, I.F.; data curation, K.M., C.D., L.B., I.F.; writing—original draft preparation, K.M., I.F.; writing—review and editing, K.M., I.F., B.D.; visualization, K.M.; supervision, I.F.; project administration, I.F., B.D.; funding acquisition, I.F., B.D. All authors have read and agreed to the published version of the manuscript.

Funding: Open Access Funding by the Austrian Science Fund (FWF) [Project PHBecol—The ecological role of poly-hydroxybutyrate in cyanobacteria, grant no. I 4082-B25], Austrian Research Promotion Agency [Projects CO2USE—Utilization of CO₂ from flue gas by photosynthetic biomass, project no. 834422; CO2USE+EPP—Increasing the economic viability of utilizing CO₂ from flue gas to produce biogas and bioplastic with photoautotrophic cyanobacteria, e.g., grant no. 848783].

Institutional Review Board Statement: Not applicable.

Informed Consent Statement: Not applicable.

Data Availability Statement: Not applicable.

Acknowledgments: The authors thank the colleagues at the Institute for Environmental Biotechnology at IFA-Tulln for their support.

Conflicts of Interest: The authors declare no conflict of interest.

Appendix A. Cycloheximide Performance Test

Mixed incubation in BG-I medium with addition of 100 mg L⁻¹ cycloheximide was tested in a preliminary experiment. For this purpose, mixed cultures were prepared from pure cultures and incubated in parallel in BG-I medium with and without cycloheximide. From the flasks with cycloheximide, only cyanobacteria were found after five days of incubation, but no living green algae (Figure A1). From all wild strain isolates where cyanobacteria were still detectable in the microscope after at least two media transfers, parallel mounts were incubated in BG-I medium with cycloheximide. In none of these 29 preparations were living cells still found after 5–6 days of incubation.

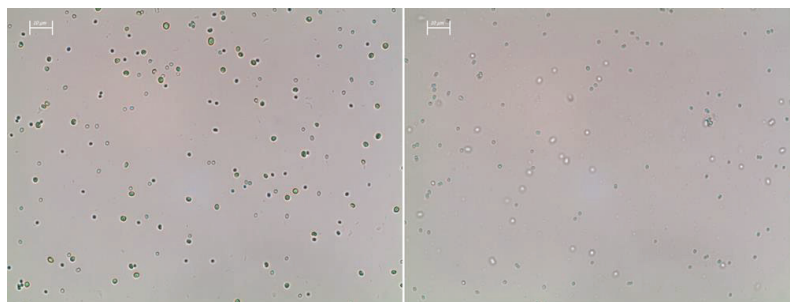


Figure A1. Mixed culture of *Muriella* sp. and *Synechocystis* sp. cultivated 5 days in BG-I medium. (left): without cycloheximide, (right): medium with 100 mg cycloheximide per liter. Scale bar: 10 μ m.

Appendix B. Sequences of Cyanobacteria Isolates

>Beninar4

GGCTGGAaCGGTCGCTanCnCccgaTGTGCCGgnnGgTGAAATATTTATAGCCtgtgga
TGAGCTTGCCTGTGATTAGCTAGTTGGAGTGGTAAACGGCACACCAAGGCGACAATC
AGTAACTGGTCTgAGAGGATGACCAGTCACACTGGGaCTGAGAnncGGCccaGACTCC
TACCGGAGGCAGCAGTGGGGAATTTCCGCAATGGGCGAAAGCCTGACGGAGCAA
TACCGCGTGAGGGATGAAGGTTCTGTTGATTGTAACCTCTTTTTTCAGGGAAGaTAA
TGACGGTACCTGAAGAATAAGCATCGGCTAACTCCGTGCCAGCAGCCGCGGTAAGA
CGGAGgaTGCAAGCGTTATCCGGAATTATTGGGCGTAAAGCGTACGCAGGTGGCCCA
TCAAGTCTATTGTCAAagAGCAGAGCTCAACTCTGTAAAGGCGATAGAACTGGTGA
GCTAGAGTATGGTAGGGGACAGGAGGAATCCCAGTGTAGCGGTGAAATGCGTAGAT
ATTGGGAAGAACCAGtGGCGAAAgCGTCTGCCAaGCCAAAAGTgACACTCATGTA
cgAAAgCTAGGgagnAAaaggaTTAnntACCCcAGTAGTCAa

>Greifenstein1

gcGtcagTTGagnnCcAGCAGgacGCTTtCGCCACTggtGTTCTTCCAGATATCTACGCA
TTTCACCGCTACACCTGGAATTCCTCCTGCCCTATCTCTCTAGTCTCACAGTTTCC
ATTGCCGATCCAAGGTTGAGCCTCGGCTTTGACAACAGACTTATCAAACAGCCTAC
GTACGCTTACGCCCAATAATTCCGGATAACGCTTGCATCCTCCGTCTTACCGCGGT
GCTGGCACGGAGTTAGCCGATGCTTATTCTGTTAGGTACCGTCATTATCTTCCCTAACA
AAAGAGGTTTACAACCCACAGGCCTTCGTCCCTCACGCGGATTGCTCCGTCAGGCT
TTCGCCATTGCGGAAAATTCCCCACTGCTGCCTCCCGTAGGAGTCTGGGCCGTGTC
TCAGTCCCAGTGTGACTGGTCATCCTCTCAGACCAGTTATCGATCGTCGCCATGGTAG
GCCGTTACCCACCATCTAGCTAATCGAACGCAAGCTCATCTACAGGCATTAAAACCT
TCACCCGAAGGCATATCCGGTATTAGCAGTCATTTCTAACTGTTGCCGAACCTATAG
GTAGATTCTTACGCGTTancaaCCngTCCGa

>Greifenstein2

cngcGtcagTTGAgaTCcAGCAGGacGCTTtCGCCACTGgtGTTCTTCCAGATATCTACG
CATTTACCGCTACACCTGGAATTCCTCCTGCCCTATCTCTCTAGTCTCACAGTTT
CCATTGCCTTTACAAGGTTGAGCCTCGCGCTTTGACAACAGACTTATCAAACAGCCT
ACGTACGCTTACGCCCAATAATTCCGGATAACGCTTGCATCCTCCGTCTTACCGCGG
CTGCTGGCACGGAGTTAGCCGATGCTTATTCTGTTAGGTACCGTCATTATCTTCCCTAA
CAAAAAGAGGTTTACAATCCACAGACCTTCGTCCCTCACGCGGATTGCTCCGTCAGG
CTTTGCCCATTTGCGGAAAATTCCCCACTGCTGCCTCCCGTAGGAGTCTGGGCCGT
GTCTCAGTCCCAGTGTGACTGGTCATCCTCTCAGACCAGTTATCGATCGTCGCCATG
GTAGGCCGTTACCCACCATCTAGCTAATCGAACGCAAGCTCATCTACAGGCATTAA
AACTTTACCCGAAGGCACATCCGGTATTAGCAGTCATTTCTAACTGTTGCCGAA
CCTATAGGTAGATTCTTAncGTancaaCCcGTCCGa

>Grönland3

tgnnCGTcaGTTatGGCCcAGCAGAGCGCCTTCGCCACTggtGTTCTTCCCGATATCTA
CGCATTTACCGCTACACCGGGAATTCCTCCTGCCCTACACACTCAAGCCTTGTA
GTTTCCATCGCTGAAATGGAGTTAAGCTCCACGCTTAAACGACAGACTTACAAGGCC
GCCTGCGGACGCTTACGCCCAATAATTCCGGATAACGCTTGCCTCCCGTATTACC
GCGGCTGCTGGCACGGAATTAGCCGTGGCTTATTCTCAAGTACCGTCATGTCTTCT
CCTTGAGAAAAGAGGTTTACAGCCCAGAGGCCTTATCCCTCACGCGGCGTGTCTCC
GTCAGGTTTTCGCCATTGCGGAAAATTCCCCACTGCTGCCTCCCGTAGGAGTCTGG
GCCGTGCTCAGTCCCAGTGTGGCTGATCATCCTCTCAGACCAGTACTGATCGTCG
CCTTGGTGGCCATTACCCACCAACTAGCTAATCAGACGCGGCTCATCTCAGGC
GAAATTCATTTACCTCTCGGCATATGGGTTATTAGCGGCCGTTTCCGGCCGTTATCC
CCCTCCTGAGGGCAaTTCCCAcgcGTTanc

>großeTulln1

tnagCGtCaGTTGagatCCAGCAGgaCGCTTtCGCCACTggtGTTCTTCCAGATATCTA
CGCATTTACCGCTACACCTGGAATTCCTCCTGCCCTATCTCTCTAGTCTCACAG
TTTCCATTGCCGATCCAAGGTTGAGCCTCGGGCTTTGACAACAGACTTATCAAACAG
CCTACGTACGCTTTACGCCCAATAATTCCGGATAACGCTTGCATCCTCCGTCTTACCG
CGGCTGCTGGCACGGAGTTAGCCGATGCTTATTCTGTTAGGTACCGTCATTATCTTCC
TAACAAAAGAGGTTTACAACCCACAGGCCTTCGTCCCTCACGCGGATTGCTCCGTC

AGGCTTTCGCCATTGCGGAAAATCCCCACTGCTGCCCTCCCGTAGGAGTCTGGGCC
 GTGTCTCAGTCCCAGTGTGACTGGTCATCCTCTCAGACCAGTTATCGATCGTCGCCAT
 GGTAGGCCATTACCCACCATCTAGCTAATCGAACGCAAGCTCATCTACAGGCATTA
 AAACCTTTCACCCGAAGGCATATCCGGTATTAGCAGTCATTTCTAACTGTTGTCCCGAA
 CCTATAGGTAGATTCTTACGCGTtc

>großeTulln3

gtcngTtGAGatcncGCAGGAcGcnTTTcnGCcACTGGTGTtncTTCnAGATATCTACGC
 ATTTACCGCTACACCTGgAaTTCCCTCTGCCCTATCTCTCTAGTCTCACAGTTTC
 CATTGCCGATCCAAGGTTGAGCCTCGGGCTTTGACAAACAGACTTATCAAACAGCCT
 ACGTACGCTTTACGCCAATAATTCCGGATAACGCTTGCATCCTCCGCTTACCAGCG
 GCTGTGGCACGGAGTTAGCCGATGCTTATTTCGTTAGGTACCGTCATTATCTTCCCTA
 ACAAAGAGGTTTACAACCCACAGGCCTTCGTCCCTCACGCGGTATtGCTCCGTCA
 GGCTTTCGCCCATTTGCGGAAAATCCCCACTGCTGCCTCCCGTAGGAGTCTGGGCC
 GTGTCTCAGTCCCAGTGTGACTGGTCATCCTCTCAGACCAGTTATCGATCGTCGCCA
 TGGTAGGCCATTACCCACCATCTAGCTAATCGAACGCAAGCTCATCTACAGGCATT
 AAAACTTTCACCCGAAGGCATATCCGGTATTAGCAGTCATTTCTAACTGTTGTCCCG
 AACCTATAGGTAGATTCTTACGCGTta

>IFATeich1

anTTGCGGCCTAGCAGAGCGCTTtCGCCACCGgtgTTCTTCTGATCTCTACGCAT
 TTCACCGCTACACCAGGAATTCCCTCTGCCCGAACGCACTCTAGTCTTGTAGTTTC
 CACTGCCCTTATGCGGTTAAGCCGCACGCTTTAAACAATAGACTTACAAAACCACCTG
 CGGACGCTTTACGCCAATCATTCCGGATAACGCTTGCATCCTCCGTATTACCAGCGG
 CTGCTGGCACGGAGTTAGCCGATGCTTATTCTCAGGTACCGTCATCATCTTCCCTGA
 GAAAAGAGGTTTACAACCCAAGAGCCTTCTCCCTCACGCGGTATTGCTCCGTGAG
 GCTTTCGCCCATTTGCGGAAAATCCCCACTGCTGCCTCCCGTAGGAGTCTGGACCGT
 GTCTCAGTTCAGTGTGGCTGATCATCCTCTCAGACCAGCTACTGATCGCAGCCTTG
 GTAGTCCATTACACCACCAACTAGCTAATCAGACGCGAGCTCATCTCTTGGCAATTA
 ATCTTTCACCCGTAGGCACATCCGGTATTAGCAGCCGTTTCCAACCTGTTGTCCCGAA
 CCAAAAAGGCAGATTCTCACGCGTta

>IFATeich3

CctcagtGtcagTTtcaGCCAGTAGCACGCTTtCGCCACCGATGTTCTTCCCAATATC
 TACGCATTTACACCGCTACACTGGGAATTCCTGCTACCCCTACTGACTCTAGTCTTGC
 AGTTTCCACCGCTCTTATGGAGTTAAGCTCCATTCTTTAACAGCAGACTTGCAAAAC
 CACCTACGGACGCTTTACGCCAATAATTCCGGATAACGCTTGCATCCTCCGTATTAC
 CGCGGCTGCTGGCACGGAGTTAGCCGATGCTTATTATCAGGTACCGTCATTTTTTTC
 TTCCCTGATAAAAAGAGGTTTACAATCCAAGGACCTTCTCCCTCACGCGGTATTGCT
 CCGTCAGGCTTTCGCCCATTTGCGGAAAATCCCCACTGCTGCCTCCCGTAGGAGTCT
 GGGCCGTGTCTCAGTCCAGTGTGGCTGCTCATCCTTTCAGAACAGACTACTGATCGT
 TGCCATGGTAGGCTTTACCCACCATCTAGCTAATCAGACGCGAGCCCATCTTCAG
 ACGATAAATCTTTCACCTTTCGGCACATTGGGTATTAGCAGTCGTTTCCAACCTGTTGT
 CCCCATTCTGAAGGCAGGTTCTCACGCG

>IFATeich4

ttCngcGTcagTTGAGATCCAGCAGGACGCTTtCGCCACTggtGTTCTTCCAGATATC
 TACGCATTTACCGCTACACCTGGAATTCCTCTGCCCTATCTCTCTAGTCTCAC
 AGTTTCCATTGCCGATCCAAGGTTGAGCCTCGGGCTTTGACAAACAGACTTATGAAAC
 AGCTACGTACGCTTTACGCCAATAATTCCGGATAACGCTTGCATCCTCCGTCTTAC
 CGCGGCTGCTGGCACGGAGTTAGCCGATGCTTATTTCGTTAGGTACCGTCATTATCTTC
 CCTAACAAAAGAGGTTTACAACCCACAGGCCTTCGTCCCTCACGCGGTATtGCTCCG
 TCAGGCTTTCGCCCATTTGCGGAAAATCCCCACTGCTGCCTCCCGTAGGAGTCTGGG
 CCGTGTCTCAGTCCCAGTGTGACTGGTCATCCTCTCAGACCAGTTATCGATCGTCGC
 CATGTTAGGCCGTTACCCACCATCTAGCTAATCGAACGCAAGCTCATCTACAGGC
 ATAAAACCTTTCACCCGAGGGCATATCCGGTATTAGCAGTCATTTCTAACTGTTGTCC
 CGAACCTATAGGTAGATTCTTACGCGt

>Steg2

aCGGCCGgAaCGGCCGCTAaTACCCcATATGCCGagaGGTGAAATGAATTCGCTT
gaggatGAGCCCCGCTGCTGATTAGCTAGTTGGTGGGGTAATGGCCACCAAGGCGACG
ATCAGTAGCTGGTCTGAGAGGATGATCAGCCACACTGGGACTGAGACACGGCCCA
GACTCCTACGGGAGGCAGCAGTGGGGAATTTCCGCAATGGGCGAAAGCCTGACG
GAGCAACGCGCGTGAGGGATGAAGGCCCTCTGGGCTGTAAACCTCTTTTCTCAAGG
AAGAAGACATGACGGTACTTGAGGAATAAGCCACGGCTAATTCGCTGCCAGCAGC
CGCGGTAATACGGGAGTGGCAAGCGTTATCCGGAATTATTGGGCGTAAAGCGTCCG
CAGGCGGCCTTGTAAGTCTGTCTGTTAAAGCGTGGAGCTTAACTCCATTGAGCGATG
GAAACTACAAGGCTTGAGTGTGGTAGGGGCAGAGGGAATTCGCGGTGTAGCGGTG
AAATGCGTAGATATCGGGAAGAACACCAGTGGCGAAGGCGCTCTGCTGGGCCATA
ACTGACGCTCATGGACGAAAGCCAGGGGAGcAaAGGGATTAGATACCCcGTAgtaa

>Steg1

ttncgcAAAtggGCGAAAGCCTGACGGAGCAACGCCGCGTGAGGGATGAAGGCCTC
TGGGCTGTAAACCTCTTTTCTCAAGGAAGAAGACATGACGGTACTTGAGGAATAAG
CCACGGCTAATTCCTGTCCAGCAGCCGCGTAATACGGGAGTGGCAAGCGTTATCC
GGAATTATTGGGCGTAAAGCGTCCGACGGCGCCTTGTAAGTCTGTCTGTTAAAGCG
TGGAGCTTAACTCCATTGAGCGATGGAAACTACAAGGCTTGAGTGTGGTAGGGGC
AGAGGGAATTCGCGGTGTAGCGGTGAAATTCGCTAGATATCGGGAAGAACACCAGT
GGCGAAGGCGCTCTGntnGGCCAtaActgaCg

>Admont5

cngcGTtagTtgagaTCCAGCAGcngcCTTTCGCCACTggTGTCTTCCAGATATCTACG
CAITTCACCGCTACACCTTggaAaTTCCTCTGCCCTATCTCTCTAGTCTCACAGTTT
CCATTGCCGATCCAAGGTTGAGCCTCGGGCTTTGACAACAGACTTATCAAAACAGCC
TACGTACGCTTTACGCCCAATAATTCGGATAACGCTTGCATCTCCGTCTTACCGCG
GCTGCTGGCACGGAGTTAGCCGATGCTTATTCGTTAGGTACCGTCATTATCTTCCCTA
ACAAAAGAGGTTTACAACCCACAGGCCTTCGTCCCTCACGCGGTATTGCTCCGTCA
GGCTTTCGCCATTGCGGAAAATTCCCCACTGCTGCCTCCCGTAGGAGTCTGGGCC
GTGTCTCAGTCCAGTGTGACTGGTCATCTCTCAGACCAGTTATCGATCGTCGCCA
TGGTAGGCCATTACCCACCATCTAGCTAATCGAACGCAAGCTCATCTACAGGCATT
AAAACTTTACCCGAAGGCATATCCGGTATTAGCAGTCATTTCTAACTGTTGTCCCG
AACTATAGGTAGATTCTTACGCGTACTCACCCGTCCGgA

>grosseTulln2

CGTtagTTATGGCCcaGCAGAGCGCCTTCGCCACTGGTGTCTTCCCGATATCTAC
GCATTTACCGCTACACCGGAATTCCTCTGCCCTACCACACTCAAGCCTTGTAG
TTTCCATCGCTGAAATGGAGTTAAGTCCACGCTTTAACGACAGACTTACAAGGCC
GCCTGCGGACGCTTTACGCCCAATAATTCGGATAACGCTTGGCACTCCCGTATTAC
CGCGGTGTGGCACGGAATTAGCCGTGGCTTATTCCTCAAGTACCGTCATGTCTTC
TTCCTTGAGAAAAGAGGTTTACAGCCAGAGGCCCTTACCCCTACGCGCGGTTGC
TCCGTACGGCTTTCGCCATTGCGGAAAATTCCCCACTGCTGCCTCCCGTAGGAGTC
TGGGCCGTGTCTCAGTCCCAGTGTGGCTGATCATCTCTCAGACCAGCTACTGATCG
TCGCCTTGGTGGGCCATTACCCACCAACTAGCTAATCAGACGCGGGCTCATCTCA
GGCGAAATTCATTCACCTCTCGGCATATGGGGTATTAGCGGCCGTTTCCGGCCGT
ATCCCCCTCTGAGGGCAGATTcnnACGCGTACTCACCCGTCCGgA

>Branna1

agngTcnGTTacGgCCTAGCagagCGCCTTCGCCACCgggtTCTTCCtgaTCTCTACGC
ATTTACCGCTACACCAGGAaTTCCTCTGCCCGAACGTACTCTAGCTGTGTAGTTT
CCACTGCTTTTATGAGGTTAAGCCTCACTCTTTAACAGCAGACTTACATTGCCACCT
GCGGACGCTTTACGCCAATCATTCGGATAACGCTTGCATCTCCGTATTACCGCG
GCTGCTGGCACGGAGTTAGCCGATGCTTATTCCTCAAGTACCTTACGTTCTTATTCT
TGAGAAAAGAGGTTTACAACCCAAAGAGCCTTCTCCCTCACGCGGTATTGCTCCGT
CAGGCTTTCGCCATTGCGGAAAATTCCCCACTGCTGCCTCCCGTAGGAGTCTGGG
CCGTGTCTCAGTCCCAGTGTGGCTGATCATCTCTCAGACCCTACTGATCGTTCGC
CTAGGTGCGCTTACCACACCTACTAGCTAATCAGACGCGAGCTCATCTTACGGCA

GTTAACCTTTCACCTTTCGGCACATCCGGTATTAGCCACCGTTTCCAGTGGTTGTCCC
CGACCTCAAGCTAGannTCACgmnTTACTCACCCGTCGGgaga

>Branna2

tnGtCCtnagTGtcagTtaCGGCCTAGCAGAGCGCCTTCGCCACCGGTGTTCTCCTG
ATCTCTACGCATTTACCGCTACACCAGGAATTCCTCTGCCCCGAACGTA CTCTAG
CTGTGTAGTTTCCACTGCTTTTATGAGGTTAAGCCTCACTCTTTAACAGCAGACTTAC
ATTGCCACCTGCGGACGCTTTACGCCAATCATTCCGGATAACGCTTGCATCCTCCG
TATTACCGCGGCTGCTGGCACGGAGTTAGCCGATGCTTATTCCTCAAGTACCTTCAG
TTCTTATTCTTGAGAAAAGAGGTTTACAACCCAAGAGCCTTCCTCCCTCACGCGGT
ATTGCTCCGTCAGGCTTTTCGCCATTGCGGAAAATTCCTCACTGCTGCCTCCCGTAG
GAGTCTGGGCCGTGCTCAGTCCCAGTGTGGCTGATCATCCTCTCAGACCAGACTACT
GATCGTCGCCTAGGTGCGCTTTACCACACCTACTAGCTAATCAGACGCGAGCTCAT
CTTCAGGCAGTTAACCTTTCACCTTTCGGCACATCCGGTATTAGCCACCGTTTCCAG
TGTTGTCCCCGACCTCAAGCTAGATTCTCAcGCGTIncaaCCgtCCGa

>Branna3

annGTcaGTTacGGCCTAGCAGAgCGCCTTCGCCACCGGTGTTCTCCTGATCTCTA
CGCATTTACCGCTACACCAGGAATTCCTCTGCCCCGAACGTA CTCTAGCTGTGTA
GTTTCCACTGCTTTTATGAGGTTAAGCCTCACTCTTTAACAGCAGACTTACATTGCCA
CCTGCGGACGCTTTACGCCAATCATTCCGGATAACGCTTGCATCCTCCGTATTACC
GCGGCTGCTGGCACGGAGTTAGCCGATGCTTATTCTCAAGTACCTTCAGTTCTTATT
CCTTGAGAAAAGAGGTTTACAACCCAAGAGCCTTCCTCCCTCACGCGGTATTGCTC
CGTCAGGCTTTCGCCATTGCGGAAAATTCCTCACTGCTGCCTCCCGTAGGAGTCTG
GGCCGTGTCTCAGTCCCAGTGTGGCTGATCATCCTCTCAGACCAGCTACTGATCGTC
GCCTAGGTGCGCTTTACCACACCTACTAGCTAATCAGACGCGAGCTCATCTTCAGG
CAGTTAACCTTTCACCTTTCGGCACATCCGGTATTAGCCACCGTTTCCAGTGGTTGTC
CCCCACCTCAAGCTAagannnnnCGCGTTACTnaaCCCCGTCCG

>Branna4

GTcnGTTAcGGCCTAGCAGAGCGCCTTCGCCACCGGTGTTCTTCctgaTCTCTACG
CATTTACCGCTACACCAGgAaTTCCCTCTGCCCCGAACGTA CTCTAGCTGTGTAGTT
TCCACTGCTTTTATGAGGTTAAGCCTCACTCTTTAACAGCAGACTTACATTGCCACC
TGCGGACGCTTTACGCCAATCATTCCGGATAACGCTTGCATCCTCCGTATTACCCG
GGCTGCTGGCACGGAGTTAGCCGATGCTTATTCTCAAGTACCTTCAGTTCTTATTCC
TTGAGAAAAGAGGTTTACAACCCAAGAGCCTTCCTCCCTCACGCGGTATTGCTCCG
TCAGGCTTTCGCCATTGCGGAAAATTCCTCACTGCTGCCTCCCGTAGGAGTCTGGG
CCGTGTCTCAGTCCCAGTGTGGCTGATCATCCTCTCAGACCAGCTACTGATCGTCGC
CTAGGTGCGCTTTACCACACCTACTAGCTAATCAGACGCGAGCTCATCTTCAGGCA
GTTAACCTTTCACCTTTCGGCACATCCGGTATTAGCCACCGTTTCCAGTGGTTGTCCC
CGACCTCAAGCTAGaTtnncACGCGTTaccaCCCCGTCCGa

>Branna5

cagtGtcagTTGCGGCCTAGCAGAGCGCTTcGCCACCGgtGTTCTCCTGATCTCTA
CGCATTTACCGCTACACCAGGAATTCCTCTGCCCCGAACGTA CTCTAGCTGTGTA
GTTTCCACTGCCCTTATGCGGTTAAGCCGCACGCTTTAACAAATAGACTTACAAAACC
ACCTGCGGACGCTTTACGCCAATCATTCCGGATAACGCTTGCATCCTCCGTATTAC
CGCGGTGCTGGCACGGAGTTAGCCGATGCTTATTCTCAGGTACCGTCACTCATCTT
CCCTGAGAAAAGAGGTTTACAACCCAAGAGCCTTCCTCCCTCACGCGGTATTGCTC
CGTCAGGCTTTCGCCATTGCGGAAAATTCCTCACTGCTGCCTCCCGTAGGAGTCTG
GACCGTGTCTCAGTTCAGTGTGGCTGATCATCCTCTCAGACCAGCTACTGATCGCA
GCCTTGGTAGTCCATTACACCACCACTAGCTAATCAGACGCGAGCTCATCTTTGG
CAATTAATCTTTCACCCGTAGGCACATCCGGTATTAGCAGCCGTTTCCA ACTGTTGTC
CCGAACCAAAAAGGCAGannntCACgngTTACtCACCCGTCCg

>Branna6

agcgtcngTTGagatCCAGCAGgacgCTTTCGCCACTggtgTTCTTCCAGATATCTACGCA
TTTACCCGCTACACCTGGAATTCCTCCTGCCCTATCTCTCTCTAGTCTCACAGTTTC
CATTGCCTTTCCAAGGTTGAGCCTCGGGCTTTGACAACAGACTTATAAAACAGCCTA

CGTACGCTTACGCCAATAATCCGGATAACGCTTGCATCCTCCGTCTTACCGCG
CTGCTGGCACGGAGTTAGCCGATGCTTATTCGTTAGGTACCGTCATTATCTCCCTAA
CAAAAGAGGTTTACAATCCACAGACCTTCGTCCCTACACGGGATTGCTCCGTCAG
GCTTTCGCCATTGCGGAAAATCCCCACTGCTCCCTCCCGTAGGAGTCTGGACCGT
GTCTCAGTTCAGTGTGACTGGTATCCTCTCAGACCAGTTACCGATCGTCGCCATG
GTGTGCCGTTACCACTCCATCTAGCTAATCGGACGCAAGCTCATCTACAGGCATTTA
AACTTTCACCCGAAGGCACATCCGGTATTAGCAGTCATTCTAACTGTTGCCGAA
CCTATAGGTAGATTCTTACGcnTtacna

>Heinrichs1

agnGtcagTTCaGGCCcAGTAGAGCGCTTtCGCCACTGGTGTCTTCCAGATATCTAC
GCATTTACCCGCTACACCTGGAATTCCTCTACCCCTACCGAACTCTAGTCTCTCAG
TTTCCACTCCCTTTACAAGGTTAAGCCTCGCGCTTTGAAAGCAGACTTGATAAAACA
CCTGCGGACGCTTTACGCCAATAATCCGGATAACGCTTGCATCCTCCGTCTTACC
GCGGCTGTGGCACGGAGTTAGCCGATGCTTATTCCTCAGGTACCGTCAGGTTTCTT
CCCTGAGAAAAGAGGTTTACGACCCAAGAGCCTTCTTCCCTCACGCGGTATTGCTC
CGTCAGGCTTTCGCCATTGCGGAAAATCCCCACTGCTGCCTCCCGTAGGAGTCTG
GGCGGTGCTCAGTCCCAGTGTGGCTGATCATCCTCTCAGACCAGCTACTGATCATT
GCCTTGGACGGCTTTACCCCAACCAACTAGCTAATCAGACGCGAGCACTTCCCTTG
GCAATAAATCTTTACCTTTCGGCACATTCGGTATTAGCAGTCGTTTCCAAGTGTGT
CCCGAACCAAGGGGCGGTTTCTCACGCGTTTaccacCCCGTCCGaana

>Heinrichs3

agtGTcnGTaTnGTCCTAGCAGAGCGCTTtCGCCACCGGTGTTCTTCCCAATCTCTA
CGCATTTACCCGCTACACTGGGAATTCCTCTACCCCTAACATACTCTAGTCTTATAG
TTTCCACTGCCTGTATGTGTTGAGCCACACGCTTTAACAGCAGACTTACAAAACCA
CCTGCGGACGCTTTACGCCAATCATTCCGGATAACGCTTGCATCCTCTGATTACCG
CGGCTGTGGCACAGAGTTAGCCGATGCTTATTCCTCAAGTACCGTCAtnATCTTCTT
TGAGAAAAGAGGTTTACGACCCAAAAGCCTTCGTCCCTCACGCGGTATTGCTCCGT
CAGGCTTTCGCCATTGCGGAAAATCCCCACTGCTGCCTCCCGTAGGAGTCTGGA
CCGTGTCTCAGTTCAGTGTGGCTGATCGTCTCTCAGACCAGCTACAGATCGATGC
CTAGGTAGTCTCTTACACCACCTACTAGCTAATCTGACGCGGAGTCAaTtnCAGGCAA
TTAATCTTACCTTTCGGCACATTCGGTATTAGCAGTCATTCTAACTGTTGCCG
GACCTGAAGanaGATTCTCACGCGTTTaccacCCCGTCCGa

>Heinrichs4

gnCCtnaggtcagTTGCAGCCTAGCAGGgCGCTTTCGCCACCggtgTTCTTCTGATC
TCTACGATTTACCCGCTACACCAGgAaTCCCCCTGCCCGAATGCACTCTAGTTAC
ACAGTTTCCACTGCCTTTATGCGGTTGAGCCGCACGCTTTGACAATAGACTTGCATC
ACCACCTACGGACGCTTTACGCCAATCATTCCGGATAACGCTTGCATCCTCCGTAT
TACCAGGCTGTGGCACGGAGTTAGCCGATGCTTCTTCTCAGGTACCGTACCTC
TTCTTCCCTGAGAAAAGAGGTTTACAACCCAAGAGCCTTCTCCCTCACGCGGTATT
GCTCCGTACAGGCTTTCGCCATTGCGGAAAATCCCCACTGCTGCCTCCCGTAGGA
GTCTGGGCCGTGTCTCAGTCCCAGTGTGGCTGATCATCCTCTCAGACCAGCTACTGA
TCGTGCCATGGTAGGCTCTTACCCACCATCTAGCTAATCAGACGCGAGCTCATCT
CTAGGCAGCTAGCCTTTCACCTTTCGGCACATTCGGTATTAGCCACCGTTTCCAGT
GGTGTCCCGAACCTAGAGCCAGATTCTCACGCGTTTcaCCCGTCCGa

>Heinrichs6

gTcaGTnnTAGCCcAGTAGAGTGCCTTCGCCATCGGTGTTCTTTCCAATATCTACG
CATTTACCCGCTCCACTGgAAaTTCCTCTACCCCTACTATACTCAAgTtCCCAGTTT
CCAATGCTGAATTGAGGTTGAGCCTCAAGGTTAACAGTGGACTTAAGAAACCACC
TGCAGACGCTTTACGCCAGTAATCCGGATAACACTTGCATCCTCCGTCTTACCGC
GGCTAGTGGCACGGaGTTAGCCGATGCTTCGTCTCTAAGTAACGTCAGATCTTCT
CCTTAGGTAAACAGAGGTTTACAACCTCAGTAAGCCTTCTTCCCTCACGCGGTATTGCT
CTGTGAGGCTTTCGCCATTGCGAGaaaTTCCTCACTGCTGCCcCCcGTAGGAGTCTGG
ACCGTGTCTCAGTTCAGTGTGGCTGATCGTCTCTCAGACCAGCTACTGATCGTGC
CCTTGGTAGGCCTTACCCACCAACTAGCTAATCAGCCGCGAGCTTCTCTTAGGC

AGATTTCTCTGTTGACCCGAAGGCATATGGAGTTTATAGCAGGTGTTTCCCCCTGTTA
TCCTCCTCTAAA GnnAaTTCTCACGCGTTacnaaCc

>Mondteich1

agtGTcaGTaTtGTCTAGCAGAGCGCTTtCGCCACCggtGTTCTTCCCAATCTCTAC
GCAITTCACCGCTACACTGGGAATTCCTCTACCCCTAACATACTCTAGTCTTATAGT
TTCCACTGCCTGTATGTGGTTGAGCCACACGCTTTAACAGCAGACTTACAAAACCA
CCTGCGGACGCTTACGCCCAATCATTCCGGATAACGCTTGCATCCTCTGTATTACCG
CGGCTGCTGGCACAGAGTTAGCCGATGCTTATCCTCAAGTACCGTCatnATCTTCT
TGAGAAAAGAGGTTTACGACCCAAAAGCCTTCGTCCCTCACGCGGTATTGCTCCGT
CAGGCTTTCGCCATTGCGGAAAATTCCCCACTGCTGCCTCCCGTAGGAGTCTGGA
CCGTGCTCAGTTCAGTGGGTGATCGTCTCTCAGACCAGCTACAGATCGATGC
CTAGGTAGTCTTTACACCACCTACTAGCTAATCTGACGCGAGCTCaATnCAGGCAA
TtAATCTTTCACCTTTCGGCACATCCGGTATTAGCAGTCAATTTCTAACTGTTGTCCCC
ACCTGAAGGataGATTCTCACGCGTTnca

>Mondteich2

cagnGTcnGTaTtGTCTAGCAGAGCGCTTtCGCCACCggtGTTCTTCCCAATCTCTA
CGCATTTACCGCTACACTGGGAATTCCTCTACCCCTAACATACTCTAGTCTTATAG
TTTCCACTGCCTGTATGTGGTTGAGCCACACGCTTTAACAGCAGACTTACAAAAC
ACCTGCGGACGCTTACGCCCAATCATTCCGGATAACGCTTGCATCCTCTGTATTACC
GCGGCTGCTGGCACAGAGTTAGCCGATGCTTATCCTCAAGTACCGTCatnATCTTCC
TTGAGAAAAGAGGTTTACGACCCAAAAGCCTTCGTCCCTCACGCGGTATTGCTCCG
TCAGGCTTTCGCCATTGCGGAAAATTCCCCACTGCTGCCTCCCGTAGGAGTCTGGA
CCGTGTCTCAGTTCAGTGGGTGATCGTCTCTCAGACCAGCTACAGATCGATGC
CTAGGTAGTCTTTACACCACCTACTAGCTAATCTGACGCGAGCTCaATnCAGGCAA
TTAATCTTTCACCTTTCGGCACATCCGGTATTAGCAGTCAATTTCTAACTGTTGTCCCC
GACCTGAAGanaGATTCTCACGCGTTatcaaCCcgTCCGangaa

>Pyhrabruck1

cagnGTcnGTaTtGTCTAGCAGAGCGCTTtCGCCACCggtGTTCTTCCCAATCTCTA
CGCATTTACCGCTACACTGGGAATTCCTCTACCCCTAACATACTCTAGTCTTATAG
TTTCCACTGCCTGTATGTGGTTGAGCCACACGCTTTAACAGCAGACTTACAAAACCA
CCTGCGGACGCTTACGCCCAATCATTCCGGATAACGCTTGCATCCTCTGTATTACC
CGGCTGCTGGCACAGAGTTAGCCGATGCTTATCCTCAAGTACCGTCatnATCTTCT
TGAGAAAAGAGGTTTACGACCCAAAAGCCTTCGTCCCTCACGCGGTATTGCTCCGT
CAGGCTTTCGCCATTGCGGAAAATTCCCCACTGCTGCCTCCCGTAGGAGTCTGGA
CCGTGTCTCAGTTCAGTGGGTGATCGTCTCTCAGACCAGCTACAGATCGATGC
CTAGGTAGTCTTTACACCACCTACTAGCTAATCTGACGCGAGCTCaATnCAGGCAA
TtAATCTTTCACCTTTCGGCACATCCGGTATTAGCAGTCAATTTCTAACTGTTGTCCCC
ACCTGAAGGacaGATTea

>Pyhrabruck2

gCGTcaGTTGAGnTCnAGCAGgacGCTTTCGCCACTGGTGTCTTCCAGATATCTA
CGCATTTACCGCTACACCTGGAATTCCTCCTGCCCTATCTCTCTAGTCTCACAG
TTTCCATGCGGATCCAAGGTTGAGCCTCGGGCTTTGACAACAGACTTATCAAAACA
GCCTACGTACGCTTACGCCCAATAATTCCGGATAACGCTTGCATCCTCCGTCTTACC
GCGGCTGCTGGCACGGAGTTAGCCGATGCTTATTCGTATTAGGTACCGTATTATCTTCC
CTAAACAAAAGAGGTTTACAACCCACAGGCCTTCGTCCCTCACGCGGTATTGCTCCG
TCAGGCTTTCGCCATTGCGGAAAATTCCCCACTGCTGCCTCCCGTAGGAGTCTGGG
CCGTGTCTCAGTCCCAGTGTGACTGGTCATCCTCTCAGACCAGTTATCGATCGTCCG
CATGGTAGGCCATTACCCACCATCTAGCTAATCGAACGCAAGCTCATCTACAGGC
ATTAAAACCTTTCACCCGAAGGCATATCCGGTATTAGCAGTCAATTTCTAACTGTTGTCC
CGAACCTATAGGTAGATTCTTACGgTtAcTcACCCGTCCGanga

>Pyhrabruck3

ctctgantGTcaGTanTAGCCcAGTAGAGTGCCTTCGCCATCGGTGTTCTTCCCAAT
CTACGCATTTACCGCTCCACTGGAAAATTCCTCTACCCCTACTATACTCAAGTTTCC
CAGTTTCCAATGCTGAATTGAGGTTGAGCCTCAAGGTTAACAGTGGACTTAAGAA

ACCACCTGCAGACGCTTACGCCAGTAATCCGGATAACACTTGCATCCTCCGCT
TACCGCGGCTGCTGGCACGGAGTTAGCCGATGCTTCGTCTCCTAAGTAACGTCAGAT
CTTCCTCCTTAGGTAACAGAGGTTTACAACACTAGTAAGCCTTCTCCCTCACGCGGT
ATTGCTCTGTAGGCTTTCGCCCAATTGCAGAAAATTCCTACTGCTGCCCTCCCGTAG
GAGTCTGGACCGTGTCTCAGTTCAGTGTGGCTGATCGTCTCTCAGACCAGCTACT
GATCGTCGCCTTGGTAGGCCTTACCCACCAACTAGCTAATCAGCCGCGAGCTTCT
CTTTAGGCAGATTTCTCTGTTTGACCCGAAGGCATATGGAGTTTATAGCAGGTGTTTCC
CCCTGTTATCCTCCTCTAAAGGCGAantCTCAgcGTTACTACCCGTCGGa

>LoipTeich2

cGtCCtnagTGtgcgTTaCGGCCTAGCAGAGCGCTTtCGCCACCGGTGTTCTCTGTA
TCTCTACGCATTTACCCGCTACACCAGGAATTCCTCTGCCCGAACGTAAGTACTTACG
TCTGTAGTTTCCACTGCCTTTACAAGGTTGAGCCTTGCTCTTAAACAGCAGACTTACA
GTGCCACCTGCGGACGCTTACGCCCAATCATTCCGGATAACGCTTGCATCCTCCGT
ATTACCGCGGCTGCTGGCACGGAGTTAGCCGATGCTTATTCCTCAGGTACCTTCATT
TTTTATTCCCTGAGAAAAGAGGTTTACAACCCAAGAGCCTTCTCCCTCACGCGGTA
TTGCTCCGTCAGGCTTTCGCCCAATTGCGGAAAATTCCTCCTGCTGCCTCCCGTAGG
AGTCTGGGCCGTGTCTCAGTCCCAGTGTGGCTGATCATCCTCTCAGACCAGCTACTG
ATCGTCGCCTTGGTGGCCTTACCACACCAACTAGCTAATCAGACGCGAGCTATC
TCTAGGCAATAAAATCTTTCACCTTTCGGCACATCCGGTATTAGCCACCGTTTCCAGTG
GTTGTCCCCGACCTagAGCTaaattctCnnncGTTACTACCCGTCGGa

>LoipTeich3

agngTcaGTTacGGCCTAGcagAGCGCTTtCGCCACCGgtgTtCTTCTgaTCTCTACGCA
TTTACCCGCTACACCAGGAaTTCCTCTGCCCGAACGTAAGTACTTACGCTCTGTAGTTT
CACTGCCTTTACAAGGTTGAGCCTTGCTCTTAAACAGCAGACTTACAGTGCCACCTG
CGGACGCTTTACGCCCAATCATTCCGGATAACGCTTGCATCCTCCGATTACCGCGG
CTGCTGGCACGGAGTTAGCCGATGCTTATTCCTCAGGTACCTTCATTTTTTATTCCT
GAGAAAAGAGGTTTACAACCCAAGAGCCTTCTCCCTCACGCGGATTGCTCCGTC
AGGCTTTCGCCCAATTGCGGAAAATTCCTCCTGCTGCCTCCCGTAGGAGTCTGGGCC
GTGTCTCAGTCCCAGTGTGGCTGATCATCCTCTCAGACCAGCTACTGATCGTCGCCT
TGGTGGCCTTACCACACCAACTAGCTAATCAGACGCGGAGCTCATCTCTAGGCAA
TAAATTTTACCTTTCGGCACATCCGGTATTAGCCACCGTATTCCAGTGGTTGTTTTCC
GACCTAGAGCTaanTTCTCangCGTTaccaCCCCGTCcggAGa

>LoipTeich5

CntCCtnagcGtgcgTTGTTGGCCcagtAGAGCGCTTtCGCCACTgggtTtCTTCCCATA
TCTACGCATTTACCCGCTACACCAGGAATTCCTCTACCCCTACCACACTTAGTCA
ACCAGTTTCCATTGCCGATCCACAGTTGAGCTGTGACCTTTGACAACAGACTTAATT
AACCCTGCGGACGCTTACGCCCAATAATTCCGGATAACGCTTGCCTCCTCCGTC
TTACCGGGCTGCTGGCACGGAGTTAGCCGAGGCTTATTCCTCAGGTACCCTCAGTT
CTTCTCCCTGAGAAAAGAGGTTTACAACCCCTAAGGCCTTCTCCCTCACGCGGG
TTGCTCCGTCAGGCTTGGCGCCATTGCGGAAAATTCCTCCTGCTGCCTCCCGTAGG
AGTCTGGGCCGTGTCTCAGTCCCAGTGTGGCTGATCATCCTCTTAGACCAGCTACTG
ATCGTCGCCTTGGTAAGCTTACCCACCAACTAGCTAATCAGACGCGAGTTTCATC
CTCAGGCGATATAACATTTACCTCTCGGCATATGGGGTATTAGCAGTCGTTTCCAAC
TGTGTCCCCCTCCTAAGGGCAGATCCTCACCGgTtACTACCCGTCGGa

>LoipTeich6

agTGtnagTTaCGGCCTAGCAGAGCGCTTtCGCCACCGGTGTTCTTCTGATCTCTA
CGCATTTACCCGCTACACCAGGAATTCCTCTGCCCGAACGTAAGTACTTACGCTCTGTA
GTTTCCACTGCCTTTACAAGGTTGAGCCTTGCTCTTAAACAGCAGACTTACAGTGCC
ACCTGCGGACGCTTACGCCCAATCATTCCGGATAACGCTTGCATCCTCCGATTACC
GCGGCTGTGGCACGGAGTTAGCCGATGCTTATTCCTCAGGTACCTTCATTTTTTAT
TCCCTGAGAAAAGAGGTTTACAACCCAAGAGCCTTCTCCCTCACGCGGATTGCT
CCGTCAGGCTTTCGCCCAATTGCGGAAAATTCCTCCTGCTGCCTCCCGTAGGAGTCT
GGGCCGTGTCTCAGTCCCAGTGTGGCTGATCATCCTCTCAGACCAGCTACTGATCGT
CGCTTGGTGGCTCTTACCACACCAACTAGCTAATCAGACGCGGAGCTCATCTCTAG

GCAATAAATCTTTCACCTTTCGGCACATCCGGTATTAGCCACCGTTTCCAGTGGTGT
CCCCGACCTaanGCTAGATTtCACGCGTTaccanCCCCGTCCGa
>LoipTeich7
agngTcaGTTacGGCCTAGCagaGCGCTTtCGCCACCgggtTtCTTCTGATCTCTACGC
AATTCACCGCTACACCAGGAaTTCCCTCTGCCCGAACGTACTCTAGCTCTGTAGTTT
CCACTGCCTTTACAAGGTTGAGCCTTGCTCTTTAACAGCAGACTTACAGTGCCACCT
GCGGACGCTTTACGCCAATCATTCCGGATAACGCTTGCATCTCCGTATTACCGCG
GCTGCTGGCACGGAGTTAGCCGATGCTTATTCCTCAGGTACCTTCATTTTTTATTCC
CTGAGAAAAGAGGTTTACAACCCAAGAGCCTTCTCCCTCACGCGGTATTGCTCCG
TCAGGCTTTCGCCATTGCGGAAAATTCCCCACTGCTGCCTCCCGTAGGAGTCTGGG
CCGTGCTACGTCCCAGTGTGGCTGATCATCTCTAACAGCAGACTGATCGTCCGC
CTTGGTGCCTCTTACCACACCAACTAGCTAATCAGACGCGAGCTCATCTTAGGCA
ATAAATCTTTCACCTTTCGGCACATCCGGTATTAGCCACCGTTTCCAGTGGTGTCC
CGACCTAGAGTaanTTCTCACGCGTTACTCCACCCGTCCGa
>LoipTeich8
cnGtGTenGTTaCGGCCTAGCAGAGCGCTTtCGCCACCgggtTtCTTCTGATCTCTA
CGCATTTACCGCTACACCAGGAATTCCTCTGCCCGAACGTACTCTAGCTCTGTA
GTTTCCACTGCCCTTACAAGGTTGAGCCTTGCTTTAACAGCAGACTTACAGTGCC
ACCTGCGGACGCTTTACGCCAATCATTCCGGATAACGCTTGCATCTCCGTATTAC
CGCGGTGCTGGCACGGAGTTAGCCGATGCTTATTCTCAGGTACCTTCATTTTTTTA
TTCCCTGAGAAAAGAGGTTTACAACCCAAGAGCCTTCTCCCTCACGCGGTATTGC
TCCGTCAGGCTTTCGCCATTGCGGAAAATTCCCCACTGCTGCCTCCCGTAGGAGTC
TGGGCCGTGTCTCAGTCCCAGTGTGGCTGATCATCTCTCAGACCAGCTACTGATCG
TCGCCTTGGTGCCTCTTACCACACCAACTAGCTAATCAGACGCGAGCTCATCTCTA
GGCAATAAATCTTTCACCTTTCGGCACATCCGGTATTAGCCACCGTTTCCAGTGGT
GTCCCCGACCTAGAGCTAGattCTCACGcnTtAcTcaCCCCGTCCGa
>LoipZulauf2
agcGTCaGTTGTGGCCnaGTAGAGCGCCTTCGCCACTGGTGTtCTTCCCGATATCTA
CGCATTTACCGCTACACCGGGAATTCCTCTACCCCTACCACACTCAAGTTCACCA
GTTTCCATTGCCGATCCACAGTTGAGCTGTGGGCTTTGACAACAGACTTAATAAAC
GCCTGCGGACGCTTTACGCCAATAATTCCGGATAACGCTTGCCTCTCCGTCTTAC
CGCGGTGCTGGCACGGAGTTAGCCGAGGCTTATTCTCTGGTACCGTCAGTTCTTC
TTCCAGAGAAAAGAGGTTTACAACCCTAAGGCCTTCTCCCTCACGCGGCGTTGC
TCCGTCAGGCTTTCGCCATTGCGGAAAATTCCCCACTGCTGCCTCCCGTAGGAGTC
TGGGCCGTGTCTCAGTCCCAGTGTGGCTGATCATCTCTTAGACCAGCTACTGATCG
TCGCCTTGGTAGTCCATTACACTACCAACTAGCTAATCAGACGCGAGTTCATCCTTA
GGCGAAAAACATTTACCTCTCGGCATATGGGGCATTAGCAGTCCGTTTCCAACCTG
TTGTTCCCTCCTAAGGGCAGATCTCACGCGTTaccacCCCCGTCCGa
>LoipTeich1
tCCtnagTGttagTGCagaCCcAGTaaCaCGCTTtCGCCGCTGGTGTtCTTCCCAATATC
TACGCATTTACCGCTACACTGGGAATTCCTGTTACCCCTATCGCACTCTAGTTCATC
AGTTTCCACTGCCCTTATGCGGTTAAGCCGCACGCTTTGACAGCAGACTTGATAAAC
CACCTACGGACGCTTTACGCCAATAATTCCGGATAACGCTTGCATCTCCGTATTAC
CGCGGTGCTGGCACGGAGTTAGCCGATGCTGATTATCAGGTACCGTACCGTATCGATT
TTCCCTGATAAAAAGAGGTTTACAACCCAAAAGCCGTCCTCCCTCACGCGGTATTGC
TCCGTCAGGCTTTCGCCATTGCGGAAAATTCCCCACTGCTGCCTCCCGTAGGAGTC
TGGACCGTGTCTCAGTTCAGTGTGCCTGGTATCCTCTCAGACCAAGTACAGATCG
TCGCCTTGGTGTGCCGTTACCCTCAACTAGCTAATCTGACGCGAGCCAATCTCTA
GACAATTAATCTTTCACCCTAAGGCACATTCGGTATTAGCAGTCCGTTTCCAACCTGTC
TCCCAATCTAAAGGCaag
>IFATeich1
tcagTGtnagTTGCGGCCTAGCAGAGCGCTTtCGCCACCGGTGTTCTTCTGATC
TCTACGCATTTACCGCTACACCAGGAATTCCTCTGCCCGaAaCGCaCTAGTCTT
GTAGTTTCCaCTGCCCTTATGCGGTTAAGCCGCacGCTTTAACAAATAGACTTACAAAA

CcaCCTGCGGACGCTTTACGCCAATCATTCCGGATAACGCTTGATCCTCCGTATTA
 CCGCGGCTGCTGGCACGGAGTTAGCCGATGCTTATTCCTCAGGTACCGTCATCATCT
 TCCCTGAGAAAAGAGGTTTACAACCCAAGAGCCTTCCTCCCTCACGCGGTATTGCT
 CCGTCAGGCTTTCGCCCAATTGCGGAAAATTCCCcACTGCTGCCTCCCGTAGGAGTC
 TGGACCGTGTCTCAGTTCAGTGTGGCTGATCATCTCTCAGACCAGCTACTGATCG
 CAGCCTTGGTAGTCCATTACACCACCAACTAGCTAATCAGACGCGAGCTCATCTCT
 TGGCAATTAATCTTTCACCCGTAGGCACATCCGGTATTAGCAGCCGTTTCCAACGTG
 TGCCCCGAACCAAAGGCAGattCTCACGCGTTACTcACCcGTcggng

>Admont1

anttnagCGTCagTTGAgaTCCAGCAGGACGCTTtCGCCACTGgTGTtCTCCAGATA
 TCTACGCATTTACCCGTACACCTGGAATTCCTCTGCCCTATCTCTCTAGTCTC
 ACAGTTTCCATTGCCGATCCAAGGTTGAGCCTCGGGCTTTGACAACAGACTTATGA
 AACAGCCTACGTACGCTTTACGCCAATAATTCCGGATAACGCTTGATCCTCCGTC
 TTACCGCGGCTGCTGGCACGGAGTTAGCCGATGCTTATTGTTAGGTACCGTCATTA
 TCTTCCCTAACAAAAGAGGTTTACAATCCACAGACCTTCGTCCCTCACGCGGTATTG
 CTCCGTCAGGCTTTCGCCCAATTGCGGAAAATTCCCcACTGCTGCCTCCCGTAGGAGT
 CTGGGCCGTGTCTCAGTCCCAGTGTGACTGGTCATCTCTCAGACCAGTTACCGATC
 GTCGCCATGGTGGCCATTACCACTCCATCTAGCTAATCGGACCGCAAGCTCATCTAC
 AGATGATAAATCTTTCACCCGAAGGCATATCCGGTATTAGCAGTCGTTTCCAACGTG
 TGCCCCGAGTCTGTAGGTAGannnTTAcacGTTAcAcCcgTCCgag

>Admont2

gtanTTcnGCGtcagTTGagaTcAGCAGGACGCTTtCGCCACTGGTGTtCTCCAGAT
 ATCTACGCATTTACCCGTACACCTGGAATTCCTCTGCCCTATCTCTCTAGCCT
 CACAGTTTCCATTGCCTTTCcAAGGTTGAGCCTCGGGCTTTGACAACAGACTTATGA
 AACAGCCTACGTACGCTTTACGCCAATAATTCCGGATAACGCTTGATCCTCCGTC
 TTACCGCGGCTGCTGGCACGGAGTTAGCCGATGCTTATTGTTAGGTACCGTCATTA
 CTTCCCTAACAAAAGAGGTTTACAATCCACAGACCTTCGTCCCTCACGCGGTATTG
 CTCCGTCAGGCTTTCGCCCAATTGCGGAAAATTCCCcACTGCTGCCTCCCGTAGGAGT
 CTGGGCCGTGTCTCAGTCCCAGTGTGACTGGTCATCTCTCAGACCAGTTATCGATC
 GTCGCCATGGTGGCCGTtACCACTCCATCTAGCTAATCGAAGCAAGCTCATCTAC
 AGGCATTAaAACTTTCACCCGAAGGCATATCCGGTATTAGCAGTCATTTCTAACTGT
 TGCCCCGAACCTATAGGTAGATTCTTACGCGTtAtncncngtCcGg

>Greifenstein3

acTTcngCGTcagTTGAGaTCCAGCAGGACGCTTtCGCCACTggTGTtCTCCAGATAT
 CTACGCATTTACCCGTACACCTGGAATTCCTCTGCCCTATCTCTCTAGTCTCA
 CAGTTTCCATTGCCGATCCAAGGTTGAGCCTCGGGCTTTGACAACAGACTTATCAA
 ACAGCCTACGTACGCTTTACGCCAATAATTCCGGATAACGCTTGATCCTCCGTC
 TACCGCGGCTGCTGGCACGGAGTTAGCCGATGCTTATTGTTAGGTACCGTCATTA
 CTTCCCTAACAAAAGAGGTTTACAACCCACAGGCCTTCGTCCCTCACGCGGTATTG
 CTCCGTCAGGCTTTCGCCCAATTGCGGAAAATTCCCcACTGCTGCCTCCCGTAGGAG
 TCTGGGCCGTGTCTCAGTCCCAGTGTGACTGGTCATCTCTCAGACCAGTTATCGAT
 CGTCGCCATGGTAGGCCGTtACCCcACCATCTAGCTAATCGAAGCAAGCTCATCTA
 CAGGCATTAaAACTTTCACCCGAAGGCATATCCGGTATTAGCAGTCATTTCTAACTG
 TTGTCCCGAACCTATAGGTAGATTCTTACGCGTtAcACCCGTCCgA

>LoipQuelleF

caGTGTCaGTTGCAGCCTAGCAGGgCGCTTtCGCCACCggtGTTCTTCTGATCTC
 TACGCATTTACCCGTACACCAGGAATTCCTCTGCCCGAATGCACTCTAGTTACA
 CAGTTTCCACTGCCTTtATGCGGTTGAGCCGCACGCTTTGACAATAGACTTGCATCA
 CCACCTACGGACGCTTTACGCCAATCATTCCGGATAACGCTTGATCCTCCGTTAT
 ACCGCGGCTGCTGGCACGGAGTTAGCCGATGCTTCTTCTCAGGTACCGTCATCTCT
 TCTTCCCTGAGAAAAGAGGTTTACAACCCAAGAGCCTTCCTCCCTCACGCGGTATT
 GCTCCGTCAGGCTTTCGCCCAATTGCGGAAAATTCCCcACTGCTGCCTCCCGTAGGA
 GTCTGGGCCGTGTCTCAGTCCCAGTGTGGCTGATCATCTCTCAGACCAGCTACTGA
 TCGTCGCCATGGTAGGCTCTTACCCcACCATCTAGCTAATCAGACGCGAGCTCATCT

CTAGGCAGCTAGCCTTTCACCTCTTCGGCACATCCGGTATTAGCCACCGTTTCCAGT
GGTTGTCCCGAACCTAGAGCCAGaTTCTCACGgTaccanCccgTCCGa

>Branna1

gtGtcagTTaCGGCCTAGCAGAGCGCCTTCGCCACCGgtgTTCTTCTGATCTCTACG
CAITTCACCGCTACACCAGGAATTCCTCTGCCCGAACGTACTCTAGCTGTGTAGT
TTCCACTGCTTTTATGAGGTTAAGCCTCACTCTTTAACAGCAGACTTACATTGCCAC
CTGCGGACGCTTTACGCCAATCATTCCGGATAACGCTTGCATCCTCCGTATTACCG
CGGCTGCTGGCACGGAGTTAGCCGATGCTTATTCTCAAGTACCTTCAGTTCTTATTC
CTTGAGAAAAGAGGTTTACAACCCAAGAGCCTTCTCCCTCACGCGGATTGCTCC
GTCAGGCTTTCGCCATTGCGGAAAATTCCCCACTGCTGCCTCCCGTAGGAGTCTG
GGCCGTGCTCAGTCCAGTGTGGCTGATCATCCTCAGACCAGCTAGCTGATCGTC
GCCTAGGTGCGCTTTACCACACCTACTAGCTAATCAGACGCGAGCTCATCTTCAG
GCAGTTAACCTTTCACCTTTCGGCACATCCGGTATTAGCCACCGTTTCCAGTGGTTG
TCCCCGACCTCAAGCTagatnencACGCGTTACtcaCccgTCCGnn

>Branna2

cGtCctnagTGtcagTTaCGGCCTAGCAGAGCGCCTTCGCCACCGGTGTTCTTCTG
ATCTCTACGCATTTACCGCTACACCAGGAATTCCTCTGCCCGAACGTACTCTAG
CTGTGTAGTTCCACTGCTTTTATGAGGTTAAGCCTCACTCTTTAACAGCAGACTTAC
ATTGCCACCTGCGGACGCTTTACGCCAATCATTCCGGATAACGCTTGCATCCTCCG
TATTACCGCGGCTGCTGGCACGGAGTTAGCCGATGCTTATTCTCAAGTACCTTCAG
TTCTTATTCTTGAGAAAAGAGGTTTACAACCCAAGAGCCTTCTCCCTCACGCGG
TATTGCTCCGTCAGGCTTTCGCCATTGCGGAAAATTCCCCACTGCTGCCTCCCGTA
GGAGTCTGGGCCGTGTCTCAGTCCCAGTGTGGCTGATCATCCTCTCAGACCAGCTA
CTGATCGTCGCTAGGTGCGCTTTACCACACCTACTAGCTAATCAGACGCGAGCTC
ATCTCAGGCAGTTAACCTTTCACCTTTCGGCACATCCGGTATTAGCCACCGTTTCCA
GTGGTTGTCCCCGACCTCAAGCTAAatnCTCACg

>Branna8

tCctnngtGTcaGTTGCGGCCTAGCAGAGCGCCTTCGCCACCGGTGTTCTTCTGAT
CTCTACGCATTTACCGCTACACCAGGAATTCCTCTGCCCGAACGTACTCTAGTC
TTGTAGTTTCCACTGCCCTTATGCGGTTAAGCCGACGCTTAAACAATAGACTTACA
AAACCTTCGCGACGCTTTACGCCAATCATTCCGGATAACGCTTGCATCCTCCG
TATTACCGCGGCTGCTGGCACGGAGTTAGCCGATGCTTATTCTCAGGTACCGTCAT
CATCTTCCCTGAGAAAAGAGGTTTACAACCCAAGAGCCTTCTCCCTCACGCGGTA
TTGCTCCGTCAGGCTTTCGCCATTGCGGAAAATTCCCCACTGCTGCCTCCCGTAGG
AGTCTGGACCGTGTCTCAGTCCAGTGTGGCTGATCATCCTCTCAGACCAGCTACTG
ATCGCAGCCTTGGTAGTCCATTACACCACCACTAGCTAATCAGACGCGAGCTCATC
TCTTGgCAATtAATCTTTCACCCGTAgGCACATCCGGTATTAncAGCCGTTTCCAAC
GntGTCCCCGAACCAaAAA

>Branna9

caGTGTenGTTaCGGCCTAGCAGAGCGCCTTCGCCACCGgtGTTCTTCTGATCT
CTACGCATTTACCGCTACACCAGGAATTCCTCTGCCCGAACGTACTCTAGCTGT
GTAGTTTCCACTGCTTTTATGAGGTTAAGCCTCACTCTTTAACAGCAGACTTACATTG
CCACTGCGGACGCTTTACGCCAATCATTCCGGATAACGCTTGCATCCTCCGTATT
ACCGCGGCTGCTGGCACGGAGTTAGCCGATGCTTATTCTCAAGTACCTTCAGTTCT
TATTCTTGAGAAAAGAGGTTTACAACCCAAGAGCCTTCTCCCTCACGCGGTATTG
CTCCGTCAGGCTTTCGCCATTGCGGAAAATTCCCCACTGCTGCCTCCCGTAGGAGT
CTGGGCCGTGTCTCAGTCCCAGTGTGGCTGATCATCCTCTCAGACCAGCTACTGATC
GTCGCTAGGTGCGCTTTACCACACCTACTAGCTAATCAGACGCGAGCTCATCTTC
AGGCAGTTAACCTTTCACCTTTCGGCACATCCGGTATTAGCCACCGTTTCCAGTGGT
TGTTCCCCGACCTCAAGCTaaatnCtanCGCGTTACTcACCCGTCcgg

>Steg3

tCnTGagCGTcaGTtaTGGCCcaGCaaGAGCGCCTTCGCCACTGGTGTCTTCCCCGAT
ATCTACGCATTTACCGCTACACCAGGAATTCCTCTGCCCGAACGTACTCTAGCTGT
TTGTAGTTTCCATCGCTCAAATGGAGTTAAGCTCCACGCTTTAACGACAGACTTACA

AGGCCGCTGCGGACGCTTTACGCCCAATAATCCGGATAACGCTTGCCACTCCCG
 TATTACCGCGGCTGCTGGCACGGAATTAGCCGTGGCTTATTCTCAAGTACCGTCAT
 GTCTTCTCCTTGAGAAAAGAGGTTTACAGCCAGGCGCTTCATCCCTCACGCGG
 CGTTGCTCCGTACGGCTTTCGCCCATTGCGGAAAATCCCACTGCTGCCTCCCGTA
 GGAGTCTGGGCCGTGTCTCAGTCCCAGTGTGGCTGATCATCTCTCAGACCAGCTA
 CTGATCGTCGCCCTGGTGGGCCATTACCCACCAACTAGCTAATCAGACGCGGGCT
 CATCCTCAGGCGAAATTCATTTACCTCTCGGCATATGGGGTATTAGCGGCCGTTTC
 CGGCCGTTATCCCCCTCCTGAGGGCagATTCCCACGCGTTACtcaCCCCTCcgga

Appendix C. Growth Test in a 5 L Tubular Photobioreactor

The laboratory tubular reactor was built from a PVC garden hose of 16 mm inner diameter and ca. 22 m length, a conventional indoor fountain pump and a 2 L glass beaker. The reactor was intentionally kept as simple as possible. *Synechocystis* sp. IFA-3 and *Chlorogloeopsis* sp. Heinrichs-4 were both cultivated in this reactor during April and May 2019 outdoors in Tulln, Austria. Typical night temperatures were around +4 to +8 °C and day temperatures were in the range of +15 to +25 °C, colder during rainy days. At sunny days the culture suspension in the beaker reached up to +45 °C.

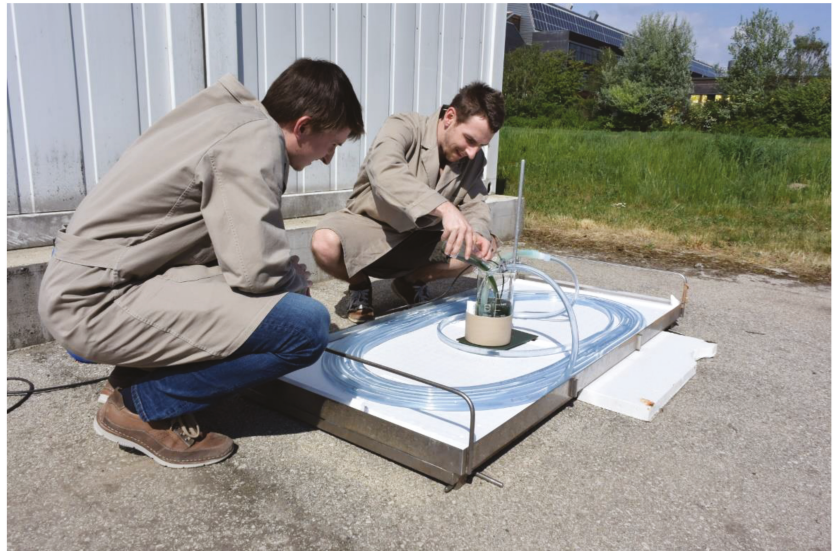


Figure A2. Inoculation of the 5-L tubular photobioreactor in Tulln with *Synechocystis* sp. IFA-3 for outdoors operation.

References

1. Zhanga, C.H.; Showb, P.-L.; Ho, S.-H. Progress and perspective on algal plastics—A critical review. *Bioresour. Technol.* **2019**, *289*, 121700. [[CrossRef](#)]
2. Narayanan, M.; Kandasamy, S.; Kumarasamy, S.; Gnanavel, K.; Ranganathan, M.; Kandasamy, G. Screening of polyhydroxybutyrate producing indigenous bacteria from polluted lake soil. *Heliyon* **2020**, *6*, e05381. [[CrossRef](#)]
3. Saratale, R.G.; Cho, S.-K.; Saratale, G.D.; Kadam, A.A.; Ghodake, G.S.; Kumar, M.; Bharagava, R.N.; Kumar, G.; Kim, D.S.; Mulla, S.I.; et al. A comprehensive overview and recent advances on polyhydroxyalkanoates (PHA) production using various organic waste streams. *Bioresour. Technol.* **2021**, *325*, 124685. [[CrossRef](#)] [[PubMed](#)]
4. Haas, C.; El-Najjar, T.; Virgolini, N.; Smerilli, M.; Neureiter, M. High cell-density production of poly(3-hydroxybutyrate) in a membrane bioreactor. *New Biotechnol.* **2017**, *37 Pt A*, 117–122. [[CrossRef](#)]

5. Drog, B.; Fritz, I.; Gattermayr, F.; Silvestrini, L. Photo-autotrophic Production of Poly(hydroxyalkanoates) in Cyanobacteria. *Chem. Biochem. Eng. Q.* **2015**, *29*, 145–156. [\[CrossRef\]](#)
6. Balaji, S.; Gopi, K.; Muthuvelan, B. A review on production of poly β hydroxybutyrate from cyanobacteria for the production of bio plastics. *Algal Res.* **2013**, *2*, 278–285. [\[CrossRef\]](#)
7. Campbell, J.; Stevens, S.E.; Balkwill, D.L. Accumulation of Poly-3-Hydroxybutyrate in *Spirulina platensis*. *J. Bacteriol.* **1982**, *149*, 361–363. [\[CrossRef\]](#)
8. Kovalcik, A.; Meixner, K.; Mihalic, M.; Zeilinger, W.; Fritz IFuchs, W.; Kucharczyk, P.; Stelzer, F.; Drog, B. Characterization of polyhydroxyalkanoates produced by *Synechocystis salina* from digestate supernatant. *Int. J. Biol. Macromol.* **2017**, *102*, 497–504. [\[CrossRef\]](#)
9. Schirmermeister, B.E.; Gugger, M.; Donoghue, P.C. Cyanobacteria and the Great Oxidation Event: Evidence from genes and fossils. *Palaeontology* **2015**, *58*, 769–785. [\[CrossRef\]](#)
10. Troschl, C.; Meixner, K.; Fritz, I.; Leitner, K.; Palacios Romero, A.; Kovalcik, A.; Sedlacek, P.; Drog, B. Pilot-scale production of poly- β -hydroxybutyrate with the cyanobacterium *Synechocystis* sp. CCALA192 in a non-sterile tubular photobioreactor. *Algal Res.* **2018**, *34*, 116–125. [\[CrossRef\]](#)
11. Singh, A.K.; Sharma, L.; Mallick, N.; Mala, I. Progress and challenges in producing polyhydroxyalkanoate biopolymers from cyanobacteria. *J. Appl. Phycol.* **2017**, *29*, 1213–1232. [\[CrossRef\]](#)
12. Carpine, R.; Olivieri, G.; Hellingwerf, K.J.; Pollio, A.; Marzocchella, A. Industrial Production of Poly- β -hydroxybutyrate from CO₂: Can Cyanobacteria Meet this Challenge? *Processes* **2020**, *8*, 323. [\[CrossRef\]](#)
13. Panuschka, S.; Drog, B.; Ellersdorfer, M.; Meixner, K.; Fritz, I. Photoautotrophic production of poly-hydroxybutyrate—First detailed cost estimations. *Algal Res.* **2019**, *41*, 101558. [\[CrossRef\]](#)
14. Meixner, K.; Fritz, I.; Daffert, C.; Markl, K.; Fuchs, W.; Drog, B. Processing recommendations for using low-solids digestate as nutrient solution for poly- β -hydroxybutyrate production with *Synechocystis salina*. *J. Biotechnol.* **2016**, *240*, 61–67. [\[CrossRef\]](#)
15. Meixner, K.; Kovalcik, A.; Sykacek, E.; Gruber-Brunhumer, M.; Zeilinger, W.; Markl, K.; Haas, C.; Fritz, J.I.; Mundigler, N.; Stelzer, F.; et al. Cyanobacteria Biorefinery—Production of poly(3-hydroxybutyrate) with *Synechocystis salina* and utilisation of residual biomass. *J. Biotechnol.* **2018**, *265*, 46–53. [\[CrossRef\]](#)
16. Gradissimo, D.G.; Xavier, L.P.; Santos, A.V. Cyanobacterial Polyhydroxyalkanoates: A Sustainable Alternative in Circular Economy. *Molecules* **2020**, *25*, 4331. [\[CrossRef\]](#)
17. Rueda, E.; García, J. Optimization of the phototrophic Cyanobacteria polyhydroxybutyrate (PHB) production by kinetic model simulation. *Sci. Total Environ.* **2021**, *800*, 149561. [\[CrossRef\]](#)
18. Yashavanth, P.R.; Meenakshi, D.; Maiti, S.K. Recent progress and challenges in cyanobacterial autotrophic production of polyhydroxybutyrate (PHB), a bioplastic. *J. Environ. Chem. Eng.* **2021**, *9*, 105379. [\[CrossRef\]](#)
19. Troschl, C.; Fritz, I.; Sodnikar, K.; Drog, B. Contaminations in mass cultivation of cyanobacteria: Highly resilient *Colpoda steinii* leads to rapid crash of *Synechocystis* sp. cultures and is inhibited by partially anoxic conditions. *Algal Res.* **2017**, *28*, 229–234. [\[CrossRef\]](#)
20. Vu, C.H.T.; Lee, H.-G.; Chang, Y.K.; Oh, H.-M. Axenic Cultures for Microalgal Biotechnology: Establishment, Assessment, Maintenance, and Applications. *Biotechnol. Adv.* **2018**, *36*, 380–396. [\[CrossRef\]](#)
21. Temraleeva, A.D.; Dronova, S.A.; Moskalenko, S.V.; Didovich, S.V. Modern Methods for Isolation, Purification, and Cultivation of Soil Cyanobacteria. *Microbiology* **2016**, *85*, 389–399. [\[CrossRef\]](#)
22. Rippka, R.; Deruelles, J.; Waterbury, J.B.; Herdman, M.; Stanier, R.Y. Generic Assignments, Strain Histories and Properties of Pure Cultures of Cyanobacteria. *J. Gen. Microbiol.* **1979**, *111*, 1–61. [\[CrossRef\]](#)
23. Meixner, K.; Daffert, C.; Dalnodar, D.; Mrazova, K.; Hrubanova, K.; Krzyzaneck, V.; Nebesarova, J.; Samek, O.; Šedřilová, Z.; Slaninova, E.; et al. Glycogen, poly(3-hydroxybutyrate) and pigment accumulation in three *Synechocystis* strains when exposed to a stepwise increasing salt stress. *J. Appl. Phycol.* **2022**. [\[CrossRef\]](#)
24. Brányiková, I.; Maršálková, B.; Doucha, J.; Brányik, T.; Bišová, K.; Zachleder, V.; Vítová, M. Microalgae—Novel Highly Efficient Starch Producers. *Biotechnol. Bioeng.* **2011**, *108*, 766–776. [\[CrossRef\]](#)
25. Ganz, T. LYSOZYME. In *Encyclopedia of Respiratory Medicine*; Laurent, G.J., Shapiro, S.D., Eds.; Academic Press: Oxford, UK, 2006; pp. 649–653, ISBN 978-0-12-370879-3.
26. Ferris, M.J.; Hirsch, C.F. Method for Isolation and Purification of Cyanobacteria. *Appl. Environ. Microbiol.* **1991**, *57*, 1448–1452. [\[CrossRef\]](#)
27. Devine, P.J.; Petrillo, S.K.; Cortvrindt, R. 11.29—In Vitro Ovarian Model Systems. In *Comprehensive Toxicology*, 2nd ed.; McQueen, C.A., Ed.; Elsevier: Oxford, UK, 2010; pp. 543–559, ISBN 978-0-08-046884-6.
28. Hariri, K. *Phylogenetische Untersuchung an Historischen Herbarien Als Methodik zu Einer Neufassung (Revision) der Taxonomie von Cyanobakterien*; Carl von Ossietzky Universität Oldenburg: Oldenburg, Germany, 2012.
29. Nübel, U.; Garcia-Pichel, F.; Muyzer, G. PCR Primers to Amplify 16S rRNA Genes from Cyanobacteria. *Appl. Environ. Microbiol.* **1997**, *63*, 3327–3332. [\[CrossRef\]](#)
30. Karr, D.B.; Waters, J.K.; Emerich, D.W. Analysis of Poly- β -Hydroxybutyrate in *Rhizobium Japonicum* Bacteroids by Ion-Exclusion High-Pressure Liquid Chromatography and UV Detection. *Appl. Environ. Microbiol.* **1983**, *46*, 1339–1344. [\[CrossRef\]](#)

31. Carmichael, W.W.; Gorham, P.R. An Improved Method for Obtaining Axenic Clones of Planktonic Blue-Green Algae1,2. *J. Phycol.* **1974**, *10*, 238–240. [[CrossRef](#)]
32. Sarchizian, I.; Ardelean, I.I. Improved Lysozyme Method to Obtain Cyanobacteria in Axenic Cultures. *Rom. J. Biol.–Plant Biol.* **2010**, *55*, 143–150.
33. Arnfield, A.J. Köppen-Geiger-Pohl Climate Classification. Available online: <https://www.britannica.com/science/Koppen-climate-classification> (accessed on 1 February 2022).
34. Varuni, P.; Menon, S.N.; Menon, G.I. Phototaxis as a Collective Phenomenon in Cyanobacterial Colonies. *Sci. Rep.* **2017**, *7*, 17799. [[CrossRef](#)]

Communication

In Situ Quantification of Polyhydroxybutyrate in Photobioreactor Cultivations of *Synechocystis* sp. Using an Ultrasound-Enhanced ATR-FTIR Spectroscopy Probe

Philipp Doppler ¹, Christoph Gasser ², Ricarda Kriechbaum ¹, Ardita Ferizi ² and Oliver Spadiut ^{1,*}

- ¹ Research Division Biochemical Engineering, Institute of Chemical, Environmental and Bioscience Engineering, TU Wien, Gumpendorfer Strasse 1a, 1060 Vienna, Austria; philipp.doppler@tuwien.ac.at (P.D.); ricarda.kriechbaum@tuwien.ac.at (R.K.)
- ² usePAT GmbH, Schönbrunner Strasse 231/2.01, 1120 Vienna, Austria; christoph.gasser@usepat.com (C.G.); ardita.ferizi@usepat.com (A.F.)
- * Correspondence: oliver.spadiut@tuwien.ac.at; Tel.: +43-1-58801-166473

Abstract: Polyhydroxybutyrate (PHB) is a very promising alternative to most petroleum-based plastics with the huge advantage of biodegradability. Biotechnological production processes utilizing cyanobacteria as sustainable source of PHB require fast in situ process analytical technology (PAT) tools for sophisticated process monitoring. Spectroscopic probes supported by ultrasound particle traps provide a powerful technology for in-line, nondestructive, and real-time process analytics in photobioreactors. This work shows the great potential of using ultrasound particle manipulation to improve spectroscopic attenuated total reflection Fourier-transformed mid-infrared (ATR-FTIR) spectra as a monitoring tool for PHB production processes in photobioreactors.

Keywords: polyhydroxyalkanoates; PHB; PAT; *Synechocystis* sp. PCC 6714; process monitoring; ultrasound particle manipulation

Citation: Doppler, P.; Gasser, C.; Kriechbaum, R.; Ferizi, A.; Spadiut, O. In Situ Quantification of Polyhydroxybutyrate in Photobioreactor Cultivations of *Synechocystis* sp. Using an Ultrasound-Enhanced ATR-FTIR Spectroscopy Probe. *Bioengineering* **2021**, *8*, 129. <https://doi.org/10.3390/bioengineering8090129>

Academic Editor: Martin Koller

Received: 20 July 2021

Accepted: 17 September 2021

Published: 21 September 2021

Publisher's Note: MDPI stays neutral with regard to jurisdictional claims in published maps and institutional affiliations.



Copyright: © 2021 by the authors. Licensee MDPI, Basel, Switzerland. This article is an open access article distributed under the terms and conditions of the Creative Commons Attribution (CC BY) license (<https://creativecommons.org/licenses/by/4.0/>).

1. Introduction

Every day, huge quantities of petroleum-based plastics are produced. The majority is for single-use purposes, not recycled and not biodegradable. Their production and disposal by incineration releases high amounts of the greenhouse gas carbon dioxide (CO₂) into the atmosphere. Nonbiodegradable plastics carelessly disposed in nature are polluting almost all habitats on earth. Plastic slowly breaks down into microplastics, threatening life in water and on land [1]. In times of serious climate change, the Paris Agreement on limiting global warming, the single-use plastics ban of the European Union, and other initiatives to avoid accumulation of plastics all over the planet, research on new technologies and materials is essential [2]. These developments should help to satisfy the Sustainable Development Goals (SDGs) proposed by the United Nations for a more sustainable future of human society [3].

One possible solution to simultaneously reduce the atmospheric CO₂ concentration and generate biodegradable plastics are cyanobacteria. Several species of cyanobacteria produce different types of polyhydroxyalkanoates (PHAs) photoautotrophically, i.e., solely out of light energy and CO₂ [4]. PHAs are alternatives to most petroleum-based plastics, and they are fully biodegradable [5]. An important representative is polyhydroxybutyrate (PHB). Alongside glycogen, PHB is accumulated by some cyanobacterial species as carbon and energy storage compound [6–8]. It is produced during nutrient starvation (nitrogen or phosphorus) or other stress-inducing factors [9,10].

The reason these bioplastics from cyanobacteria did not find their way into applications yet is that scaling-up the production processes is challenging. Usually, externally illuminated glass reactors with a high surface-to-volume ratio are used [7,11,12]. For every step during scale-up, the availability of CO₂, nutrients, and most importantly, light is

different, and biomass growth and PHB productivity strongly vary [13]. Thus, in situ quantification tools used as process analytical technology (PAT) to determine the PHB content in real-time are inevitable. Karmann et al. utilized flow cytometry for at-line PHB quantification [14], and Gutschmann et al. investigated the use of photon density wave spectroscopy for in-line PHB monitoring [15]. Vibrational spectroscopy represents another powerful technique for probing liquid as well as solid samples in a nondestructive manner, and it is also capable of in-line operation. Attenuated total reflection Fourier-transformed mid-infrared (ATR-FTIR) spectroscopy can be used to quantify the amount of PHB or glycogen accumulated within the cell [16].

In a typical in-line ATR probe, light in the mid-IR region from 400–4000 cm^{-1} is totally reflected within the diamond tip. This results in an evanescent field that penetrates approximately 1–2 μm of the cultivation broth and interacts with all molecules [17]. The changes in light intensities are recorded, and the spectra can be evaluated by univariate calibration or chemometric tools [16,18]. ATR-FTIR instruments are commercially available, and applications for in-line, on-line, or at-line monitoring are established PAT tools, e.g., for *P. chrysogenum* or *E. coli* processes [19–21]. Further, ATR-FTIR studies were done for characterization of PHAs [22], and for PHB production processes using bacteria [23–25]. In general, a specific cell spectrum in liquid culture is only achievable if the evanescent field is mainly populated by cells. Usually in stirred cultivation broths, only the liquid constituents are accessible. Different strategies were employed to selectively enhance the signal attributed to the cells, e.g., using an on-line loop to bring medium through a flow cell equipped with an ATR-element. By selectively stopping the flow, cells settle on the ATR element and are then accessible for analysis with ATR-FTIR spectroscopy. This was shown for quantification of PHB in *E. coli* [24]. After the measurement, the cells are resuspended as flow is re-established. This prolonged procedure could influence the cells due to oxygen or nutrient limitations, as well as produce biofilms as cells are not efficiently resuspended. To avoid these effects in biotechnological processes ultrasound (US) particle manipulation devices can be used [26].

It is, however, desirable to have a fast in-line measurement of the PHB content for process monitoring and control. By using spectroscopic probes and acoustic traps, which can perform in-line particle (cell) manipulation, cells can be directly accumulated in the evanescent field of an ATR probe, making them available for measurement. These acoustic traps use US standing wave fields to trap cells in the fermentation broth [27]. By alternating US frequencies, the acoustic pressure nodes carrying the cells can be moved and the cells are pushed onto the ATR diamond for direct acquisition of IR cell spectra. US particle manipulation in combination with an ATR-FTIR probe was successfully used to generate cell spectra containing quantitative information of accumulated carbohydrates in *S. cerevisiae* cultivations [28,29].

Here, we present a US particle manipulation device to enhance the quality of in situ ATR-FTIR spectra of *Synechocystis* sp. PCC 6714 during PHB accumulation. It was directly inserted into the bioreactor, enabling in-line measurement of PHB and glycogen content of the cyanobacterial cells. We did photobioreactor cultivations to evaluate the applicability of the technology as a real-time PAT tool for monitoring, and to avoid time-consuming and laborious PHB off-line analytics involving toxic chemicals.

2. Materials and Methods

2.1. Strain, Media, and Preculture Preparation

An axenic culture of wild-type *Synechocystis* sp. PCC 6714 accumulating PHB under nitrogen-limiting conditions was used [30,31]. The precultures for inoculation of photobioreactor cultivations were grown in 250 mL Erlenmeyer flasks containing 50 mL BG11 medium with 1.5 $\text{g}\cdot\text{L}^{-1}$ NaNO_3 [32]. The cells were incubated in a Minित्रon incubation shaker (Infors, Basel, Switzerland) at 28 °C, 150 rpm (25 mm amplitude) with 3% CO_2 atmosphere under continuous illumination of 50 $\mu\text{mol}\cdot\text{m}^{-2}\cdot\text{s}^{-1}$.

2.2. Bioreactor Cultivations

For photobioreactor experiments a Ralf bioreactor system (Bioengineering, Wald, Switzerland) with 6.7 L total volume respectively 5.4 L working volume was equipped with two 65 mm turbine impellers, and LED strips for external, continuous illumination via the glass jacket. 10 m of warm-white LED stripes (Paulmann, Völkens, Germany) carrying 200 LEDs with a total light power of 1,920 lm were uniformly wrapped around the vessel. The inner diameter of the reactor was 148 mm, and the illumination provided in the center, measured in cell-free BG11 medium, was $250 \mu\text{mol}\cdot\text{m}^{-2}\cdot\text{s}^{-1}$. pH was measured in-line via an EasyFerm Plus pH probe (Hamilton, Bonaduz, Switzerland). Pressurized air and CO₂ were separately controlled by two type 4850 mass flow controllers (Brooks Instruments, Hatfield, PA, USA) operated by the 0254 control unit (Brooks Instruments, Hatfield, PA, USA).

5.4 L BG11 medium containing approx. $750 \text{ mg}\cdot\text{L}^{-1}$ NaNO₃ was filled into the vessel prior to autoclaving [32]. Aeration flow of the 5% CO₂-enriched air was in total $270 \text{ mL}\cdot\text{min}^{-1}$ (0.05 vvm). The pH was controlled at 8.5 ± 0.05 via automatic addition of 2 N KOH throughout the whole process. Temperature was set to 28 °C and the stirring speed to 180 rpm. For inoculation, the preculture was added via septum to a final optical density at 750 nm (OD₇₅₀) of 0.12. Samples were drawn in regular intervals every day until the end of process. To monitor cell growth OD₇₅₀ was determined for every sample in 1 mL cuvettes on a Nanodrop One photometer (Thermo Fisher Scientific, Waltham, MA, USA). Dry cell weight (DCW) was estimated via following correlation found in previous studies [33]:

$$\text{DCW} [\text{mg}\cdot\text{L}^{-1}] = 168.9 * \text{OD}_{750} \quad (1)$$

Nitrate concentrations in the medium were determined on an ICS-6000 ion chromatography system with an IonPac AS11 column (Thermo Fisher Scientific, Waltham, MA, USA). The method was recently described in detail elsewhere [34].

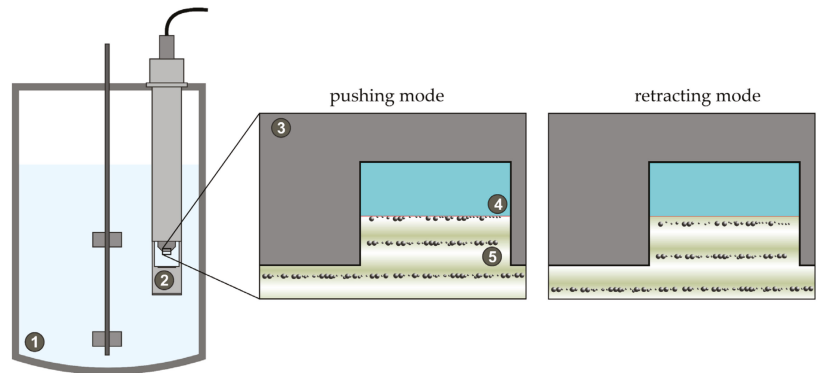
2.3. In-Line Ultrasound-Enhanced ATR-FTIR Measurements

A ReactIR 45m spectrometer with plug-and-play interface was connected to a 1.5 m silver halide optical fiber ATR probe with diamond tip (Mettler Toledo, Columbus, OH, USA). It was used for collecting mid-IR spectra between 800 and $1,800 \text{ cm}^{-1}$ at a resolution of 4 cm^{-1} . The detector was constantly cooled by liquid nitrogen and the device purged with dry air. For data acquisition, the software iC IR 4.2 (Mettler Toledo, Columbus, OH, USA) was used. As a background, cultivation medium before inoculation was measured. A spectrum was recorded every minute with 256 scans.

The ATR probe head together with the soniccatch add-on (usePAT GmbH, Vienna, Austria) formed a US trap (see Scheme 1). The created standing wave US field held cells in place directly in the reactor. By accurate control of the field parameters via the US transducer through the US amplifier sonicamp (usePAT GmbH, Vienna, Austria), the cells could either be pushed into the evanescent field of the ATR or retracted from it, enabling a selective in-situ FTIR measurement of the cells and their PHB and glycogen content. The distance of ATR surface to US transducer was 2.8 mm, the frequency of the driving amplifier was set to 2.18 MHz. The used trapping protocol involved four steps: firstly, cells were trapped at a catching frequency, followed by a successive stepwise ramp to push the cells into the evanescent field. Afterwards, the frequency was adjusted back to retract the cells. Finally, the cells were released, and the cycle started anew. This ensured the catching and measurement of new cells from the fermentation broth.

Spectra treatment and evaluation was done in Python 3.8 using the numpy, scipy, and pandas libraries. Spectra were smoothed using a Savitzky–Golay filter with a window length of 15 and a third order polynomial. Catching of cells was verified by evaluating the integrated intensity of the Amide II band (ca. 1540 cm^{-1}), since this absorption band is characteristic of the cells. Pristine cell spectra were obtained by subtracting consecutive spectra of retracted and pushed cells, leading to drift-free absorbance spectra. Since the amount of caught and pushed cells varied, for the determination of PHB and glycogen

content the spectra were normalized to the Amide II band. For PHB quantification, the most important band at 1738 cm^{-1} , corresponding to the carbonyl stretch, was integrated, and correlated to the amount of PHB in the cells determined by the reference method. Since this band is not overlapped by any other substance in the matrix, a simple univariate calibration was possible. The determination of glycogen was performed analogously using the absorption band at 1030 cm^{-1} .



Scheme 1. Experimental setup: (1) a glass bioreactor with stirrer. (2) The sonic-catch add-on in combination with the ReactIR 45m diamond ATR probe formed the US trap. (3) Detail of ATR probe tip (4), where the US standing wave field (shaded in green, (5)) catches cells in pressure nodal points. By accurate control of this US field, cells can either be pushed into evanescent field of ATR or retracted from it.

2.4. Off-Line Quantification of PHB and Glycogen

After centrifugation of 1 mL culture aliquots, the cell pellets were dried at $75\text{ }^{\circ}\text{C}$ for 24 h, and directly used for PHB and glycogen sample preparation and measurement [33]. Briefly, PHB was quantified on an UltiMate 3000 HPLC system (Thermo Fisher Scientific, Waltham, MA, USA) with an Aminex HPX-87 H column (Bio-Rad Laboratories, Hercules, CA, USA). Glycogen was determined on an ICS-6000 ion chromatography system with a CarboPac PA10 column (Thermo Fisher Scientific, Waltham, MA, USA).

3. Results

3.1. Photobioreactor Cultivations

For accumulation of PHB within the wild-type *Synechocystis* sp. PCC 6714 strain photobioreactor cultivations were conducted, and biomass growth and nitrate content monitored (Figure 1).

During the biomass growth phase, growth was almost linear within the first seven days (168 h) with an average growth rate $\mu_{\text{linear}} = 0.15\text{ g}\cdot\text{L}^{-1}\cdot\text{d}^{-1}$ to a value of $1.06\text{ g}\cdot\text{L}^{-1}$. The available nitrate in the medium of 9.0 mM was consumed after 168 h, which resulted in an average biomass per spent nitrate yield of $1.87\text{ g}\cdot\text{g}^{-1}$. Following the depletion of nitrogen, PHB production started. After a maximum of $1.39\text{ g}\cdot\text{L}^{-1}$ biomass was reached at 309 h, the cell concentration started to decline, and thus, the process was stopped at a final DCW of $1.33\text{ g}\cdot\text{L}^{-1}$ after 344 h (Figure 1).

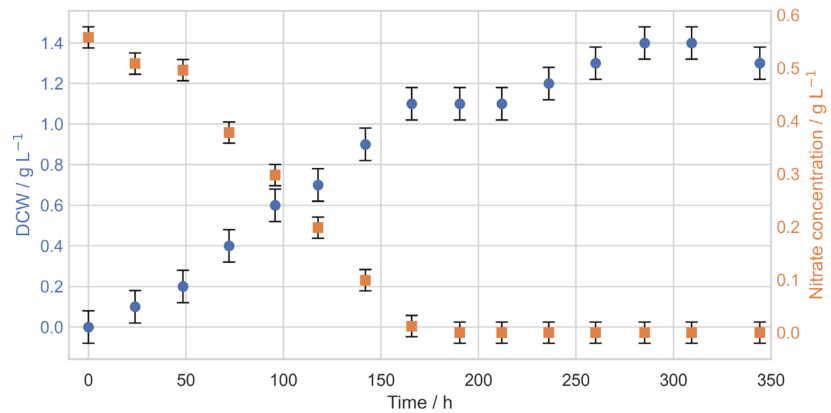


Figure 1. A photobioreactor cultivation of *Synechocystis* sp. PCC 6714 under nitrogen-limiting conditions showing the DCW (blue) and nitrate concentration (orange) during process. Error bars reflect the error of calibration curve.

3.2. Ultrasound-Enhanced ATR-FTIR Spectra

Figure 2a depicts typical process FTIR spectra, with the orange spectrum at the top representing a spectrum in retracted state and the spectrum in blue representing the pushing state. Clear bands attributed to specific vibrational transitions in organic material, and in this case, cells can be seen in the blue spectrum, e.g., the Amide I band at 1650 cm^{-1} , the Amide II band at 1540 cm^{-1} , or the fingerprint region from $990\text{--}1200\text{ cm}^{-1}$. Figure 2b shows the integrated intensity of the Amide II band at 1540 cm^{-1} . When the cells were pushed into the evanescent field of the ATR, the intensity raised, and when the cells were pulled out again, it decreased. The resulting modulation was stable and allowed for the subtraction of a pair of differently manipulated spectra, which yielded a pristine spectrum of the cells, shown at the bottom of Figure 2a in green. As indicated in Figure 2b, the intensity of the Amide II band was used to automatically detect pairs for spectra subtraction, as it was not affected as strongly by shifts of the OH-deformation band of water at 1650 cm^{-1} compared to that of the Amide I band.

In these subtracted spectra, the accumulation of PHB in the cell during the nitrogen deprived cultivation became clearly visible, as the band attributed to the carbonyl stretch of the PHB at 1738 cm^{-1} was free standing and could thus be used directly for determination of the PHB content. It was in good agreement with the reference spectrum obtained by direct measurement of PHB powder (Figure 3).

3.3. In Situ Quantification of PHB Content

Cell spectra obtained during the cultivations revealed a steady increase in the intensity of the PHB absorption band at 1738 cm^{-1} , as shown in Figure 3. These spectra were normalized to the Amide II band to accommodate the fact that during catching of new cells, not the exact same amount of material could be caught and was pushed into the evanescent field of the ATR for FTIR measurement. In this case, we used nonoverlapping bands as an internal standard for intensity correction, and the Amide II band was not affected by either PHB or glycogen, or other components of the cultivation broth. For calibration, reference values were needed. For the characterization of the cultivation at different time intervals, offline samples were taken and analyzed for PHB and glycogen content. Because the timestamp of the offline reference samples and the in-line measurements did not necessarily coincide, the offline references were used to fit a model describing its evolution over time. With the obtained reference points, a univariate calibration (band integral at 1738 cm^{-1} for PHB, band height at 1025 cm^{-1} for glycogen) was performed.

This resulted in coefficients of determination (R^2) and limit of quantifications (LOQ) of 0.91 and $18.3 \text{ mg}\cdot\text{g}^{-1}$ and 0.90 and $71.2 \text{ mg}\cdot\text{g}^{-1}$ for PHB and glycogen, respectively, as summarized in Table 1.

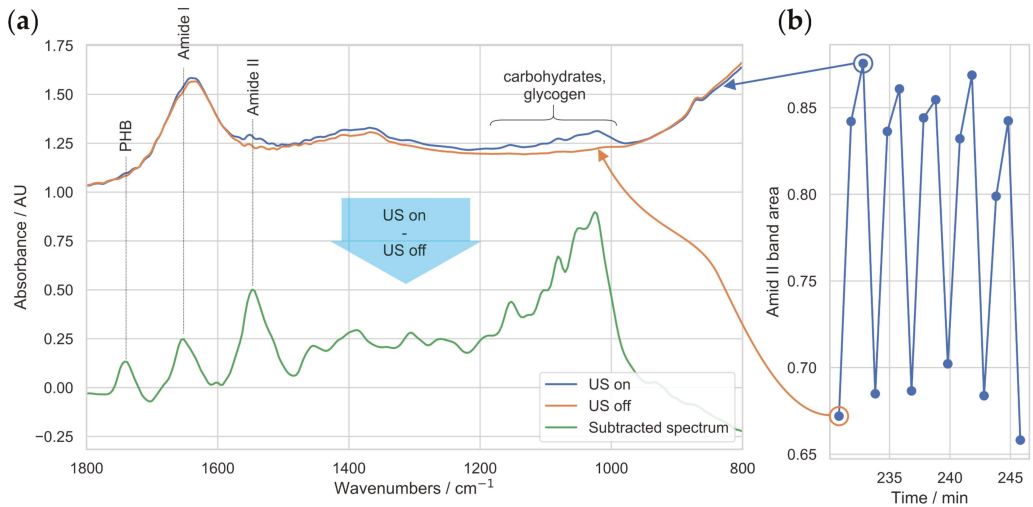


Figure 2. Typical process FTIR spectra. (a) Two selected spectra with activated (blue) and deactivated US capture (orange) are depicted on top. Subtraction yielded pure spectra of *Synechocystis* sp. 6714, shown at bottom (green). (b) Integrated signal from the Amide II band, showing modulation occurring when US trap was in pushing mode vs. retracting mode.

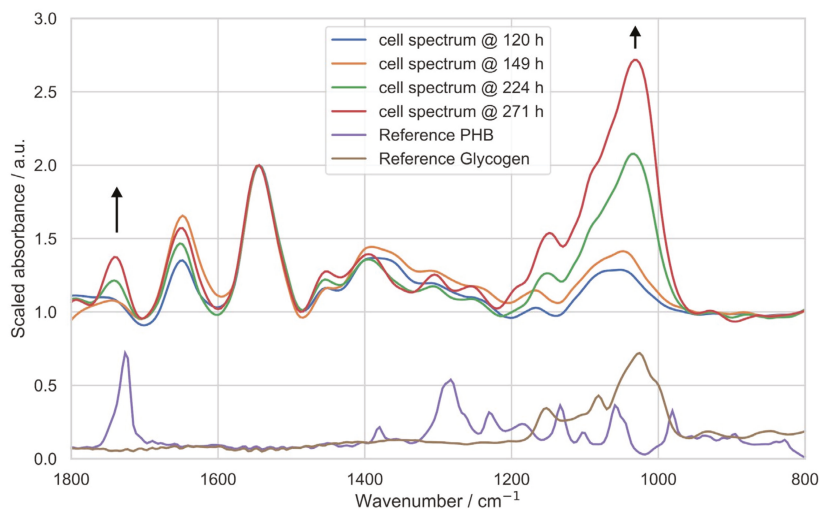


Figure 3. Top: in-line spectra of cells during different times in fermentation. PHB and glycogen bands were increasing steadily. Bottom: reference spectra of dry PHB and glycogen powder, showing approximate position of specific absorption bands.

Table 1. Calibration results for PHB and glycogen in situ quantification.

Analyte	Method	Adj. R ² [-]	LOQ [mg·g ⁻¹]
PHB	Band integration (1705–1774 cm ⁻¹), baseline corrected	0.91	18.3
Glycogen	Band height at 1025 cm ⁻¹ , baseline corrected	0.90	71.2

With an established calibration, the trends of accumulated PHB and glycogen during the cultivation were plotted (Figure 4). The in-line determined PHB and glycogen content were in good agreement with the references obtained from offline analytics.

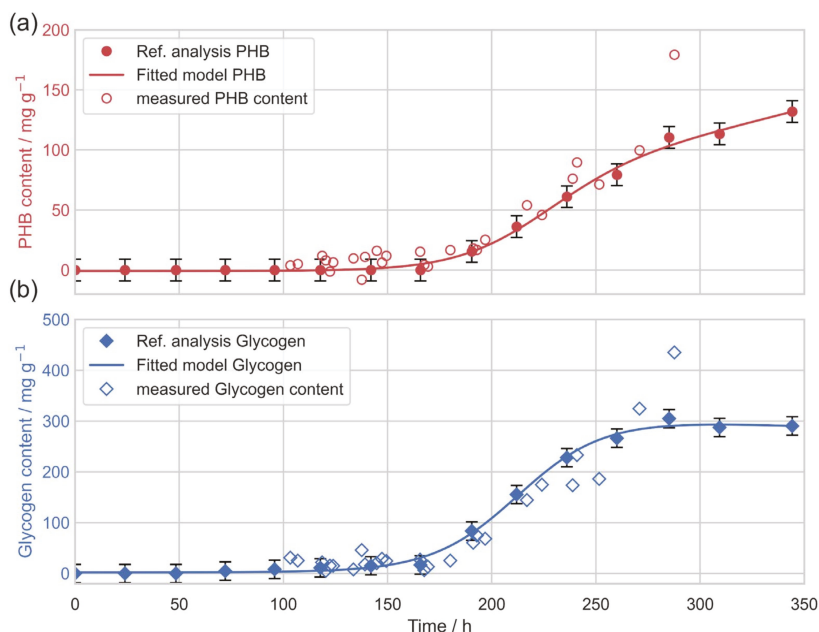


Figure 4. Trend of accumulated storage compounds during *Synechocystis* sp. PCC 6714 cultivation. (a) In-cell PHB; (b) glycogen content. Reference analysis was performed offline (filled markers). Profile was modeled to extracted reference points for caught spectra. In-line measured quantities are depicted as unfilled markers. Error bars reflect error of calibration curve.

4. Discussion

For the production of PHB classical two-phase cultivation processes were performed. During the first stage, the biomass growth phase, linear growth with an average rate of 0.15 g·L⁻¹·d⁻¹ was observed until 168 h of process time. Linear photoautotrophic growth is typical for stirred photobioreactors since the cells are usually light-limited [12]. This is due to the long distances photons have to travel in the wide vessel, and it occurs even in diluted cultures [35,36]. After 168 h, the nitrate was completely consumed. This initiated the PHB production phase to a maximum intracellular product content of 132 mg·g⁻¹ (13.2%) of DCW, respectively a volumetric PHB concentration of 175 mg·L⁻¹, which is in the range of published values for this strain [30]. The process was stopped after biomass concentration started to decline after 344 h.

Throughout the cultivation, the frequency of the US trap was alternated according to the proposed four-step protocol for trapping, pushing, retracting and releasing. By this, different ATR-FTIR spectra were obtained, which yielded pristine spectra of caught

Synechocystis sp. PCC 6714 cells. Specific bands for PHB at 1738 cm^{-1} (C-O stretch) and the characteristic region for glycogen between 950 and 1200 cm^{-1} (combinations of C-O, C-C and C-O-H stretch) could be assigned by comparison to that of off-line spectra of respective pure standard material and literature values [37,38]. The shift between measured in-line spectra of PHB compared to that of pure, dry PHB powder was ascribed to different IR absorption maxima of amorphous and crystalline PHB. Thus, the PHB accumulated within *Synechocystis* sp. PCC 6714 was predominantly amorphous [24]. After correlating off-line to in situ acquired spectral data, LOQ values for cellular PHB and glycogen content of 18.3 and $71.2\text{ mg}\cdot\text{g}^{-1}$ were calculated. The possibility to directly measure PHB in the cell by simply using the characteristic band intensity of PHB is a straightforward univariate analysis technique, void of complex chemometric modelling. This allows for straight interpretation of the acquired spectra.

We successfully utilized a US particle manipulation device to enhance ATR-FTIR spectra quality for PHB and glycogen quantification in situ in a photobioreactor. The accumulation of these compounds was quantified and monitored throughout the cultivation process. This work shows the great potential of this method as a real-time PAT monitoring tool for PHB production processes.

Author Contributions: Conceptualization, P.D., C.G. and O.S.; methodology, P.D., C.G., R.K. and A.F.; software, P.D., C.G. and A.F.; validation, C.G. and A.F.; formal analysis, P.D. and C.G.; investigation, P.D., C.G., R.K. and A.F.; resources, C.G.; data curation, C.G.; writing—original draft preparation, P.D. and C.G.; writing—review and editing, P.D., C.G., R.K. and O.S.; visualization, P.D. and C.G.; supervision, C.G. and O.S.; project administration, C.G. and O.S.; funding acquisition, O.S. All authors have read and agreed to the published version of the manuscript.

Funding: We thank Interreg Project Plastocyan ATCZ260 for funding. TU Wien is acknowledged for funding the doctoral college bioactive. Open Access Funding by TU Wien Bibliothek.

Institutional Review Board Statement: Not applicable.

Informed Consent Statement: Not applicable.

Data Availability Statement: The data presented in this study are available on request from the corresponding author.

Conflicts of Interest: The authors declare no conflict of interest.

References

- Prata, J.C.; da Costa, J.P.; Lopes, I.; Duarte, A.C.; Rocha-Santos, T. Environmental exposure to microplastics: An overview on possible human health effects. *Sci. Total Environ.* **2020**, *702*, 134455. [CrossRef]
- Hoegh-Guldberg, O.; Jacob, D.; Taylor, M.; Guillen Bolanos, T.; Bindi, M.; Brown, S.; Camilloni, I.A.; Diedhiou, A.; Djalante, R.; Ebi, K.; et al. The human imperative of stabilizing global climate change at $1.5\text{ }^{\circ}\text{C}$. *Science* **2019**, *365*, eaaw6974. [CrossRef]
- United Nations. The 17 Sustainable Development Goals. Available online: <https://sdgs.un.org/goals> (accessed on 19 July 2021).
- Ansari, S.; Fatma, T. Cyanobacterial polyhydroxybutyrate (PHB): Screening, optimization and characterization. *PLoS ONE* **2016**, *11*, 1–20. [CrossRef]
- Mergaert, J.; Anderson, C.; Wouters, A.; Swings, J.; Kersters, K. Biodegradation of polyhydroxyalkanoates. *FEMS Microbiol. Lett.* **1992**, *103*, 317–321. [CrossRef]
- Troschl, C.; Meixner, K.; Drosig, B. Cyanobacterial PHA Production-Review of Recent Advances and a Summary of Three Years' Working Experience Running a Pilot Plant. *Bioengineering* **2017**, *4*, 26. [CrossRef]
- Koller, M. A review on established and emerging fermentation schemes for microbial production of polyhydroxyalkanoate (PHA) biopolyesters. *Fermentation* **2018**, *4*, 30. [CrossRef]
- Markl, E.; Grünbichler, H.; Lackner, M. Cyanobacteria for PHB Bioplastics Production: A Review. *Algae (IntechOpen)* **2019**. [CrossRef]
- Koch, M.; Berendzen, K.W.; Forchhammer, K. On the role and production of polyhydroxybutyrate (Phb) in the cyanobacterium *synechocystis* sp. pcc 6803. *Life* **2020**, *10*, 47. [CrossRef] [PubMed]
- Mendhulkar, V.D.; Shetye, L.A. Synthesis of biodegradable polymer polyhydroxyalkanoate (PHA) in cyanobacteria *Synechococcus elongatus* under mixotrophic nitrogen- and phosphate-mediated stress conditions. *Ind. Biotechnol.* **2017**, *13*, 85–93. [CrossRef]
- Fu, J.; Huang, Y.; Liao, Q.; Xia, A.; Fu, Q.; Zhu, X. Photo-bioreactor design for microalgae: A review from the aspect of CO_2 transfer and conversion. *Bioresour. Technol.* **2019**, *292*, 121947. [CrossRef] [PubMed]

12. Doppler, P.; Spadiut, O. Introduction to autotrophic cultivation of microalgae in photobioreactors. In *The Autotrophic Biorefinery*; Kourist, R., Schmidt, S., Eds.; Walter de Gruyter GmbH: Berlin, Germany, 2021. [\[CrossRef\]](#)
13. Socher, M.L.; Löser, C.; Schott, C.; Bley, T.; Steingroewer, J. The challenge of scaling up photobioreactors: Modeling and approaches in small scale. *Eng. Life Sci.* **2016**, *16*, 598–609. [\[CrossRef\]](#)
14. Karmann, S.; Follonier, S.; Bassas-Galia, M.; Panke, S.; Zinn, M. Robust at-line quantification of poly(3-hydroxyalkanoate) biosynthesis by flow cytometry using a BODIPY 493/503-SYTO 62 double-staining. *J. Microbiol. Methods* **2016**, *131*, 166–171. [\[CrossRef\]](#) [\[PubMed\]](#)
15. Gutschmann, B.; Schiewe, T.; Weiske, M.T.H.; Neubauer, P.; Hass, R.; Riedel, S.L. In-line monitoring of polyhydroxyalkanoate (PHA) production during high-cell-density plant oil cultivations using photon density wave spectroscopy. *Bioengineering* **2019**, *6*, 85. [\[CrossRef\]](#) [\[PubMed\]](#)
16. Lourenço, N.D.; Lopes, J.A.; Almeida, C.F.; Sarraguça, M.C.; Pinheiro, H.M. Bioreactor monitoring with spectroscopy and chemometrics: A review. *Anal. Bioanal. Chem.* **2012**, *404*, 1211–1237. [\[CrossRef\]](#) [\[PubMed\]](#)
17. Griffiths, P.R.; De Haseth, J.A. Attenuated Total Reflection. *Fourier Transform. Infrared Spectrom. Second. Ed.* **2007**, 321–348. [\[CrossRef\]](#)
18. Doppler, P.; Veiter, L.; Spadiut, O.; Herwig, C.; Rajamanickam, V. A Chemometric Tool to Monitor and Predict Cell Viability in Filamentous Fungi Bioprocesses Using UV Chromatogram Fingerprints. *Processes* **2020**, *8*, 461. [\[CrossRef\]](#)
19. Koch, C.; Posch, A.E.; Goicoechea, H.C.; Herwig, C.; Lendl, B. Multi-analyte quantification in bioprocesses by Fourier-transform-infrared spectroscopy by partial least squares regression and multivariate curve resolution. *Anal. Chim. Acta* **2014**, *807*, 103–110. [\[CrossRef\]](#)
20. Koch, C.; Posch, A.E.; Herwig, C.; Lendl, B. Comparison of Fiber Optic and Conduit Attenuated Total Reflection (ATR) Fourier Transform Infrared (FT-IR) Setup for In-Line Fermentation Monitoring. *Appl. Spectrosc.* **2016**, *70*, 1965–1973. [\[CrossRef\]](#) [\[PubMed\]](#)
21. Kastenhofer, J.; Libiseller-egger, J.; Rajamanickam, V.; Spadiut, O. Monitoring, E. coli Cell Integrity by ATR-FTIR Spectroscopy and Chemometrics: Opportunities and Caveats. *Processes* **2021**, *9*, 422. [\[CrossRef\]](#)
22. Xu, J.; Guo, B.H.; Yang, R.; Wu, Q.; Chen, G.Q.; Zhang, Z.M. In situ FTIR study on melting and crystallization of polyhydroxyalkanoates. *Polymer* **2002**, *43*, 6893–6899. [\[CrossRef\]](#)
23. Wendlandt, K.D.; Geyer, W.; Mirschel, G.; Al-Haj Hemidi, F. Possibilities for controlling a PHB accumulation process using various analytical methods. *J. Biotechnol.* **2005**, *117*, 119–129. [\[CrossRef\]](#) [\[PubMed\]](#)
24. Jarute, G.; Kainz, A.; Schroll, G.; Baena, J.R.; Lendl, B. On-line determination of the intracellular poly(β -hydroxybutyric acid) content in transformed *Escherichia coli* and glucose during PHB production using stopped-flow attenuated total reflection FT-IR spectrometry. *Anal. Chem.* **2004**, *76*, 6353–6358. [\[CrossRef\]](#)
25. Porras, M.A.; Cubitto, M.A.; Villar, M.A. A new way of quantifying the production of poly(hydroxyalkanoate)s using FTIR. *J. Chem. Technol. Biotechnol.* **2015**, *91*, 1240–1249. [\[CrossRef\]](#)
26. Radel, S.; Schnöller, J.; Lendl, B.; Gröschl, M.; Benes, E. Anwendung der Ultraschall-Teilchen-Manipulation für die Online-Infrarot-Spektroskopie von (Zell-)Suspensionen. *Elektrotechnik Und Inf.* **2008**, *125*, 76–81. [\[CrossRef\]](#)
27. Radel, S.; Brandstetter, M.; Lendl, B. Observation of particles manipulated by ultrasound in close proximity to a cone-shaped infrared spectroscopy probe. *Ultrasonics* **2010**, *50*, 240–246. [\[CrossRef\]](#)
28. Koch, C.; Brandstetter, M.; Lendl, B.; Radel, S. Ultrasonic Manipulation of Yeast Cells in Suspension for Absorption Spectroscopy with an Immersible Mid-Infrared Fiberoptic Probe. *Ultrasound Med. Biol.* **2013**, *39*, 1094–1101. [\[CrossRef\]](#)
29. Koch, C.; Brandstetter, M.; Wechselberger, P.; Lorantfy, B.; Plata, M.R.; Radel, S.; Herwig, C.; Lendl, B. Ultrasound-Enhanced Attenuated Total Reflection Mid-infrared Spectroscopy In-Line Probe: Acquisition of Cell Spectra in a Bioreactor. *Anal. Chem.* **2015**, *87*, 2314–2320. [\[CrossRef\]](#)
30. Kamravamanesh, D.; Pflüg, S.; Nischkauer, W.; Limbeck, A.; Lackner, M.; Herwig, C. Photosynthetic poly- β -hydroxybutyrate accumulation in unicellular cyanobacterium *Synechocystis* sp. PCC 6714. *AMB Express* **2017**, *7*, 143. [\[CrossRef\]](#) [\[PubMed\]](#)
31. Doppler, P.; Kriechbaum, R.; Singer, B.; Spadiut, O. Make microalgal cultures axenic again—A fast and simple workflow utilizing fluorescence-activated cell sorting. *J. Microbiol. Methods* **2021**, *186*, 106256. [\[CrossRef\]](#)
32. Stanier, R.Y.; Kunisawa, R.; Mandel, M.; Cohen-Bazire, G. Purification and properties of unicellular blue-green algae (order Chroococcales). *Bacteriol. Rev.* **1971**, *35*, 171–205. [\[CrossRef\]](#) [\[PubMed\]](#)
33. Mittermair, S.; Richer, J.; Doppler, P.; Trenzinger, K.; Nicoletti, C.; Forsich, C.; Spadiut, O.; Herwig, C.; Lackner, M. Impact of exoD gene knockout on the polyhydroxybutyrate overaccumulating mutant Mt_a24. *Int. J. Biobased Plast.* **2021**, *3*, 1–18. [\[CrossRef\]](#)
34. Doppler, P.; Kornpointner, C.; Halbwirth, H.; Remias, D.; Spadiut, O. Tetraedron minimum, first reported member of hydrodictyaceae to accumulate secondary carotenoids. *Life* **2021**, *11*, 107. [\[CrossRef\]](#)
35. Schuurmans, R.M.; Matthijs, J.C.P.; Hellingwerf, K.J. Transition from exponential to linear photoautotrophic growth changes the physiology of *Synechocystis* sp. PCC 6803. *Photosynth. Res.* **2017**, *132*, 69–82. [\[CrossRef\]](#)
36. Ogbonna, J.C.; Yada, H.; Masui, H.; Tanaka, H. A novel internally illuminated stirred tank photobioreactor for large-scale cultivation of photosynthetic cells. *J. Ferment. Bioeng.* **1996**, *82*, 61–67. [\[CrossRef\]](#)

37. Quilès, F.; Polyakov, P.; Humbert, F.; Francius, G. Production of extracellular glycogen by *Pseudomonas fluorescens*: Spectroscopic evidence and conformational analysis by biomolecular recognition. *Biomacromolecules* **2012**, *13*, 2118–2127. [[CrossRef](#)]
38. Kansiz, K.; Billman-Jacobe, H.; McNaughton, D. Quantitative determination of the biodegradable polymer poly(β -hydroxybutyrate) in a recombinant *Escherichia coli* strain by use of mid-infrared spectroscopy and multivariate statistics. *Appl. Environ. Microbiol.* **2000**, *66*, 3415–3420. [[CrossRef](#)]

Article

Modelling Mixed Microbial Culture Polyhydroxyalkanoate Accumulation Bioprocess towards Novel Methods for Polymer Production Using Dilute Volatile Fatty Acid Rich Feedstocks

Alan Werker ^{1,2,*}, Laura Lorini ³, Marianna Villano ³, Francesco Valentino ⁴ and Mauro Majone ³¹ Promiko AB, Briggatan 16, 23442 Lomma, Sweden² School of Chemical Engineering, The University of Queensland, Brisbane, QLD 4072, Australia³ Department of Chemistry, Sapienza University of Rome, Piazzale Aldo Moro 5, 00185 Rome, Italy;

laura.lorini@uniroma1.it (L.L.); marianna.villano@uniroma1.it (M.V.); mauro.majone@uniroma1.it (M.M.)

⁴ Department of Environmental Sciences, Informatics and Statistics, Cà Foscari University of Venice, Via Torino 155, 30172 Venice, Italy; francesco.valentino@unive.it

* Correspondence: alan@werker.se

Abstract: Volatile fatty acid (VFA) rich streams from fermentation of organic residuals and wastewater are suitable feedstocks for mixed microbial culture (MMC) Polyhydroxyalkanoate (PHA) production. However, many such streams have low total VFA concentration (1–10 gCOD/L). PHA accumulation requires a flow-through bioprocess if the VFAs are not concentrated. A flow through bioprocess must balance goals of productivity (highest possible influent flow rates) with goals of substrate utilization efficiency (lowest possible effluent VFA concentration). Towards these goals, dynamics of upshift and downshift respiration kinetics for laboratory and pilot scale MMCs were evaluated. Monod kinetics described a hysteresis between the upshift and downshift responses. Substrate concentrations necessary to stimulate a given substrate uptake rate were significantly higher than the concentrations necessary to sustain the attained substrate uptake rate. A benefit of this hysteresis was explored in Monte Carlo based PHA accumulation bioprocess numerical simulations. Simulations illustrated for a potential to establish continuous flow-through PHA production bioprocesses even at a low (1 gCOD/L) influent total VFA concentration. Process biomass recirculation into an engineered higher substrate concentration mixing zone, due to the constant influent substrate flow, enabled to drive the process to maximal possible PHA production rates without sacrificing substrate utilization efficiency.

Keywords: polyhydroxyalkanoates (PHA); polyhydroxybutyrate (PHB); mixed microbial cultures; activated sludge; respiration kinetics; Monod kinetics; oxygen mass balance; hysteresis; process modelling

Citation: Werker, A.; Lorini, L.; Villano, M.; Valentino, F.; Majone, M. Modelling Mixed Microbial Culture Polyhydroxyalkanoate Accumulation Bioprocess towards Novel Methods for Polymer Production Using Dilute Volatile Fatty Acid Rich Feedstocks. *Bioengineering* **2022**, *9*, 125. <https://doi.org/10.3390/bioengineering9030125>

Academic Editor: Giorgos Markou

Received: 9 February 2022

Accepted: 16 March 2022

Published: 21 March 2022

Publisher's Note: MDPI stays neutral with regard to jurisdictional claims in published maps and institutional affiliations.



Copyright: © 2022 by the authors. Licensee MDPI, Basel, Switzerland. This article is an open access article distributed under the terms and conditions of the Creative Commons Attribution (CC BY) license (<https://creativecommons.org/licenses/by/4.0/>).

1. Introduction

Polyhydroxyalkanoates (PHAs) are a family of semi-crystalline polyesters that are naturally accumulated by many species of bacteria, for carbon and energy intermediate storage [1]. Accumulated polymer is stored in bacteria as intracellular granules. The recoverable pure polymers are biodegradable and have thermoplastic properties of interest for bioplastics and chemical industries [2]. PHA properties can be manipulated based on monomer composition, monomer distribution, and polymer molecular mass distribution. As such, PHAs are tagged as a biobased renewable resource with broad potential for services and products of value for society [3].

Limited types and amounts of PHAs are available commercially today [4], with supplies principally generated by pure culture production methods and refined feedstocks. PHAs can also be produced as a by-product of organic residual (waste) management using pure microbial cultures, as well as with open cultures of bacterial biomass that are enriched with the PHA-storing phenotype [5,6]. Open culture bioprocess environments

can generate selection pressures. These selection pressures can favour preferred survival of populations of species of PHA-accumulating microorganisms due to competitive advantage with rapid substrate uptake and metabolism via PHA storage. Bioprocesses by design, or by coincidence, will generate selection pressures, for PHA-accumulating microorganisms, related to factors such as substrate type and feeding methods [7], operating temperature [8], and/or the process environments engineered for wastewater contaminant removal [9,10]. Significant storage capacities of PHAs in open or so-called mixed microbial cultures (MMCs) have been accomplished in the laboratory and up to pilot scale in the range from 40 to 90% gPHA per gram of biomass volatile solids [11,12]. The present work concerns bioprocess challenges for industrial scale PHA production using MMCs. Specifically, this work addresses the idea to develop bioprocess methods which allow producing PHA in MMCs with continuous influent flow constant volume bioprocesses using moderate to low concentration volatile fatty acid (VFA) rich feedstocks as substrate.

MMCs can be made to accumulate PHA with VFA rich feedstocks. Effluents of suspended solids separated acidogenic fermentation liquors from wastewater and sludges, dominated by (C2 to C5) VFAs, are typically found to result in co-polymer blends of poly(3-hydroxybutyrate-co-3-hydroxyvalerate) [13]. Other types of more complex MMC co-polymer blends have also been reported [14–16]. The VFA composition strongly influences the accumulated co-polymer monomer distribution and, thereby, resultant co-polymer blend crystallinity. Even full-scale waste municipal activated sludge has been shown to be directly applicable to produce commercial quality PHAs [17]. Evidence was given for engineering polymer properties and maintaining quality control with VFA feedstocks produced from fermented sludge and industrial waste at pilot scale. Extent of maximum polymer crystallinity was steered predictably over a wide range by the feedstock composition for consistently applied accumulation methods. Crystallinity influences microstructure with concomitant influence on thermal, physical, and mechanical properties to suit many kinds of applications.

Pilot scale projects have repeatedly demonstrated technical feasibility for commercial scale PHA production based on direct accumulation of surplus biomass treating wastewater or using biomass produced with selection pressures specifically for MMC PHA production [11]. Notwithstanding, specific considerations to address underlying expected challenges of bioprocess methods for industrial scale MMC PHA production are lacking in the research literature. Considerations of upscaled process have been given for acclimation towards augmented polymer storage [18], for mitigating influence of autotrophic flanking populations [19] and for influences of changes in process temperature [20] during the PHA accumulation, for examples. Robust industrial scale mixed culture PHA accumulation processes will be needed wherein methods are specifically independent, or at least insensitive, to feedstock VFA concentration. This independence would allow the same facility to have flexibility to produce polymers with “direct accumulation” [11] biomass fed with available regional VFA-rich feedstock. Such a facility would need to accommodate variability of feedstock VFA composition and concentration. Consideration of approach for industrial scale continuous flow through PHA accumulation, especially for cases with substrates of lower VFA concentrations (<10 gCOD/L), have not been found to be addressed in the research literature.

Pure culture methods for PHA production classically rely on fed-batch fermentation processes with concentrated feedstocks. A mass of organic substrate is to be delivered to a microbial biomass to achieve as high a titre of PHA containing bacteria as possible, in the shortest possible time, and within the limits of the available bioprocess volume [21]. Batch systems for pure culture PHA production methods may often be with starting broth organic substrate concentrations of between 10 and 20 g/L. The source feedstocks have an order of magnitude higher concentration. In this way, a high mass of substrate can be added with small additions of liquid volume. Ideas and methods for continuous production are evolving [22]. These continuous methods are applied to achieve gains in volumetric

productivity if batch to batch down times are reduced. Higher concentrated feedstocks are nevertheless still desirable towards facilitating pure culture PHA process operations.

MMC PHA production methods must similarly strive to achieve as high a productivity as possible in mass polymer produced per unit volume and time. Acidogenic fermentation effluents can be sourced from commonly available regional sources of municipal and/or industrial organic wastewater and sludge. However, a challenge is that these typically available fermentation feedstocks do not often have high total VFA concentrations. VFA rich feedstocks from fermented organic waste streams from industrial and municipal sources may often, and in own direct experience with examples over 20 years, be in the low VFA concentration range between 0.5 to 10 g/L [23]. Higher VFA concentrations are possible with fermentations in selected limited cases such as dairy [24,25] and fishing [26] industry residues. However, these examples may not be sufficiently large enough VFA sources to promote wide generic implementation of MMC PHA production at industrial scale. For broad implementation of MMC PHA production, one must consider to exploit commonly available surplus organic residues that societies generate, collect and process. Bioprocess methods that are applicable over a wide range of VFA concentration are anticipated to offer greater flexibility to source a wider diversity of regionally available MMC feedstocks to produce PHA within the same generic industrial facility.

If VFAs are the product for transport and sale, then innovations in methods of VFA up concentration as part of recovery are required [27]. VFA extraction during acidogenic fermentation is furthermore reported to improve yields in acidogenic fermentation [28]. However, when PHA is the end product, MMC PHA accumulation processes are the up concentration unit process due to biochemical conversion (soluble VFA to PHA granules) and biomass separability. Therefore, so long as the dilute VFA rich feedstock supplies do not require undue transportation, it is only necessary that a sufficient VFA mass is available, even if it is in a dilute form. A sufficient VFA mass is to be delivered in a volumetric flow at industrial scale to exploit the PHA storing potential of a MMC biomass such as surplus municipal activated sludge [17]. Activated sludge thickened (concentrated) biomass solids, with at least 5 to 10% dry solids content, may be brought within reasonable distance to the site of PHA production where available VFA sources exist. In the present work, MMC biomass respiration has been investigated for development of industrial scale PHA production methods with dilute VFA-rich feedstocks.

With dilute VFA-rich feedstocks it is anticipated that the feed volumes will be larger than the available bioprocess working volume. The feed volume must flow through the process, and it is required that the biomass is retained in the process by, for example, membranes [29] or gravity settling [17]. The effluent from the accumulation process should have as low a VFA concentration as possible to limit waste of substrate and effluent management costs. However, substrate uptake rate depends on substrate concentration. Therefore, high productivity, with high volumetric rates of PHA production, supposes high sustained process substrate concentrations with reference to the modelled process using Monod kinetics [30]. Higher steady state concentrations of substrate in the effluent, for flow through accumulation processes, trade-off the goal of greater substrate utilization efficiency with the goal of greater volumetric productivity.

In previous research, it was observed that traditional Monod kinetics could not adequately describe the dynamics of response of a MMC biomass during fed-batch PHA accumulation [31]. Consequently, methods of process for industrial scale accumulation were anticipated based on replicated observations of an interpreted hysteresis in the biomass dynamics of respiration with pulse wise substrate additions. Industrial methods were introduced, and these included mixing zones with higher substrate concentration for stimulating high substrate uptake rates, while maintaining these higher rates in mixing zones of significantly lower substrate concentrations. However, these previous observations were not systematically evaluated for enrichment MMCs from different sources. They were also not brought into a frame of a predictive process model.

The objective in the present work was to systematically evaluate and confirm a model for stimulation and attenuation of substrate uptake rates during PHA accumulation. Specifically, it was of interest to assess if a common model framework could be applied to two distinctly different MMCs enriched for PHA accumulation. The goal was to refine insight for conditions and principles of bioprocess engineering to maintain both high substrate utilization efficiency and optimal volumetric productivity during continuous feed mixed culture PHA production. The approach is intended to be flexible and to work well in cases for PHA production with low VFA concentration feedstock at industrial scale.

Dynamics of respiration for laboratory and pilot scale MMC enrichment cultures were characterized by oxygen and chemical oxygen demand (COD) mass balances as a function of initial substrate concentration. Acetic acid and acetate mixtures were used as the model substrate. The dynamic response of the biomass was translated into a process model that was applicable to both cultures. This process model was then applied by means of Monte Carlo numerical simulations to experiment with ideas of a constant volume, flow through, PHA production bioprocess design. The numerical simulations expressed how stimulation and maintenance mixing zones could, in principle, be applied for achieving high rates of PHA production while still maintaining low effluent substrate concentrations.

2. Materials and Methods

2.1. Biomass from a Lab-Scale SBR

A PHA-storing mixed microbial culture was produced in a 1.0 L working volume aerobic sequencing batch reactor (SBR) at room temperature (20 to 25 °C). A mechanical stirrer provided complete mixing of the culture medium without any settling, and oxygen was delivered through air pumps connected to an array of ceramic diffusers. The SBR was inoculated with activated sludge from the “Roma Nord” (Rome, Italy) full-scale municipal wastewater treatment plant (WWTP). At the time of the present study, the enrichment culture was established under steady state conditions for 3 months (12 h cycle and organic loading rate (OLR) of 8.5 gCOD/L/d). The biomass was characterized with a PHA accumulation potential in the range from 0.63 to 0.70 gPHA/gVSS. Full details of the SBR operations and performances are reported elsewhere [32].

The SBR cycle program sequence with timer controlled peristaltic pumps was as follows: (a) feast substrate feeding (10 min; 0.42 L), (b) feast reaction phase (150 min), (c) surplus biomass (mixed liquor) withdrawal (3 min; 0.50 L), (d) famine substrate feeding (5 min; 0.08 L), (e) famine reaction phase (552 min). The 1-day sludge retention time (SRT) was equal to the hydraulic retention time (HRT) due to no applied settling phase. The feast substrate was an 85:15 mixture (COD basis) of acetic and propionic acids in a mineral medium at 10.12 gCOD/L. The substrate was trimmed to pH 6.0 with NaOH from a 3.0 M stock solution. The famine substrate comprised ammonium sulphate at 7.33 g/L, and with 80 mL addition per cycle, giving a nitrogen loading of 249 mgN/d. A net excess nitrogen loading was established per cycle given a C/N balance of 34 gCOD/gN. The mineral medium composition was (mg/L): K₂HPO₄ (334), KH₂PO₄ (259), MgSO₄·7H₂O (100), CaCl₂·2H₂O (50), thiourea (20), Na₂EDTA (3), FeCl₃·6H₂O (2), H₃BO₃ (0.3), CoCl₂·6H₂O (0.2), ZnSO₄·7H₂O (0.1), MnCl₂·4H₂O (0.03), NaMoO₄·2H₂O (0.03), NiCl₂·6H₂O (0.02) and CuCl₂·2H₂O (0.01). Stability of feast and famine selection conditions were routinely monitored from dissolved oxygen (DO) trends (WTW Cell Oxi 3310).

The biomass source for replicate respiration response experiments in the present work was the withdrawn surplus biomass (c) after feast reaction (b) as described above. The 500 mL withdrawn mixed liquor was directed to an aerated vessel with the added nitrogen rich famine substrate that the wasted biomass would otherwise have experienced for the remaining cycle segments (d and e). Famine conditions were maintained for at least 8 h before the biomass was then used for replicate respiration experiments. Experiments were conducted at room temperature after the applied famine period and these experiments were completed within 26 h of the biomass withdrawal from the SBR. The famine condition for the biomass was confirmed from measured nitrogen uptake during famine, and consistent

performance in PHA content cycling (Fourier transform infrared spectroscopy (FTIR) measurements). Famine biomass in the present work refers to the biomass after famine conditions were applied for at least 8 h.

2.2. Biomass from a Pilot-Scale SBR

The pilot scale biomass was produced in an SBR (120 L working volume) operated with automatic control (Labview, National Instruments, Austin, TX, USA). The SBR was inoculated with activated sludge from Treviso full-scale WWTP (northeast Italy). The PHA-accumulating biomass exhibited typical accumulating potential between 0.40 to 0.46 gPHA/gVSS. Full details of the pilot SBR operations and performances are reported elsewhere [33].

The selection SBR was fed with filtrate coming from fermentation of a 33:67 (%v/v) mixture of the organic fraction of municipal solid waste (OFMSW) and excess waste activated sludge (WAS). Both organic input streams were produced and managed within the Treviso municipality. The fermentate used to produce the biomass was characterized with 75% soluble COD as VFA, and a VFA composition dominated by butyric and acetic acids followed by propionic and other organic acids. The SBR was operated continuously (6-h cycle and 1 d HRT and SRT) with no biomass settling phase. Aeration, with linear membrane blowers (Bibus EL-S-250), provided oxygen and mixing. The 6-h aerobic cycle was as follows: (a) surplus biomass (mixed liquor) withdrawal (0.5 min), (b) delay (10 min), (c) feed (0.5 min), and (d) reaction (349 min). Temperature (22–25 °C, maintained with immersion heater) and pH (8.0–8.5) trends were monitored, but not controlled. OLR with VFA was 3.3 ± 0.7 gCOD/L/d with variations due to VFA level and composition fluctuations from the feedstock fermentation process [33].

Two-liter grab samples from the withdrawn surplus biomass were sent chilled by overnight courier from the pilot plant in Treviso to the laboratory of the present work at La Sapienza in Rome. The received biomass was stored at 4 °C and used for experiments within 24 h after its arrival. Prior to experiments, the stored famine biomass was acclimated by warming to room temperature (23 °C) over a few hours with continuous aeration and mixing. The famine condition for the biomass was confirmed with assessment for negligible biomass PHA content (FTIR measurements).

2.3. Pulse-Stimulation Respiration Experiments

A stock of mixed liquor with the famine biomass was maintained aerated and well-mixed at constant temperature (24 ± 1 °C). For each pulse-stimulation experiment a grab sample of mixed liquor of defined dilution and volume (50 to 100 mL) was mixed to target a biomass suspended solids concentration measured as VSS (volatile suspended solids). Dilutions were made with the same media (laboratory scale MMC) or matrix (pilot scale MMC) of the mixed liquor, containing no or negligible biomass and no added organic substrate. pH was at the level established in the respective SBRs and not adjusted. For the pilot scale mixed liquor, biomass suspended solids were separated by gravity separation and decantation to generate dilution media with the same matrix. The source of dilution media was maintained similarly to the famine biomass source with constant aeration and at the same temperature. Respiration experiments were conducted with and without constant aeration, and initial substrate concentrations over a range from 5 to 500 mgCOD/L. Biomass concentrations were in the order of 1 and 2 gVSS/L for the laboratory and pilot biomass experiments, respectively.

For each experiment, the defined mixed liquor volume containing famine biomass was disposed directly to a vessel with magnetic coupled stirrer (600 rpm). This vessel was maintained with a pre-set level of constant aeration (0 to 1 mL/min air). Air flow from standard aquarium pumps was regulated through a Dwyer Series VF flowmeter. DO and pH trends were logged starting upon mixed liquor addition to the vessel and for a period of pre-aeration lasting at least 2-min. Then, a defined volume (pulse) of substrate (0.20 to 2 mL) from a concentrated stock solution was injected as an impulse to the defined

mixed liquor volume. The time point of substrate injection was tagged to the log file. DO and pH trends were followed until dissolved oxygen concentration increased again asymptotically upon substrate consumption. Such a pulse-stimulation experiment lasted anywhere from a few minutes to the better part of 1 h. This duration was expected to be dependent on the biomass source, the mass of substrate added, and the concentration of the biomass. The added aliquots of substrate stock solutions were defined mixtures of acetic acid and/or sodium acetate generated from 2 M stock solutions of acetic acid and sodium acetate trihydrate (Sigma-Aldrich > 99%), respectively.

2.4. Analytical Methods

Suspended solids from selected famine mixed liquor samples (1.5 mL Eppendorf) having negligible soluble COD were separated by microcentrifugation (RCF of $12,000\times g$ for 10 min). The supernatant was decanted to another Eppendorf tube by a single inversion, and residual hanging liquid was carefully wicked out of the tube with tissue. The pellet was either resuspended back to 1.5 mL with deionized water, or it was dried overnight at 105 °C. The suspended solids concentration was evaluated based on chemical oxygen demand (COD), for the resuspended pellet solution. The mixed liquor supernatant was stored at 4 °C pending ammonia analysis. COD measurements were with Spectroquant[®] (Merck, Milano, Italy) 25–1500 and 300–3500 mg/L kits and procedure in combination with a Spectroquant[®] NOV60A spectrophotometer (Merck, Milano, Italy). Calibration was based on an acetic acid stock solution dilution series. The COD of the famine biomass was converted to volatile suspended solids (VSS) based on the assumed biomass composition of $C_5H_7O_2N$ with 1.42 mgCOD/mgVSS. Ammonium ions were measured on supernatant samples spectrophotometrically at 420 nm by the direct Nessler method [34]. PHA content for the laboratory (feast and famine) and pilot (famine) biomass was evaluated qualitatively by FTIR on the dried pellet. FTIR measurements were performed on ground dried biomass pellets with an Alpha ATR-FTIR (Bruker, Lund, Sweden) with diamond crystal as previously reported [35].

Dissolved oxygen and pH-millivolt signals were measured continuously during experiments and logged at 0.1 Hz (HQ40d, LDO101, PHC201, Hach Lange, Solna, Sweden). The pH-millivolt signal was 4-point calibrated (pH 4, 7, 9 and 10). Probe dynamic response characteristic was based on measured instantaneous shift-up and shift-down changes: pH was logged for the trends in shifts between 0.01 molar phosphate buffer solutions. Phosphate buffer solutions were prepared with KH_2PO_4 and K_2HPO_4 at pH 5 and 9. In a similar way, DO probe dynamics were estimated from trends by moving the probe between mixed non-aerated and mixed aerated SBR media solutions. The media solutions were at low ($DO \approx 0$ mg/L, mixed, non-aerated, with biomass suspended solids) and high ($DO = 8.3$ mg/L mixed, aerated, without biomass suspended solids) steady state DO levels. Shift up and down trends were evaluated in triplicate, and the first order response time constants were estimated for the pH and DO probes from least squares non-linear regression analysis of the first order exponential asymptotic trends (Prism, Version 9, Graphpad Software, San Diego, CA, USA). The probe first order time constants were found to be 0.35 ± 0.02 s⁻¹ (pH), and 0.14 ± 0.02 s⁻¹ (DO). The logged pH and DO signals were processed by a Savitsky-Golay [36] second order 7-point filter for signal smoothing and the first derivatives. The interpreted actual trends of DO and pH were the measured signal values, corrected for probe response dynamics based on the empirically determined first order probe response time constants [37].

2.5. Dissolved Oxygen and Chemical Oxygen Demand Mass Balance

The model for the data analysis was based on a mass balance for dissolved oxygen and chemical oxygen demand concentrations. It considered a defined impulse addition of substrate to a defined amount of active biomass (VSS), in a constant volume system with constant aeration. The initial biomass was a famine biomass meaning that the biomass existed with a low background level of endogenous aerobic respiration after being subjected

to a long period without exogenous organic substrate supply. The mass balance assumed that the famine biomass would exhibit a feast response. A feast response means a sudden increase in aerobic respiration levels due to the added organic substrate. This increased level of aerobic respiration was assumed to be due to substrate uptake for PHA storage only (no active biomass growth). In particular, exogenous supplied acetic acid is converted into intracellular stored polyhydroxybutyrate granules (PHB) during the feast response. DO concentration changes in the control volume were linked to processes of aeration, endogenous aerobic respiration, aerobic respiration in substrate consumption, and aerobic respiration on stored PHA:

$$\frac{dC_o}{dt} = Q_{oa} - (Q_{oe} + Q_{os} + Q_{op}) \tag{1}$$

where C_o is the DO concentration (mgO_2/L) as a function of time (t in minutes), Q_{os} is the DO uptake rate ($\text{mgO}_2/\text{L}/\text{min}$) due to substrate consumption, Q_{op} is the DO uptake rate ($\text{mgO}_2/\text{L}/\text{min}$) due to activity on stored polymer, Q_{oe} is the biomass endogenous respiration rate ($\text{mgO}_2/\text{L}/\text{min}$), and Q_{oa} is the DO supply rate ($\text{mgO}_2/\text{L}/\text{min}$) due to constant air flow with coarse bubble aeration.

The specific substrate uptake rate (q_s , $\text{mgCOD}/\text{gVSS}/\text{min}$) was assumed to be coupled to oxygen uptake rate by a constant (average) yield (Y_{os}) for oxygen consumed per amount of substrate consumed ($\text{mgO}_2/\text{mgCOD}$):

$$q_s = \frac{q_{os}}{Y_{os}} = \frac{Q_{os}}{Y_{os} \cdot X_a} \tag{2}$$

where q_{os} is specific oxygen uptake rate ($\text{mgO}_2/\text{gVSS}/\text{min}$), and X_a is the initial (active) biomass concentration (gVSS/L). DO supply rate, governed by the conditions of volume, aeration, and mixing, was:

$$Q_{oa} = k_a(C_o^* - C_o) \tag{3}$$

where k_a is the estimated aeration oxygen mass transfer rate ($1/\text{min}$) with constant air flow and volume, and C_o^* is the apparent maximum oxygen (saturation) concentration (mgO_2/L). Aerobic respiration activity on stored polymer was assumed to ensue upon depletion of exogenous substrate. As substrate supply becomes exhausted, respiration shifts rapidly to famine and the subsequent consumption of stored polymer [30]. A switching function was used to describe this shift from aerobic respiration on exogenous substrate to the initial level of respiration activity on the amount of stored PHA as endogenous substrate:

$$Q_{op} = X_a \cdot q_{op} \left(\frac{k_s}{k_s + C_s}, \frac{C_o}{k_o + C_o} \right)_{\min} \tag{4}$$

where k_s is the Monod apparent affinity constant on substrate concentration (mgCOD/L), k_o is the Monod apparent affinity constant on oxygen concentration (mgO_2/L), C_s is the exogenous substrate concentration (mgCOD/L) as a function of time, q_{op} is the initial specific aerobic respiration rate on stored polymer ($\text{mgO}_2/\text{gVSS}/\text{min}$), and $(a,b)_{\min}$ is minimum of a and b . Thus, maximum aerobic respiration levels required that DO concentration was not limiting.

Aerobic respiration rate (DO consumption rate) on polymer was expected to be a function of the amount of polymer stored by the biomass [30]. Respiration on stored polymer results in a decrease of the stored polymer content. However, it was only the initial respiration rate on stored polymer that was estimated as the exogenous substrate supply became depleted. Therefore, any decrease in polymer content directly after substrate consumption was neglected and it is only the initial estimated level of respiration on the maximum amount of polymer stored directly after substrate depletion represented by Q_{op} .

For the COD mass balance, amount of polymer produced was determined from the average yield on substrate given polymer storage and assuming no active growth following similar previous model developments [38]:

$$X_p = (1 - Y_{os}) \cdot (C_{si} - C_s) \tag{5}$$

where X_p is the PHA concentration as function of time (mgCOD/L), and C_{si} is the initial substrate concentration (mgCOD/L).

Specific substrate consumption rate was represented by Haldane-Monod kinetics given sufficient dissolved oxygen concentration:

$$q_s = q_s^e \cdot \left(\frac{C_s}{k_s + C_s + \frac{C_s^2}{k_h}} \cdot \frac{C_o}{k_o + C_o} \right)_{min} \tag{6}$$

where k_h is the apparent Haldane substrate inhibition factor (mgCOD/L), and q_s^e is the extant maximum specific substrate uptake rate (mgCOD/gVSS/min). Directly after substrate addition, a transient phase was observed. An extant maximum specific rate was used because of this lag period before the biomass responded in its upshift to the full extent of respiration and substrate uptake rates due to C_{si} . The biomass extant maximum substrate uptake rate is a function of the stimulating (upshift) substrate concentration (C_{si}) and time. The transient phase could be described explicitly as a function of time [39]. However, in the model development it was found to be simpler to maintain a time implicit representation for all equations, including the upshift lag phase kinetics:

$$q_s^e = q_s^m \cdot \left(1 - f_i \frac{k_i}{k_i + (C_{si} - C_s)} \right) \tag{7}$$

where q_s^m is the maximum specific substrate uptake rate (mgCOD/gVSS/min), f_i represents the initial respiration level with respect to the maximum reached substrate uptake rate ($0 < f_i < 1$), and k_i is the respiration induction substrate concentration constant (mgCOD/L). The initial substrate uptake (q_s^i) is therefore:

$$q_s^i = q_s^m \cdot (1 - f_i) \tag{8}$$

k_i relates to the amount of substrate consumed by the biomass to reach q_s^m with respiration rate initially starting from q_s^i at time, $t = 0$. The maximum expressed substrate uptake rate q_s^m was interpreted to be dependent on the initial substrate concentration (C_{si}):

$$q_s^m = q_s^r + q_s^u \cdot \frac{C_{si}}{k_u + C_{si}} \tag{9}$$

where q_s^r is an inherent biomass capacity for substrate uptake, q_s^u is a capacity for increase in substrate uptake rate, and k_u is an apparent half-saturation constant (mgCOD/L) for an upshift in substrate uptake rate given C_{si} as the peak (initial) exogenous substrate concentration.

Specific uptake rates were estimated based on the measured stock biomass (gVSS/L) and substrate (gCOD/L) concentrations that were corrected for the known media dilutions that were used for each respiration experiment. Model exploration for assessing the mass balance with measured DO concentration trends was performed with Berkeley Madonna (Version 10, Berkeley, CA, USA). Data analysis for estimation of model parameters, by nonlinear least squares regression analyses, was performed with custom scripts written in MATLAB (Version 2020b, Mathworks, Kista, Sweden), or with model equations defined and fitted by non-linear regression analyses in Prism (Version 9, Graphpad Software, San Diego, CA, USA).

2.6. Monte Carlo Accumulation Process Simulation

A Monte Carlo model was developed wherein a population of biomass suspended solid elements were modelled for PHA accumulation with no active microbial growth. Substrate concentration change as a function of time was calculated based on volumetric flow and mass balance differential equations for two connected well-mixed control volumes (Figure 1). This configuration represented a subsection of an idealised module

for an industrial scale constant volume accumulation process. The process implements zones for stimulation and maintenance of biomass aerobic respiration levels as previously discussed [31]; biomass mixed liquor was continuously recirculated from a maintenance volume V_m to a stimulation mixing zone V_s receiving influent substrate. In V_s , the influent substrate, and recirculated biomass mixed liquor, are mixed in proportions to reach elevated substrate concentrations to stimulate a maximal substrate uptake rate (Equation (9)). In V_m , high substrate uptake rates are to be maintained at low substrate concentration (Equation (6)). The model represented a process subsection because in practice multiple parallel stimulation zones could be applied to service one larger, or several parallel, maintenance volumes in a larger volume industrial process.

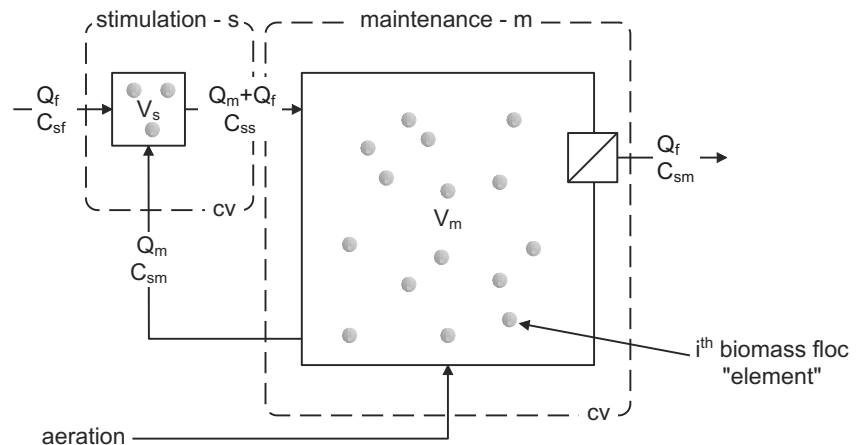


Figure 1. Model system for PHA accumulation comprising 2 process zones as completely mixed biomass stimulation and maintenance control volumes (cv), V_s and V_m respectively.

In Figure 1, a feedstock with substrate concentration C_{sf} is disposed to V_s at a flow rate of Q_f and the flow Q_m maintains a defined continuous exchange and recirculation of the mixed liquor from the main volume V_m to the mixing zone of V_s and back again. This recirculation generates the concentration C_{ss} in V_s . The V_m hydraulic residence time is $HRT_m = V_m/Q_m$. Similarly, the maximum HRT_s is V_s/Q_m .

Biomass suspended solids are retained in V_m by an ideal separator. Process effluent from V_m is at the influent flow rate of Q_f . Effluent has substrate concentration C_{sm} . Concentration C_{ss} of substrate in V_s is a function of Q_f , Q_m , C_{sm} and C_{sf} based on the flow and mass balances. Oxygen uptake rates were calculated and oxygen was assumed to be maintained at levels that were not limiting for microbial activity in V_m . Influent flow rate was set to achieve a target organic loading rate with respect to the process theoretically maximum possible substrate uptake rate (Equation (9)).

The model applied the system of equations according to the above presented oxygen and chemical oxygen demand mass balances. Model parameters in Equations (1)–(9) used for the process simulations were determined as part of the biomass characterizations reported in the first part of the present investigation.

The respiration and substrate uptake rates for each individual biomass element was dependent on its history of exposure to dissolved substrate concentration. The capacity for substrate uptake rate for each biomass element was therefore determined by the highest most recently experienced substrate concentration (Equation (9)) in combination with the history of conditions of substrate concentration after that maximum substrate exposure (Equation (6)). The total process substrate uptake rate was determined by the sum of uptake rates for all the elements in the maintenance zone. Thus, substrate uptake rates in V_s were assumed to be negligible due to anticipated DO limitation.

Uptake rates were driven with k_i dependent up-shift kinetics (Equation (9)) for biomass elements seeing a history of constant or progressively increasing substrate concentrations. Substrate uptake rates were driven by k_s dependent downshift kinetics (Equation (6)) for elements seeing a decrease in substrate concentration from a recent maximum value. For numerical stability, but also for practical representation based on previous work, the biomass elements were given a first order transient response time constant of 5 s. This meant that 95% of the expected response in respiration rate would be reached for a sustained change in substrate concentration after 15 s.

Numerical integration of governing differential equations was made for each time step to update stimulation “s” and maintenance “m” control volume substrate concentrations:

$$\frac{dC_{ss}}{dt} = \frac{Q_f \cdot C_{sf} + Q_m \cdot C_{sm} - (Q_m + Q_f) \cdot C_{ss}}{V_s} \tag{10}$$

$$\frac{dC_{sm}}{dt} = \frac{(Q_m + Q_f) \cdot C_{ss} - Q_m \cdot C_{sm} - Q_f \cdot C_{sm} - \sum_{i=1}^{n_m} x_a \cdot q_{si}}{V_m} \tag{11}$$

The element specific substrate uptake rates, q_{si} (mgCOD/gVSS/min), were according to Equation (2) and with respect to the element mass x_a (gVSS/element) for the elements found in V_m at each time step. Haldane kinetics (k_h) and induction kinetics (k_i) were neglected due to the modelled process time scales and anticipated low substrate concentrations in V_m .

The biomass elements were assumed to be ideally mixed in respective control volumes. Transport of biomass elements between V_m and V_s was made at each time step by random element selection and in proportion to flow rate and suspended solids concentrations. The biomass element statistics of residence time, respiration, polymer storage, and substrate uptake rate were estimated and evaluations of the process performance were made. The model and simulations were made with MATLAB (Version 2020b, Version 2020b, Mathworks, Kista, Sweden). Numerical integration of differential equations was with the ode45 solver, using a relative tolerance of 10^{-3} , and a maximum time step of 0.05 s. The random number generator was uniquely seeded for each simulation run.

In keeping with previous work modelling MMC PHA production, the biomass maximum element specific substrate uptake rate q_{si}^m (mgCOD/gVSS/min) was adjusted for PHA content [30]:

$$q_{si}^m = q_s^m \cdot \left(1 - \frac{f_{PHAi}}{f_{PHA}^m} \right)^\alpha \tag{12}$$

where f_{PHAi} is the average PHA to active biomass mass ratio for the i th biomass element, and f_{PHA}^m is the maximum possible PHA to active biomass ratio for the biomass. The inhibition exponent α is reported to range [30]. A value of 1.24 [40] was applied for these model simulations. The influent flow Q_f was adjusted to provide a mass input rate of substrate based on C_{sf} to give a constant substrate organic loading rate with respect to the maximum biomass uptake capacity (Equation (12)). Thus, the applied substrate organic loading rate was set to a relative constant level:

$$Q_f \cdot C_{sf} = f_L \cdot \sum_{i=1}^{n_m} x_a \cdot q_{si}^m \tag{13}$$

where f_L is the applied fraction of the maximum possible organic loading rate ($0 < f_L < 1$) with respect to the system maximum capacity in substrate uptake rate.

3. Results and Discussion

3.1. Laboratory and Pilot MMC Enrichment Biomass Characterization

Ten sets of experiments were performed with the laboratory scale SBR biomass harvested after the feast phase with a subsequent applied period of famine. All the respiration

experiments on the laboratory scale famine biomass were spread over 3 months of steady state SBR operations. Two sets of replicate experiments were performed for the pilot scale MMC biomass harvested after famine. Consistency of the biomass condition before experiments was evaluated. FTIR measurements were performed on dried biomass samples from the laboratory biomass directly after feast harvesting. The laboratory and pilot famine biomass were also assessed by FTIR before experiments. Consistency of added ammonia uptake after laboratory feast biomass harvesting was confirmed.

Based on the experience from previously reported studies [35,41], FTIR measurements qualitatively confirmed a consistency of laboratory SBR operations with respect to post feast significant biomass PHA content, and a famine biomass with low to negligible PHA content (Figure 2). For the harvested laboratory biomass, progression to famine aerobic respiration by consumption of stored polymer was facilitated with added ammonia-nitrogen during 8 h of famine. Levels of ammonia after famine were $26.0 \pm 3.5 \text{ mgNH}_4\text{-N/L}$ down from $62 \text{ mgNH}_4\text{-N/L}$ added just after feast harvesting. The pilot scale biomass was harvested after the famine cycle on site. Pilot scale famine biomass was similarly confirmed by FTIR to contain negligible PHA content before the start of the respiration experiments (Figure 2).

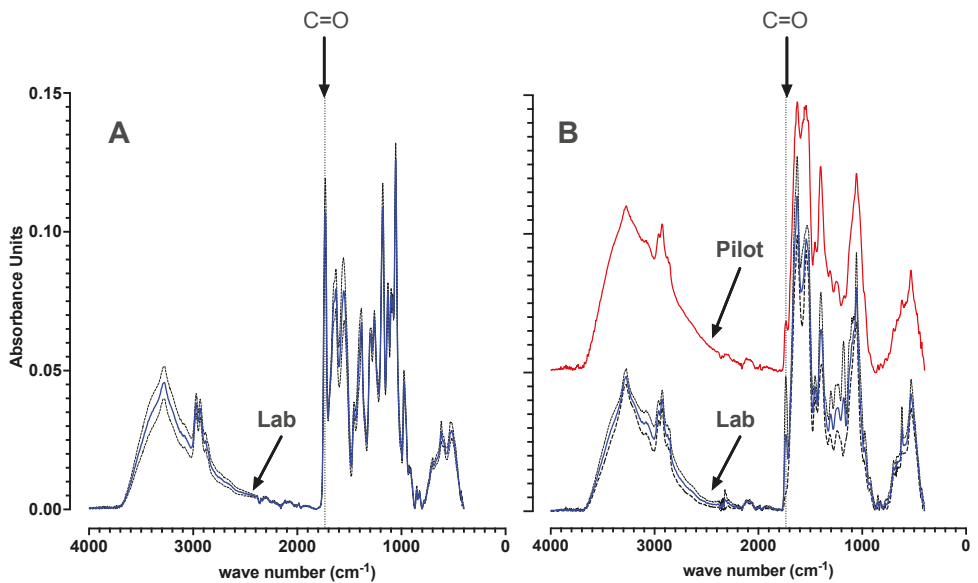


Figure 2. Background corrected and vector normalized FTIR spectra. Spectra are shown for the laboratory scale SBR dried biomass directly after biomass harvesting at the end of feast (A). Low PHA content was confirmed for laboratory and pilot famine biomass before start of respiration experiments (B). For the laboratory biomass, average spectra (solid line) are shown with standard deviation (dashed line) from biomass samples taken over the course of 10 distinct experiments carried out over 3 months. Significant or low PHA content is qualitatively represented by a characteristic large or small C=O absorbance peak ($\approx 1735 \text{ cm}^{-1}$). See [41] for further explanation.

3.1.1. Model Evaluation with No Active Aeration

The oxygen and COD mass balance model was first evaluated with the laboratory scale SBR biomass in experiments with no active aeration ($k_a \approx 0$) (Figure 3). Respiration rates were always referenced to the initial observed endogenous respiration rate. Any minor contribution of passive oxygen transfer would introduce a slight negative bias to the estimation of the reference background level of endogenous respiration rate.

For initial substrate concentrations (C_{si}) larger than about 20 mgCOD/L, dissolved oxygen levels were insufficient for complete removal of added substrate (Figure 3A). For these larger starting substrate COD levels, a progressively increasing respiration rate from an initial starting level was observed. This induction of increase in respiration rates above the reference endogenous levels, could be described implicitly in time by applying respective parameter constants of f_i and k_i given in Equations (7) and (8). Further, it was possible to establish that k_o was negligible (<0.1 mgO₂/L) for this MMC biomass dominated by finely dispersed suspended solids. A non-readily settling biomass was expected because enrichment was applied without requirement for settling as part of the selection pressure (HRT = SRT).

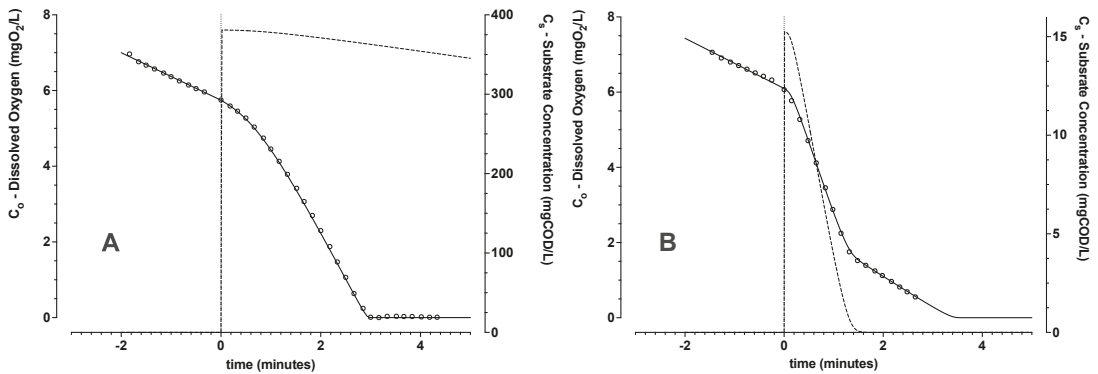


Figure 3. Trends of measured (o) and modelled (solid line) dissolved oxygen concentration, as a function of time for C_{si} levels starting ($t = 0$) at 381 (A) and 15 (B) mgCOD/L. Modelled trends of COD concentration C_s (dashed line) from the mass balance are shown. These batch respiration experiments were conducted without active aeration using laboratory scale SBR enrichment biomass.

For lower starting C_{si} levels (<20 mgCOD/L), initial dissolved oxygen concentrations were high enough to support complete added substrate COD removal (Figure 3B). Parameters describing the trends of respiration on the added substrate mass and kinetics for complete substrate removal could be readily estimated. Experiments replicated with 3 distinct batches of surplus biomass for C_{si} concentrations of 5, 10 and 15 mgCOD/L gave an average oxygen yield on substrate Y_{os} of 0.23 ± 0.03 ($n = 7$) gO₂/gCOD. This estimated yield coincides with the previously reported theoretical Y_{os} level of 0.26 gO₂/gCOD [42] for PHA storage. Therefore, the resultant estimated yield of oxygen consumed for substrate removed supported the assumption of polymer storage without active biomass growth. This interpreted polymer storage dominating response was notwithstanding availability of ammonia-nitrogen and ortho-phosphate in the medium.

Transport of acetate into the cell and its activation is estimated to cost 1 ATP per Cmol of acetate [43]. Acetate transport into the cell can be both passive and active depending on substrate concentration and/or external conditions of pH [44]. Thus, conditions that promote for greater extent of passive transport would result in reduced oxygen demand for PHA accumulation, and consequently Y_{os} values can also be lower than the estimated theoretical level of 0.26 gO₂/gCOD.

A consistently low k_s value of 0.110 ± 0.004 mgCOD/L was estimated for the cases with low starting substrate concentrations. A low apparent substrate affinity constant (k_s) was expected. In previous work [40], an arbitrarily low k_s value of 0.2 Cmmol/L (6.2 mgCOD/L) was selected, and not estimated explicitly to avoid numerical problems in other parameter determination. The present work suggests an affinity constant for acetate in the substrate consumption (Equation (6)) that is an order of magnitude lower.

3.1.2. Model Evaluation with Active Aeration

Assessment of biomass respiration response over a wider range of initial substrate concentration required oxygen supply. Constant aeration maintained dissolved oxygen levels greater than 1 mgO₂/L, and, thereby, they were significantly greater than the estimated k_o . The model represented observed trends of dissolved oxygen, for an initial substrate concentration (Figure 4). Even if substrate concentration as a function of time was not measured explicitly, the endpoint of substrate consumption was implicitly determined according to the model by the maximum in the rate of change (inflection point) of dissolved oxygen concentration given constant air flow rate. When substrate becomes exhausted, oxygen levels will increase first rapidly and then asymptotically to a higher dissolved oxygen level due to the shift to lower respiration rates.

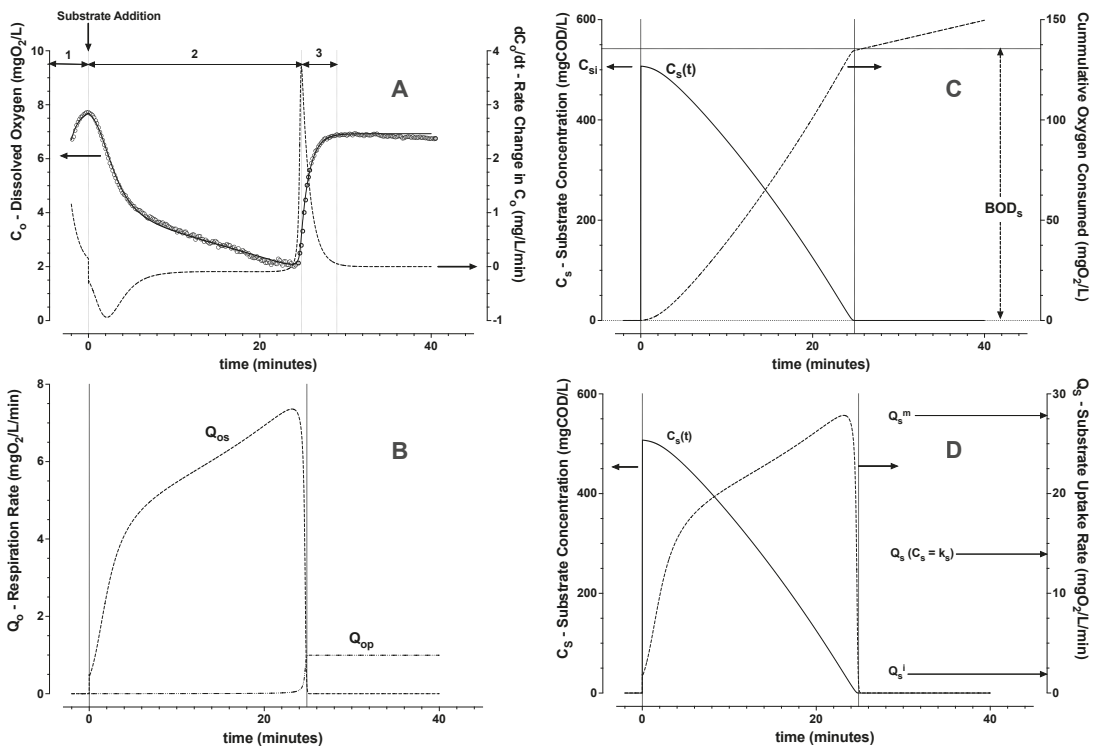


Figure 4. Typical example for trends of measured (o) and modelled (—) dissolved oxygen (A) with Zone 1 (pre-aeration), Zone 2 (substrate consumption), and Zone 3 (re-aeration). From estimated oxygen mass transfer rate (k_a , Zone 3), and endogenous respiration Q_{oc} (Zone 1), respiration rates on substrate and polymer were calculated (B). Average yield Y_{os} was given by estimated oxygen demand (BOD_s) for added substrate removal (C). Trends of substrate uptake rate could thereby be estimated from the mass balance (D).

Each experimental data set was divided into 3 zones for the model parameter estimation (see Figure 4A): Zone 1—pre-aeration before substrate addition, Zone 2—substrate consumption after its sudden pulse wise addition, and Zone 3—post aeration after the above mentioned inflection point. Only the first 4 min of Zone 3 were included in the data analysis. In this way, the re-aeration trend with the average (approximately constant) respiration rate on the maximum level of stored polymer was estimated. To avoid a risk for uncertainty in parameter value prediction, a progressive approach towards robust

step-wise parameter estimation was applied. The 8 parameters ($k_a, f_i, k_i, k_s, k_H, Y_{os}, Q_{op}, q_s^m$) were estimated in 6 steps:

1. From Zone 3, the re-aeration C_o trend (Equations (1) and (3)) was fit by non-linear least squares regression with assumption of constant Q_{oe} and Q_{op} . From the fitted trend, the oxygen mass transfer coefficient k_a was estimated;
2. From Zone 1, the average reference level of endogenous respiration, Q_{oe} (Equations (1) and (3)), was then estimated assuming negligible Q_{op} ;
3. From Zone 3, Q_{op} , the average respiration rate on stored polymer directly after substrate depletion, was then calculated (Equations (1) and (3));
4. From Zone 2, the trend of respiration rate on substrate, Q_{os} , was then estimated (Equations (1) and (3));
5. From Zone 2, the integral of Q_{os} , the cumulative biochemical oxygen demand (BOD_s) due to substrate removal, was estimated. Then the average yield Y_{os} and the trend of substrate concentration were calculated (Equation (2));
6. From Zone 2, the trend of substrate uptake rate as a function of estimated substrate concentration was then used to determine remaining parameters (Equations (6)–(8)). The induction and downshift substrate affinity constants (k_i and k_s , respectively) were interpolated from the derived trend of substrate uptake rate as a function of interpreted substrate concentration. Remaining parameters were estimated by nonlinear least squares regression analysis (see Figures 4 and 5).

The laboratory scale SBR biomass was characterised in triplicate with distinct famine biomass batches over a week of steady SBR operations (Figure 5A,C). The pilot scale SBR biomass was similarly characterized with replicate evaluations from one grab sample of the pilot surplus activated sludge (Figure 5B,D). Summary of experiments and outcomes for the biomass evaluations with respect to the parameters of the model (Equations (1)–(9)) are given in Table 1 and depicted in Figure 5.

The estimated average yield of oxygen on substrate Y_{os} (Table 1) reproduced outcomes reported above for cases without active aeration. Y_{os} for the pilot biomass was also found to be close to theoretical predictions for microbial activity due to polymer storage only [42]. The assumption to neglect active growth in the model evaluation was therefore supported also for the pilot scale biomass. The oxygen mass transfer coefficient (k_a) was determined independently for each experiment with consistent outcomes. A lower air flow rate was applied for the pilot scale biomass experiments due to lower levels of respiration rate.

Table 1. Characterization of laboratory and pilot scale SBR MMC enrichment biomass with data from respiration experiments with oxygen and chemical oxygen demand mass balance modelling when active constant aeration was applied. Values in the brackets give the number of measurements or experiments used in estimation of means with standard deviations.

Parameter	Units	Laboratory Scale	Pilot Scale
Temperature	°C	24.6 ± 0.3 (24)	23.8 ± 0.6 (17)
pH ($t = 0$)	-	9.2 ± 0.1 (24)	9.0 ± 0.1 (17)
X_a	gVSS/L	1.0 ± 0.1 (11)	1.71 ± 0.04 (2)
k_a	1/min	1.11 ± 0.14 (24)	0.60 ± 0.15 (17)
q_{oe}	mgO ₂ /gVSS/min	0.64 ± 0.12 (24)	0.25 ± 0.07 (17)
Y_{os}	gO ₂ /gCOD	0.26 ± 0.02 (24)	0.23 ± 0.05 (17)
k_s	mgCOD/L	2.0 ± 0.7 (24)	1.8 ± 0.4 (17)
k_H	mgCOD/L	38 ± 7 (24)	20 ± 2 (17)
q_s^f	mgCOD/gVSS/min	7.4 ± 0.1 (24)	2.5 ± 0.2 (17)
q_s^H	mgCOD/gVSS/min	21.1 ± 1.1 (24)	6.8 ± 0.2 (17)

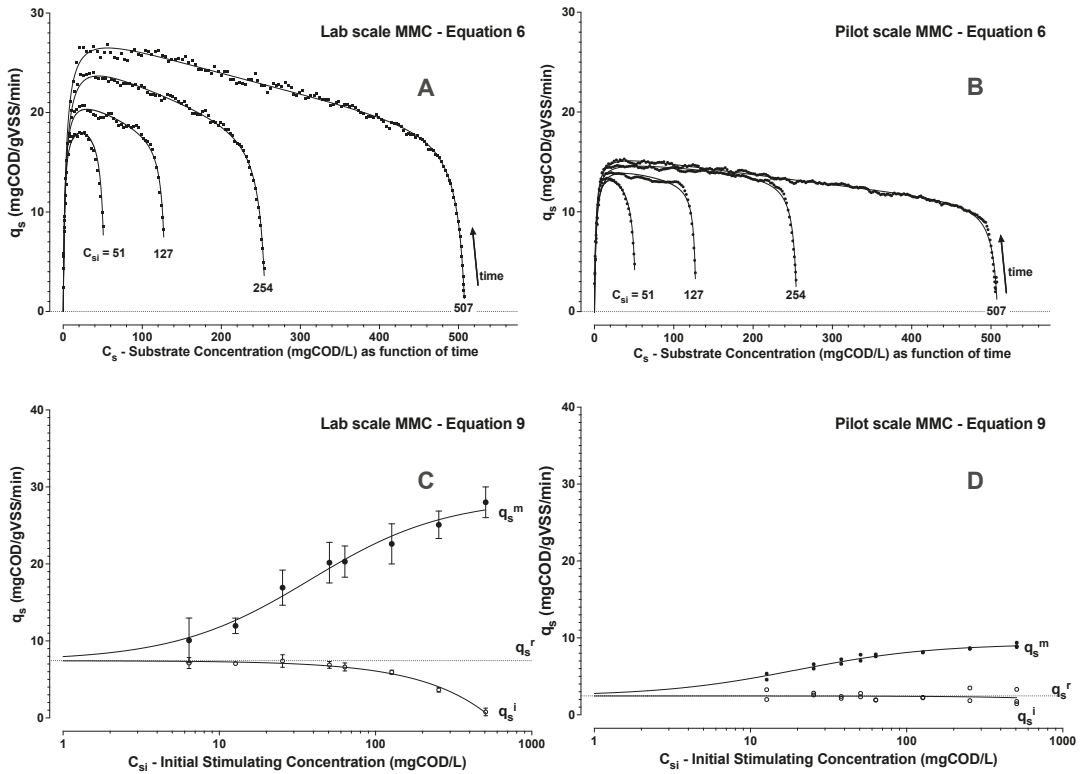


Figure 5. Figures show typical results for the laboratory (A) and pilot (B) scale MMCs experiments with respective trends of interpreted specific substrate uptake rate (q_s) as a function of C_{si} , and with substrate concentration changing implicitly in time. Points (\bullet) correspond to the rates and concentrations derived from DO concentration data and the trend lines are the curves fit by least squares regression analysis to Equation (6). Results of estimated initial (\circ , q_s^i) and maximum (\bullet , q_s^m) specific substrate uptake rates for laboratory (C) and pilot (D) scale MMCs are shown as a function of initial acetic acid substrate concentrations (C_{si}). The trend of maximum substrate uptake rate follows Equation (9) by least squares regression analysis. The initial specific substrate uptake rate decreased linearly with increasing initial acetic acid concentration.

A reproducible low substrate affinity constant (k_s) was observed for both biomass sources. The k_s value, about 2 mgCOD/L, was higher than the value estimated for experiments reported above without active aeration at low initial C_{si} values. The k_s (without active aeration) was reproducible and estimated by non-linear least squares regression model analysis. The k_s (with active aeration) was estimated pragmatically as the interpolated concentration at half the maximum substrate uptake rate from the 6-step derived trend of C_s with time. The value of about 2 mgCOD/L was considered to be a conservative estimate of what may actually be a lower affinity constant in reality. A k_s of 2 mgCOD/L is still much lower than previously assumed [40]. k_s has significant bearing on the performance of a flow through PHA accumulation bioprocess. A lower k_s means, with all other parameters being equal, that similarly high polymer production rates can be maintained with lower substrate concentrations. Lower substrate concentration means less substrate lost in the effluent of a flow-through process giving a better substrate utilisation efficiency.

As expected, the maximum observed substrate uptake rates were dependent on the initial applied substrate concentration. Contrary to trends of substrate consumption, the

affinity constant for stimulating an upshift to a maximum substrate uptake rate (k_u) was found to be significantly larger than k_s (Table 1). Thus, the hysteresis that was anticipated from previous work [31] was confirmed from the model that could be similarly applied for two distinct MMC cultures. Levels of substrate concentration that are necessary to stimulate to a maximum rate of substrate uptake are predicted to be higher than the concentration levels that are necessary to maintain a substrate uptake rate once it has been established. The upshift kinetics (Equation (9)) and downshift kinetics (Equation (6)) both similarly follow a Monod model but they did not follow the same path.

Enrichment MMC biomass sourced from laboratory and pilot SBRs revealed a similar behaviour, but the pilot MMC exhibited about one third the specific maximum rate to assimilate substrate. The trends of maximum substrate uptake rate further suggested an inherent starting (resting) capacity for substrate uptake rate (q_s^r). This capacity can be seen in the trends shown in Figure 5C,D. The maximum substrate uptake rates approached the initial inherent rates with decreasing C_{si} . However, when dosing with acetic acid, Figure 5 also shows how the initial levels of substrate uptake rate (q_s^i) decreased below the estimated q_s^r in direct proportion to added amounts of acetic acid.

Higher initial levels of acetic acid suggested apparent substrate inhibition during substrate uptake, as depicted in Figure 5A,B and this inhibition could be described by applying a Haldane inhibition constant k_h (Equation (6)). Since, the acetic acid addition included both organic substrate and acid addition, it was unclear if COD levels, and/or acid addition were causative factors to observed substrate inhibition. Additional respiration experiments were performed with the laboratory SBR biomass using acetic acid and acetate blends. These experiments suggested that, in the range of conditions tested, it was the amount of acid addition and not the initial COD concentration that promoted the decrease in q_s^i with respect to q_s^r (Figure 6B,C).

The buffer capacity of the mixed liquor involves contribution from dissolved solids as well as the biomass suspended solids. Initial pH change due to acid addition could be characterized with respect to the specific acid addition. The buffer capacity for mmol/L H^+ added with respect to X_a concentration is shown in Figure 6A. Results suggested that even if the pilot SBR biomass exhibited lower buffer capacity (higher pH change for the same specific acid addition), similar levels of specific acid addition resulted in a similar induction lag phase described by k_i (Figure 6B). Thus, the amount of specific acid addition causing sudden pH change may be of more direct influence on the initial biomass response to organic acid dosing rather than the absolute initial pH change. An influence of the amount of acid addition on uptake rate was also inferred by comparison of pH and uptake rate trends (Figure 6C,D). A lower k_h (higher apparent Haldane substrate inhibition) was observed for acetic acid versus acetate additions in experiments for approximately the same starting COD concentration.

The relatively small increment in PHA content that accumulated in the biomass after a small pulse of substrate was not measured directly as part of the study. The median applied substrate pulse for the experiments was 57 mgCOD/L acetic acid concentration. From Table 1, and the COD mass balance (Equation (5)), the expected increment of biomass polyhydroxybutyrate content can be estimated. Assuming an active biomass concentration (X_a) of 1 gVSS/L, 57 mgCOD/L of acetic acid would result in about 2.5 percent gPHA/gVSS. Even though the biomass PHA content was not measured explicitly, it was of interest to evaluate if the independently determined level of biomass respiration after substrate consumption corresponded to the model predicted level of PHA produced (X_p). Directly after substrate consumption the residual elevated respiration rate Q_{op} was estimated from Equations (1) and (3). Q_{op} should be directly related to aerobic metabolism on stored PHA [30,38]. The residual respiration rate levels were found to follow an expected two-thirds power law trend (Figure 7) as a function of the estimated specific polymer concentration (X_p/X_a). This outcome suggests an internal model consistency and supports previous research findings for microbial activity during famine [30].

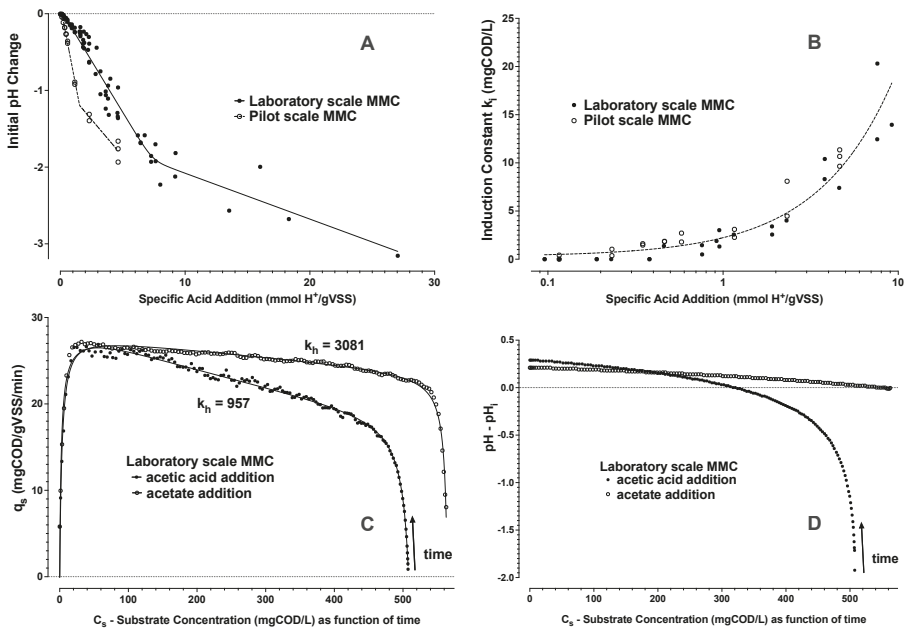


Figure 6. Initial pH changes are shown due to specific acid addition with the substrate (A). Corresponding to this acetic acid and/or acetate addition, the linear trend of influence (shown on a log scale) for the induction (lag phase) constant (k_i) is similarly shown as a function of the specific acid addition (B). An example for the dynamics of substrate uptake rate during COD consumption as an implicit function of time for addition of acetic acid or acetate is given (C) with information of the measured trend in pH (D) with respect to the initial pH level (pH_i) during the same time.

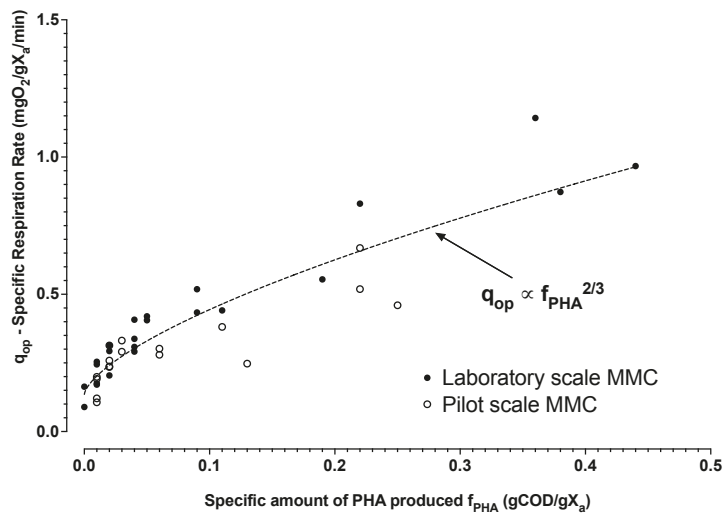


Figure 7. Estimated levels of biomass specific respiration rate after substrate consumption with respect to the estimated levels of PHA calculated from added substrate and yield of oxygen on substrate assuming no active biomass growth. The trend line is the least squares regression estimate for combined laboratory (•) and pilot (◊) data.

3.1.3. Monte Carlo Simulation of PHA Accumulation in MMC Enrichment Biomass

Sets of PHA accumulation numerical simulations were performed to explore the implication of the interpreted stimulation-maintenance hysteresis due to upshift and downshift substrate affinities given by:

1. the stimulation of respiration rates due to the highest most recent substrate concentration as influenced by k_u in Equation (9), and
2. the maintenance of an attained respiration rate with decreasing substrate concentrations as influenced by k_s in Equation (6).

Simulations comprised an aerated maintenance volume V_m of 500 L, containing 5000 mgVSS/L active biomass with PHA accumulation potential of 0.6 gPHA/gVSS. The biomass suspended solids were divided into 10^5 individually followed floc elements ($x_a = 25$ mgVSS active biomass per element). The estimated average kinetic parameters of the laboratory scale biomass were applied (Table 1). An influent feedstock with a low C_{sf} of 1000 mgCOD/L was supplied continuously with adjusted flow Q_f to maintain a targeted fraction of the biomass maximum substrate uptake rate (f_L). Q_m flow rates were set to a defined HRT_m , and V_s was adjusted to ensure an HRT_s of 30 s based on Q_m in all cases. Simulations were maintained for up to 1 h modelled time by which time steady trends were well-developed and polymer content approached levels in the order of 0.3 gPHA/gVSS.

An influence of stimulation-maintenance hysteresis is illustrated in Figure 8 for cases of HRT_m equal to 10, 40, and 640 min and a constant relative substrate loading rate of f_L equal to 0.7 in all three cases. For increasing HRT_m , the frequency that any given floc element recirculates to the V_s influent mixing zone, decreases progressively. At longer HRT_m the system approaches limiting conditions of Q_f effectively flowing directly into V_m . For influent flowing directly to V_m , biomass respiration rates will initially increase due to increase of C_{sm} in V_m and the active biomass will respond with a corresponding increase in respiration rate (Equation (9)). C_{sm} will increase and approach a steady state value when the substrate mass inflow rate matches the sum of the effluent mass outflow rate plus the biological mass uptake rate for PHA storage. Loading the modelled laboratory biomass at f_L equal to 0.7 resulted in such a predicted steady state effluent substrate concentration of about 50 mgCOD/L with longer HRT_m . In these cases, the process dynamics are driven only by Equation (9). The system settles, in this example, at "A" in Figure 8.

For reduced HRT_m , flocs of biomass are more frequently and repeatedly stimulated to a higher respiration rate due to exposure to C_{ss} in V_s . Over a period of about $3 \times HRT_m$, essentially all the biomass suspended solids should have been disposed to respiration stimulation in V_s . Increasing Q_m to give a 10-min HRT_m , f_L equal to 0.7, resulted in C_{ss} in the order of 500 mgCOD/L in V_s . This level is significant for stimulating maximal respiration rates for the laboratory scale biomass (Table 1). Initially, C_{sm} substrate concentrations increased in V_m , and two populations of biomass activity developed in parallel. Some flocs were respiring at a level due exposure to the increasing C_{sm} levels in V_m (Equation (9)). However, a second population of flocs developed increasingly over $3 \times HRT_m$. These flocs had passed through V_s . This population respired at higher levels due to contact to C_{ss} in V_s (Equation (9)), and subsequent C_{sm} in V_m (Equation (6)). In this way, the system settled at an order of magnitude lower steady state C_{sm} in V_m of 6 mgCOD/L ("B" in Figure 8). This lower effluent concentration was approached as all biomass elements passed through V_s at least once. A similar overall level of substrate uptake rate resulted at "B" as for "A", but with a significantly improved substrate utilization efficiency. By floc element exposure to respiration stimulation to near maximal rates in V_s a higher respiration was maintained down to lower substrate concentrations (Figure 5A,C). For increasing HRT_m , it takes longer for the system to reach steady state due a longer V_m volumetric turnover time ("C" in Figure 8). Thus, lower HRT_m served to stimulate all process biomass as quickly as possible.

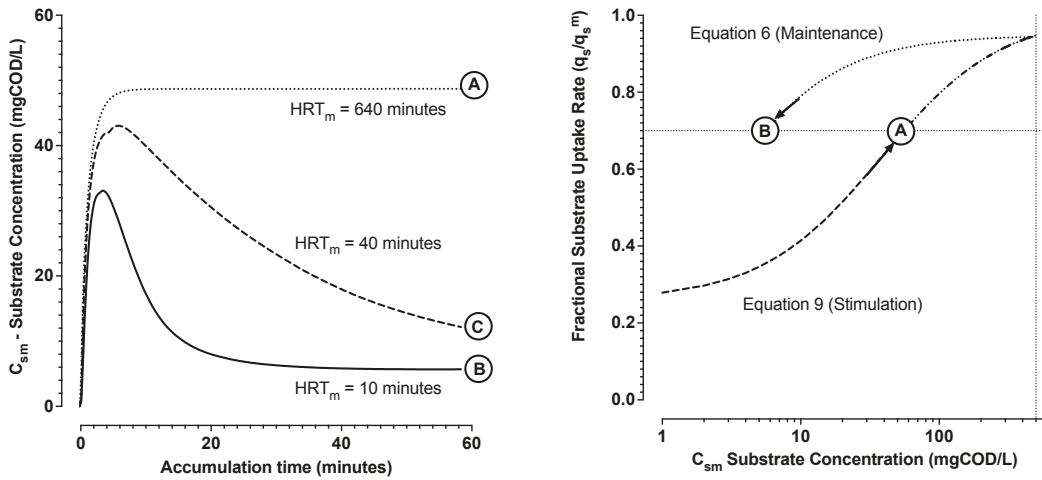


Figure 8. Simulation results for a fractional substrate loading rate of f_L equal to 0.7 while varying the recirculation flow rate for higher and lower HRT_m levels. Higher HRT_m levels approach conditions of effective substrate feed directly into V_m (A). For lower HRT_m , influence of C_{ss} uptake rate stimulation in V_s enables for higher uptake rates maintained at lower C_{sm} concentration (B). Moderate HRT_m levels require longer times for all the biomass to be exposed to C_{ss} in V_s (C).

3.1.4. Future Research Perspectives and Challenges

This strategy for engineering accumulation bioprocess with internal, or external, recirculation and contact to elevated substrate concentrations that exist in the influent mixing zone(s) becomes increasingly more relevant the lower the influent substrate concentration becomes. Stimulation of respective biomass elements is asynchronous in time because not all biomass elements experience “stimulation” at the same time. Monte Carlo modelling can be applied as a way to understand the nature of the distribution of activities for discrete floc elements. In contrast, the typical approach for PHA accumulation with laboratory and pilot scale systems in the reviewed research literature [11,12] has been by dosing often concentrated substrate directly into a well-mixed aerated vessel containing PHA accumulating biomass. This is a synchronous strategy for stimulating high respiration rates because all the process biomass is subject to the same substrate concentration history at the same time.

Typically, dissolved oxygen [25,45,46], redox conditions [47], or pH [48] can be used with feedback control for timing the frequency of pulse feeding events. When substrate is concentrated, the process may be fed-batch and initiated with lower starting volume with a more concentrated biomass [49]. Furthermore, when the feedstock is concentrated then small pulse wise volume inputs can be added to bring the entire working volume quickly to substrate levels that result in maximum substrate uptake rates. Even in such cases, the process volume may not be sufficiently large to be able to supply enough VFA mass to reach saturation of PHA content in the process biomass. Intermittent settling and decanting cycles have been suggested as one strategy to extend the process capacity to enable delivery of more substrate [50]. However, periodic batch decanting of excess volume introduces a dead time to the accumulation process. This added time for intermittent settling and decanting is a disadvantage because it reduces volumetric productivity. Continuous feed MMC PHA production methods therefore need further attention for the industrial developments.

Additions of substrate in MMC accumulation cannot be too large due to a risk for inhibition [46]. Larger additions of substrate also increase the availability of substrate. Availability of substrate (without other limiting factors) can stimulate for active growth of the accumulating as well as flanking heterotrophic biomass populations [51]. Methods

for dosing substrate based on pH control results in sustained elevated substrate concentrations [52] that are anticipated to contribute to stimulate for unwanted flanking growth. Continuous feeding methods for MMC production methods require to be developed and undertaken in ways that do not unduly reduce the yield of product formation by promoting unwanted flanking biomass growth.

Smaller pulse-wise substrate additions can be made in a fed-batch process with peak substrate concentrations that are just sufficient to stimulate high average substrate uptake rates [17]. This semi-continuous feeding approach can be performed with fed-batch or flow through process methods. However, fed-batch methods with many smaller pulses also introduce a dwell time between successive inputs. The dwell time between onset of substrate depletion from one pulse, and the control system triggering for the next pulse of substrate, has been observed in own developments to introduce a significant accumulated dead time with lower substrate uptake rate. This dead time decreases process volumetric productivity. More frequent interruption of substrate addition leading to punctuation of loss in respiration rate has been observed to furthermore risk to result in PHA of lower average molecular weight [31]. Therefore, the most optimal approach for MMC PHA accumulation is a process with continuous feeding that maintains the highest possible substrate uptake rate with the lowest possible effluent substrate concentration.

Methods supporting the development of industrial MMC PHA accumulation with continuous feed supply and as a flow through bioprocess have not been found to be reported in the research literature. Initial outcomes in published work for fed-batch methods applying constant feed based on predetermined rates without feedback control were not found to be satisfactory [46]. Since then pulse-wise feeding methods have become the standard practice in approach for MMC PHA production. Notwithstanding, continuous flow methods are desirable for continued advancements because they offer an optimal sustained volumetric productivity.

As an example, numerical simulations were performed to explore how the application of a stimulation zone could influence substrate utilisation efficiency while pushing the system towards theoretical limits of maximum PHA production rates with a feedstock VFA concentration of 1000 mgCOD/L (Figure 9). Higher applied organic loading rates drive the system biomass to maximum possible substrate uptake and polymer production rates (volumetric productivity). Without benefit of the stimulation effect (case of $HRT_m = 250$ min in Figure 9), higher volumetric productivity results in a direct trade-off with loss of substrate utilisation efficiency. Increasing amounts of substrate are discharged in the effluent. With all other things begin equal, substrate losses are significantly mitigated if the biomass has been stimulated to higher respiration rate (case of $HRT_m = 5$ min in Figure 9). For the modelled process scenario, a targeted organic loading rate of greater than about f_L equal to 0.9 was a break point. Progressive losses in substrate utilisation efficiency result without further gains in volumetric productivity beyond the break point.

The stochastic modelling of the observed MMC biomass response in stimulation of respiration and substrate uptake rates suggests potential to understand and develop optimal operational conditions for robust continuous feed methods at industrial scale. Characteristics for any biomass may be readily determined by the methods of the respiration experiments that were replicated for both the laboratory and pilot scale SBR enrichment biomass sources in the present investigation. This kind of characterisation of the biomass dynamic response is recommended towards innovation in the bioprocess that can address challenges for maximising productivity and for avoiding growth of flanking populations.

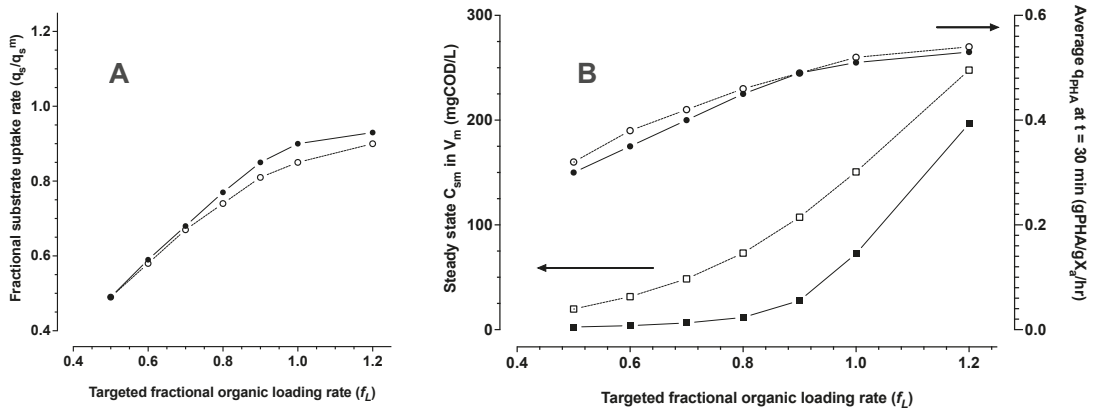


Figure 9. The targeted fraction of the system maximum possible substrate uptake rate (f_L —see Equation (13)), versus the actual fraction of maximum uptake rate achieved in the process (A). Maintenance volume (V_m) steady state substrate concentration C_{sm} (squares), and average specific PHA production rates after 30 min accumulation (circles) as a function of the targeted fraction of the system maximum possible substrate uptake rate (B). Closed and open symbols are for HRT_m of 5 and 250 min, respectively.

In the present work, the dynamic response characterisation for two biomass sources revealed a similar inhibition effect of specific acid dosing (Figure 6B,C). This suggests a benefit of dosing substrate to higher concentrations of biomass. If biomass retention is by gravity separation, then recirculation and stimulation could be achieved by influent mixing with the return thickened biomass suspended solids coming from the clarifier. Higher suspended solids concentration brings added buffer capacity to the stimulation mixing zone.

Recirculation to V_s using as low a HRT_m as possible helps to initially stimulate all the process biomass as quickly as possible. Feeding exclusively to the stimulation zone becomes less critical to maintain if all the process biomass has been “stimulated”. Once all the process biomass is stimulated the process control objective is to ensure a feeding rate to sustain sufficient but still relatively low substrate concentration levels (ca. 5 to 25 mgCOD/L, based on the estimated K_s of about 2 mgCOD/L). Thus a challenge is to establish feedback control for optimum feeding rate without over or under feeding the process.

In the model simulations, the required influent flow rate was calculated. In practice, the feeding rate must be determined from the process monitoring. Recirculating to the stimulation zone with known flows, mixing ratios and characteristic time constants, can serve needs for monitoring and feed rate feedback control [31]. V_s and V_m zones can be monitored in parallel with sensor signals (dissolved oxygen, pH, ORP, IR-spectroscopy, and so forth) that are related directly or indirectly to substrate concentrations, biomass respiration levels, and/or PHA content. The V_s zone provides a dynamic reference measurement because water quality parameters, including but not limited to, buffer capacity, and ionic composition will change in time. Changes will be due to the feedstock water quality and also the intense PHA accumulation biological activity in V_m . So-called soft-sensing process control strategies [53] are anticipated to become necessary. The process modelling methods applied in the present work can be adapted to test principles of control strategies for the polymer production. Addressing the challenges of developing robust and relevant strategies for the MMC accumulation process monitoring and control will be essential for successful industrial scale process implementations.

4. Conclusions

There are three main outcomes as conclusions from this study and with novelty in contributions from the investigation efforts to characterize and model dynamics of substrate uptake rate for MMCs during PHA accumulation:

1. A property of hysteresis in the dynamic response of MMCs storing PHA could be demonstrated for two distinct enrichment cultures using dissolved oxygen and chemical oxygen demand mass balance experiments.
2. This hysteresis could be modelled with readily identifiable parameters using Monod equations describing the distinct upshift and downshift dynamics in substrate uptake rates as a function of substrate concentrations and as a function of time. It was found that the substrate concentration, required to stimulate a substrate uptake rate, was higher than the substrate concentration required to maintain an attained substrate uptake rate.
3. The system of equations in numerical simulations suggest for an opportunity to exploit this property of hysteresis in industrial scale bioprocesses for PHA production. MMC PHA production processes can be operated with continuous feeding strategies, even with low concentration feedstocks. The model simulations found that engineered stimulation zones can be applied in continuous flow PHA production bioprocesses as a strategy to reach maximum possible performance in volumetric productivity without sacrificing performance in substrate utilization efficiency.

Applying ideas and principles revealed by the model simulations is a future challenge with applications in practice. Methods for process monitoring are required in combination with feedback control to maintain optimal organic loading rates during the PHA accumulation process.

Author Contributions: Conceptualization, A.W.; methodology, A.W., L.L., F.V. and M.M.; software, A.W.; validation, A.W.; formal analysis, A.W.; investigation, A.W., L.L., F.V., M.V. and M.M.; resources L.L., F.V. and M.M.; data curation, A.W.; writing—original draft preparation, A.W.; writing—review and editing, A.W., M.V. and M.M.; visualization, A.W.; supervision, A.W. and M.M.; project administration, M.M.; funding acquisition, M.M. All authors have read and agreed to the published version of the manuscript.

Funding: Funding support that facilitated the availability of laboratory and pilot scale enrichment MMC for PHA production was due to the REsources from URban Bio-waSte"-RESURBIS (GA 7303499) project in the European Horizon2020 (Call CIRC-05-2016) program. Alan Werker was funded as a Visiting Professor at Sapienza University of Rome from 13 March 2018 to 15 June 2018.

Institutional Review Board Statement: Not applicable.

Informed Consent Statement: Not applicable.

Data Availability Statement: The data presented in this study are available on request from the corresponding author.

Acknowledgments: Alan Werker is grateful for the opportunity and kind support from Mauro Majone, and Sapienza University of Rome, to be a visiting Professor in the spring of 2018 enabling undertaking the practical experiments used for the presented study.

Conflicts of Interest: The authors declare no conflict of interest.

Abbreviations

The following abbreviations and symbols are used in this manuscript:

ATR-FTIR	attenuated total reflection-FTIR
BOD	biochemical oxygen demand
COD	chemical oxygen demand
DO	dissolved oxygen
FTIR	Fourier transform infrared spectroscopy
HRT	hydraulic retention time
MMC	mixed microbial culture
PHA	polyhydroxyalkanoate
PHB	polyhydroxybutyrate
SBR	sequencing batch reactor
SRT	solids retention time
VFA	volatile fatty acid
VSS	volatile suspended solids
WWTP	wastewater treatment plant
α	PHA accumulation inhibition exponent
C_o	DO concentration (mgO ₂ /L)
C_o^*	apparent maximum DO (saturation) concentration (mgO ₂ /L)
C_s	exogenous dissolved substrate concentration (mgCOD/L)
C_{s_i}	initial or peak upshift C_s (mgCOD/L)
$1 - f_i$	q_s^i / q_s^m
k_a	aeration oxygen mass transfer coefficient (1/min)
k_h	Haldane substrate inhibition constant (mgCOD/L)
k_i	substrate induction constant (mgCOD/L)
k_o	Monod apparent affinity constant on DO concentration (mgO ₂ /L)
k_s	Monod apparent downshift affinity constant on substrate concentration (mgCOD/L)
k_u	Monod apparent upshift affinity constant on peak substrate concentration (mgCOD/L)
Q_{oa}	DO supply rate due to aeration (mgO ₂ /L/min)
Q_{oe}	DO consumption rate due to endogenous respiration (mgO ₂ /L/min)
Q_{op}	DO consumption rate due to stored PHA (mgO ₂ /L/min)
Q_{os}	DO consumption rate due to substrate consumption (mgO ₂ /L/min)
q_{op}	specific Q_{op} (mgO ₂ /gVSS/min)
q_{os}	specific Q_{os} (mgO ₂ /gVSS/min)
q_s^r	biomass resting specific substrate uptake rate (mgCOD/gVSS/min)
q_s	specific substrate uptake rate (mgCOD/gVSS/min)
q_s^e	maximum extant specific substrate uptake rate (mgCOD/gVSS/min)
q_s^i	initial maximum extant specific substrate uptake rate (mgCOD/gVSS/min)
q_s^m	maximum specific substrate uptake rate (mgCOD/gVSS/min)
t	time (minutes)
q_s^r	biomass maximum upshift in specific substrate uptake rate (mgCOD/gVSS/min)
X_a	active biomass concentration (gVSS/L)
X_p	PHA concentration (gCOD/L)
Y_{os}	yield of oxygen consumed with substrate (mgO ₂ /mgCOD)
C_{sf}	influent feedstock substrate concentration (mgCOD/L)
C_{sm}	maintenance volume substrate concentration (mgCOD/L)
C_{ss}	stimulation volume substrate concentration (mgCOD/L)
f_L	applied fraction of maximum possible organic loading rate

f_{PHAi}	i th-active biomass element specific PHA level (x_p/x_a)
f_{PHA}^m	active biomass maximum PHA level for x_p/x_a
HRT_m	HRT in V_m due to Q_m (min)
HRT_s	HRT in V_s due to Q_m (min)
n_m	number of biomass elements in V_m
Q_f	substrate feed (and effluent) flow rate (L/min)
Q_m	recirculation flow rate (L/min)
q_{si}^m	i th-biomass element maximum specific substrate uptake rate (mgCOD/gVSS/min)
V_m	maintenance volume (L)
V_s	stimulation volume (L)
x_a	element specific active biomass (gVSS/element)
x_p	element specific PHA content (gPHA/element)

References

- Anderson, A.J.; Dawes, E.A. Occurrence, Metabolism, Metabolic Role, and Industrial Uses of Bacterial Polyhydroxyalkanoates. *Microbiol. Rev.* **1990**, *54*, 450–472. [[CrossRef](#)] [[PubMed](#)]
- Laycock, B.; Halley, P.; Pratt, S.; Werker, A.; Lant, P. The chemomechanical properties of microbial polyhydroxyalkanoates. *Prog. Polym. Sci.* **2014**, *39*, 397–442. [[CrossRef](#)]
- Hatti-Kaul, R.; Nilsson, L.J.; Zhang, B.; Rehnberg, N.; Lundmark, S. Designing Biobased Recyclable Polymers for Plastics. *Trends Biotechnol.* **2020**, *38*, 50–67. [[CrossRef](#)]
- Vandi, L.J.; Chan, C.M.; Werker, A.; Richardson, D.; Laycock, B.; Pratt, S. Wood-PHA Composites: Mapping Opportunities. *Polymers* **2018**, *10*, 751. [[CrossRef](#)] [[PubMed](#)]
- Nikodinovic-Runic, J.; Guzik, M.; Kenny, S.T.; Babu, R.; Werker, A.; O'Connor, K.E. Carbon-rich wastes as feedstocks for biodegradable polymer (polyhydroxyalkanoate) production using bacteria. *Adv. Appl. Microbiol.* **2013**, *84*, 139–200. [[CrossRef](#)]
- Saratale, R.G.; Cho, S.K.; Saratale, G.D.; Kadam, A.A.; Ghodake, G.S.; Kumar, M.; Bharagava, R.N.; Kumar, G.; Kim, D.S.; Mulla, S.I.; et al. A comprehensive overview and recent advances on polyhydroxyalkanoates (PHA) production using various organic waste streams. *Bioresour. Technol.* **2021**, *325*, 124685. [[CrossRef](#)]
- Marang, L.; van Loosdrecht, M.C.; Kleerebezem, R. Enrichment of PHA-producing bacteria under continuous substrate supply. *New Biotechnol.* **2018**, *41*, 55–61. [[CrossRef](#)]
- Stouten, G.R.; Hogendoorn, C.; Douwenga, S.; Kiliyas, E.S.; Muyzer, G.; Kleerebezem, R. Temperature as competitive strategy determining factor in pulse-fed aerobic bioreactors. *ISME J.* **2019**, *13*, 3112–3125. [[CrossRef](#)]
- Anterrieu, S.; Quadri, L.; Geurkink, B.; Dinkla, I.; Bengtsson, S.; Arcos-Hernandez, M.; Alexandersson, T.; Morgan-Sagastume, F.; Karlsson, A.; Hjort, M.; et al. Integration of biopolymer production with process water treatment at a sugar factory. *New Biotechnol.* **2014**, *31*, 308–323. [[CrossRef](#)]
- Bengtsson, S.; Karlsson, A.; Alexandersson, T.; Quadri, L.; Hjort, M.; Johansson, P.; Morgan-Sagastume, F.; Anterrieu, S.; Arcos-Hernandez, M.; Karabegovic, L.; et al. A process for polyhydroxyalkanoate (PHA) production from municipal wastewater treatment with biological carbon and nitrogen removal demonstrated at pilot-scale. *New Biotechnol.* **2017**, *35*, 42–53. [[CrossRef](#)]
- Estevez-Alonso, A.; Pei, R.; Loosdrecht, M.C.M.V.; Kleerebezem, R.; Werker, A. Scaling-up microbial community-based polyhydroxyalkanoate production: Status and challenges. *Bioresour. Technol.* **2021**, *327*, 124790. [[CrossRef](#)] [[PubMed](#)]
- Valentino, F.; Morgan-Sagastume, F.; Campanari, S.; Villano, M.; Werker, A.; Majone, M. Carbon recovery from wastewater through bioconversion into biodegradable polymers. *New Biotechnol.* **2017**, *37*, 9–23. [[CrossRef](#)] [[PubMed](#)]
- Lemos, P.C.; Serafim, L.S.; Reis, M.A.M. Synthesis of polyhydroxyalkanoates from different short-chain fatty acids by mixed cultures submitted to aerobic dynamic feeding. *J. Biotechnol.* **2006**, *122*, 226–238. [[CrossRef](#)] [[PubMed](#)]
- Bengtsson, S.; Pisco, A.R.; Johansson, P.; Lemos, P.C.; Reis, M.A. Molecular weight and thermal properties of polyhydroxyalkanoates produced from fermented sugar molasses by open mixed cultures. *J. Biotechnol.* **2010**, *147*, 172–179. [[CrossRef](#)]
- Mel, B.; Torres-giner, S.; Reis, M.A.M.; Silva, F.; Matos, M.; Cabedo, L. Blends of Poly(3-Hydroxybutyrate-co-3-Hydroxyvalerate) with Fruit Pulp Biowaste Derived Poly(3-Hydroxybutyrate-co-3-Hydroxyvalerate-co-3-Hydroxyhexanoate) for Organic Recycling Food Packaging. *Polymers* **2021**, *13*, 1155.
- Silva, F.; Matos, M.; Pereira, B.; Ralo, C.; Pequito, D.; Marques, N.; Carvalho, G.; Reis, M.A. An integrated process for mixed culture production of 3-hydroxyhexanoate-rich polyhydroxyalkanoates from fruit waste. *Chem. Eng. J.* **2022**, *427*, 131908. [[CrossRef](#)]
- Werker, A.; Bengtsson, S.; Johansson, P.; Magnusson, P.; Gustafsson, E.; Hjort, M.; Anterrieu, S.; Karabegovic, L.; Karlsson, A.; Morgan-Sagastume, F.; et al. Production Quality Control of Mixed Culture Poly(3-hydroxybutyrate-co-3-hydroxyvalerate) blends using full-scale municipal activated sludge and non-chlorinated solvent extraction. In *The Handbook of Polyhydroxyalkanoates: Kinetics, Bioengineering, and Industrial Aspects*, 1st ed.; Koller, M., Ed.; CRC Press: Boca Raton, FL, USA, 2020; pp. 329–386.
- Morgan-Sagastume, F.; Valentino, F.; Hjort, M.; Zanolli, G.; Majone, M.; Werker, A. Acclimation Process for Enhancing Polyhydroxyalkanoate Accumulation in Activated-Sludge Biomass. *Waste Biomass Valorization* **2019**, *10*, 1065–1082. [[CrossRef](#)]
- Estévez-Alonso, Á.; van Loosdrecht, M.C.; Kleerebezem, R.; Werker, A. Simultaneous nitrification and denitrification in microbial community-based polyhydroxyalkanoate production. *Bioresour. Technol.* **2021**, *337*, 125420. [[CrossRef](#)]

20. Grazia, G.D.; Quadri, L.; Majone, M.; Morgan-Sagastume, F.; Werker, A. Influence of temperature on mixed microbial culture polyhydroxyalkanoate production while treating a starch industry wastewater. *J. Environ. Chem. Eng.* **2017**, *5*, 5067–5075. [[CrossRef](#)]
21. Koller, M. A review on established and emerging fermentation schemes for microbial production of polyhydroxyalkanoate (PHA) biopolyesters. *Fermentation* **2018**, *4*, 30. [[CrossRef](#)]
22. Koller, M.; Braunnegg, G. Potential and prospects of continuous polyhydroxyalkanoate (PHA) production. *Bioengineering* **2015**, *2*, 94–121. [[CrossRef](#)] [[PubMed](#)]
23. Silva, F.C.; Serafim, L.S.; Nadais, H.; Arroja, L.; Capela, I. Acidogenic Fermentation towards Valorisation of Organic Waste Streams into Volatile Fatty Acids. *Chem. Biochem. Eng. Q.* **2013**, *27*, 467–476.
24. Lagoa-Costa, B.; Kennes, C.; Veiga, M.C. Cheese whey fermentation into volatile fatty acids in an anaerobic sequencing batch reactor. *Bioresour. Technol.* **2020**, *308*, 123226. [[CrossRef](#)] [[PubMed](#)]
25. Valentino, F.; Karabegovic, L.; Majone, M.; Morgan-Sagastume, F.; Werker, A. Polyhydroxyalkanoate (PHA) storage within a mixed-culture biomass with simultaneous growth as a function of accumulation substrate nitrogen and phosphorus levels. *Water Res.* **2015**, *77*, 49–63. [[CrossRef](#)] [[PubMed](#)]
26. Bermúdez-Penabaz, N.; Kennes, C.; Veiga, M.C. Anaerobic digestion of tuna waste for the production of volatile fatty acids. *Waste Manag.* **2017**, *68*, 96–102. [[CrossRef](#)]
27. Atasoy, M.; Owusu-Agyeman, I.; Plaza, E.; Cetecioglu, Z. Bio-based volatile fatty acid production and recovery from waste streams: Current status and future challenges. *Bioresour. Technol.* **2018**, *268*, 773–786. [[CrossRef](#)] [[PubMed](#)]
28. Jones, R.J.; Fernández-Feito, R.; Massanet-Nicolau, J.; Dinsdale, R.; Guwy, A. Continuous recovery and enhanced yields of volatile fatty acids from a continually-fed 100 L food waste bioreactor by filtration and electro dialysis. *Waste Manag.* **2021**, *122*, 81–88. [[CrossRef](#)]
29. Burniol-Figols, A.; Pinelo, M.; Skiadas, I.V.; Gavala, H.N. Enhancing polyhydroxyalkanoate productivity with cell-retention membrane bioreactors. *Biochem. Eng. J.* **2020**, *161*, 107687. [[CrossRef](#)]
30. Tamis, J.; Marang, L.; Jiang, Y.; van Loosdrecht, M.C.M.; Kleerebezem, R. Modeling PHA-producing microbial enrichment cultures-towards a generalized model with predictive power. *New Biotechnol.* **2014**, *31*, 324–334. [[CrossRef](#)]
31. Werker, A.; Bengtsson, S.; Karlsson, A. Method for Accumulation of Polyhydroxyalkanoates in Biomass with On-Line Monitoring for Feed Rate Control and Process Termination. U.S. Patent US8748138B2, 10 June 2014.
32. Lorini, L.; di Re, F.; Majone, M.; Valentino, F. High rate selection of PHA accumulating mixed cultures in sequencing batch reactors with uncoupled carbon and nitrogen feeding. *New Biotechnol.* **2020**, *56*, 140–148. [[CrossRef](#)]
33. Valentino, F.; Moretto, G.; Lorini, L.; Bolzonella, D.; Pavan, P.; Majone, M. Pilot-Scale Polyhydroxyalkanoate Production from Combined Treatment of Organic Fraction of Municipal Solid Waste and Sewage Sludge. *Ind. Eng. Chem. Res.* **2019**, *58*, 12149–12158. [[CrossRef](#)]
34. APHA. *Standard Methods for the Examination of Water and Wastewater*; American Public Health Association: Washington DC, USA, 1998.
35. Chan, C.M.; Johansson, P.; Magnusson, P.; Vandi, L.J.L.J.; Arcos-Hernandez, M.; Halley, P.; Laycock, B.; Pratt, S.; Werker, A. Mixed culture polyhydroxyalkanoate-rich biomass assessment and quality control using thermogravimetric measurement methods. *Polym. Degrad. Stab.* **2017**, *144*, 110–120. [[CrossRef](#)]
36. Savitzky, A.; Golay, M.J. Smoothing and Differentiation of Data by Simplified Least Squares Procedures. *Anal. Chem.* **1964**, *36*, 1627–1639. [[CrossRef](#)]
37. Spanjers, H.; Olsson, G. Modelling of the dissolved oxygen probe response in the improvement of the performance of a continuous respiration meter. *Water Res.* **1992**, *26*, 945–954. [[CrossRef](#)]
38. Krishna, C.; Loosdrecht, M.C.V. Substrate flux into storage and growth in relation to activated sludge modeling. *Water Res.* **1999**, *33*, 3149–3161. [[CrossRef](#)]
39. Panikov, N.S. *Microbial Growth Kinetics*; Chapman & Hall: London, UK, 1995.
40. Johnson, K.; Kleerebezem, R.; van Loosdrecht, M.C. Model-based data evaluation of polyhydroxybutyrate producing mixed microbial cultures in aerobic sequencing batch and fed-batch reactors. *Biotechnol. Bioeng.* **2009**, *104*, 50–67. [[CrossRef](#)]
41. Arcos-Hernandez, M.V.; Gurieff, N.; Pratt, S.; Magnusson, P.; Werker, A.; Vargas, A.; Lant, P. Rapid quantification of intracellular PHA using infrared spectroscopy: An application in mixed cultures. *J. Biotechnol.* **2010**, *150*, 372–379. [[CrossRef](#)]
42. Beun, J.J.; Dircks, K.; Loosdrecht, M.C.V.; Heijnen, J.J. Poly-beta-hydroxybutyrate metabolism in dynamically fed mixed microbial cultures. *Water Res.* **2002**, *36*, 1167–1180. [[CrossRef](#)]
43. van Aalst-van Leeuwen, M.A.; Pot, M.A.; van Loosdrecht, M.C.; Heijnen, J.J. Kinetic Modeling of Poly (beta-hydroxybutyrate) Production and Consumption by Paracoccus pantotrophus under Dynamic Substrate Supply. *Biotechnol. Bioeng.* **1997**, *55*, 773–782. [[CrossRef](#)]
44. Jolkver, E.; Emer, D.; Ballan, S.; Krämer, R.; Eikmanns, B.J.; Marin, K. Identification and characterization of a bacterial transport system for the uptake of pyruvate, propionate, and acetate in *Corynebacterium glutamicum*. *J. Bacteriol.* **2009**, *191*, 940–948. [[CrossRef](#)]
45. Gurieff, N. *Production of Biodegradable Polyhydroxyalkanoate Polymers Using Advanced Biological Wastewater Treatment Process Technology*; The University of Queensland: Brisbane, Australia, 2007.

46. Serafim, L.S.; Lemos, P.C.; Oliveira, R.; Reis, M.A. Optimization of polyhydroxybutyrate production by mixed cultures submitted to aerobic dynamic feeding conditions. *Biotechnol. Bioeng.* **2004**, *87*, 145–160. [[CrossRef](#)] [[PubMed](#)]
47. Moretto, G.; Russo, I.; Bolzonella, D.; Pavan, P.; Majone, M.; Valentino, F. An urban biorefinery for food waste and biological sludge conversion into polyhydroxyalkanoates and biogas. *Water Res.* **2020**, *170*, 115371. [[CrossRef](#)] [[PubMed](#)]
48. Tamis, J.; Lužkov, K.; Jiang, Y.; van Loosdrecht, M.C.M.; Kleerebezem, R. Enrichment of *Plasticumulans acidivorans* at pilot-scale for PHA production on industrial wastewater. *J. Biotechnol.* **2014**, *192*, 161–169. [[CrossRef](#)] [[PubMed](#)]
49. Morgan-Sagastume, F.; Bengtsson, S.; Grazia, G.D.; Alexandersson, T.; Quadri, L.; Johansson, P.; Magnusson, P.; Werker, A. Mixed-culture polyhydroxyalkanoate (PHA) production integrated into a food-industry effluent biological treatment: A pilot-scale evaluation. *J. Environ. Chem. Eng.* **2020**, *8*, 104469. [[CrossRef](#)]
50. Albuquerque, M.G.; Concas, S.; Bengtsson, S.; Reis, M.A. Mixed culture polyhydroxyalkanoates production from sugar molasses: The use of a 2-stage CSTR system for culture selection. *Bioresour. Technol.* **2010**, *101*, 7112–7122. [[CrossRef](#)]
51. Marang, L.; van Loosdrecht, M.C.M.; Kleerebezem, R. Modeling the competition between PHA-producing and non-PHA-producing bacteria in feast-famine SBR and staged CSTR systems. *Biotechnol. Bioeng.* **2015**, *112*, 2475–2484. [[CrossRef](#)]
52. Mulders, M.; Tamis, J.; Stouten, G.R.; Kleerebezem, R. Simultaneous growth and poly(3-hydroxybutyrate) (PHB) accumulation in a *Plasticumulans acidivorans* dominated enrichment culture. *J. Biotechnol.* **2020**, *8*, 100027. [[CrossRef](#)]
53. Haimi, H.; Mulas, M.; Corona, F.; Vahala, R. Data-derived soft-sensors for biological wastewater treatment plants: An overview. *Environ. Model. Softw.* **2013**, *47*, 88–107. [[CrossRef](#)]

Article

Cell Retention as a Viable Strategy for PHA Production from Diluted VFAs with *Bacillus megaterium*

Milos Kacanski ¹, Lukas Pucher ¹, Carlota Peral ², Thomas Dietrich ² and Markus Neureiter ^{1,*}

¹ Department of Agrobiotechnology, Institute of Environmental Biotechnology, University of Natural Resources and Life Sciences, Vienna, Konrad-Lorenz-Str. 20, 3430 Tulln, Austria; milos.kacanski@boku.ac.at (M.K.); lukas.pucher@students.boku.ac.at (L.P.)

² TECNALIA, Basque Research and Technology Alliance (BRTA), Parque Tecnológico de Álava, Leonardo Da Vinci 1, 01510 Minano, Spain; carlota.peral@tecnalia.com (C.P.); thomas.dietrich@tecnalia.com (T.D.)

* Correspondence: markus.neureiter@boku.ac.at; Tel.: +43-1-47654-97441

Abstract: The production of biodegradable and biocompatible materials such as polyhydroxyalkanoates (PHAs) from waste-derived volatile fatty acids (VFAs) is a promising approach towards implementing a circular bioeconomy. However, VFA solutions obtained via acidification of organic wastes are usually too diluted for direct use in standard batch or fed-batch processes. To overcome these constraints, this study introduces a cell recycle fed-batch system using *Bacillus megaterium* uyuni S29 for poly(3-hydroxybutyrate) (P3HB) production from acetic acid. The concentrations of dry cell weight (DCW), P3HB, acetate, as well as nitrogen as the limiting substrate component, were monitored during the process. The produced polymer was characterized in terms of molecular weight and thermal properties after extraction with hypochlorite. The results show that an indirect pH-stat feeding regime successfully kept the strain fed without prompting inhibition, resulting in a dry cell weight concentration of up to 19.05 g/L containing 70.21% PHA. After appropriate adaptations the presented process could contribute to an efficient and sustainable production of biopolymers.

Keywords: polyhydroxyalkanoates; poly(3-hydroxybutyrate); cell retention; volatile fatty acids; *Bacillus megaterium*

Citation: Kacanski, M.; Pucher, L.; Peral, C.; Dietrich, T.; Neureiter, M. Cell Retention as a Viable Strategy for PHA Production from Diluted VFAs with *Bacillus megaterium*. *Bioengineering* **2022**, *9*, 122. <https://doi.org/10.3390/bioengineering9030122>

Academic Editor: Martin Koller

Received: 25 February 2022

Accepted: 14 March 2022

Published: 16 March 2022

Publisher's Note: MDPI stays neutral with regard to jurisdictional claims in published maps and institutional affiliations.



Copyright: © 2022 by the authors. Licensee MDPI, Basel, Switzerland. This article is an open access article distributed under the terms and conditions of the Creative Commons Attribution (CC BY) license (<https://creativecommons.org/licenses/by/4.0/>).

1. Introduction

There is a growing crisis related to the depletion of non-renewable resources and their impact on the environment. A way to address this challenge is to utilize waste materials from existing processes to decrease the environmental impact and create new products. To achieve this, it will be necessary to develop processes for valuable products that are either already on the market or have the capacity to be environmentally friendly alternatives to existing solutions. One approach is to produce biodegradable and biocompatible materials from renewable resources. In this regard, polyhydroxyalkanoates (PHAs) are good candidates because of their material properties [1] and lower impact [2,3] on the environment.

PHAs are intracellular polymers that help bacteria and archaea survive environmental challenges [4] and they are produced when there is an excess of available carbon and a simultaneous limitation of an essential nutrient such as nitrogen or phosphorous [5]. They are elastomeric or thermoplastic polyesters that are biocompatible and biodegradable [1]. Since their constitutive monomers influence their properties, they are broadly classified as either short chain length (3–5 carbon atoms in the monomer backbone), medium-chain length (6–14 carbon atoms in monomer backbone) or long-chain length PHAs (more than 14 carbon atoms) [6,7]. Exact material properties are also determined by polymer aspects such as average molecular weight and polydispersity index [1]. The most basic and most common type of PHA is poly(3-hydroxybutyrate) (P3HB), a highly crystalline and brittle material with thermoplastic behavior [8].

Current production schemes for PHA involve raw materials that are either unsustainably expensive or they divert resources from food production [2,3,9]. It is clear that the right way forward for PHA is to utilize cheap waste materials for the production and recently this concept has received a lot of attention. Various raw materials such as grass silage [10], crude glycerol [11], surplus whey [12] as well as chicory root hydrolysate [13], and desugared molasses [14] have been identified as suitable for production. Notably, production from volatile fatty acids (VFAs) has also been successfully demonstrated in various cases and scenarios, including pure as well as mixed culture approaches [15–20]. VFAs are very promising substrates for PHA production, since—in contrast to wastes with specific composition—they can be readily obtained from multiple wastes through already established digestion processes. Sludges from municipal wastewater are available in abundant volumes and there is rapid development for their use for VFA production [21]. In addition, food waste is also disposed in significant quantities and often studied for its VFA potential [22]. Industrial wastes, e.g., from agricultural, dairy, pulp and paper industries are also evaluated as perspective sources of VFAs [23,24]. Chemicals that can be derived from multiple renewable sources are deemed as platform chemicals within the biorefinery concept [25] and developing production processes around VFAs fits well within this context. They are already on the market to a significant extent [26], and there is also substantial research to optimize their output from renewable sources [22,26,27]. This aspect would also contribute to the robustness of PHA production, as constant availability of raw material throughout the year is less of an issue if it can be obtained from various sources.

The critical disadvantage of renewable carbon sources for PHA biosynthesis is that they are usually too diluted for productive batch and fed-batch processes [12,13,28–31]. A straightforward approach to tackle this issue would be to concentrate the substrates. However, this makes the process less favorable from an economic and ecological perspective, due to the additional energy input and costs of the concentration step and the risk of accumulating various substances that may inhibit microbial growth [9,13,30]. There is an alternative approach in the form of a cell recycle reactor, where the working volume is kept constant, with all the biomass in it, while the substrate flows through the process, according to the selected feeding regime. This has been demonstrated in a study with a recombinant *E.coli* fed by whey [28] and similar approaches employed *Cupriavidus necator* to produce PHA with carbohydrates [32,33]. Membrane-based biopolymer production with organic acids is mentioned only in one study with food scraps digestate that contained mostly lactic and butyric acid [34]. Volatile fatty acids, in particular, have an additional constraint, since they can inhibit the producing microbes [34,35]. However, this can be solved by implementing a properly controlled feeding regime. Cell recycling is a powerful approach for working with diluted carbon sources, especially when the desired product is accumulated inside the cells. Ultimately, the concentrated cell mass will result in high productivities, which could be further increased by establishing a fully continuous process.

Regarding the active culture, there is a choice between processes based on aseptic pure cultures and mixed microbial consortia (MMC). The MMC approach is generally cheaper and more robust. There is no requirement for sterility, and the adaptation of the microbial consortium is a necessary and expected part of the process. This allows for flexibility in substrate quality, which is an important aspect in fed-batch approaches from complex waste-based substrates. However, MMC processes come with certain drawbacks, which call for the development of pure culture processes. The MMC approach requires more effort to guarantee specific material properties related to the composition and distribution of monomeric units and molecular weight and related aspects such as crystallinity [20,31,36]. In addition, pure cultures offer more potential with regard to the use of metabolic and genetic engineering for improving all aspects important for PHA production.

However, there is a possibility to transfer some advantages of the MMC approach to pure culture processes with certain design choices. The impact of dissolved inhibitive substrate components [31] is less relevant in cell recycle processes, as they are less likely to accumulate due to washout. Furthermore, the use of extremophilic production strains can

reduce to some extent the dependence on successful sterilization and proper protection from contamination during the long processes [9]. *Bacillus megaterium* uyuni S29, a halophilic organism isolated from a Bolivian Salt Lake, has the potential to adequately address this function. This strain was already reported to accumulate P3HB at relatively high content (up to 60% of dry cell weight) [37], including a study with waste-based media [14].

The objective of this work was to establish P3HB production from a VFA-based substrate using *Bacillus megaterium* uyuni S29 as the production strain. The process was designed as a cell recycle fed-batch system with an indirect pH-stat feeding regime.

2. Materials and Methods

2.1. Microorganisms and Media for Cultivation

The working strain in this study, *Bacillus megaterium* uyuni S29 (CECT 7922), was cultivated for preculture on nutrient broth (NB) agar plates (5 g/L peptone from meat, 3 g/L meat extract, 15 g/L agar-agar) at 30 °C. For long term storage, the organism was kept at −80 °C as cryo-stock in modified beef extract medium (10 g/L peptone from casein, 10 g/L meat extract, 5 g/L NaCl) with 10% glycerol.

The preculture was inoculated from a plate and cultivated in a rotary shaker (Infors Multitron) at 35 °C and 130 rpm for 24 h in 300 mL baffled shake flasks containing 100 mL of fermentation media. To achieve the goals of this study, we designed a synthetic medium containing acetate as the main carbon and energy source alongside some additional nutrients in the form of yeast extract and citric acid (present only at the beginning). These nutrients were added to speed up initial growth as they are known to promote growth of *Bacillus megaterium* strains [38]. Acetate content was kept below a value of 5 g/L to avoid inhibition. The medium composition was as follows: 10 g/L NaCl, 1.5 g/L KH₂PO₄, 4 g/L Na₂HPO₄, 0.025 g/L CaCl₂, 0.025 g/L NH₄Fe(III) citrate, 0.04 g/L MgSO₄·7H₂O, 1 mL/L of 5 × SL6 trace elements solution, 5 g/L (NH₄)₂SO₄, 5 g/L yeast extract, 0.75 g/L citric acid and 4 g/L sodium acetate. The 5 × SL6 trace elements solution contained: 0.5 g/L ZnSO₄·7 H₂O, 0.15 g/L MnCl₂·4 H₂O, 1.5 g/L H₃BO₃, 1g/L CoCl₂·6 H₂O, 0.05 g/L CuCl₂·2 H₂O, 0.1 g/L NiCl₂·6 H₂O and 0.15 g/L Na₂MoO₄·2 H₂O. pH was set to 7.0 and the media was autoclaved at 121 °C for 20 min. Phosphates and ammonium sulfate were autoclaved separately to avoid precipitation.

Consumed acetate was replenished via the feed medium (10 g/L NaCl, 0.5 g/L KH₂PO₄, 1 g/L Na₂HPO₄, 0.025 g/L, CaCl₂, 0.025 g/L NH₄Fe(III) citrate, 1 mL/L of 5 × SL6 trace elements solution and 20 g/L Na acetate, pH: 7.0). The medium was designed to induce nitrogen limitation by excluding (NH₄)₂SO₄ and yeast extract. A concentration of 20 g/L sodium acetate (14.63 g/L of acetic acid) was chosen to mimic the concentration of carbon source expected from acidification processes. Phosphate content in the feed was decreased to evade precipitation. The acid control solution was 2 M H₂SO₄ with the addition of 8 g/L of MgSO₄·7 H₂O to evade precipitation. The first batch of feed media was sterile filtered in a 10 L bottle. Subsequent batches were not sterilized, since there was only a low risk for contamination due to low nitrogen and high acetate content.

2.2. Fermentation Setup

The experiments were conducted in a fermenter with 5 L working volume (B. Braun Biotech International GmbH, Melsungen, Germany) operating at a working volume of 4 L. Aeration (2–10 L/min) and stirring (200–800 rpm) were controlled stepwise by feedback from the dissolve oxygen (DO) probe against a setpoint of 20% DO. The reactor was connected with the membrane system, as shown in Figure 1. We used a 0.02 mm pore size microfiltration membrane (CFP-2-E-4MA, 420 cm² membrane area, GE healthcare, Amersham, UK) sterilized by flushing 2 M NaOH for 2 h. Before connecting to the reactor, NaOH was removed by flushing with sterile water. During the process, a crossflow pump was operated at 1750 mL/min. Transmembrane pressure was measured before the membrane as well as on the permeate side. The pumps for the crossflow and the permeate

were set to automatically reverse the flow every 20 min for 1 min to avoid intensive fouling of the membrane by the biomass.

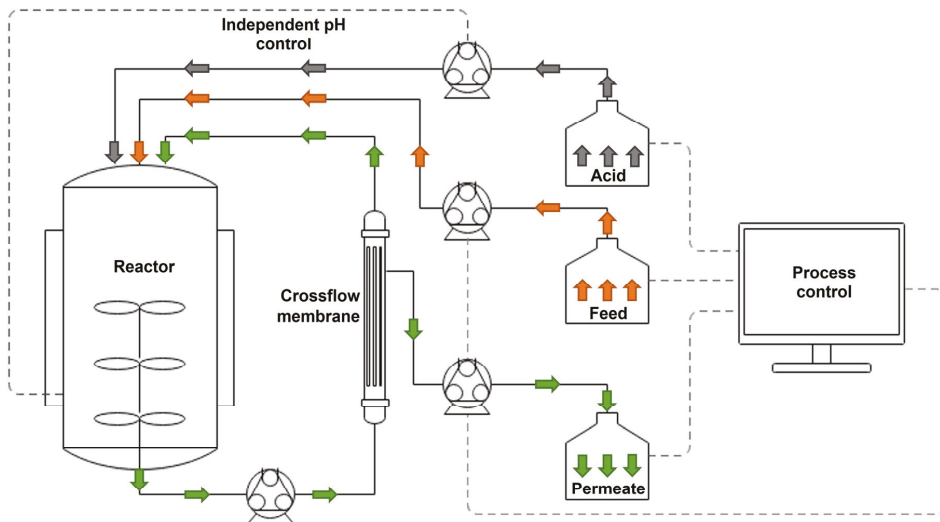


Figure 1. Schematic representation of the cell recycle system. Addition of acid (grey) and VFA feed (orange) and removal of permeate (green) via pumps is recorded by scales and controlled by the process control system in order to keep process values stable and maintain a constant volume in the reactor.

Feed, permeate removal and pH were programmed with a control system (1769 CompactLogix Controller, Rockwell Automation, Milwaukee, WI, USA) to pump out the permeate, as measured by the weight of the permeate bottle, at the exact amount of liquid supplied via the feed and acid control, as measured by the respective weights of feed and acid solution bottles. Since the change in pH in the reactor is the result of acetate consumption, the feed was linked to the pH control by following the current addition rate of acid solution. A control interface table provided the system with information about the current rate of feed addition based on the current acid consumption. The setpoint for the feed rate was defined to correspond to a range of acid consumption.

2.3. Analytical Methods

Samples of the fermentation broth were taken 3 times per day and separated into triplicates of 5 mL each, from which further analysis was performed. Samples were centrifuged (Centrifuge 5810, Eppendorf, Hamburg, Germany) at $2724 \times g$ for 15 min and the supernatant was frozen at 20 °C for subsequent analysis. The precipitated biomass was washed and dried for 48 h at 105 °C to determine the dry cell weight (DCW) and subsequently the P3HB content.

Acetate concentration was determined by HPLC (1100 series with refractive index detector, Agilent, Santa Clara, CA, USA; ION 300 column, Transgenomic, New Haven, CT, USA; column temperature: 45 °C; eluent: 0.005 M H_2SO_4 , flow rate: 0.325 mL/min; pressure: 46 bar).

The total amount of nitrogen available for consumption to the strain was determined as total Kjeldahl nitrogen. Approximately 1.5 mL of fermentation supernatant was dissolved in 20 mL concentrated sulfuric acid and 1 Kjeltab (Thomson & Capper, Cheshire, UK). Following digestion in a Digest Automat K-438 (Büchi, Flawil, Switzerland), the nitrogen concentration was determined by titration with an AutoKjeldahl Unit K-370 (Büchi, Flawil, Switzerland).

Biopolymer production was quantified by oxidation to crotonic acid [39] determined by HPLC using the same setup described for the determination of acetic acid. This method

was considered sufficient to quantify the produced polymer, as this strain was shown to produce only P3HB under the conditions applied in the experiments [14].

2.4. Polymer Extraction and Characterization

The polymer was extracted via biomass digestion with sodium hypochlorite [40]. Centrifuged biomass was suspended in 0.2 M H₂SO₄ and left overnight at room temperature. After 24 h, the pH value of the suspension was set to 13.0 to break up the cell membrane and after another hour a 10% solution of sodium hypochlorite was added to double the volume, yielding the final hypochlorite concentration of 5%. After one hour, the suspensions were centrifuged, and the precipitate was dried at 105 °C. The resulting powder was P3HB, which was used for further characterization.

Weight average (M_w) and number average (M_n) molecular weight were determined using gel permeation chromatography (GPC) PL-GPC-50 (Agilent Technologies, Santa Clara, CA, USA) equipped with an IR detector. The column was a RESIPORE 3 μ m (300 \times 7.5 mm) heated to 25 °C and the mobile phase was chloroform (flow rate: 1 mL/min). The standard EasiCal Polystyrene pre-prepared calibration kit, PS-2 Part Number PL2010-0605 (Agilent Technologies, Santa Clara, CA, USA) was used. The polydispersity was calculated as the ratio between the weight- and number-average molecular weights. Sample injection volumes of 20 μ L were used.

Melting temperature T_M as well as glass transition temperature T_G were determined via differential scanning calorimetry (DSC). Samples (3–4 mg) were weighed in aluminum pans, which were sealed and then heated in a DSC calorimeter (TA Instruments, New Castle, DE, USA) at a constant rate of 10 °C/min from 20 °C to 220 °C, cooled down to –50 °C, and heated up again to 220 °C. An empty pan was used as a reference. Dry nitrogen was used as a purge gas at 50 mL/h.

Thermal degradation was studied by TGA using a SDT 2960 Simultaneous DTA-TGA/DSC-TGA (TA Instruments, New Castle, DE, USA). The polymer sample was heated from 20 °C to 500 °C at a rate of 2 °C/min in an active nitrogen atmosphere at a flow rate of 20 mL/min.

3. Results and Discussion

3.1. Growth and Polymer Production

This study examined growth and polymer production of *Bacillus megaterium* uyuni S29 from a dilute substrate in a cell recycle setup with a crossflow membrane. Growth and polymer production over the duration of the fermentation process (90 h) are shown in Figure 2. After a lag phase, there is a linear increase in DCW until 48 h. A continued, but less steep ascent can be observed until 72 h, reaching a maximum value of 19.05 g/L, after which there is a decline to 17.55 g/L at the end of the process. Polymer production followed the same profile as biomass, peaking at 72 h with 13.38 g/L (70.21% of DCW) and declining towards the end to 12.25 g/L (69.61% of DCW). The maximal PHB productivity was 0.058 g/Lh, with a corresponding yield of 0.23 g/g reached after 48 h into the process.

Nitrogen was not provided in the feed solution and became a limiting factor after 30 h, when its level dropped below 0.1 g/L. The acetate level in the fermenter stabilized at a level below 1 g/L between 12 and 60 h, with a minimal concentration of 0.22 g/L after 30 h. Thereafter, it slowly increased, reaching its maximal value of 2.22 g/L at the end.

A repetition of the experiment shows similar growth and polymer production (Figure 3). In this case, the linear growth phase was shorter and lasted until 36 h. DCW continued to increase at a smaller rate until 70 h, reaching a maximum value of 16.20 g/L, after which there was a sharp decline for the final value of 13.34 g/L. Polymer production followed the same trend, with low levels already present at the start of the experiment and reflecting course of biomass through the 70 h peak at 12.24 g/L (76% of DCW) all the way to the final concentration of 9.58 g/L (71.78% of DCW). The maximal productivity was 0.062 g/Lh with a corresponding yield of 0.26 g/g, which was again reached when the curve began to flatten (36 h). After 30 h, the nitrogen concentration dropped below 0.07 g/L, indicating limitation.

In this experiment, an accumulation of acetic acid was observed after the feed was started, since an additional sampling point after 6 h was added. Acetic acid concentration then decreased steadily to a minimum value of 0.12 g/L at 30 h, and increased thereafter to the final concentration of 2.07 g/L.

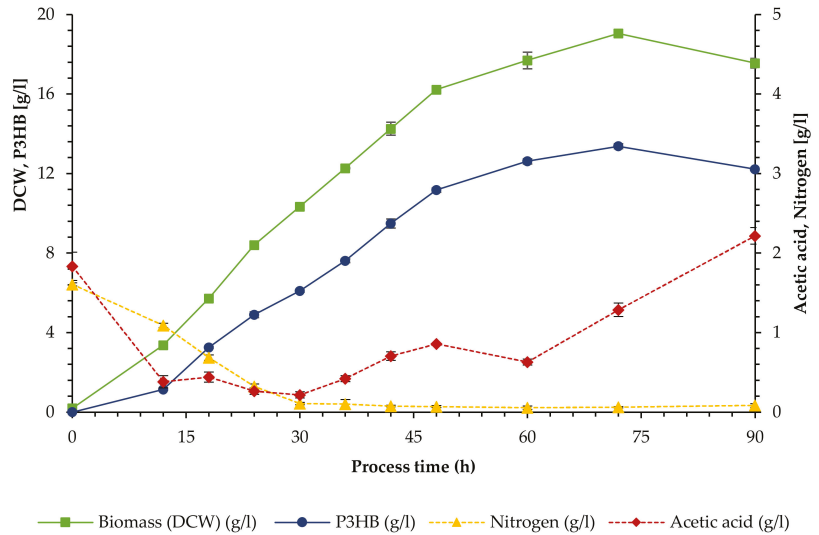


Figure 2. Cultivation of *Bacillus megaterium* uyuni S29 in a cell recycle process (I). Biomass (as DCW) and polymer (P3HB) concentration (left axis) and concentration of acetic acid and nitrogen (as TKN) (right axis). Error bars represent standard deviation from triplicate samples.

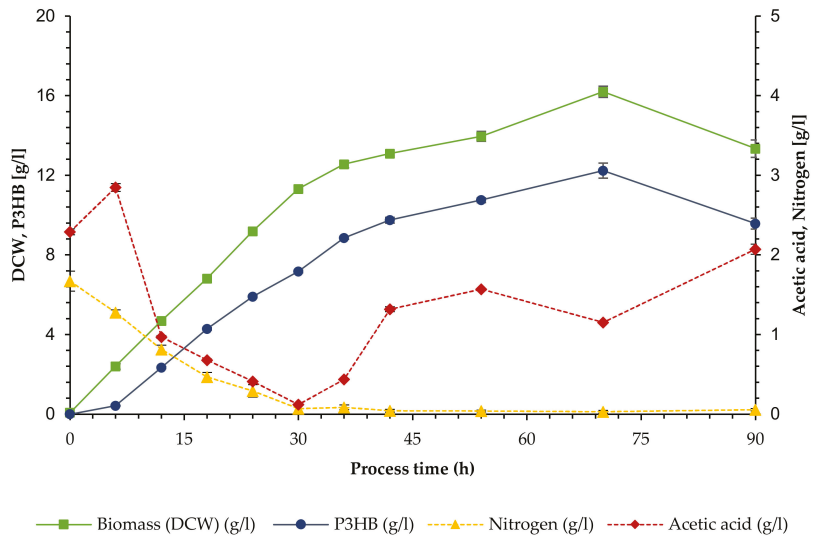


Figure 3. Cultivation of *Bacillus megaterium* uyuni S29 in a cell recycle process (II, replicate). Biomass (as DCW) and polymer (P3HB) concentration (left axis) and concentration of acetic acid and nitrogen (as TKN) (right axis). Error bars represent standard deviation from triplicate samples.

The selection of a halophilic strain and the cell retention design open the possibility of non-sterile processes with pure cultures. A high salt concentration combined with a strong and adapted inoculum could keep potential contaminants at bay during the initial phase, while the nutrient limitation would not allow for significant growth of competing organisms in the later stages of the process. This strategy was partially implemented in the present work, where sterilization procedures were applied only for the initial reactor volume and the first 10 L of feed. No contamination could be detected when checked under the microscope.

In the literature, most work on the conversion of volatile fatty acids to PHA relates to the application of mixed microbial consortia. This approach requires a sequential batch approach and, in most cases, results are less favorable compared to pure culture approaches [40,41]. The most successful PHA production from VFAs to date was achieved by Huschner et al. in a regular fed-batch with *Ralstonia eutropha* H16 (different designation for *Cupriavidus necator*) using a concentrated VFA solution resulting in cell densities of 112 g/L with 83% polymer content [18]. The feeding regime was a combination of pH-stat with acid solution and DO-stat with VFA salts. The feed solution contained organic acids in the approximate range of 300–600 g/L and organic salts at about 350 g/L. While ideal for fed-batch processes, it is questionable whether feed concentrations in this range can be obtained from renewable resources in an economically feasible way. More comparable with the present study is the work of Du et al., who achieved 22.7 g/L of DCW with 72.6% polymer in a similar setup with *C. necator*. With respect to the production strain it is notable that the achieved DCW and polymer concentrations in our study are comparable with values for *Bacillus megaterium* on a sugar rich substrate [14].

The large constraint to reaching higher cell densities and productivities in our study was nitrogen content [42]. Due to the way the system is configured, a part of the nitrogen is washed out with the permeate. This design made nitrogen a much more limiting factor compared to the fed-batch version of the same process. Based on the data from nitrogen measurements and feed addition it can be calculated that approximately 0.79 g/L of the initial nitrogen content was consumed by the cells.

In order to improve the productivity [18], it will be necessary to optimize the nitrogen supply to accumulate more biomass [42]. This could be achieved by starting with a higher nitrogen concentration in the medium or by introducing a nitrogen source with the feed solution. However, it must be considered that faster growth will result in higher feed rates and consequently a faster washout of nutrients, which ultimately limits this approach. The addition of nitrogen to the feed should be further investigated, however, this needs to be carefully optimized with nutrient limitations in mind [42].

Due to the inhibitive properties of acetate at elevated concentrations, an overfeed of the system was identified as a potential risk during operation [18,35]. The feeding regime is a calculation-based pH-stat and there is a possibility that small errors in calculation or feed preparation amplify. Therefore, it is critical to align the pH of the feed and pH setting of the process control, as this could easily create a negative or positive feedback loop. However, during operation the system turned out to run stably without any issues in this regard. This could be explained by a partial compensation of changes in broth composition due to the washout via the permeate. Additionally, a low acetate content in the feed prevents the acetate content in the reactor from suddenly increasing in the case of systemic glitches in the process control.

A major disadvantage of VFA as a raw material compared to sugar based substrates is the low productivity [31]. A continuous mode of operation could lead these processes towards higher productivities. MMC processes are currently being rapidly developed in this regard [36,43]. Various pure culture based processes have also been investigated [44–46] and the process scheme in the present work would surely benefit in terms of productivity from continuous mode. The most straightforward way to convert this process to continuous mode would be the continuous removal of the fermentation broth, creating a chemostat [31]. This should be possible with this strain, since it produces a polymer during the growth

stage. There would be no typical PHB accumulation phase, and all of the polymer would have to be produced during exponential growth, requiring a dual limitation strategy [42] and imposing some limit on the desired increase in productivity. Another option would involve the coupling of two cell recycling processes, with a first reactor dedicated for unlimited biomass production and a second reactor with optimal conditions for polymer accumulation. Different volumes in the reactors would determine the residence time/dilution factor to achieve the goals of each step [31].

3.2. Membrane Performance

The membrane behavior in both experiments is shown in Figure 4. The performance was stable, but there is an increase in transmembrane pressure over time due to fouling. The membrane backflush protocol allowed for uninterrupted operation for the duration of the process. However, if the process reached higher cell densities and required a faster feed rate, an exchange of a membrane module might be necessary. For a practical full-scale application, specialized membrane technology could enable more robust operation, but the module used proved to be sufficiently functional for the lab-scale process.

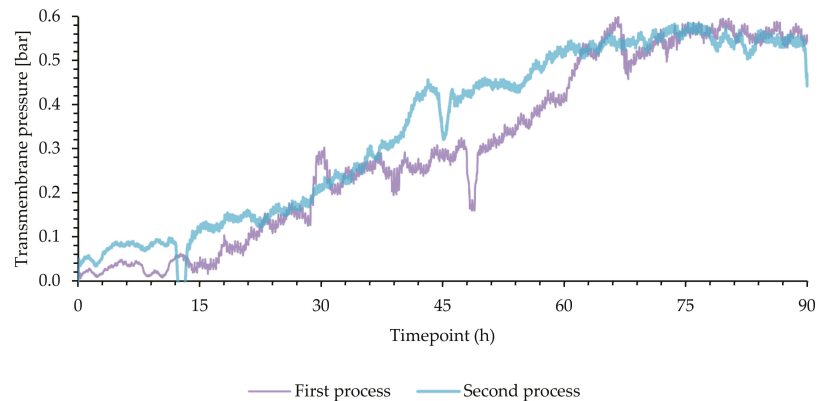


Figure 4. Transmembrane pressure of the two cell recycle processes with *Bacillus megaterium* uyuni S29. The membrane pressure curves are shown as 60 min rolling averages.

3.3. Polymer Characterization

The polymer was separated from the biomass by digestion of the surrounding biomass using hypochlorite. The obtained molecular weights and results of the DSC (Figure S1, Table S1) and TGA (Figure S2) of the extracted polymer are shown in Table 1 together with values that were obtained from polymers of the same strain in other studies, and commercial products. The results indicate that the grade of the extracted polymer is lower than what might be normally expected from polymers of this strain. This is most likely a consequence of the hypochlorite extraction, which tends to degrade the polymer and reduce the molecular weight. This is also indicated by the PDI, which is very low compared to values previously obtained with the same strain [46]. The thermal properties follow this trend and are considerably poor. Therefore, the possible applications for such a polymer are very limited. As material properties can be influenced by both cultivation and extraction, it is likely that a higher-quality polymer can be obtained with an adapted purification process.

Table 1. Material properties produced by the same strain in different studies in comparison with commercially available products.

Sample Origin	M _w [kg/mol]	PDI	T _m (°C)	T _g (°C)	T _d (°C)
This study	56.83	1.29	154.30	−23.27	184.50
This study	59.65	1.43	151.84	−24.02	194.97
<i>B. megaterium</i> S29 [47]	350	2.76	178	1.8	238.7
<i>B. megaterium</i> S29 [48]	600–125	nd	161	−11	nd
<i>B. megaterium</i> S29 [48]	600–125	nd	136.8	−16	nd
Mirel TM F1005 Mirel [49]	71.7	2.1	166.7	nd	283.3
Mirel TM F1006 Mirel [49]	71.4	2.2	165.7	nd	275.5
Enmat Y1000 [49]	77.6	2.6	168.9	nd	272.8

M_w: weight average molecular weight; PDI: polydispersity index; T_m: melting temperature; T_g: glass transition temperature; T_d: degradation temperature; nd: not determined.

4. Conclusions

It could be demonstrated that a cell recycling fed-batch system can be operated in a stable manner to produce P3HB from acetate with *Bacillus megaterium*. While the process indicators were within the anticipated range, there is still room for improvement. The development of a more suitable nitrogen feeding regime is expected to increase biomass concentrations and consequently the productivity of the process. The hypochlorite extraction used for purification had a negative impact on the material properties of the obtained polymer, which underlines the importance of selecting an appropriate extraction process. When applied to waste-derived VFA mixtures, the presented process has the potential to contribute to a sustainable and efficient production of biopolymers.

Supplementary Materials: The following supporting information can be downloaded at: <https://www.mdpi.com/article/10.3390/bioengineering9030122/s1>, Figure S1: Differential scanning calorimetry (DSC) of the extracted polymers; Figure S2: Thermogravimetric analysis (TGA) of the extracted polymers; Table S1: Results differential scanning calorimetry (DSC) of the extracted polymers.

Author Contributions: Conceptualization—M.K. and M.N.; methodology—M.K. and M.N.; formal analysis—M.K.; investigation—M.K., L.P., C.P.; resources—M.N. and T.D.; data curation—M.K., C.P.; writing—original draft preparation—M.K.; writing—review and editing—M.N. and T.D.; visualization—M.K.; supervision—M.N.; project administration—T.D. and M.N.; funding acquisition—T.D. and M.N. All authors have read and agreed to the published version of the manuscript.

Funding: This work was supported by the European project ‘Volatile—Biowaste-derived volatile fatty acid platform for biopolymers, bioactive compounds and chemical building blocks’ and has received funding from the European Union’s Horizon 2020 research and innovation program under grant agreement number 720777.

Institutional Review Board Statement: Not applicable.

Informed Consent Statement: Not applicable.

Data Availability Statement: Essential data are contained within the article. The raw data are available on request from the corresponding author.

Acknowledgments: The authors would like to thank Maximilian Schmid for providing his expertise in the handling of *Bacillus megaterium* uyuni S29, Wilhelm Müllner for programming and customization of the process control system, and Marcus Pruckner for his help with chemical analytics and maintenance of equipment.

Conflicts of Interest: The authors declare no conflict of interest. The funders had no role in the study’s design, in the collection, analyses, or interpretation of data, in the writing of the manuscript, or in the decision to publish the results.

References

- Bugnicourt, E.; Cinelli, P.; Lazzeri, A.; Alvarez, V. Polyhydroxyalkanoate (PHA): Review of Synthesis, Characteristics, Processing and Potential Applications in Packaging. *Express Polym. Lett.* **2014**, *8*, 791–808. [\[CrossRef\]](#)
- Yadav, B.; Pandey, A.; Kumar, L.R.; Tyagi, R.D. Bioconversion of Waste (Water)/Residues to Bioplastics—A Circular Bioeconomy Approach. *Bioresour. Technol.* **2020**, *298*, 122584. [\[CrossRef\]](#) [\[PubMed\]](#)
- Dietrich, K.; Dumont, M.J.; Del Rio, L.F.; Orsat, V. Producing PHAs in the Bioeconomy—Towards a Sustainable Bioplastic. *Sustain. Prod. Consum.* **2017**, *9*, 58–70. [\[CrossRef\]](#)
- Obruca, S.; Sedlacek, P.; Koller, M.; Kucera, D.; Pernicova, I. Involvement of Polyhydroxyalkanoates in Stress Resistance of Microbial Cells: Biotechnological Consequences and Applications. *Biotechnol. Adv.* **2018**, *36*, 856–870. [\[CrossRef\]](#) [\[PubMed\]](#)
- Philip, S.; Keshavarz, T.; Roy, I. Polyhydroxyalkanoates: Biodegradable Polymers with a Range of Applications. *J. Chem. Technol. Biotechnol.* **2007**, *82*, 233–247. [\[CrossRef\]](#)
- Taguchi, S.; Doi, Y. Evolution of Polyhydroxyalkanoate (PHA) Production System by “Enzyme Evolution”: Successful Case Studies of Directed Evolution. *Macromol. Biosci.* **2004**, *4*, 145–156. [\[CrossRef\]](#)
- Licciardello, G.; Catara, A.F.; Catara, V. Production of Polyhydroxyalkanoates and Extracellular Products Using *Pseudomonas corrugata* and *P. mediterranea*: A Review. *Bioengineering* **2019**, *6*, 105. [\[CrossRef\]](#)
- Albuquerque, P.B.S.; Malafaia, C.B. Perspectives on the Production, Structural Characteristics and Potential Applications of Bioplastics Derived from Polyhydroxyalkanoates. *Int. J. Biol. Macromol.* **2018**, *107*, 615–625. [\[CrossRef\]](#)
- Koller, M.; Maršálek, L.; de Sousa Dias, M.M.; BrauneGG, G. Producing Microbial Polyhydroxyalkanoate (PHA) Biopolyesters in a Sustainable Manner. *N. Biotechnol.* **2017**, *37*, 24–38. [\[CrossRef\]](#)
- Koller, M.; Bona, R.; Hermann, C.; Horvat, P.; Martinz, J.; Neto, J.; Pereira, L.; Varila, P.; BrauneGG, G. Biotechnological Production of Poly(3-Hydroxybutyrate) with *Wautersia eutropha* by Application of Green Grass Juice and Silage Juice as Additional Complex Substrates. *Biocatal. Biotransformation* **2005**, *23*, 329–337. [\[CrossRef\]](#)
- BrauneGG, G.; Bona, R.; Koller, M. Sustainable Polymer Production. *Polym. Plast. Technol. Eng.* **2004**, *43*, 1779–1793. [\[CrossRef\]](#)
- Koller, M.; Hesse, P.; Bona, R.; Kutschera, C.; Atlić, A.; BrauneGG, G. Potential of Various Archae- and Eubacterial Strains as Industrial Polyhydroxyalkanoate Producers from Whey. *Macromol. Biosci.* **2007**, *7*, 218–226. [\[CrossRef\]](#) [\[PubMed\]](#)
- Haas, C.; Steinwandter, V.; De Apodaca, E.D.; Madurga, B.M.; Smerilli, M.; Dietrich, T.; Neureiter, M. Production of PHB from Chicory Roots—Comparison of Three *Cupriavidus necator* Strains. *Chem. Biochem. Eng. Q.* **2015**, *29*, 99–112. [\[CrossRef\]](#)
- Schmid, M.T.; Song, H.; Raschbauer, M.; Emerstorfer, F.; Omann, M.; Stelzer, F.; Neureiter, M. Utilization of Desugared Sugar Beet Molasses for the Production of Poly(3-Hydroxybutyrate) by Halophilic *Bacillus megaterium* uyuni S29. *Process Biochem.* **2019**, *86*, 9–15. [\[CrossRef\]](#)
- Werker, A.; Bengtsson, S.; Korving, L.; Hjort, M.; Anterrieu, S.; Alexandersson, T.; Johansson, P.; Karlsson, A.; Karabegovic, L.; Magnusson, P.; et al. Consistent Production of High Quality PHA Using Activated Sludge Harvested from Full Scale Municipal Wastewater Treatment-PHARIO. *Water Sci. Technol.* **2018**, *78*, 2256–2269. [\[CrossRef\]](#)
- Tamis, J.; Mulders, M.; Dijkman, H.; Rozendal, R.; van Loosdrecht, M.C.M.; Kleerebezem, R. Pilot-Scale Polyhydroxyalkanoate Production from Paper Mill Wastewater: Process Characteristics and Identification of Bottlenecks for Full-Scale Implementation. *J. Environ. Eng.* **2018**, *144*, 04018107. [\[CrossRef\]](#)
- Cerrone, F.; Choudhari, S.K.; Davis, R.; Cysneiros, D.; O’Flaherty, V.; Duane, G.; Casey, E.; Guzik, M.W.; Kenny, S.T.; Babu, R.P.; et al. Medium Chain Length Polyhydroxyalkanoate (mcl-PHA) Production from Volatile Fatty Acids Derived from the Anaerobic Digestion of Grass. *Appl. Microbiol. Biotechnol.* **2014**, *98*, 611–620. [\[CrossRef\]](#)
- Huschner, F.; Grousseau, E.; Brigham, C.J.; Plassmeier, J.; Popovic, M.; Rha, C.; Sinskey, A.J. Development of a Feeding Strategy for High Cell and PHA Density Fed-Batch Fermentation of *Ralstonia eutropha* H16 from Organic Acids and Their Salts. *Process Biochem.* **2015**, *50*, 165–172. [\[CrossRef\]](#)
- Follonier, S.; Riesen, R.; Zinn, M. Pilot-Scale Production of Functionalized Mcl-PHA from Grape Pomace Supplemented with Fatty Acids. *Chem. Biochem. Eng. Q.* **2015**, *29*, 113–121. [\[CrossRef\]](#)
- Chalima, A.; De Castro, L.F.; Burgstaller, L.; Sampaio, P.; Carolas, A.L.; Gildemyn, S.; Velghe, F.; Ferreira, B.S.; Pais, C.; Neureiter, M.; et al. Waste-Derived Volatile Fatty Acids as Carbon Source for Added-Value Fermentation Approaches. *FEMS Microbiol. Lett.* **2021**, *368*, fnab054. [\[CrossRef\]](#)
- Lee, W.S.; Chua, A.S.M.; Yeoh, H.K.; Ngoh, G.C. A Review of the Production and Applications of Waste-Derived Volatile Fatty Acids. *Chem. Eng. J.* **2014**, *235*, 83–99. [\[CrossRef\]](#)
- Strazzera, G.; Battista, F.; Garcia, N.H.; Frison, N.; Bolzonella, D. Volatile Fatty Acids Production from Food Wastes for Biorefinery Platforms: A Review. *J. Environ. Manage.* **2018**, *226*, 278–288. [\[CrossRef\]](#) [\[PubMed\]](#)
- Koutinas, A.A.; Vlysidis, A.; Pleissner, D.; Kopsahelis, N.; Lopez Garcia, I.; Kookos, I.K.; Papanikolaou, S.; Kwan, T.H.; Lin, C.S.K. Valorization of Industrial Waste and By-Product Streams via Fermentation for the Production of Chemicals and Biopolymers. *Chem. Soc. Rev.* **2014**, *43*, 2587–2627. [\[CrossRef\]](#) [\[PubMed\]](#)
- Bengtsson, S.; Hallquist, J.; Werker, A.; Welander, T. Acidogenic Fermentation of Industrial Wastewaters: Effects of Chemostat Retention Time and PH on Volatile Fatty Acids Production. *Biochem. Eng. J.* **2008**, *40*, 492–499. [\[CrossRef\]](#)
- Choi, S.; Song, C.W.; Shin, J.H.; Lee, S.Y. Biorefineries for the Production of Top Building Block Chemicals and Their Derivatives. *Metab. Eng.* **2015**, *28*, 223–239. [\[CrossRef\]](#)

26. Atasoy, M.; Owusu-Agyeman, I.; Plaza, E.; Cetecioglu, Z. Bio-Based Volatile Fatty Acid Production and Recovery from Waste Streams: Current Status and Future Challenges. *Bioresour. Technol.* **2018**, *268*, 773–786. [[CrossRef](#)] [[PubMed](#)]
27. Moretto, G.; Valentino, F.; Pavan, P.; Majone, M.; Bolzonella, D. Optimization of Urban Waste Fermentation for Volatile Fatty Acids Production. *Waste Manag.* **2019**, *92*, 21–29. [[CrossRef](#)]
28. Ahn, W.S.; Park, S.J.; Lee, S.Y. Production of Poly(3-Hydroxybutyrate) from Whey by Cell Recycle Fed-Batch Culture of Recombinant *Escherichia coli*. *Biotechnol. Lett.* **2001**, *23*, 235–240. [[CrossRef](#)]
29. Bhattacharyya, A.; Saha, J.; Haldar, S.; Bhowmic, A.; Mukhopadhyay, U.K.; Mukherjee, J. Production of Poly-3-(Hydroxybutyrate-Co-Hydroxyvalerate) by *Haloferax mediterranei* Using Rice-Based Ethanol Stillage with Simultaneous Recovery and Re-Use of Medium Salts. *Extremophiles* **2014**, *18*, 463–470. [[CrossRef](#)]
30. Obruca, S.; Benesova, P.; Marsalek, L.; Marova, I. Use of Lignocellulosic Materials for PHA Production. *Chem. Biochem. Eng. Q.* **2015**, *29*, 135–144. [[CrossRef](#)]
31. Koller, M. A Review on Established and Emerging Fermentation Schemes for Microbial Production of Polyhydroxyalkanoate (PHA) Biopolyesters. *Fermentation* **2018**, *4*, 30. [[CrossRef](#)]
32. Haas, C.; El-Najjar, T.; Virgolini, N.; Smerilli, M.; Neureiter, M. High Cell-Density Production of Poly(3-Hydroxybutyrate) in a Membrane Bioreactor. *N. Biotechnol.* **2017**, *37*, 117–122. [[CrossRef](#)]
33. Ienczak, J.L.; Schmidt, M.; Quines, L.K.; Zanfonato, K.; da Cruz Pradella, J.G.; Schmidell, W.; de Aragao, G.M.F. Poly(3-Hydroxybutyrate) Production in Repeated Fed-Batch with Cell Recycle Using a Medium with Low Carbon Source Concentration. *Appl. Biochem. Biotechnol.* **2016**, *178*, 408–417. [[CrossRef](#)] [[PubMed](#)]
34. Du, G.; Yu, J. Green Technology for Conversion of Food Scraps to Biodegradable Thermoplastic Polyhydroxyalkanoates. *Environ. Sci. Technol.* **2002**, *36*, 5511–5516. [[CrossRef](#)] [[PubMed](#)]
35. Zeb, B.S.; Mahmood, Q.; Ping, Z.; Lin, Q.; Lu, H.F.; Tingting, C.; Abbas, G. Assessment of Toxicity of Volatile Fatty Acids to Photobacterium phosphoreum. *Microbiol. Russian Fed.* **2014**, *83*, 510–515. [[CrossRef](#)]
36. Albuquerque, M.G.E.; Martino, V.; Pollet, E.; Avérous, L.; Reis, M.A.M. Mixed Culture Polyhydroxyalkanoate (PHA) Production from Volatile Fatty Acid (VFA)-Rich Streams: Effect of Substrate Composition and Feeding Regime on PHA Productivity, Composition and Properties. *J. Biotechnol.* **2011**, *151*, 66–76. [[CrossRef](#)]
37. Pradhan, S.; Dikshit, P.K.; Moholkar, V.S. Production, Ultrasonic Extraction, and Characterization of Poly(3-Hydroxybutyrate) (PHB) Using *Bacillus megaterium* and *Cupriavidus necator*. *Polym. Adv. Technol.* **2018**, *29*, 2392–2400. [[CrossRef](#)]
38. Täubel, M.; Kämpfer, P.; Buczolits, S.; Lubitz, W.; Busse, H.J. *Bacillus barbaricus* sp. nov., Isolated from an Experimental Wall Painting. *Int. J. Syst. Evol. Microbiol.* **2003**, *53*, 725–730. [[CrossRef](#)]
39. Karr, D.B.; Waters, J.K.; Emerich, D.W. Analysis of Poly-β-Hydroxybutyrate in *Rhizobium japonicum* Bacteroids by Ion-Exclusion High-Pressure Liquid Chromatography and UV Detection. *Appl. Environ. Microbiol.* **1983**, *46*, 1339–1344. [[CrossRef](#)]
40. Mannina, G.; Presti, D.; Montiel-Jarillo, G.; Carrera, J.; Suárez-Ojeda, M.E. Recovery of Polyhydroxyalkanoates (PHAs) from Wastewater: A Review. *Bioresour. Technol.* **2020**, *297*, 122478. [[CrossRef](#)]
41. Kourmentza, C.; Plácido, J.; Venetsaneas, N.; Burniol-Figols, A.; Varrone, C.; Gavala, H.N.; Reis, M.A.M. Recent Advances and Challenges towards Sustainable Polyhydroxyalkanoate (PHA) Production. *Bioengineering* **2017**, *4*, 55. [[CrossRef](#)] [[PubMed](#)]
42. Zinn, M.; Witholt, B.; Egl, T. Dual Nutrient Limited Growth: Models, Experimental Observations, and Applications. *J. Biotechnol.* **2004**, *113*, 263–279. [[CrossRef](#)]
43. Chen, Z.; Huang, L.; Wen, Q.; Guo, Z. Efficient Polyhydroxyalkanoate (PHA) Accumulation by a New Continuous Feeding Mode in Three-Stage Mixed Microbial Culture (MMC) PHA Production Process. *J. Biotechnol.* **2015**, *209*, 68–75. [[CrossRef](#)] [[PubMed](#)]
44. Atlić, A.; Koller, M.; Scherzer, D.; Kutschera, C.; Grillo-Fernandes, E.; Horvat, P.; Chiellini, E.; Brauneegg, G. Continuous Production of Poly([R]-3-Hydroxybutyrate) by *Cupriavidus necator* in a Multistage Bioreactor Cascade. *Appl. Microbiol. Biotechnol.* **2011**, *91*, 295–304. [[CrossRef](#)] [[PubMed](#)]
45. Du, G.; Chen, J.; Yu, J.; Lun, S. Continuous Production of Poly-3-Hydroxybutyrate by *Ralstonia eutropha* in a Two-Stage Culture System. *J. Biotechnol.* **2001**, *88*, 59–65. [[CrossRef](#)]
46. Yue, H.; Ling, C.; Yang, T.; Chen, X.; Chen, Y.; Deng, H.; Wu, Q.; Chen, J.; Chen, G.Q. A Seawater-Based Open and Continuous Process for Polyhydroxyalkanoates Production by Recombinant *Halomonas campaniensis* LS21 Grown in Mixed Substrates. *Biotechnol. Biofuels* **2014**, *7*, 108. [[CrossRef](#)]
47. Schmid, M.T.; Sykacek, E.; O'Connor, K.; Omann, M.; Mundigler, N.; Neureiter, M. Pilot Scale Production and Evaluation of Mechanical and Thermal Properties of P(3HB) from *Bacillus megaterium* Cultivated on Desugared Sugar Beet Molasses. *J. Appl. Polym. Sci.* **2022**, *139*, 51503. [[CrossRef](#)]
48. Rodríguez-Contreras, A.; Koller, M.; Miranda-de Sousa Dias, M.; Calafell-Monfort, M.; Brauneegg, G.; Marqués-Calvo, M.S. High Production of Poly(3-Hydroxybutyrate) from a Wild *Bacillus megaterium* Bolivian Strain. *J. Appl. Microbiol.* **2013**, *114*, 1378–1387. [[CrossRef](#)]
49. Meixner, K.; Kovalcik, A.; Sykacek, E.; Gruber-Brunhumer, M.; Zeilinger, W.; Markl, K.; Haas, C.; Fritz, I.; Mundigler, N.; Stelzer, F.; et al. Cyanobacteria Biorefinery—Production of Poly(3-Hydroxybutyrate) with *Synechocystis salina* and Utilisation of Residual Biomass. *J. Biotechnol.* **2018**, *265*, 46–53. [[CrossRef](#)]

Review

Review of the Developments of Bacterial Medium-Chain-Length Polyhydroxyalkanoates (mcl-PHAs)

V. Uttej Nandan Reddy ¹, S. V. Ramanaiah ², M. Venkateswar Reddy ³ and Young-Cheol Chang ^{4,*}

¹ Department of Biotechnology, Koneru Lakshmaiah Education Foundation, Guntur 522502, Andhra Pradesh, India; vemireddyuttej@gmail.com

² Food and Biotechnology Research Lab, South Ural State University (NRU), 76, Lenin Prospekt, Chelyabinsk 454080, Russia; ramanasudarsan@gmail.com

³ Center for Biotechnology and Interdisciplinary Studies, Rensselaer Polytechnic Institute, 110 8th Street, Troy, NY 12180, USA; motakv@rpi.edu

⁴ Course of Chemical and Biological Engineering, Muroran Institute of Technology, Hokkaido 050-8585, Japan

* Correspondence: ychang@mmm.muroran-it.ac.jp

Abstract: Synthetic plastics derived from fossil fuels—such as polyethylene, polypropylene, polyvinyl chloride, and polystyrene—are non-degradable. A large amount of plastic waste enters landfills and pollutes the environment. Hence, there is an urgent need to produce biodegradable plastics such as polyhydroxyalkanoates (PHAs). PHAs have garnered increasing interest as replaceable materials to conventional plastics due to their broad applicability in various purposes such as food packaging, agriculture, tissue-engineering scaffolds, and drug delivery. Based on the chain length of 3-hydroxyalkanoate repeat units, there are three types PHAs, i.e., short-chain-length (scl-PHAs, 4 to 5 carbon atoms), medium-chain-length (mcl-PHAs, 6 to 14 carbon atoms), and long-chain-length (lcl-PHAs, more than 14 carbon atoms). Previous reviews discussed the recent developments in scl-PHAs, but there are limited reviews specifically focused on the developments of mcl-PHAs. Hence, this review focused on the mcl-PHA production, using various carbon (organic/inorganic) sources and at different operation modes (continuous, batch, fed-batch, and high-cell density). This review also focused on recent developments on extraction methods of mcl-PHAs (solvent, non-solvent, enzymatic, ultrasound); physical/thermal properties (Mw, Mn, PDI, Tm, Tg, and crystallinity); applications in various fields; and their production at pilot and industrial scales in Asia, Europe, North America, and South America.

Keywords: polyhydroxyalkanoates; mcl-PHAs; scl-PHAs

Citation: Reddy, V.U.N.; Ramanaiah, S.V.; Reddy, M.V.; Chang, Y.-C. Review of the Developments of Bacterial Medium-Chain-Length Polyhydroxyalkanoates (mcl-PHAs). *Bioengineering* **2022**, *9*, 225. <https://doi.org/10.3390/bioengineering9050225>

Academic Editor: Martin Koller

Received: 10 April 2022

Accepted: 17 May 2022

Published: 21 May 2022

Publisher's Note: MDPI stays neutral with regard to jurisdictional claims in published maps and institutional affiliations.



Copyright: © 2022 by the authors. Licensee MDPI, Basel, Switzerland. This article is an open access article distributed under the terms and conditions of the Creative Commons Attribution (CC BY) license (<https://creativecommons.org/licenses/by/4.0/>).

1. Introduction

Polyhydroxyalkanoates (PHAs) are a type of biopolymer developed as intracellular carbon/energy storage materials which have a wide range of material characteristics. PHAs are identified as granular inclusion bodies after extraction from cells, these are becoming popular as prospective replacements for traditional plastics in various applications, including food packaging industries, cultivational fields, scaffold preparation, and biomaterial implants [1,2]. PHAs are classified based on the length of the 3-hydroxyalkanoate (3HA) repeat units, the repeat units of PHAs with short chain length (scl-PHAs) are generally 4–5 carbon atoms long (e.g., 3-hydroxybutyrate, 3HB and 3-hydroxyvalerate, 3HV units), medium chain length (mcl-PHAs) are 6–14 carbon atoms long (e.g., 3-hydroxyhexanoate, 3HHx, 3-hydroxyheptanoate, 3HHo), and long chain length (lcl-PHA) are more than 14 carbon atoms (e.g., 3-hydroxyhexadecanoate) [3,4]. Rakkan et al. (2022) reported the production of mcl-co-lcl PHAs (72 to 75% of DCW) from *Enterobacter* sp. strains TS3 and TS1L using glucose [5]. Mcl-PHAs are soft, elastomeric, and have less crystallinity, a lower melting point, and lower glass transition temperature [6]. Nutrient limiting conditions are required for PHA generation in *Pseudomonas oleovorans*, *Pseudomonas putida*, and *Ralstonia*

eutropha, but not in recombinant *Escherichia coli* and *Alcaligenes latus* [7]. High manufacturing costs are a key impediment to the commercialization of PHAs. Carbon conversion yield (g/g), titer or volumetric yield (g/L), and productivity (g/L/h) are crucial in this scenario [8]. Aside from production criteria, low-cost downstream processing techniques and PHA manufacturing that fulfils cost performance standards have remained difficult to achieve. This has prompted researchers to focus on improving PHA fermentation and downstream processing efficiency to lower total costs [9,10]. The PHA production and degradation cycle is explained in Figure 1.

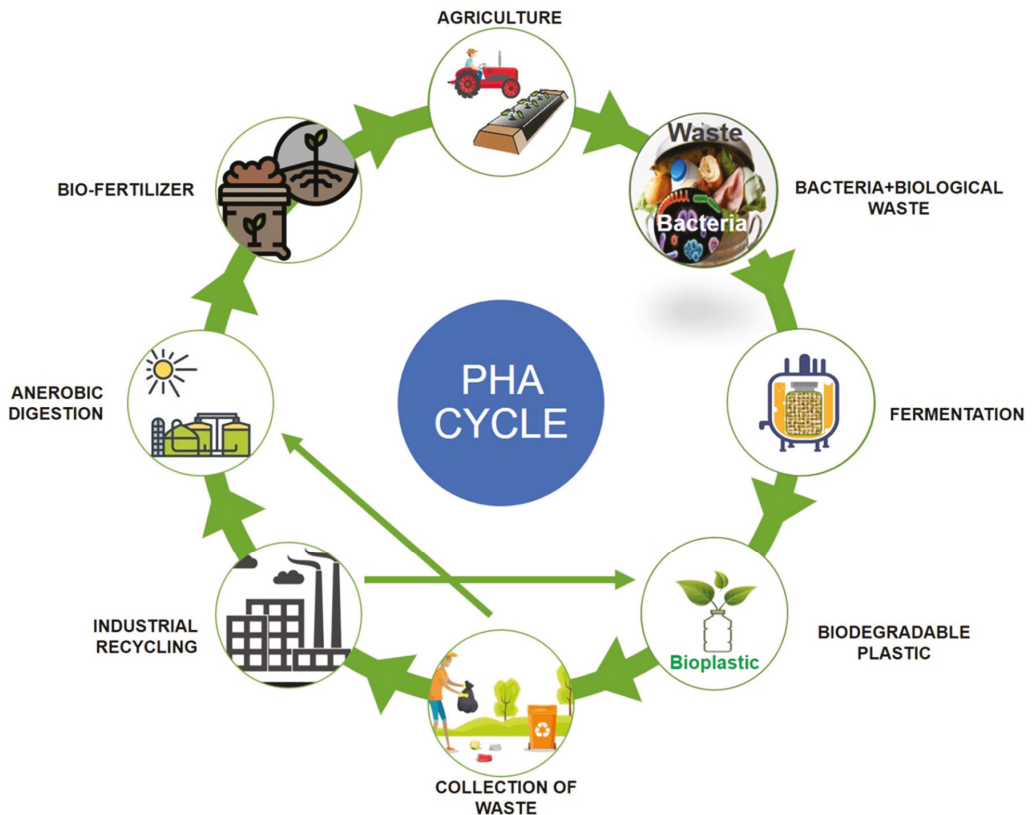


Figure 1. Polyhydroxyalkanoates (PHA) production and degradation cycle.

A significant aim for PHA synthesis is to obtain high yields in high cell-density cultures (HCDCs). Bioethanol and yeast that produces single-cell proteins were used to construct HCDC in the beginning. Because of its benefits, such as reduced culture volume and residual liquid, cheaper production costs, and lower capital investment, HCDC technique is favored over low cell density technologies [11,12]. Dry cell weight (DCW) above 100 g/L is termed HCDC for PHA synthesis, a DCW above 50 g/L is regarded high for recombinant protein production [11,13,14]. More details on PHA production through HCDC were provided in Section 3.2. The species of *Bacillus* and *C. necator* are generally known to produce scl-PHAs, whilst *Pseudomonas* species known to produce mcl-PHAs. PHAs including Scl and Mcl can be developed by the species of *Alcaligenes* and *Rhodococcus*. PHAs have been used to construct a variety of drug carriers, cardiac patches, vascular grafts, nerve conduits, heart valves, artificial blood vessels, subcutaneous implants, orthopaedical pins, stents, wound dressings, and slings [15]. In addition, the FDA authorized P4HB

for medical usage as absorbable sutures in the year 2007 [16]. Poly-3-hydroxyhexanoate (P3HO) has been used for soft (cardiovascular and neurologic) and hard (bone) tissue engineering [17,18]. By lowering mitochondrial damage, methyl esters of 3HB were used as drugs to treat Alzheimer's disease [19]. Memory enhancers have also been shown to be sodium salts of 3HB monomers [20].

Unlike other polymers used before, which degrade through bulk degradation, PHAs degrade through controlled surface erosion [15]. Controlled degradation must be used to preserve implant integrity in vivo. PHAs have been thoroughly tested both inside and outside of the labs to confirm that they are biodegradable. PHAs also degrade far slower than polylactic acid (PLA), making them suited for long-term applications. This review article focused on mcl-PHA production using organic/inorganic carbon sources and various types of the fermentation strategies. We also discussed recent developments on cost-effective downstream processing methods, thermal/mechanical properties of mcl-PHAs, applications of mcl-PHAs, and their worldwide production at pilot and industrial scale.

2. Mcl-PHA production

2.1. Inorganic Carbon Sources

It is crucial to employ natural substrates for microbial PHA synthesis to reduce manufacturing costs. The ideal feedstock is one that does not compete with human food. Syngas is a carbon monoxide and hydrogen mixture that may be produced by pyrolyzing organic waste. PHAs may be synthesized by a variety of microorganisms using syngas. Heinrich et al. (2016) genetically engineered the *Rhodospirillum rubrum* S1 to create a heteropolymer of 3-hydroxydecanoic acid and 3-hydroxyoctanoic acid [P(3HD-co-3HO)] from artificial syngas including CO and CO₂ [21]. Three genes—3-hydroxyacyl-ACP thioesterase (*phaG*), mcl-fatty acid CoA ligase (PP 0763), and a PHA synthase (*phaC1*)—from *P. putida* KT2440 were chosen for overexpression. To investigate the impact of syngas-mediated gene overexpression, the CO-inducible P_{cooF} promoter was employed. A recombinant mutant produced P(3HD-co-3HO) up to 7.1% (wt/wt) of the DCW. Furthermore, enhanced mcl-PHA synthesis and increased gene expression via the P_{cooF} promoter resulted in a greater molar fraction of 3HO in the generated copolymer than the Plac promoter, which regulated expression on the original vector. The polymer has a molecular mass of 124.3 kDa, melting point of 49.6 °C, and glass transition temperature of 41.1 °C. According to GC analysis, the polymer-isolate fractions were 55.6 mol % 3HD, 44.2 mol % 3HO, and less than 0.2 mol % 3HH. The partial disintegration of the accumulated polymer might be connected to the activity of a lipase identified in *R. rubrum*, as these enzymes have been shown to digest PHAs with varying chain lengths [22]. Figure 2 depicts the metabolic pathway carried in the production of mcl-PHAs from CO₂ in recombinant *R. rubrum*. After entering into the cytoplasmic membrane, CO₂ is fixed via ribulose 1,5-bisphosphate carboxylase through the Calvin cycle and generates glyceraldehyde-3-phosphate, which is subsequently converted to the pyruvate. Pyruvate is further converted into acetyl-CoA by the action of the enzyme pyruvate synthase. Acetyl-CoA is then entered into the fatty acid de novo synthesis cycle and generates 3-hydroxyacyl-ACP. The thiolysis of 3-hydroxyacyl-ACP is catalyzed by the 3-hydroxyacyl-ACP thioesterase and produces 3-hydroxy fatty acid. Activation of 3-hydroxy fatty acids occurred by the addition of CoA, which is catalyzed by the enzyme mcl-fatty acid CoA ligase. The enzyme PHA synthase polymerizes the 3-hydroxyacyl-CoA into mcl-PHA [21].

PHAs were produced using *C. glutamicum* B-10646 with scl-mcl monomer units [23,24]. The cells were grown on a mineral medium with a main growth substrate (gas) comprising a 1:2:7 ratio of CO₂: O₂: H₂ (by volume). The gas mixture was continuously pushed through the culture at a rate of 10–12 L/min in a 10 L bioreactor, the oxygen volume coefficient of mass transfer was 460 h⁻¹ (kLa). By varying the butyrolactone concentration (3–5 g/L), copolymers with varying molar fractions of 3HB/4HB (10.0 to 51.3%), 3HV (0.3–0.5%), and 3HHx (0–0.4%) were obtained. Tanaka et al. (2021) used recombinant *C. necator* strains and a mineral salts medium [25]. A sterile filter was employed to introduce a substrate gas

mixture with a ratio of $H_2/O_2/CO_2 = 8:1:1$. The quantity of PHAs were determined by gas chromatography analysis. In all the cultures investigated, the PHAs generated are a copolyester of 3HB and 3HHx (47.7%). Löwe et al. (2017) used synthetic bacterial co-culture to generate mcl-PHAs (C6, C8, C10, and C12) from CO_2 [26]. *P. putida* cscAB fixes CO_2 and changes it to sucrose, and then transfers into the culture filtrate, this sugar serves as a carbon source for *Synechococcus elongatus* cscB, which converts it to PHAs that accumulate in the cytoplasm. Using a nitrogen-limited method, they were able to achieve a maximum PHA production rate of 23.8 mg/L/day and a maximum titer of 156 mg/L.

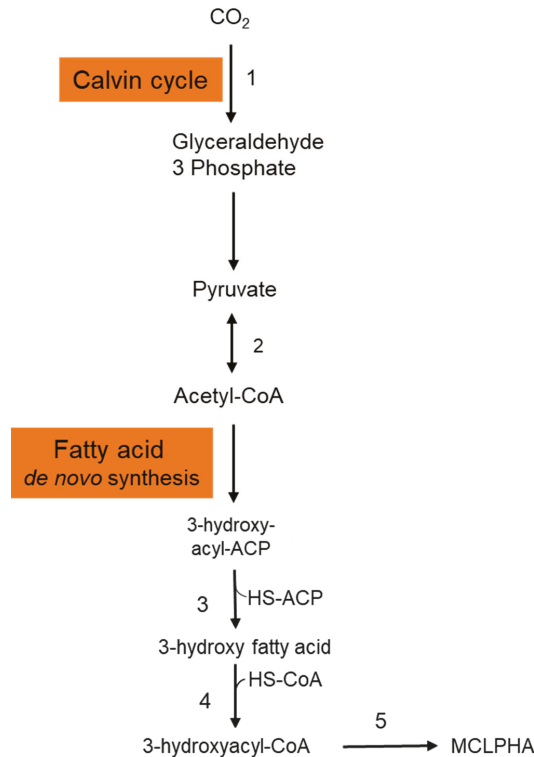


Figure 2. Metabolic pathway involved in the synthesis of mcl-PHA from CO_2 in *Rhodospirillum rubrum*. This figure was generated with the information from [21]. 1: Ribulose 1,5-bisphosphate carboxylase; 2: Pyruvate synthase; 3: 3-hydroxyacyl-ACP thioesterase; 4: MCL fatty acid CoA ligase; 5: PHA synthase.

2.2. Organic Carbon Sources

Mcl-PHA production from various organic carbon sources were summarized in Table 1.

Table 1. Mcl-PHA production using various carbon sources from literature reports.

Bacteria	Carbon Source	DCW (g/L)	PHA Conc. (g/L)	PHA (%)	PHA Composition	Productivity (g/L/h)	Time (h)	References
<i>P. putida</i> KT2442	Oleic acid	141	72	51	C6-C8-C10-C12-C14	1.91	38	[10]
<i>P. putida</i> KT2440	Glucose + nonanoic acid	98	32	33	C9-C7	3.1	32	[13]
Recombinant <i>R. eutropha</i>	Palm oil	139	102	74	Mcl-PHA	1.2	96	[27]

Table 1. Cont.

Bacteria	Carbon Source	DCW (g/L)	PHA Conc. (g/L)	PHA (%)	PHA Composition	Productivity (g/L/h)	Time (h)	References
<i>P. putida</i> KT2440	Waste cooking oil	159	58	36	C6-C8-C10-C12-C14	1.93	30	[28]
<i>P. putida</i> KT2440	Glucose + nonanoic acid + acrylic acid	71	53	75	C9-C7	1.8	30	[29]
<i>P. putida</i> LS46	Octanoic acid	29	17	61	C6-C8-C10-C12	0.66	27	[30]
<i>P. putida</i> KT2440	Glucose + nonanoic acid	71	40	56	C5-C7-C9	1.44	28	[31]
<i>P. putida</i> IPT 046	Glucose + fructose	50	31	63	Mcl-PHA	0.8	42	[32]
<i>P. oleovorans</i>	n-octane	112	5.6	5	Mcl-PHA	0.091	61	[33]
<i>P. putida</i> KT2442	Octanoic acid	51	18	35	C8	0.41	43	[34]
<i>P. putida</i> KT2442	Oleic acid	90	18	20	C6-C8-C10-C12-C14	0.57	32	[34]
<i>P. oleovorans</i>	n-octane	12	3.4	28	Mcl-PHA	0.58	120	[35]
<i>P. oleovorans</i>	n-octane	37	12	33	Mcl-PHA	0.25	48	[36]

P. = *Pseudomonas*; DCW = Dry cell weight; PHA conc. = polyhydroxyalkanoates concentration; *R.* = *Ralstonia*.

2.2.1. Fatty Acids

R. eutropha grown on animal fat waste produced 45 g/L biomass which contains 60% PHA [37]. In the *R. eutropha* recombinant strain, the *R. aetherivorans* has expressed I24 PHA synthase gene, and PHA with HHx units is produced by *P. aeruginosa* hydratase gene (*phaI*) [27]. The total biomass produced was 139 g/L with 74% of co-polymer, P (3HB-co-19 mol % 3HHx). Sato et al. observed that, in utilizing butyrate and palm kernel oil as carbon and energy sources, recombinant *C. necator* H16 produced good amount of P (3HB-co-19 mol % 3HHx). Furthermore, the scientists demonstrated that the 3-HHx% in KNK005 *phaA*-deactivated mutant strains is boosted by the butyrate. This culture environment produces higher biomass (171 g/L) and HHx copolymer in the cells (81%) with PHA titers of 139 g/L [38]. Cai et al. (2009) produced a *P. putida* KTMQ01 recombinant. The recombinant's DCW was 86% mcl-PHA [39]. Genetically altered *P. putida* KT2440 employs inexpensive substrates, such as xylose and octanoic acid, to produce mcl-PHA at a low cost. The cells accumulated mcl-PHA to a level of 20% [40].

A PHA-negative mutant of *R. eutropha* was created using the *phaC* gene from *Aeromonas caviae*, produced 3HB copolymer comprising 5 mol % 3HHx using soybean oil (20 g/L) in fed-batch mode [41]. DCW and % PHA were 133 g/L, 72.5% respectively. *A. hydrophila* 4AK4 produced P(3HB-co-3HHx), which contains 15% HHx from dodecanoate [42]. The co-expression of *phaC* with *phaP* and *phaJ* resulted in a 3HHx level of 34 mol % in the copolymer. When dodecanoate was used as the only carbon source, 54 g/L DCW and 52.7% PHA were observed [43]. The wild-type strain produced 40.4 g/L of DCW, and 54.6% of P(3HB-co-3HHx) [44]. This modified strain used plant oils successfully, produced 88.3 g/L dry biomass with a polymer content of 57% (3HB-co-3HHx) [45]. Tufail et al. investigated the use of leftover braising liquid as a substrate for PHA production using *P. aeruginosa* (KF270353) for 72 h. PHAs (53.2%) and DCW (23.7 g/L) were detected in the highest amounts in waste braising liquid [46]. Ruiz et al. (2019) produced 159.4 g/L of DCW, and 57 g/L of mcl-PHA using fatty acids generated from waste cooking oil as the carbon source, and *P. putida* KT2440 as biocatalyst [28].

2.2.2. Carbohydrates

P(3HB-co-3HHx) with 14 mol % HHx units was produced with gluconate using recombinant *A. hydrophila* 4AK4 strain [47]. Poblete-Castro et al. (2014) produced PHA using *gad* (gluconate dehydrogenase) deleted mutant, *P. putida* KT2440 [48] under fed-batch mode. The DO-stat feeding method generated the 67% of mcl-PHA with 62 g/L DCW [46].

Fed-batch cultivation of *P. putida* KT2440 on mixed substrates of acrylic acid, nonanoic acid, and glucose (0.05: 1.25: 1) generated 71 g/L of DCW with 75% of PHA which contains the 89 mol % 3HN [29]. However, the concentration of 3HN was decreased to 65 mol % in the absence of acrylic acid. The amount of mcl-PHA produced increased 10-fold when dodecanoic acid was utilized as the feedstock by Zhao et al. (2020) [49]. Liu et al. (2019) reported that *Pseudomonas-Saccharomyces* produced up to 152.3 mg/L mcl-PHA using xylose as a carbon root [50]. The inclusion of *S. cerevisiae* in the consortium produced cell mass sedimentation. Sugarcane biorefinery derived sucrose hydrolysate and decanoic acid used in fed-batch cell cultivations produced 33% PHA in 53.4 g/L of DCW using *P. putida* KT2440 [51]. A β -oxidation metabolism in the *R. eutropha* mutant was studied for P(3HB-co-3-HHx) development from soybean oil [52]. The removal of *fadB1* (enoyl-CoA hydratase/3HACoA dehydrogenase) in *R. eutropha* recombinant strains with additional genes generating (R)-enoyl-CoA hydratases resulted in a 6–21% 3-HHx content in the copolymer [52]. Figure 3 depicts how the metabolic pathway operates in the production of mcl-PHAs from sugars.

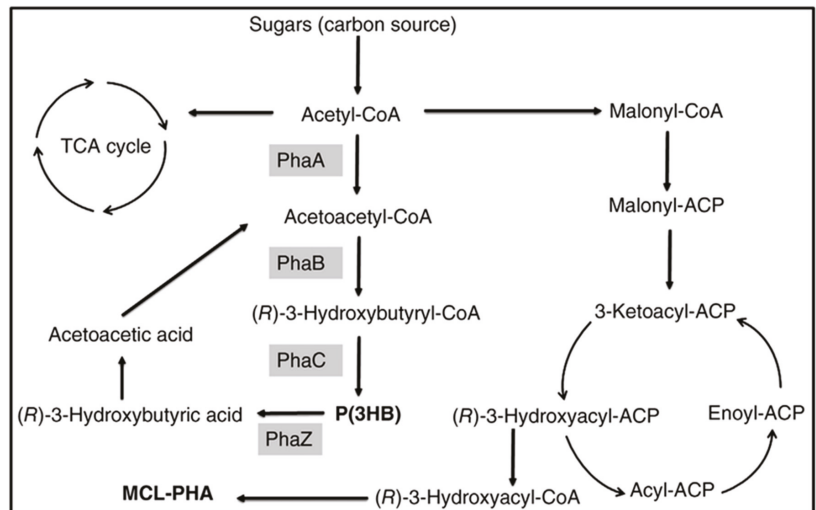


Figure 3. Metabolic pathway involved in the synthesis of PHAs from sugars. PhaA: β -ketothiolase; PhaB: β -ketoacyl-CoA reductase; PhaC: PHA synthase; PhaZ: PHA depolymerase.

2.2.3. Organic Residues/Wastes and Others

PHA production was carried out using organic acids/or sugar-based compounds derived from renewable waste materials [53]. Davis et al. (2013) produced mcl-PHA (25–34%) from perennial ryegrass biomass using *P. fluorescens* 555 and *P. putida* W619 [54]. Awasthi et al. (2021) reported about the mcl-PHA production using watermelon waste residues [55]. Muhr et al. (2013 a,b) produced mcl-PHA (22–30% DCW) from *P. chlororaphis* DSM 50083 and animal-derived waste [6,56]. Grape pulp was used to produce mcl-PHA from *P. resinovorans* in a 3.7 L bioreactor [57]. Chicken feathers were used to produce mcl-PHA with *P. putida* KT2440, the polymer consisted of 3-HHx (27.2 mol %) and 3-HHo (72.8 mol %) monomer units [58]. Apple pomace, the residue which is left out after processing of apple serves as a potential carbon source to produce PHAs [59]. Blanco et al. (2021) reviewed the PHA production using various substrates [60]. Apart from the above-mentioned carbon sources, there is a scope to produce mcl-PHAs from waste materials such as food waste, molasses, lingo-cellulosic biomass, cannery waste, biodiesel industry waste, paper-mill wastewater, coffee waste, and cheese whey [61]. As an example,

production from cheese whey shown in Figure 4. PHAs were produced using synthetic substrates, waste materials, and toxic compounds [62–72].

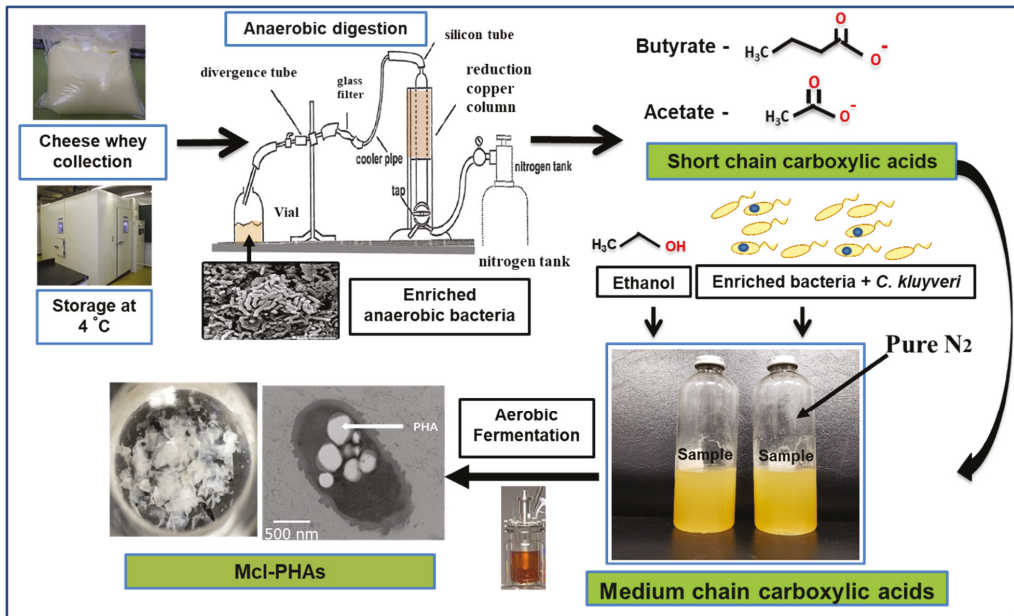


Figure 4. Hypothetical flow chart describing steps involved in mcl-PHA production from cheese whey.

2.2.4. Vegetable Oils

Coconut oil containing both medium (C6–C14) and long (>C14) chain length fatty acids, lauric acid (C12:0) and myristic acid (C14:0) (up to 55%) are the main fatty acids [73]. *Pseudomonas* sp. is recognized to produce PHAs through fatty acids. Fatty acids are shortened by basically 2, 4, or 6 carbon atoms after each cycle of β -oxidation. In nature, *Pseudomonas* sp. is known for its adaptability, and it can make mcl-PHAs from a range of carbon feedstocks. PHAs (58% DCW) were produced in 20 L bioreactor in a batch mode by *P. mendocina* CH50 (NCIMB 10541) using coconut oil at a concentration of 20 g/L [74]. The optical density increased to 31 after 48 h, and the pH decreased slightly during fermentation, nitrogen content declined from 0.12 g/L to 0.015 g/L shows that the fermentation took place in a nitrogen-limiting environment. The mcl-PHAs terpolymer was composed of 3HO-3HD-3HDD. P(3HO-3HD-3HDD) has a molecular weight of 333 kDa and a PDI (polydispersity index) of 2.37, whereas mcl-PHAs with both unsaturated and saturated groups have an average molecular weight of 60–410 kDa [75]. *Pseudomonas* sp. GI01 was used to produce mcl-PHA using palm oil and waste rapeseed oil. The purified polymers consisted of monomers ranging from C6 to C16 [76,77]. Song et al. (2008) used *Pseudomonas* sp. strain DR2 and the waste vegetable oil to produce mcl-PHA in the range of 24–38% [78]. Previous studies find out the importance of C/N balance for PHA production [79–81]. Carbon and nitrogen concentrations play a major role in PHA production. Mohan and Reddy (2013) applied design of experimental methodology using Taguchi orthogonal array to evaluate the influence and specific function of eight important factors and mentioned that glucose at 6 g/L and NH_4Cl at 100 mg/L concentrations are best for higher PHA accumulation [80]. Reddy et al. (2015) reported that *phaC* gene expression was 5.37 folds higher at 100 mg/l nitrogen concentration than other concentrations [63]. The precursor molecules required for mcl-PHA synthesis in bacteria are generated through three different

metabolic routes, which depend on the type of carbon source that existed in the medium. If carbohydrates are the main carbon source, the de novo fatty acid pathway is dominant, and fatty acids are the main carbon source, the β -oxidation pathway is dominant. The third pathway is chain elongation, and this pathway utilizes the precursors produced from both carbohydrates (acetyl-CoA) and fatty acids (acyl-CoA). All the three metabolic pathways generate different intermediate precursors—such as (R)-3-hydroxyacyl-acyl carrier protein, 2-trans-enoyl-CoA, (S)-3-hydroxyacyl-coA, and 3-ketoacyl-CoA—which are involved in the mcl-PHA synthesis. The hypothesis is that the (S)-3-hydroxyacyl-CoA, and 3-ketoacyl-CoA are subsequently converted to (R)-3-hydroxyacyl-CoA by the action of enzymes, 3-hydroxyacyl-coA epimerase, and 3-ketoacyl-ACP reductase respectively. The enzyme, (R)-specific enoyl-CoA hydratase (*PhaJ*)—which catalyzes the 2-trans-enoyl-CoA to (R)-3-hydroxyacyl-coA—plays a critical role in supplying monomer units from β -oxidation to PHA synthesis. (R)-3-hydroxyacyl-ACP-CoA transferase (*PhaG*), which has been identified in *P. putida* and *P. aeruginosa* plays, an important role in the metabolic connection of de novo fatty acid biosynthesis with mcl-PHA synthesis. *PhaG* catalyzes the conversion of (R)-3-hydroxyacyl-ACP to (R)-3-hydroxyacyl-CoA and contribute to mcl-PHA synthesis from gluconate or other carbohydrate sources. In the final step of mcl-PHA synthesis, the enzyme PHA synthase (*PhaC*) catalyzes the conversion of (R)-3-hydroxyacyl-CoA molecules into mcl-PHA [6,28,40,48,52,54,56].

3. Mcl-PHA Production at Various Modes of Operations

Mcl-PHA yields are optimized in batch, fed-batch, and continuous operation methods (Table 2). Sugar has been the most common carbon source used by most industries to manufacture PHAs during the last 20 years. Sugar can be produced from several biomass sources such as sugarcane, beet, molasses, and bagasse. They are plentiful and simple to obtain, and bacteria can swiftly digest and convert them to PHAs. Large PHA enterprises have selected this strategy due to the ample availability of raw materials and the ease of operation.

Table 2. Mcl-PHA production at various modes of operations from literature reports.

Bacteria	Substrate	Mode of Operation	PHA Production	Reference
<i>P. putida</i> KT2440	Glucose and nonanoic acid	Fed-batch mode	32%	[13]
<i>P. mendocina</i>	Octanoate	Batch mode	31%	[82]
<i>P. oleovorans</i>	n-octane	Continuous mode	63%	[83]
<i>P. putida</i>	Oleic acid	Fed-batch mode	51%	[84]
<i>P. putida</i> LS46	Octanoic acid	Fed-batch mode	61%	[30]
<i>P. putida</i> KT2440	Decanoic and acetic acids	Fed-batch mode	74%	[85]
<i>P. putida</i> KT2440	Glucose and nonanoic acid	Fed-batch mode	56%	[31]
<i>P. putida</i> CA-3	Decanoic and butyric acid	Fed-batch mode	65%	[86]
<i>P. putida</i> KT2440	Nonanoic acid	Fed-batch mode	75%	[87]
<i>P. oleovorans</i>	Octanoic acid	Fed-batch mode	62%	[88]
<i>P. putida</i> BM01	Glucose and octanoate	Fed-batch mode	66%	[89]

3.1. Batch Mode

In batch mode, carbon/nitrogen sources will be added into the reactor at initial hours of incubation, and no extra nutrients will be introduced afterwards [90]. Batch

fermentation procedures, in general, lead to a lower PHA yields. This is due to the breakdown of PHAs that produced in the cultivation process [91]. Under batch conditions, Rai et al. (2011) achieved a DCW of 0.8 g/L which contains 31% homopolymer, P3HO using *P. mendocina* [82].

3.2. Continuous Mode

This mode maintains a constant growth rate of microbes under ideal conditions. Consequently, by continuing to cultivate at high specific growth rates, production may be enhanced. Continuous culture is also beneficial since it reduces the need for bioreactor shutdowns and cleaning. Furthermore, the continuous culture prevents washout even at high dilution rates; therefore, product concentration and production may rise. The continuous culture is maintained by new media to the reactor, which feeds the cells with new nutrients. Products and effluent are continuously removed to maintain a consistent bioreactor workload. Jung et al. used *P. oleovorans* to derive mcl-PHAs from n-octane in a two-step continuous process. With two-stage fermentation, one can focus on accumulating PHAs in one reactor while accumulating biomass in another. Under these conditions, 18 g/L DCW, 63% of PHAs were achieved [83]. Egli et al. (1991) employed chemostat cultivation atmosphere to produce PHAs from *P. putida* GPo1 [92]. According to this study, PHAs may form if nitrogen limitation is applied [93].

3.3. Fed-Batch Mode

In the fed-batch method, cells proliferate until the desired cell density is attained with a steady supply of carbon sources and necessary nutrients. The feeding of nutrients and carbon sources maintains a consistent rate of growth, limiting the formation of by-products. There are two different types of feed-batch operations, one is the development of growth-related products, and the other one is product formation that occurs only under the non-growth associated conditions. PHA development usually occurs in two stages. First, the log stage is performed so that the cells gained the sufficient biomass. The second stage of polymer synthesis entails feeding all the essential materials into the bioreactor [94]. The second stage usually occurs when an essential nutrient, such as nitrogen, phosphorous, and oxygen limited conditions.

Most of the mcl-PHA production studies were conducted in a batch-fed mode. The pH and DO stats are utilized during the fermentation process to keep the pH and DO at specific levels. Lee et al. (2000) got 51% of PHAs, 141 g/L of DCW, using *P. putida* and oleic acid [84]. Davis et al. (2015) employed *P. putida* KT2440 in a two-stage fed-batch mode with glucose and nonanoic acid [13]. Cells were fed glucose during the biomass developing phase, while nonanoic acid was provided during the PHAs developmental phase and obtained 32% of PHAs, 102 g/L of DCW [13]. An oxygen-limited fed-batch growth approach with *P. putida* LS46 and octanoic acid as a substrate in a 7 L bioreactor achieved 29 g/L of DCW, 61% of PHA [30]. Octanoic acid toxicity in *P. putida* LS46 cells might explain the low biomass accumulation. Gao et al. (2016) created mcl-PHA using a mixture of decanoic and acetic acids in a fed-batch culture of *P. putida* KT2440 [85]. Acetic acid used to inhibit the crystallization of decanoic acid. Different glucose/acetic acid/decanoic acid ratios were used to find co-feed ratios that resulted in higher mcl-PHA yields. At the ideal ratio (4:1:5), 75 g/L of total DCW and 74% of PHA content were attained. Sun et al. (2009) demonstrated that *P. putida* KT2440 developed mcl-PHA by co-feeding glucose and nonanoic acid [31]. After exponential, as well as subsequent constant feed, with 1:1 (*w/w*) nonanoic acid: glucose, 71 g/L of total DCW and 56% of PHA were observed. Cerrone et al. (2014) demonstrated that the *P. putida* CA-3 HCDC was formed in a two-stage fermentation using decanoic and butyric acid [86]. To boost the maximal yield of mcl-PHA, the isolates were cultivated first on butyric acid (biomass growth phase) and then on a combination of butyric and decanoic acid (20:80 *v/v* ratio) during the PHA synthesis stage. This approach resulted in 71.3 g/L of DCW with 65% of PHA [86].

Sun et al. (2007) used the *P. putida* KT2440 to manufacture mcl-PHA from nonanoic acid, obtained 70 g/L of DCW with 75% PHAs [87]. Diniz et al. (2004) employed *P. putida* IPT 046 to explore various feeding patterns such as exponential preceded by constant feed for production of mcl-PHA [32]. The exponential feeding method yields a maximum 40 g/L DCW and a 21% of PHAs. However, when phosphate was limited, 50 g/L of DCW with 63% PHAs was obtained [32]. *P. oleovorans* ATCC 29347 was cultivated under pH-stat fed-batch conditions with octanoic acid as the carbon source and reported 63 g/L of DCW with 62% PHAs [88]. Kim et al. (1997) investigated a two-stage fed-batch approach using *P. putida* BM01 [89]. Glucose and octanoate were supplied in growth and PHAs development stages. This approach yielded 55 g/L of DCW with 66% of PHA. Higher DCW (125.6 g/L) with 55% PHAs observed using *P. putida* KT2440 [95].

4. Industries Producing PHAs

Scl-PHA are produced by various industries; however, very few industries produce mcl-PHAs. In this section, we provide information regarding industries that produce PHAs in various regions.

4.1. Europe

In 2007, Biomer Biotechnology Co. (Starnberg, Germany) produced 10 tonnes of Biomer bio polyester. Biomer's objective has been to integrate with agricultural food industries, which they believe will offer the technology needed to create PHAs from its waste [96]. Bio-on founded LUX-ON with the purpose of generating PHAs using CO₂ as organic load. The system also gathers sustainable solar energy to power the bioproduction process. Sugar cane molasses, sugar cane, food wastes, waste cooking oil, glycerol, and carbohydrates are among the feedstocks utilized [97]. Paques, a Dutch company, employs natural bacteria and methods to generate biodegradable PHBV biopolymers from waste streams [98]. Bioextrax is a Sweden-based company producing PHAs using bacteria from sucrose [99]. BASF is a German-based company producing biopolymer, Ecovio® with special material properties such as flexibility and toughness. Guzik (2021) summarized the recent developments occurred in Jerzy Haber Institute of Catalysis and Surface Chemistry of the Polish Academy of Sciences in collaboration with other groups [100].

4.2. Asia

Tianan Biologic [101] is a biopolymer specialist in the production and use of PHBV and PHB. To make the copolymer, *C. necator* is fermented with D-glucose and propionic acid. The fermentation facilities are in the city of Ningbo, China. Since its founding in 2000, the company has generally been recognized as the largest maker of PHBV, with an annual capacity of 2000 metric tons. In 2004, they were the first company in the world to commercially synthesize PHBV using water-based extraction technology. The extraction method has been patent-protected. Tianjin GreenBio Material Co. is China's first company to produce 10,000 tonnes of PHAs per year. They have developed completely biodegradable granules for the manufacturing of blown film (SoGreen 2013). They also developed PHAs foam pellets, which can be converted into completely biodegradable foams for usage in food service and appliance packaging. The PHAs are created using a P(3HB-co-4HB) copolymer.

Mitsubishi (Tokyo, Japan) manufactures P(3HB) at both research and pilot scales under the brand name Biogreen® [102]. Kaneka Corporation (Tokyo, Japan) manufactures P(3HB-co-3HHx) under the brand names Kaneka PHBH® and AONILEX®, with an annual capacity of 100 tonnes. To make it, plant oils and fatty acids are used as the primary raw material in a microbial fermentation process [103]. Metabolix, located in Massachusetts, has completed the sale of its PHA biopolymer intellectual property to an associate company, CJ Cheil Jedang Co (Seoul, Korea) for 10 million USD. The acquisition includes patents on production and application, as well as microbes used in Metabolix's manufacturing procedures [104].

4.3. North and South America

PHAs are being commercialized for high-value biological applications by several PHA manufacturers. These firms include Terra Verdae Bioworks (Edmonton, AB, Canada), PolyFerm (Kingston, ON, Canada), and Tephra Inc. (Lexington, MA, USA). Among the products provided are heart valves, scaffolds, ecological sutures, and materials for regulated distribution. These product categories have lower volume but higher profit margins. Polyferm Canada [105] produces mcl-PHAs under the brand name. Versa Mer™ using naturally selected microorganisms and basic materials such as vegetable oils and sugars. The applications they are now working on include medical devices, sealants, adhesives, and polymer modifiers. Danimer Scientific manufactures produces PHAs under the trade name Nodax™ in the United States (Bainbridge, GA, USA). They entered the PHAs industry in 2007 after receiving knowledge from Procter & Gamble (Cincinnati, OH, USA). Danimer created a copolymer with a 3HB unit and a mcl-PHA repeat unit [106]. Nodax™ PHAs are manufactured from easily accessible feedstock and are completely renewable. Mango Materials, a company based in the United States, is producing PHAs from methane.

PHB Industrial S/A is a Brazil based company that manufactures and sells Biocycle® disposable polymers, PHB, and P (3HB-co-3HV) since September 2000 [107]. Until 2015, the firm functioned on a small scale and sold its commodities to Japan. Metabolix, Inc. released Yield10 in 2015, and it was listed on NASDAQ. PHB and its copolymers are manufactured by Yield10 Bioscience under the Miller™ brand [108]. Miller™ was marketed by Telles, a joint venture between Archer Daniels Midland Firm and Metabolix. TephraFLEX® produces P4HB. After detoxification, P4HB is converted into healthcare products such as films, sutures, and fabrics [109]. P4HB is digested to yield 4HB, a naturally occurring element of the vertebrate body. Tephra's TephELAST is more elastic than TephraFLEX and has been employed in the production of medical devices. These polymers are created using pilot and research platforms. Newlight Technologies developed a unique biocatalyst to produce PHAs from CO₂ and biogas using microorganisms obtained from the Pacific Ocean. Newlight created the AirCarbon polymer by combining methane from a California cattle farm with air [110,111].

5. News on PHAs

The PHAs market is predicted to reach 121 million USD by 2025, according to *Markets and Markets* [112]. The rising demand for PHAs in various industries—such as packaging, biomedical, and agricultural—is driving market expansion. Several factors will propel the PHAs sector, including public awareness of the depletion of hydrocarbons and the development of sustainable, eco-friendly bioplastics. Europe is the world's largest PHAs market in terms of volume and value, followed by North America and Asia. PHAs are more expensive than standard polymers, which is one of the key impediments to the market's growth. Biodegradable polymers, such as PHAs, have higher production costs than normal plastics, ranging from 20% to 80% more. This is mostly due to the high polymerization cost of biodegradable polymers, which is because most of the technologies are still in the research stage. These bio-based manufacturing methods and materials are still in the early stages of development and have not yet achieved the level of commercialization that their petroleum-based equivalents have.

The company Mars plans to reduce virgin plastic use by 25% by the year 2025 and make all plastic packaging reusable, recyclable, or biodegradable [113]. Mars is aiming for 100% biodegradable, recyclable, or biological plastic packaging by 2025, as well as a 25% reduction in virgin plastic consumption, a 30% average recycled content in plastic packaging, and recycling requirements for customers in all important markets. Maltesers replaced the plastic interior of the candy box with a water-based coating, reducing 82 metric tons of plastic waste. The first-ever Mars Wrigley Gum bottle with 30% recycled content is now available on the German market. This is an industry-leading move, reducing unused plastic use by approximately 350 tons annually. Orbit Megapack has released an on-pack recycling guide on How2Recycle, which provides a step-by-step guide on whether and how

to recycle each part of the gum pack. Balisto has partnered with German retailer EDEKA Minden-Hannover to offer the first chocolate bar with paper-based packaging, reducing packaging plastic use by approximately 440 kg. M&M's launched recyclable packaging in the M&M's Choco 300 g pouch in France. Mars Wrigley partnered with Danimer Scientific, a leading developer and manufacturer of biodegradable materials, to develop an innovative home compostable packaging for its products. Colgate designed recyclable toothpaste tubes so they can go into curbside recycling bins. This could eventually keep a billion tubes out of landfills each year [114].

6. Extraction of PHAs

In terms of product quality, price, and environmental effect, downstream processing is a significant stage in PHAs manufacture. Following fermentation, there are two fundamental ways for recovering PHAs: (i) dissolve the biomass in acid, alkaline solutions, detergents, protease and extracting the pellets; or (ii) direct solvent separation of PHAs from the bacteria [115]. Enzymatic degradation of non-PHA biomass is one solvent-free approach for releasing PHA granules from cells. Certain proteins have been found on the membrane of PHA granules, such proteins include synthases, PHA depolymerize enzymes, polymer membrane expressed protein (e.g., phasins), and other proteins that influence pellet organelle distribution [116]. The chemical composition of PHAs determines their soluble nature in various solvents, mcl-PHAs are mostly soluble in a lot of solvents which include acetone and ethyl acetate. Another critical aspect of PHA pellet separation appears to be that the processes used must allow the polymers' molecular size to change as little as possible.

6.1. Solvent Extraction

This was a popular technique because of its easy of usage with accessibility. Solvents induce the cellular surface to rupture, and increase diffusivity. Fluid interaction with PHA particles causes polymer solubilization. To recover the item, it should be precipitated with a non-solvent. Acetone and ethyl acetate are the solvents preferred for the separation of mcl-PHAs, whereas cold methanol or ethanol are acceptable non-solvents used for precipitation. The advantage of solvent separation is that it yields high-purity PHAs with nearly no change in particle size [117]. Many extraction methods use chloroform, although it is dangerous and increases the cost of the process. Endotoxin content is low in chloroform extracted PHAs, which is crucial for PHAs used in pharmaceutical applications. In several countries, chlorinated agents are no longer permitted in consumer goods. At room temperature, mcl-PHAs can be isolated using diethyl ether, tetrahydrofuran, or acetone [118]. Endotoxins (e.g., lipopolysaccharides) must be removed during PHA separation, especially if the product is to be used as a pharmaceutical. Thermally controlled separation procedures, as reported by Ferrer et al. (2007) for isolation of P(3HO-co-3HHx) from *Pseudomonas putida* GPo1, are one possible approach [119]. Organic solvents such as 2-propanol and n-hexane were used to achieve PHAs quality of more than 97% (*w/w*) and very less endotoxin limits (i.e., 10–15 endotoxin units per gram of PHO). PHO was also redissolved in 2-propanol at a temperature of 45 °C and precipitated at a temperature of 10 °C, providing a high purity product with low endotoxicity (2 per gram PHO). Green PHA isolation processes will necessitate less energy requirement, no harmful chemical usage, and excellent purity and yields [120]. Yabueng et al. (2018) examined green solvents such as 1,3-propanediol, 2-methyltetrahydrofuran, ethyl lactate, and 1,3-dioxolane for PHA separation from *Cupriavidus necator* [121].

6.2. Ultrasound-Assisted and Aqueous Two-Phase Extraction

Ishak et al. (2016) used ultra-high-frequency sound to irradiate mcl-PHAs with cells mixed with an excellent and minimal non-solute-solvent combination [122]. When that solvent is mixed in a sufficient proportion with a suitable solvent, the PHAs stay in suspension [123]. If the marginal solvent concentration is raised, the PHAs will be dissolved. These

researchers evaluated impacts of ultrasonic irradiation maximal dissipation on energy, solvent/marginal non-solvent ratio, and time on mcl-PHA removal efficiencies. Furthermore, employing ultrasound during PHA extraction decreases solvent quantities, allowing safer solvents to be used, and it also shortens process times [124].

Aqueous two-phase extraction (ATPE) has the advantage of having a larger water concentration (up to 90% *w/w*), which makes biopolymer separation more ecologically friendly. Furthermore, the phase-separation components of ATPE can be harmless and relatively favorable. ATPE is said to be a scalable, cost-effective PHAs separation technique [9,125,126]. Leong et al. reexamined the parameters for purifying PHA from *C. necator* [127]. Additional centrifugation stages were avoided under these circumstances, and the recovery yield and purity factor increased by 72.2% and 1.61-fold, respectively [127]. As previously stated, non-PHA organic matter was removed to isolate PHAs from *C. necator* H16. The procedure was optimized using EOPO 3900 (5%), pH 6, and a fermenting temperature of 30 °C, purity factor and recovery yield were 1.36 and 97.6%, respectively [128].

6.3. Chemical and Enzymatic Digestion Method

By dissolving non-PHA cell material (NPCM), enzymatic and chemical digestion techniques aim to preserve unbroken PHA granules. The idea behind these methods is to break down microbial cell walls and release PHAs from the microorganism [129,130]. Early research looked towards removing NPCM from cells using powerful oxidizing agents such as sodium hydroxide and sodium hypochlorite. Extreme circumstances favorable for oxidation of both NPCM and PHAs—and therefore keen command of oxidizing agent content, heat generated, and reaction rate—is critical to this technique (i.e., reduced molecular weight). Dong et al. investigated surfactant and sodium hypochlorite mixtures for recovering PHAs from *Azotobacter cerococcid* G-3 [131]. Proteolytic enzymes catalyze hydrolytic processes involving proteins. According to preliminary research, lysozyme, bromelain, and trypsin are the most promising enzymes for this procedure. Yasotha et al. recovered and purified mcl-PHAs using alcalase, SDS, EDTA, and lysozyme [132]. Studies demonstrated that alcalase was the most important element in NPCM degradation and mcl-PHA purification. The counter flow filtration process successfully eliminated NPCM and allowed for high-purity mcl-PHA recovery [132]. PHA was purified by an enzyme method, according to Kachrimanidou et al. (2016) they developed a blend of unrefined enzyme to catalysis of *C. necator* lysis and release the PHAs compound using solid-state cultivation of *Aspergillus oryzae*. The enzymatic reaction was carried out at 48 °C with no control of pH. The product yield and quality of PHA achieved is 98% and 96.7%, respectively [133]. For the extraction of PHAs, Israni et al. took use of *Streptomyces albus* strong lytic activity [134]. *S. albus* and PHAs producing cultures are injected together into a reactor. The lytic enzymes from *S. albus* are added for PHA extraction in the second stage.

7. Properties of PHAs

One of the most significant characteristics for processing and producing polymers' end-use is their thermal and physical qualities. The molecular structure of polymers is largely responsible for their physical and thermal characteristics. The physicochemical features of scl/mcl PHAs are distinct. Because PHAs are susceptible to increasing in temperature and breaking down during the melt process, their heat stability is essential. Plasticizers can help to prevent PHAs from degrading too much during the melting process [135]. Both P3HO and P3HO-P3HD have higher thermal degradation kinetic parameters than PHB and PHBV due to complexation on the development of six-membered transitional configuration. The thermal breakdown temperatures of P3HO with epoxy and hydroxy groups are varied. The P3HO with epoxy pendant groups might have a higher heat breakdown temperature after raising the temperature due to the bridging potential of epoxy groups.

7.1. Melting Point, Crystallization, Gas Barrier, and Solubility

Polymer performance is influenced by their crystallization kinetics. In PHAs, the length of the side chains can have a big impact on how they crystallize; for example, mcl-PHAs can form a layered crystal structure, increasing the side chain length of mcl-PHAs (e.g., C7 or more) and resulting in the formation of a new smectic liquid crystalline phase [136]. Both the main and side chains of mcl-PHAs with smectic crystals can cause cold crystallization during heating [32]; therefore, two melting points in mcl-PHAs have been found, which can be ascribed to the development of two distinct crystal phases (phase I and phase II) [137]. Crystallization rates have been shown to be improved by reactive chemical modification of PHAs. When compared to unmodified PHAs, modified PHAs with lengthy chain branching and low cross-linking densities demonstrated enhanced crystallization rates [138–140]. These chemical alterations also enhanced the rheological characteristics and processability of the material. Scl-PHAs require halogenated solvents to dissolve due to their high crystallinity [141]. The low crystallinity of mcl-PHAs permits them to be dissolved in non-halogenated solvents. The extraction, purification, and recycling of mcl-PHA copolymers are made easier and more cost-effective because of their solubility profile. Sobieski et al. (2017) reported the physical gel formation of P(3HB-co-3HHx) copolymer, and the gel's thermal reversibility was established by heating it to 85 °C [142]. The composition of 3HHx in P(3HB-co-3HHx) might affect physical and mechanical strength, and rheological qualities in addition to polymer concentration. P(3HB-co-3HHx) gels with a low concentration of 3HHx (3.9 mol %) exhibit a greater opacity and better structure preservation when tilted than gels with a higher 3HHx content (13 mol %). After removing the solvent, the PHBHx gels revealed a sub-micron scale interconnected porous topology, indicating a viable material for biological applications such as tissue engineering [142].

When varying monomers with three carbon units, the melting point and crystallinity were reduced [143]. The quantity of side-chain carbons affects their melting and glass transition temperatures [144]. By copolymerizing P3HB with mcl-PHAs, the glass transition temperature of P3HB may be greatly decreased. The glass transition temperature of the mcl-PHAs generated from the C1–C7 side chain was between 0 °C and 50 °C, with a melting point of 175–69 °C [136]. Mcl-PHAs with slow crystallization rate and low melting point have limited melt processability; reactive modifications—including crosslinking, mixing with other polymers, and grafting techniques—can be used to solve these problems in the PHAs [145].

The oxygen and water vapor barrier qualities of polymers are important as their physical and thermal properties when it comes to using them for effective packaging applications such as food packing. When compared to traditional polymers, such as polypropylene and polyethylene, PHAs have better gas barrier qualities [146]. In particular, PHA copolymers have significantly better oxygen, carbon dioxide, and odor barrier characteristics than polyethylene and polypropylene [106]. PHBV has the best resistance to oxygen and water vapor penetration among biodegradable polymers [147]. When compared to PLA and PBS, the PHBV offers good potential for usage in fruit, and vegetable packaging as it has an appropriate oxygen and water vapor transfer rate [147]. However, the PHBV's gas barrier qualities are insufficient for the packaging of meat, cheese, and coffee. Graphene oxide and clay supplementation to PHAs has been found to increase barrier characteristics by creating a convoluted route for gas molecules [148].

7.2. Mechanical Properties of PHAs

Because of their molecular weight and chemical makeup, the mechanical characteristics of PHAs can vary greatly. Tensile strength and Young's modulus are 43 MPa and 3.5 GPa, respectively, for a typical P3HB with a molecular weight of less than 1000 Kda [149]. Because of secondary crystallization at room temperature, the brittleness of the P3HB was demonstrated to rise even more with age [150]. Copolymerization with other monomers can compensate for P3HB's lack of toughness [149]. It was also shown that employing a modified *E. coli* strain to increase the molecular weight of the P3HB (2200 KDa) during

synthesis might improve the mechanical qualities even further [151,152]. Molecular weight of the mcl-PHAs, varies from 45 to 462 Kda. Mw, Mn, and PDI of mcl-PHAs produced using various carbon sources and bacteria were summarized in Table 3. Mcl-PHAs are soft, flexible, sticky depending on the monomer composition. Copolymerization using as little as 5 mol % mcl monomers can improve the attributes of scl-PHAs (P3HB), such as toughness and thermal properties [143,153]. When P3HB was copolymerized with 17 mol % 3HHx, the elongation at break rose from 6% to 850%, while the P3HB's tensile strength reduced from 43 to 20 MPa [153]. PHA copolymers with differing side group chain lengths or co-monomer compositions have variable modulus and elongation properties, as predicted.

Table 3. Gel permeation chromatography (GPC) results of mcl-PHAs from literature reports.

Bacteria	Carbon Source	Mw (kDa)	Mn (kDa)	PDI	References
<i>P. putida</i> KT2440	Waste cooking oil	45	22	2.04	[28]
<i>P. putida</i> KT2440	Nonanoic acid + undecanoic acid	115	-	1.8	[31]
<i>P. putida</i> KT2442	Oleic acid	135	49	2.76	[34]
<i>P. putida</i> KT2442	Octanoic acid	187	78	2.4	[34]
<i>P. putida</i> KT2442	Vegetable-free fatty acids	168	65	2.68	[34]
<i>P. putida</i> KT2442	Animal-free fatty acids	180	71	2.53	[34]
<i>P. putida</i> KT2440	Biodiesel-derived crude glycerol	462	193	2.4	[154]
<i>P. putida</i> LS46	Hexanoic acid	49	22	2.3	[155]
<i>P. putida</i> LS46	Heptanoic acid	82	35	2.3	[155]
<i>P. putida</i> LS46	Octanoic acid	115	54	2.2	[155]
<i>P. putida</i> LS46	Nonanoic acid	55	26	2.3	[155]
<i>P. putida</i> LS46	Decanoic acid	49	21	2.4	[155]
<i>P. putida</i> LS46	Lauric acid	131	63	2.1	[155]
<i>P. putida</i> LS46	Myristic acid	86	44	2.0	[155]
<i>P. putida</i> KT2442 mutant	Dodecanoic acid (15%)	100	80	1.25	[156]
<i>P. putida</i> KT2442 mutant	Dodecanoic acid (39%)	157	108	1.45	[156]
<i>P. putida</i> KT2442 mutant	Tetradecanoic acid (49%)	95	67	1.43	[156]
<i>P. corrugat</i>	Coconut oil	343	74	4.6	[157]
<i>P. resinovorans</i>	Coconut oil	165	101	1.63	[158]
<i>P. resinovorans</i>	Sunflower oil	112	65	1.72	[158]
<i>P. resinovorans</i>	Soybean oil	127	70	1.81	[158]
<i>P. oleovorans</i>	Octanoic acid	189	51	3.69	[159]
<i>P. oleovorans</i>	Soybean oil	130	72	1.70	[159]
<i>P. oleovorans</i>	Undecanoic acid	260	135	1.92	[159]

P. = pseudomonas; Mw = molecular weight; Mn = molecular number; PDI = polydispersity index.

8. Applications of PHAs

PHAs have shown considerable promise in various applications over the last two decades in the packaging, agricultural, and medical sectors in applications such as drug carriers, medical implants, and biocontrol agents [160]. The key criteria that govern the use of PHAs are their molecular weights and co-monomer concentration [143]. When compared to P3HB, P3HBV copolymer offers superior physical qualities such as impact resistance, hardness, flexibility, lower processing temperature, and a wider processing window [161]. Mcl-PHAs can be used as adhesives [162], coatings [163], plasticizers, medical devices, fibers [164], non-woven composites [165], and as bio-carriers in the slow release of fertilizers [166].

Crosslinking improves the mechanical qualities of PHAs, they can be employed in cartilage and ligament substitutes [167]. TEPHA Medical Devices Inc., based in the United States, has been manufacturing FDA-approved PHA sutures for medical absorbable sutures under the TephafLEX[®] brand since 2007 [168]. Unilever developed and launched PHA micro powder-based sun creams in 2019 to improve sun creams' water resistance while lowering their environmental effect. This sun lotion is a natural alternative to microbead-based sunscreens, which can damage the seas and oceans. Danimer Scientific and Cove have produced entirely biodegradable straw and bottles made of PHAs. Nestle has also teamed up with Danimer Scientific to develop biodegradable water bottles, with the goal of making all plastic packaging recyclable or reusable by 2025 [169]. Overall, PHAs have applications in plasticizers, fishing lines [170], wastewater treatment [171], food packaging, and fertilizers [172].

Research on mcl-PHAs and their derivatives, which are more elastomeric, has intensified in recent years. Due to the limitations of large-scale production of mcl-PHAs, most recent studies have focused on the copolymers P(3HB-co-3HHx) and P(3HO), which have better mechanical characteristics and many more elastomers than scl-PHAs in addition to having been manufactured in considerable amounts. Because many organs in the body have elastomeric qualities, mcl-PHA polymer scaffolds that can withstand and retake from numerous structures without harming other nearby tissue can be used. Tim et al. employed a polymeric scaffold made up of two components fashioned into a tubular conduit, the inner layer was made using a polyglycolic acid mesh and the outer layer was made with three layers of non-porous P(3HO-co-3HHx) with 10% 3HHx for tissue engineering studies [172].

P(3HB-co-3HHx) scaffolds can thus be employed for vascular grafting, according to these findings [173]. Sodian et al. conducted one of the first investigations employing an elastomeric P(3HO) for the creation of a tri-leaflet heart valve scaffold [174]. Based on the findings of these experiments, it was shown that P(3HO) manufactured TEHV may be implanted in the pulmonary location and operate properly for 120 days in lambs [174]. Stock et al. (2000) investigated the possibility of developing three-leaflet, valved pulmonary conduits in lambs using autologous ovine vascular cells and thermoplastic P(3HO) [175]. Sodian et al. (2002) employed a new stereolithography manufacturing approach to create P(4HB) and P(3HO) scaffolds of cuspid and semilunar valves based on X-ray computed tomography and appropriate software [176]. Wu et al. (2007) created unique hybrid valves made of decellularized swine aortic valves covered with PVC (3HB-co-3HHx) [177]. Yang et al. (2002) conducted one of the first experiments on P(3HB-co-3HHx) as a nerve regeneration conduit material [178]. Ying et al. (2008) used electro spun copolymers of P(3HB-co-5 mol % 3HHx), P(3HB-co-7 mol % 4HB) and P(3HB-co-97 mol % 4HB) to make nanostructured fibrous scaffolds [179]. The generated scaffolds have tensile strength and Young's modulus in the ranges of 5–30 and 15–150 MPa, which are equivalent to human skin. P3HO homopolymer fabricated 2D films were also investigated as a matrix material for skin tissue engineering. Wang et al. (2004) tested the in vitro biocompatibility of rabbit bone marrow cells injected on PLA, P3HB, and P(3HB-co-3HHx) 3D scaffolds [180]. On the P(3HB-co-3HHx) scaffolds, the cells proliferated the most. Several studies on three-dimensional polymer scaffold systems using a blend of P(3HB) and P(3HB-co-3HHx) for use as a matrix for cartilage tissue engineering have been conducted [181–183]. Wang et al. conducted one of the things is to first investigations of the use of PHA with dendrimer matrix for effective skin drug delivery systems (SDS) [184]. Vermeer et al. (2021) demonstrated a new application of PHAs in self-healing concrete [185]. Harazna et al. (2020) used ceramic-polymer bounded diclofenac with the biocompatible P(3HO) [186].

9. Conclusions and Future Perspectives

This review summarized the recent developments in mcl-PHA production using organic/inorganic carbon sources and various types of the fermentation strategies such as batch, continuous, and fed-batch. We also discussed downstream processing methods,

properties and applications of mcl-PHAs, and their worldwide production at an industrial scale. Current mcl-PHA production through fermentation is facing several problems, such as high levels of foaming in the reactor due to toxicity of fatty acids which are used as a carbon source, inconsistency in the PHA titers (varying from 3 to 102 g/L), polymer property alterations due to fluctuations in molecular weights (from 45 to 462 Kda of Mw). Fatty acid (high) concentration in the fermentation broth inhibiting the growth of microorganisms and creating problems in down-stream processing, such as centrifugation and lyophilization. High-cell-density fermentation requires a continuous oxygen supply (7 L/min) which is expensive and creates safety issues in large-scale fermentation. Before scaling-up the mcl-PHA production process, researchers should focus on solving the above-mentioned problems by using recombinant strains and wild type bacteria other than *Pseudomonas*.

Author Contributions: Conceptualization, M.V.R. and Y.-C.C.; Writing—original draft preparation, V.U.N.R. and M.V.R.; Writing—review and editing, S.V.R. and Y.-C.C. All authors have read and agreed to the published version of the manuscript.

Funding: This research received no external funding.

Institutional Review Board Statement: Not applicable.

Informed Consent Statement: Not applicable.

Data Availability Statement: Data is contained within the article or corresponding author.

Conflicts of Interest: The authors declare no conflict of interest.

References

- Lemoigne, M. Dehydration and polymerization product of β -oxybutyric acid. *Bull. Soc. Chim. Biol.* **1926**, *8*, 770–782.
- Muhammadi, S.; Muhammad, A.; Shafqat, H. Bacterial polyhydroxyalkanoates-eco-friendly next generation plastic: Production, biocompatibility, biodegradation, physical properties and applications. *Green Chem. Lett. Rev.* **2015**, *8*, 56–77. [[CrossRef](#)]
- Lee, S.Y.; Chang, H.N. Production of poly (hydroxy alkanolic acid). *Adv. Biochem. Eng. Biotechnol.* **1995**, *52*, 27–58.
- Choonut, A.; Prasertsan, P.; Klomklao, S.; Sangkharak, K. A Novel Green Process for Synthesis of 3-Hydroxyalkanoate Methyl Ester Using Lipase and Novel mcl-co-1cl PHA as Catalyst and Substrate. *J. Polym. Environ.* **2021**, *30*, 1423–1434. [[CrossRef](#)]
- Rakkan, T.; Chana, N.; Chirapongsatonkul, N.; Sangkharak, K. Screening and identification of newly isolated basic red 9-degrading bacteria from textile wastewater and their ability to produce medium-co-long-chain-length polyhydroxyalkanoates. *J. Polym. Environ.* **2022**, *30*, 415–423. [[CrossRef](#)]
- Muhr, A.; Rechberger, E.M.; Salerno, A.; Reiterer, A.; Schiller, M.; Kwicien, M.; Adamus, G.; Kowalczyk, M.; Strohmeier, K.; Schober, S.; et al. Biodegradable latexes from animal-derived waste: Biosynthesis and characterization of mcl-PHA accumulated by *P. citronellolis*. *React. Funct. Polym.* **2013**, *73*, 1391–1398. [[CrossRef](#)]
- Nitschke, M.; Costa, S.G.V.A.O.; Contiero, J. Rhamnolipids and PHAs: Recent reports on *Pseudomonas*-derived molecules of increasing industrial interest. *Process Biochem.* **2011**, *46*, 621–630. [[CrossRef](#)]
- Chen, G.-Q.; Jiang, X.-R. Engineering bacteria for enhanced polyhydroxyalkanoates (PHA) biosynthesis. *Synth. Syst. Biotechnol.* **2017**, *2*, 192–197. [[CrossRef](#)]
- Kourmentza, C.; Plácido, J.; Venetsaneas, N.; Burniol-Figols, A.; Varrone, C.; Gavala, H.N.; Reis, M.A.M. Recent advances and challenges towards sustainable polyhydroxyalkanoate (PHA) production. *Bioengineering* **2017**, *4*, 55. [[CrossRef](#)]
- Lee, S.Y.; Wong, H.H.; Choi, J.; Lee, S.H.; Lee, S.C.; Han, C.S. Production of Medium-Chain-Length Polyhydroxyalkanoates by High-Cell-Density Cultivation of *Pseudomonas putida* Under Phosphorus Limitation. *Biotechnol. Bioeng.* **2000**, *68*, 466–470. [[CrossRef](#)]
- Riesenberger, D.; Guthke, R. High-cell-density cultivation of microorganisms. *Appl. Microbiol. Biotechnol.* **1999**, *51*, 422–430. [[CrossRef](#)]
- Cavalheiro, J.M.B.T.; Raposo, S.R.; Almeida, M.C.M.D.; Sevrin, M.T.C.C.; Grandfils, C.; Fonseca, M.M.R. Effect of cultivation parameters on the production of poly (3-hydroxybutyrate-co-4-hydroxybutyrate) and poly (3-hydroxybutyrate-4-hydroxybutyrate-3-hydroxyvalerate) by *Cupriavidus necator* using waste glycerol. *Bioresour. Technol.* **2012**, *111*, 391–397. [[CrossRef](#)] [[PubMed](#)]
- Davis, R.; Duane, G.; Kenny, S.T.; Cerrone, F.; Guzik, M.W.; Babu, R.P.; Casey, E.; O'Connor, K.E. High cell density cultivation of *Pseudomonas putida* KT2440 using glucose without the need for oxygen enriched air supply. *Biotechnol. Bioeng.* **2015**, *112*, 725–733. [[CrossRef](#)] [[PubMed](#)]
- Ryu, H.W.; Hahn, S.K.; Chang, Y.K.; Chang, H.N. Production of poly(3-hydroxybutyrate) by high cell density fed-batch culture of *Alcaligenes eutrophus* with phosphate limitation. *Biotechnol. Bioeng.* **1997**, *55*, 25–32. [[CrossRef](#)]

15. Chen, G.-O.; Zhang, J. Microbial polyhydroxyalkanoates as medical implant biomaterials. *Artif. Cells Nanomed. Biotechnol.* **2018**, *46*, 1–18. [[CrossRef](#)]
16. Williams, S.F.; Rizk, S.; Martin, D.P. Poly-4-hydroxybutyrate (P4HB): A new generation of resorbable medical devices for tissue repair and regeneration. *Biomed. Eng.* **2013**, *58*, 439–452. [[CrossRef](#)]
17. Skibiński, S.; Cichoń, E.; Harażna, K.; Marcello, E.; Roy, I.; Witko, M.; Ślósarczyk, A.; Czechowska, J.; Guzik, M.; Zima, A. Functionalized tricalcium phosphate and poly (3-hydroxyoctanoate) derived composite scaffolds as platforms for the controlled release of diclofenac. *Ceram. Int.* **2021**, *47*, 3876–3883. [[CrossRef](#)]
18. Cichoń, E.; Harażna, K.; Skibiński, S.; Witko, T.; Zima, A.; Ślósarczyk, A.; Zimowska, M.; Witko, M.; Leszczyński, B.; Wróbel, A.; et al. Novel bioresorbable tricalcium phosphate/polyhydroxyoctanoate (TCP/PHO) composites as scaffolds for bone tissue engineering applications. *J. Mech. Behav. Biomed. Mater.* **2019**, *98*, 235–245. [[CrossRef](#)]
19. Zhang, J.; Cao, Q.; Li, S.; Lu, X.; Zhao, Y.; Guan, J.-S.; Chen, J.-C.; Wu, Q.; Chen, G.-Q. 3-Hydroxybutyrate methyl ester as a potential drug against Alzheimer’s disease via mitochondria protection mechanism. *Biomaterials* **2013**, *34*, 7552–7562. [[CrossRef](#)]
20. Xiao, X.-Q.; Zhao, Y.; Chen, G.-Q. The effect of 3-hydroxybutyrate and its derivatives on the growth of glial cells. *Biomaterials* **2007**, *28*, 3608–3616. [[CrossRef](#)]
21. Heinrich, D.; Raberg, M.; Fricke, P.; Kenny, S.T.; Gamez, L.M.; Babu, R.P.; O’Connor, K.; Steinbüchel, A. Synthesis gas (syngas)-derived medium-chain-length polyhydroxyalkanoate synthesis in engineered *Rhodospirillum Rubrum*. *Appl. Environ. Microbiol.* **2016**, *82*, 6132–6140. [[CrossRef](#)] [[PubMed](#)]
22. Jaeger, K.E.; Steinbüchel, A.; Jendrossek, D. Substrate specificities of bacterial polyhydroxyalkanoate depolymerases and lipases: Bacterial lipases hydrolyze poly(ω -hydroxyalkanoates). *Appl. Environ. Microbiol.* **1995**, *61*, 3113–3118. [[CrossRef](#)] [[PubMed](#)]
23. Volova, T.G.; Kiselev, E.G.; Shishatskaya, E.I.; Zhila, N.O.; Boyandin, A.N.; Syrvacheva, D.A.; Vinogradova, O.N.; Kalacheva, G.S.; Vasiliev, A.D.; Peterson, I.V. Cell growth and accumulation of polyhydroxyalkanoates from CO₂ and H₂ of a hydrogen-oxidizing bacterium, *Cupriavidus eutrophus* B-10646. *Bioresour. Technol.* **2013**, *146*, 215–222. [[CrossRef](#)] [[PubMed](#)]
24. Volova, T.G.; Shishatskaya, E.I.; Zhila, N.O.; Shishatskii, O.N.; Kiselev, Y.G.; Mironov, P.V.; Vasiliev, A.D.; Peterson, I.V.; Sinskey, A.J. Fundamental basis of production and application of biodegradable polyhydroxyalkanoates. *J. Sib. Fed. Univ. Biol.* **2012**, *3*, 280–299.
25. Tanaka, K.; Yoshida, K.; Orita, I.; Fukui, T. Biosynthesis of Poly (3-hydroxybutyrate-co-3-hydroxyhexanoate) from CO₂ by a recombinant *Cupriavidus necator*. *Bioengineering* **2021**, *8*, 179. [[CrossRef](#)]
26. Löwe, H.; Hobmeier, K.; Moos, M.; Kremling, A.; Pflüger-Grau, K. Photoautotrophic production of polyhydroxyalkanoates in a synthetic mixed culture of *Synechococcus elongatus* cscB and *Pseudomonas putida* cscAB. *Biotechnol. Biofuels* **2017**, *10*, 1–14. [[CrossRef](#)]
27. Riedel, S.L.; Bader, J.; Brigham, C.J.; Budde, C.F.; Yusof, Z.A.; Rha, C.; Sinskey, A.J. Production of poly (3-hydroxybutyrate-co-3-hydroxyhexanoate) by *Ralstonia eutropha* in high cell density palm oil fermentations. *Biotechnol. Bioeng.* **2012**, *109*, 74–83. [[CrossRef](#)]
28. Ruiz, C.; Kenny, S.T.; Babu, P.R.; Walsh, M.; Narancic, T.; O’Connor, K.E. High cell density conversion of hydrolyzed waste cooking oil fatty acids into medium chain length polyhydroxyalkanoate using *Pseudomonas putida* KT2440. *Catalysts* **2019**, *9*, 468. [[CrossRef](#)]
29. Jiang, X.J.; Sun, Z.; Ramsay, J.A.; Ramsay, B.A. Fed-batch production of MCL-PHA with elevated 3-hydroxynonanoate content. *AMB Express* **2013**, *50*, 1–18. [[CrossRef](#)]
30. Blunt, W.; Dartiailh, C.; Sparling, R.; Gapes, D.J.; Levin, D.B.; Cicek, N. Development of high cell density cultivation strategies for improved medium chain length polyhydroxyalkanoate productivity using *Pseudomonas putida* LS46. *Bioengineering* **2019**, *6*, 89. [[CrossRef](#)]
31. Sun, Z.; Ramsay, J.A.; Guay, M.; Ramsay, B.A. Enhanced yield of medium-chain-length polyhydroxyalkanoates from nonanoic acid by co-feeding glucose in carbon-limited, fed-batch culture. *J. Biotechnol.* **2009**, *143*, 262–267. [[CrossRef](#)] [[PubMed](#)]
32. Diniz, S.C.; Taciro, M.K.; Gomez, J.G.C.; Pradella, J.G. High-cell-density cultivation of *Pseudomonas putida* IPT 046 and medium-chain-length polyhydroxyalkanoate production from sugarcane carbohydrates. *Appl. Biochem. Biotechnol.* **2004**, *119*, 1–69. [[CrossRef](#)]
33. Kellerhals, M.B.; Hazenberg, W.; Witholt, B. High cell density fermentations of *Pseudomonas oleovorans* for the production of mcl-PHAs in two-liquid phase media. *Enz. Microbiol. Technol.* **1999**, *24*, 111–116. [[CrossRef](#)]
34. Kellerhals, M.B.; Kessler, B.; Witholt, B.; Tchouboukov, A.; Brand, H. Renewable long-chain fatty acids for production of biodegradable medium-chain-length polyhydroxyalkanoates (mcl-PHAs) at laboratory and pilot plant scales. *Macromolecules* **2000**, *33*, 4690–4698. [[CrossRef](#)]
35. Preusting, H.; Hazenberg, W.; Witholt, B. Continuous production of poly(3-hydroxyalkanoates) by *Pseudomonas oleovorans* in a high-cell-density, two-liquid-phase chemostat. *Enzym. Microb. Technol.* **1993**, *15*, 311–316. [[CrossRef](#)]
36. Preusting, H.; Houten, R.; Hoefs, A.; Langenberghe, E.K.; Favre-Bulle, O.; Witholt, B. High cell density cultivation of *Pseudomonas oleovorans*: Growth and production of poly (3-hydroxyalkanoates) in two-liquid phase batch and fed-batch systems. *Biotechnol. Bioeng.* **1993**, *41*, 550–556. [[CrossRef](#)] [[PubMed](#)]
37. Riedel, S.L.; Jahns, S.; Koenig, S.; Bock, M.C.; Brigham, C.J.; Bader, J.; Stahl, U. Polyhydroxyalkanoates production with *Ralstonia eutropha* from low quality waste animal fats. *J. Biotechnol.* **2015**, *214*, 119–127. [[CrossRef](#)]

38. Sato, S.; Maruyama, H.; Fujiki, T.; Matsumoto, K. Regulation of 3-hydroxyhexanoate composition in PHBH synthesized by recombinant *Cupriavidus necator* H16 from plant oil by using butyrate as a co-substrate. *J. Biosci. Bioeng.* **2015**, *120*, 246–251. [[CrossRef](#)]
39. Cai, L.; Yuan, M.Q.; Liu, F.; Jian, J.; Chen, G.Q. Enhanced production of medium-chain-length polyhydroxyalkanoates (PHA) by PHA depolymerase knockout mutant of *Pseudomonas putida* KT2442. *Bioresour. Technol.* **2009**, *100*, 2265–2270. [[CrossRef](#)]
40. LeMeur, S.; Zinn, M.; Egli, T.; Thöny-Meyer, L.; Ren, Q. Production of medium-chain-length polyhydroxyalkanoates by sequential feeding of xylose and octanoic acid in engineered *Pseudomonas putida* KT2440. *BMC Biotechnol.* **2012**, *12*, 53.
41. Kahar, P.; Tsuge, T.; Taguchi, K.; Doi, Y. High yield production of polyhydroxyalkanoates from soybean oil by *Ralstonia eutropha* and its recombinant strain. *Polym. Degrad. Stab.* **2004**, *83*, 79–86. [[CrossRef](#)]
42. Jing, H.; Yuan-Zheng, Q.; Dai-Cheng, L.; Guo-Qiang, C. Engineered *Aeromonas hydrophila* for enhanced production of poly (3-hydroxybutyrate-co-3-hydroxyhexanoate) with alterable monomers composition. *FEMS Microbiol. Lett.* **2004**, *239*, 195–201.
43. Ouyang, S.; Han, J.; Qiu, Y.; Qin, L.; Chen, S.; Wu, Q.; Leski, M.L.; Chen, G. Poly (3-hydroxybutyrate-co-3-hydroxyhexanoate) production in recombinant *Aeromonas hydrophila* 4ak4 harboring phba, phbb and vgb genes. *Macromol. Symp.* **2005**, *224*, 21–34. [[CrossRef](#)]
44. Budde, C.F.; Riedel, S.L.; Willis, L.B.; Rha, C.; Sinskey, A.J. Production of poly (3-hydroxybutyrate-co-3-hydroxyhexanoate) from plant oil by engineered *Ralstonia eutropha* strains. *Appl. Environ. Microbiol.* **2011**, *77*, 2847–2854. [[CrossRef](#)] [[PubMed](#)]
45. Thinagarani, L.; Sudesh, K. Evaluation of sludge palm oil as feedstock and development to efficient method for its utilization to produce polyhydroxyalkanoate. *Waste Biomass Valoriz.* **2017**, *10*, 709–720. [[CrossRef](#)]
46. Tufail, S.; Munir, S.; Jamil, N. Variation analysis of bacterial polyhydroxyalkanoates production using saturated and unsaturated hydrocarbons. *Braz. J. Microbiol.* **2017**, *48*, 629–636. [[CrossRef](#)]
47. Qiu, Y.Z.; Han, J.; Guo, J.J.; Chen, G.Q. Production of poly (3-hydroxybutyrate-co-3-hydroxyhexanoate) from gluconate and glucose by recombinant *Aeromonas hydrophila* and *Pseudomonas putida*. *Biotechnol. Lett.* **2005**, *27*, 1381–1386. [[CrossRef](#)]
48. Poblete-Castro, I.; Rodriguez, A.L.; Lam, C.M.; Kessler, W. Improved production of medium-chain-length polyhydroxyalkanoates in glucose-based fed-batch cultivations of metabolically engineered *Pseudomonas putida* strains. *J. Microbiol. Biotechnol.* **2014**, *24*, 59–69. [[CrossRef](#)]
49. Zhao, F.; He, F.; Liu, X.; Shi, J.; Liang, J.; Wang, S.; Yang, C.; Liu, R. Metabolic engineering of *Pseudomonas mendocina* NK-01 for enhanced production of medium-chain-length polyhydroxyalkanoates with enriched content of the dominant monomer. *Int. J. Biol. Macromol.* **2020**, *154*, 1596–1605. [[CrossRef](#)]
50. Liu, C.; Qi, L.; Yang, S.; He, Y.; Jia, X. Increased sedimentation of a *Pseudomonas–Saccharomyces* microbial consortium producing medium chain length polyhydroxyalkanoates. *Chin. J. Chem. Eng.* **2019**, *27*, 1659–1665. [[CrossRef](#)]
51. Oliveira, G.H.D.; Zaiat, M.; Rodrigues, J.A.D.; Ramsay, J.A.; Ramsay, B.A. Towards the production of mcl-pha with enriched dominant monomer content: Process development for the sugarcane biorefinery context. *J. Polym. Environ.* **2020**, *28*, 844–853. [[CrossRef](#)]
52. Insomphun, C.; Mifune, J.; Orita, I.; Numata, K.; Nakamura, S.; Fukui, T. Modification of β -oxidation pathway in *Ralstonia eutropha* for production of poly(3-hydroxybutyrate-co-3-hydroxyhexanoate) from soybean oil. *J. Biosci. Bioeng.* **2014**, *117*, 184–190. [[CrossRef](#)]
53. Serafim, L.S.; Lemos, P.C.; Albuquerque, M.G.; Reis, M.A. Strategies for PHA production by mixed cultures and renewable waste materials. *Appl. Microbiol. Biotechnol.* **2008**, *81*, 615–628. [[CrossRef](#)] [[PubMed](#)]
54. Davis, R.; Kataria, R.; Cerrone, F.; Woods, T.; Kenny, S.; O'Donovan, A.; Guzik, M.; Shaikh, H.; Duane, G.; Gupta, V.K.; et al. Conversion of grass biomass into fermentable sugars and its utilization for medium chain length polyhydroxyalkanoate (mcl-PHA) production by *Pseudomonas* strains. *Bioresour. Technol.* **2013**, *150*, 202–209. [[CrossRef](#)] [[PubMed](#)]
55. Awasthi, M.K.; Kumar, V.; Yadav, V.; Sarsaiya, S.; Awasthi, S.K.; Sindhu, R.; Zhang, Z. Current state of the art biotechnological strategies for conversion of watermelon wastes residues to biopolymers production: A review. *Chemosphere* **2022**, *290*, 133310. [[CrossRef](#)]
56. Muhr, A.; Rechberger, E.M.; Salerno, A.; Reiterer, A.; Malli, K.; Strohmeier, K.; Koller, M. Novel description of mcl-PHA biosynthesis by *Pseudomonas chlororaphis* from animal-derived waste. *J. Biotechnol.* **2013**, *165*, 45–51. [[CrossRef](#)] [[PubMed](#)]
57. Andler, R.; Valdés, C.; Urtuvia, V.; Andreeßen, C.; Diaz-Barrera, A. Fruit residues as a sustainable feedstock for the production of bacterial polyhydroxyalkanoates. *J. Clean. Prod.* **2021**, *307*, 127236. [[CrossRef](#)]
58. Pernicova, I.; Enev, V.; Marova, I.; Obruca, S. Interconnection of waste chicken feather biodegradation and keratinase and mcl-PHA production employing *Pseudomonas putida* KT2440. *Appl. Food Biotechnol.* **2019**, *6*, 83–90.
59. Liu, H.; Kumar, V.; Jia, L.; Sarsaiya, S.; Kumar, D.; Juneja, A.; Awasthi, M.K. Biopolymer poly-hydroxyalkanoates (PHA) production from apple industrial waste residues: A review. *Chemosphere* **2021**, *284*, 131427. [[CrossRef](#)]
60. Blanco, F.G.; Hernández, N.; Rivero-Buceta, V.; Maestro, B.; Sanz, J.M.; Mato, A.; Prieto, M.A. From residues to added-value bacterial biopolymers as nanomaterials for biomedical applications. *Nanomaterials* **2021**, *11*, 1492. [[CrossRef](#)]
61. Yadav, B.; Pandey, A.; Kumar, L.R.; Tyagi, R.D. Bioconversion of waste (water)/residues to bioplastics-A circular bioeconomy approach. *Bioresour. Technol.* **2020**, *298*, 122584. [[CrossRef](#)] [[PubMed](#)]
62. Chang, Y.C.; Venkateswar Reddy, M.; Imura, K.; Onodera, R.; Kamada, N.; Sano, Y. Two-Stage polyhydroxyalkanoates (PHA) production from cheese whey using *Acetobacter pasteurianus* C1 and *Bacillus* sp. CYR1. *Bioengineering* **2021**, *8*, 157. [[CrossRef](#)] [[PubMed](#)]

63. Chang, Y.C.; Venkateswar Reddy, M.; Choi, D.B. Cometary degradation of toxic trichloroethene or *cis*-1,2-dichloroethene with phenol and production of poly- β -hydroxybutyrate (PHB). *Green Chem.* **2021**, *23*, 2729–2737. [[CrossRef](#)]
64. Reddy, M.V.; Watanabe, A.; Onodera, R.; Mawatari, Y.; Tsukiori, Y.; Watanabe, A.; Kudou, M.; Chang, Y.C. Polyhydroxyalkanoates (PHA) production using single or mixture of fatty acids with *Bacillus* sp. CYR1: Identification of PHA synthesis genes. *Bioresour. Technol. Rep.* **2020**, *11*, 100483–100491. [[CrossRef](#)]
65. Reddy, M.V.; Mawatari, S.; Onodera, R.; Nakamura, Y.; Yajima, Y.; Chang, Y.C. Bacterial conversion of waste into polyhydroxybutyrate (PHB): A new approach of bio-circular economy for treating waste and energy generation. *Bioresour. Technol. Rep.* **2019**, *7*, 100246–100254. [[CrossRef](#)]
66. Reddy, M.V.; Mawatari, Y.; Onodera, R.; Nakamura, Y.; Yajima, Y.; Chang, Y.C. Polyhydroxyalkanoates (PHA) production from synthetic waste using *Pseudomonas pseudoflava*: PHA synthase enzyme activity analysis from *P. pseudoflava* and *P.alleronii*. *Bioresour. Technol.* **2017**, *234*, 99–105. [[CrossRef](#)]
67. Reddy, M.V.; Mawatari, Y.; Yajima, Y.; Satoh, K.; Venkata Mohan, S.; Chang, Y.C. Production of poly-3-hydroxybutyrate (P3HB) and poly-3-(hydroxybutyrate-co-hydroxyvalerate) P(3HB-co-3HV) from synthetic wastewater using *Hydrogenophaga alleronii*. *Bioresour. Technol.* **2016**, *215*, 155–162. [[CrossRef](#)]
68. Amulya, K.; Venkateswar Reddy, M.; Rohit, M.V.; Mohan, S.V. Wastewater as renewable feedstock for polyhydroxyalkanoates (PHA) production: Understanding the role of reactor microenvironment and system pH. *J. Clean. Prod.* **2016**, *112*, 4618–4627. [[CrossRef](#)]
69. Amulya, K.; Venkateswar Reddy, M.; Mohan, S.V. Acidogenic spent wash valorization through polyhydroxyalkanoate (PHA) synthesis coupled with fermentative biohydrogen production. *Bioresour. Technol.* **2014**, *158*, 336–342. [[CrossRef](#)]
70. Reddy, M.V.; Mohan, S.V. Influence of aerobic and anoxic microenvironments on polyhydroxyalkanoates (PHA) production from food waste and acidogenic effluents using aerobic consortia. *Bioresour. Technol.* **2012**, *103*, 313–321. [[CrossRef](#)]
71. Srikanth, S.; Venkateswar Reddy, M.; Mohan, S.V. Microaerophilic microenvironment at biocathode enhances electrogenesis with simultaneous synthesis of polyhydroxyalkanoates (PHA) in bioelectrochemical system (BES). *Bioresour. Technol.* **2012**, *125*, 291–299. [[CrossRef](#)] [[PubMed](#)]
72. Mohan, S.V.; Venkateswar Reddy, M.; Subhash, G.V.; Sarma, P.N. Fermentative effluents from hydrogen producing bioreactor as substrate for poly (β -OH) butyrate production with simultaneous treatment: An integrated approach. *Bioresour. Technol.* **2010**, *101*, 9382–9386. [[CrossRef](#)] [[PubMed](#)]
73. Appaiah, P.; Sunil, L.; Prasanth Kumar, P.K.; Gopala Krishna, A.G. Composition of Coconut Testa, Coconut Kernel and its Oil. *J. Am. Oil Chem. Soc.* **2014**, *91*, 917–924. [[CrossRef](#)]
74. Basnett, P.; Marcello, E.; Lukasiewicz, B.; Panchal, B.; Nigmatullin, B.; Knowles, J.C.; Roy, I. Biosynthesis and characterization of a novel, biocompatible medium chain length polyhydroxyalkanoate by *Pseudomonas mendocina* CH50 using coconut oil as the carbon source. *J. Mater. Sci. Mater. Med.* **2018**, *29*, 1–11. [[CrossRef](#)]
75. Valappil, S.P.; Misra, S.K.; Boccaccini, A.R.; Roy, I. Biomedical applications of polyhydroxyalkanoates (PHAs), an overview of animal testing and in vivo responses. *Expert Rev. Med. Devices* **2006**, *3*, 853–868. [[CrossRef](#)]
76. Mozejko, J.; Ciesielski, S. Saponified waste palm oil as an attractive renewable resource for mcl-polyhydroxyalkanoate synthesis. *J. Biosci. Bioeng.* **2013**, *116*, 485–492. [[CrossRef](#)]
77. Mozejko, J.; Wilke, A.; Przybylek, G.; Ciesielski, S. Mcl-PHAs produced by *Pseudomonas* sp. Gl01 using fed-batch cultivation with waste rapeseed oil as carbon source. *J. Microbiol. Biotechnol.* **2012**, *22*, 371–377. [[CrossRef](#)]
78. Song, J.H.; Jeon, C.O.; Choi, M.H.; Yoon, S.C.; Park, W.J. Polyhydroxyalkanoate (PHA) production using waste vegetable oil by *Pseudomonas* sp. strain DR2. *J. Microbiol. Biotechnol.* **2008**, *18*, 1408–1415.
79. Reddy, M.V.; Yajima, Y.; Mawatari, Y.; Hoshino, T.; Chang, Y.C. Degradation and conversion of toxic compounds into useful bioplastics by *Cupriavidus* sp. CY-1: Relative expression of PhaC gene under phenol and nitrogen stress. *Green Chem.* **2015**, *17*, 4560–4569. [[CrossRef](#)]
80. Mohan, S.V.; Venkateswar Reddy, M. Optimization of critical factors to enhance polyhydroxyalkanoates (PHA) synthesis by mixed culture using Taguchi design of experimental methodology. *Bioresour. Technol.* **2013**, *128*, 409–416. [[CrossRef](#)]
81. Reddy, M.V.; Mohan, S.V. Effect of substrate load and nutrients concentration on the Polyhydroxyalkanoates (PHA) production using mixed consortia through wastewater treatment. *Bioresour. Technol.* **2012**, *114*, 573–582. [[CrossRef](#)] [[PubMed](#)]
82. Rai, R.; Keshavarz, T.; Roether, J.A.; Boccaccini, A.R.; Roy, L. Medium chain length polyhydroxyalkanoates, promising new biomedical materials for the future. *Mater. Sci. Eng. R Rep.* **2011**, *72*, 29–47. [[CrossRef](#)]
83. Jung, K.; Hazenberg, W.; Prieto, M.; Witholt, B. Two-stage continuous process development for the production of medium-chain-length poly(3-hydroxyalkanoates). *Biotech. Bioeng.* **2001**, *71*, 19–24. [[CrossRef](#)]
84. Lee, M.Y.; Park, W.H.; Lenz, R.W. Hydrophilic bacterial polyesters modified with pendant hydroxyl groups. *Polymer* **2000**, *41*, 1703–1709. [[CrossRef](#)]
85. Gao, J.; Ramsay, J.A.; Ramsay, B.A. Fed-batch production of poly-3-hydroxydecanoate from decanoic acid. *J. Biotechnol.* **2016**, *218*, 102–107. [[CrossRef](#)]
86. Cerrone, F.; Duane, G.; Casey, E.; Davis, R.; Belton, I.; Kenny, S.T.; Guzik, M.W.; Woods, T.; Babu, R.P.; O'Connor, K. Fed-batch strategies using butyrate for high cell density cultivation of *Pseudomonas putida* and its use as a biocatalyst. *Appl. Microbiol. Biotechnol.* **2014**, *98*, 9217–9228. [[CrossRef](#)]

87. Sun, Z.; Ramsay, J.A.; Guay, M.; Ramsay, B.A. Carbon-limited fed-batch production of medium-chain-length polyhydroxyalkanoates from nonanoic acid by *Pseudomonas putida* KT2440. *Appl. Microbiol. Biotechnol.* **2007**, *74*, 69–77. [CrossRef]
88. Kim, B.S. Production of medium chain length polyhydroxyalkanoates by fed-batch culture of *Pseudomonas oleovorans*. *Biotechnol. Lett.* **2002**, *24*, 125–130. [CrossRef]
89. Kim, G.J.; Lee, I.Y.; Yoon, S.C.; Shin, Y.C.; Park, Y.H. Enhanced yield and a high production of medium-chain-length poly(3-hydroxyalkanoates) in a two-step fed-batch cultivation of *Pseudomonas putida* by combined use of glucose and octanoate. *Enzym. Microb. Technol.* **1997**, *20*, 500–505. [CrossRef]
90. Kaur, G.; Roy, I. Strategies for large-scale production of polyhydroxyalkanoates. *Chem. Biochem. Eng. Q.* **2015**, *29*, 157–172. [CrossRef]
91. Zinn, M.; Witholt, B.; Egli, T. Occurrence, synthesis and medical application of bacterial polyhydroxyalkanoate. *Adv. Drug. Del. Rev.* **2001**, *53*, 5–21. [CrossRef]
92. Egli, T. On multiple-nutrient-limited growth of microorganisms, with special reference to dual limitation by carbon and nitrogen substrates. *Antonie Van Leeuwenhoek* **1991**, *60*, 225–234. [CrossRef] [PubMed]
93. Huijberts, G.N.M.; Eggink, G. Production of poly(3-hydroxyalkanoates) by *Pseudomonas putida* KT2442 in continuous cultures. *Appl. Microbiol. Biotechnol.* **1996**, *46*, 233–239. [CrossRef]
94. McNeil, B.; Harvey, L.M. *Fermentation, a Practical Approach*; IRL: Tokyo, Japan, 1990.
95. Andin, N.; Longieras, A.; Veronese, T.; Marcato, F.; Molina-Jouve, C.; Uribelarrea, J.-L. Improving carbon and energy distribution by coupling growth and medium chain length polyhydroxyalkanoate production from fatty acids by *Pseudomonas putida* KT2440. *Biotechnol. Bioprocess Eng.* **2017**, *22*, 308–318. [CrossRef]
96. Bio-On Declares Bankruptcy. Available online: <http://www.plasticsnews.com/news/bio-declares-bankruptcy> (accessed on 3 January 2020).
97. A Bio-on e a Hera Cria a Lux-on, o Novo Desafio Para Produzir Bioplástico a Partir de CO₂. Available online: <http://www.bio-on.it/project.php?lin=portoghese> (accessed on 10 December 2018).
98. Upcycling Waste to Natural Biopolymers. Available online: <http://www.paquesbiomaterials.nl> (accessed on 10 December 2018).
99. Bioextrax develops world-leading bio-based technologies – accelerating the transition to a sustainable global economy. Available online: <http://bioextrax.com> (accessed on 25 March 2022).
100. Guzik, M.W. Polyhydroxyalkanoates, bacterially synthesized polymers, as a source of chemical compounds for the synthesis of advanced materials and bioactive molecules. *Appl. Microbiol. Biotechnol.* **2021**, *105*, 7555–7566. [CrossRef]
101. Titan An Biopolymers/Enmat. Available online: <http://www.titanan-enmat.com/> (accessed on 25 March 2022).
102. Mitsubishi Gas Chemical (MGC). Available online: <https://www.mgc.co.jp/> (accessed on 25 March 2022).
103. Completion of Kaneka Biodegradable Polymer PHBHT[™] Plant with Annual Production of 5,000 Tons. Available online: <http://www.kaneka.co.jp/en/service/news/nr20191219/> (accessed on 19 December 2019).
104. CJ Acquires Intellectual Property and Lab Equipment from US Venture Firm. Available online: <http://www.ajudaily.com/view/20160823101739592> (accessed on 23 August 2016).
105. Polymeron. Available online: <http://www.polymerofcanada.com/versamerphas.html> (accessed on 25 March 2022).
106. Noda, I.; Lindsey, S.B.; Caraway, D. Nodax[™] class PHA copolymers: Their properties and applications. In *Plastics from Bacteria: Natural Functions and Applications*; Chen, G.-Q., Ed.; Springer: Berlin/Heidelberg, Germany, 2010; pp. 237–255.
107. Biocycle. Available online: <http://www.biocycle.com.br> (accessed on 25 March 2022).
108. Yield10 BIOSCIENCE. Available online: <http://www.yield10bio.com> (accessed on 25 March 2022).
109. Tepha Medical Devices. Tepha Medical Devices. Available online: <http://www.tepha.com/technology/polymer-processing-material-attributes> (accessed on 25 March 2022).
110. Jennifer, B.; Emily, G. Plastic from thin air. *Popul. Sci.* **2014**, *285*, 24.
111. Can Plastic Be Made Environmentally Friendly? Available online: <http://www.scientificamerican.com/article/can-plastic-be-made-environmentally-friendly> (accessed on 29 January 2014).
112. Polyhydroxyalkanoate (PHA) Market by Type (Short Chain Length, Medium Chain Length), Production Method (Sugar Fermentation, Vegetable Oil Fermentation, Methane Fermentation), Application, and Region - Global Forecast to 2025. Available online: <http://www.marketsandmarkets.com/Market-Reports/pha-market-395.html> (accessed on 1 February 2021).
113. MARS. Available online: <http://www.mars.com/sustainability-plan/healthy-planet/sustainable-packaging> (accessed on 25 March 2022).
114. After 149 Years, Colgate's Toothpaste Tubes are Finally Recyclable. Available online: <http://www.fastcompany.com/90713412/after-149-years-colgates-toothpaste-tubes-are-finally-recyclable> (accessed on 19 January 2022).
115. Kosseva, M.R.; Rusbandi, E. Trends in the biomanufacturer of polyhydroxyalkanoates with focus on downstream processing. *Int. J. Biol. Macromol.* **2018**, *107*, 762–778. [CrossRef]
116. Bresan, S.; Sznajder, A.; Hauf, W.; Forchhammer, K.; Pfeiffer, D.; Jendrossek, D. Polyhydroxyalkanoate (PHA) granules have no phospholipids. *Sci. Rep.* **2016**, *6*, 26612. [CrossRef]
117. Jacquel, N.; Lo, C.W.; Wei, Y.H.; Wu, H.S.; Wang, S.S. Isolation and purification of bacterial poly(3-hydroxyalkanoates). *Biochem. Eng. J.* **2008**, *39*, 15–27. [CrossRef]
118. Koller, M.; Niebelschütz, H.; Braunnegg, G. Strategies for recovery and purification of poly[(R)-3-hydroxyalkanoates] (PHA) biopolyesters from surrounding biomass. *Eng. Life Sci.* **2013**, *13*, 549–562. [CrossRef]

119. Furrer, P.; Panke, S.; Zimm, M. Efficient recovery of low endotoxin medium-chain length poly([R]-3-hydroxyalkanoate) from bacterial biomass. *J. Microbiol. Methods* **2007**, *69*, 206–213. [[CrossRef](#)] [[PubMed](#)]
120. Chemat, F.; Vian, M.A.; Cravotto, G. Green extraction of natural products: Concept and principles. *Int. J. Mol. Sci.* **2012**, *13*, 8615–8627. [[CrossRef](#)] [[PubMed](#)]
121. Yabueng, N.; Napathom, S.C. Toward non-toxic and simple recovery process of poly (3-hydroxybutyrate) using the green solvent 1,3-dioxolane. *Process Biochem.* **2018**, *69*, 197–207. [[CrossRef](#)]
122. Ishak, K.A.; Annuar, M.S.M.; Heidelberg, T.; Gumel, A.M. Ultrasound-assisted rapid extraction of bacterial intra cellular medium-chain-length poly(3-hydroxyalkanoates) (mcl-phas) in medium mixture of solvent/marginal non-solvent. *Arab. J. Sci. Eng.* **2016**, *41*, 33–44. [[CrossRef](#)]
123. Noda, I. Process for Recovering Polyhydroxyalkanoates Using Air Classification. U.S. Patent US5849854A, 15 December 1998.
124. Vilku, K.; Mawson, R.; Simons, L.; Bates, D. Applications and opportunities for ultrasound assisted extraction in the food industry-A review. *Innov. Food Sci. Emerg. Technol.* **2008**, *9*, 161–169. [[CrossRef](#)]
125. Leong, Y.K.; Koroh, F.E.; Show, P.L.; Lan, J.C.W.; Loh, H.S. Optimization of extractive bioconversion for green polymer via aqueous two-phase system. *Chem. Eng. Trans.* **2015**, *45*, 1495–1500.
126. Leong, Y.K.; Lan, J.C.W.; Loh, H.S.; Ling, T.C.; Ooi, C.W.; Show, P.L. Cloud-point extraction of green-polymers from *Cupriavidus necator* lysate using thermo separating-based aqueous two-phase extraction. *J. Biosci. Bioeng.* **2016**, *123*, 3270–3375.
127. Leong, Y.K.; Show, P.L.; Lan, J.C.-W.; Loh, H.-S.; Yap, Y.-J.; Ling, T.C. Extraction and purification of polyhydroxyalkanoates (PHAs): Application of thermo separating aqueous two-phase extraction. *J. Polym. Res.* **2017**, *24*, 158. [[CrossRef](#)]
128. Leong, K.; Show, P.L.; Lan, J.C.W.; Krishna Moorthy, R.; Chu, D.T.; Nagarajan, D.; Yen, H.W.; Chang, J.S. Application of thermo-separating aqueous two-phase system in extractive bioconversion of polyhydroxyalkanoates by *Cupriavidus necator* H16. *Bioresour. Technol.* **2019**, *287*, 121474. [[CrossRef](#)]
129. López-Abelairas, M.; García-Torreiro, M.; Lú-Chau, T.; Lema, J.M.; Steinbüchel, A. Comparison of several methods for the separation of poly(3-hydroxybutyrate) from *Cupriavidus necator* H16 cultures. *Biochem. Eng. J.* **2015**, *93*, 250–259. [[CrossRef](#)]
130. Gumel, A.M.; Annuar, M.S.M.; Chisti, Y. Recent advances in the production, recovery, and applications of polyhydroxyalkanoates. *J. Polym. Environ.* **2013**, *21*, 580–605. [[CrossRef](#)]
131. Dong, Z.; Sun, X.; Zhaolin, D.; Xuenan, S.U.N. A new method of recovering polyhydroxyalkanoate from *Azotobacter chroococcum*. *Chin. Sci. Bull.* **2000**, *45*, 252–256. [[CrossRef](#)]
132. Yasotha, K.; Aroua, M.K.; Ramachandran, K.B.; Tan, I.K.P. Recovery of medium-chain-length polyhydroxyalkanoates (PHAs) through enzymatic digestion treatments and ultrafiltration. *Biochem. Eng. J.* **2006**, *30*, 260–268. [[CrossRef](#)]
133. Kachrimanidou, V.; Kopsahelis, N.; Vlysidis, A.; Papanikolaou, S.; Kookos, I.K.; Martínez, B.M.; Rondan, M.C.E.; Kautinas, A.A. Downstream separation of poly(hydroxyalkanoates) using crude enzyme consortia produced via solid state fermentation integrated in a biorefinery concept. *Food Bioprod. Process* **2016**, *100*, 323–334. [[CrossRef](#)]
134. Israni, N.; Thapa, S.; Shivakumar, S. Biolytic extraction of poly (3-hydroxybutyrate) from *Bacillus megaterium* T13 using the lytic enzyme of *Streptomyces albus* Tia1. *J. Genet. Eng. Biotechnol.* **2018**, *16*, 265–271. [[CrossRef](#)]
135. Panaitecu, D.M.; Lupescu, I.; Frone, A.N.; Chiulan, I.; Nicolae, C.A.; Tofan, V.; Stefanu, A.; Somoghi, R.; Trusca, R. Medium chain-length polyhydroxyalkanoate copolymer modified by bacterial cellulose for medical devices. *Biomacromolecules* **2017**, *18*, 3222–3232. [[CrossRef](#)]
136. Abe, H.; Ishii, N.; Sato, S.; Tsuge, T. Thermal properties and crystallization behaviors of medium-chain-length poly (3-hydroxyalkanoate) s. *Polymer* **2012**, *53*, 3026–3034. [[CrossRef](#)]
137. Chen, G.Q. A microbial polyhydroxyalkanoates (PHA) based bio and material industry. *Chem. Soc. Rev.* **2009**, *38*, 2434–2446. [[CrossRef](#)]
138. Gopi, S.; Kontopoulou, M.; Ramsay, B.A.; Ramsay, J.A. Manipulating the structure of medium-chain-length polyhydroxyalkanoate (MCL-PHA) to enhance thermal properties and crystallization kinetics. *Int. J. Biol. Macromol.* **2018**, *119*, 1248–1255. [[CrossRef](#)]
139. Nerkar, M.; Ramsay, J.A.; Ramsay, B.A.; Kontopoulou, M. Melt compounded blends of short and medium chain-length poly-3-hydroxyalkanoates. *J. Polym. Environ.* **2014**, *22*, 236–243. [[CrossRef](#)]
140. Xiang, H.; Chen, W.; Chen, Z.; Sun, B.; Zhu, M. Significant accelerated crystallization of long chain branched poly (3-hydroxybutyrate-co-3-hydroxyvalerate) with high nucleation temperature under fast cooling rate. *Compos. Sci. Technol.* **2017**, *142*, 207–213. [[CrossRef](#)]
141. Noda, I.; Schechtman, L.A. Solvent extraction of polyhydroxyalkanoates from biomass. U.S. Patent 5,942,597, 24 August 1999.
142. Sobieski, B.J.; Gong, L.; Aubuchon, S.R.; Noda, I.; Chase, D.B.; Rabolt, J.F. Thermally reversible physical gels of poly[(R)-3-hydroxybutyrate-co-(R)-3-hydroxyhexanoate]: Part 1 gelation in dimethylformamide. *J. Polym.* **2017**, *131*, 217–223. [[CrossRef](#)]
143. Noda, I.; Green, P.R.; Satkowski, M.M.; Schechtman, L.A. Preparation and properties of a novel class of polyhydroxyalkanoate copolymers. *Biomacromolecules* **2005**, *6*, 580–586. [[CrossRef](#)]
144. Tanadchangsaeng, N.; Tsuge, T.; Abe, H. Comonomer compositional distribution, physical properties, and enzymatic degradability of bacterial poly (3-hydroxybutyrate-co-3-hydroxy-4-methylvalerate) polyesters. *Biomacromolecules* **2010**, *11*, 1615–1622. [[CrossRef](#)] [[PubMed](#)]
145. Kolahchi, A.R.; Kontopoulou, M. Chain extended poly (3-hydroxybutyrate) with improved rheological properties and thermal stability, through reactive modification in the melt state. *Polym. Degrad. Stab.* **2015**, *121*, 222–229. [[CrossRef](#)]

146. Muthuraj, R.; Misra, M.; Mohanty, A.K. Biodegradable compatibilized polymer blends for packaging applications: A literature review. *J. Appl. Polym. Sci.* **2018**, *135*, 45726. [CrossRef]
147. Wu, F.; Misra, M.; Mohanty, A.K. Challenges and new opportunities on barrier performance of biodegradable polymers for sustainable packaging. *Prog. Polym. Sci.* **2021**, *117*, 101395. [CrossRef]
148. Xu, P.; Yang, W.; Niu, D.; Yu, M.; Du, M.; Dong, W.; Chen, M.; Lemstra, P.J.; Ma, P. Multifunctional and robust polyhydroxyalkanoate nanocomposites with superior gas barrier, heat resistant and inherent antibacterial performances. *Chem. Eng. J.* **2020**, *382*, 122864. [CrossRef]
149. Choi, S.Y.; Cho, I.J.; Lee, Y.; Kim, Y.; Kim, K.; Lee, S.Y. Microbial polyhydroxyalkanoates and nonnatural polyesters. *Adv. Mater.* **2020**, *32*, 1907138. [CrossRef]
150. Bugnicourt, E.; Cinelli, P.; Lazzeri, A.; Alvarez, V.A. Polyhydroxyalkanoate (PHA): Review of synthesis, characteristics, processing and potential applications in packaging. *Express Polym. Lett.* **2014**, *8*, 791–808. [CrossRef]
151. Kusaka, S.; Abe, H.; Lee, S.; Doi, Y. Molecular mass of poly [(R)-3-hydroxybutyric acid] produced in a recombinant *Escherichia coli*. *Appl. Microbiol. Biotechnol.* **1997**, *47*, 140–143. [CrossRef] [PubMed]
152. Choi, J.; Lee, S.Y. High level production of supra molecular weight poly (3-hydroxybutyrate) by metabolically engineered *Escherichia coli*. *Biotechnol. Bioprocess Eng.* **2004**, *9*, 196–200. [CrossRef]
153. Doi, Y.; Kitamura, S.; Abe, H. Microbial synthesis and characterization of poly (3-hydroxybutyrate-co-3-hydroxyhexanoate). *Macromolecules* **1995**, *28*, 4822–4828. [CrossRef]
154. Acuña, J.M.; Rohde, M.; Saldias, C.; Castro, I.P. Fed-Batch mcl-Polyhydroxyalkanoates production in *Pseudomonas putida* KT2440 and phaZ mutant on biodiesel-derived crude glycerol. *Front. Bioeng. Biotechnol.* **2021**, *9*, 1–10.
155. Dartailh, C.; Blunt, W.; Sharma, P.K.; Liu, S.; Cicek, N.; Levin, D.B. The thermal and mechanical properties of medium chain-length polyhydroxyalkanoates produced by *Pseudomonas putida* LS46 on various substrates. *Front. Bioeng. Biotechnol.* **2021**, *8*, 1–9. [CrossRef]
156. Liu, W.; Chen, G.Q. Production and characterization of mediumchain-length polyhydroxyalkanoate with high 3-hydroxytetradecanoate monomer content by fadB and fadA knockout mutant of *Pseudomonas putida* KT2442. *Appl. Microbiol. Biotechnol.* **2007**, *76*, 1153–1159. [CrossRef]
157. Solaiman, D.K.Y.; Ashby, R.D.; Foglia, T.A. Physiological characterization and genetic engineering of *Pseudomonas corrugata* for medium-chain-length polyhydroxyalkanoates synthesis from triacylglycerols. *Curr. Microbiol.* **2002**, *44*, 189–195. [CrossRef]
158. Ashby, R.D.; Foglia, T.A. Poly(hydroxyalkanoate) biosynthesis from triglyceride substrates. *Appl. Microbiol. Biotechnol.* **1998**, *49*, 431–437. [CrossRef]
159. Hazer, D.B.; Hazer, B.; Kaymaz, F. Synthesis of microbial elastomers based on soybean oily acids. Biocompatibility studies. *Biomed. Mater.* **2009**, *4*, 1–9. [CrossRef]
160. Kalia, V.C.; Patel, S.K.S.; Shanmugam, R.; Lee, J.K. Polyhydroxyalkanoates: Trends and advances toward biotechnological applications. *Bioresour. Technol.* **2021**, *326*, 124737. [CrossRef]
161. Dill, S.; Demicheva, M.; Fleschutz, B.; Weinlein, R.; Demicheva, M.; Fleschutz, B.; Weinlein, R. Influence of polyhydroxybutyrate content on the crystallization behavior of polyamide 6-polyhydroxybutyrate blends. *Macromol. Symp.* **2019**, *384*, 1800170. [CrossRef]
162. Wang, S.; Chen, W.; Xiang, H.; Yang, J.; Zhou, Z.; Zhu, M. Modification and potential application of short-chain-length polyhydroxyalkanoate (SCL-PHA). *Polymers* **2016**, *8*, 273. [CrossRef] [PubMed]
163. Rastogi, V.; Samyn, P. Bio-based coatings for paper applications. *Coatings* **2015**, *5*, 887–930. [CrossRef]
164. Xiang, H.; Chen, Z.; Zheng, N.; Zhang, X.; Zhu, L.; Zhou, Z.; Zhu, M. Melt-spun microbial poly (3-hydroxybutyrate-co-3-hydroxyvalerate) fibers with enhanced toughness: Synergistic effect of heterogeneous nucleation, long-chain branching and drawing process. *Int. J. Biol. Macromol.* **2019**, *122*, 1136–1143. [CrossRef] [PubMed]
165. Wagner, A.; Poursorkhabi, V.; Mohanty, A.K.; Misra, M. Analysis of porous electrospun fibers from poly (l-lactic acid)/Poly (3-hydroxybutyrate-co-3-hydroxyvalerate) blends. *ACS Sustain. Chem. Eng.* **2014**, *2*, 1976–1982. [CrossRef]
166. Ivanov, V.; Stabnikov, V.; Ahmed, Z.; Dobrenko, S.; Saliuk, A. Production, and applications of crude polyhydroxyalkanoate-containing bioplastic from the organic fraction of municipal solid waste. *Int. J. Environ. Sci. Technol.* **2015**, *12*, 725–738. [CrossRef]
167. Ang, S.L.; Sivashankari, R.; Shaharuddin, B.; Chuah, J.-A.; Tsuge, T.; Abe, H.; Sudesh, K. Potential applications of polyhydroxyalkanoates as a biomaterial for the aging population. *Polym. Degrad. Stab.* **2020**, *181*, 109371. [CrossRef]
168. Tefha Medical Devices Overview. Available online: <http://www.tepha.com/technology/overview/> (accessed on 25 March 2022).
169. Development of Biodegradable Water Bottle. Available online: <http://www.foodpackagingforum.org/news/development-of-biodegradable-water-bottle> (accessed on 23 January 2019).
170. Wang, Y.; Yin, J.; Chen, G.-Q. Polyhydroxyalkanoates, challenges and opportunities. *Curr. Opin. Biotechnol.* **2014**, *30*, 59–65. [CrossRef]
171. Choonut, A.; Prasertsan, P.; Klomkiao, S.; Sangkharak, K. An environmentally friendly process for textile wastewater treatment with a medium-chain-length polyhydroxyalkanoate film. *J. Polym. Environ.* **2021**, *29*, 3335–3346. [CrossRef]
172. Tim, D.S.; Stock, U.; Hrkach, J.; Shinoka, T.; Lien, B.; Moses, M.A.; Stamp, A.; Taylor, G.; Moran, A.M.; Landis, W.; et al. Tissue engineering of autologous aorta using a new biodegradable polymer. *Ann. Thorac. Surg.* **1999**, *68*, 2298–2305.

173. Zhang, L.; Zheng, Z.; Xi, J.; Gao, Y.; Ao, Q.; Gong, Y.; Zhao, N.; Zhang, X. Improved mechanical property and biocompatibility of poly(3-hydroxybutyrate-co-3-hydroxyhexanoate) for blood vessel tissue engineering by blending with poly(propylene carbonate). *Eur. Polym. J.* **2007**, *43*, 2975–2986. [[CrossRef](#)]
174. Sodian, R.; Hoerstrup, S.P.; Sperling, J.S.; Daebritz, S.; Martin, D.P.; Moran, A.M.; Kim, B.S.; Schoen, F.J.; Vacanti, J.P.; Mayer Jr, J.E. Early in vivo experience with tissue-engineered trileaflet heart valves. *Circulation* **2007**, *102*, 22–29.
175. Stock, U.A.; Nagashima, M.; Kahalil, P.N.; Nollert, G.D.; Herden, T.; Sperling, J.S.; Moran, A.M.; Lien, B.; Martin, D.P.; Schoen, F.J.; et al. Tissue-engineered valved conduits in the pulmonary circulation. *J. Thorac. Cardiovasc. Surg.* **2000**, *119*, 732–740. [[CrossRef](#)]
176. Sodian, R.; Loebe, M.; Hein, A.; Martin, D.P.; Hoerstrup, S.P.; Potapov, E.V.; Hausmann, H.; Leuth, T.; Hetzer, R. Application of stereolithography for scaffold fabrication for tissue engineered heart valves. *ASAIO J.* **2002**, *48*, 12–16. [[CrossRef](#)] [[PubMed](#)]
177. Wu, S.; Liu, Y.L.; Cui, B.; Qu, X.H.; Chen, G.Q. Study on decellularized porcine aortic valve/poly (3-hydroxybutyrate-co-3-hydroxyhexanoate) hybrid heart valve in sheep model. *Artif. Organs* **2007**, *31*, 689–697. [[CrossRef](#)] [[PubMed](#)]
178. Yang, Y.; Li, X.; Li, G.; Zhao, N.; Zhang, X. Study on chitosan and PHBHHx used as nerve regeneration conduit material. *J. Biomed. Eng.* **2002**, *19*, 25–29.
179. Ying, H.T.; Ishii, D.; Mahara, A.; Murakami, S.; Yamaoka, T.; Sudesh, K.; Samian, R.; Fujita, M.; Maeda, M.; Iwata, T. Scaffolds from electrospun polyhydroxyalkanoate copolymers: Fabrication, characterization, bioabsorption and tissue response. *Biomaterials* **2008**, *29*, 1307–1317. [[CrossRef](#)]
180. Wang, Y.W.; Wu, Q.O.; Chen, G.Q. Attachment, proliferation and differentiation of osteoblasts on random biopolyester poly(3-hydroxybutyrate-co-3-hydroxyhexanoate) scaffolds. *Biomaterials* **2004**, *25*, 669–675. [[CrossRef](#)]
181. Zhao, K.; Deng, Y.; Chen, J.C.; Chen, G.Q. Polyhydroxyalkanoate (PHA) scaffolds with good mechanical properties and biocompatibility. *Biomaterials* **2003**, *24*, 1041–1054. [[CrossRef](#)]
182. Deng, Y.; Zhao, K.; Zhang, X.F.; Hu, P.; Chen, G.Q. Study on the three-dimensional proliferation of rabbit articular cartilage-derived chondrocytes on polyhydroxyalkanoate scaffolds. *Biomaterials* **2002**, *23*, 4049–4056. [[CrossRef](#)]
183. Deng, Y.; Lin, X.J.; Zheng, Z.; Deng, J.G.; Chen, J.C.; Ma, H.; Chen, G.Q. Poly(hydroxybutyrate-co-hydroxyhexanoate) promoted production of extracellular matrix of articular cartilage chondrocytes in vitro. *Biomaterials* **2003**, *24*, 4273–4281. [[CrossRef](#)]
184. Wang, Z.; Itoh, Y.; Hosaka, Y.; Kobayashi, I.; Nakano, Y.; Maeda, I.; Umeda, F.; Yamakawa, J.; Kawase, M.; Yagi, K. Novel transdermal drug delivery system with polyhydroxyalkanoate and starburst polyamidoamine dendrimer. *J. Biosci. Bioeng.* **2003**, *95*, 541–543. [[CrossRef](#)]
185. Vermeer, C.M.; Rossi, E.; Tamis, J.; Jonkers, H.M.; Kleerebezem, R. From waste to self-healing concrete: A proof-of-concept of a new application for polyhydroxyalkanoate. *Resour. Conserv. Recycl.* **2021**, *164*, 105206. [[CrossRef](#)]
186. Harażna, K.; Cichoń, E.; Skibiński, S.; Witko, T.; Solarz, D.; Kwiecień, I.; Guzik, M. Physicochemical and biological characterisation of diclofenac oligomeric poly (3-hydroxyoctanoate) hybrids as β -TCP ceramics modifiers for bone tissue regeneration. *Int. J. Mol. Sci.* **2020**, *21*, 9452. [[CrossRef](#)]

Article

Poly(3-mercapto-2-methylpropionate), a Novel α -Methylated Bio-Polythioester with Rubber-like Elasticity, and Its Copolymer with 3-hydroxybutyrate: Biosynthesis and Characterization

Lucas Vinicius Santini Ceneviva ¹, Maierwufu Mierzati ¹, Yuki Miyahara ¹, Christopher T. Nomura ², Seiichi Taguchi ³, Hideki Abe ⁴ and Takeharu Tsuge ^{1,*}

¹ Department of Materials Science and Engineering, Tokyo Institute of Technology, 4259 Nagatsuta, Midori-ku, Yokohama 226-8502, Japan; santini.l.aa@m.titech.ac.jp (L.V.S.C.); mirzat.m.aa@m.titech.ac.jp (M.M.); miyahara.y.aa@m.titech.ac.jp (Y.M.)

² Department of Biological Sciences, College of Science, University of Idaho, 875 Perimeter Dr., Moscow, ID 83844-3010, USA; ctnomura@uidaho.edu

³ Graduate School of Science, Technology and Innovation, Kobe University, 1-1 Rokkodai-cho, Nada, Kobe 657-8501, Japan; staguchi86@people.kobe-u.ac.jp

⁴ Bioplastic Research Team, RIKEN Center for Sustainable Resource Science, 2-1 Hirosawa, Wako, Saitama 351-0198, Japan; habe@riken.jp

* Correspondence: tsuge.t.aa@m.titech.ac.jp

Citation: Ceneviva, L.V.S.; Mierzati, M.; Miyahara, Y.; Nomura, C.T.; Taguchi, S.; Abe, H.; Tsuge, T. Poly(3-mercapto-2-methylpropionate), a Novel α -Methylated Bio-Polythioester with Rubber-like Elasticity, and Its Copolymer with 3-hydroxybutyrate: Biosynthesis and Characterization. *Bioengineering* **2022**, *9*, 228. <https://doi.org/10.3390/bioengineering9050228>

Academic Editor: Martin Koller

Received: 13 April 2022

Accepted: 17 May 2022

Published: 23 May 2022

Publisher's Note: MDPI stays neutral with regard to jurisdictional claims in published maps and institutional affiliations.



Copyright: © 2022 by the authors. Licensee MDPI, Basel, Switzerland. This article is an open access article distributed under the terms and conditions of the Creative Commons Attribution (CC BY) license (<https://creativecommons.org/licenses/by/4.0/>).

Abstract: A new polythioester (PTE), poly(3-mercapto-2-methylpropionate) [P(3M2MP)], and its copolymer with 3-hydroxybutyrate (3HB) were successfully biosynthesized from 3-mercapto-2-methylpropionic acid as a structurally-related precursor. This is the fourth PTE of biological origin and the first to be α -methylated. P(3M2MP) was biosynthesized using an engineered *Escherichia coli* L5BJ, which has a high molecular weight, amorphous structure, and elastomeric properties, reaching 2600% elongation at break. P(3HB-co-3M2MP) copolymers were synthesized by expressing 3HB-supplying enzymes. The copolymers were produced with high content in the cells and showed a high 3M2MP unit incorporation of up to 77.2 wt% and 54.8 mol%, respectively. As the 3M2MP fraction in the copolymer increased, the molecular weight decreased and the polymers became softer, more flexible, and less crystalline, with lower glass transition temperatures and higher elongations at break. The properties of this PTE were distinct from those of previously biosynthesized PTEs, indicating that the range of material properties can be further expanded by introducing α -methylated thioester monomers.

Keywords: polythioester; polyhydroxyalkanoate; 3-hydroxybutyrate; bioplastic; biopolymer; alpha-methylated; rubber-like elasticity

1. Introduction

Global plastic production reached 367 million tons by 2020 [1]. Between 1950 and 2015, only 9% of plastic waste was recycled, with 12% incinerated and 79% accumulated in landfills and the environment [2]. There is increasing concern regarding plastic waste pollution, particularly in oceans, as 80% of these plastics are of land origin [3]. Thus, it is projected that by 2050, there will be more plastics than fish in the oceans [4].

The development of biodegradable and bio-based plastics, known as “bioplastics”, has gained attention [5]. Polyhydroxyalkanoates (PHAs) are a family of aliphatic polyesters naturally produced from sugars, fatty acids, and amino acids by bacteria as intracellular energy reserves in the presence of excess carbon sources and limited nutrients [6,7]. Bioplastics exhibit intrinsic biodegradability and biocompatibility in any medium or marine environment [8–10]. PHAs also exhibit extraordinary versatility, as polyesters from more

than 160 different monomers can be produced by wild-type or engineered bacteria from structurally related or unrelated carbon sources [11].

Poly(3-hydroxybutyrate) [P(3HB)], the most common PHA in natural PHA-producing bacteria [6], is stiff and brittle [12] and has low thermal stability [13]; numerous methods have been investigated to improve its properties, including thermal processing, blending, fiber inclusion, and copolymerization [14]. Most copolymerization approaches have focused on the biosynthesis of 3HB-based copolymers with medium-chain length monomers, such as 3-hydroxyhexanoate, as their elastomeric characteristics can result in a softer and more flexible structure than those of P(3HB) [15] or PHA monomers containing shorter chain lengths (i.e., 2-hydroxyalkanoate monomers), fluorine, or ring-structures [16–18]. Recently, the α -methylated structure of poly(3-hydroxy-2-methylbutyrate) [P(3H2MB)] was used to fabricate PHA materials with high flexibility and superior thermal stability because of its fast crystallization behavior and highest melting temperature (T_m) among PHAs [19].

Polythioesters (PTEs) were first chemically synthesized approximately 70 years ago [20]; however, they have never been produced on an industrial scale and established commercially because of their high production costs, low yields, and use of toxic substances [21]. In 2001, by using structurally related thioester precursors and other carbon sources, Lütke-Eversloh et al. [22] identified that a copolymer of 3HB and 3-mercaptopropionate (3MP) could be biosynthesized by *Ralstonia eutropha* H16 via its inherent P(3HB) synthesis pathway, making it the eighth class of biological polymers. In sequence, copolymers of 3HB with 3-mercaptopbutyrate (3MB) [23] and 3-mercaptopvalerate (3MV) [24] were synthesized from their structurally related precursors in *R. eutropha*. Notably, their homopolymers, P(3MP), P(3MB) and P(3MV), could be biosynthesized by constructing a recombinant strain of *Escherichia coli* via a non-natural pathway containing butyrate kinase to phosphorylate 3-mercaptopalkanoate precursors, phosphotransbutyrylase to convert 3-mercaptopalkanoate-Pi esters to 3-mercaptopalkanoate-CoA thioesters, and PHA synthase to polymerize these thioesters by releasing CoA [25]. Comparison of the properties of biosynthesized PTE homopolymers and those of their structurally analogous oxyester PHAs indicated that they can have a higher glass transition temperature (T_g) and/or higher T_m than their oxygen analogs [25]. PTE homopolymers may also have higher elongations at break, as copolymers of 3MP with 3HB showed higher elasticity than those of 3HB with an equivalent oxyester [26].

In this study, we biosynthesized a new PTE homopolymer and its copolymers with 3HB by an engineered *E. coli* and using 3-mercaptop-2-methylpropionic acid as the thioester precursor, making it the fourth PTE to be biosynthesized and the first α -methylated PTE. P(3M2MP) and its copolymers had their chemical structure confirmed by nuclear magnetic resonance (NMR), and their thermal and mechanical properties were also investigated by differential scanning calorimetry (DSC) and tensile tests.

2. Materials and Methods

2.1. Bacterial Strain and Plasmids

The host strain, plasmids, and biosynthesis strategies used in this study were the same as in the previous studies [19,27]. The host strain for PHA/PTE accumulation was *E. coli* LSBJ, a *fadB* and *fadJ* knockout mutant of *E. coli* LS5218, which enables control of the repeating unit composition in PHA biosynthesis [28]. For P(3HB-co-3M2MP) biosynthesis, two plasmids were introduced into the host strains, pTTQ19PCT and pBBR1phaP(D4N)C_{J_{Ac}}AB_{Re} NSDG. pTTQ19PCT contains the propionyl-CoA transferase (PCT) gene from *Megasphaera elsdenii*, which supplies 3M2MP-CoA, whereas pBBR1phaP(D4N)C_{J_{Ac}}AB_{Re} NSDG contains the phasin (PhaP_{Ac}) gene from *Aeromonas caviae* with the point mutation D4N that enables high PHA accumulation by enhancing the expression of the *phaPCJ* operon [29], PHA synthase (PhaC_{Ac}) gene from *A. caviae* with N149S and D171G point mutations that enhance incorporation of the second monomer unit of the 3HB-based copolymer [30], (R)-specific enoyl-CoA hydratase gene (*phaJ_{Ac}*), and genes for the enzymes, 3-ketothiolase (PhaA_{Re}) and acetoacetyl-CoA reductase (PhaB_{Re}) from *R. eutropha* H16 that supply the

3HB precursor for PhaC_{Ac} polymerization. For P(3M2MP) homopolymer biosynthesis, the plasmid pTTQ19PCT was also introduced, while the other plasmid had the deletion of the *phaAB*_{Re} and *phaJ*_{Ac} genes, becoming the plasmid pBBR1phaP(D4N)CJ_{Ac} NSDG. To obtain pBBR1phaP(D4N)CJ_{Ac}AB_{Re} NSDG using PCR primer sets (5'-gttgggcaggcaaacacgggtt-3' and 5'-gatccactagtcttagagcgcc-3'). The resulting PCR fragment was treated with the Mighty Cloning Reagent Set Blunt End Kit (Takara Bio, Shiga, Japan) and self-ligated using a DNA Ligation Kit (Takara). Figure 1 illustrates the proposed biosynthetic pathways for P(3HB-co-3M2MP) and P(3M2MP).

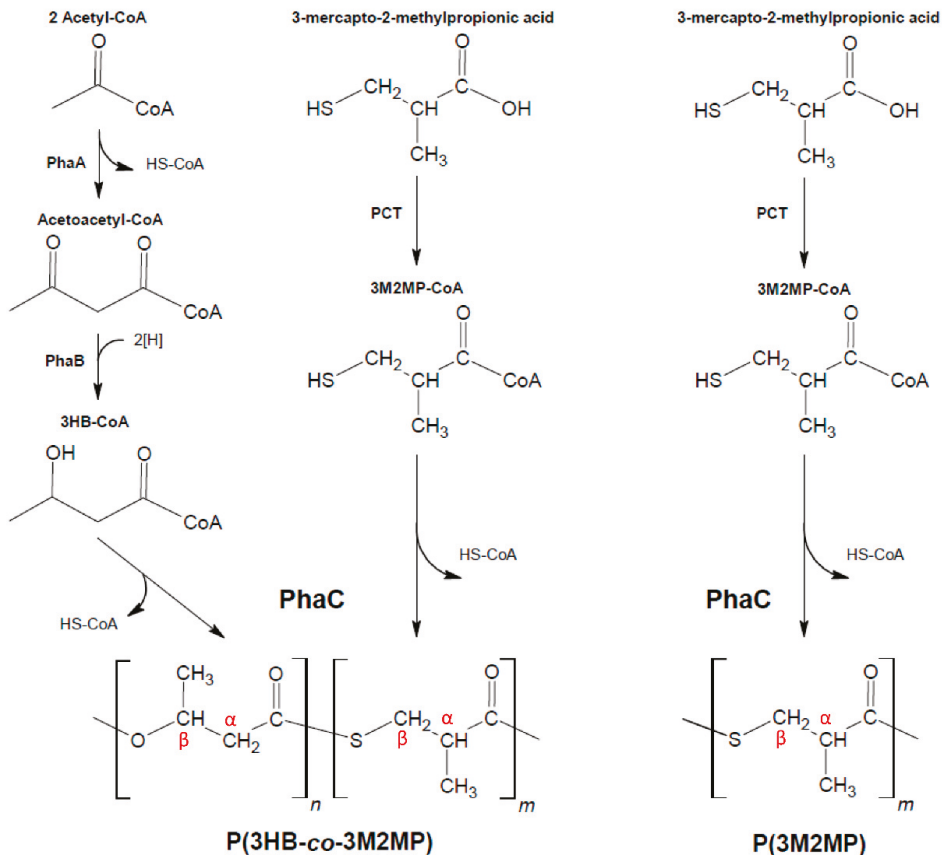


Figure 1. P(3HB-co-3M2MP) and P(3M2MP) biosynthetic pathway.

2.2. P(3HB-co-3M2MP) and P(3M2MP) Biosynthesis, Harvest, and Polymer Content

For copolymer production, recombinant *E. coli* LSBJ was pre-cultivated for 18 h at 30 °C with reciprocal shaking at 160 rpm in a 50 mL flask containing 20 mL of lysogeny broth (LB) medium (i.e., 10 g NaCl, 10 g tryptone, and 5 g bacto-yeast extract per liter of distilled water) with 50 mg/L kanamycin and 50 mg/L carbenicillin. Thereafter, 10 mL/L of pre-culture was inoculated into 500 mL shake flasks containing approximately 100 mL of M9-modified medium (17.1 g/L Na₂HPO₄·12H₂O, 3 g/L KH₂PO₄, 2.5 g/L bacto-yeast extract, 0.5 g/L NaCl) containing 2 mL/L of 1 M MgSO₄·7H₂O, 0.1 mL/L of 1 M CaCl₂, 50 mg/L kanamycin, 50 mg/L carbenicillin, 20 g/L glucose, and different concentrations of (*R,S*)-3-mercapto-2-methylpropionic acid (Tokyo Kasei Kogyo Co., Tokyo, Japan;

0.25–2.5 g/L) as a 3M2MP precursor, with the pH adjusted to 7.0 using NaOH. Gene expression was induced by adding 1 mM isopropyl β -D-1-thiogalactopyranoside (IPTG). The culture for P(3HB-co-3M2MP) production was maintained for 72 h at 30 °C with reciprocal shaking at 130 rpm.

Based on the results of Watanabe et al. [27] and Furutate et al. [19], several changes were made in the concentrations of the culture medium used for P(3M2MP) homopolymer biosynthesis. First, an additional pre-cultivation step was performed, in which recombinant *E. coli* LSBJ was inoculated into 1.7 mL of LB medium containing 50 mg/L kanamycin and 50 mg/L carbenicillin in 5 mL test tubes for 4 h at 37 °C with reciprocal shaking at 160 rpm. This seed culture (0.2 mL) was further inoculated into a 50 mL flask containing 20 mL LB medium, 50 mg/L kanamycin, and 50 mg/L carbenicillin for an additional 18 h at 30 °C with reciprocal shaking at 160 rpm. The pre-culture (5 mL) was inoculated into 500 mL shake flasks containing approximately 100 mL of M9-modified medium with 2 mL/L 1 M $\text{MgSO}_4 \cdot 7\text{H}_2\text{O}$, 0.1, 1 M CaCl_2 , 50 mg/L kanamycin, and 50 mg/L carbenicillin, and grown without precursors and IPTG for 4 h at 30 °C with reciprocal shaking at 130 rpm. Thereafter, 3.75 g/L glucose, 1.2 g/L pH-neutralized 3-mercapto-2-methylpropionic acid, and 1 mM IPTG were added to the culture medium, and cultivation was continued until a total biosynthesis time of 76 h was reached.

After cultivation, the cells were harvested by centrifugation, washed twice with distilled water, and lyophilized for 72 h in previously weighed tubes to obtain the dry cell weight. The polymer content was determined by ultrasonication extraction as described previously with some modifications [31]. Approximately 100 mg of lyophilized cells was added to 50 mL plastic tubes and resuspended in 20 mL of distilled water. Subsequently, 13 mL 10% sodium dodecyl sulfate (SDS) was added to a final concentration of approximately 4% SDS. This solution was ultrasonicated continuously for 4 min at an output level of 4 (15 W), harvested by centrifugation with three rinsing steps (20 mL distilled water, 5 mL methanol, and 20 mL distilled water), and lyophilized for 24 h to determine the polymer content.

To produce sufficient polymers for characterization, biosynthesis was performed at a larger scale in 2 L shake flasks containing 1 L M9-modified medium at the same concentrations as described above, except that the reciprocal shaking speed was adjusted to 103 rpm. For the second step of pre-cultivation, the scale was increased to 500 mL shake flasks containing 100 mL of LB medium with 50 mg/L kanamycin and 50 mg/L carbenicillin, and the reciprocal shaking speed was adjusted to 130 rpm.

2.3. Polymer Film Preparation

The polymers produced on a larger scale were harvested by centrifugation, lyophilized for 72 h, extracted with chloroform for 72 h at room temperature, and purified by precipitation with methanol. The purified polymers were dissolved in chloroform to prepare the polymer films. The polymer solution was filtered once or twice with 0.45 μm polytetrafluoroethylene filter membranes and added to a perfluoroalkoxy alkane (PFA) Petri dish with an internal diameter of approximately 7.7 cm. After solvent evaporation, the polymer films were aged for at least three weeks at room temperature before characterizing their thermal and mechanical properties.

2.4. Polymer Structure Characterization

For one-dimensional ^1H NMR, two-dimensional ^1H - ^1H correlation spectroscopy (^1H - ^1H COSY), and ^1H - ^{13}C heteronuclear single quantum coherence (^1H - ^{13}C HSQC) NMR, 10–20 mg of the purified and filtered polymers was dissolved in 1 mL of CDCl_3 and filtered through 0.45 μm polyvinylidene fluoride filter membranes. In contrast, for one-dimensional ^{13}C NMR, 20–40 mg was dissolved in 1 mL of CDCl_3 and filtered through 0.45 μm polyvinylidene fluoride filter membranes (NMR; 400 Hz; BioSpin AVANCE III 400A, or 500 MHz AVANCE III HD with CryoProbe, Bruker, Billerica, MA, USA). The chemical structure was determined using ^1H and ^{13}C NMR and confirmed using ^1H - ^1H

COSY and ^1H - ^{13}C HSQC. The 3M2MP unit content of the P(3HB-co-3M2MP) copolymers was determined by integrating the methine ($>\text{CH}-$) peaks in the ^1H NMR spectra. The sequence distribution was investigated by calculating the D value [32] by integrating the carbonyl groups in the ^{13}C NMR spectra, and the peaks for the four possible combinations of the copolymer units were assigned using ^1H - ^{13}C heteronuclear multiple bond correlation (^1H - ^{13}C HMBC). Finally, Fourier transform infrared (FTIR) spectroscopy using an FT/IR-4600 spectrometer (Jasco, Tokyo, Japan) with attenuated total reflection (ATR) (model ATR PRO400-S, Jasco, Tokyo, Japan) was performed to confirm the presence of thioester chemical groups in the polymer molecule.

2.5. Molecular Weight

For molecular weight determination, 2–3 mg of the polymer samples were dissolved in HPLC-grade chloroform at 1 mg/mL, filtered through 0.45 μm polyvinylidene fluoride filter membranes, and analyzed using gel permeation chromatography (GPC) on a Shimadzu Nexera 40 GPC system (Kyoto, Japan) with a Shodex RI-504 refractive index detector (Shanghai, China). The gel permeation chromatography system was operated in a column oven at 40 $^\circ\text{C}$. HPLC-grade chloroform was used as the eluent at a flow rate of 0.3 mL/min. Each sample was analyzed for 28 min. Calibration curves were plotted using polystyrene standards with low polydispersity.

2.6. Thermal Properties

The thermal properties of the polymers were analyzed using DSC 8500 (Perkin-Elmer, Waltham, MA, USA) under a nitrogen atmosphere. Each sample (5–7 mg) was encapsulated in an aluminum pan and subjected to two heating steps. The samples were heated from -50 $^\circ\text{C}$ to 200 $^\circ\text{C}$ at 20 $^\circ\text{C}/\text{min}$ (1st heating scan). The melted samples were heated at 200 $^\circ\text{C}$ for 1 min, rapidly decreased to -50 $^\circ\text{C}$, and then heated from -50 $^\circ\text{C}$ to 200 $^\circ\text{C}$ at 20 $^\circ\text{C}/\text{min}$ (2nd heating scan). The T_m and enthalpy of fusion (ΔH_m) were determined from the 1st heating scan curve, whereas the T_g and cold crystallization temperature (T_{cc}) were determined from the 2nd heating scan curve.

2.7. Mechanical Properties

The tensile strength, yield strength, Young's modulus, and elongation at break of the polymers were determined using the stress–strain curves measured with a Shimadzu EZ-S 500N testing machine at a strain rate of 5 mm/min. The samples were dumbbell-shaped using a super dumbbell cutter (SDMP-1000, ISO 37-4/ISO 527-2-5B) with a gauge length of 10 mm, width of 2 mm, and thickness of approximately 100 μm .

3. Results

3.1. P(3HB-co-3M2MP) and P(3M2MP) Biosynthesis and Polymer Content

Copolymers of P(3HB-co-3M2MP) were biosynthesized by recombinant *E. coli* LSBJ containing the plasmids pTTQ19PCT (for *pct* expression) and pBBR1phaP(D4N)J_{Ac}AB_{Re} NSDG (for *phaPCJ* and *phaAB* expression) with glucose and increasing concentrations of 3-mercapto-2-methylpropionic acid (0.25–2.5 g/L) as carbon source and 3M2MP precursor, respectively. Use of 0.25–1.5 g/L of 3-mercapto-2-methylpropionic acid led to stable cell growth and a polymer content of approximately 3.5 g/L and 68 wt%, respectively. The 3M2MP content also increased from 5.5 mol% to 53.9 mol%, as summarized in Table 1. However, when the concentrations exceeded 2.0 g/L, cell growth and the polymer content were significantly increased, with ranges of 4.29–5.06 g/L and 72.1–77.2 wt%, respectively. Notably, the 3M2MP content reached a maximum of 54.8% at 2 g/L and then decreased sharply to 10.7 mol% at 2.5 g/L.

The P(3M2MP) homopolymer was biosynthesized by recombinant *E. coli* LSBJ containing the plasmids pTTQ19PCT and pBBR1phaP(D4N)J_{Ac} NSDG cultured with 3.75 g/L of glucose and 1.2 g/L of 3-mercapto-2-methylpropionic acid. As expected, the cell growth

and polymer content of P(3M2MP) were significantly lower than those of the 3HB-based copolymer, with 1.28 g/L of cell growth and 8.4 wt% of P(3M2MP) content.

Table 1. P(3HB-co-3M2MP) and P(3M2MP) biosynthesis by recombinant *E. coli* LSBJ.

PhaAB and PhaJ Expression	Precursor (g/L) ¹	Dry Cell wt. (g/L)	Polymer Content (wt%)	Monomer Composition (mol%) ²		Sample ID
				3HB	3M2MP	
+ ³	0.25	3.50 ± 0.03	69.1 ± 1.9	94.5	5.5	1
+ ³	0.50	3.69 ± 0.25	68.7 ± 1.0	89.9	10.1	2
+ ³	1.00	3.48 ± 0.02	67.3 ± 0.1	65.8	34.2	3
+ ³	1.50	3.63 ± 0.02	69.1 ± 0.2	46.1	53.9	4
+ ³	2.00	4.29 ± 0.07	72.1 ± 0.8	45.2	54.8	5
+ ³	2.50	5.06 ± 0.04	77.2 ± 0.3	89.3	10.7	6
− ⁴	1.20	1.28 ± 0.01	8.4 ± 1.3	0	100	7

3HB, 3-hydroxybutyrate; 3M2MP, 3-mercapto-2-methylpropionate. Results are expressed as the mean ± standard deviation ($n = 3$). ¹ (R,S)-3-Mercapto-2-methylpropionic acid. ² Determined by comparison of the methine (>CH-) peaks in the ¹H NMR spectra. ³ Strain harboring pTTQ19PCT and pBBR1phaP(D4N)_{Ac}AB_{Re} NSDG. Cells were cultured in 100 mL M9-modified medium containing 0.25–2.5 g/L precursor (3-mercapto-2-methylpropionic acid), 20 g/L glucose, and 1 mM IPTG at 30 °C for 72 h. ⁴ Strain harboring pTTQ19PCT and pBBR1phaP(D4N)_{Ac} NSDG. Cells were cultured in 100 mL M9-modified medium at 30 °C for 4 h, and 1.2 g/L precursor (3-mercapto-2-methylpropionic acid), 3.75 g/L glucose, and 1 mM IPTG were added before further culture for 72 h.

3.2. Chemical Structure and Sequence Distribution Characterization

Based on ¹H NMR analysis of the P(3M2MP) homopolymer, four peaks directly associated with its structure, A, B, and C, were identified with peak integrations of 0.99–1.00, at 3.14, 3.01, and 2.86 ppm, and D with a peak integration of 3.16 at 1.25 ppm. Other significant peaks at 7.26, 1.58, and 0 ppm corresponded to the solvent *d*-chloroform, water moisture, and internal standard tetramethylsilane, respectively. ¹H–¹H COSY NMR revealed correlations between A and B and between C and D. Based on this result and those of ¹H NMR integration, A and B were identified as the two protons of the methylene group, C was the proton of the methine group, and D was the proton of the methyl group. Using ¹³C NMR, peaks E, F, G, and H at 201.3, 48.4, 31.6, and 17.6 ppm, respectively, were found to be directly associated with its structure, which was confirmed using ¹H–¹³C HSQC NMR. This result indicates that A and B correlate with G, serving as the methylene group, C correlates with F as the methine group, D correlates with H as the methyl group, and E serves as the protonless carbonyl group, confirming the expected structure of the homopolymer structurally related to 3-mercapto-2-methylpropionic acid. Figure 2a shows the ¹H NMR, Figure 2b ¹H–¹H COSY NMR, Figure 2c ¹³C NMR, and Figure 2d ¹H–¹³C HSQC NMR spectra. Moreover, based on the ATR-FTIR results shown in Figure 3, the thioester group was confirmed based on the peaks at 1682 and 956 cm^{−1}, which were associated with dialkyl thioester carbonyl stretching (1700–1680 cm^{−1}) and dialkyl thioester C–S stretching (1035–930 cm^{−1}), respectively [33].

Based on ¹H NMR analysis of the copolymers P(3HB-co-3M2MP) in Figure 4, the 3HB chemical shifts were similar to those found by Lütke-Eversloh et al. [22] for the copolymer, P(3HB-co-3MP). However, because of the presence of a methyl group in the 3M2MP unit, overlap with the methyl group of 3HB was observed. Therefore, the comonomer composition was estimated by integrating the methine groups.

Based on the sequence distribution of the polymer, as a copolymer with two different units, four types of unit combinations can occur, 3HB-3M2MP, 3HB-3HB, 3M2MP-3M2MP, and 3M2MP-3HB, with the carbonyl group split into four peaks using a Bernoullian statistical model. The sequence distribution was predicted from the parameter “D” [32] as follows. For simplification, 3HB is expressed as “O” and 3M2MP as “S”.

$$D = \frac{F_{OO} \cdot F_{SS}}{F_{OS} \cdot F_{SO}} \quad (1)$$

where F_{XY} is the mole fraction of the carbonyl group in the XY sequence in the ^{13}C NMR spectrum. Therefore, when $D = 1$, the copolymer is statistically random. However, when D is markedly larger than 1, the copolymer is blocky, and when it is markedly smaller than 1, it is an alternating copolymer [32].

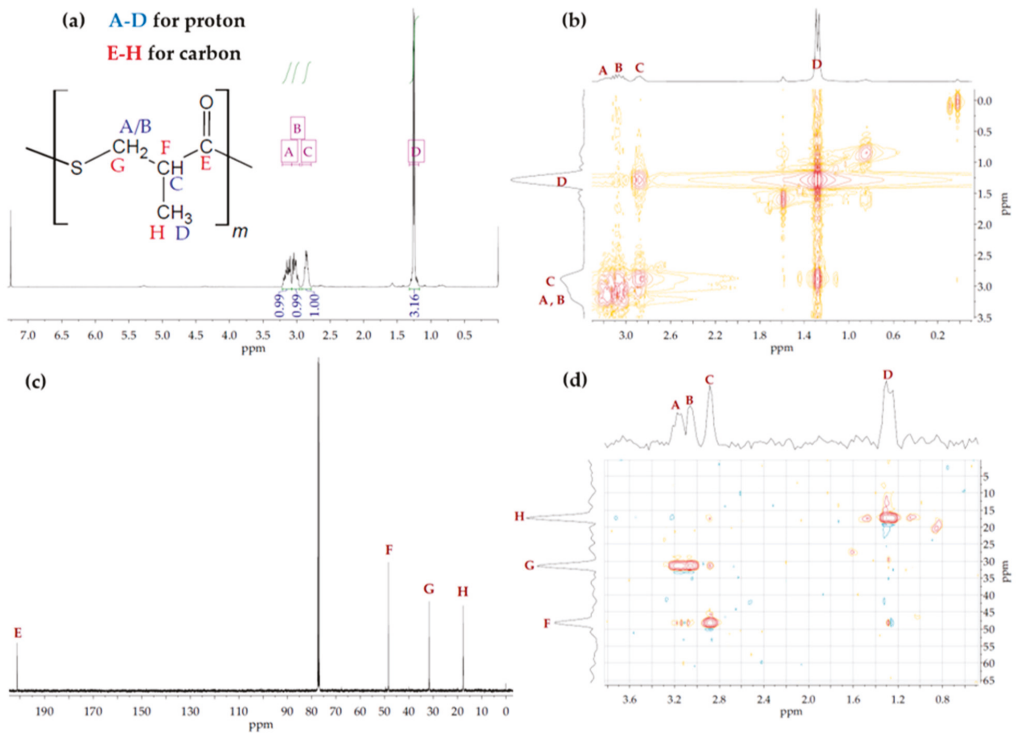


Figure 2. NMR spectra of P(3M2MP). (a) ^1H NMR; (b) ^1H - ^1H COSY NMR; (c) ^{13}C NMR; and (d) ^1H - ^{13}C HSQC NMR.

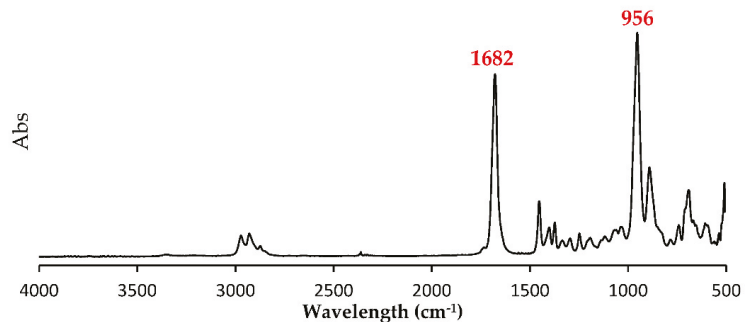


Figure 3. FTIR spectra of P(3M2MP).

The ^{13}C NMR spectra of the copolymer samples showed two extra peaks 195.2 and 173.5 ppm that were not present in the spectra of their homopolymers. Thereafter, based on the ^1H - ^{13}C HMBC for the copolymer samples, these peaks were found to interact with the protons of the 3M2MP and 3HB units. Accordingly, these are the carbonyl peaks of 3M2MP-3HB and 3HB-3M2MP diad, respectively. Figure 5a shows the ^{13}C NMR spectrum

and Figure 5b the ^1H - ^{13}C HMBC spectrum of Sample 5. The D parameter was calculated for the copolymer samples using the carbonyl peaks detected in the ^{13}C NMR spectra. Table 2 presents the results for the F_{XY} and D parameters for each sample and shows that all samples had D values significantly greater than 1, indicating that they have blocky sequence distributions. When the amount of the 3M2MP precursor added to the medium was small, the degree of the block sequence tended to be high.

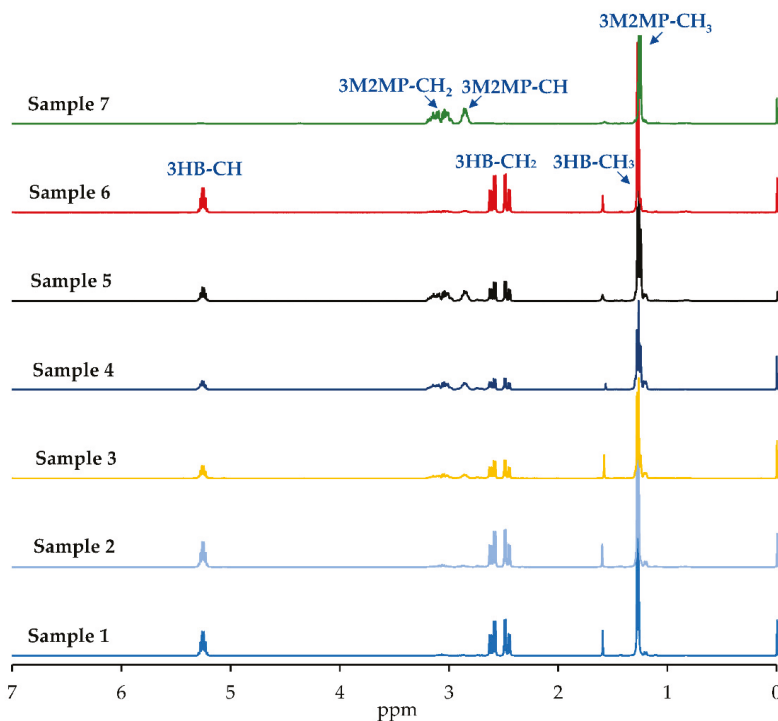


Figure 4. ^1H NMR spectra of Sample 1 (3M2MP 5.5 mol%), Sample 2 (10.1 mol%), Sample 3 (34.2 mol%), Sample 4 (53.9 mol%), Sample 5 (54.8 mol%), Sample 6 (10.7 mol%), and Sample 7 (100 mol%).

Table 2. D value and sequence distribution of P(3HB-co-3M2MP) samples.

Sample ID	3M2MP (mol%)	Diad Sequence Distribution				D	Degree of Block Sequence ¹
		F_{OO}	F_{OS}	F_{SO}	F_{SS}		
1	5.5	0.960	0.016	0.009	0.015	100	High
2	10.1	0.934	0.012	0.006	0.048	623	High
3	34.2	0.741	0.006	0.037	0.216	720	High
4	53.9	0.329	0.182	0.152	0.337	4	Low
5	54.8	0.449	0.067	0.045	0.439	65	Medium
6	10.7	0.868	0.057	0.021	0.054	39	Medium

¹ $1 < D < 10$: low, $10 \leq D < 100$: medium, $100 \leq D$: high.

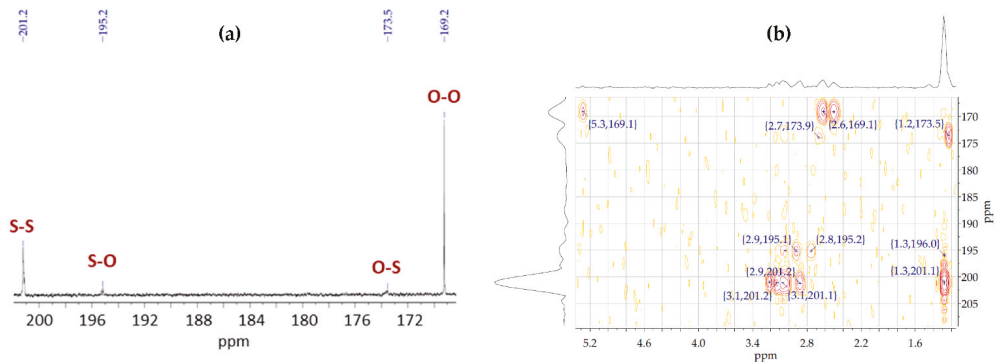


Figure 5. (a) ^{13}C NMR of Sample 5 (3M2MP 54.8 mol%) showing combination peaks; (b) ^1H - ^{13}C HMBC of Sample 5.

3.3. Molecular Weight and Thermal Properties

The weight-average molecular weight (M_w) of the samples was considered high, varying from 7.7×10^5 to 17.5×10^5 g/mol. The values are in the upper limit of the 1 to 20×10^5 g/mol range commonly found for biosynthesized P(3HB) [34]. In contrast, other PTE and PTE copolymers with 3HB have markedly smaller M_w and M_w/M_n , as reported previously [22–26]. Moreover, except for in Sample 4, decreasing M_w and increasing M_w/M_n trends were observed, possibly because of the increasing amounts of unreacted 3-mercapto-2-methylpropionic acid; at increasing dosage concentrations, this reagent acted as a chain-transfer agent, ultimately decreasing the average molecular weight of the polymer and increasing the number of synthesized chains because of its chain termination function [34].

Based on the thermal properties, the homopolymer (Sample 7) displayed clear amorphous behavior, with a negative T_g and no melting or cold crystallization peaks. Consequently, in Samples 1–3, with increasing amounts of 3M2MP incorporated into the polymer structure, T_g and ΔH_m decreased until only T_g remained, resulting in amorphous characteristics for Sample 4. Samples 5 and 6 exhibited different behaviors. The 3M2MP unit content of Sample 5 was similar to that of Sample 4 but was not amorphous. Sample 5 had two T_g peaks with lower ΔH_m and T_{cc} values but a higher T_m compared with those of Sample 3. This finding may be related to differences in its microstructure compared with that of Sample 4. The T_g and T_{cc} of Sample 6 were similar to those of Sample 1; however, this sample exhibited a higher T_m and ΔH_m , possibly because of its higher crystallinity, higher M_w and M_w/M_n , and lower 3M2MP fraction, despite the higher precursor addition. Moreover, as there are no published reports of biosynthesis and material property of its equivalent oxoester polymer [35,36], we could not confirm the high thermal stability of P(3M2MP). However, compared with other bio-PTE homopolymers, P(3M2MP) is the first amorphous PTE [25].

Table 3 shows the results of the molecular weight and thermal property analyses of the samples, whereas Figure 6a,b show the 1st and 2nd heating scans, respectively.

Table 3. Molecular weight and thermal properties of the samples.

Sample ID	3M2MP (mol%)	M_w ($\times 10^5$)	M_w/M_n	T_g ($^{\circ}\text{C}$)	T_{cc} ($^{\circ}\text{C}$)	T_m ($^{\circ}\text{C}$)	ΔH_m (J/g)
P(3HB) ¹	0	5.2	2.3	4.0	NA	176	79
1	5.5	14.6	3.3	8.1	57	150, 164	28
2	10.1	12.0	3.2	6.6	62	149, 164	26
3	34.2	10.0	3.6	5.4	70	159, 173	13
4	53.9	13.7	4.4	-1.2	-	-	-
5	54.8	7.7	4.2	-3.1, 7.0	65	167, 179	9
6	10.7	17.5	5.6	8.4	50	166, 181	51
7	100	15.0	2.6	-3.1	-	-	-

NA: not available, -: not detectable. ¹ Data from Ref. [19].

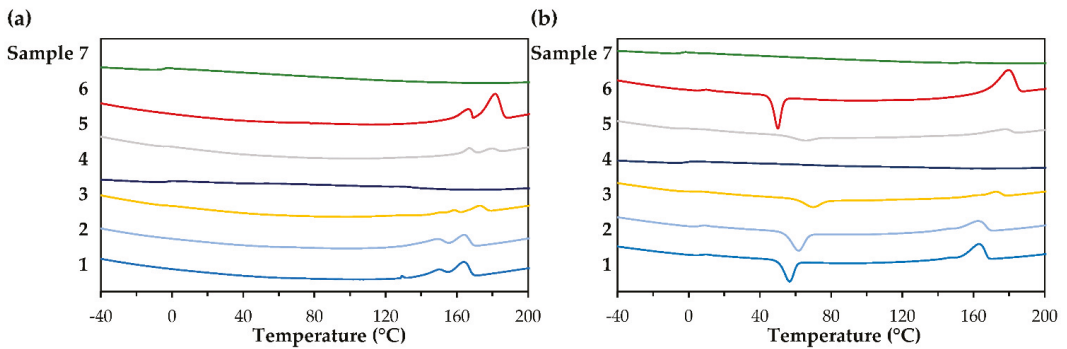


Figure 6. DSC thermogram of Samples 1 (3M2MP 5.5 mol%), 2 (10.1 mol%), 3 (34.2 mol%), 4 (53.9 mol%), 5 (54.8 mol%), 6 (10.7 mol%), and 7 (100 mol%). (a) 1st heating scan; (b) 2nd heating scan.

3.4. Physical and Mechanical Properties

Figure 7 shows the physical aspects of the polymer films as the 3M2MP fraction increased from 5.5 mol% to 100 mol%. Accordingly, the polymers became more transparent and softer as the 3M2MP content increased. Notably, the homopolymer tends to be very sticky, leading to handling difficulties.

Table 4 shows the mechanical properties based on the physical observations. As the 3M2MP fraction increased from Samples 1 to 7, the yield strength, tensile strength, and Young’s modulus decreased, whereas elongation at break increased. Sample 6 differed from the other samples, as explained above. The 3M2MP unit conferred the copolymers with great flexibility, allowing them to achieve over 1500% elongation at break with only 53.9 mol% of 3M2MP. Although Sample 5 showed similar 3M2MP contents to Sample 4, it exhibited a significantly lower elongation of break. This difference may be related to its lower molecular weight and differences in the degree of the block sequence (Tables 2 and 3). Therefore, the sequence distribution may greatly affect the mechanical properties of the copolymers [37]. The stress–strain curves of all samples are shown in Figure 8.

The homopolymer also showed exceptional elasticity, with 2605% of elongation at break. Notably, most deformation was instantly recoverable. Figure 9 shows the elongation and recovery after manual deformation.

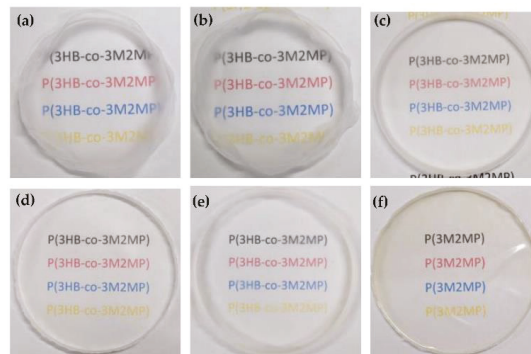


Figure 7. Polymer solvent cast films with increasing 3M2MP units. (a) Sample 1 (5.5 mol% 3M2MP); (b) Sample 2 (10.1 mol%); (c) Sample 3 (34.2 mol%); (d) Sample 4 (53.9 mol%); (e) Sample 5 (54.8 mol%); (f) Sample 7 (100 mol%).

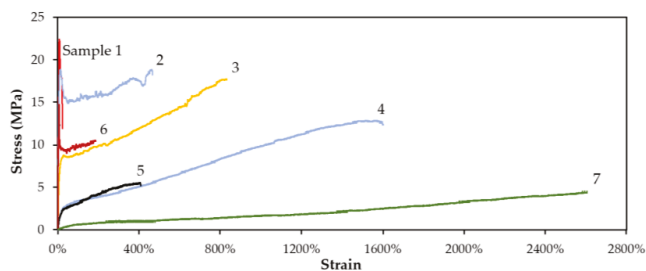


Figure 8. Stress–strain curve of Samples 1 (3M2MP 5.5 mol%), 2 (10.1 mol%), 3 (34.2 mol%), 4 (53.9 mol%), 5 (54.8 mol%), 6 (10.7 mol%), and 7 (100 mol%).

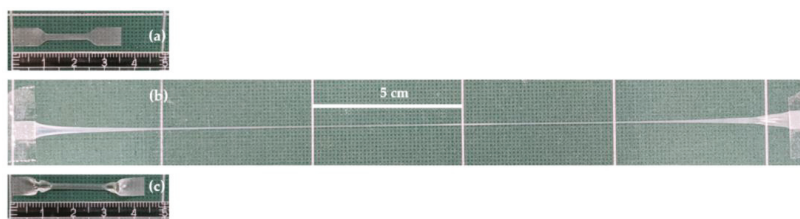


Figure 9. Elongation of P(3M2MP) (Sample 7) by manual deformation. (a) Before deformation; (b) during deformation; (c) after deformation.

Table 4. Mechanical properties of the samples ($n = 3$).

Sample ID	3M2MP (mol%)	Yield Strength (MPa)	Tensile Strength (MPa)	Elongation at Break (%)	Young’s Modulus (MPa)
P(3HB) ¹	0	NA ²	58 ± 7	12 ± 0	1420 ± 80
1	5.5	13.6 ± 2.0	23.0 ± 2.3	24 ± 13	880 ± 75
2	10.1	14.6 ± 2.2	19.3 ± 3.0	470 ± 131	644 ± 41
3	34.2	6.5 ± 0.3	17.1 ± 0.8	825 ± 21	87 ± 8
4	53.9	2.2 ± 0.1	12.7 ± 0.2	1549 ± 103	13 ± 1
5	54.8	1.3 ± 0.2	5.8 ± 0.4	436 ± 49	18 ± 1
6	10.7	8.2 ± 3.5	15.5 ± 1.4	158 ± 58	709 ± 303
7	100	1.0 ± 0.1	4.2 ± 0.5	2605 ± 4	0.8 ± 0.1

¹ Ref. [19], ² Not available.

4. Discussion

NMR spectroscopy confirmed that P(3M2MP) homopolymer and copolymers with 3HB were biosynthesized by recombinant *E. coli* LSBJ using a similar method to previous studies to produce P(3H2MB) and its copolymers [19,38]. The biosynthesis data indicated that the maximum uptake of 3-mercapto-2-methylpropionic acid by the cells occurred under the culture conditions used in this study, unlike those observed for other sulfuric fatty acids [22–24]. Notably, the polymer content achieved for copolymer production was markedly higher than that observed for other P(3HB-co-3-mercaptoalkanoate)s [22–24], demonstrating that the point mutation D4N in PhaP_{Ac} and double-point mutations NSDG in PhaC_{Ac} lead to high polymer accumulation and high incorporation of 3M2MP unit into the 3HB copolymer. These findings indicate the relatively high polymerization activity of PhaC_{Ac} NSDG for 3M2MP unit. The lower production of the homopolymer relative to its 3HB copolymers suggests that the presence of 3HB unit facilitates the polymerization of 3M2MP unit by PhaC_{Ac} NSDG.

In contrast to P(3MP) and other bio-PTEs [25,39], P(3M2MP) can be easily dissolved in chloroform for extraction; however, the range of solvent solubility, which may impact

its recovery from cells, remains unclear. Thakor et al. [40] efficiently extracted a PTE homopolymer from cells containing up to 45 wt% polymer by adding SDS to the cultivation broth, performing intensive stirring for 20 min at 90 °C, and conducting centrifugation and water rinsing cycles. This extraction method may also be applied to P(3M2MP).

Based on the sequence distribution, the D values of the copolymers were markedly higher than those typically found for most PHA copolymers [32,41,42] and other P(3HB-co-3-mercaptopalkanoate)s [26,43], indicating a high block sequence distribution. When the amount of 3M2MP precursor added to the medium was small, the degree of the block sequence tended to be high (Table 2) because polymerization of the 3HB monomer was prioritized over that of the 3M2MP monomer. Therefore, increasing the amount of 3M2MP precursor increased the intracellular 3M2MP concentration, which facilitated the polymerization of 3M2MP, thereby reducing the degree of block sequence in the biosynthesized copolymers. However, as the copolymers were not fractionated with a solvent depending on the solubility difference between the 3M2MP and 3HB units, some polymer samples may be blends of copolymers with different comonomer compositions.

The molecular weight of the copolymers was exceptionally high compared with that of normally biosynthesized P(3HB) but showed a decreasing trend with higher addition of 3M2MP precursor, which may induce a chain-transfer reaction during polymerization [34]. Moreover, regarding its thermal properties, in contrast to other bio-PTEs [25], P(3M2MP) exhibited amorphous behavior, possibly because a racemic 3M2MP precursor was used. Therefore, as the 3M2MP fraction in the copolymer increased, T_g and ΔH_m decreased. On the other hand, Huang et al. [44] demonstrated that the higher thioester linkage contents in 3HB-based copolymers may lead to higher thermal stability by reducing thermal degradation by hindering random scission of the polymer chain. Thus, thermal degradation study of P(3M2MP) and its copolymers are of interest as a potential target for thermostable material.

P(3M2MP) showed extraordinary elongation at break and instant recovery, indicating that its elasticity is higher than those of most commercial elastomeric polymers, such as natural or synthetic rubber (typically ranging from 100% to 800%) [45–47], or well-known elastic PHAs, such as poly(4-hydroxybutyrate), which have copolymer and/or homopolymer elongations of approximately 1000% [48]. Because P(3HB-co-3MP) also has significant elastic properties [26], the superior elasticity of PTE may be related to the sulfur atom in the polymer backbone. Because the Pauling electronegativity of the sulfur atom (2.58) is markedly lower than that of the oxygen atom (3.44) and closer to the carbon atom (2.55) [25], the smaller difference in electronegativity may enable easier mobilization of the polymer structure during stretching [26]. α -Carbon methylation of 3M2MP may also affect its mechanical properties by hindering packing of the polymer structure.

Despite the lack of oxoester-equivalent polymers for analogy, a unique property of α -methylated monomers in their materials can be identified relative to those in other PTEs. It is interesting to study the biodegradability of P(3M2MP) because P(3MP), a non- α -methylated PTE, does not show biodegradability [49]. Bacterial PTEs are now considered non-biodegradable biopolymers [50]. Although the biodegradability of P(3MB) and P(3MV) has not been evaluated, other enzymatically polymerized PTEs were reported to be degradable with lipase [51].

Author Contributions: Conceptualization, L.V.S.C., M.M. and T.T.; methodology, L.V.S.C., M.M., Y.M. and T.T.; software, L.V.S.C. and M.M.; validation, M.M., H.A. and T.T.; formal analysis, L.V.S.C. and M.M.; investigation, L.V.S.C. and M.M.; resources, C.T.N., S.T. and T.T.; data curation, L.V.S.C.; writing—original draft preparation, L.V.S.C.; writing—review and editing, T.T.; visualization, L.V.S.C. and T.T.; supervision, T.T.; project administration, T.T.; funding acquisition, T.T. All authors have read and agreed to the published version of the manuscript.

Funding: This paper is based on the results obtained from a project, JPNP18016, commissioned by the New Energy and Industrial Technology Development Organization (NEDO) and partially supported by a Grant-in-Aid for Scientific Research (KAKENHI, 21H03640), Japan.

Institutional Review Board Statement: Not applicable.

Informed Consent Statement: Not applicable.

Data Availability Statement: Not applicable.

Acknowledgments: The authors acknowledge the Biomaterials Analysis Division and Materials Analysis Division, Open Facility Center, Tokyo Institute of Technology, for their support with DNA sequencing analysis and NMR measurements, respectively.

Conflicts of Interest: The authors declare no conflict of interest.

References

1. PlasticsEurope. Plastics the Facts-2021. Available online: <https://plasticseurope.org/wp-content/uploads/2021/12/Plastics-the-Facts-2021-web-final.pdf> (accessed on 16 February 2022).
2. Geyer, R.; Jambeck, J.R.; Law, K.L. Production, use, and fate of all plastics ever made. *Sci. Adv.* **2017**, *3*, e1700782. [[CrossRef](#)] [[PubMed](#)]
3. Kaza, S.; Yao, L.; Bhada-Tata, P.; van Woerden, P. *What a Waste 2.0: A Global Snapshot of Solid Waste Management to 2050. Urban Development Series*; World Bank: Washington, DC, USA, 2018; ISBN 978-1-4648-1347-4.
4. World Economic Forum; Ellen MacArthur Foundation; McKinsey & Company. The New Plastics Economy—Rethinking the Future of Plastics. Available online: <https://emf.thirdlight.com/link/faarmdpz93ds-5vmvdf/@/preview/1?o> (accessed on 16 February 2022).
5. Ross, G.; Ross, S.; Tighe, B.J. Bioplastics: New routes, new products. In *Brydson's Plastics Materials*, 8th ed.; Gilbert, M., Ed.; Butterworth-Heinemann: Cambridge, MA, USA, 2017; pp. 631–652. ISBN 978-0-323-35824-8.
6. Chen, G.-Q.; Hajnal, I.; Wu, H.; Lv, L.; Ye, J. Engineering biosynthesis mechanisms for diversifying polyhydroxyalkanoates. *Trends Biotechnol.* **2015**, *33*, 565–574. [[CrossRef](#)] [[PubMed](#)]
7. Anjum, A.; Zuber, M.; Zia, K.M.; Noreen, A.; Anjum, M.N.; Tabasum, S. Microbial production of polyhydroxyalkanoates (PHAs) and its copolymers: A review of recent advancements. *Int. J. Biol. Macromol.* **2016**, *89*, 161–174. [[CrossRef](#)] [[PubMed](#)]
8. Choi, S.Y.; Cho, I.J.; Lee, Y.; Kim, Y.-J.; Kim, K.-J.; Lee, S.Y. Microbial polyhydroxyalkanoates and nonnatural polyesters. *Adv. Mater.* **2020**, *32*, 1907138. [[CrossRef](#)] [[PubMed](#)]
9. Suzuki, M.; Tachibana, Y.; Kasuya, K.I. Biodegradability of poly (3-hydroxyalkanoate) and poly (ϵ -caprolactone) via biological carbon cycles in marine environments. *Polym. J.* **2021**, *53*, 47–66. [[CrossRef](#)]
10. Narancic, T.; Verstichel, V.; Chaganti, S.R.; Morales-Gamez, L.; Kenny, S.T.; De Wilde, B.; Padamati, R.B.; O'Connor, K.E. Biodegradable plastic blends create new possibilities for end-of-life management of plastics but they are not a panacea for plastic pollution. *Environ. Sci. Technol.* **2018**, *52*, 10441–10452. [[CrossRef](#)]
11. Choi, S.Y.; Rhie, M.N.; Kim, H.T.; Joo, J.C.; Cho, I.J.; Son, J.; Lee, Y. Metabolic engineering for the synthesis of polyesters: A 100-year journey from polyhydroxyalkanoates to non-natural microbial polyesters. *Metab. Eng.* **2020**, *58*, 47–81. [[CrossRef](#)]
12. Taguchi, S.; Iwata, T.; Abe, H.; Doi, Y. Poly(hydroxyalkanoate)s. In *Polymer Science: A Comprehensive Reference*, 1st ed.; Matyjaszewski, K., Möller, M., Eds.; Elsevier: Amsterdam, The Netherlands, 2012; pp. 157–182. ISBN 978-0-08-087862-1.
13. McAdam, B.; Fournet, M.B.; McDonald, P.; Mojicevic, M. Production of Polyhydroxybutyrate (PHB) and Factors Impacting Its Chemical and Mechanical Characteristics. *Polymers* **2020**, *12*, 2908. [[CrossRef](#)]
14. Yeo, J.C.C.; Muiruri, J.K.; Thitsartarn, W.; Li, Z.; He, C. Recent advances in the development of biodegradable PHB-based toughening materials: Approaches, advantages and applications. *Mater. Sci. Eng. C Mater. Biol. Appl.* **2018**, *92*, 1092–1116. [[CrossRef](#)]
15. Sudesh, K.; Abe, H.; Doi, Y. Synthesis, structure and properties of polyhydroxyalkanoates: Biological polyesters. *Prog. Polym. Sci.* **2000**, *25*, 1503–1555. [[CrossRef](#)]
16. Taguchi, S.; Matsumoto, K. Evolution of polyhydroxyalkanoate synthesizing systems toward a sustainable plastic industry. *Polym. J.* **2021**, *53*, 67–79. [[CrossRef](#)]
17. Ishii-Hyakutake, M.; Mizuno, S.; Tsuge, T. Biosynthesis and characteristics of aromatic polyhydroxyalkanoates. *Polymers* **2018**, *10*, 1267. [[CrossRef](#)] [[PubMed](#)]
18. Brydson, J.A. Silicone and other heat-resisting polymers. In *Plastics Materials*, 7th ed.; Brydson, J.A., Ed.; Butterworth-Heinemann: Oxford, UK, 1999; pp. 814–852. ISBN 0-7506-4132-0.
19. Furutate, S.; Kamoi, J.; Nomura, C.T.; Taguchi, S.; Abe, H.; Tsuge, T. Superior thermal stability and fast crystallization behavior of a novel, biodegradable α -methylated bacterial polyester. *NPG Asia Mater.* **2021**, *13*, 31. [[CrossRef](#)]
20. Marvel, C.S.; Kotch, A. Polythioesters. *J. Am. Chem. Soc.* **1951**, *73*, 1100–1102. [[CrossRef](#)]
21. Xia, Y.; Wübbeler, J.H.; Qi, Q.; Steinbüchel, A. Employing a recombinant strain of *Advenella mimigardefordensis* for biotechnical production of homopolythioesters from 3,3'-dithiodipropionic acid. *Appl. Environ. Microbiol.* **2012**, *78*, 3286–3297. [[CrossRef](#)]
22. Lütke-Eversloh, T.; Bergander, K.; Luftmann, H.; Steinbüchel, A. Identification of a new class of biopolymer: Bacterial synthesis of a sulfur-containing polymer with thioester linkages. *Microbiol. Read.* **2001**, *147*, 11–19. [[CrossRef](#)]
23. Lütke-Eversloh, T.; Bergander, K.; Luftmann, H.; Steinbüchel, A. Biosynthesis of poly(3-hydroxybutyrate-co-3-mercaptoputyrate) as a sulfur analogue to poly(3-hydroxybutyrate) (PHB). *Biomacromolecules* **2001**, *2*, 1061–1065. [[CrossRef](#)]

24. Lütke-Eversloh, T.; Steinbüchel, A. Novel precursor substrates for polythioesters (PTE) and limits of PTE biosynthesis in *Ralstonia eutropha*. *FEMS Microbiol. Lett.* **2003**, *221*, 191–196. [CrossRef]
25. Lütke-Eversloh, T.; Fischer, A.; Remminghorst, U.; Kawada, J.; Marchessault, R.H.; Bögershausen, A.; Kalwei, M.; Eckert, H.; Reichelt, R.; Liu, S.J.; et al. Biosynthesis of novel thermoplastic polythioesters by engineered *Escherichia coli*. *Nat. Mater.* **2002**, *1*, 236–240. [CrossRef]
26. Yu, F.; Dong, T.; Zhu, B.; Tajima, K.; Yazawa, K.; Inoue, Y. Mechanical properties of comonomer-compositionally fractionated poly[(3-hydroxybutyrate)-*co*-(3-mercaptopropionate)] with low 3-mercaptopropionate unit content. *Macromol. Biosci.* **2007**, *7*, 810–819. [CrossRef]
27. Watanabe, Y.; Ishizuka, K.; Furutate, S.; Abe, H.; Tsuge, T. Biosynthesis and characterization of novel poly(3-hydroxybutyrate-*co*-3-hydroxy-2-methylbutyrate): Thermal behavior associated with α -carbon methylation. *RSC Adv.* **2015**, *5*, 58679. [CrossRef]
28. Tappel, R.C.; Wang, Q.; Nomura, C.T. Precise control of repeating unit composition in biodegradable poly(3-hydroxyalkanoate) polymers synthesized by *Escherichia coli*. *J. Biosci. Bioeng.* **2012**, *113*, 480–486. [CrossRef] [PubMed]
29. Ushimaru, K.; Watanabe, Y.; Hiroe, A.; Tsuge, T. A single-nucleotide substitution in phasin gene leads to enhanced accumulation of polyhydroxyalkanoate (PHA) in *Escherichia coli* harboring *Aeromonas caviae* PHA biosynthetic operon. *J. Gen. Appl. Microbiol.* **2015**, *61*, 63–66. [CrossRef] [PubMed]
30. Tsuge, T.; Watanabe, S.; Shimada, D.; Abe, H.; Doi, Y.; Taguchi, S. Combination of N149S and D171G mutations in *Aeromonas caviae* polyhydroxyalkanoate synthase and impact on polyhydroxyalkanoate biosynthesis. *FEMS Microbiol. Lett.* **2007**, *277*, 217–222. [CrossRef]
31. Arikawa, H.; Sato, S.; Fujiki, T.; Matsumoto, K. Simple and rapid method for isolation and quantitation of polyhydroxyalkanoate by SDS-sonication treatment. *J. Biosci. Bioeng.* **2017**, *124*, 250–254. [CrossRef] [PubMed]
32. Kamiya, N.; Yamamoto, Y.; Inoue, Y.; Chujo, R.; Doi, Y. Microstructure of bacterially synthesized poly(3-hydroxybutyrate-*co*-3-hydroxyvalerate). *Macromolecules* **1989**, *22*, 1676–1682. [CrossRef]
33. Socrates, G. The Carbonyl Group: C=O. In *Infrared and Raman Characteristic Group Frequencies: Tables and Charts*, 3rd ed.; Socrates, G., Ed.; John Wiley & Sons, Ltd.: Chichester, UK, 2001; pp. 115–156. ISBN 978-0-470-09307-8.
34. Tsuge, T. Fundamental factors determining the molecular weight of polyhydroxyalkanoate during biosynthesis. *Polym. J.* **2016**, *48*, 1051–1057. [CrossRef]
35. Marx, A.; Poetter, M.; Buchholz, S.; May, A.; Siegert, H.; Alber, B.; Fuchs, G.; Eggeling, L. Microbiological Production Of 3-Hydroxyisobutyric Acid. Available online: <https://patentimages.storage.googleapis.com/1a/8f/54/e04f10eb8e2206/CA2654133A1.pdf> (accessed on 27 February 2022).
36. Vermeer, C.M.; Bons, L.J.; Kleerebezem, R. Production of a newly discovered PHA family member with an isobutyrate-fed enrichment culture. *Appl. Microbiol. Biotechnol.* **2022**, *106*, 605–618. [CrossRef]
37. Kajita, T.; Noro, A.; Matsushita, Y. Design and properties of supramolecular elastomers. *Polymer* **2017**, *128*, 297–310. [CrossRef]
38. Furutate, S.; Abe, H.; Tsuge, T. Thermal properties of poly(3-hydroxy-2-methylbutyrate-*co*-3-hydroxybutyrate) copolymers with narrow comonomer-unit compositional distributions. *Polym. J.* **2021**, *53*, 1451–1457. [CrossRef]
39. Kawada, J.; Lütke-Eversloh, T.; Steinbüchel, A.; Marchessault, R.H. Physical properties of microbial polythioesters: Characterization of poly(3-mercaptopalkanoates) synthesized by engineered *Escherichia coli*. *Biomacromolecules* **2003**, *4*, 1698–1702. [CrossRef]
40. Thakor, N.; Lütke-Eversloh, T.; Steinbüchel, A. Application of the BPEC pathway for large-scale biotechnological production of poly(3-mercaptopropionate) by recombinant *Escherichia coli*, including a novel in situ isolation method. *Appl. Environ. Microbiol.* **2005**, *71*, 835–841. [CrossRef]
41. Hu, D.; Chung, A.L.; Wu, L.P.; Zhang, X.; Wu, Q.; Chen, J.C.; Chen, G.Q. Biosynthesis and characterization of polyhydroxyalkanoate block copolymer P3HB-*b*-P4HB. *Biomacromolecules* **2011**, *12*, 3166–3173. [CrossRef]
42. Tripathi, L.; Wu, L.P.; Chen, J.; Chen, G.Q. Synthesis of Diblock copolymer poly-3-hydroxybutyrate -block-poly-3-hydroxyhexanoate [PHB-*b*-PHHx] by a β -oxidation weakened *Pseudomonas putida* KT2442. *Microb. Cell Fact.* **2012**, *11*, 11. [CrossRef]
43. Impallomeni, G.; Steinbüchel, A.; Lütke-Eversloh, T.; Barbuzzi, T.; Ballistreri, A. Sequencing microbial copolymers of 3-hydroxybutyric and 3-mercaptopalkanoic acids by NMR, electrospray ionization mass spectrometry, and size exclusion chromatography NMR. *Biomacromolecules* **2007**, *8*, 985–991. [CrossRef]
44. Huang, P.; Furutate, S.; Mizuno, S.; Tsuge, T. Thermal degradation behavior of bacterial poly (3-hydroxybutyrate-*co*-3-mercaptopropionate). *Polym. Degrad. Stab.* **2019**, *165*, 35–42. [CrossRef]
45. Goff, J.; Sulaiman, S.; Arkles, B.; Lewicki, J.P. Soft Materials with Recoverable Shape Factors from Extreme Distortion States. *Adv. Mater.* **2016**, *28*, 2393–2398. [CrossRef]
46. Arkles, B.; Goff, J.; Sulaiman, S.; Sikorsky, A. Ultra-High Elongation Silicone Elastomers. Available online: <https://www.gelest.com/wp-content/uploads/2019/08/High-Elongation-Silicone-Elastomers.pdf> (accessed on 27 February 2022).
47. Hiroe, A.; Ishii, N.; Ishii, D.; Kabe, T.; Abe, H.; Iwata, T.; Tsuge, T. Uniformity of monomer composition and material properties of medium-chain-length polyhydroxyalkanoates biosynthesized from pure and crude fatty acids. *ACS Sustain. Chem. Eng.* **2016**, *4*, 6905–6911. [CrossRef]
48. Saito, Y.; Doi, Y. Microbial synthesis and properties of poly(3-hydroxybutyrate-*co*-4-hydroxybutyrate) in *Comamonas acidovorans*. *Int. J. Biol. Macromol.* **1994**, *16*, 99–104. [CrossRef]

49. Kim, D.Y.; Lütke-Eversloh, T.; Elbanna, K.; Thakor, N.; Steinbüchel, A. Poly(3-mercaptopropionate): A nonbiodegradable biopolymer? *Biomacromolecules* **2005**, *6*, 897–901. [[CrossRef](#)]
50. Steinbüchel, A. Non-biodegradable biopolymers from renewable resources: Perspectives and impacts. *Curr. Opin. Biotechnol.* **2005**, *16*, 607–613. [[CrossRef](#)]
51. Kato, M.; Toshima, K.; Matsumura, S. Preparation of aliphatic poly(thioester) by the lipase-catalyzed direct polycondensation of 11-mercaptoundecanoic acid. *Biomacromolecules* **2005**, *6*, 2275–2280. [[CrossRef](#)]

Article

Subcritical Water as a Pre-Treatment of Mixed Microbial Biomass for the Extraction of Polyhydroxyalkanoates

Liane Meneses ¹, Asiyah Esmail ^{2,3}, Mariana Matos ^{2,3}, Chantal Sevrin ⁴, Christian Grandfils ⁴, Susana Barreiros ¹, Maria A. M. Reis ^{2,3}, Filomena Freitas ^{2,3,*} and Alexandre Paiva ^{1,*}

- ¹ LAQV-REQUIMTE, Department of Chemistry, School of Science and Technology, NOVA University Lisbon, 2819-516 Caparica, Portugal; lp.meneses@campus.fct.unl.pt (L.M.); sfb@fct.unl.pt (S.B.)
² UCIBIO—Applied Molecular Biosciences Unit, Department of Chemistry, School of Science and Technology, NOVA University Lisbon, 2819-516 Caparica, Portugal; a.esmail@campus.fct.unl.pt (A.E.); m.matos@campus.fct.unl.pt (M.M.); amr@fct.unl.pt (M.A.M.R.)
³ Associate Laboratory i4HB-Institute for Health and Bioeconomy, School of Science and Technology, NOVA University Lisbon, 2819-516 Caparica, Portugal
⁴ CEIB-Interfaculty Research Centre of Biomaterials, University of Liege, B-4000 Liege, Belgium; csevrin@uliege.be (C.S.); c.grandfils@uliege.be (C.G.)
* Correspondence: a4406@fct.unl.pt (F.F.); abp08838@fct.unl.pt (A.P.)

Abstract: Polyhydroxyalkanoate (PHA) recovery from microbial cells relies on either solvent extraction (usually using halogenated solvents) and/or digestion of the non-PHA cell mass (NPCM) by the action of chemicals (e.g., hypochlorite) that raise environmental and health hazards. A greener alternative for PHA recovery, subcritical water (SBW), was evaluated as a method for the dissolution of the NPCM of a mixed microbial culture (MMC) biomass. A temperature of 150 °C was found as a compromise to reach NPCM solubilization while mostly preventing the degradation of the biopolymer during the procedure. Such conditions yielded a polymer with a purity of 77%. PHA purity was further improved by combining the SBW treatment with hypochlorite digestion, in which a significantly lower hypochlorite concentration (0.1%, *v/v*) was sufficient to achieve an overall polymer purity of 80%. During the procedure, the biopolymer suffered some depolymerization, as evidenced by the lower molecular weight (M_w) and higher polydispersity of the extracted samples. Although such changes in the biopolymer's molecular mass distribution impact its mechanical properties, impairing its utilization in most conventional plastic uses, the obtained PHA can find use in several applications, for example as additives or for the preparation of graft or block co-polymers, in which low- M_w oligomers are sought.

Keywords: polyhydroxyalkanoate (PHA); poly(3-hydroxybutyrate-co-3-hydroxyvalerate) (P(HB-co-HV)); mixed microbial culture (MMC); hypochlorite digestion; subcritical water (SBW)

Citation: Meneses, L.; Esmail, A.; Matos, M.; Sevrin, C.; Grandfils, C.; Barreiros, S.; Reis, M.A.M.; Freitas, F.; Paiva, A. Subcritical Water as a Pre-Treatment of Mixed Microbial Biomass for the Extraction of Polyhydroxyalkanoates. *Bioengineering* **2022**, *9*, 302. <https://doi.org/10.3390/bioengineering9070302>

Academic Editor: Martin Koller

Received: 31 May 2022

Accepted: 6 July 2022

Published: 8 July 2022

Publisher's Note: MDPI stays neutral with regard to jurisdictional claims in published maps and institutional affiliations.



Copyright: © 2022 by the authors. Licensee MDPI, Basel, Switzerland. This article is an open access article distributed under the terms and conditions of the Creative Commons Attribution (CC BY) license (<https://creativecommons.org/licenses/by/4.0/>).

1. Introduction

Over the past few decades, polyhydroxyalkanoate (PHA) production has drawn considerable attention and intensive work has been undertaken to convert these biodegradable and biocompatible polymers into viable competitors of oil-based plastics. Production processes have been optimized and their costs have already decreased significantly [1]. However, the downstream processes for polymer recovery from cells, and their purification, still hinder PHAs' wider implementation [2,3]. Given the intracellular nature of PHAs, their release from the surrounding biomass requires cells to rupture, allowing the subsequent separation of the polymer from the non-PHA cell mass (NPCM) [4]. The procedures currently used consist of solvent extraction or digestion methods. Solvent extraction mainly requires halogenated solvents (e.g., chloroform, methylene chloride, 1,2-dichloroethane) for PHAs' dissolution, which results in high extraction yields and highly pure biopolymers with low endotoxin contents [4–6]. Digestion methods, on the other hand, target the NPCM

by the action of chemicals (e.g., sodium hypochlorite, acids), surfactants, enzymes, or biological agents, as reviewed by Pérez-Rivero et al. (2019) [6]. Although the digestion methods present a lower toxicity for human health and require a lower investment, they can affect the polymers' properties while producing high volumes of wastewater which raise environmental concerns with recycling difficulties [6].

Due to its strong oxidizing properties, hypochlorite has been frequently used to degrade most of the NPCM (proteins, lipids, carbohydrates, nucleic acids) into water-soluble compounds. However, most of the studies reported in the literature are referring to a large range of this oxidation agent, making comparison very difficult between these investigations. However, in general, sodium hypochlorite was used at concentrations ranging from 1.05 wt.% to 12.1 wt.% [7–11], and large volumes of the reactant solution were required. Variable extraction yields (70–100 wt.%) and polymer purities (88–98%) were attained depending on the reaction time (1–12 h) and temperature (from room temperature to 37 °C) [7–11]. Although the procedure's conditions can be adjusted to reach high extraction yields (>70 wt.%) and polymer purities (up to 98%), the treatment with hypochlorite affects the quality of the obtained PHA by impacting its molecular weight (M_w) and polydispersity index (PDI) [2,3,12]. Hypochlorite digestion was reported to decrease the biopolymer's M_w and to raise its PDI. Such alterations of PHAs' quality may compromise the final polymer applications [5], particularly in terms of mechanical and thermal properties [11,13,14]. Indeed, PHAs with a M_w below 400 kDa have a lower resistance to mechanical stress [13,14], with a M_w above 600 kDa representing a threshold to fit to thermoplastic applications [11]. Another drawback of the procedure is the difficulty in completely removing traces of hypochlorite from the recovered PHA. Moreover, the utilization of hypochlorite can generate toxic halogenated compounds [4].

In line with this, considerable efforts have been made to develop alternative and greener methods for PHA recovery with high yields and purity degrees, comparable to those obtained with the use of organic solvents. Alternative solvents, such as ionic liquids [15] and supercritical CO_2 [16], have been proposed but did not reach the desired PHA yield or purity degree. Due to its dissolution and hydrolysis capacity, subcritical water (SBW) has been used for the extraction of several added value compounds from different sources. At high pressure and temperature in the liquid state, the properties of water change: its density is slightly decreased when compared to water at an ambient pressure and temperature (around 900 mg/L), its dielectric constant also decreases with temperature, and its ionic product increases—reaching values as high as -12 , while water at ambient conditions reaches -14 [17]. Such changes confer water with the ability to dissolve or even hydrolyze several macromolecules, including proteins, polysaccharides, and lipids [18]. SBW has been used for the extraction of phenolic compounds and carbohydrates from red and white wine grape pomace [19,20], as well as from cork [21]. It has also been used to obtain purified cellulose from sesame seed hulls [22]. Moreover, SBW has also demonstrated its capacity to extract proteins, peptides, and amino acids from codfish frames [23]. Therefore, due to its characteristics, SBW shows the potential to be used as a green solvent for PHA extraction, since it can hydrolyze and dissolve NPCM components such as the cell membrane's proteins [23] and phospholipids [24].

This work focused on evaluating the feasibility of applying SBW for PHA recovery from the biomass of a mixed microbial culture (MMC). SBW treatment was applied at different temperatures for NPCM solubilization and the procedure's efficiency was evaluated in terms of recovery yield and polymer purity, and through the polymer's physical–chemical properties. Furthermore, the SBW treatment was also combined with hypochlorite digestion as a strategy to improve the extraction procedure. The obtained polymers were characterized for their composition, molecular mass distribution, thermal properties, and crystallinity. To the best of our knowledge, this work reports, for the first time, the use of SBW for PHA extraction in a manner that minimizes the utilization of harmful chemicals such as hypochlorite.

2. Materials and Methods

2.1. Biomass Production

The PHA-containing biomass was obtained by cultivation of an MMC in a three-stage bioprocess, as described in [25], using fermented fruit waste as a feedstock. To prevent PHA degradation, the cultivation broth collected from the final stage was acidified to pH 2–3 and stored at 4 °C until further use. Prior to the extraction experiments, the acidified cultivation broth was neutralized by the addition of NaOH 5 M and centrifuged ($10,375\times g$, for 10 min, at 20 °C). The supernatant was discarded, while the biomass pellet was washed with deionized water and centrifuged again under the same conditions. The washed biomass was lyophilized for 48 h, at $-50\text{ }^{\circ}\text{C}$ and 0.8 mBar. The freeze-dried biomass was stored in closed plastic bags at $-20\text{ }^{\circ}\text{C}$ until required for the extraction experiments.

2.2. Polymer Extraction with Chloroform

Solvent extraction with chloroform was used as the reference extraction method, as well as to purify the PHA obtained from the different extraction methods, before the characterization processes. The polymer was extracted from the lyophilized biomass in a Soxhlet apparatus, as described in [26]. Briefly, 5 g of dried biomass was extracted with 250 mL chloroform, at 80 °C, over 24 h. The obtained polymer solution was left in a fume hood overnight for partial solvent evaporation. Afterwards, the polymer was precipitated in cold ethanol (1:10, *v/v*), under vigorous stirring. Finally, the polymer was dried at room temperature until reaching a constant weight.

2.3. NPCM Digestion with Sodium Hypochlorite

The lyophilized biomass (~0.2 g) was suspended in 5 mL of a sodium hypochlorite solution at a concentration of 5.0% (*v/v*). The digestion was conducted at room temperature, for 3 h as described in [9], under constant stirring (200 rpm). The samples were centrifuged ($7012\times g$, 10 min, 20 °C) and the pellets were washed with deionized water until a neutral pH was reached. Finally, the polymer samples were freeze dried and kept in closed flasks, at room temperature.

2.4. Subcritical Water-Assisted Extraction

The lyophilized biomass was subjected to SBW treatment at different temperatures between 130 and 200 °C, using an SBW apparatus (Figure 1) operated as described in [20]. Briefly, the HiP stainless-steel reactor was filled with lyophilized biomass between two layers of glass spheres (6 mm diameter) and placed inside the electric oven. Water was pumped into the reactor through a high-pressure tube at a flow rate of 10 mL/min, using a Knauer 40 preparative pump 1800 coupled to a Rheonik Rhe 01.03 unit. After pressurizing the system, the heating cords and the oven were turned on. The water temperature increased at an average rate of 1.2 °C/min until the desired value was reached and maintained for 30 min. The pressure of the entire system was maintained by a Tescom back pressure regulator (BPR), set at 80 bar. The recovered biomass was collected from the reactor and dried in an oven at 60 °C, until it reached a constant weight. The polymer content in the samples was determined by Soxhlet extraction with chloroform, as described in Section 2.1.

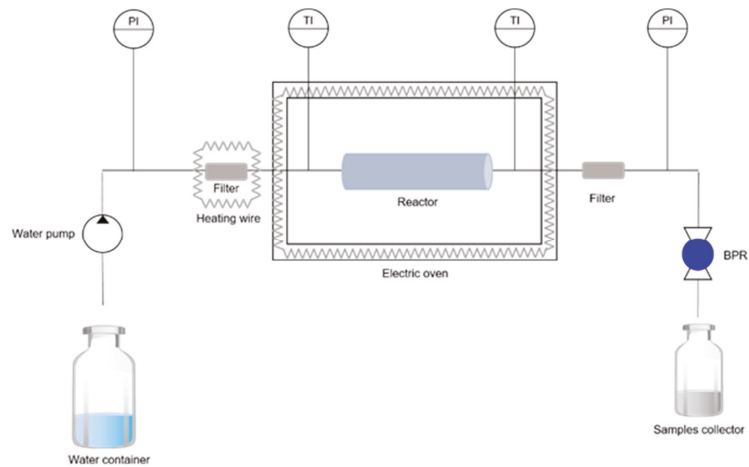


Figure 1. Schematic representation of the SBW apparatus used for SBW treatment. PI: pressure indicators; TI: temperature indicators.

2.5. Hypochlorite Digestion of the SBW Treated Biomass

Dried SBW-treated (150 °C) biomass samples (~0.2 g) were suspended in deionized water (5 mL) and digested with different hypochlorite contents, namely, 0.1, 0.5, 3.0, and 5.0% (v/v). The digestion was conducted as described in Section 2.3. The polymer samples were freeze dried and kept in closed flasks, at room temperature.

2.6. Calculations

For each procedure, the recovery yield (%) was determined as follows:

$$\text{Recovery yield} = \frac{m_{\text{product}}}{m_{\text{biomass}}} \times 100 \% \quad (1)$$

where m_{product} is the dry mass of the sample (g) obtained with each extraction procedure and m_{biomass} is the mass of the dry biomass (g) used for each procedure. In the case of the standard extraction with chloroform, the recovery yield corresponds to the extracted PHA. For the SBW treatments and hypochlorite extraction, the recovery yield corresponds to a mixture of PHA and NPCM. The purity of the samples was determined by gas chromatography (GC) as described in [26], with slight modifications. Briefly, samples (2–5 mg) were hydrolyzed with 1 mL 20% (v/v) sulfuric acid in methanol solution and 1 mL heptadecane in chloroform (1 g/L), at 100 °C for 3.5 h. After hydrolysis, 1 mL of deionized water was added. After separation of the organic and aqueous phases, the organic phase, with the resulting methyl esters, was analyzed in a chromatograph 430-GC Bruker equipped with a Crossbond, Stabilwax column (Restek, Bellefonte, PA, USA). Analysis was performed at a constant 14.5 psi pressure, using helium as a carrier gas. The calibration curve was prepared with poly(3-hydroxybutyrate-co-3-hydrovalerate), P(HB-co-HV), (Sigma-Aldrich, Saint Louis, MA, USA, 88 mol% 3-HB, 12 mol% 3-HV) dissolved in chloroform at concentrations ranging from 0.053 to 6.750 g/L, with heptadecane as an internal standard (1.0 g/L).

2.7. Polymer Characterization

All polymer samples used for characterization procedures were previously purified from the remaining NPCM, using Soxhlet extraction with chloroform as described in Section 2.1.

2.7.1. Composition

The polymers' compositions were determined by GC as described in Section 2.6.

2.7.2. Molecular Mass Distribution

The polymers' molecular weight (M_w and M_n) and polydispersity index (PDI) were analyzed by size exclusion chromatography (SEC). For this analysis, 15 mg polymer samples was dissolved in 15 mL of chloroform for 18 h at room temperature. The samples were then filtered with glass fiber filters (47 mm, PALL). The analysis was performed in a Waters Millennium system with chloroform as an eluent with a rate of 1 mL/min. Relative average molecular weights were determined against polystyrene standards using the universal calibration curve.

2.7.3. Thermal Properties

Differential scanning calorimetry (DSC) analysis was performed using a differential scanning calorimeter DSC 131 (Setaram, Caluire, France). The samples were placed in aluminum crucibles and analyzed in a temperature range between -90 and 220 °C, with heating and cooling speeds of 10 °C/min. Thermogravimetric analysis (TGA) was performed using the thermogravimetric equipment Labsys EVO (Setaram, Caluire, France). Samples were placed in aluminum crucibles and analyzed in a temperature range between 25 and 500 °C, at 10 °C/min. The crystallinity index (X_c , %) of the samples was estimated as the ratio between the melting enthalpy (ΔH_m , J g⁻¹) of its melting peak and the melting enthalpy of 100% crystalline P(3HB), previously reported to be 146 J g⁻¹ [27].

3. Results and Discussion

3.1. Solvent Extraction with Chloroform and Hypochlorite Digestion

The original biomass had a PHA content of 66 wt.%, which was determined by Soxhlet extraction with chloroform. The obtained polymer was a 3-hydroxybutyrate and 3-hydroxyvalerate (3-HB/3-HV) co-polymer, P(HB-co-HV), with a 3-HV content of 18 wt.% (Figure S1), which is within the range reported for P(HB-co-HV) produced by MMC from several agri-food wastes (13–24 wt.%) [25,28–30].

Soxhlet extraction with chloroform, of the original biomass, was performed as a reference method for the comparison of the original polymer's properties with those obtained with hypochlorite digestion and SBW treatments. The procedure resulted in an extraction yield of 66 wt.% and a purity of 91 wt.% (Table 1). The chloroform-extracted polymer had a M_w of 3.0×10^5 g/mol and a low PDI of 1.3 (Table 1), which shows its homogeneity in terms of molecular chain length. These values are of the same order of magnitude as those reported for P(HB-co-HV) obtained from MMC by extraction with chloroform (M_w between 2.5×10^5 and 6.4×10^5 g/mol; PDI between 1.3 and 2.5) [25,28–30]. The polymer's thermal properties, melting temperature (T_m) of 153 °C and degradation temperature (T_{deg}) of 283 °C (Table 1), are also within the values reported for other P(HB-co-HV) samples extracted from MMC biomass, namely, a T_m between 147 and 168 °C and T_{deg} between 247 and 278 °C [28,29]. The polymer presented an X_c of 34%, which is in agreement with the values reported for other P(HB-co-HV) samples (18–69%) [31–33].

Hypochlorite digestion of the MMC biomass resulted in a higher recovery yield (75 wt.%) compared to the chloroform extraction procedure (66 wt.%), but the sample's purity was considerably lower (77 wt.%, compared to 91 wt.% for the chloroform-extracted sample) (Table 1), showing that the solubilization of NPCM by hypochlorite was not complete. Nevertheless, this procedure took only 3 h at room temperature, while the Soxhlet extraction with chloroform took 24 h at a temperature of 80 °C (Table 1). Moreover, simpler equipment is used, and sodium hypochlorite is not as hazardous as chloroform, with a lower environmental impact. The polymer's M_w (3.2×10^5 g/mol) and its PDI (1.3) were in the same order of magnitude as those reported for P(HB-co-HV) recovered from biomass by hypochlorite digestion (3.6×10^5 – 6.3×10^5 g/mol and 1.7, respectively) [34,35]. These data show there was no impact on the polymer's molecular mass distribution

compared to the chloroform-extracted sample; however, a decrease in the sample's T_m to 140 °C (Table 1) was observed, as well as a reduction in crystallinity from 34% to 21% (Table 1).

Table 1. Thermal properties and molecular mass distribution of the samples obtained with the different extraction methods tested (T_m , melting temperature; T_{deg} , degradation temperature; M_w , average molecular weight; PDI, polydispersity index; X_c , crystallinity index; 3HV, 3-hydroxyvalerate; RT, room temperature).

Extraction Method	Recovery Yield (%)	Polymer Purity (%)	3-HV Content (wt.%)	M_w (g/mol)	PDI	T_m (°C)	T_{deg} (°C)	X_c (%)
Chloroform (Soxhlet, 80 °C, 24 h)	66 ± 0.92	91 ± 0.82	18 ± 1.1	3.0 × 10 ⁵	1.3	153	283	34
Hypochlorite (5.0%, RT, 3 h)	75 ± 1.1	77 ± 0.91	17 ± 0.10	3.2 × 10 ⁵	1.3	140	277	21
SBW-assisted extraction								
SBW treatment								
130 °C	94 ± 1.3	67 ± 0.67	18 ± 1.1	1.2 × 10 ⁵	5.1	150	278	35
150 °C	88 ± 1.4	77 ± 0.77	17 ± 0.10	5.0 × 10 ⁴	6.0	147	295	40
165 °C	77 ± 1.4	75 ± 0.79	16 ± 0.91	2.3 × 10 ⁴	7.4	141	294	48
180 °C	58 ± 1.0	66 ± 1.06	15 ± 1.3	7.0 × 10 ³	3.9	127	291	51
200 °C	2	(*)	(*)	(*)	(*)	(*)	(*)	(*)
SBW treatment (150 °C) + Hypochlorite								
0.1%	85 ± 1.4	80 ± 0.80	17 ± 1.1	3.0 × 10 ⁴	7.5	136	290	62
0.5%	83 ± 1.3	81 ± 0.59	17 ± 1.1	3.0 × 10 ⁴	4.8	139	287	48
3.0%	83 ± 1.2	82 ± 0.67	17 ± 1.2	3.0 × 10 ⁴	3.1	140	282	49
5.0%	81 ± 1.3	84 ± 0.69	17 ± 1.1	2.8 × 10 ⁴	3.9	141	276	59

(*) The sample was degraded.

3.2. SBW-Assisted Extraction

3.2.1. SBW Treatment

SBW treatment was applied to the MMC biomass samples at temperatures in the range of 130–200 °C. An example of the SBW process is shown in Figure 2. Briefly, the water flow was initiated at room temperature (18–20 °C), and, after being pressurized, the system was heated until the water exiting the reactor attained the desired temperature, which was maintained for 30 min. Approximately 2 h of heating was required for the water exiting the reactor to achieve the desired temperature (in this case, 150 °C), although at the inlet it was reached within less than 1 h. Within the nearly 2 h heating phase of the experiment, there was a mass loss of 0.7 g from the initial 11.5 g of biomass placed inside the reactor, while during the 30 min treatment phase at 150 °C, a further 0.65 g was removed. This corresponds to an overall mass loss of 12%.

As shown in Table 1, by increasing the temperature of the SBW treatment from 130 to 150 °C, there was a decrease in the recovery yield from 94 wt.% to 88 wt.%, accompanied by an increase in the sample's purity from 67 wt.% to 77 wt.%. This indicates that the mass lost during the SBW treatment resulted mostly from the solubilization/hydrolysis of NPCM. However, a reduction in the polymer's M_w , concomitant with an increase in its PDI, was observed for both samples compared to the chloroform and the hypochlorite-extracted samples. This impact was more pronounced for the SBW treatment at 150 °C, in which the obtained polymer had a M_w of 5.0 × 10⁴ g/mol and a PDI of 6.0 (Table 1). These results indicate that the PHA molecules were depolymerized to some extent during the SBW treatment. Moreover, this depolymerization appeared to be correlated with the applied temperature, being accentuated when raising the extraction temperature.

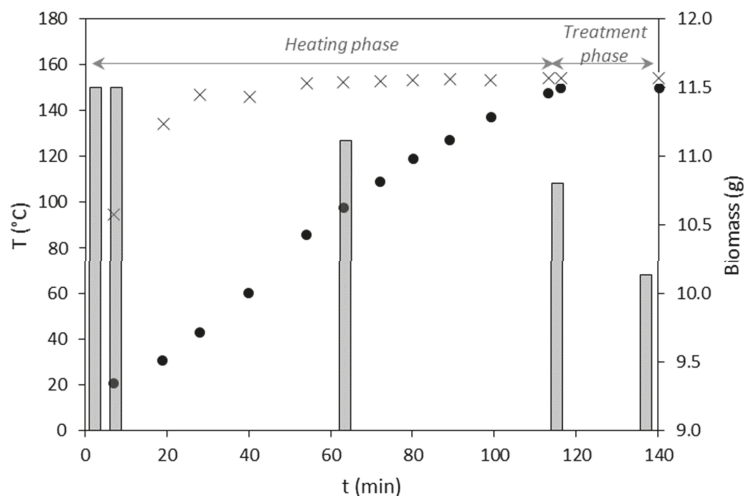


Figure 2. Heating profile of the SBW system (temperature of the water entering (×) and exiting (●) the reactor) and mass of the sample (bars) in the reactor during the assay performed at 150 °C.

The thermal degradation of PHA occurs mainly by random chain scission of the ester bonds, resulting in a gradual reduction in M_w by the formation of smaller polymer fractions, including short oligomers and monomers [36,37]. Studies on P(3HB) show that at temperatures between 160 and 180 °C, there is a significant decrease in the polymer's thermal stability which becomes drastic at temperatures above 200 °C [37,38]. Regarding the co-polymer P(HB-co-HV), which has a higher thermal stability than the homopolymer, a significant decrease in residual mass was only observed at 230 °C [39]. Even though these authors did not observe significant mass alterations, the analysis of M_w and PDI showed that, when the polymer was subjected to 180 °C for 30 min, the M_w decreased by 80%. Increasing the temperature caused even larger decreases in M_w [39]. Hence, exceeding the polymer's melting point seems to be the trigger to initiate chain scissions [39] and, with the exception of SBW treatment at 130 °C, all the temperatures applied in this study were close to, or above, the T_m of P(HB-co-HV). Moreover, the combination of multiple factors can lead to an accelerated degradation process. In this work, we combined temperature and pressure in the SBW treatment, which can explain the reduction in M_w and increase in PDI, even at lower temperatures than those found in the literature.

Increasing the temperature of the SBW treatment to 165 and 180 °C resulted in lower recovery yields (77 and 58 wt.%, respectively) and a lower polymer purity (75 and 66 wt.%, respectively), which suggests that the thermal depolymerization led to the release of soluble monomers and/or short oligomers, which were removed from the sample. This is supported by the observation that the sample extracted at 180 °C had the lowest M_w (7.0×10^3 g/mol), but the PDI was also lower (3.9) (Table 1), suggesting that the short oligomers generated during the procedure were probably solubilized in SBW and washed away.

Further increasing the SBW temperature to 200 °C led to the destruction of the sample and no polymer was recovered after SBW treatment. These results agree with the reported stability of P(HB-co-HV) co-polymers [38,39].

These changes in polymers' molecular chains impacted their thermal properties, with a gradual decrease in the T_m when raising the temperature during the SBW treatment. As highlighted in Table 1, the polymers recovered from the MMC biomass subjected to 165 °C and 180 °C had their T_m decreased by almost 10 °C and over 20 °C, respectively. However, between 130 and 150 °C, the T_m decreased by only 3 °C. These changes in the thermal

characteristics of the polyesters were also noticed in terms of crystallinity percentage. The SBW treatment of 130 °C displayed X_c values (35%) closer to that of P(HB-co-HV) extracted with chloroform (34%). In contrast, materials submitted to SBW treatments at higher temperatures presented higher X_c values, increasing from 6% for 150 °C, to 14% for 165 °C, and 17% for 180 °C (Table 1). Figure 3 shows the P(HB-co-HV) obtained at the temperatures that caused an increase in X_c , and the changes to its visual aspect are also noticeable: the PHA becomes harder and glossier. Such phenomena have been reported for other biopolymers extracted by SBW, e.g., cellulose [22]. Interestingly, no significant changes were observed for the samples regarding the T_{deg} of these polymers, which ranged between 287 and 294 °C, whatever the experimental conditions of purification.

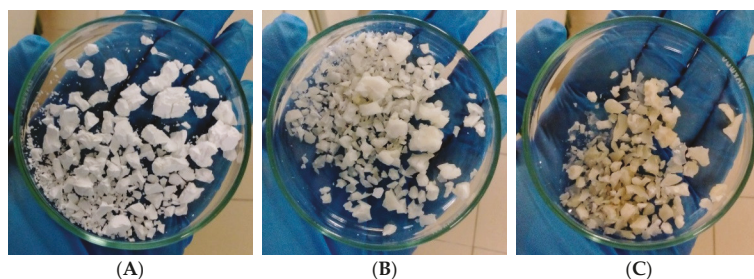


Figure 3. Images of the samples obtained after the SBW treatment of MMC biomass at (A) 150 °C, (B) 165 °C, and (C) 180 °C.

The PHA's thermal properties, especially T_m , are related to other properties, namely, M_w , the presence of side chains, or the presence of other functional groups [40]. A direct relation between T_m and M_w , has been proposed by some authors [41], and it has been reported that for low- M_w PHA (10^3 – 10^4 g/mol), the correspondent T_m values are within 146–153 °C [42], corroborating the relation between the decrease in T_m with the decrease in M_w .

Combining the highest recovery yield (88 wt.%) and polymer purity (77 wt.%), the SBW treatment at 150 °C was selected for subsequent tests. Although there was a reduction in the polymer's M_w and an increase in its PDI, the thermal properties remained practically unchanged, compared to the chloroform-extracted PHA.

3.2.2. Extraction of PHA from the SBW-Treated Biomass with Hypochlorite

Being demonstrated to be effective, SBW treatment was employed at 150 °C as a pre-treatment of the MMC biomass prior to digestion with sodium hypochlorite.

Hypochlorite concentrations ranging from 0.1 to 5.0% (*v/v*) were used to determine the most appropriate conditions to improve the polymer's recovery yield and purity compared to the SBW treatment alone. As shown in Table 1, a higher polymer purity (84 wt.%) was achieved for the SBW-treated samples subjected to the highest hypochlorite concentration (5.0% *v/v*). For the other concentrations tested, 3.0, 0.5, and 0.1% (*v/v*), higher recovery yields were obtained (83–85 wt.%), with a reduction in the polymer's purity (80–82 wt.%). Even though the purity values achieved with the combination of SBW and hypochlorite digestion are not as high as those obtained with chloroform extraction (91 wt.%), they are still higher than those achieved with hypochlorite digestion alone (77 wt.%).

This two-step purification technique had no impact on the P(HB-co-HV) composition, with all polymers having the same 3HV content for the sample obtained with the SBW treatment at 150 °C (17 wt.%) (Table 1). On the other hand, the polymers' crystallinity index values were noticed to rise with the combined treatment method (48–62%, Table 1) in parallel with only using SBW. This can be linked to the greater purity of the extracted polymers. Regarding the M_w , it remained the same for all tested conditions (2.8×10^4 – 3.0×10^4 g/mol, respectively) and was only slightly lower than the 150 °C

SBW-treated sample (5.0×10^4 g/mol). However, even though the M_w decreased, with the exception of the sample digested with 0.1% hypochlorite, the extracted polymer became more homogeneous, as evidenced by the decrease in the PDI, from 6 (after SBW 150 °C) to 3.1–4.8, for 5.0, 3.0, and 0.5% (*v/v*) hypochlorite. These changes could be assigned to the higher extraction of the lower M_w PHA oligomers formed during the SBW treatment upon treating with hypochlorite. The sample digested with the lowest hypochlorite concentration (0.1%, *v/v*) was characterized by having a higher PDI (7.5), indicating that these conditions yielded a polymer with a wide variety of chain sizes. The lower hypochlorite concentration might not have been enough to solubilize and wash away the smaller PHA oligomers that were thus retained within the recovered sample.

The impact of the different hypochlorite concentrations tested might be related to the alkalinity afforded by this oxidant compound. Berger et al. (1989) previously reported that when using a hypochlorite solution with pH 10, the obtained polymer had a M_w 2.5 times higher than when using the hypochlorite solution without pH correction (13.6) [7]. The pH of the hypochlorite solutions used was 9.1, 8.6, 7.3, and 6.7 for 5, 3, 0.5, and 0.1% (*v/v*) hypochlorite, respectively.

As has been previously discussed, these changes in the size of the polymeric chains are also evidenced by the alterations in the thermal properties of the P(HB-co-HV). There was a decrease in the polymers' T_m by 6–11 °C compared to the polymer obtained directly after SBW at 150 °C, and 12–17 °C when compared to the original polymer (Table 1). These changes might be related to alterations on the samples' M_w and PDI [38,41–43]. The polymers' thermal degradation was apparently not affected, with the T_{deg} still in the range of 276–290 °C.

3.3. Overall Assessment of the SBW-Hypochlorite Procedure

These findings show that, after being subjected to the SBW treatment at 150 °C, a hypochlorite concentration 50 times lower can be used to reach a higher PHA recovery yield and a higher polymer purity, compared to hypochlorite digestion alone. Examples in the literature show that using only hypochlorite extraction, some authors were able to achieve purities of 90% (using 1% NaOCl, for 3 h, at room temperature) [34]. Others [10] were even able to scale up the extraction to 50 L, maintaining a purity of 93%; however, this method employed a higher hypochlorite concentration (13% NaOCl), for 1 h at room temperature. To achieve polymers with even higher purity degrees, hypochlorite can be combined with organic solvents (chloroform or acetone), or even surfactants (sodium dodecyl sulfate or triton X-100).

SBW hydrolysis alone was not a suitable method for PHA extraction, since the low temperatures tested (130 °C) had a low solubilization capacity, while the higher temperatures (180–200 °C) caused severe polymer degradation. Intermediate temperatures, on the other hand, caused some polymer degradation, as shown by the lower M_w and higher PDI of the extracted samples. Coupling the SBW treatment with hypochlorite digestion allowed a reduction of the amount of hypochlorite required to reach a good extraction yield and polymer purity, which renders this an approach of interest.

The observed decrease in the PHA's M_w impairs the utilization of the biopolymer in most of the conventional applications of plastics due to the loss of mechanical properties. Nevertheless, there are specific applications for which low- M_w PHAs are of interest, such as their utilization as plasticizers [44] and surfactants, or for the preparation of graft and block co-polymers, which are useful for the fabrication of bio-adhesives, drug-delivery systems, drug-coating systems, and tissue-engineering materials [45–47]. Nevertheless, for biomedical and pharmaceutical uses, the biopolymers would require further purification to meet the requirements of such high-value areas. For such applications, the PHA molecules are depolymerized into monomers or short oligomers (10^2 – 10^4 g/mol) by physical (e.g., thermal decomposition), chemical methods (e.g., acid hydrolysis, alcoholysis), and/or enzymatic methods [46–48]. The developed SBW-hypochlorite digestion methodology could be of great value for the extraction of the biopolymer with the appropriate M_w for

use in such areas of application, without the need to resort to the chemical hydrolysis of high- M_w PHA.

4. Conclusions

To minimize the impact of harmful chemicals in the purification process of PHA, the use of SBW was validated in this work. It was observed that a two-step purification process integrating SBW pre-treatment at 150 °C, which showed the best compromise between NPCM solubilization and PHA properties, and hypochlorite digestion allowed the dissolution of the rest of the NPCM material. This approach showed that, after the SBW treatment, it was possible to recover the PHA with 50 times less hypochlorite, with a purity higher than that obtained with hypochlorite alone. Moreover, the impact on the PHA's M_w was mostly due to the SBW treatment, since after the hypochlorite extraction, the difference was less significant. Reducing the utilization of chemicals, such as hypochlorite, is of the utmost importance due to their environmental burden. The low- M_w PHA generated can find use as additives, surfactants, and graft or block co-polymers, among other uses. With this work, it was shown that it is possible to develop methods for the extraction of PHA using green solvents, with a lower environmental impact than the conventional solvents used.

Supplementary Materials: The following supporting information can be downloaded at: <https://www.mdpi.com/article/10.3390/bioengineering9070302/s1>, Figure S1: GC chromatogram of the P(HB-co-HV) sample obtained by Soxhlet extraction with chloroform, to illustrate the typical profile obtained.

Author Contributions: Conceptualization, A.P. and F.F.; methodology, L.M., A.E., M.M., C.S., and C.G.; writing—original draft preparation, L.M.; writing—review and editing, A.E., M.M., F.F., and A.P.; funding acquisition, S.B., M.A.M.R., F.F., and A.P. All authors have read and agreed to the published version of the manuscript.

Funding: This work was financed by national funds from FCT-Fundação para a Ciência e a Tecnologia, I.P., in the scope of projects UIDP/04378/2020 and UIDB/04378/2020 of the Research Unit on Applied Molecular Biosciences—UCIBIO, and the project LA/P/0140/2020 of the Associate Laboratory Institute for Health and Bioeconomy—i4HB, and by the Associate Laboratory for Green Chemistry—LAQV (UIDB/50006/2020). Liane Meneses, Asiyah Esmail, and Alexandre Paiva also acknowledge FCT I.P. for financial support through SFRH/BD/148510/2019, 2021.05014.BD, and IF/01146/2015, respectively.

Institutional Review Board Statement: Not applicable.

Informed Consent Statement: Not applicable.

Data Availability Statement: The data presented in this study are available on request from the corresponding authors.

Conflicts of Interest: The authors declare no conflict of interest.

References

1. Kourmentza, C.; Plácido, J.; Venetsaneas, N.; Burniol-Figols, A.; Varrone, C.; Gavala, H.N.; Reis, M.A.M. Recent Advances and Challenges towards Sustainable Polyhydroxyalkanoate (PHA) Production. *Bioengineering* **2017**, *4*, 55. [CrossRef]
2. Mannina, G.; Presti, D.; Montiel-Jarillo, G.; Suárez-Ojeda, M.E. Bioplastic Recovery from Wastewater: A New Protocol for Polyhydroxyalkanoates (PHA) Extraction from Mixed Microbial Cultures. *Bioresour. Technol.* **2019**, *282*, 361–369. [CrossRef] [PubMed]
3. Samorì, C.; Abbondanzi, F.; Galletti, P.; Giorgini, L.; Mazzocchetti, L.; Torri, C.; Tagliavini, E. Extraction of Polyhydroxyalkanoates from Mixed Microbial Cultures: Impact on Polymer Quality and Recovery. *Bioresour. Technol.* **2015**, *189*, 195–202. [CrossRef] [PubMed]
4. Koller, M.; Niebelschütz, H.; Braunnegg, G. Strategies for Recovery and Purification of Poly [(R)-3-Hydroxyalkanoates] (PHA) Biopolyesters from Surrounding Biomass. *Eng. Life Sci.* **2013**, *13*, 549–562. [CrossRef]
5. Pagliano, G.; Galletti, P.; Samorì, C.; Zaghini, A.; Torri, C. Recovery of Polyhydroxyalkanoates from Single and Mixed Microbial Cultures: A Review. *Front. Bioeng. Biotechnol.* **2021**, *9*, 624021. [CrossRef]

6. Pérez-Rivero, C.; López-Gómez, J.P.; Roy, I. A Sustainable Approach for the Downstream Processing of Bacterial Polyhydroxyalkanoates: State-of-the-Art and Latest Developments. *Biochem. Eng. J.* **2019**, *150*, 107283. [[CrossRef](#)]
7. Berger, E.; Ramsay, B.A.; Ramsay, J.A.; Chavarie, C. PHA Recovery by Hypochlorite Digestion of Non-PHB Biomass. *Biotechnol. Tech.* **1989**, *3*, 227–232. [[CrossRef](#)]
8. López-Abelairas, M.; García-Torreiro, M.; Lú-Chau, T.; Lema, J.M.; Steinbüchel, A. Comparison of Several Methods for the Separation of Poly(3-Hydroxybutyrate) from *Cupriavidus necator* H16 Cultures. *Biochem. Eng. J.* **2015**, *93*, 250–259. [[CrossRef](#)]
9. Villano, M.; Valentino, F.; Barbetta, A.; Martino, L.; Scandola, M.; Majone, M. Polyhydroxyalkanoates Production with Mixed Microbial Cultures: From Culture Selection to Polymer Recovery in a High-Rate Continuous Process. *New Biotechnol.* **2014**, *31*, 289–296. [[CrossRef](#)]
10. Heinrich, D.; Madkour, M.H.; Al-Ghamdi, M.A.; Shabbaj, I.I.; Steinbüchel, A. Large Scale Extraction of Poly (3-Hydroxybutyrate) from *Ralstonia eutropha* H16 Using Sodium Hypochlorite. *AMB Express* **2012**, *2*, 1–6. [[CrossRef](#)]
11. Lorini, L.; Martinelli, A.; Pavan, P.; Majone, M.; Valentino, F. Downstream Processing and Characterization of Polyhydroxyalkanoates (PHAs) Produced by Mixed Microbial Culture (MMC) and Organic Urban Waste as Substrate. *Biomass Convers. Biorefinery* **2021**, *11*, 693–703. [[CrossRef](#)]
12. Kunasundari, B.; Sudesh, K. Isolation and Recovery of Microbial Polyhydroxyalkanoates. *Express Polym. Lett.* **2011**, *5*, 620–634. [[CrossRef](#)]
13. Guzik, M.; Witko, T.; Steinbüchel, A.; Wojnarowska, M.; Sołtysik, M.; Wawak, S. What Has Been Trending in the Research of Polyhydroxyalkanoates? A Systematic Review. *Front. Bioeng. Biotechnol.* **2020**, *87*, 137–146. [[CrossRef](#)]
14. Serafim, L.S.; Queirós, D.; Rossetti, S.; Lemos, P.C. Biopolymer Production by Mixed Microbial Cultures: Integrating Remediation with Valorization. In *Recent Advances in Biotechnology Microbial Biopolyester, Vol. 1: Production, Performance and Processing Microbiology, Feedstocks, and Metabolism*; Koller, M., Ed.; Bentham Science: Sharjah, United Arab Emirates, 2016; Volume 1, p. 226. [[CrossRef](#)]
15. Kobayashi, D.; Fujita, K.; Nakamura, N.; Ohno, H. A Simple Recovery Process for Biodegradable Plastics Accumulated in Cyanobacteria Treated with Ionic Liquids. *Appl. Microbiol. Biotechnol.* **2015**, *99*, 1647–1653. [[CrossRef](#)] [[PubMed](#)]
16. Hejazi, P.; Vasheghani-farahani, E.; Yamini, Y. Supercritical Fluid Disruption of *Ralstonia eutropha* for Poly (-Hydroxybutyrate) Recovery. *Biotechnol. Prog.* **2003**, *19*, 15191523. [[CrossRef](#)]
17. Kruse, A.; Dinjus, E. Hot Compressed Water as Reaction Medium and Reactant. *Properties and Synthesis Reactions. J. Supercrit. Fluids* **2007**, *39*, 361–379. [[CrossRef](#)]
18. Brunner, G. Near Critical and Supercritical Water. *Part I. Hydrolytic and Hydrothermal Processes. J. Supercrit. Fluids* **2009**, *47*, 373–381. [[CrossRef](#)]
19. Pedras, B.; Salema-Oom, M.; Sá-Nogueira, I.; Simões, P.; Paiva, A.; Barreiros, S. Valorization of White Wine Grape Pomace through Application of Subcritical Water: Analysis of Extraction, Hydrolysis, and Biological Activity of the Extracts Obtained. *J. Supercrit. Fluids* **2017**, *128*, 138–144. [[CrossRef](#)]
20. Pedras, B.M.; Regalin, G.; Sá-Nogueira, I.; Simões, P.; Paiva, A.; Barreiros, S. Fractionation of Red Wine Grape Pomace by Subcritical Water Extraction/Hydrolysis. *J. Supercrit. Fluids* **2020**, *160*, 104793. [[CrossRef](#)]
21. Cunha, M.; Lourenço, A.; Barreiros, S.; Paiva, A.; Simões, P. Valorization of Cork Using Subcritical Water. *Molecules* **2020**, *25*, 4695. [[CrossRef](#)]
22. Zhang, R.Y.; Liu, H.M.; Hou, J.; Yao, Y.G.; Ma, Y.X.; Wang, X. De Cellulose Fibers Extracted from Sesame Hull Using Subcritical Water as a Pretreatment. *Arab. J. Chem.* **2021**, *14*, 103178. [[CrossRef](#)]
23. Melgosa, R.; Marques, M.; Paiva, A.; Bernardo, A.; Fernández, N.; Sá-Nogueira, I.; Simões, P. Subcritical Water Extraction and Hydrolysis of Cod (*Gadus Mmorhua*) Frames to Produce Bioactive Protein Extracts. *Foods* **2021**, *10*, 1222. [[CrossRef](#)] [[PubMed](#)]
24. Tran Nguyen, P.L.; Go, A.W.; Huynh, L.H.; Ju, Y.H. A Study on the Mechanism of Subcritical Water Treatment to Maximize Extractable Cellular Lipids. *Biomass Bioenergy* **2013**, *59*, 532–539. [[CrossRef](#)]
25. Matos, M.; Cruz, R.A.P.; Cardoso, P.; Silva, F.; Freitas, E.B.; Carvalho, G.; Reis, M.A.M. Combined Strategies to Boost Polyhydroxyalkanoate Production from Fruit Waste in a Three-Stage Pilot Plant. *ACS Sustain. Chem. Eng.* **2021**, *9*, 8270–8279. [[CrossRef](#)]
26. Cruz, M.V.; Araújo, D.; Alves, V.D.; Freitas, F.; Reis, M.A.M. Characterization of Medium Chain Length Polyhydroxyalkanoate Produced from Olive Oil Deodorizer Distillate. *Int. J. Biol. Macromol.* **2016**, *82*, 243–248. [[CrossRef](#)]
27. Morais, C.; Freitas, F.; Cruz, M.V.; Paiva, A.; Dionísio, M.; Reis, M.A.M. Conversion of Fat-Containing Waste from the Margarine Manufacturing Process into Bacterial Polyhydroxyalkanoates. *Int. J. Biol. Macromol.* **2014**, *71*, 68–73. [[CrossRef](#)]
28. Albuquerque, M.G.E.; Martino, V.; Pollet, E.; Avérous, L.; Reis, M.A.M. Mixed Culture Polyhydroxyalkanoate (PHA) Production from Volatile Fatty Acid (VFA)-Rich Streams: Effect of Substrate Composition and Feeding Regime on PHA Productivity, Composition and Properties. *J. Biotechnol.* **2011**, *151*, 66–76. [[CrossRef](#)]
29. Duque, A.F.; Oliveira, C.S.S.; Carmo, I.T.D.; Gouveia, A.R.; Pardelha, F.; Ramos, A.M.; Reis, M.A.M. Response of a Three-Stage Process for PHA Production by Mixed Microbial Cultures to Feedstock Shift: Impact on Polymer Composition. *New Biotechnol.* **2014**, *31*, 276–288. [[CrossRef](#)]
30. Matos, M.; Cruz, R.A.P.; Cardoso, P.; Silva, F.; Freitas, E.B.; Carvalho, G.; Reis, M.A.M. Sludge Retention Time Impacts on Polyhydroxyalkanoate Productivity in Uncoupled Storage/Growth Processes. *Sci. Total Environ.* **2021**, *799*, 149363. [[CrossRef](#)]

31. Sankhla, I.S.; Bhati, R.; Singh, A.K.; Mallick, N. Poly(3-Hydroxybutyrate-Co-3-Hydroxyvalerate) Co-Polymer Production from a Local Isolate, *Brevibacillus invocatus* MTCC 9039. *Bioresour. Technol.* **2010**, *101*, 1947–1953. [[CrossRef](#)]
32. Bossu, J.; Angellier-Coussy, H.; Totee, C.; Matos, M.; Reis, M.; Guillard, V. Effect of the Molecular Structure of Poly (3-Hydroxybutyrate-Co-3-Hydroxyvalerate) (P (3HB-3HV)) Produced from Mixed Bacterial Cultures on Its Crystallization and Mechanical Properties. *Biomacromolecules* **2020**, *21*, 4709–4723. [[CrossRef](#)] [[PubMed](#)]
33. Esmail, A.; Pereira, J.R.; Sevrin, C.; Grandfils, C.; Menda, U.D.; Fortunato, E.; Oliva, A.; Freitas, F. Preparation and Characterization of Porous Scaffolds Based on Poly (3-Hydroxybutyrate) and Poly (3-Hydroxybutyrate-Co-3-Hydroxyvalerate). *Life* **2021**, *11*, 935. [[CrossRef](#)] [[PubMed](#)]
34. Martínez-Abad, A.; Cabedo, L.; Oliveira, C.S.S.; Hilliou, L.; Reis, M.A.M.; Lagarón, J.M. Characterization of Polyhydroxyalkanoate Blends Incorporating Unpurified Biosustainably Produced Poly (3-Hydroxybutyrate-Co-3-Hydroxyvalerate). *J. Appl. Polym. Sci.* **2016**, *133*, 42633. [[CrossRef](#)]
35. Pradhan, S.; Dikshit, P.K.; Moholkar, V.S. Production, Characterization, and Applications of Biodegradable Polymer: Polyhydroxyalkanoates. In *Advances in Sustainable Polymers. Materials Horizons: From Nature to Nanomaterials*; Katiyar, V., Kumar, A., Mulchandani, N., Eds.; Springer: Singapore, 2020. [[CrossRef](#)]
36. Naser, A.Z.; Deia, I.; Darras, B.M. Poly (lactic acid) (PLA) and polyhydroxyalkanoates (PHAs), green alternatives to petroleum-based plastics: A review. *RSC Adv.* **2021**, *11*, 17151. [[CrossRef](#)] [[PubMed](#)]
37. Lorini, L.; Martinelli, A.; Capuani, G.; Frison, N.; Reis, M.; Ferreira, B.S.; Villano, M.; Majone, M.; Valentino, F. Characterization of Polyhydroxyalkanoates Produced at Pilot Scale from Different Organic Wastes. *Front. Bioeng. Biotechnol.* **2021**, *9*, 628719. [[CrossRef](#)] [[PubMed](#)]
38. Wang, S.; Chen, W.; Xiang, H.; Yang, J.; Zhou, Z.; Zhu, M. Modification and Potential Application of Short-Chain-Length Polyhydroxyalkanoate (SCL-PHA). *Polymers* **2016**, *8*, 273. [[CrossRef](#)]
39. Xiang, H.; Wen, X.; Miu, X.; Li, Y.; Zhou, Z.; Zhu, M. Thermal Depolymerization Mechanisms of Poly(3-Hydroxybutyrate-Co-3-Hydroxyvalerate). *Prog. Nat. Sci. Mater. Int.* **2016**, *26*, 58–64. [[CrossRef](#)]
40. Palmieri, S.; Tittarelli, F.; Sabbatini, S.; Cespi, M.; Bonacucina, G.; Eusebi, A.L.; Fatone, F.; Stipa, P. Effects of Different Pre-Treatments on the Properties of Polyhydroxyalkanoates Extracted from Sidestreams of a Municipal Wastewater Treatment Plant. *Sci. Total Environ.* **2021**, *801*, 149633. [[CrossRef](#)]
41. Stanley, A.; Murthy, P.S.K.; Vijayendra, S.V.N. Characterization of Polyhydroxyalkanoate Produced by *Halomonas venusta* KT832796. *J. Polym. Environ.* **2020**, *28*, 973–983. [[CrossRef](#)]
42. Cha, S.H.; Son, J.H.; Jamal, Y.; Zafar, M.; Park, H.S. Characterization of Polyhydroxyalkanoates Extracted from Wastewater Sludge under Different Environmental Conditions. *Biochem. Eng. J.* **2016**, *112*, 1–12. [[CrossRef](#)]
43. Martínez-Herrera, R.E.; Alemán-Huerta, M.E.; Almaguer-Cantú, V.; Rosas-Flores, W.; Martínez-Gómez, V.J.; Quintero-Zapata, I.; Rivera, G.; Rutiaga-Quiñones, O.M. Efficient Recovery of Thermostable Polyhydroxybutyrate (PHB) by a Rapid and Solvent-Free Extraction Protocol Assisted by Ultrasound. *Int. J. Biol. Macromol.* **2020**, *164*, 771–782. [[CrossRef](#)] [[PubMed](#)]
44. Hong, S.G.; Hsu, H.W.; Ye, M.T. Thermal Properties and Applications of Low Molecular Weight Polyhydroxybutyrate. *J. Therm. Anal. Calorim.* **2013**, *111*, 1243–1250. [[CrossRef](#)]
45. Yu, G.-E. Process of Producing Low Molecular Weight Poly (Hydroxyalkanoate)s from High Molecular Weight Poly (Hydroxyalkanoate)s. U.S. 7361725B2, 22 April 2008.
46. Chaber, P.; Kwiecień, M.; Zięba, M.; Sobota, M.; Adamus, G. The heterogeneous selective reduction of PHB as a useful method for preparation of oligodiols and surface modification. *RSC Adv.* **2017**, *7*, 35096–35104. [[CrossRef](#)]
47. Kanmani, P.; Kumaresan, K.; Aravind, J.; Karthikeyan, S.; Balan, R. Enzymatic degradation of polyhydroxyalkanoate using lipase from *Bacillus subtilis*. *Int. J. Environ. Sci. Technol.* **2016**, *13*, 1541–1552. [[CrossRef](#)]
48. Don, T.-M.; Liao, K.-H. Studies on the alcoholysis of poly(3-hydroxybutyrate) and the synthesis of PHB-b-PLA block copolymer for the preparation of PLA/PHB-b-PLA blends. *J. Polym. Res.* **2018**, *25*, 38. [[CrossRef](#)]

Article

Improved Processability and Antioxidant Behavior of Poly(3-hydroxybutyrate) in Presence of Ferulic Acid-Based Additives

Lionel F. Longé¹, Laurent Michely², Antoine Gallos^{1,*}, Agustin Rios De Anda², Henri Vahabi³, Estelle Renard², Michel Latroche², Florent Allais¹ and Valérie Langlois^{2,*}

¹ URD Agro-Biotechnologies Industrielles (ABI), CEBB, AgroParisTech, F-51110 Pomacle, France; lionel.longe@orange.fr (L.F.L.); florent.allais@agroparistech.fr (F.A.)

² Université Paris Est Creteil, CNRS, ICMPE, F-94010 Creteil, France; michely@icmpe.cnrs.fr (L.M.); agustin.rios-de-anda@u-pec.fr (A.R.D.A.); e.renard@u-pec.fr (E.R.); latroche@icmpe.cnrs.fr (M.L.)

³ Université de Lorraine, Centrale Supélec, LMOPS, F-57000 Metz, France; henri.vahabi@univ-lorraine.fr

* Correspondence: antoine.gallos@agroparistech.fr (A.G.); langlois@u-pec.fr (V.L.)

Abstract: Poly(3-hydroxybutyrate), PHB, has gathered a lot of attention for its promising properties—in particular its biobased nature and high biodegradability. Although PHB is prime candidate for the packaging industry, the applications are still limited by a narrow processing window and thermal degradation during melt processing. In this work, three novel additives based on ferulic acid esterified with butanediol, pentanediol, and glycerol (BDF, PDF, and GTF, respectively) were used as plasticizers and antioxidative additives to improve mechanical properties of PHB. Elongation at break up to 270% was obtained in presence of BDF and the processing window was improved nearly 10-fold. The Pawley method was used to identify the monoclinic space group P2 of the BDF. The estimated crystallite size (71 nm) agrees with a crystalline additive. With PHB₇₀BDF₃₀ blends, even higher elongations at break were obtained though dwindled with time. However, these properties could be recovered after thermal treatment. The high thermal stability of this additive leads to an increase in the fire retardancy property of the material, and the phenolic structure induced antioxidant properties to the samples as demonstrated by radical scavenging tests, further highlighting the possibilities of the PHB/additive blends for packaging applications.

Keywords: PHB; polyhydroxybutyrate; biopolymer; plasticizer; ferulic acid

Citation: Longé, L.F.; Michely, L.; Gallos, A.; Rios De Anda, A.; Vahabi, H.; Renard, E.; Latroche, M.; Allais, F.; Langlois, V. Improved Processability and Antioxidant Behavior of Poly(3-hydroxybutyrate) in Presence of Ferulic Acid-Based Additives. *Bioengineering* **2022**, *9*, 100. <https://doi.org/10.3390/bioengineering9030100>

Academic Editor: Martin Koller

Received: 20 January 2022

Accepted: 19 February 2022

Published: 28 February 2022

Publisher's Note: MDPI stays neutral with regard to jurisdictional claims in published maps and institutional affiliations.



Copyright: © 2022 by the authors. Licensee MDPI, Basel, Switzerland. This article is an open access article distributed under the terms and conditions of the Creative Commons Attribution (CC BY) license (<https://creativecommons.org/licenses/by/4.0/>).

1. Introduction

Since their production method was streamlined a few decades ago, poly(3-hydroxyalkanoate)s (PHAs), which are produced by a fermentation process, have shown a growing amount of interest [1–3]. Indeed, PHAs are one of the most promising renewable biocompatible and biodegradable polyesters [4–8]. Produced by microorganisms in presence of natural substrates, they offer an excellent alternative to petroleum-based plastics. Poly(3-hydroxybutyrate), PHB, is one of the simplest members of the PHAs family. PHB is a linear semi-crystalline isotactic polyester with high crystallinity, high melting temperature, and excellent resistance to solvents. Similarly, to other PHAs, PHB exhibits complete biodegradability [9–14]. However, its industrial applications are still limited today due to its high brittleness, low value for elongation at break and thermal degradation during melt processing. The short permanence above melting point induces degradation that involves a cis-elimination reaction and the formation of crotonic acid [15]. To improve PHB thermal and mechanical properties, a lot of efforts have been put to find different solutions such as formulations with additives [16]. A common workaround is to synthesize copolyesters of PHB with other 3-hydroxyalkanoates moieties, such as 3-hydroxyvalerate and 3-hydroxyhexanoate [17]. Poly(3-hydroxyvalerate) (PHBHV) is the most common

co-monomer for industrial application and the resulting copolymer, PHBHV, exhibits significant improvement in the elongation at break depending on monomers ratio. Internal plasticization of PHB have been developed using the bacterial fermentation of copolymers.

On the other hand, the external plasticization is an efficient and rapid method to improve some mechanical properties of polymers. Additives as plasticizers, blend partners, fillers, and crosslinkers may also affect the processing and mechanical properties [18]. Blending PHB with plasticizers may offer the advantage to improve the processability. Plasticizing additives for PHB are diverse, and include aromatic compounds, fatty acids, alcohols, ester, and polymers themselves [19–30]. Vegetable oils and their derivatives have also been extensively studied as promising additives into PHA formulations [31–34]. Semi-interpenetrated networks in which PHB is embedded in network based on sunflower oil and trithiol exhibited a toughening improvement of this polyester [33]. Plasticized PHB formulations were recently prepared with monoterpenes such as linalool, geraniol, and geranyl acetate [34]. Blending with terpenes leads to a decrease of the glass transition temperature (T_g) values and a remarkable increase in the elongation at break combined with a decrease in Young's modulus with regard to pure PHB. The effect is more pronounced with geranyl acetate thanks to the presence of the segment bearing ester group that increases free volume and molecular mobility. However, there are still challenges to be overcome to open the new applications to PHB. Ferulic acid is a biobased compound that can be extracted through different processes from lignocellulosic biomass. Due to the various functional groups, it can be easily functionalized and its phenol group usually carry on antioxidant properties even after functionalization. Ferulic acid derivatives were recently found to have plasticizing effects on polylactic acid (PLA) and polycaprolactone (PCL) [35–37].

The objective of this study is to develop the appropriate plasticizer for improving mechanical properties. We aim at preparing plasticized PHB with ferulic derivatives. The bis-O-dihydroferuloyl 1,4-butanediol (BDF) was blended with PHB to have a direct comparison with the observed plasticizing effect of BDF in PLA. Two others ferulic acid derivatives (bis-O-dihydroferuloyl 1,5-pentanediol, and tris-O-dihydroferuloyl glycerol), hereafter named PDF and GTF, were also blended with PHB to study the effect of various molecular designs. PHB was melt-blended with BDF, PDF, and GTF using extrusion process. The influence of the chemical structure of these compounds on the thermal properties, mechanical properties, dynamic mechanical properties, thermal stability, and flammability behavior of PHB was studied. A special attention was paid to the evolution of the mechanical properties and recrystallization of the blends over time.

2. Materials and Methods

PHB powder (Batch T19) without any plasticizer was kindly supplied by BIOMER, Schwalbach am Taunus, Germany ($M_w = 230,000 \text{ g}\cdot\text{mol}^{-1}$). Ferulic acid was acquired from Biosynth-Carbosynth, Eching, Germany. Palladium (10%) on activated charcoal, 2,2-diphenyl-1-picrylhydrazyl and sodium chloride were purchased from Fisher Scientific, Illkirch, France. Hydrochloric acid (37%), anhydrous magnesium sulphate, sodium bicarbonate, celite, acetone, ethanol, methanol, dichloromethane, and ethyl acetate were obtained from VWR, Fontenay-sous-Bois, France. Ferulic acid ($\geq 99\%$ purity) was purchased from Sigma-Aldrich. Butane-1,4-diol, pentane-1,5-diol and glycerol were acquired from Alfa Aesar, Kandel, Germany. Solid supported Cal-B (Novozyme 435) was procured from Novozymes, Le Pecq, France. Deuterated acetone and deuterated chloroform were ordered from Eurisotop, Saint-Aubin, France.

2.1. Synthesis of Ferulate Derivatives

Synthesis of the different additives was performed in three steps. First, in a round bottom flask, ferulic acid (150 g, 0.77 mol) was dissolved in large excess of ethanol (600 mL). The mixture is vigorously stirred, then concentrated hydrochloric acid (37% w/w , 8.8 mL, 0.12 mol), was added into the solution under constant stirring. The reaction was allowed to proceed at reflux overnight. The mixture is then allowed to cool down and ethanol

is removed under reduced pressure and replaced by ethyl acetate (600 mL). The organic phase is then washed three times with saturated sodium carbonate solution (3×100 mL) and once with brine solution (100 mL). The organic layer is then recovered and dried over anhydrous magnesium sulphate. An aliquot of the solution was taken, and ethyl acetate was removed under reduced pressure to yield ethyl ferulate. Purity was measured higher than 99% by NMR and yield was calculated to be 98.0% (168.2 g, 0.76 mol). Secondly, the round bottom flask containing the ethyl ferulate (168.2 g, 0.76 mol) solution was sealed with a septum and nitrogen was bubbled through for 15 min. Palladium on activated charcoal (8.4 g) was quickly added to the flask then nitrogen was further bubbled for 5 min. Dihydrogen was then flushed constantly in the round bottom flask, under constant gentle stirring, until hydrogenation was completed (ca. 48 h). The mixture is then filtered over celite, and ethyl acetate was removed under reduced pressure to yield hydrogenated ethyl ferulate (163.8 g, 0.73 mol), 96.5% yield, >99.9% purity. Finally, hydrogenated ethyl ferulate (2) (163.8 g, 0.73 mol) and butane-1,4-diol (21 mL, 0.24 mol) were vigorously mixed in a round bottom flask. Solid supported Cal-B (16.3 g) was poured in the mixture under constant stirring. Heating was set to 75 °C and the round bottom flask was connected to high vacuum pump and left overnight with gentle stirring. After being allowed to cool down, acetone was used to dissolve and filter the mixture to remove solid supported Cal-B. Acetone was then removed under reduced pressure to yield a white solid. Recrystallization in ethanol (500 mL) yielded BDF (67.86 g, 0.15 mol), 69.1% yield, 97.2% purity. Yield can be greatly increased by further recrystallization. For PDF synthesis, similar reaction was performed with pentanediol instead of butanediol. Hydrogenated ethyl ferulate (150 g, 0.67 mol) and pentane-1,5-diol (23 mL, 0.22 mol) were added to a round bottom flask and vigorously stirred until complete homogenization. Solid supported Cal-B (15.0 g) was added in the mixture under constant stirring. Heating was set to 75 °C and the round bottom flask was connected to high vacuum pump and left overnight with gentle stirring. After being allowed to cool down, acetone was used to dissolve and filter the mixture to remove solid supported Cal-B. Acetone was then removed under reduced pressure to yield a yellow oil. Purification was easily done by flash chromatography. The product was loaded on silica with acetone and the following solvent profile was applied to purify the mixture: 5 column volumes (CV) with a 95/5 cyclohexane/isopropanol, then increase to 80/20 during another 5CV. PDF can be collected during the second phase of the purification, while some remaining ethyl ferulate can be collected during the first phase. Total yield for PDF 84.1% (85.19 g, 0.19 mol), purity > 99%.

2.2. Extrusion Process

Extrusion of polymer-additives formulation was performed on a compounding extruder HAAKE™ MiniLab II twin screw, screw diameter 16 mm, 24 mm. Screws are set in co-rotation, at 60 rpm. Extrusion temperature was set to 170 °C. HAAKE MiniJet Pro piston injection molding system was used for the injection molding of sample specimens. DMA test bar mold was used, with dimensions of $60 \times 10 \times 1$ mm. The mold was maintained at 45 °C during injection.

2.3. Characterization

Tensile specimens were prepared using a cutting die mounted on an arbor press. Specimen were prepared according to ISO 527-2 specification, type 5B. Traction tests were performed on an INSTRON 5965 dual column tabletop testing systems set to tensile testing. The equipment was fitted with 2530 series static load cells, 100 N or 2 kN when required. Strain rate was set to 1 mm/min. Tests were performed in triplicate at room temperature. Dynamic mechanical analyses (DMA) were conducted on a TA Instrument DMA Q800 in tension deformation mode. Frequency was set to 1 Hz and strain to 0.06%. Temperature was raised from -140 °C to 170 °C at a ramp of 3 °C/min. The samples had dimensions ($20 \times 5 \times 0.92$ mm) and all tests were done under air. The storage modulus (E'), loss modulus (E''), and loss factor ($\tan \delta$) of each specimen were obtained as a function of temperature.

X-ray diffraction (XRD) was performed using a Bruker D8 advance diffractometer (Cu-K α radiation), in the 2 θ -range from 7 to 55° with a step size of 0.02°. Crystallographic properties of the patterns were analyzed by the Pawley and Rietveld methods using TOPAS 4 [38]. Powder density was obtained by a manometric method with an ULTRAPYC 1200e helium pycnometer from Quantachrome.

Differential scanning calorimetry (DSC) measurements were recorded on a TA Instruments DSC25. A first heating run from −80 °C to 200 °C with a heating rate of 10 °C/min was performed to determine the melting temperature (T_m) and the fusion enthalpy (ΔH_m). This was followed by a cooling run to −80 °C with a cooling ramp of 200 °C/min. The T_g was obtained in a second heating run from −80 °C to 200 °C at 10 °C/min. The degree of crystallinity χ_c may be calculated via the total enthalpy method according to Equation (1)

$$\chi_c = \frac{\Delta H_m}{W_{PHB}\Delta H_m^o} \times 100 \quad (1)$$

where ΔH_m is the specific enthalpy of melting of the sample studied, W_{PHB} the weight fraction of the PHB in the blend and ΔH_m^o represents the specific enthalpy of melting for the 100% crystalline PHB, taken as 146 J/g. The degree of crystallinity χ_c was calculated as a function of the real amount of PHB in each sample.

2.4. Antioxydant Activity and Flammability Measurements

Radical scavenging activity (RSA) was measured by simple test with 2,2-diphenyl-1-picrylhydrazyl (DPPH). A solution of DPPH at 0.1 mM in ethanol was prepared fresh and kept away from light. A sample of the polymer blend was then placed in a test tube along with 3 mL of the DPPH solution (immersion length 3.2 cm, i.e., total surface in contact with solution 7.14 cm²). After one hour in total darkness and at room temperature the absorption at 515 nm was measured and compared to the absorption of the original solution. The radical scavenger ability (RSA) was then calculated as in Equation (2)

$$RSA (\%) = \frac{Abs_{reference} - Abs_{sample}}{Abs_{reference}} \times 100 \quad (2)$$

where $Abs_{reference}$ is the absorbance of the 0.1 mM of DPPH solution without a sample and Abs_{sample} is the absorbance of the 0.1 mM solution of DPPH with the polymer sample.

A pyrolysis combustion flow calorimeter analysis (PCFC) apparatus from Fire Testing Technology (FTT) Company-UK, was used to evaluate the flammability behavior of samples. A small quantity of samples, between 2 and 4 mg, were pyrolyzed up to 750 °C. The heating rate was fixed at 1 °C/s. Then, gases obtained from sample pyrolysis were collected and transferred into another compartment for combustion at 900 °C containing 20% of oxygen. Huggett's relation (1 kg of consumed oxygen corresponds to 13.1 MJ of released energy) allowed obtaining of the most important parameters related to flammability: peak of heat release rate (pHRR), temperature at pHRR (T_{pHRR}), and total heat release (THR). For each sample three tests were performed, and the related accuracy was estimated around 5%.

3. Results and Discussion

3.1. Synthesis of the Additives Based on Ferulic Acid

Three esters have been synthesized from ferulic acid (Figure 1). The first step is an esterification of ferulic acid in presence of ethanol, followed by the hydrogenation of the non-aromatic double bond. The transesterification in the presence of butanediol, pentanediol or glycerol is then catalyzed by solid supported Cal-B to obtain ferulic derivatives called butanediol diferulate, BDF (A), pentanediol diferulate, PDF (B), and glycerol triferulate GTF (C) respectively. BDF and PDF are diesters while GTF, obtained in presence of glycerol is the triester of ferulic acid. Physical properties of BDF, GTF, and PDF are reported in Table 1.

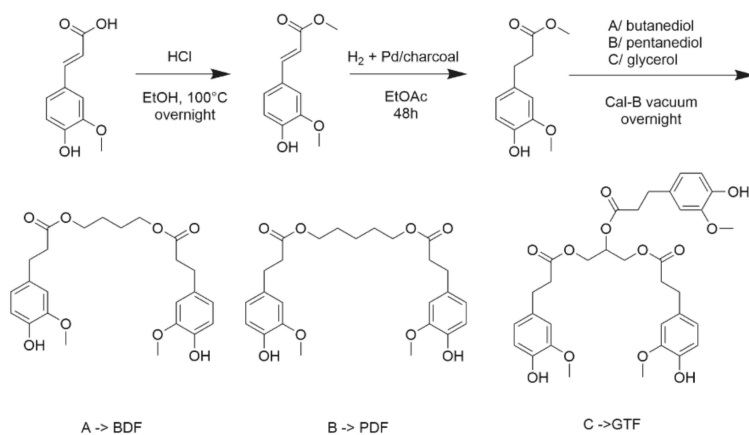


Figure 1. Synthesis of BDF, PDF, and GTF additives from ferulic acid.

Table 1. Molar masses and thermal properties of ferulic acid derivatives determined by DSC.

	M (g·mol ⁻¹)	T _g (°C)	T _m (°C)	ΔH _m (J/g)
BDF	446.2	−19	112	108
PDF	460.2	−22	-	-
GTF	626.2	+42	-	-

The three compounds exhibit a glass transition temperature which was attributed to some medium-long range order in the material as the compound form a non-covalent oligomer by π -stacking of the aromatic rings. As expected, the longer five carbon chain in PDF decreases the T_g compared to BDF which has only four carbon chain. Yet, that one carbon difference is also responsible for a completely different crystallization behavior. This seems sufficient to have different intermolecular interactions (polar interaction between the ester groups, aromatic groups, hydroxyl functions, etc.) that could explain this difference between BDF and PDF. BDF has a T_m at 110 °C while analysis by DSC could not detect any T_m for PDF, suggesting different intermolecular interactions for those two compounds. GTF, being synthesized around a short triol, displays a much higher T_g at 42 °C due to the presence of the three aromatic rings that stiffens the system. We then observed an exudation of the PDF on the surface of our samples during their storage. This observation allowed us not to retain PDF for the rest of our study because the blends are not stable.

3.2. PHB/Additives Blends and Their Mechanical Properties

The major drawback of PHB during hot melt extrusion is that the melting point and the extrusion temperature are very close to the degradation temperature. Therefore, if PHB residence time in the extruder is prolonged, temperature and shear stress will start to degrade the polymer, causing oxidation (i.e., seen as samples browning), distinctive odor release attributed to crotonic acid and loss of mechanical properties. To overcome this inconvenient, PHB and the ferulic acid-based additives were combined by hot melt extrusion in a twin-screw mini-extruder and injected directly into a mold. By using a mini-extruder, PHB residence time is diminished, which limits the polymer degradations. Different formulations of PHB_xBDF_y blends were prepared to study the influence of BDF concentrations (Table 2).

Table 2. Formulations and thermal properties of different PHBxBDF100-x blends determined by DSC after different times since the extrusion process.

PHB _x BDF _{100-x}	Time after extrusion (day)	T _g theo. (°C)	T _g (°C)	T _m PHB (°C)	ΔH _m PHB (J/g)	T _m BDF (°C)	ΔH _m BDF (J/g)
PHB ₁₀₀ BDF ₀	7	-	+0.9	177	101	-	-
PHB ₉₅ BDF ₅	7	-0.2 ^b	-0.7	173	98	-	-
PHB ₉₀ BDF ₁₀	7	-1.2 ^b	-1.5	172	99	-	-
PHB ₈₀ BDF ₂₀	7	-3.2 ^b	-4.1	168	98	100	9
PHB ₇₀ BDF ₃₀	0.25	-5.3 ^b	-17	167	93	102	9
PHB ₇₀ BDF ₃₀	1	-5.3 ^b	-17	168	97	96	37
PHB ₇₀ BDF ₃₀	7	-5.3 ^b	-18	167	91	95	56
PHB ₀ BDF ₁₀₀	7	-17.7 ^a	-19.0	-	-	112	108

(^a) Calculated by $T_g = 2/3 T_m$. (^b) Determined by Fox equation.

Theoretical glass transition temperature of BDF (-17.7 °C) matches quite closely with the experimental T_g measured by DSC (-19 °C). Furthermore, the measured T_g for the PHB_x/BDF_{100-x} blends also line up closely to the theoretical values determined by the Fox equation when the blends contain less than 30 wt % of BDF. The crystallinity of the PHB is nearly unchanged whatever the content of BDF, as shown by the values of the melting enthalpies in the different blends. Even if the BDF concentrations above 20% start to hinder PHB crystallization, the BDF interference with PHB is only limited to a shift in melting point T_m from 177 °C to 167 °C. This decrease of T_m is certainly due to the decrease of crystallite sizes as the total amount of crystalline PHB part remains constant. The diffraction pattern of PHB is shown in Figure 2. The phase is crystalline though a broadening of the diffraction peaks is observed in the range 20–25° in 2θ. The diffraction pattern was indexed with the orthorhombic cell proposed by Kawaguchi and Doi [39]. The structure was refined with the atomic positions given by Brückner et al. [40] in space group P212121. The cell parameters obtained from the Rietveld and Loopstra method [41] are given in Table 3. The estimated crystallite size (286 nm) agrees with a semi-crystalline material. For the X-ray pattern of BDF, the phase is crystalline though the diffraction peaks are relatively broad. The Pawley method [42] was used to determine the space group and cell parameters of BDF. The diffraction lines can be fully indexed with a monoclinic space group P2 and the cell parameters are given in Table 3.

Table 3. Crystallographic parameters of BDF and PHB determined by X-ray diffraction (estimated standard deviations (esd) given between brackets apply to the last digits).

Phase	Space Group	a (Å)	b (Å)	c (Å)	β (°)	Crystal Size (nm)
BDF	P2 (N°3)	13.055 (2)	11.029 (2)	8.682 (2)	112.30 (2)	71 (5)
PHB	P2 ₁ 2 ₁ 2 ₁	5.713 (2)	13.171 (5)	6.055 (3)	-	286 (49)

The estimated crystallite size (71 nm) agrees with a crystalline material. The calculated density (1.282) of BDF deduced from the chemical formula C₂₄H₃₀O₈ (M = 446.5 g) and the cell volume obtained by the Pawley method (V = 1156.7 Å³) is in good agreement with the measured one (1.277), assuming Z = 2. The diffraction pattern of the PHB₇₀/BDF₃₀ is also shown as prepared (1 day) in Figure 2. The pattern can be described by a combination of the two single phases BDF and PHB, though BDF looks much less crystalline than the pristine material. All diffraction peaks can be accounted, and the sample can be seen as a physical mixture of the two phases without significant chemical reactions between them. It can be stated that introducing 30% BDF lowers the melting temperature of PHB by 10 °C, which allows to decrease the processing temperature of the samples by extrusion. It is possible that BDF not only acts as a chain spacer in the amorphous phase of PHB but plays the same role during the melting and extrusion process. By spacing the chains, BDF

can reduce the polymers viscosity and melting point, leading to lower overall processing temperatures. This is beneficial as the heat extrusion effect on the polymer degradation is reduced. For the remaining of the investigation, a concentration of 30% of additive in the blends was considered.

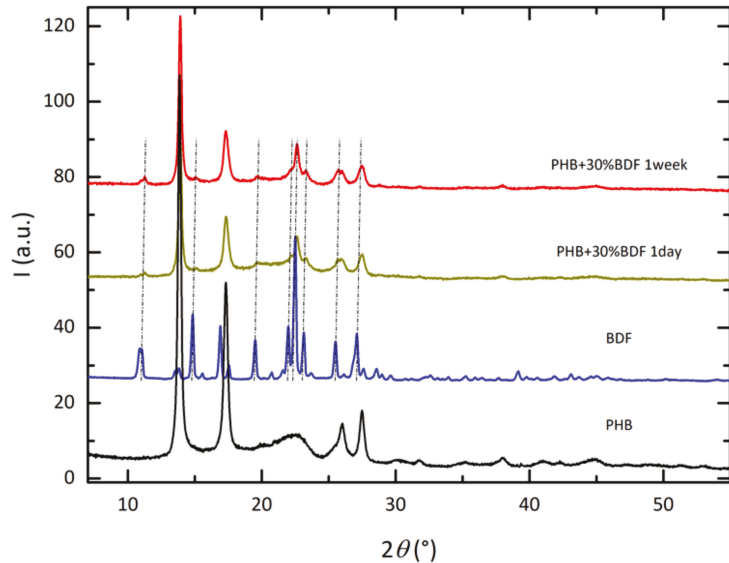


Figure 2. X-ray diffraction patterns of (from bottom to top) PHB (black), BDF (blue), PHB₇₀BDF₃₀ as-prepared (one day), and PHB₇₀BDF₃₀ after one week. Vertical dotted lines added for BDF are a guide for the eyes.

Mechanical properties showed that the incorporation of the ferulic acid-based additives induces a substantial increase in the elongation at break of the material which was measured three hours after extrusion in the case of PHB₇₀GTF₃₀ and PHB₇₀BDF₃₀. For PHB₇₀GTF₃₀, it jumps from 11% for pure PHB to 178% (Figure 3, Table 4). This increase is paralleled by a decline of the Young’s modulus E and of the stress at break or. Indeed, or decreases from 29.7 for pure PHB to 5.8 MPa for PHB₇₀GTF₃₀. This means that both GTF and BDF act also as mechanical plasticizers, yielding toughened PHB formulations. For PHB₇₀PDF₃₀, no increase of the elongation at break could be detected compared to pure PHB. Additionally, it was found that during storage at room temperature, some oily substance exuded from the samples. Unlike BDF and GTF, PDF is a liquid at room temperature which explains that this behavior is not observed for these compounds. For those reasons, PDF could not be considered as a good candidate for improving the toughening mechanical properties of PHB or for medium-long term packaging applications contrary to BDF and GTF.

Table 4. Mechanical properties of PHB and blends three hours after extrusion.

	Young Modulus (MPa)	Stress at Break (MPa)	Elongation at Break (%)
PHB ₁₀₀	1169 ± 38	29.7 ± 1.6	11 ± 1.6
PHB ₇₀ BDF ₃₀	417 ± 38	11.4 ± 1.1	42 ± 13.9
PHB ₇₀ PDF ₃₀	510 ± 82	12.3 ± 1.7	12 ± 5.5
PHB ₇₀ GTF ₃₀	211 ± 93	5.8 ± 0.8	178 ± 48.7

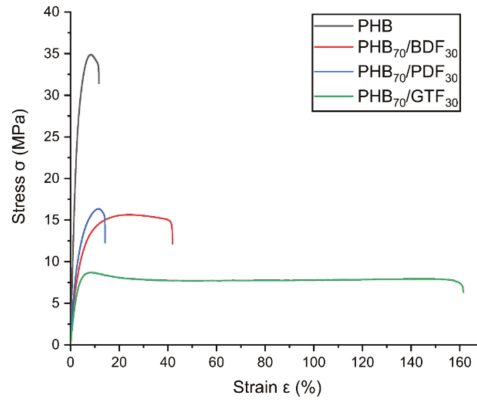


Figure 3. Strain–stress curve of PHB/additive samples, three hours after extrusion: PHB₇₀BDF₃₀, PHB₇₀PDF₃₀, PHB₇₀GTF₃₀, and pure PHB.

3.3. Evolution of Mechanical Properties over Time

PHB mechanical properties are known to quickly evolve with time after solidifying. After three hours, PHB properties are usually mostly settled but can still slightly evolve. By blending additives into PHB, the phenomenon kinetics might vary. As such, the blends mechanical properties were monitored by DMA over a period of one week for PHB₇₀BDF₃₀ and PHB₇₀GTF₃₀ (Table 5, Figure 4). Values of tan δ measured by DMA show important changes for PHB-GTF blends for which a sharp decrease in intensity can be noted. Furthermore, the presence of two peaks in the signal can also be detected, one at 30 °C characteristic of PHB, and a second one at 60 °C for GTF. After one week, the material properties changed significantly as only the peak at 60 °C remains. This shift in tan δ peak temperature and intensity is due to an increase of the crystallization ratio of the blend. Indeed, as the chains reorganize and crystallize, the material becomes more brittle (i.e., diminishing tan δ intensity) and the *T_g* increases (i.e., tan δ peak shifts to higher temperatures). This phenomenon also accounts for the jump in *E'* at 40 °C, from 45 to 4510 MPa. However, the hardening of the samples leads to high brittleness. Specimens for traction test could no longer be prepared as samples shattered upon handling. Therefore, it was concluded that GTF was not suitable as an additive for PHB. In the case of PHB₇₀BDF₃₀ samples, the maximum of tan δ was observed at −1 °C. The peak is also much wider and asymmetrical. The shoulder discerned at higher temperature, around 20 °C, is attributed to the presence of BDF. A reorganization of the material occurs between the two measurements with an overall stiffening of the material as manifested by the increase of *E'* at 40 °C from 540 to 1630 MPa. This value is yet close to the initial value for PHB, 2120 MPa.

Table 5. Thermo-mechanical properties of different PHB-additive blends measured by DMA after (a) 3 h and (b) 1 week.

	<i>E'</i> at 20 °C (MPa)	<i>E'</i> at 40 °C (MPa)	<i>E''</i> Tα (°C)	<i>E''</i> Tβ (°C)	Tan δ (°C)
PHB ₇₀ BDF ₃₀ (a)	820	540	−5		−1
PHB ₇₀ BDF ₃₀ (b)	2190	1630	−7		−2
PHB ₇₀ GTF ₃₀ (a)	2000	45	24	−100	31
PHB ₇₀ GTF ₃₀ (b)	6140	4510	47	−86	60

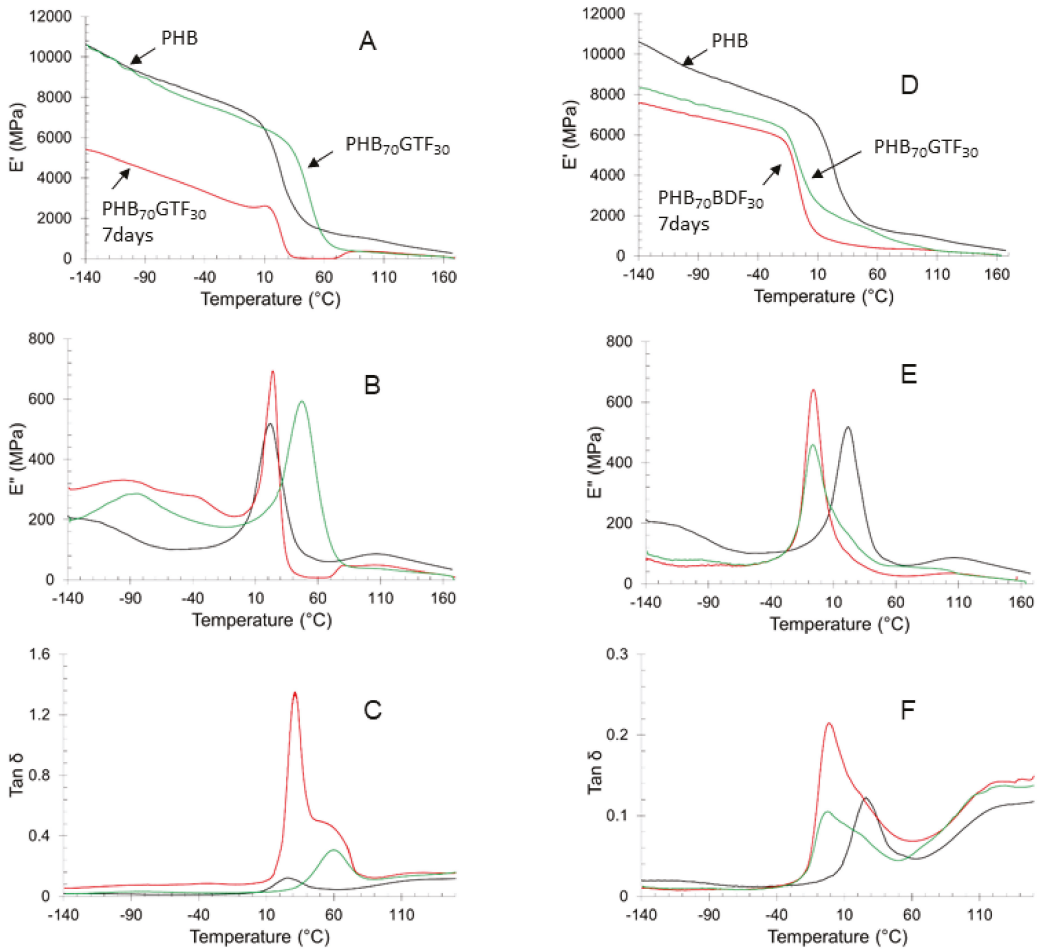


Figure 4. DMA analysis. (A) Storage modulus, (B) loss modulus, and (C) tan delta of PHB after extrusion (in dark), PHB₇₀GTF₃₀ 1/2 h after extrusion (in red), PHB₇₀GTF₃₀ 7 days after extrusion (in green). (D) Storage modulus, (E) loss modulus, and (F) tan delta of PHB after extrusion (in dark), PHB₇₀BDF₃₀ 0.5 h after extrusion (in red), PHB₇₀BDF₃₀ 7 days after extrusion (in green).

Consequently, the addition of BDF to PHB reduces the stiffening of the material during storage. This behavior is advantageous as PHB alone is stiff and brittle. For better understanding of the BDF and PHB crystallization, their structures were studied by X-ray diffraction. After one week, the diffraction pattern of the PHB₇₀BDF₃₀ mixture does not show significant evolution with time (Figure 2). The amorphous contribution observed for the as-prepared sample seems however significantly reduced for the one-week sample, indicating some possible recrystallization phenomenon. This fact was confirmed by DSC measurements (Figure 5).

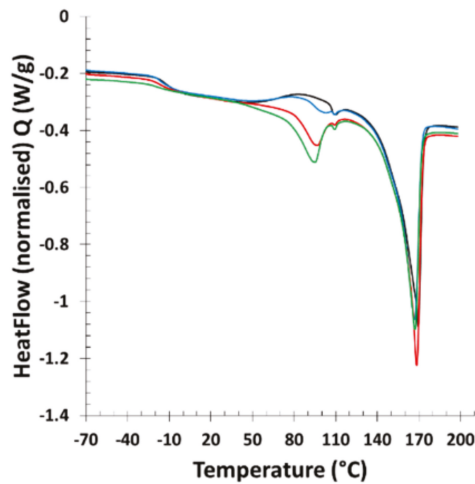


Figure 5. DSC analysis of PHB₇₀BDF₃₀ after extrusion after 30 min (in dark), PHB₇₀BDF₃₀ 0.25 day after extrusion (in blue), PHB₇₀BDF₃₀ one day after extrusion (in red), PHB₇₀BDF₃₀ seven days after extrusion (in green).

Analysis by DSC over the one-week period of the PHB₇₀BDF₃₀ samples highlights a BDF crystallization after 24 h. This crystallization is responsible for the property changes as they are closely linked to the reorganization of the macromolecular chains of the amorphous into crystalline domains. The BDF crystallizes in the sample over time which causes a change in the mechanical properties of the PHB/BDF blends which become stiffer and much less flexible.

Mechanical tests very quickly after extrusion because we observed a very important flexibility of the PHB samples which contain BDF. It is really very difficult to prevent crystallization of PHB, which has a very fast crystallization rate but the strain at break of PHB₇₀BDF₃₀ is around 253% although the strain at break of the PHB is around 11% just after extrusion.

The evolution of the mechanical properties was therefore followed over time and to see if this phenomenon is reversible, the samples were subjected to thermal treatments at 120 °C, i.e., above the T_m of BDF but well below the T_m of PHB. It turns out that three anneals at 120 °C for 5 min were necessary for the sample to recover its initial properties, i.e., an elongation at break of 260%, as shown in Figure 6. Five minutes after extrusion, PHB samples already have low elongation at break around 11%, while for PHB₇₀BDF₃₀ it is 25 times higher, at 253%. This value decreases rapidly, and after one hour it is already down to 27%. Simultaneously the BDF was observed to crystallize in the sample as the normalized fusion enthalpy increases steadily to a plateau around 65 J/g. Even though the two phenomena seem connected, they do not happen concomitantly. Indeed, the decline in elongation at break occurs marginally before the increase of ΔH_m . After one week, the samples were annealed 5 min at 120 °C. Elongation at break increased by 34%, five times higher than annealed PHB. Following three anneals, properties like the fresh samples could be recovered (Table 6). 262% of elongation at break was measured five minutes after annealing, and 190% after one hour. Compared to the non-annealed samples, the drop in ϵ_{break} was about 10 times slower, while, at the same time, the crystallization kinetic was slightly faster.

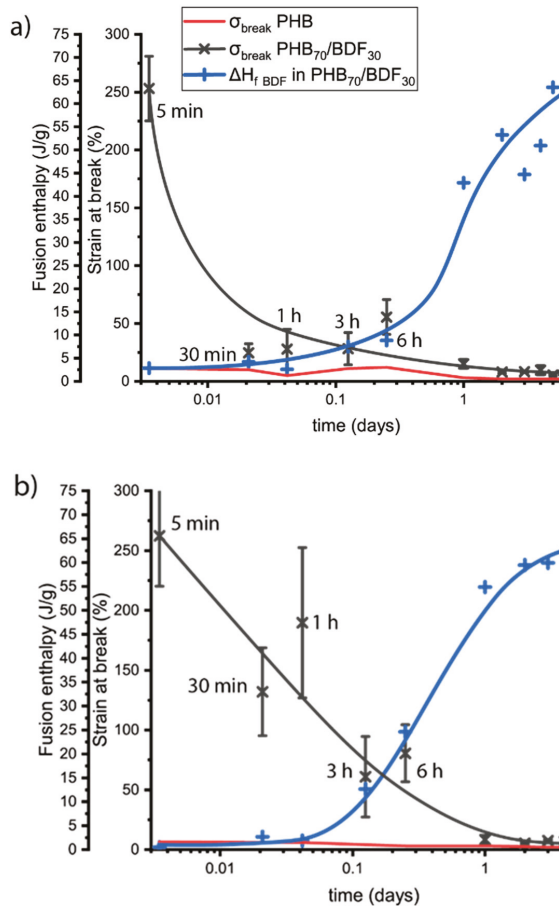


Figure 6. Follow up of polymer deformation at break for PHB (gray) and PHB₇₀BDF₃₀ (red) (a) after extrusion and (b) after annealing at 120 °C. Blue dashed line represents the fusion enthalpy of BDF in the PHB₇₀BDF₃₀.

Table 6. Effects of successive anneals at 120 °C on mechanical properties.

Number of Anneals	$\epsilon_{\text{break PHB}_{70}\text{BDF}_{30}}$ (%)	$\epsilon_{\text{break PHB}_{100}}$ (%)	$\sigma_{\text{break PHB}_{70}\text{BDF}_{30}}$ (MPa)	$\sigma_{\text{break PHB}_{100}}$ (MPa)
0	253 ± 20	11 ± 0.2	12.5 ± 1.3	22.8 ± 0.5
1	34 ± 14	6 ± 0.2	17.0 ± 0.4	36.1 ± 1.9
2	54 ± 13	5 ± 0.8	15.2 ± 0.8	36.3 ± 2.8
3	262 ± 42	7 ± 2.0	18.1 ± 1.1	28.8 ± 1.2

3.4. Antioxidant Properties and Thermal Stability

BDF is a phenolic compound that exhibits two phenol groups per molecule. As such, some radical-scavenging property is expected. Accordingly, by blending BDF and PHB the resulting material is anticipated to exhibit antioxidant behavior. Radical scavenging activity (RSA) can be measured by reduction of DPPH in solution. The DPPH radical scavenging assay is widely used to assess the antioxidant activity of phenolic compounds [43,44]. At 517 nm, this relaxation and swelling control radical has an absorbance maximum. When this molecule reacts with a hydrogen donor such as an antioxidant, the absorbance decreases

and a change in color of the solution from purple to yellow is observed. As shown in Figure 7, concentration as low as 5%w/w was found to reduce 81% of DPPH in solution. With 20% and above, 94% radical scavenging activity can be obtained. This behavior makes BDF a promising additive for applications where antioxidant properties are sought after.

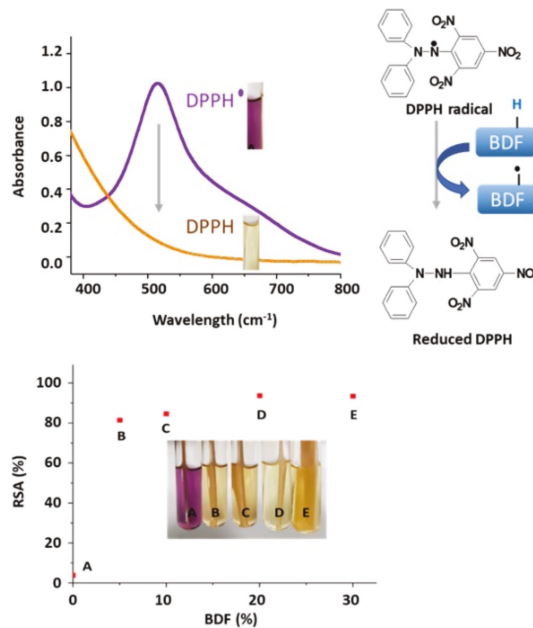


Figure 7. Radical scavenging activity of (A) pure PHB, (B) PHB₉₅BDF₅, (C) PHB₉₀BDF₁₀, (D) PHB₈₀BDF₂₀, and (E) PHB₇₀BDF₃₀.

The TGA shows the loss of mass as a function of temperature. This loss of mass is due to the loss of volatile fragments following the important degradations of polymer chains leading to small molecules. On Figure 8 the temperature at which 20% mass loss is observed is 280 °C for PHB and 360 °C for BDF. The introduction between 5% and 40% of BDF increases the thermal stability by 10 °C and the 20% mass loss is now observed at 290 °C. Pyrolysis combustion flow calorimetry (PCFC) tests were performed according to ASTM D7309 to evaluate the flammability of PHB, PHB₈₀BDF₂₀ and PHB₇₀BDF₃₀ samples [45]. Figure 9 displays the curves of heat release rate as a function of temperature and several parameters extracted from these curves, including peak of heat release rate (pHRR), total heat release (THR), and temperature at pHRR, summarized in Table 7. Pure PHB shows a highly flammable character demonstrated by an intense pHRR 1074 W/g at 305 °C. The presence of BDF in PHB significantly changed the flammability behavior of PHB. The slope of HRR curves were decreased by increasing the percentage of BDF. Moreover, the pHRR was meaningfully decreased and reached 723 W/g and 659 W/g for PHB₈₀BDF₂₀ and PHB₇₀BDF₃₀, respectively. Furthermore, the temperature at pHRR was increased from 305 °C for pure PHB to 310 °C for PHB₇₀BDF₃₀, while for PHB₈₀BDF₂₀ it remained similar that of pure PHB, at 305.5 °C. It was also noticed that there is quite no change in THR for samples containing BDF compared to pure PHB.

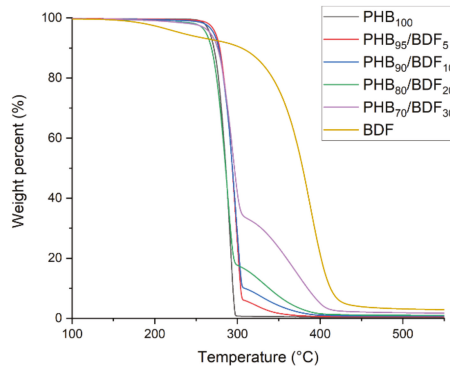


Figure 8. Thermal stabilities of different PHB-BDF blends measured by TGA.

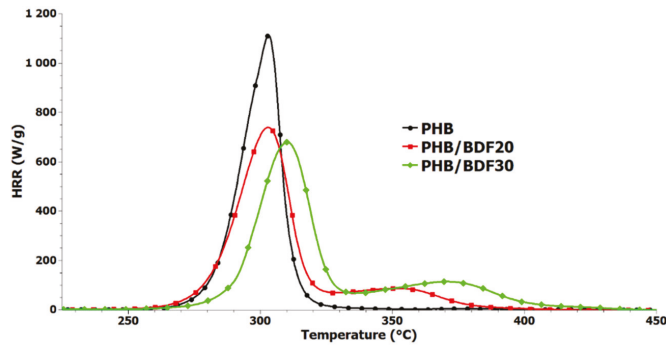


Figure 9. Heat release rate (HRR) curves for PHB, PHB₈₀BDF₂₀, and PHB₇₀BDF₃₀ obtained from pyrolysis combustion flow calorimeter analysis (PCFC) tests.

Table 7. Summary of results obtained in PCFC tests for PHB, PHB₈₀BDF₂₀, and PHB₇₀BDF₃₀.

	pHRR (W/g)	T _{pHRR}	THR (kJ/g)	Reduction in pHRR (%)
PHB	1074	305	22.3	-
PHB ₈₀ /BDF ₂₀	723	305.5	22.8	33
PHB ₇₀ /BDF ₃₀	659	310	23	39

4. Conclusions

Among the three ferulic acid derivatives, only BDF and GTF showed a plasticizing effect of PHB with a clear increase in elongation at break unlike PDF. However, the mechanical properties of the mixtures vary with time due to the crystallization of the additives. This effect is very important in the case of GTF because the specimens become so brittle after one week that it is no longer possible to handle them. The BDF is very pro-mising because it increases the elongation at break from 11% for PHB to 260% for the PHB₇₀BDF₃₀ blend. Although this value is not stable over time, it is possible to recover this property after a short five-minute heat treatment of PHB at a temperature much lower than the melting temperature of PHB but just above the melting temperature of BDF. For this purpose, an X-ray diffraction study has allowed for the first time to specify the crystal structure and the lattice parameters of BDF. This derivative which had already shown its properties as plasticizer for PCL and PLA confirms here all its interest during the formulation of PHB. The reversibility of the mechanical properties according to the temperature combine with the antioxidant properties and the resistance to the flammability will undoubtedly

allow to consider new applications for the PHB. The incorporation of BDF decrease the hydrophobicity of PHB surface as it was shown by the values of contact angle with water from 70° to 63.5° in presence of BDF. The effect of ferulic acid-based derivatives on the kinetics of enzymatic and hydrolytic degradations required a further study to precise the long-term behavior of these biodegradable polyesters.

Author Contributions: Conceptualization, A.G. and V.L.; Methodology, L.F.L., L.M., H.V., A.R.D.A., E.R. and M.L.; Validation, A.G., M.L. and V.L.; Original draft preparation, L.F.L., A.R.D.A., M.L. and V.L.; Project administration, F.A. and V.L. All authors have read and agreed to the published version of the manuscript.

Funding: This research received no external funding.

Institutional Review Board Statement: Not applicable.

Informed Consent Statement: Informed consent was obtained from all subjects involved in the study.

Data Availability Statement: Not applicable.

Acknowledgments: Financial support from ANR PRCI (SeaBioP Project, France) is sincerely acknowledged. The Région Grand Est, the Conseil Départemental de la Marne and the Grand Reims are gratefully acknowledged for supporting these works.

Conflicts of Interest: The authors declare no conflict of interest.

References

- Steinbüchel, A.; Valentin, H.E. Diversity of Bacterial Polyhydroxyalkanoic Acids. *FEMS Microbiol. Lett.* **1995**, *128*, 219–228. [[CrossRef](#)]
- Sudesh, K.; Abe, H.; Doi, Y. Synthesis, Structure and Properties of Polyhydroxyalkanoates: Biological Polyesters. *Prog. Polym. Sci.* **2000**, *10*, 1503–1555. [[CrossRef](#)]
- Lenz, R.W.; Marchessault, R.H. Bacterial Polyesters: Biosynthesis, Biodegradable Plastics and Biotechnology. *Biomacromolecules* **2005**, *6*, 1–8. [[CrossRef](#)]
- Akaraonye, E.; Keshavarz, T.; Roy, I. Production of Polyhydroxyalkanoates: The Future Green Materials of Choice. *J. Chem. Technol. Biotechnol.* **2010**, *85*, 732–743. [[CrossRef](#)]
- Chen, G.Q.; Chen, X.Y.; Wu, F.Q.; Chen, J.C. Polyhydroxyalkanoates (PHA) toward cost competitiveness and functionality. *Adv. Ind. Eng. Polym. Res.* **2020**, *3*, 1–7. [[CrossRef](#)]
- Koller, M. Biodegradable and Biocompatible Polyhydroxy-alkanoates (PHA): Auspicious Microbial Macromolecules for Pharmaceutical and Therapeutic Applications. *Molecules* **2018**, *23*, 362. [[CrossRef](#)]
- Zhang, J.; Shishatskaya, E.I.; Volova, T.G.; Da Silva, F.L.; Chen, G.Q. Polyhydroxyalkanoates for therapeutic applications. *Mater. Sci. Eng. C Mater. Biol. Appl.* **2018**, *86*, 144–150. [[CrossRef](#)]
- Rai, R.; Keshavarz, T.; Roether, J.A.; Boccaccini, A.R.; Roy, I. Medium chain length polyhydroxyalkanoates, promising new biomedical materials for the future. *Mater. Sci. Eng.* **2011**, *72*, 29–47. [[CrossRef](#)]
- Guerin, P.; Renard, E.; Langlois, V. Degradation of Natural and Artificial Poly[(R)-3-Hydroxyalkanoate]s: From Biodegradation to Hydrolysis. In *Plastics from Bacteria; Microbiology Monographs*; Springer: Berlin/Heidelberg, Germany, 2010; pp. 283–321.
- Jendrossek, D.; Handrick, R. Microbial Degradation of Polyhydroxyalkanoates. *Annu. Rev. Microbiol.* **2002**, *56*, 403–432. [[CrossRef](#)]
- Renard, E.; Walls, M.; Guérin, P.; Langlois, V. Hydrolytic Degradation of Blends of Polyhydroxyalkanoates and Functionalized Polyhydroxyalkanoates. *Polym. Degrad. Stab.* **2004**, *85*, 779–787. [[CrossRef](#)]
- Tokiwa, Y.; Calabia, B.P. Review Degradation of Microbial Polyesters. *Biotechnol. Lett.* **2004**, *26*, 1181–1189. [[CrossRef](#)] [[PubMed](#)]
- Numata, K.; Abe, H.; Iwata, T. Biodegradability of Poly(hydroxyalkanoate) Materials. *Materials* **2009**, *2*, 1104–1126. [[CrossRef](#)]
- Volova, T.; Prudnikova, S.V.; Vinogradova, O.N.; Syrvacgheva, D.A.; Shihatskaya, E.I. Microbial degradation of polyhydroxyalkanoates with different chemical compositions and their biodegradability. *Microb. Ecol.* **2017**, *73*, 353–367. [[CrossRef](#)] [[PubMed](#)]
- Grassie, N.; Murray, E.J.; Holmes, P.A. The Thermal Degradation of Poly(-d)-β-Hydroxybutyric Acid): Part 2-Changes in Molecular Weight. *Polym. Degrad. Stab.* **1984**, *6*, 95–103. [[CrossRef](#)]
- Gigante, V.; Cinneli, P.; Segginai, M.; Alavarez, V.A.; Lazzar, A. Processing and thermomechanical properties of PHA. In *The Handbook of Polyhydroxyalkanoates*; CRC Press: Boca Raton, FL, USA, 2020; ISBN 9781003087663.
- Qiu, Y.Z.; Han, J.; Quo, J.-J.; Chen, G.-Q. Production of Poly(3-hydroxybutyrate-co-3-hydroxyhexanoate) from Gluconate and Glucose by Recombinant *Aeromonas hydrophila* and *Pseudomonas putida*. *Biotechnol. Lett.* **2005**, *27*, 1381–1386. [[CrossRef](#)]
- Jost, V. Mechanical and permeation properties of PHA-based blends and composites. In *The Handbook of Polyhydroxyalkanoates*; CRC Press: Boca Raton, FL, USA, 2020; ISBN 9781003087663.
- Vieira, M.G.A.; da Silva, M.A.; dos Santos, L.O.; Beppu, M.M. Natural-Based Plasticizers and Biopolymer Films: A Review. *Eur. Polym. J.* **2011**, *47*, 254–263. [[CrossRef](#)]

20. Hong, S.-G.; Hsu, H.-W.; Ye, M.-T. Thermal Properties and Applications of Low Molecular Weight Polyhydroxybutyrate. *J. Therm. Anal. Calorim.* **2012**, *111*, 1243–1250. [[CrossRef](#)]
21. Brunel, D.G.; Pachekoski, W.M.; Dalmolin, C.; Agnelli, J.A.M. Natural additives for poly (hydroxybutyrate-CO-hydroxyvalerate)-PHBV: Effect on mechanical properties and biodegradation. *Mater. Res.* **2014**, *17*, 1145–1156. [[CrossRef](#)]
22. Choi, J.S.; Park, W.H. Effect of Biodegradable Plasticizers on Thermal and Mechanical Properties of poly(3-Hydroxybutyrate). *Polym. Test.* **2004**, *23*, 455–460. [[CrossRef](#)]
23. Mekonnen, T.; Mussone, P.; Khalil, H.; Bressler, D. Progress in Bio-Based Plastics and Plasticizing Modifications. *J. Mater. Chem. A* **2013**, *1*, 13379–13398. [[CrossRef](#)]
24. Parra, D.F.; Fusaro, J.; Gaboardi, F.; Rosa, D.S. Influence of Poly (ethylene Glycol) on the Thermal, Mechanical, Morphological, Physical–chemical and Biodegradation Properties of Poly (3-Hydroxybutyrate). *Polym. Degrad. Stab.* **2006**, *91*, 1954–1959. [[CrossRef](#)]
25. Erceg, M.; Kovačić, T.; Klarić, I. Thermal Degradation of poly(3-Hydroxybutyrate) Plasticized with Acetyl Tributyl Citrate. *Polym. Degrad. Stab.* **2005**, *90*, 313–318. [[CrossRef](#)]
26. Baltieri, R.C.; Innocentini Mei, L.H.; Bartoli, J. Study of the Influence of Plasticizers on the Thermal and Mechanical Properties of poly(3-Hydroxybutyrate) Compounds. *Macromol. Symp.* **2003**, *197*, 33–44. [[CrossRef](#)]
27. Jost, V.; Langowski, H.-C. Effect of Different Plasticisers on the Mechanical and Barrier Properties of Extruded Cast PHBV Films. *Eur. Polym. J.* **2015**, *68* (Suppl. C), 302–312. [[CrossRef](#)]
28. Arrieta, M.; López, J.; Hernández, A.; Rayón, E. Ternary PLA-PHB-Limonene Blends Intended for Biodegradable Food Packaging Applications. *Eur. Polym. J.* **2013**, *50*, 255–270. [[CrossRef](#)]
29. Persico, P.; Ambrogio, V.; Baroni, A.; Santagata, G.; Carfagna, C.; Malinconico, M.; Cerruti, P. Enhancement of poly (3-hydroxybutyrate) thermal and processing stability using a bio-waste derived additive. *Int. J. Biol. Macromol.* **2012**, *51*, 1151–1158. [[CrossRef](#)]
30. Auriemma, M.; Piscitelli, A.; Pasquino, R.; Cerruti, P.; Malinconico, M.; Grizzuti, N. Blending poly(3-Hydroxybutyrate) with Tannic Acid: Influence of a Polyphenolic Natural Additive on the Rheological and Thermal Behavior. *Eur. Polym. J.* **2015**, *63*, 123–131. [[CrossRef](#)]
31. Audic, J.-L.; Lemiègre, L.; Corre, Y.-M. Thermal and Mechanical Properties of a Polyhydroxyalkanoate Plasticized with Biobased Epoxidized Broccoli Oil. *J. Appl. Polym. Sci.* **2014**, *131*, 1–7. [[CrossRef](#)]
32. Garcia-Garcia, D.; Ferri, J.M.; Montanes, N.; Lopez-Martinez, J.; Balart, R. Plasticization Effects of Epoxidized Vegetable Oils on Mechanical Properties of poly(3-Hydroxybutyrate). *Polym. Int.* **2016**, *65*, 1157–1164. [[CrossRef](#)]
33. Mangeon, C.; Modjinou, T.; Rios de Anda, A.; Thevenieau, F.; Renard, E.; Langlois, V. Renewable Semi-Interpenetrating Polymer Networks Based on Vegetable Oils Used as Plasticized Systems of Poly(3-hydroxyalkanoate)s. *ACS Sustain. Chem. Eng.* **2018**, *6*, 5034–5042. [[CrossRef](#)]
34. Mangeon, C.; Michely, L.; Rios de Anda, A.; Thevenieau, F.; Renard, E.; Langlois, V. Natural Terpenes Used as Plasticizers for Poly(3-hydroxybutyrate). *ACS Sustain. Chem. Eng.* **2018**, *6*, 16160–16168. [[CrossRef](#)]
35. Gallos, A.; Paës, G.; Legland, D.; Beaugrand, J.; Allais, F. Microstructural and Chemical Approach to Highlight How a Simple Methyl Group Affects the Mechanical Properties of a Natural Fibers Composite. *ACS Sustain. Chem. Eng.* **2017**, *5*, 10352–10360. [[CrossRef](#)]
36. Gallos, A.; Crowet, J.-M.; Michely, L.; Raghuvanshi, V.S.; Mention, M.M.; Langlois, V.; Dauchez, M.; Garnier, G.; Allais, F. Blending ferulic acid derivatives and polylactic acid into biobased and transparent elastomeric materials with shape memory properties. *Biomacromolecules* **2021**, *22*, 1568–1578. [[CrossRef](#)] [[PubMed](#)]
37. Kasmi, S.; Gallos, A.; Beaugrand, J.; Paës, G.; Allais, F. Ferulic acid derivatives used as biobased powders for a convenient plasticization of polylactic acid in continuous hot-melt process. *Eur. Polym. J.* **2019**, *110*, 293–300. [[CrossRef](#)]
38. Bruker AXS. *Topas V4. 2: General Profile and Structure Analysis Software for Powder Diffraction Data AXS Bruker*; Bruker AXS: Karlsruhe, Germany, 2009.
39. Kawaguchi, Y.; Doi, Y. Structure of native poly(3-hydroxybutyrate) granules characterized by X-ray diffraction. *FEMS Microbiol. Lett.* **1990**, *70*, 151–156. [[CrossRef](#)]
40. Brückner, S.; Meille, S.V.; Malpezzi, L.; Cesàro, A.; Navarini, L.; Tomblini, R. The structure of Poly(D-(-)-β-hydroxybutyrate). A Refinement based on the Rietveld method. *Macromolecules* **1988**, *21*, 967–971. [[CrossRef](#)]
41. Rietveld, H.M. A profile refinement method for nuclear and magnetic structures. *J. Appl. Crystallogr.* **1969**, *2*, 65–71. [[CrossRef](#)]
42. Le Bail, A. Whole powder pattern decomposition methods and applications: A retrospection. *Powder Diffr.* **2005**, *20*, 316–326. [[CrossRef](#)]
43. Sureshkumar, M.; Lee, P.-N.; Lee, C.-K. Facile preparation of a robust and flexible antioxidant film based on self-polymerized dopamine in a microporous battery separator. *RSC Adv.* **2012**, *2*, 5127–5129. [[CrossRef](#)]
44. Engman, L.; Persson, J.; Vessman, K.; Ekström, M.; Berglund, M.; Andersson, C.-M. Organotellurium compounds as efficient retarders of lipid peroxidation in methanol. *Free Radic. Biol. Med.* **1995**, *19*, 441–452. [[CrossRef](#)]
45. Sonnier, R.; Vahabi, H.; Ferry, L.; Lopez-Cuesta, J.-M. Pyrolysis-combustion flow calorimetry: A powerful tool to evaluate the flame retardancy of polymers. *Fire Polym. VI New Adv. Flame Retard. Chem. Sci.* **2012**, *1118*, 361–390.

Article

Antioxidant Network Based on Sulfonated Polyhydroxyalkanoate and Tannic Acid Derivative

Laura Brelle, Estelle Renard and Valerie Langlois *

Univ Paris Est Creteil, CNRS, ICMPE, UMR 7182, 2 rue Henri Dunant, 94320 Thiais, France; brelle@icmpe.cnrs.fr (L.B.); renard@icmpe.cnrs.fr (E.R.)

* Correspondence: langlois@u-pec.fr

Abstract: A novel generation of gels based on medium chain length poly(3-hydroxyalkanoate)s, *mcl*-PHAs, were developed by using ionic interactions. First, water soluble *mcl*-PHAs containing sulfonate groups were obtained by thiol-ene reaction in the presence of sodium-3-mercapto-1-ethanesulfonate. Anionic PHAs were physically crosslinked by divalent inorganic cations Ca^{2+} , Ba^{2+} , Mg^{2+} or by ammonium derivatives of gallic acid $\text{GA-N}(\text{CH}_3)_3^+$ or tannic acid $\text{TA-N}(\text{CH}_3)_3^+$. The ammonium derivatives were designed through the chemical modification of gallic acid GA or tannic acid TA with glycidyl trimethyl ammonium chloride (GTMA). The results clearly demonstrated that the formation of the networks depends on the nature of the cations. A low viscoelastic network having an elastic around 40 Pa is formed in the presence of Ca^{2+} . Although the gel formation is not possible in the presence of $\text{GA-N}(\text{CH}_3)_3^+$, the mechanical properties increased in the presence of $\text{TA-N}(\text{CH}_3)_3^+$ with an elastic modulus G' around 4200 Pa. The $\text{PHOSO}_3^-/\text{TA-N}(\text{CH}_3)_3^+$ gels having antioxidant activity, due to the presence of tannic acid, remained stable for at least 5 months. Thus, the stability of these novel networks based on PHA encourage their use in the development of active biomaterials.

Keywords: polyhydroxyalkanoate; PHOU; water soluble PHA; network; tannic acid

Citation: Brelle, L.; Renard, E.; Langlois, V. Antioxidant Network Based on Sulfonated Polyhydroxyalkanoate and Tannic Acid Derivative. *Bioengineering* **2021**, *8*, 9. <https://doi.org/10.3390/bioengineering8010009>

Received: 10 November 2020

Accepted: 23 December 2020

Published: 8 January 2021

Publisher's Note: MDPI stays neutral with regard to jurisdictional claims in published maps and institutional affiliations.



Copyright: © 2021 by the authors. Licensee MDPI, Basel, Switzerland. This article is an open access article distributed under the terms and conditions of the Creative Commons Attribution (CC BY) license (<https://creativecommons.org/licenses/by/4.0/>).

1. Introduction

Poly(3-hydroxyalkanoate)s (PHAs) are natural polymers produced by microorganisms as carbon and energy storage compounds when they are placed under special growth conditions. PHAs are naturally occurring aliphatic polyesters that have a high structural diversity related to the alkyl pendant group [1–3]. The length of this side chain group is decisive for their final thermal and mechanical properties. PHAs can be divided into three main types depending on the number of carbon atoms in the monomer unit: short-chain-length PHAs (*scl*-PHA), with monomers consisting of 3–5 carbon atoms, medium-chain-length PHAs (*mcl*-PHA), with monomers consisting of 6–14 carbon atoms, and long chain length PHAs (*lcl*-PHA), which are obtained from long chain fatty acids with more than 14 carbon atoms. The former display physical properties associated with highly crystalline thermoplastics while the latter generally possess low crystallinity and elastomeric character. Due to their biodegradability [4,5] and biocompatibility, they constitute a very promising group of natural biomaterials for various biomedical applications including drug delivery and tissue engineering [6–9].

In order to enlarge the potential in biomedical applications, chemical modifications of *mcl*-PHAs have been performed. One of the first studies concerning the chemical modification of PHAs started with the production of poly(3-hydroxyoctanoate-*co*-3-hydroxyundecenoate) (PHOU) that contained unsaturated groups in the side chains [10,11]. The chemical modifications of the unsaturated groups of PHOU have already been reported [12–17]. The introduction of polar groups, such as hydroxyl, carboxylic and ammonium groups, makes it possible to modify the hydrophilic/hydrophobic balance of the polymer. Amphiphilic PHAs-PEG copolymers that were synthesized by esterification [18–20] and by click chemistry [21–24] have shown the ability to self-associate in aqueous medium

to form micelles, vesicular structures or polymersomes. Water soluble PHAs obtained by introducing PEG [18], ammonium groups [25], or sulfonate functions [26,27] retained their biocompatible and non-cytotoxic character and the presence of PEG and propyleneglycol (PPG) segments provided hydrophilicity, blood compatibility [28], and thermo-sensitivity respectively [29,30].

Networks based on PHAs were prepared by photoactivated reaction in the presence of PEG-monoacrylate [28] or PEG-diacryloyl [31]. Chen et al. [32] recently reported PHA gel via photo-crosslinking based on a thiol-ene reaction with PEG-dithiol as a photo-cross-linker. Although some structures from chemically cross-linked PHAs have already been described in the literature, there is to our knowledge no study on the gels with PHAs bearing sulfonate groups. These novel materials should constitute an interesting support in the biomedical field because of the biological interactions of the sulfonate groups due to their anticoagulant, antiangiogenic, and antimitogenic properties. These active anionic sites are known to interact with proteins, such as fibronectin [33–36].

In our paper, we describe the synthesis of PHA sulfonate, PHOSO_3^- , by a photoactivated thiol-ene process in the presence of sodium-2-mercapto-1-ethanesulfonate and the elaboration of crosslinked structures by combination with bivalent cations or organic polycationic molecules (Figure 1).

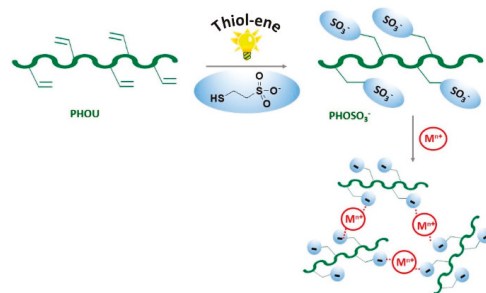


Figure 1. Gelation process of PHOSO_3^- induced by cationic species as Ca^{2+} , Mg^{2+} , Ba^{2+} , and gallic and tannic acid derivatives.

Among the bivalent cations that have the capability of forming a gel by ionic interactions with anionic polymers, Ca^{2+} , Ba^{2+} , and Mg^{2+} present interesting properties in biomedical applications [37–39]. In particular, the gelation of an alginate solution with a multivalent ion of opposite charge such as Ca^{2+} allows to obtain a resistant and biocompatible hydrogel.

To increase the numbers of ionic interactions, we report here the synthesis of ammonium derivatives of gallic acid and tannic acid. Gallic acid (GA) is a natural trihydroxybenzoic acid extracted from plants and evaluated as an antioxidant, antibacterial, and antiviral compound [40,41]. Tannic acid (TA) is a kind of natural polyphenol that is commonly found in high herbaceous and woody plants that is a well-known bio-based molecule for its antioxidant and antibacterial activity [42–44]. Moreover, polyphenols due to their cyclic structure and the presence of a large content of hydroxyl groups are good candidates for the development of stable physical gels and offer the possibility to be easily modifiable through these accessible functions. Tannic acid has already shown the ability to make gels or hydrogels with good mechanical structures by different interactions such as supramolecular interactions by hydrogen bonds [45], coordination with transition metals [46,47], and a self-assembly method by redox reaction [48,49]. A series of bio-based UV-curable antibacterial resins were synthesized through modifying tannic acid with glycidyl methacrylate (GMA) [50]. In this study, ammonium groups were introduced on GA and TA through reaction with glycidyl trimethyl ammonium chloride (GTMA). The presence of ammonium groups on GA and TA increases both the number of cationic charges compared to divalent cations and the rigidity by the presence of the aromatic rings. Gels

were formed by ionic interactions of the oppositely charged polyelectrolytes PHOSO_3^- and Ca^{2+} , Ba^{2+} and Mg^{2+} , and $\text{GA-N}(\text{CH}_3)_3^+$ and $\text{TA-N}(\text{CH}_3)_3^+$. The viscoelastic properties of the gels and their antioxidant activity were studied.

2. Materials and Methods

2.1. Materials

Poly(3-hydroxyoctanoate-co-3-hydroxyundecenoate) with 33% double bonds PHOU was provided from the Swiss Federal Laboratory for Materials Testing and Research (EMPA, Switzerland, $M_n = 40,000$ g/mol, Polydispersity index 1.7). The different comonomers are randomly distributed. CaCl_2 , BaCl_2 , MgCl_2 , and Sodium 2-mercapto-1-ethanesulfonate (98%) were purchased from Aldrich. Tannic acid was purchased from Alfa Aesar. Tetrahydrofuran (THF), dimethylsulfoxide (DMSO), methanol, and ethanol absolute anhydrous were purchased from Carlo Erba. Gallic acid, 2,2-dimethoxy-2-phenylacetophenone (DMPA, Irgacure 651), glycidyltrimethyl ammonium (GTMA), triphenylphosphine (TPP), and methyl hydroxyquinone (MEHQ), were supplied from Sigma-Aldrich and were used without prior purification. Butylacetate was supplied from Merck. Tannic acid was purchased from Alfa Aesar.

2.2. Synthesis of PHO Sulfonate, PHOSO_3^-

A total of 0.2 g PHOU was solubilized in 12 mL THF under agitation at room temperature. Five molar equivalents (relative to the double bonds of PHOU) of sodium 2-mercapto-1-ethanesulfonate (98%) and 0.5 eq. molar DMPA were solubilized in 18 mL of a MeOH/THF (2/1 v/v) mixture. The mixture placed at 11 cm was irradiated for 300 s at room temperature with a mercury xenon ($180 \text{ Mw}\cdot\text{cm}^{-2}$) Lightning cure LC8 (L8251) lamp from Hamamatsu coupled with a flexible light guide. During the entire irradiation process the mixture was kept under stirring. After irradiation, 25 mL DMSO was added. The resulting product was dialyzed in a 1000 Da cut-off dialysis tube against distilled water, which was changed three times daily for 4 d.

2.3. Synthesis of Trimethyl Ammonium Gallic Acid: $\text{GA-N}(\text{CH}_3)_3^+$

In a two-neck round-bottom flask, 2.125 g of gallic acid, 4.996×10^{-2} moles of GTMA, 0.1456 g of triphenylphosphine (TPP) and 0.0097 g of methyl hydroxyquinone (MEHQ) were solubilized in 5 mL of anhydrous ethanol and butyl acetate 1:2 (v:v), under an inert atmosphere. The mixture was stirred at 100°C for 48 h. After 48 h, the mixture was precipitated in acetone to remove solvent and then purified by flash column chromatography using methanol as an eluent.

2.4. Synthesis of Trimethyl Ammonium Tannic Acid: $\text{TA-N}(\text{CH}_3)_3^+$

In a flask, 4.25 g of tannic acid, 0.25 moles of GTMA, 0.09 g of triphenylphosphine (TPP) and 0.0075 g of methyl hydroxyquinone (MEHQ) were solubilized in 10 mL of an anhydrous ethanol and butyl acetate 1:2 (v:v) mixture, under an inert atmosphere. The mixture was stirred at 100°C for 48 h. Then it was solubilized in an H_2O /ethanol mixture (25:75) and centrifuged. The precipitate containing the $\text{TA-N}(\text{CH}_3)_3^+$ was recovered and dried in a vacuum chamber at 40°C for one night. The molar mass of the monomeric unit of the polymer is $M_0 = (0.67 \times 142) + (0.33 \times 323) = 201 \text{ g}\cdot\text{mol}^{-1}$.

2.5. Elaboration of Network Based on PHOSO_3^-

$\text{PHOSO}_3^-/\text{Ca}^{2+}$. Networks were prepared according to the following protocol. A total of 0.05 mL of CaCl_2 0.2 M was added to 0.25 mL of PHOSO_3^- with a concentration of $27 \text{ g}\cdot\text{L}^{-1}$. The mixture was vortexed for 30 s allowing the instantaneous formation of the network.

$\text{PHOSO}_3^-/\text{TA-N}(\text{CH}_3)_3^+$. A total of 0.2 mL of PHOSO_3^- with a concentration of $96 \text{ g}\cdot\text{L}^{-1}$ and 0.01 g of $\text{TA-N}(\text{CH}_3)_3^+$ were introduced into a haemolysis tube. After an agitation with a vortex, a sticky, brown gel was formed.

2.6. DPPH Test

The radical scavenging activity (RSA) of the networks was determined by using 2,2-diphenyl-1-picrylhydrazyl. A total of 37 mg of the $\text{PHOSO}_3^-/\text{TA-N}(\text{CH}_3)_3^+$ were immersed in 3 mL of 0.1 mM of DPPH solution in methanol in the dark for 60 min at room temperature. The RSA was measured by using a Varian Cary 50 Bio UV-Visible spectrophotometer controlled by the CaryWinUV software. RSA was therefore determined by monitoring the decrease of the absorbance at 517 nm (Equation (1)):

$$\text{RSA (\%)} = ((A_{\text{ref}} - A_s)/A_{\text{ref}}) \times 100 \quad (1)$$

where A_{ref} corresponds to the absorbance of the 0.1 mM of DPPH solution without a sample and A_s corresponds to the absorbance of the 0.1 mM solution of DPPH with 37 mg samples of tannic derivatives.

2.7. Characterization

The molar mass of the $\text{PHO}_{(67)}\text{U}_{(33)}$ was determined by Size Exclusion Chromatography in THF using a Shimadzu LC-10AD pump with two Shodex GPC K-805L columns (5 μm Mixte-C) at a concentration of 10 mg·mL⁻¹. A Wyatt Technology Optilab Rex interferometric refractometer (Toulouse, France) was used as a detector, and low polydispersity index polystyrene standards (3×10^4 – 2×10^6 g/mol) were used for PHOU analysis. ¹H NMR spectra (400 MHz) were performed with a Bruker AV 400M spectrometer (Wissembourg, France). In a disposable spectrophotometer cell, 10 μL of CaCl_2 (0.2 M) was added to 0.250 mL of PHOSO_3^- at 37 g·L⁻¹, in a constant manner. After manual stirring, the transmittance was measured at 600 nm with a UV-vis Cary50 Bio Varian UV–visible spectrometer supplied by Varian (Agilent, Les Ulis, France) recording controlled by Cary Win UV software in the range 250–800 nm. Rheological properties were determined with a hybrid rheometer (DISCOVERY HR-2) (Guyancourt, France) using a cone and plate geometry (20 mm, 1°). Rheological tests were performed at 25 °C (room temperature) and the Peltier temperature control system was used to keep the temperature constant throughout the analysis. The evaporation of the water contained in the 3D network was limited by the presence of a solvent trap. For $\text{PHOSO}_3^-/\text{M}^{2+}$ networks, the elastic modulus (G') and viscous modulus (G'') were plotted against frequency from 0.1 to 100 rad·s⁻¹ for an applied strain at 20% on 0.350 mL of a 3D network. In addition, for the $\text{PHOSO}_3^-/\text{TA-N}(\text{CH}_3)_3^+$ network frequency sweep tests were done between 0.1 and 100 Hz for an applied strain at 1%. These measurements were carried out three times to ensure the repeatability of the results and the viability of the tests.

3. Results and Discussion

3.1. Synthesis of Poly(3-Hydroxyalkanoate) Sulfonate, PHOSO_3^- , Ammonium Derivatives of Gallic Acid $\text{GA-N}(\text{CH}_3)_3^+$ and Tannic Acid, $\text{TA-N}(\text{CH}_3)_3^+$

Poly(3-hydroxyoctanoate-co-3-hydroxyundecenoate) PHOU is a hydrophobic polyester composed of long alkyl side chains and lateral unsaturated groups. Sulfonate groups were grafted to the terminal double bonds of the PHOU, to both provide an amphiphilic character to the PHA and to induce non-covalent binding of SO_3^- ions to cationic species to form ionic crosslinking (Figure 1).

Poly(3-hydroxyoctanoate-co-3-hydroxyundecenoate), PHOU was first characterized by ¹H NMR (Figure 2) to determine the percentage of terminal unsaturation by integrating protons corresponding to the CH peak (2) at 5.1 ppm, and the signal relating to the terminal alkene group of side chain (7) at 5.7 ppm. Sodium-3-mercapto-1-ethanesulfonate was grafted under photochemical activation, using 5 molar equivalents of sulfonate groups. After purification by dialysis, the polymers were dried by freeze-drying and then analyzed by ¹H NMR. The presence of the signals relating to the two CH_2 methylene (c, d), which are characteristic of sulfonate groups, appeared at 2.66 ppm and the total disappearance of the peaks relating to the terminal alkene group of side chains (7) and (8) indicated the success

of the formation of PHOSO_3^- . We previously showed that no chain scission occurred during this thiol-ene reaction and the PHOSO_3^- is water soluble [26,27].

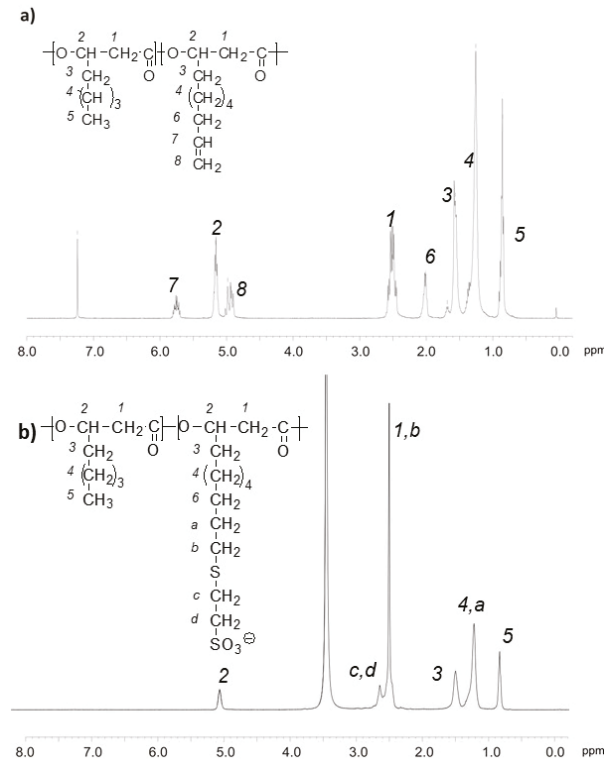


Figure 2. ^1H NMR spectra: (a) PHOU in CDCl_3 ; (b) PHOSO_3^- in dimethyl sulfoxide, $\text{DMSO}-d_6$.

Ammonium derivative of gallic acid $\text{GA}-\text{N}(\text{CH}_3)_3^+$ and tannic acid $\text{TA}-\text{N}(\text{CH}_3)_3^+$ were synthesized through the reaction with glycidyl trimethylammonium chloride GTMA (Figure 3). ^1H NMR spectra (Figure 4) showed that GTMA was grafted to phenol groups of the TA due to the disappearance of the peak at 3.1 ppm (a) which correspond to the epoxide groups of GTMA and the appearance of peaks at 3.5–4.6 ppm, which correspond to the $-\text{CH}_2-\text{CH}(\text{OH})-\text{CH}_2-\text{N}(\text{CH}_3)_3^+$ units (a', b', c'). The number of ammonium groups $\text{N}(\text{CH}_3)_3^+$ was calculated from the area ratio of the peaks at 6.7–7.5 ppm ($I_{1,2}$), which corresponds to the protons on the aromatic group of tannic acid, and the peak at 3.2 ppm (I_d), which are characteristic of the protons on the ammonium groups (Equation (2)). The conversion of the grafting reaction is defined by Equation (3).

$$\text{N}(\text{CH}_3)_3^+ = \frac{I_{1,2} \times 20}{I_d \times 9} \quad (2)$$

$$\text{Conversion (\%)} = \frac{\text{N}(\text{CH}_3)_3^+}{25} \times 100 \quad (3)$$

The substitution degree of TA was calculated as around 76% (which corresponds to 19 N^+ per molecule) and $\text{TA}-\text{N}(\text{CH}_3)_3^+$ is totally soluble in water. The substitution reaction of GA determined by NMR is quantitative. The degree of substitution was calculated as the ratio of the integration of the peak (d) at 3.3 ppm to the number of hydrogens carried by the nitrogen atom (N^+), i.e., nine. Integration of peaks b and c confirmed that there were

4 N⁺ per molecule. As a consequence, we can further study the influence of the numbers of ammonium groups on the gel formation.

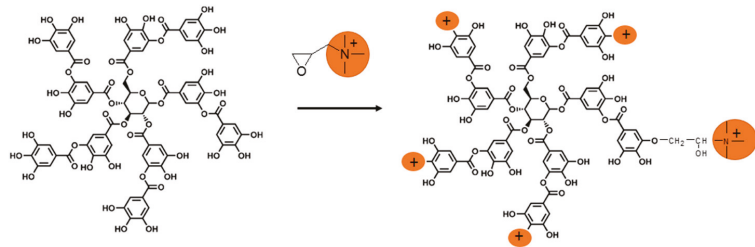


Figure 3. Schematic representation of TA-N(CH₃)₃⁺ by chemical modification of tannic acid in the presence of GTMA.

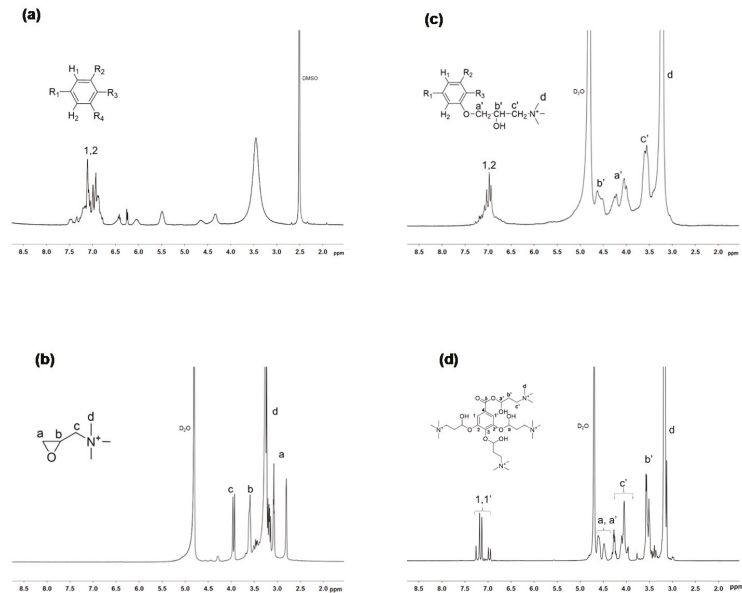


Figure 4. ¹H NMR spectra of (a) tannic acid in DMSO, (b) GTMA in D₂O, (c) TA-N(CH₃)₃⁺ in D₂O, and (d) GA-N(CH₃)₃⁺ in D₂O.

3.2. Effects of the Nature of Cations on the Formation of Gels

Networks were spontaneously formed after a few seconds of mixing PHOSO₃[−] and cationic species. The influence of the nature of divalent cations as Mg²⁺, Ba²⁺, and Ca²⁺ was first studied. In the presence of Mg²⁺ no gel formation was observed regardless of the concentration. Mg²⁺ therefore does not have sufficient interaction energy and attractive power [51]. The Ba²⁺ did not allow the formation of a gel and gave rise to a precipitate even at very low concentrations. This result may be due to the bigger size of the barium atom nucleus combined with an insufficient proportion of sulfonate functions [52]. PHOSO₃[−], which is completely soluble in water (27 g·L^{−1}; 1.1 × 10^{−5} moles), instantly forms a network in the presence of a sufficient molar concentration of Ca²⁺. The variation of transmittance as a function of the number of moles of Ca²⁺ showed three well-defined zones (Figure 5). A first zone is defined between 0 to 1.5 × 10^{−5} moles, showing that the polymer remains in solution. Between 1.5 × 10^{−5} and 2.5 × 10^{−5} moles, the transmittance

drops sharply from 98% to 20%, respectively, attesting to the gel formation. The addition of Ca^{2+} beyond this concentration does not modify the transmittance, which remains constant at 20%. The presence of precipitate is then observed when the moles of salt are greater than 2.6×10^{-5} moles.

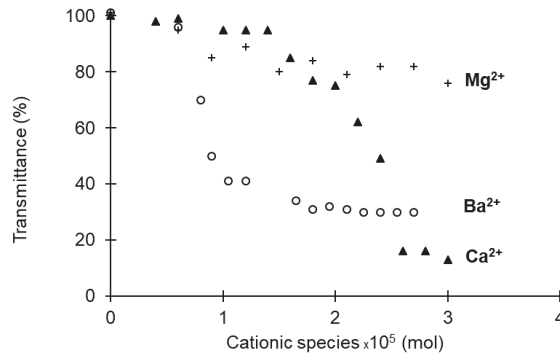


Figure 5. Effect of the cationic species on the network formation with a PHOSO_3^- (concentration of $27 \text{ g}\cdot\text{L}^{-1}$).

The gel formation conditions were studied next in the presence of Ca^{2+} , gallic acid and tannic acid derivatives. Under our conditions, no gel was formed in the presence of $\text{GA-N}(\text{CH}_3)_3^+$ whereas gels formed very easily in the presence of $\text{TA-N}(\text{CH}_3)_3^+$, which allows us to affirm that the number of positive charges is very important during gel formation. Therefore, in order to be able to compare the conditions of gel formation in the presence of Ca^{2+} and the $\text{TA-N}(\text{CH}_3)_3^+$ derivative, Figure 6 shows the different zones observed for the gels as a function of the number of positive and negative charges. To perform this study we added increasing volumes of positive charge solution (Ca^{2+} or $\text{TA-N}(\text{CH}_3)_3^+$) from the same initial solution. The results obtained are very different because there are three zones in the case of Ca^{2+} (liquid, gel and precipitate), whereas there are only two zones for $\text{TA-N}(\text{CH}_3)_3^+$ (liquid and gel). In the presence of Ca^{2+} , the gels were formed in the stoichiometric conditions of the number of moles of positive and negative charges. On the other hand, in the presence of $\text{TA-N}(\text{CH}_3)_3^+$, the experimental conditions were different because it is enough that the number of moles of sulfonate groups and positive charges are greater than 2.296×10^{-5} moles and 0.483×10^{-5} moles, respectively.

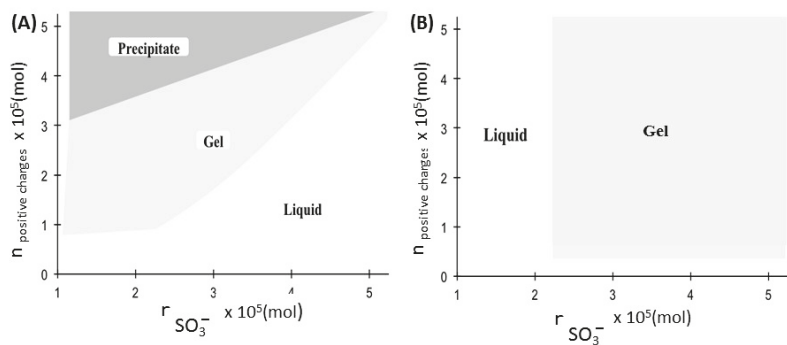


Figure 6. Schematic representation of the effect of the number of positive charges for Ca^{2+} (A) or $\text{TA-N}(\text{CH}_3)_3^+$ (B) as a function of the amount of SO_3^- in the gel formation.

3.3. Structure of Networks and Antioxidant Properties

The mechanical properties of the $\text{PHOSO}_3^- / \text{Ca}^{2+}$ networks are strongly dependent of the polymer and CaCl_2 concentration (Table 1). Dynamic viscoelastic measurement results show that at the higher frequency region G' is larger than G'' , showing that these gels present predominantly elastic properties. The modulus G' depends on the concentration of CaCl_2 and increases linearly with the concentration of PHOSO_3^- , which shows the influence of hydrophobic interactions between chains and undoubtedly the presence of entanglements. This effect is superimposed on the ionic bonds between the polymer and Ca^{2+} . However, the elastic modulus obtained remains low and does not exceed 40 Pa. Although the network keeps its structure for a week, the addition of water led to the deterioration of the network. The low percentage of SO_3^- groups (33%) did not allow the formation of enough ionic interactions with Ca^{2+} . The use of other calcium salts such as CaCO_3 was studied, but its low solubility in water did not allow the formation of the network, or even $\text{CaSO}_4 \cdot 2\text{H}_2\text{O}$ in the presence of Na_2HPO_4 , which is often used as a gelation accelerator [38].

Table 1. Influence of PHO-SO_3^- concentration on gel mechanical properties of $\text{PHOSO}_3^- / \text{Ca}^{2+}$ networks at 10 Hz.

$[\text{PHO-SO}_3^-]$ (g/L)	$n_{\text{SO}_3^-} \times 10^5$	$n_{\text{Ca}^{2+}} \times 10^5$	n Positive Charges $\times 10^5$	G' (Pa)	G'' (Pa)
47	1.93	1.4	2.8	4.01	3.93
59	2.42	1.5	3.0	14.62	11.26
68	2.79	1.4	2.8	24.20	12.78
71	2.91	1.8	3.6	38.38	24.92

Although the formation of a tannic acid-based network often requires a certain pH value necessary to have the phenolate groups [44–46], the advantage of our system is that there is no pH-dependence of the gel formation. In the physiological medium, the tannic acid derivative $\text{TA-N}(\text{CH}_3)_3^+$ and the sulfonate PHA always have quaternary amine and sulfonate groups, respectively. The $\text{PHOSO}_3^- / \text{TA-N}(\text{CH}_3)_3^+$ network has better mechanical properties than the gel obtained in the presence of Ca^{2+} (Figure 7). Indeed, the viscoelastic modulus at 100 Hz was much larger than those of the $\text{PHOSO}_3^- / \text{Ca}^{2+}$ network. The elastic modulus of the $\text{PHOSO}_3^- / \text{TA-N}(\text{CH}_3)_3^+$ network was stable even after 5 months. This was due to the presence of polyphenolic moieties that gave the network a very high stability and remarkable mechanical properties despite the low proportion of SO_3^- . Unlike the $\text{PHOSO}_3^- / \text{Ca}^{2+}$ network, the addition of water to the $\text{PHOSO}_3^- / \text{TA-N}(\text{CH}_3)_3^+$ network did not disrupt the structure of the network, and the network structure was maintained even after the rheological studies. Moreover, the formation of the network was a completely reversible process even after freeze-drying without any change of the viscoelastic modulus.

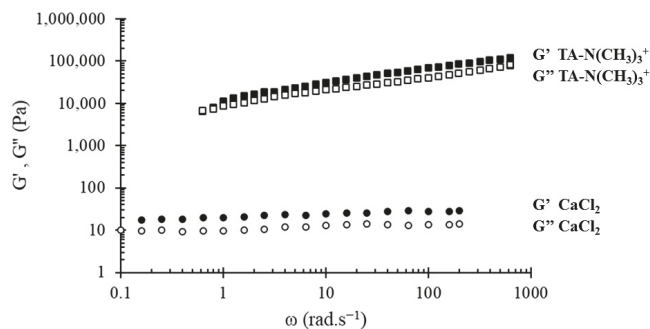


Figure 7. Frequency dependences of the storage modulus G' and loss modulus G'' of PHOSO_3^- at $96 \text{ g} \cdot \text{L}^{-1}$ with CaCl_2 and $\text{TA-N}(\text{CH}_3)_3^+$.

The antioxidant capacity was assessed using the DPPH radical scavenging assay. This method consists in performing a reduction of the DPPH radical to its non-radical form in the presence of tannic acid, a hydrogen donating compound (Figure 8). The solution containing DPPH has a purple color, corresponding to a UV-visible absorbance at 517 nm. In the presence of TA, TA-N(CH₃)₃⁺, and PHOSO₃⁻/TA-N(CH₃)₃⁺, the solutions became yellow and presented significant antiradical activity with a radical scavenging activity (% RSA) superior to 82%.

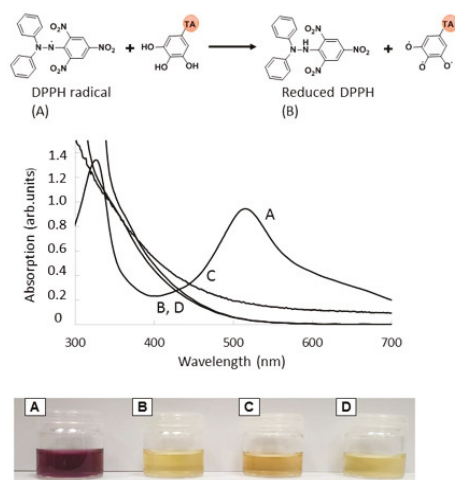


Figure 8. Absorption UV spectra in the presence of DPPH (A) and reduced DPPH after reaction with TA (B), TA-N(CH₃)₃⁺ (C), and PHOSO₃⁻/TA-N(CH₃)₃⁺ (D).

4. Conclusions

A copolymer based on unsaturated PHAs was functionalized with the polar SO₃⁻ sulfonate groups to promote, on the one hand, its solubility in water [26,27], and on the other hand, ionic interactions with cations. An efficient and reproducible method for the synthesis of copolymer of water soluble PHOSO₃⁻ was developed by thiol-ene reaction in the presence of sodium-3-mercapto-1-ethanesulfonate. This copolymer was further used for the preparation of network by ions' interaction with different cations, namely Ca²⁺, Ba²⁺, and Mg²⁺. Among them, only Ca²⁺ presented the ability to form a gel in the well-defined contents. To reinforce the mechanical properties and stability of the gels, a polycationic derivative of tannic acid was synthesized by reaction with glycidyl trimethyl ammonium chloride (GTMA). The presence of aromatic groups and cationic charges improved the elastic modulus from 40 Pa obtained with Ca²⁺ to 4200 Pa in the presence of TA-N(CH₃)₃⁺. The antioxidant networks based on PHOSO₃⁻/TA-N(CH₃)₃⁺ were stable for 5 months in a buffered physiological environment and constitute a new generation of soft biomaterials.

Author Contributions: Conceptualization, L.B., E.R. and V.L.; methodology, L.B., E.R.; investigation, L.B., E.R. and V.L.; writing—original draft preparation, L.B., E.R. and V.L.; supervision, E.R. and V.L. All authors have read and agreed to the published version of the manuscript.

Funding: Financial support from ANR PRCI (SeaBioP Project, France).

Institutional Review Board Statement: Not applicable.

Informed Consent Statement: Not applicable.

Data Availability Statement: Not applicable.

Acknowledgments: Financial support from ANR PRCI (SeaBioP Project, France) is sincerely acknowledged.

Conflicts of Interest: The authors declare no conflict of interest

References

- Steinbüchel, A.; Valentin, H.E. Diversity of bacterial polyhydroxyalkanoic acids. *FEMS Microbiol. Lett.* **1995**, *128*, 219–228. [[CrossRef](#)]
- Sudesh, K.; Abe, H.; Doi, Y. Synthesis, structure and properties of polyhydroxyalkanoates: Biological polyesters. *Prog. Polym. Sci.* **2000**, *25*, 1503–1555. [[CrossRef](#)]
- Lenz, R.W.; Marchessault, R.H. Bacterial Polyesters: Biosynthesis, Biodegradable Plastics and Biotechnology. *Biomacromolecules* **2005**, *6*, 1–8.
- Numata, K.; Abe, H.; Iwata, T. Biodegradability of Poly(hydroxyalkanoate) Materials. *Materials* **2009**, *2*, 1104–1126. [[CrossRef](#)]
- Volova, T.G.; Prudnikova, S.V.; Vinogradova, O.N.; Syrvacheva, D.A.; Shishatskaya, E.I. Microbial Degradation of Polyhydroxyalkanoates with Different Chemical Compositions and Their Biodegradability. *Microb. Ecol.* **2017**, *73*, 353–367. [[CrossRef](#)]
- Zhang, J.; Shishatskaya, E.I.; Volova, T.G.; Silva, L.F.; Chen, G.-Q. Polyhydroxyalkanoates (PHA) for therapeutic applications. *Mater. Sci. Eng. C* **2018**, *86*, 144–150. [[CrossRef](#)]
- Rai, R.; Keshavarz, T.; Roether, J.; Boccaccini, A.R.; Roy, I. Medium chain length polyhydroxyalkanoates, promising new biomedical materials for the future. *Mater. Sci. Eng. R Rep.* **2011**, *72*, 29–47. [[CrossRef](#)]
- Koller, M. Biodegradable and Biocompatible Polyhydroxy-alkanoates (PHA): Auspicious Microbial Macromolecules for Pharmaceutical and Therapeutic Applications. *Molecules* **2018**, *23*, 362. [[CrossRef](#)] [[PubMed](#)]
- Williams, S.F.; Martin, D.P. Applications of Polyhydroxyalkanoates (PHA). *Med. Pharm.* **2002**, *10*, 91–121.
- Bear, M.M.; Renard, E.; Randriamahefa, S.; Langlois, V.; Guérin, P. Preparation of a bacterial polyester with carboxy groups in side chains. *C. R. l'Academie. Sci. Ser. IIC Univers.* **2001**, *4*, 289–293.
- Chen, G.-Q.; Chen, X.-Y.; Wu, F.-Q.; Chen, J.-C. Polyhydroxyalkanoates (PHA) toward cost competitiveness and functionality. *Adv. Ind. Eng. Polym. Res.* **2020**, *3*, 1–7. [[CrossRef](#)]
- Renard, E.; Poux, A.; Timbart, L.; Langlois, A.V.; Guérin, P. Preparation of a Novel Artificial Bacterial Polyester Modified with Pendant Hydroxyl Groups. *Biomacromolecules* **2005**, *6*, 891–896. [[CrossRef](#)] [[PubMed](#)]
- Eroğlu, M.S.; Hazer, B.; Ozturk, T.; Çaykara, T. Hydroxylation of pendant vinyl groups of poly(3-hydroxy undec-10-enoate) in high yield. *J. Appl. Polym. Sci.* **2005**, *97*, 2132–2139. [[CrossRef](#)]
- Stigers, J.D.; Tew, G.N. Poly(3-hydroxyalkanoate)s Functionalized with Carboxylic Acid Groups in the Side Chain. *Biomacromolecules* **2003**, *4*, 193–195. [[CrossRef](#)]
- Renard, E.; Timbart, L.; Vergnol, G.; Langlois, V. Role of carboxyl pendant groups of medium chain length poly(3-hydroxyalkanoate)s in biomedical temporary applications. *J. Appl. Polym. Sci.* **2010**, *117*, 1888–1896. [[CrossRef](#)]
- Park, W.H.; Lenz, R.W.; Goodwin, S. Epoxidation of Bacterial Polyesters with Unsaturated Side Chains. I. Production and Epoxidation of Polyesters from 10-Undecenoic Acid. *Macromolecules* **1998**, *31*, 1480–1486. [[CrossRef](#)]
- Hazer, B.; Steinbüchel, A. Increased diversification of polyhydroxyalkanoates by modification reactions for industrial and medical applications. *Appl. Microbiol. Biotechnol.* **2007**, *74*, 1–12. [[CrossRef](#)]
- Domenek, S.; Langlois, V.; Renard, E. Bacterial polyesters grafted with poly(ethylene glycol): Behaviour in aqueous media. *Polym. Degrad. Stab.* **2007**, *92*, 1384–1392. [[CrossRef](#)]
- Renard, E.; Tanguy, P.-Y.; Samain, E.; Guérin, P. Synthesis of novel graft polyhydroxyalkanoates. *Macromol. Symp.* **2003**, *197*, 11–18. [[CrossRef](#)]
- Renard, E.; Ternat, C.; Langlois, V.; Guérin, P. Synthesis of Graft Bacterial Polyesters for Nanoparticles Preparation. *Macromol. Biosci.* **2003**, *3*, 248–252. [[CrossRef](#)]
- Babinot, J.; Renard, E.; Langlois, V. Preparation of Clickable Poly(3-hydroxyalkanoate) (PHA): Application to Poly(ethylene glycol) (PEG) Graft Copolymers Synthesis. *Macromol. Rapid Commun.* **2010**, *31*, 619–624. [[CrossRef](#)] [[PubMed](#)]
- Babinot, J.; Renard, E.; Le Droumaguet, B.; Guigner, J.-M.; Mura, S.; Nicolas, J.; Couvreur, P.; Langlois, V.; Patrick, C. Facile Synthesis of Multicompartment Micelles Based on Biocompatible Poly(3-hydroxyalkanoate). *Macromol. Rapid Commun.* **2012**, *34*, 362–368. [[CrossRef](#)] [[PubMed](#)]
- Babinot, J.; Renard, E.; Langlois, V. Controlled Synthesis of Well Defined Poly(3-hydroxyalkanoate)s-based Amphiphilic Diblock Copolymers Using Click Chemistry. *Macromol. Chem. Phys.* **2010**, *212*, 278–285. [[CrossRef](#)]
- Babinot, J.; Guigner, J.-M.; Renard, E.; Langlois, V. Poly(3-hydroxyalkanoate)-derived amphiphilic graft copolymers for the design of polymersomes. *Chem. Commun.* **2012**, *48*, 5364–5366. [[CrossRef](#)] [[PubMed](#)]
- Sparks, J.; Scholz, C. Synthesis and Characterization of a Cationic Poly(β -hydroxyalkanoate). *Biomacromolecules* **2008**, *9*, 2091–2096. [[CrossRef](#)]
- Modjinou, T.; Lemechko, P.; Babinot, J.; Versace, D.L.; Langlois, V.; Renard, E. Poly(3-hydroxyalkanoate) sulfonate: From nanoparticles toward water soluble polyesters. *Eur. Polym. J.* **2015**, *68*, 471–479.
- Jain-Beuguel, C.; Li, X.; Renault, L.H.; Modjinou, T.; Colin, C.S.; Gref, R.; Renard, E.; Langlois, V. Water-Soluble Poly(3-hydroxyalkanoate) Sulfonate: Versatile Biomaterials Used as Coatings for Highly Porous Nano-Metal Organic Framework. *Biomacromolecules* **2019**, *20*, 3324–3332. [[CrossRef](#)]
- Chung, C.W.; Kim, H.W.; Kim, Y.B.; Rhee, Y.H. Poly(ethylene glycol)-grafted poly(3-hydroxyundecenoate) networks for enhanced blood compatibility. *Int. J. Biol. Macromol.* **2003**, *32*, 17–22. [[CrossRef](#)]

29. Jiang, L.; Luo, Z.; Loh, X.J.; Wu, Y.-L.; Li, Z. PHA-Based Thermogel as a Controlled Zero-Order Chemotherapeutic Delivery System for the Effective Treatment of Melanoma. *ACS Appl. Bio Mater.* **2019**, *2*, 3591–3600. [[CrossRef](#)]
30. Le Fer, G.; Babinot, J.; Versace, D.-L.; Langlois, V.; Renard, E. An Efficient Thiol-Ene Chemistry for the Preparation of Amphiphilic PHA-Based Graft Copolymers. *Macromol. Rapid Commun.* **2012**, *33*, 2041–2045. [[CrossRef](#)]
31. Hao, J.; Deng, X. Semi-interpenetrating networks of bacterial poly(3-hydroxybutyrate) with net-poly(ethylene glycol). *Polymer* **2001**, *42*, 4091–4097. [[CrossRef](#)]
32. Zhang, X.; Li, Z.; Che, X.; Yu, L.; Jia, W.; Shen, R.; Chen, J.; Ma, Y.; Chen, G.Q. Synthesis and Characterization of Polyhydroxyalkanoate Organo/Hydrogels. *Biomacromolecules* **2019**, *20*, 3303–3312. [[CrossRef](#)] [[PubMed](#)]
33. Pavon-Djavid, G.; Gamble, L.J.; Ciobanu, M.; Gueguen, V.; Castner, D.G.; Mignonney, V. Bioactive Poly(ethylene terephthalate) Fibers and Fabrics: Grafting, Chemical Characterization, and Biological Assessment. *Biomacromolecules* **2007**, *8*, 3317–3325. [[CrossRef](#)] [[PubMed](#)]
34. Silver, J.H.; Hart, A.P.; Williams, E.C.; Cooper, S.L.; Charef, S.; Labarre, D.; Jozefowicz, M. Anticoagulant effects of sulphonated polyurethanes. *Biomaterials* **1992**, *13*, 339–344. [[CrossRef](#)]
35. Palarasah, Y.; Skjoedt, M.O.; Vitved, L.; Koch, C. Sodium Polyanethole Sulfonate as an Inhibitor of Activation of Complement Function in Blood Culture Systems. *J. Clin. Microbiol.* **2010**, *48*, 908–914. [[CrossRef](#)]
36. Meder, F.; Brandes, C.; Treccani, L.; Rezwani, K. Controlling protein–particle adsorption by surface tailoring colloidal alumina particles with sulfonate groups. *Acta Biomater.* **2013**, *9*, 5780–5787. [[CrossRef](#)]
37. Li, G.; Zhang, G.; Sun, R.; Wong, C.-P. Mechanical strengthened alginate/polyacrylamide hydrogel crosslinked by barium and ferric dual ions. *J. Mater. Sci.* **2017**, *52*, 8538–8545. [[CrossRef](#)]
38. Larsen, B.E.; Bjørnstad, J.; Pettersen, E.O.; Tønnesen, H.H.; Melvik, J.E. Rheological characterization of an injectable alginate gel system. *BMC Biotechnol.* **2015**, *15*, 29. [[CrossRef](#)]
39. Espona-Noguera, A.; Ciriza, J.; Cañibano-Hernández, A.; Fernandez, L.; Ochoa, I.; Saenz del Burgo, L.; Pedraz, J.L. Tunable injectable alginate-based hydrogel for cell therapy in Type 1 Diabetes Mellitus. *Int. J. Biol. Macromol.* **2018**, *107*, 1261–1269.
40. Badhani, B.; Sharma, N.; Kakkur, R. Gallic acid: A versatile antioxidant with promising therapeutic and industrial applications. *RSC Adv.* **2015**, *5*, 27540–27557. [[CrossRef](#)]
41. Zahrani, N.A.A.L.; El-Shishtawy, R.M.; Asiri, A.M. Recent developments of gallic acid derivatives and their hybrids in medicinal chemistry: A review European. *J. Med. Chem.* **2020**, *204*, 112609–112646. [[CrossRef](#)] [[PubMed](#)]
42. Glaive, A.-S.; Modjinou, T.; Versace, D.-L.; Abbad-Andaloussi, S.; Dubot, P.; Langlois, V.; Renard, E. Design of Antibacterial and Sustainable Antioxidant Networks Based on Plant Phenolic Derivatives Used As Delivery System of Carvacrol or Tannic Acid. *ACS Sustain. Chem. Eng.* **2017**, *5*, 2320–2329. [[CrossRef](#)]
43. Bhone, K.; Lim, M.; Sing, C.; Wei, Z. Tannic Acid as Phytochemical Potentiator for Antibiotic Resistance Adaptation. *APCBEE Procedia* **2013**, *7*, 175–181.
44. Xie, Y.; Chen, S.; Zhang, X.; Shi, Z.; Wei, Z.; Bao, J.; Zhao, W.; Zhao, C. Engineering of Tannic Acid Inspired Antifouling and Antibacterial Membranes through Co-deposition of Zwitterionic Polymers and Ag Nanoparticles. *Ind. Eng. Chem. Res.* **2019**, *58*, 11689–11697. [[CrossRef](#)]
45. Fan, H.; Wang, L.; Feng, X.; Bu, Y.; Wu, D.; Jin, Z. Supramolecular Hydrogel Formation Based on Tannic Acid. *Macromolecules* **2017**, *50*, 666–676. [[CrossRef](#)]
46. Fan, H.; Wang, J.; Zhang, Q.; Jin, Z. Tannic Acid-Based Multifunctional Hydrogels with Facile Adjustable Adhesion and Cohesion Contributed by Polyphenol Supramolecular Chemistry. *ACS Omega* **2017**, *2*, 6668–6676. [[CrossRef](#)]
47. Zheng, L.-Y.; Shi, J.-M.; Chi, Y.-H. Tannic Acid Physically Cross-Linked Responsive Hydrogel. *Macromol. Chem. Phys.* **2018**, *219*. [[CrossRef](#)]
48. Guo, J.; Sun, W.; Kim, J.P.; Lu, X.; Li, Q.; Lin, M.; Mrowczynski, O.; Rizk, E.B.; Cheng, J.; Qian, G.-Y.; et al. Development of tannin-inspired antimicrobial bioadhesives. *Acta Biomater.* **2018**, *72*, 35–44. [[CrossRef](#)]
49. Park, K.; Jeong, H.; Tanum, J.; Yoo, J.-C.; Hong, J. Developing regulatory property of gelatin-tannic acid multilayer films for coating-based nitric oxide gas delivery system. *Sci. Rep.* **2019**, *9*, 1–8. [[CrossRef](#)]
50. Liu, R.; Zheng, J.; Guo, R.; Luo, J.; Yuan, Y.; Liu, X. Synthesis of New Biobased Antibacterial Methacrylates Derived from Tannic Acid and Their Application in UV-Cured Coatings. *Ind. Eng. Chem. Res.* **2014**, *53*, 10835–10840. [[CrossRef](#)]
51. Assifaoui, A.; Lerbret, A.; Huynh, U.T.D.; Neiers, F.; Chambin, O.; Loupiac, C.; Cousin, F.; Uyen, H.T.D. Structural behaviour differences in low methoxy pectin solutions in the presence of divalent cations (Ca²⁺ and Zn²⁺): A process driven by the binding mechanism of the cation with the galacturonate unit. *Soft Matter* **2015**, *11*, 551–560. [[CrossRef](#)] [[PubMed](#)]
52. Huynh, U.T.D.; Lerbret, A.; Neiers, F.; Chambin, O.; Assifaoui, A. Binding of Divalent Cations to Polygalacturonate: A mechanism Drien by the Hydration Water. *J. Phys. Chem.* **2016**, *120*, 1021–1032. [[CrossRef](#)] [[PubMed](#)]

Review

A New Wave of Industrialization of PHA Biopolyesters

Martin Koller^{1,2,*} and Anindya Mukherjee^{3,4}

¹ Office of Research Management and Service, c/o Institute of Chemistry, University of Graz, NAWI Graz, Heinrichstrasse 28/IV, 8010 Graz, Austria

² ARENA—Association for Resource Efficient and Sustainable Technologies, Inffeldgasse 21b, 8010 Graz, Austria

³ Global Organization for PHA (GO!PHA), Oudebrugsteeg 9, 1012 JN Amsterdam, The Netherlands; anindya.mukherjee@gopha.org

⁴ PHAXTEC, Inc., Wake Forest, NC 27587, USA

* Correspondence: martin.koller@uni-graz.at; Tel.: +43-316-380-5463

Abstract: The ever-increasing use of plastics, their fossil origin, and especially their persistence in nature have started a wave of new innovations in materials that are renewable, offer the functionalities of plastics, and are biodegradable. One such class of biopolymers, polyhydroxyalkanoates (PHAs), are biosynthesized by numerous microorganisms through the conversion of carbon-rich renewable resources. PHA homo- and heteropolyesters are intracellular products of secondary microbial metabolism. When isolated from microbial biomass, PHA biopolymers mimic the functionalities of many of the top-selling plastics of petrochemical origin, but biodegrade in soil, freshwater, and marine environments, and are both industrial- and home-compostable. Only a handful of PHA biopolymers have been studied in-depth, and five of these reliably match the desired material properties of established fossil plastics. Realizing the positive attributes of PHA biopolymers, several established chemical companies and numerous start-ups, brand owners, and converters have begun to produce and use PHA in a variety of industrial and consumer applications, in what can be described as the emergence of the “PHA industry”. While this positive industrial and commercial relevance of PHA can hardly be described as the first wave in its commercial development, it is nonetheless a very serious one with over 25 companies and start-ups and 30+ brand owners announcing partnerships in PHA production and use. The combined product portfolio of the producing companies is restricted to five types of PHA, namely poly(3-hydroxybutyrate), poly(4-hydroxybutyrate), poly(3-hydroxybutyrate-co-3-hydroxyvalerate), poly(3-hydroxybutyrate-co-4-hydroxybutyrate), and poly(3-hydroxybutyrate-co-3-hydroxyhexanoate), even though PHAs as a class of polymers offer the potential to generate almost limitless combinations of polymers beneficial to humankind. To date, by varying the co-monomer type and content in these PHA biopolymers, their properties emulate those of the seven top-selling fossil plastics, representing 230 million t of annual plastics production. Capacity expansions of 1.5 million t over the next 5 years have been announced. Policymakers worldwide have taken notice and are encouraging industry to adopt biodegradable and compostable material solutions. This wave of commercialization of PHAs in single-use and in durable applications holds the potential to make the decisive quantum leap in reducing plastic pollution, the depletion of fossil resources, and the emission of greenhouse gases and thus fighting climate change. This review presents setbacks and success stories of the past 40 years and the current commercialization wave of PHA biopolymers, their properties, and their fields of application.

Citation: Koller, M.; Mukherjee, A. A New Wave of Industrialization of PHA Biopolyesters. *Bioengineering* **2022**, *9*, 74. <https://doi.org/10.3390/bioengineering9020074>

Academic Editor: Jason A. Burdick

Received: 5 January 2022

Accepted: 8 February 2022

Published: 15 February 2022

Publisher’s Note: MDPI stays neutral with regard to jurisdictional claims in published maps and institutional affiliations.



Copyright: © 2022 by the authors. Licensee MDPI, Basel, Switzerland. This article is an open access article distributed under the terms and conditions of the Creative Commons Attribution (CC BY) license (<https://creativecommons.org/licenses/by/4.0/>).

Keywords: biopolymers; commercialization; copolyester; homopolyester; polyhydroxyalkanoate

1. Introduction

Plastics based on fossil resources have proven their valuable role in increasing our quality of life in various sectors, as shown by their wide-spread application as packaging materials for food and other perishable goods; in the medical and pharmaceutical field;

and in the transportation sector, e.g., in automobiles or aircraft, where plastics have enabled novel technological and safety-related improvements. Thus, it is undisputed that plastics, which ubiquitously accompany us in our daily lives, have made our society more convenient. However, the persistence of fossil plastics at their end of life, the insufficiency of collection and recycling systems, and their leakage into terrestrial and aquatic environments, ultimately leading to microplastic pollution of the eco- and biosphere, are omnipresent threats to all life on earth [1]. A UN study in 2005 concluded that plastic waste in oceans would result in the formation of microplastics and that these microplastics constituted the next environmental threat so great that it had the potential to be the next epic threat [2]. These and the topic of greenhouse gas emissions connected to the production and incineration of fossil plastics have raised significant awareness among consumers and finally among policymakers. While regulations are being put in place to reduce the use of plastics, not all of these measures are necessarily beneficial to the environment and practical from a convenience standpoint. For a real cure to the plastic pollution predicament, real, sustainable solutions are needed [1]. It is important that such solutions forgo the negative environmental and logistical impacts of plastics while retaining their benefits. Alternatives that fulfill all of these criteria have been provided by nature, and such materials already exist. Polyhydroxyalkanoate (PHA) biopolyesters, produced by and playing multifaceted metabolic roles in numerous bacteria and archaea, are expedient examples of materials that bridge the desired benefits of plastics without endangering the environment. For illustration, a recent study by Dilkes-Hoffman et al. reports the complete degradation of PHA bottles in marine environments within 1.5 to 3.5 years, in contrast to the decades or even centuries that disintegration of petro-plastic bottles would take [3].

Similar to other biopolymers such as carbohydrates, nucleic acids, and proteins, PHA biopolymers have been established as macromolecules embedded into the closed cycles of producing and degrading materials in nature: PHAs are produced by living organisms (“biosynthesized” materials) and they biodegrade. Moreover, PHAs are produced from renewable raw materials, thus originating from natural substrates instead of fossil resources. Importantly, PHAs are biocompatible to humans and other life forms and are readily metabolized to non-toxic compounds when ingested by living organisms [4].

The ecological concerns of fossil plastics, together with ongoing limitations of fossil resources, have now opened the door for PHA biopolymers to play a front-running role for industry and society while maintaining nature’s cycle of circularity and sustainability. The skyrocketing crude oil prices in the 1970s prompted the first commercialization efforts in PHAs. However, much of that effort slowed down after the recovery of crude oil prices, although the scientific research continued. Price and availability were identified as the primary obstacles to the continued development and commercialization of PHAs. They were identified as not being price competitive to well-established fossil plastics, and certain challenges in their processability also had to be overcome. The material properties of PHAs do not exactly match those of the fossil-based competitors; in other words, they were not drop-ins for fossil plastics, although they cover a substantial spectrum of their property profile [5]. Now, many decades later, after having accumulated significant knowledge on production, processability, and end-of-life outcomes of PHA, we finally are on the threshold of serious and sustained commercialization efforts of these biopolymers. It is now better understood how the production price can be lowered by resorting to inexpensive or even near zero-cost carbon sources [6,7], which natural microbes are best suited to produce the various types of PHA from a given substrate [8], how microorganisms can be tailored using systems biology and metabolic engineering approaches [9,10], how bioprocesses can be rendered to consume less energy by running PHA production under low-sterility or nonsterile conditions with extremophilic microorganisms [11], and how to optimize downstream processing for recovery of intracellular PHA [12]. In addition, a large body of knowledge has been generated on fine-tuning the (co)polymer composition and thus tailoring the product properties during the bioprocess [13] and on facilitating PHA processing by blending appropriate chemical additives and other polymers [14].

Indeed, a growing number of companies spread over different global regions have started commercial-scale PHA biopolymer production for processing towards vendible items by melt extrusion, injection molding, 3D printing, electrospinning, etc. [15,16]. This new wave of PHA commercialization is increasingly becoming an integral part of current concepts of the bioeconomy and circular economy, which, as postulated by the European “Green Deal” [17], are characterized by the replacement of “end-of-pipe products” such as fossil plastics, especially for single-use applications, by biodegradable alternatives based on renewable carbon to drastically reduce plastic pollution and greenhouse gas emissions and to curb global warming [1]. In fact, calculations based on a plethora of life cycle studies estimate that replacement of 1 kg fossil plastic by PHA could salvage on average CO₂ emissions by 2 kg and around 30 MJ of fossil resources on an energy basis [18].

Material properties of PHA biopolymers are dependent on the type and distribution of various monomeric building blocks; PHAs are a versatile group of biomaterials, with characteristics that range from elastomeric to semicrystalline thermoplastic-like polymers [19]. Despite the discovery of more than 150 different hydroxyalkanoate (HA) building blocks that constitute the PHA biopolymer family, only a limited number of PHA copolymer types have reached industrial maturity. As shown in the subsequent sections, we currently witness considerable activities in different regions globally towards commercialization of a few PHA biopolymers, namely the homopolymer poly(3-hydroxybutyrate) (P(3HB)); the copolymers poly(3-hydroxybutyrate-co-3-hydroxyvalerate) (P(3HB-co-3HV)), poly(3-hydroxybutyrate-co-4-hydroxybutyrate) (P(3HB-co-4HB)), and poly(3-hydroxybutyrate-co-3-hydroxyhexanoate) (P(3HB-co-3HHx)); and, to a minor extent, the homopolymer poly(4-hydroxybutyrate) (P(4HB)) and some medium-chain-length PHA (*mcl*-PHA) copolymers. The chemical structures of these biopolyesters are illustrated in Figure 1.

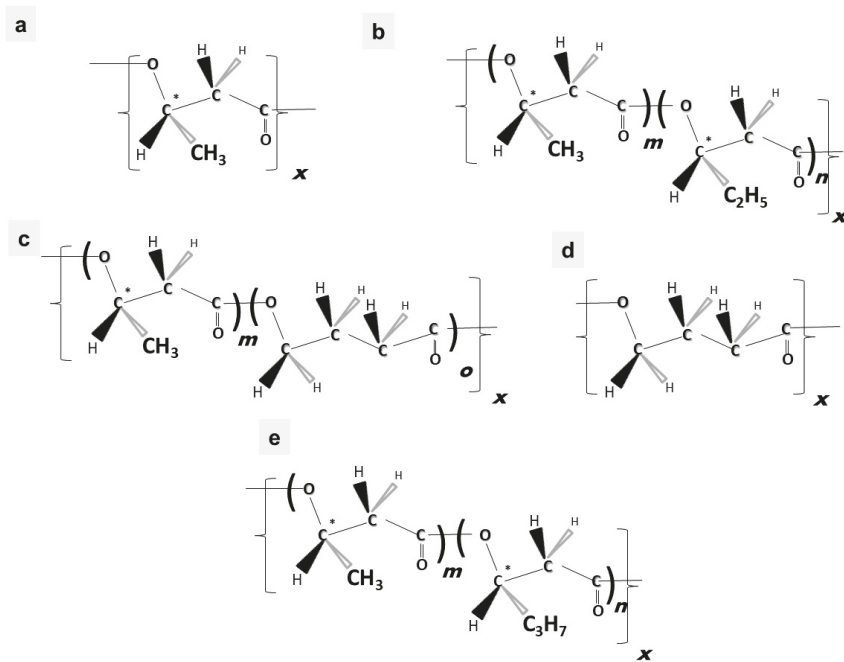


Figure 1. Chemical structures of “bulk PHA” types: (a) P(3HB); (b) P(3HB-co-3HV); (c) P(3HB-co-4HB); (d) P(4HB); (e) P(3HB-co-3HHx). Asterisks (*) indicate chiral centers of PHA building blocks.

While it is challenging to estimate the current volume of PHA produced industrially, it has, to the best of our knowledge, not yet exceeded 10,000 t annually at the time of submis-

sion of the present article (January 2022); however, capacity expansions of over 1.5 million t have already been announced for the next 5–10 years, and an additional 1 million t are in the planning stages. Compared with the estimated global plastic production of roughly 400 Mt per year, the share of PHA is negligible [20]. Therefore, this review is dedicated to drawing a clear current and developing picture of a very old biopolymer platform that is transforming into the new “PHA industry”. The intent here is to take the reader on a journey through the history of PHA commercialization attempts, highlighting the obstacles and stumbling blocks that often made this path difficult and the targeted applications where PHA is intended to be commercialized.

2. Industrializing Poly(3-hydroxybutyrate) (P(3HB) or PHB)

2.1. Challenges of Processing and Commercializing P(3HB)

P(3HB) constitutes the by far best-studied representative of the PHA family. It is also the type of PHA biopolyester that is produced by the largest number of microbes in nature from simple feedstocks such as carbohydrates, alcohols such as glycerol, or fatty acids with an even number of carbon atoms. In addition, many more bacteria convert gaseous C₁-substrates like methane (by type-II methanotrophs), CO₂ (by cyanobacteria and aerobic chemolithoautotrophic hydrogen-oxidizing “knallgas bacteria” such as *Alcaligenes eutrophus*—today *Cupriavidus necator*), and syngas (generated from organic waste materials, e.g., by Rhodospirilli) into P(3HB) homopolyester (reviewed by Koller et al., 2017) [21].

PHB, however, has a very narrow melt processing window since its melting temperature is close to its degradation temperature. It is also highly crystalline; therefore, it has a low elongation at break (ϵ) and is brittle. P(3HB) suffers from slow crystallization rates and lower biodegradability rates compared to other types of PHA, which have been successfully industrially manufactured since the 1980s. However, despite the apparent property deficiencies, P(3HB) also has some beneficial features, especially for the production of hard, creep-resistant items, which do not change their properties over a broad temperature range even when stored for several years. Another beneficial aspect of P(3HB) is the adaptability of its melt viscosity for different processing techniques (reviewed by [5]). According to Urs Hänggi [22], P(3HB) outperforms many competing petrochemical plastics in UV resistance and mechanical stability.

Commercial P(3HB) is also used to blend with other biobased polymers, such as poly(lactic acid) (PLA) and thermoplastic starch (TPS), and synthetic but still biodegradable polyesters such as poly(butylene adipate terephthalate) (PBAT); resulting polymer blends achieved certifications in biodegradability (90% of carbon metabolized within 180 days under standardized conditions according to European norm EN 13432) and compostability (not more than 10% of the polymer remains in a sieve of 2 mm pore size after 180-day composting tests under standardized conditions according to EN 13432) [23]. Incorporation of additives (diverse nucleating agents to increase crystallization rates; stabilizing agents (antioxidants), and plasticizing agents such as tributyl citrate, glycerol, and sorbitol) is often used to overcome the above-discussed shortcomings of the material properties of P(3HB). Moreover, P(3HB) can be processed with filler materials such as lignocelluloses to fine-tune the properties of P(3HB), such as lowering crystallinity and density, increasing biodegradability further, and reducing the production price of the final biobased and biodegradable polymer products. Gregorova et al. [24] have demonstrated many of these improved attributes by incorporating untreated and modified (alkali, stearic acid, or hydrothermal treatment to improve the interface adhesion) beechwood flour in P(3HB). They produced films of P(3HB) blended with lignocellulose by hot compression molding which displayed significant reduction in the degree of crystallinity (66% to about 50% for the composites), while showing improved Young’s moduli, thus demonstrating the reinforcement effect of these fillers [24].

2.2. Biomer

Biomer, based in Schwalbach, Germany, was one of the first industrial producers of P(3HB) using the strain *Azohydromonas australica* (formerly known as *Alcaligenes latus*) from sucrose as the carbon feedstock. The Biomer process is based on the experimental work carried out and patented (1983 German Patent No. 379,613 and 1988 Canadian Patent No. 1,236,415) by Lafferty and Braunegg in the 1980s in Graz, Austria. These researchers discovered that *A. australica* is an outstandingly fast-growing bacterium, which accumulates PHA also during balanced growth, in parallel to the formation of catalytically active biomass [5]. The technology based on these experiments was developed by Chemie Linz/PCD Polymere GmbH in Austria in the late 1980s and was later scaled up to an annual production of 2 t P(3HB) in 1991. However, the low crude oil price at the time made PHA less competitive with fossil plastics, discouraging growth in the industrial proliferation of these biopolyesters (reviewed by da Cruz Pradella [20]).

Biomer acquired the base technology and commercialized P(3HB) in 1993. The technology includes several grades of these resins blended with low-molecular-weight softeners and nucleating agents (tributyl citrate). The products are sold to plastics processing companies. Biomer also markets pure P(3HB) in powder form for blending into other biobased polymers such as PLA. Commercial grades include Biomer P209/P209E, P226/P226E, P263/P263E, and P309. “E” refers to the presence of “polymeric nucleating agent” to overcome low crystallization rate, while the others contain boron nitride as a nucleating agent. Their degree of crystallinity (X_c) values range between 60 and 70%, melting temperatures (T_m) range between 170 and 175 °C, glass transition temperature (T_g) ranges between −5 and 5 °C, and weight average molecular weight (M_w) is 500–600 kDa. Tensile strength (σ) ranges between 8 and 27 MPa and elongation at break (ϵ) between 3.7 and 16%. The property variations are due to the additives such as nucleating agents and plasticizers added. The data show that these P(3HB) homopolyesters are rigid materials suitable for injection or compression molding or melt extrusion and are not sufficiently flexible for film blowing [25]. According to Biomer, their production capacity is 900 t per annum; these products were used for many studies developing new materials for different applications (personal communication U. Hänggi [26]). In this context, Arrieta et al. developed composites of PLA and Biomer P226, with the natural terpene limonene acting as a plasticizer, improving the processing, interaction of the polymers, and disintegration of the blend during composting. Transparent films were generated, in which P(3HB) acted as a reinforcement of the PLA matrix, resulting in a higher oxygen barrier and improved surface water resistance, which makes these materials interesting candidates for food packaging purposes. Composting studies showed that P(3HB) rather slowed down the disintegration rate of PLA, while limonene favored the composting process [27]. Recently, Biomer P304 was blended with abundantly available agave fibers and organic peroxide (to improve compatibility between P(3HB) and fibers) and processed via reactive extrusion; the flexural and impact strengths increased compared to the neat P(3HB) by 46% and 45%, respectively. Authors suggest also this material for food packaging applications [28].

2.3. PHB Industrial S.A.

Another important example of companies commercializing P(3HB) homopolyester is PHB Industrial S.A. in Brazil (PHB/ISA). Their product BIOCYLE™ is produced on an annual scale of approximately 50–100 t. In this process, *C. necator* is cultivated in fed-batch mode on hydrolyzed sucrose (equimolar mixture of glucose and fructose); this process is integrated into an energetically autarkic bioethanol and cane sugar factory [29]. This approach is based on technologies originally developed by the Copersucar Technology Center (CTC) at the Institute of Technological Research of São Paulo State (IPT), São Paulo State University, based on a research grant from 1991 for “Production of Biodegradable Plastics from Sugar via Biotechnological Route” and sold in 1995 to PHB/ISA. The PHA production process is integrated into the sugar and bioethanol factory Usina da Pedra, Serrana. Remarkably, the PHB/ISA process is energetically autarkic: lignocellulosic sugar

cane bagasse “waste” remaining after sugar extraction is used to fuel the entire industrial plant energetically—not only the bioreactor and medium sterilization and the cultivation process itself for PHA production, but also the bioethanol distillation and water evaporation for sugar crystallization. Moreover, fusel alcohols (amyl alcohol, etc.) are used for extraction of the BIOCYCLE™ PHA (trademark established in 2000) from biomass [20]. P(3HB) homopolymer is sold as “BIOCYCLE 1000” [30]. According to the company, the process proved to be economically feasible in 2004 at a volumetric productivity of about 1.7 g/(L·h) and attaining PHA concentrations of 70 g/L in a 13 m³ production bioreactor [31].

2.4. Tianan Biologic Materials Co.

In Ningbo, Zhejiang province, People’s Republic of China (PR China), Tianan Biologic Materials Co., a company normally focusing on P(3HB-co-3HV) copolymer production [32], also produces and markets P(3HB) homopolymer designated ENMAT Y3000™ (powder form) and ENMAT Y3000P™ (pellet form) for injection molding, thermoforming, and extrusion applications. Tianan produces this “100% biobased and 100% biodegradable” (manufacturer information) product using cassava starch as the raw material, which is sold in the form of slightly brown polymer pellets, containing an undisclosed nucleating agent to induce crystallinity. This product is certified as compostable by the US Biodegradable Products Institute (BPI), is listed as Food Contact Material (FCM) substance No. 744 in Table 1 of Annex I of the Plastics Regulation of the European Union, and has been EU REACH compliant since 2008 [33].

2.5. Nafigate Corporation–Hydal

An intriguing approach for P(3HB) manufacturing was developed in Brno, Czech Republic, by the Hydal consortium [34]. Using this technology, Nafigate produces P(3HB) homopolymers from waste frying oil and resorts to a polymer recovery process using oils, which, as the company claims, makes the entire process about 50% less energy-intensive compared to poly(ethylene) (PE) production. This process achieved a technological readiness level (TRL) of 9 in 2019 and is claimed by Nafigate as “*the first in the World to use 100% waste on an industrial scale ... for the production of natural PHA biopolymer*”. Undisclosed additives for stabilization are added to the biopolymer, which is sold as granules in the Czech Republic. Some recommended applications of their polymers are mulch films and 3D printing filaments. In addition, the company uses its own P(3HB) as primary (micro)plastic beads for peeling in shower milk products as a replacement for fossil plastic beads which are banned as primary microplastics in Europe as part of the Intentionally Added Microplastics Legislation. In addition, Nafigate is producing formulations using P(3HB) and substitutes polluting chemicals such as oxybenzone chemical UV filters in sunscreen creams; these products are already available on the market (“Naturetics™” products; market launch in Czech Republic in 2021) [35]. Moreover, the application of the product in biomedicine, sustainable packaging, and smart fertilizers is envisioned. As a timeline, the company expects to start P(3HB) production for biomedical applications in 2022 and to start large-scale P(3HB) production for packaging purposes in 2026. Unfortunately, the company does not disclose production volumes or the downstream processing technique applied; according to the internet site, they do not resort to solvent extraction (“*process involves the breakdown of microbial cells from which PHA granules are released*”). The bioprocess is carried out using wild-type *C. necator* as production strain [34].

Table 1. Most commercialized types of PHA (P(3HB), P(3HB-co-3HV), P(3HB-co-4HB), P(3HB-co-3HHx), P(4HB)), production strains, substrates, manufacturers, manufacturing scale/capacity, and certifications.



Type of PHA	Production Strains (Origin)	Substrates	Manufacturer	Logo	PHA Brand Name (Trade Mark)	Capacity (t/year)	Certifications/Approvals
 <p>Poly(3-hydroxybutyrate)</p>	<i>Cupriavidus necator</i> (soil bacterium)	Glucose	ICI, London, UK (technology transferred to Zeneca, Monsanto, and finally Metabolix)		BIOPOL	Stopped (was about 800 in 1996)	-
		Hydrolyzed cane sugar	PHB Industrial S.A. (PHB/ISA), Serrana, Brazil		BIOCYCLE	~100 (entire PHA production capacity)	Compostable according to DIN CERTO and Vinçotte
		Beet sucrose and by-products of sugar beet industry (molasses) plus additional surplus products from agriculture	Bio-On, Bologna, Italy		Minerv-PHA	2000 (current situation unclear!)	"Biodegradable"; according to USDA ("certified biobased product") and TÜV Austria "OK biodegradable"; according to company: "MINERV-PHA™ dissolves in normal river or sea water leaving no residue in just a few days."
	<i>Azohydromonas australica</i> (<i>Azohydromonas lata</i>) (soil bacterium)	Sucrose	Biomer Schwabach, Germany		Biomer	900 (capacity)	"Fully biodegradable and compostable"
	<i>Paraburkholderia sacchari</i> (soil bacterium)	Sucrose	PHB Industrial S.A. (PHB/ISA), Serrana, Brazil		BIOCYCLE	~100 (entire PHA production capacity)	Compostable according to DIN CERTO and Vinçotte
	<i>Halomonas</i> sp. (<i>Halomonas bluphagenensis</i> ssp.) (salt lake isolate)	Presumably glucose	COFCO, Beijing, PR China		COFCO PHA	1000 (capacity)	n.r.

Table 1. Cont.

Type of PHA	Production Strains (Origin)	Substrates	Manufacturer	Logo	PHA Brand Name (Trade Mark)	Capacity (t/year)	Certifications/Approvals
Poly(3-hydroxybutyrate-co-3-hydroxyvalerate) 	Not disclosed Methanotroph ("robust strain"; origin n.r.)	Crude biogas (CH ₄ , CO ₂ , H ₂ S)	Mango Materials, Redwood City, CA, USA		YOOP	0.25 (pilot scale; long-term goal: about 5 t per year)	"Fully biodegradable and compostable"
	"Newlight's biocatalyst 9X" (marine isolate)	CH ₄ and CO ₂ from greenhouse gases	Newlight Technologies LLC, Huntington Beach, CA, USA		AirCarbon	n.r.	"Fully biodegradable"; "readily compostable"
	"Own microbiological collection"; wild-type organisms (origin not disclosed)	Waste cooking oil (Hydal technology)	Nafigate Corporation, Prague, Czech Republic		Hydal PHA	n.r.	FDA approved for food contact (FCN 1754), "carbon-negative"; certified (ISO 14046-3 and specification for the assessment of the life cycle greenhouse gas emissions of goods and services (PAS 2050: 2008/2011)), "ocean degradable" (ASTM D6691 and D7081), "industrially compostable" (ASTM D6400)
Cupriavidis necator (soil bacterium)	Glucose plus 3HV precursor	Waste cooking oil (Hydal technology)	ICI, London, UK (technology transferred to Zeneca, Monsanto, and finally MetaboliX)		BIOPOL	Stopped (was about 600–800 in 1996)	-
	Glucose plus 3HV precursor	Telles (joint venture of MetaboliX and ADM from 2009 to 2012)	Telles (joint venture of MetaboliX and ADM from 2009 to 2012)		Mirel	50,000 (capacity in 2009; stopped in 2012)	n.r.
	Glucose plus 3HV precursor (glucose deriving from cassava starch)	Tianan Biologic Materials Co., Ningbo, PR China	Tianan Biologic Materials Co., Ningbo, PR China		ENMAT	2000	"Compostable" according to US Biodegradable Products Institute (BPI) Food Contact Material ("FCM") substance No. 744 in Table 1 of Annex I of the EU (REACH)

Table 1. Cont.

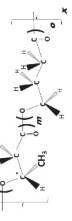





Type of PHA	Production Strains (Origin)	Substrates	Manufacturer	Logo	PHA Brand Name (Trade Mark)	Capacity (t/year)	Certifications/Approvals
<p>Poly(3-hydroxybutyrate-co-4-hydroxybutyrate)</p> 	<p><i>Halomonas</i> sp. (<i>Halomonas bluelphagensis</i> spp.) (salt lake isolate; genetically engineered)</p> <p><i>Haloflex mediterranei</i> (marine salt brine at Spanish coast)</p> <p>Rec. <i>Escherichia coli</i> (Enterobacterium)</p>	<p>Hydrolyzed cane sucrose plus propionate</p> <p>Beet sucrose and by-products of sugar beet industry (molasses) plus additional surplus products from agriculture plus 3HV precursors</p> <p>Presumably glucose plus 3HV precursor</p> <p>Sugars; starch, glycerol (no 3HV-related precursors needed)</p> <p>Glucose plus 1,4-butanediol (4HB precursor)</p>	<p>PHB Industrial S.A. (PHB/ISA) Serrana, Brazil</p> <p>Bio-On, Bologna, Italy</p> <p>PhaBuilder, Beijing, PR China</p> <p>Not commercially produced yet but high industrial potential supposed</p> <p>Tianjin GreenBio Materials Co. Ltd., Tianjin, PR China</p> <p>CJ, Seoul, Republic of Korea (technology from MetaboliX)</p>	    	<p>BIOCYCLE</p> <p>Minerv-PHA</p> <p>-</p> <p>-</p> <p>SoGreen</p> <p>Yield10</p>	<p>~100 (entire PHA production capacity)</p> <p>2000 (current situation unclear!)</p> <p>n.r.</p> <p>-</p> <p>10,000</p> <p>n.r.</p>	<p>n.r.</p> <p>"Biodegradable": according to USDA ("certified biobased product") and TÜV Austria "OK biodegradable": according to company: "MINERV-PHA™ dissolves in normal river or sea water leaving no residue in just a few days."</p> <p>n.r.</p> <p>-</p> <p>n.r.</p> <p>n.r.</p>

Table 1. Cont.

Type of PHA	Production Strains (Origin)	Substrates	Manufacturer	Logo	PHA Brand Name (Trade Mark)	Capacity (t/year)	Certifications/Approvals
Poly(3-hydroxybutyrate-co-3-hydroxyhexanoate) 	Not disclosed	Not disclosed	Tepha Medical Devices Inc., Lexington, MA, USA		TephaELAST	n.r.	FDA approved for biomedical use as implant material; the entire production process is ISO 13485 compliant
	Not disclosed	Sugar plus 4HB-related precursor	Shenzhen Ecomann Biotechnology Co. Ltd., Guangdong, PR China		Ambio	10,000 (planned; 75,000 capacity)	"OK compost" "OK compost HOME" FDA approved
	<i>Halomonas</i> sp. TD40 (salt lake isolate)	Glucose, corn steep liquor, and GBL	PhaBuilder, Beijing, PR China		mp34HB 10	1000–10,000 (entire PHA production capacity)	Biodegradable according to ASTM 6400 and EN15432
	<i>Halomonas</i> sp. (<i>Halomonas bluephagesis</i> sp.; presumably strain TD40)	Glucose, corn steep liquor, and GBL	Medpha, Beijing, PR China	n.r.	Medpha PHA	100	n.r.
	Presumably <i>Aeromonas caviae</i> or <i>Aeromonas hydrophila</i> ; other sources (Tan et al., 2021) assume rec. <i>C. necator</i> (soil bacteria)	"Inexpensive oils derived from the seeds of plants such as canola and soy"	Danimer Scientific, Bainbridge, GA, USA (formerly Meridian Holdings Group Inc. and MHG; technology originally from Proctor & Gamble, Cincinnati, OH, USA)		Nodax	10,000	Biobased (ASTM D6866; "OK biobased"); anaerobic and aerobic digestion in soil freshwater ("OK biodegradable SOIL"), freshwater ("OK biodegradable WATER"), marine environment (ASTM D6691), industrial and home composting (according to TÜV Austria and EN and ASTM norms) FDA approved for food contact

Table 1. Cont.

Type of PHA	Production Strains (Origin)	Substrates	Manufacturer	Logo	PHA Brand Name (Trade Mark)	Capacity (t/year)	Certifications/Approvals
 <p>Poly(4-hydroxybutyrate)</p>	Rec. <i>C. necator</i>	Vegetable oils	Kanegafuchi Chemical Industry Co. Ltd. (Kaneka), Tokyo, Japan				"OK compost INDUSTRIAL", "OK compost HOME", "OK biodegradable SOIL", and "OK biobased" according to TUV Austria; the "Biobased" certification for Japan; and the "Industrial Compostable" certification for Japan and USA
		Waste cooking oil	RWDC Industries Ltd., Athens, GA, USA		Solon®	4000 (expected to be expanded)	n.r.
	Rec. <i>C. necator</i> ("reprogrammed microorganism") (salt lake isolate)	"Alternative carbon source, including crops and kitchen waste", seawater	Bluepha Co. Ltd., Beijing, PR China		Bluepha PHA	1000	Readily degraded both in seawater and soil within 3–6 months
	Rec. <i>Escherichia coli</i> (Enterobacterium)	4HB-related precursor	Tepha Medical Devices Inc., Lexington, MA, USA		TephaFLEX	n.r.	FDA approved for biomedical use as implant material; the entire production process is ISO 13485 compliant

n.r.: not reported.

2.6. Newlight Technologies LLC

In the USA, the Californian company Newlight Technologies LLC, located in Huntington Beach, produces P(3HB) homopolyester by using “naturally occurring microorganisms found in the ocean”. Unfortunately, not much is disclosed by the company about its biotechnological process. Bioreactor design, biocatalyst design, purification, and material performance were optimized over a period of ten years from 2007 to 2017. Since 2019, the commercial production plant “Eagle 3” is in operation. Renewable energy is used for this process. According to the company, marine microbes (“Newlight’s 9X biocatalyst”) consume air and CO₂ from greenhouse gas to accumulate P(3HB) homopolyester, marketed under the trade name AirCarbon™. The products are FDA approved for food contact according to the norm FCN 1754 and “carbon-negative” certified according to the International Organization for Standardization (ISO 14046-3) and the specification for the assessment of the life cycle greenhouse gas emissions of goods and services (PAS 2050: 2008/2011). They are “ocean degradable” according to the American Society for Testing and Material (ASTM D6691 and D7081) and “industrially compostable” according to ASTM D6400 [36]. AirCarbon™-based P(3HB) is used as the base resin for the company’s Restore™ (foodware) and Covalent™ (fashion products) branded products. Newlight sells biodegradable food-contact items such as straws and cutlery that are blue-stained, probably to look like the ocean. The company also claims these products to be durable and dishwasher safe [37]. Products branded Covalent use AirCarbon™ P(3HB) for the production of fashionable eyewear, and even as a leather replacement in smartphone covers and other accessories. These products have been being marketed since the end of 2020. Interestingly, Covalent™ puts a “carbon date”—a unique timestamp placed on every Covalent™ product to disclose the time when the AirCarbon™ P(3HB) used to manufacture the product was biosynthesized. When entering this “carbon date” into the company’s website, the consumer can access IBM blockchain history for an individual item, making every single step from cradle to gate traceable, and calculate the carbon footprint associated with the overall production process [38].

2.7. COFCO Cooperation Ltd.

The company China Oil & Foodstuffs Corporation Cooperation Ltd. (COFCO), located in Beijing, PR China, is reported as the largest food and beverage producer in the People’s Republic of China. In addition, the company is a significant producer of biobased PLA polymers produced by their PLAneo™ technology. The plant was engineered and constructed by ThyssenKrupp Industrial Solutions and started operating in 2018 [39]. Since then, COFCO has also commercialized P(3HB) homopolyester using extremophilic production strains, many of which are genetically modified. This production concept, named the Next Generation Biotechnology (NGIB), uses robust, extremophilic production strains such as recombinant *Halomonas bluephagenesis* (originally termed *Halomonas* sp. TD01), which allows production under nonsterile conditions with continuous cultivation conditions from inexpensive feedstocks, thus saving fresh water and energy [40,41]. The current production capacity is estimated at 1000 t per annum. COFCO’s downstream processing for PHA recovery is further simplified since *Halomonas* spp. cells are easily disrupted by sodium dodecyl sulfate (SDS) washing and release PHA granules into the aqueous phase [42]. The technology used by COFCO was initially used by two other Chinese start-ups: PhaBuilder and Medpha. The P(3HB) produced is being used for the production of textile fibers (personal communication by George Chen) [43]. The company has also filed a patent application in cooperation with Tsinghua University for reusing wastewater from the PHA production process using *Halomonas* sp. [44] (Chinese patent 202010358327.1, publication date 30 June 2020).

2.8. Mango Materials

Mango Materials, a start-up led by three female entrepreneurs and located in California, produces P(3HB) under the trade name YOOP from crude biogas, a mixture of CH₄,

CO₂, and H₂S. The company is co-located at a biogas-producing wastewater treatment plant in the San Francisco Bay Area. Current weekly quantities of about 100 kg P(3HB) are being produced as disclosed by the company. The products are recommended for use in injection molding, fiber extrusion, and additive manufacturing (3D printing) [45], the last being one of the currently most emerging applications for PHA [46]. The P(3HB) production process constitutes a closed-loop system where spent PHA materials made of YOOPTM PHA can undergo conversion to biogas, generating the raw material for the next PHA-production cycle. At the moment, the company is looking for launching partnerships with various biogas producers such as landfills, wastewater treatment plants, and agricultural waste composting facilities. Production strains appear to be randomly cultured wild-type methanotrophs, although this is not revealed by the company. According to Mango Materials, no sterilization is required due to the robust nature of the strain and the process [45]. P(3HB) homopolymer is produced as the sole product, which the company claims to biodegrade in about 6 weeks in a marine environment [45].

2.9. Bio-On

Bio-On, a company located near Bologna, Italy, produced P(3HB) and P(3HB-co-3HV) for different applications under the brand name MinervTM. They used beet sucrose, by-products of beet sugar production (molasses), and other agro-industrial surplus materials and claimed an annual production of approximately 2000 t of PHA starting in 2018. Bio-On mentions using *C. necator* as their production strain on their homepage. They claim to use a downstream process for PHA recovery from the non-PHA cell mass without using organic solvents for PHA extraction. On its internet site, the company claims to possess “the world’s largest PHA production plant” [47]. However, Bio-On came under severe financial trouble in 2019, declared bankruptcy in order to avoid liquidation, and continued operations under a temporary court order [48]. Their current status and future remain unclear.

Bio-On claims to have developed and filed a patent application for its Minerv products in PHA nanoparticles to diagnose and treat cancer (Minerv BIOMEDSTM). These nanoparticles simultaneously contained two different contrast media, namely magnetic nanoparticles and gold nanocylinders, which can rapidly mark tumor mass by NMR. Moreover, such nanoparticles could additionally contain chemotherapeutics to combat tumors [49]. In the bioremediation field, Bio-On announced in 2017 that tests were successfully carried out for biological degradation of oil slicks on sea surface; here, PHA powder was put on the oil film and was used as feedstocks for different microorganisms which are capable of hydrocarbon degradation [50]. In cosmetics and personal care, Bio-On MinervTM PHA was used as microbeads in emulsions for body and face peeling, cleaning agents, and toothpaste. The company claims that these products entered the market as “Minerv Bio-CosmeticsTM” replacing primary microplastic particles made of PE. The lipophilic and hydrophobic nature of P(3HB) gives cosmetic products a creamy texture at 5 to 20 μm particle sizes, which makes such PHA microparticles particularly interesting for skin care applications, where they do not remove water from the skin, but give oily skin a natural matt appearance [51]. In addition, PHA microparticles scatter light and can also be used as sunscreens, which Bio-On claims to have marketed together with Unilever (brand name “MyKAITM”) [52]. In 2018, the company started marketing their so-called “Minerv SupertoysTM”, a form of biodegradable LEGOTM-like toy bricks made of colored Minerv PHA [53]. In 2019, Bio-On filed for a patent application for a cigarette filter containing a liquid-like P(3HB) product of PHA to replace triacetin. The patent application claims that this new filter system can retain up to 60% of dangerous reactive oxidative species from tobacco smoke [54]. Moreover, Bio-On also claims to have produced prototypes of various furniture pieces consisting of Bio-On PHA for the designer Kartell [55].

3. Industrializing P(3HB-co-3HV) Copolyesters

3.1. PHA Heteropolyesters and Their Advantages in Processing and Commercialization

P(3HB) homopolyester was considered to be the only PHA produced in nature since its discovery in the 1920s by Maurice Lemoigne [56] until Wallen and Davis isolated P(3HB-co-3HV) from dried activated sludge in the 1970s. They used chloroform to dissolve the PHA and precipitated it using ether and cooling the mixture. They then treated the resulting PHA samples with hot ethanol. The ethanol-insoluble fraction had a Fourier transform infrared spectroscopy (FTIR) spectrum and melting temperature (170 °C) of P(3HB) homopolyester, while the ethanol-soluble fraction precipitated when cooling down and had a melting point of 100–105 °C and a structure different from P(3HB) homopolyester [57]. Further research followed, and in 1984 Wallen and Rohwedder reported on the isolation of new microbial strains accumulating PHA from effluent water. Again, the properties of the PHA produced by these microbes were considerably different from the properties known from P(3HB) homopolyester; a T_m below 100 °C or solubility even in cold ethanol were findings surprising at that time. Based on GC-MS analyses, it was confirmed that the polymer contained, besides 3-hydroxybutyrate (3HB), also 3-hydroxyvalerate (3HV) units and, to a minor extent, 3-hydroxyhexanoate (3HHx). This was the first unambiguous identification of PHA building blocks different from 3HB [58]. Using techniques such as gas chromatography–mass spectroscopy (GC-MS), Findlay and White discovered 11 additional and different 3-hydroxyalkanoates (3HAs) from marine sediments and 6 more in *Bacillus megaterium* PHA in 1983 [59]. In 1981, Morikawa and Marchessault discovered that pyrolysis of 3HB- and 3HV-containing microbial PHA generates unsaturated compounds (crotonic acid and pentenoic acid, respectively), which were recognized as valuable chemical synthons [60].

The fact that P(3HB-co-3HV) copolyesters can be produced by feeding appropriate 3HV precursors was subsequently discovered and patented by Holmes, Wright, and Collins for Imperial Chemical Industry Biological (ICI) in the early 1980s (EP0052459A1), where they claimed that “*The copolymers are made microbiologically: for part of the cultivation the micro-organism is under conditions of limitation of a nutrient, e.g., nitrogen source, required for growth but not polyester accumulation. For at least part of this period of growth limitation the substrate is an acid or a salt thereof that gives the comonomer units. Propionic acid, which gives polymers where $n = 1$, $R<2> = R<3> = R<4> = H$ and $R<1> = C_2H_5$, is the preferred acid.*” [61].

In 1992, a seminal paper by Luzier summarized for the first time the advantages of P(3HB-co-3HV) copolyesters in comparison to P(3HB) homopolyester by comparing thermal and mechanical properties for different grades of PHA commercially produced that time by ICI (see next section); P(3HB) homopolyester and P(3HB-co-3HV) with 10 or 20 mol-% 3HV were studied. With increasing 3HV content, melting point T_m decreased (170 °C for P(3HB) and 140 and 130 °C for the two P(3HB-co-3HV) grades, degree of crystallinity (80, 60, and 35%), tensile strength (40, 25, and 20 MPa), flexural modulus (3.5, 1.2, and 0.8 GPa), elongation at break (8, 20, and 50%), and impact strength (60, 110, and 350 J/m). The lower T_m of the P(3HB-co-3HV) copolyesters broadened their processing windows, making them suitable especially for extrusion, injection, and blow molding, which enabled the application of the materials for injection-molded parts, bottles, extruded sheets, films, fibers, and P(3HB-co-3HV)-coated paper [62].

3.2. ICI–Zeneca–Metabolix–Telles

Imperial Chemical Industry Biological (ICI), London, UK, started P(3HB-co-3HV) production as a reaction to the sudden oil shock of the 1970s. In this process, *C. necator* (in the original patent: *Alcaligenes eutrophus* NC 1B) was used as production strain. Cultivations were performed on the main substrate glucose (formation of biomass, 3HB, and energy) and propionic acid (precursor for 3HV) up to cell concentrations exceeding 100 g/L, with P(3HB-co-3HV) fractions in cell dry mass reaching up to 80 wt.-%. Phosphate-limitation acted as the factor to provoke the switch from the phase of balanced biomass growth to the phase of PHA biosynthesis in the ICI process. Importantly, for economic and environmental reasons, the company soon switched from solvent extraction for P(3HB-co-3HV) recovery

to the use of surfactants and enzyme cocktails to disintegrate non-PHA biomass for release of the intracellular product. A limited number of copolymers having a different percentage of 3HV fraction were synthesized and obtained as a white powder. Based on customer needs, ICI then blended the various copolymer grades along with other additives to obtain the appropriate PHA compound granulates for sale to their customers. ICI started its commercial production plant that had the capacity to produce 5000 t annually and sold the products under the trade name BIOPOL™ (in the USA under the trade name PHBV™) at USD 7–8 per kilogram. Shampoo bottles (by the company Wella) and disposable razors were some of the products made with these P(3HB-co-3HV) compounds and marketed. Da Cruz Pradella estimated that in 1990 the demand for these compounds was between 5000 and 10,000 t per year [20,63].

In 1993, ICI spun off its agricultural and pharma division, including BIOPOL™, as Zeneca Ltd. Zeneca, in turn, sold all its PHA-related patents and technology to Monsanto in 1996; it was estimated that, at that time, Zeneca had a production capacity of 600–800 t per year [5,20,63]. Monsanto, however, was more interested in producing PHA in transgenic plants, a process that has not been realized on a commercial scale as of this writing. Monsanto eventually ceased BIOPOL™ production in 1999 and subsequently sold the entire ICI/Zeneca BIOPOL technology to Metabolix (based in Cambridge, Massachusetts) in 2001. Metabolix finally entered into the joint venture called Telles with Archer Daniels Midland (ADM) in 2006; Telles pursued the ambitious goal of commercializing P(3HB-co-3HV) under the trade name Mirel™. Telles launched a production plant with an annual capacity of 50,000 t in 2009. Two types of P(3HB-co-3HV) were produced: a grade suitable for thermoforming and injection molding (Mirel™ 3000 series) and a paper coating grade (Mirel™ 4000 series) [64]. Compression molding grade Mirel™ P1003 was produced through “blends of poly(R-3-hydroxybutyric acid), poly(3-hydroxybutyrate-co-4-hydroxybutyrate), proprietary mineral fillers, and proprietary biodegradable additives” [65]. Envisaged applications included shopping bags, compost bags, packaging, agriculture/horticulture films, aquatic applications, and production of various durable consumer goods. The process was based on sugars such as dextrose from hydrolyzed corn growing adjacent to the Telles fermentation plant in Clinton, Iowa [64]. ADM finally abandoned the joint venture in January 2012, which at that time was a real setback for the budding PHA industry and the numerous ambitious PHA research groups [66]. However, Metabolix carried on its activities in the biosynthesis of P(3HB) in recombinant oil plants and switchgrass, eventually developing PHA copolymers of P(3HB) and P(4HB), or P(3HB-co-4HB), including those that were elastomeric and had a high 4-hydroxybutyrate (4HB) co-monomer fraction (~50%) as reported later [42,67].

3.3. PHB Industrial S.A., Brazil

PHB Industrial S.A. (PHB/ISA), in Serrana, Brazil, also produces P(3HB-co-3HV) copolyesters from hydrolyzed sucrose from sugarcane, in addition to P(3HB) production already described above. Different 3HV-related precursors (propionic acid, valeric acid) were used to produce the copolymers [68]. PHB/ISA's P(3HB-co-3HV), sold under the labels BIOCYCLE PHBV7 and BIOCYCLE PHBV19 contains 7 and 19 mol-% 3HV, respectively [31]. The BIOCYCLE™ materials are certified as compostable according to DIN CERTO and Vinçotte [38]. Efficient copolyester production using this process may require a switch to alternative production strains different from *C. necator*, such as *Burkholderia sacchari* (wild-type isolate: IPT 101) and its mutants (strain IPT 189), allowing beneficial features such as direct utilization of sucrose, high specific growth rates above 0.4 h^{-1} , and high volumetric productivity [69]. *B. sacchari* can also be used to produce block P(3HB-co-3HV) copolyesters using xylose and levulinic acid, both inexpensive starting materials originating from bagasse, a by-product of cane sugar production [70]. As shown in 2015 by Kovalcik et al., thermoforming of BIOCYCLE P(3HB-co-3HV) produced by the company PHB/ISA with Kraft lignin resulted in highly compatible composites. In this study, lignin exerted a reinforcing effect on the copolyester and improved its rather modest thermo-oxidative

stability during melt processing, a typical problem when processing P(3HB) homopolyester and P(3HB-co-3HV) copolyesters with 3HV contents up to 15 mol-%. The new composite materials were shown to drastically increase the biopolyester's barrier performance against O₂ and CO₂, which makes such biocomposites intriguing materials for packaging films for perishable food [71].

3.4. Tianan Biologic Materials Co.

Currently, Tianan Biologic Materials Co. in Ningbo, PR China, is known as “the world's largest producer” of P(3HB-co-3HV) copolyesters with a reported production capacity of 2000 annual t [33]. These copolyesters with typically rather low fractions of 3HV (1–3 mol-%) are sold under the trade names ENMAT Y1000™ (powder form), ENMAT Y1000P™ (pellet form), and ENMAT Y1010™ (processed with “nucleating and stabilizing agent”). Some researchers have also reported higher 3HV content of 5 mol-% [72,73] and 8 mol-% [74] in ENMAT™ P(3HB-co-3HV), although the authors of the present review have no evidence of such grades being sold at present. These Tianan materials are used for producing a broad range of different marketable items via injection molding, thermoforming, and melt extrusion, with the melting temperature being slightly lower than that of the P(3HB) homopolyester ENMAT Y3000P™. The company recommends detailed conditions for processing their materials on established fossil plastic processing machines. ENMAT™ P(3HB-co-3HV) copolyesters have compostability certification (US Biodegradable Products Institute) and are listed as FCM substance No. 744 in Table 1 of Annex I of the Plastics Regulation of the European Union. They have also been EU REACH compliant since 2008 [32]. ENMAT™ P(3HB-co-3HV) copolyesters can be used for film blowing due to their higher flexibility [75]. Overall improvement in processability and improvements in flexural strength, elastic modulus, and thermal stability of ENMAT™ P(3HB-co-3HV) can be achieved by compounding them with various fractions of PLA [72] or with modified lignin [74]. Tianan also promotes PHA grades for denitrification of soil and in wastewater treatment plants and for spinning fiber and producing nonwovens [23,76]. Recently, biocomposites of ENMAT Y1000P™ and Miscanthus fibers and distillers' dried grains with solubles (DDGS) were prepared by Meereboer et al. [77] to further improve the marine degradability of the biopolyester. P(3HB-co-3HV) processed with Miscanthus showed 15 and 25% better biodegradability, respectively, compared to pure P(3HB-co-3HV). Compared to neat P(3HB-co-3HV), 85/15 and 75/25 composites of P(3HB-co-3HV) and DDGS showed 17 and 40% better biodegradability, respectively. The 75/25 P(3HB-co-3HV)/Miscanthus and 75/25 P(3HB-co-3HV)/DDGS biocomposites completely biodegraded in marine environments within 412 and 295 days, respectively [77].

3.5. Genecis Bioindustries Inc.

Genecis is one of the newest start-ups in PHA, producing their P(3HB-co-3HV) in Ontario, Canada. Genecis uses “discarded organic food waste” as raw material for its acidogenic bacterial colony to produce fatty acids. These fatty acids, in turn, are converted by PHA-producing microbes to P(3HB-co-3HV). All microbes used are reported as isolates from Canadian environmental samples. The process currently is carried out in a “large pilot bioreactor” at the University of Toronto, at the end of which they use “a chemical process to open the bacterial cells and extract the plastic particles”; the production strain(s) and capacity remain largely unrevealed. According to the company's information, it is expected that 3 t of organic waste will be converted into P(3HB-co-3HV) per week at a new demonstration plant starting in 2021. Food packaging items such as cutlery, coffee pods, and 3D printing filaments are listed as possible fields of application for their PHA materials [78].

3.6. Bioextrax

In Sweden, Bioextrax AB, founded in 2014 as a spin-off from the biotechnology department of Lund University, produces PHA as granules at “a per kg price which is

approximately 50% of other methods". According to the company, PHA produced by the Bioextrax process is recovered via "a universal, environmentally friendly and very cost-efficient recovery of PHAs from PHA producing bacteria"; "Bioextrax's patented technology produces native-shaped bioplastics granules with intact molecular weight" and can be applied to pure and mixed microbial cultures. This natural extraction process does without chemicals and solvents and leaves the nutrient-rich solubilized non-PHA biomass as a coproduct [79]. According to the underlying patent (WO2016085396A1), non-PHA biomass of the PHA producer is hydrolyzed by a *Bacillus pumilus* culture. At the moment, the company holds some patent-pending processes for the production of P(3HB-co-3HV) copolyesters and poly(3-hydroxyoctanoate) (P(3HO)) homopolymer, with production strains being kept confidential by the company. The company's business model is to license the entire technology (PHA production and downstream processing) to big industrial PHA producers (personal communication by Edvard Hall, CEO Bioextrax [80]).

4. Industrializing P(3HB-co-4HB) Copolyesters

4.1. 4-Hydroxybutyrate: An Achiral Building Block as Game Changer for PHA Properties

4-Hydroxybutyrate (4HB) is the only well-studied achiral monomer found in natural PHA. 4HB was first described as a PHA monomer by the team of Yoshiharu Doi in Japan, who discovered this novel monomer in PHA samples produced by two strains of *C. necator* when supplied with butyric acid along with the 4HB precursors 4-hydroxybutyric acid or 4-chlorobutyric acid, while feeding butyric acid alone resulted in accumulation of P(3HB) homopolymer. Depending on the feed composition and the strain selected, up to 49 mol-% 4HB was incorporated into the P(3HB-co-4HB) copolyesters. The presence of 4HB in PHA was confirmed by nuclear magnetic resonance (NMR) (both solid-state ^{13}C NMR and solution NMR were applied), and a significant decrease in crystallinity at increasing 4HB fraction in P(3HB-co-4HB) was reported, with the 49 mol-% 4HB copolymer being almost completely amorphous without any detectable crystalline regions [81]. As has been comprehensively reviewed by Utsunomia et al., these copolyesters can range from being thermoplastic to completely elastomeric depending on the 4HB fraction [82].

Doi's group carried out an in-depth investigation on the properties of this novel class of PHA using X-ray diffraction and differential scanning calorimetry (DSC), revealing that the integration of 4HB building blocks into the highly crystalline P(3HB) matrix causes a considerably stronger drop in lattice crystallinity than exhibited by 3HV fractions in P(3HB-co-3HV) copolyesters [83]. Later, the impact of different 4HB fractions in P(3HB-co-4HB) copolyesters on T_m , T_g , and storage modulus (E') was studied on compression-molded sheets, showing that all of these parameters decreased with increasing 4HB fraction. Yield stress and stress at break decreased only slightly with increasing 4HB content, while the elongation at break increased substantially, making such copolyesters highly flexible materials. Moreover, improved thermal stability was observed for melt-processed P(3HB-co-4HB) copolymer sheets with increased 4HB fractions [84].

4.2. Tianjin GreenBio Materials Co. Ltd.

Tianjin GreenBio Materials Co. Ltd. (GreenBio) in PR China was one of two companies that produced P(3HB-co-4HB). In 2009, GreenBio received a \$20 million investment from the strain collection *Deutsche Stammsammlung für Mikroorganismen und Zellkulturen* (DSMZ) to scale their PHA production from pilot- to industrial-scale bioreactors of 150 m³ volume [85]. Recombinant *Escherichia coli* was used as the production strain, and glucose was used as the primary carbon source along with 1,4-butanediol to produce the copolyesters. GreenBio used an organic solvent-based downstream process to recover the PHA copolymers followed by washing with water to remove the organic solvents. This complex downstream process was one of the primary causes for the high price of the PHA, sold under the trade name SoGreen™. Different grades of SoGreen™ were labeled as SoGreen-00X™, with "X" ranging from A to D (depending on 4HB fraction), all of them having a similar thermal decomposition temperature of about 286 to 290 °C.

According to the company's information disclosed online and in literature reports, the following SoGreen™ grades were commercially available: SoGreen-00A-1™ (3% 4HB), SoGreen-00B (12% 4HB), SoGreen-00C™ (16% 4HB), and SoGreen-00D™ (64% 4HB). SoGreen-00A-1™ had a T_m of 166 °C (manufacturer information [86]), and 150 °C according to reference [86]. SoGreen-00D™ had an outstandingly low T_m of 50 °C (manufacturer information) [85]. The standard material SoGreen-00B™ (12% 4HB) had a T_m of 125 °C (manufacturer information) [85], or 126 °C [87], while, surprisingly, SoGreen-00D™ was reported to have a comparatively high T_m of 152 °C [85]. Glass transition T_g decreased with increasing 4HB fraction (SoGreen-00A-1™: +4 °C [86], SoGreen-00C™: −8 °C [85]). Predictably, elongation at break drastically increased from 10% (SoGreen-00A™) to 775% (SoGreen-00D™) with increasing 4HB content (manufacturer information) [85]. GreenBio reportedly had a PHA production capacity of 10,000 t per year, and the company claimed it as the world's largest PHA production facility in 2021 [85]. Besides selling the pure P(3HB-co-4HB) resins, Tianjin Green Bioscience also modified their SoGreen™ products with undisclosed additives for several different applications; pellets for film blowing were sold as SoGreen 2013™ with an elongation at break of 174–180% and a tensile strength of 41–45 MPa for applications such as “fresh film, mulching film, laminating film, wrapping film, heat-shrinkable film, food packaging, shopping bags, garbage bags, gift bags, produce bags” (manufacturer information). Pellets for foam applications were sold as SoGreen 1023™ for expandable food-service ware, producing mesh foam bags for fruits, cushion pads, cushion fillers, etc. They had a tensile strength of 35 MPa, elongation at break of 300%, a flexural modulus of 1200 MPa, and a flexural strength of 48 MPa. Pellets for production of sheets, boards, and injection-molding products were commercialized as SoGreen 3001™. Mechanical properties of these products significantly differ from the more flexible products SoGreen 2013™ and 1023™: SoGreen 3001™ had a low tensile strength of 21 MPa and an elongation at break of only 42%, and it had lower flexural modulus and flexural strength of 25 MPa and 960 MPa, respectively [85].

However, GreenBio came under severe economic pressure [42]. GreenBio products did not perform as expected due to the insufficient market demand due to high product prices, which in turn was the result of high production costs, and it stopped its production about two years ago (personal communication by George Chen [43]).

4.3. Shenzhen Ecomann Biotechnology Co. Ltd.

Another Chinese P(3HB-co-4HB) manufacturer was Shenzhen Ecomann Biotechnology Co. Ltd., established in 2008 and located in Shenzhen, Guangdong. They processed their AmBio™ P(3HB-co-4HB) into customer-ready products like “aquarium biopellet filter media” (about 5000 t annual capacity, selling price ca. USD 14) and resins for film blowing (annual capacity of 5000 T; selling price 3.8–4.0 USD/kg). They also commercialized 500 t of PHA per year for biodegradable dog bags at a price below USD 0.01 per piece, and 500 t per year of PHA for the “Compostable and Biodegradable Green Bag” for shopping (USD 0.03 per piece), biodegradable bags for household and kitchen waste (“bin liners”; USD 0.02 per piece), mulch films made of PHA, biodegradable iPhone cases, and PHA 3D printing inks and filaments. All these bags were labeled “OK compost” (TÜV, Austria), indicating their home compostability [88]. The Ecomann grades of P(3HB-co-4HB) were labeled based on 4HB fraction in them such as EM 40000™ (3HB:4HB = 13:1), EM 20010™ (3HB:4HB = 18:1), and EM 10070™ (3HB:4HB = 10:1). Some blends were also sold containing PLA and fillers. Products such as EM 30000™ and EM 50000™ were also marketed, but their 4HB content was not reported. T_m values for these materials were between 140 and 160 °C (110–130 °C for EM 50000™). Tensile strength was reported to be 41–49 MPa (EM 40000™) and 38–40 MPa (EM 20010™), and degrees of crystallinity were around 15–16%. All materials were “OK compost HOME” certified and FDA approved. Raw Ecomann PHA was also sold as raw material to buyers such as BASF in China [88].

In a study by Coltelli et al. [89], Ecomann EM 5400 F™ was used to prepare skin-compatible beauty masks by blending with starch and embedding bioactive compounds to

be released to the skin under wet conditions. Calcium carbonate microparticles were added to control stickiness during molding, and their films were manufactured via compression molding. The prepared films were tested and turned out to be highly biocompatible in in vitro experiments. The authors blended Ecomann PHA with other biopolyesters such as PBAT, poly(butylene succinate-co-butylene adipate) (PBSA), and starch and prepared novel beauty masks. The ternary blends showed better processability during melt extrusion at 140 °C [89]. Their primary goal in going after their applications was to target the beauty care market, which they determined to be more than USD 5×10^{11} in 2017, with estimates of up to USD 8×10^{11} in 2025, a potentially large and important market opportunity for biocompatible and biodegradable PHA. The Ecomann P(3HB-co-4HB) grades were also tested in the biomedical field by Wu et al. [90], who prepared compression-molded membranes of this material after mixing it with chitosan in a Brabender. These materials showed high biocompatibility in a cytocompatibility test, in addition to antimicrobial activity which varied with the chitosan content, making them viable for wound dressing applications [90].

4.4. Metabolix and Cheiljedang Corporation

After the dissolution of the joint venture Telles, set up between ADM and Metabolix, Metabolix focused its attention on producing P(3HB-co-4HB) copolymers using recombinant *E. coli*. They already had experience in producing P(4HB) homopolymers which Tephra, a spin-out from Metabolix, uses in its products. Metabolix developed and produced a wide variety of P(3HB-co-4HB) copolymers starting from semicrystalline P(3HB-co-4HB) (5–15% 4HB; T_g –10 °C, T_m 119 °C, tensile strength 36 MPa) to amorphous P(3HB-co-4HB) (up to 50% 4HB; T_g –30 °C, tensile strength 1.5 MPa). The company claimed biodegradation of their products by 90% in marine environments after 120 days, depending on the 4HB fraction in the copolyesters and the thickness of the parts. Applications ranged from compostable shopping bags, rigid food containers, drinking straws, coffee capsules, mulching films, and fishing nets to formulations for controlled release of pesticides, for paper coating, and as 3D printing inks [91]. Most of the polymers were produced via contract manufacturing and no volume figures were released.

In 2016, Metabolix reorganized itself as Yield10 Biosciences, an agricultural bioscience company, led by Oliver Peoples, CEO, and Kristi Snell, CSO, both pioneers in PHA. Yield10 continues to develop PHA in camelina plants which they believe would allow them to reach price points similar to commodity plastics. In January 2021, Yield10 disclosed their successful field tests of prototype lines of the recombinant oil plant *Camelina sativa* engineered to accumulate PHA biopolymers (presumably P(3HB) homopolyester) directly in seeds, with PHA fractions in seeds reaching about 6%. For 2021, large field tests were envisaged, provided that regulatory approval by the authorities will be given [92,93].

The assets of Metabolix's microbial production of PHA along with the intellectual property were sold to CJ Cheiljedang, and CJ renamed the commercial entity CJ White Bio. CJ White Bio has recently reaffirmed their commitment to PHA and to the grades that Metabolix had come up with in many of the same markets. They have announced the establishment of a 5000 ton per year plant in Indonesia to produce P(3HB-co-4HB) [42,92].

4.5. PhaBuilder and Medpha

Several start-up companies were founded during the last several years in PR China to manufacture P(3HB-co-4HB) using the NGIB concept, similar to the COFCO process for P(3HB) homopolyester production, which has been mentioned above [39]. Among these companies, PhaBuilder produces P(3HB-co-4HB) by recombinant *Halomonas* ssp., a recombinant of the halophilic Chinese salt lake isolate *Halomonas* sp. TD01 (later: *Halomonas bluephagenesis* [94]), on an annual production scale of several tons [42]. They used a recombinant version of the strain *H. bluephagenesis* TD40, which was cultivated on a 5 m³ scale on glucose, corn steep liquor, and γ -butyrolactone (GBL) already in 2018. They reported to have obtained 100 g/L dry biomass containing 60.4% P(3HB-co-13.5 mol-%-

4HB) at a productivity of about 1.7 g/(L·h) [95]; the industrial process still uses the same feedstocks as described in this article (personal communication with George Chen) [43]. PhaBuilder's standard P(3HB-co-4HB), labeled "mP34HB 10", is a fully biodegradable and semicrystalline material. After granulation (prepared by blending with plasticizers, heat stabilizers, and processing additives), it can be used for film blowing, extrusion, injection molding, and 3D printing. mP34HB 10 is reported to biodegrade in different natural environments tested, such as seawater, freshwater, sewage, sludge, and soil, and undergoes composting. mP34HB 10 meets the requirements of biodegradation standards ASTM 6400 and EN13432. The material is also widely used in polymer modification with other compatible biobased materials such as PLA, other aliphatic polyesters (such as poly(butylene succinate) (PBS), PBSA, or PBAT), and thermoplastic starch (TPS), in addition to some non-biodegradable materials (such as TPU, PVAc, POM, PMMA, and ABS) [96].

PhaBuilder also plans to produce other types of PHA such as P(3HB), P(3HB-co-3HHx), and P(3HB-co-3HV). In addition, the company carries out extensive research for new applications of the 3HB monomer [42].

Medpha also produces P(3HB-co-4HB) biopolyesters on an industrial scale using the recombinant *Halomonas* spp. originally derived from *Halomonas* TD01; as the name indicates, this company concentrates on producing PHA explicitly for medical applications (personal communication with George Chen) [43].

4.6. Tepha Medical Devices Inc.

The linear, pliable homopolyester P(4HB) has remarkable material characteristics, which are completely different from those observed for the above-described short-chain-length (*scl*)-PHAs, such as P(3HB) and P(3HB-co-3HV). Most of all, P(4HB) has an exceptionally high elongation at break of up to 1000%, which makes it enormously stretchable and flexible. This compares favorably with other polymers such as PLA, poly(glycolic acid) (PGA), or P(3HB), which has an elongation at break of only about 3–7% [97,98], and poly(ϵ -caprolactone) (PCL), which has an elongation at break of about 60% [99]. Oriented P(4HB) fibers have tensile strength values of about 545 MPa, which is higher than for poly(propylene) (PP) sutures (410–460 MPa), making them very interesting and viable as biological fiber applications such as sutures, although P(4HB) sutures have a significantly lower Young's modulus than other marketed monofilament sutures [100].

In 2001, Metabolix Inc., Cambridge, USA, filed a patent for the production of P(4HB) and 4HB-rich copolyesters by using stable recombinant strains such as *E. coli* from inexpensive feedstocks. In 2007, the company Tepha Inc., USA, started, based on this patent, producing a range of PHA-based biomedical products in Lexington, MA, USA, e.g., P(4HB)-made TephaFLEX™ sutures, which are US Food and Drug Administration (FDA) approved in 2007 (notably, it is still the only PHA approved for biomedical application to date!) [82]. In addition, the entire production process is ISO 13485 compliant, referring to the quality management for manufacturing of medical devices; this also includes a patented downstream processing for yielding an "extremely high purity material" by a solvent–antisolvent process (US9480780B2). Tepha holds a high number of patents on production, processing, and application of their material P(4HB) homopolyester, which is produced using an engineered and recombinant *E. coli* K12 production strain. Generally, multifilament fibers, multifilament meshes, polymer tubing, and thin films can be produced from TephaFLEX™ products. A range of surgical materials based on P(4HB) or P(3HB-co-4HB) (trademark TephaELAST™), e.g., absorbable meshes (for hernia repair, wound support, tissue reinforcement), threads, or films for a variety of surgical procedures, are produced by Tepha Inc., Lexington, USA, [101], as are textile fibers for weaving, knitting, and braiding in cooperation with big textile manufacturers [102].

5. Industrializing P(3HB-co-3HHx) Copolyesters

5.1. Hybrid-Type PHA Copolyesters Consisting of *Scl*- and *Mcl*-PHA Building Blocks

Hybrid *scl-mcl*-PHA copolyesters consisting of 3HB and small amounts of medium-chain-length (*mcl*)-PHA building blocks (3HHx, 3-hydroxyoctanoate (3HO), 3-hydroxydecanoate (3HD)) were originally developed and patented by Isao Noda and coworkers. This Nodax™ type of PHA helps to overcome problems associated with well-established P(3HB-co-3HV) copolyesters, namely the “isodimorphism”, where 3HV units can be easily incorporated into the crystal 3HB-lattice and *vice versa*, thus preventing disruption of the highly crystalline matrix. *Mcl*-building blocks, in contrast, disturb the 3HB matrix even more efficiently than the achiral building block 4HB does. In particular, P(3HB-co-3HHx) with a 3HHx content of 10–17 mol-% features excellent flexibility, demonstrated through exceptionally high elongation at break of up to 850%, which outperforms commercially available P(3HB-co-3HV) with 20 mol-% 3HV [103]. Indeed, this group of PHAs currently holds great promise for a permanent industrial-scale production by different companies.

The first report on the production of such hybrid-type P(3HB-co-3HHx) copolyesters was provided by Kobayashi et al. [104], who showed production of poly(3-hydroxybutyrate-co-3-hydroxyhexanoate) (P(3HB-co-3HHx)) by *Aeromonas* spp. on fats and oils. This was a real scientific surprise at the time; before that, it became widely accepted that microbes produce either *scl*-PHA or *mcl*-PHA, simply depending on the type of PHA synthase active in a given production strain. These novel findings resulted in the first patent on such type of PHA by Shiotani and Kobayashi for Kanegafuchi (Kaneka) Chemical Industry Co. Ltd. (U.S. Patent 5,292,860, 1994), which already claimed the use of *Aeromonas caviae* as production strain. Later, patents for production of this type of PHA were filed by Procter & Gamble for the inventions in this field by Isao Noda (U.S. Patent 5,498,692, 1996; U.S. Patent 5,990,271, 1999), in addition to a patent on halogen-free processes for recovery for such *scl-mcl*-PHA copolyesters (U.S. Patent 5,942,597).

On a larger scale, such materials were for the first time produced by wild-type strain *Aeromonas hydrophila* cultivated on glucose during the balanced growth phase, followed by feeding lauric acid under phosphate limitation during the PHA accumulation phase. This strain was isolated from raw sewage samples by Sang Yup Lee’s group and turned out to produce P(3HB-co-3HHx) from lauric acid and oleic acid [105]. The large-scale process was described by Chen et al., who achieved a volumetric productivity for P(3HB-co-3HHx) containing 11 mol-% 3HHx of 0.54 g/(L·h) in a two-stage batch process on a 20 m³ scale, corresponding to a production of 100 g/L biomass containing 50% P(3HB-co-3HHx) within 46 h of cultivation [103]. Importantly, the authors underlined in this study that a typically low-productive batch cultivation mode was applied due to complications observed when running this process with *A. hydrophila* 4AK4 in fed-batch mode.

Besides wild-type *A. caviae*, genetically modified *Ralstonia eutropha* (today: *C. necator*) expressing the *Pseudomonas fluorescens* GK-13 synthase gene is also reported to accumulate *scl-mcl*-PHA hybrid copolyesters; dependent on the substrate provided (salts of different fatty acids), the generated copolyesters contained, besides 3HB, building blocks such as 3HHx, 3HO, 3HD, or 3HDD [106].

5.2. Danimer Scientific

Danimer Scientific was founded in 2004 to manufacture biobased polymers and their compounds with, for example, PLA and PHA. In 2007, Danimer Scientific purchased the assets of the Nodax™ PHA biopolymers from Procter & Gamble (P&G), Cincinnati, OH, USA. P&G had by then developed and industrially produced P(3HB-co-3HHx) biopolymers under the Nodax™ tradename based on their patents in the field. In 2013, Isao Noda joined DaniMer/Meredian Inc. after spending three decades with P&G; today, he is a member of the Board of Directors in addition to his many other responsibilities within Danimer Scientific. In 2014, Danimer and Meredian Inc. merged to form Meredian Holdings Group (MHG), which was then renamed to Danimer Scientific in 2016 and now produces Nodax™ P(3HB-co-3HHx) commercially in Bainbridge, Georgia, and Winchester, Kentucky.

The standard materials contain 5% 3HHx (T_m about 150 °C); sheets with 7.1% 3HHx (T_m 112–129 °C) and flakes/pellets with 6.5% 3HHx (T_m 121–146 °C) are also manufactured. Production is performed based on proprietary processes; not all details, e.g., bioreactor types, production strains, and downstream processing, are disclosed. Their production capacity is estimated at 10,000 t per year [20,107].

Recently, Danimer Scientific announced breaking ground in both Georgia and Kentucky for the construction of additional capacity in PHA production. A few months back, Danimer acquired the technology and assets of Novomer Inc., a start-up out of upstate New York. Novomer is reputed to have invented a pathway to produce poly(3-hydroxypropionate) (P(3HP)) polymers using a chemocatalytic pathway. P(3HP) is described to have excellent barrier properties. The beverage company Bacardi® announced that they have partnered with Danimer Scientific to convert their poly(ethylene terephthalate) (PET) bottles into PHA-based bottles, thus reducing about 3000 annual t (corresponding to 80 million bottles) of PET currently used to bottle their alcoholic drinks [107].

Production of P(3HB-co-3HHx), a hybrid *scl-mcl*-PHA, by Danimer Scientific starts from bioconversion of natural oils such as from palm, canola, or soy. There is some discrepancy about the production strain used for this process: while some sources report “presumably *A. caviae*” as production strain [20], others refer to “recombinant *R. eutropha*” [42]. According to Bacardi®, these “100% biodegradable spirit bottles” will biodegrade within 18 months in industrial composting facilities, soil, freshwater, and marine environments [108]. In addition, according to Danimer’s homepage, a “private-label manufacturer will use Danimer Scientific’s Nodax™ PHA for marine degradable straws with plans to expand into adjacent product categories”. This company appears to be Wincup®, which has now publicly announced the production and marketing of its PHA-based straws. According to a press release from December 2020, Kemira, a pulp and paper chemicals company, is currently evaluating “Danimer Scientific’s Nodax™ PHA as commercial, fully biobased alternative for polyethylene coatings to manufacture recyclable paper and board products from renewable sources” [109].

5.3. Kanegafuchi Chemical Industry Co. Ltd. (Kaneka)

Kaneka, headquartered in Minato-ku, Tokyo, is an early developer and producer of PHA biopolymers. Their PHA biopolymer PHBH™ is also P(3HB-co-3HHx), similar to Danimer Scientific, with differences in the 3HHx content in the final polymer. The above-mentioned patent (U.S. Patent 5,292,860, 1994) by Shiotani and Kobayashi for Kaneka, which claims the use of *Aeromonas* sp. for *scl-mcl*-PHA biosynthesis, forms the basis for Kaneka’s PHA biopolymer industrialization. It was later shared with Procter & Gamble, although the two companies P&G (and later Danimer Scientific) and Kaneka use different feedstocks, with Kaneka’s feedstock being palm oil and Danimer’s being Canola oil. Kaneka reportedly increased their production capacity to about 5000 t per year in 2020, an increase of about 5-fold from their previous capacity [110].

In Japan, approximately 10,000 Seven-Eleven Japan stores have started using PHBH™ drinking straws for Seven Café™ ice coffees since 2019 [111]. Moreover, in 2019, Kaneka launched the development of cosmetic containers with the company Shiseido Co. Ltd. (Tokyo, Japan); the product “AquaGel Lip Palette™”, a biodegradable container for makeup, has been commercially available since the end of 2020 [112]. In addition, many global brand holders are studying a wide range of applications for PHBH™ such as straws, plastic bags, cutlery, and food containers and packaging materials [110]. In addition, there is a project ongoing by Kaneka on teaching a polymer processing company in Kenya to produce PHBH™ waste bin liners as a contribution to reducing the plastic waste problem in developing countries [113].

Currently, Kaneka is also commercializing other grades of PHBH™ biopolymers such as rigid-grade X131A and X331N (6% 3HHx, 30% crystallinity) and semirigid grade X151A (11% 3HHx, about 5% crystallinity) [110]. Indeed, leading scientists from the PHA field such as Alexander Steinbüchel (University of Münster, Münster, Germany) currently

consider the industrialization endeavors for PHA by Kaneka the probably most promising activities for a large-scale market entry of these products (“I see only one technically reliable PHA product, the copolyester of 3HB and 3HHx produced by Kaneka in Japan, which is currently on the market.”) [114].

5.4. Bluepha

In the context of NGIB, the Chinese company Bluepha explicitly mentions on their internet site that “plastics should be from nature and go back to nature” [115]. This company uses a recombinant strain of the soil bacterium *C. necator* obtained by means of synthetic biology for production of P(3HB-co-3HHx) copolyesters (“Bluepha is programmer of cells”); a schematic of the process, presented by the company itself, is provided in Figure 2. The production scale of this plant is reported to be 1000 t annually [42]. According to the company, “alternative carbon sources” such as crops and kitchen waste are used as substrates for the cultivation, which is carried out in seawater. The Bluepha P(3HB-co-3HHx) is reported to be readily degraded both in seawater and soil within 3–6 months. The product is sold as pellets for injection molding, (aquarium) water restoration, textiles, and polymer films and as 3D-printing inks [115].

5.5. RWDC Industries Ltd.

The Singapore- and US-based company RWDC Industries Ltd. produces Solon™ PHA by upcycling waste cooking oil [116]. As a primary market, the company plans to replace an impressive quantity of “1.4 trillion (*sic!*) drinking straws by 2025” (press release; quantity and the true need for so many straws must be questioned) [117]. Based on a previously established technology, P(3HB-co-3HHx) is produced by a recombinant *C. necator* strain; on their internet site, the company discloses a PHA fraction of in cell biomass of 80%. Their new 25–50 kt plant in Athens, Georgia, is announced to be fully operational by the second half of 2021. This US-based facility is planned to initially produce about 4000 t of Solon™ per year, but the output is planned to increase to 350 kt by 2025, which would multiply the current global PHA productivity by more than 10 times. The company also plans to build more plants in Asia to meet the growing demand for biodegradable plastics in this region, which would consist of modular 25 kt production plants to be quickly installed at locations that are defined to be strategic to best serve customer demands. According to experts from the polymer industry, Solon™ PHA needs to be sold at less than USD 4 per kg in order for RWDC to succeed in the market. Besides drinking straws, the company plans to enter the market for coffee cups and lids, cutlery, light-weight shopping bags, foods containers, and textile fibers. According to the company’s CCO, Blake Lindsey, “The applications are endless and the impact is profound.” [118].

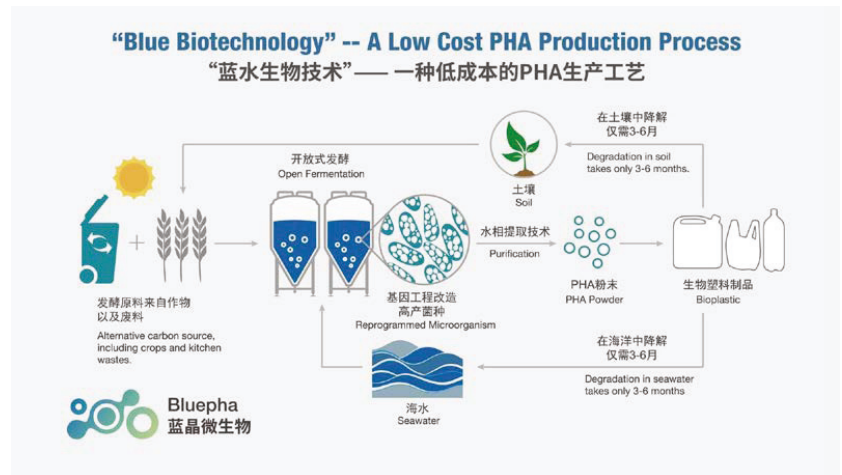


Figure 2. Illustration of the “Bluepha” process for industrial PHA production based on the principles of Next Generation Industrial Biotechnology (NGIB) [115]. The English and Chinese text are the same.

6. Industrializing *Mcl*-PHA Copolyesters

Regarding the types of PHA biopolymers produced on an industrial scale, there is, to the best of the authors’ knowledge, only one company commercializing *mcl*-PHA, a group of PHA with building blocks having at least six carbon atoms, such as 3HHx and longer monomers, at any scale: PolyFerm Canada, located in Ontario, produces VersaMer™ PHA as “irregular pieces, pellets, and latex”, encompassing, *inter alia*, P(3HO-*co*-3HHx), poly(3-hydroxyheptanoate-*co*-3-hydroxynonanoate) (P(3HHp-*co*-3HN)), and *mcl*-PHA containing also unsaturated building blocks. These materials have outstandingly low T_g (−45 to −35 °C), low T_m (45 to 65 °C), low molecular mass as is typical for *mcl*-PHA (100–150 kDa), and extraordinary high elongation at break of 1200–1400% [119]. In 2016, PolyFerm Canada licensed its technology to TerraVerdae Bioproducts, an industrial biotechnology company developing advanced bioplastics and biomaterials from C1-feedstocks. They are said to be scaling up *mcl*-PHA production based on personal communication with Bruce Ramsay, the cofounder of PolyFerm [120,121]. However, the majority of companies commercializing PHA are focusing on the “top-selling” *scl*-PHA products P(3HB), P(3HB-*co*-3HV), P(3HB-*co*-4HB), and P(3HB-*co*-3HHx), in addition to Tephra’s surgically important homopolymer P(4HB), as described in the previous sections.

7. Conclusions

As mentioned in the introduction, we are currently witnessing a significant wave of activities in PHA development and commercialization. While most of the commercial activities are focused on *scl*-PHA as bulk polymers such as P(3HB), P(3HB-*co*-3HV), P(3HB-*co*-4HB), and P(3HB-*co*-3HHx) and to a minor extent on P(4HB) and highly amorphous *mcl*-PHA copolyesters, most of these biopolymers are processed exclusively into single-use products. The next several years will draw a clearer picture about which concepts in the marketing of PHAs are indeed future-fit, be it in terms of market requirements, customer acceptance, sustainability, or economic feasibility. However, it is quite clear that the long-term success of commercial PHA needs to be grounded on some defined solid fundamentals: robust and powerful microbial production strains, optimized and simple cultivation facilities, amply available renewable feedstocks, and sustainable and inexpensive downstream processing technologies, pointing to its ease of production and acceptable price points that would allow its proliferation to serve various markets

In any case, considering the currently already well-established status of biotechnological PHA manufacturing and the far-developed understanding of the metabolic background of PHA biosynthesis, we can expect that the current wave of commercialization of PHAs has indeed started. This is in contrast to the first commercialization efforts for PHAs made several decades ago: That time, we witnessed some short-term efforts and successes in biopolymer production during periods of crude oil shortage and exploding prices of fossil resources, but rapidly declining interest in renewable-sourced polymers, chemicals, and solvents as soon as the price for fossil resources dropped again. Now, the time is ripe for a continued market presence of these biopolymers. During the next few years, it will be of utmost interest to follow which types of PHA biopolymers, industrialization concepts, production strains, raw material sources, cultivation modes, and applications (single-use or durable) will prevail in the long term.

Author Contributions: M.K., writing—original draft preparation, M.K. and A.M.; writing—review and editing, M.K.; visualization. All authors have read and agreed to the published version of the manuscript.

Funding: This research received no external funding.

Institutional Review Board Statement: Not applicable.

Informed Consent Statement: Not applicable.

Data Availability Statement: Not applicable.

Conflicts of Interest: The authors declare no conflict of interest.

References

1. Koller, M. Switching from petro-plastics to microbial polyhydroxyalkanoates (PHA): The biotechnological escape route of choice out of the plastic predicament. *EuroBiotech J.* **2019**, *3*, 32–44. [CrossRef]
2. UN General Assembly. Resolution A/60/L.22—Oceans and the Law of the Sea. Available online: https://www.un.org/en/development/desa/population/migration/generalassembly/docs/globalcompact/A_RES_60_30.pdf (accessed on 15 September 2021).
3. Dilkes-Hoffman, L.S.; Lant, P.A.; Laycock, B.; Pratt, S. The rate of biodegradation of PHA bioplastics in the marine environment: A meta-study. *Mar. Pollut. Bull.* **2019**, *142*, 15–24. [CrossRef] [PubMed]
4. Sharma, V.; Sehgal, R.; Gupta, R. Polyhydroxyalkanoate (PHA): Properties and modifications. *Polymer* **2021**, *212*, 123161. [CrossRef]
5. Braunegg, G.; Lefebvre, G.; Genser, K.F. Polyhydroxyalkanoates, biopolyesters from renewable resources: Physiological and engineering aspects. *J. Biotechnol.* **1998**, *65*, 127–161. [CrossRef]
6. Saratale, R.G.; Cho, S.K.; Saratale, G.D.; Kadam, A.A.; Ghodake, G.S.; Kumar, M.; Kim, D.S.; Mulla, S.I.; Shin, H.S. A comprehensive overview and recent advances on polyhydroxyalkanoates (PHA) production using various organic waste streams. *Bioresour. Technol.* **2021**, *325*, 124685. [CrossRef] [PubMed]
7. de Donno, M.L.; Moreno, S.; Rene, E.R. Polyhydroxyalkanoate (PHA) production via resource recovery from industrial waste streams: A review of techniques and perspectives. *Bioresour. Technol.* **2021**, *331*, 124985. [CrossRef] [PubMed]
8. Kourmentza, C.; Plácido, J.; Venetsaneas, N.; Burniol-Figols, A.; Varrone, C.; Gavala, H.N.; Reis, M.A. Recent advances and challenges towards sustainable polyhydroxyalkanoate (PHA) production. *Bioengineering* **2017**, *4*, 55. [CrossRef] [PubMed]
9. Zhang, X.; Lin, Y.; Wu, Q.; Wang, Y.; Chen, G.Q. Synthetic biology and genome-editing tools for improving PHA metabolic engineering. *Trends Biotechnol.* **2020**, *38*, 689–700. [CrossRef]
10. Zheng, Y.; Chen, J.C.; Ma, Y.M.; Chen, G.Q. Engineering biosynthesis of polyhydroxyalkanoates (PHA) for diversity and cost reduction. *Metab. Eng.* **2020**, *58*, 82–93. [CrossRef]
11. Chen, G.Q.; Chen, X.Y.; Wu, F.Q.; Chen, J.C. Polyhydroxyalkanoates (PHA) toward cost competitiveness and functionality. *Adv. Ind. Eng. Polym. Res.* **2020**, *3*, 1–7. [CrossRef]
12. Koller, M. Established and advanced approaches for recovery of microbial polyhydroxyalkanoate (PHA) biopolyesters from surrounding microbial biomass. *EuroBiotech J.* **2020**, *4*, 113–126. [CrossRef]
13. Park, S.J.; Kim, T.W.; Kim, M.K.; Lee, S.Y.; Lim, S.C. Advanced bacterial polyhydroxyalkanoates: Towards a versatile and sustainable platform for unnatural tailor-made polyesters. *Biotechnol. Adv.* **2012**, *30*, 1196–1206. [CrossRef] [PubMed]
14. Meereboer, K.W.; Misra, M.; Mohanty, A.K. Review of recent advances in the biodegradability of polyhydroxyalkanoate (PHA) bioplastics and their composites. *Green Chem.* **2020**, *22*, 5519–5558. [CrossRef]
15. Gigante, V.; Cinelli, P.; Seggiani, M.; Alavarez, V.A.; Lazzeri, A. Processing and Thermomechanical Properties of PHA. In *The Handbook of Polyhydroxyalkanoates*; Koller, M., Ed.; CRC Press: Boca Raton, FL, USA, 2020; Volume 3, pp. 91–118.

16. Puppi, D.; Chiellini, F. Additive manufacturing of PHA. In *The Handbook of Polyhydroxyalkanoates*; Koller, M., Ed.; CRC Press: Boca Raton, FL, USA, 2020; Volume 3, pp. 119–136.
17. European Commission. A European Green Deal. Available online: https://ec.europa.eu/info/strategy/priorities-2019-2024/european-green-deal_en (accessed on 7 September 2021).
18. Essel, R.; Carus, M. Meta analysis of 30 LCAs. *Bio-Plast. Mag.* **2012**, *7*, 46–49.
19. Koller, M. Chemical and biochemical engineering approaches in manufacturing polyhydroxyalkanoate (PHA) biopolyesters of tailored structure with focus on the diversity of building blocks. *Chem. Biochem. Eng. Q.* **2018**, *32*, 413–438. [CrossRef]
20. da Cruz Pradella, J.G. Economics and Industrial Aspects of PHA Production. In *The Handbook of Polyhydroxyalkanoates*; Koller, M., Ed.; CRC Press: Boca Raton, FL, USA, 2020; Volume 3, pp. 389–404.
21. Koller, M.; Maršálek, L.; Miranda de Sousa Dias, M.; Braunnegg, G. Producing microbial polyhydroxyalkanoate (PHA) biopolyesters in a sustainable manner. *N. Biotechnol.* **2017**, *37*, 24–38. [CrossRef]
22. Hänggi, U. Virgin PHB Has Thermoplastic Properties, but is not a Thermoplast. Available online: <http://www.biomer.de/K%C3%96LN2018.pdf> (accessed on 15 September 2021).
23. BASF. ecoflex®: Das Original Seit 1998–Zertifiziert Kompostierbarer Kunststoff. Available online: https://plastics-rubber.basf.com/global/de/performance_polymers/products/ecoflex.html (accessed on 10 September 2021).
24. Gregorova, A.; Wimmer, R.; Hrabalova, M.; Koller, M.; Ters, T.; Mundigler, N. Effect of surface modification of beech wood flour on mechanical and thermal properties of poly(3-hydroxybutyrate)/wood flour composites. *Holzforschung* **2009**, *63*, 565–570. [CrossRef]
25. Biomer. Injection Molded Articles Made of Renewable Raw Materials. Available online: <https://www.biomer.de/IndexE.html> (accessed on 13 September 2021).
26. Hänggi, U.; (Biomer, Schwalbach, Germany). Personal communication, 2021.
27. Arrieta, M.P.; López, J.; Hernández, A.; Rayón, E. Ternary PLA–PHB–Limonene blends intended for biodegradable food packaging applications. *Eur. Polym. J.* **2014**, *50*, 255–270. [CrossRef]
28. Smith, M.K.; Paleri, D.M.; Abdelwahab, M.; Mielewski, D.F.; Misra, M.; Mohanty, A.K. Sustainable composites from poly(3-hydroxybutyrate) (PHB) bioplastic and agave natural fibre. *Green Chem.* **2020**, *22*, 3906–3916. [CrossRef]
29. Nonato, R.; Mantelatto, P.; Rossell, C. Integrated production of biodegradable plastic, sugar and ethanol. *Appl. Microbiol. Biotechnol.* **2011**, *57*, 1–5.
30. Biocycle. BIOCYCLE 1000–Properties. Available online: http://www.biocycle.com.br/images/propriedades_1000_ing.pdf (accessed on 10 September 2021).
31. The Industry Gives Its First Steps. Available online: http://www.biocycle.com.br/imprensa_ing_01.htm (accessed on 10 September 2021).
32. TianAn Biopolymer. Available online: <http://www.tianan-enmat.com/index.html> (accessed on 14 September 2021).
33. TianAn. Available online: <http://www.tianan-enmat.com/product.html#> (accessed on 15 September 2021).
34. Nafigate. Bacteria Are the Key. Available online: <https://www.nafigate.com/hydal-biotechnology/> (accessed on 14 September 2021).
35. Nafigate. Naturetics: Cosmetics with PHA. Available online: <https://www.nafigate.com/portfolio/naturetics/> (accessed on 11 September 2021).
36. Newlight. Available online: <https://www.newlight.com/aircarbon> (accessed on 12 September 2021).
37. Newlight. Available online: <https://www.newlight.com/products> (accessed on 9 September 2021).
38. Covalent. Available online: <https://covalentfashion.com/> (accessed on 10 September 2021).
39. BioPlastics. Thyssenkrupp Commissions First Commercial Bioplastics Plant for COFCO in China. Available online: <https://www.bioplasticsmagazine.com/en/news/meldungen/20181018thyssenkrupp-commissions-first-commercial-bioplastics-plant-for-COFCO-in-China.php> (accessed on 10 September 2021).
40. Chen, G.-Q.; Jiang, X.-R. Next generation industrial biotechnology based on extremophilic bacteria. *Curr. Opin. Biotechnol.* **2018**, *50*, 94–100. [CrossRef]
41. Wu, F.; Chen, G.-Q. Next generation industrial biotechnology. In *The Handbook of Polyhydroxyalkanoates*; Koller, M., Ed.; CRC Press: Boca Raton, FL, USA, 2021; Volume 2, pp. 405–415.
42. Tan, D.; Wang, Y.; Tong, Y.; Chen, G.Q. Grand Challenges for Industrializing Polyhydroxyalkanoates (PHAs). *Trends Biotechnol.* **2021**, *39*, 953–963. [CrossRef]
43. Chen, G.Q.; (Tsinghua University, Beijing, China). Personal communication, 2021.
44. Tsinghua University; COFCO Nutrition and Health Research Institute Co., Ltd., Jilin; COFCO Biochemical Co., Ltd.; COFCO Biotechnology Co., Ltd. Chinese Patent 202010358327, 30 June 2020.
45. MangoMaterials. Available online: <https://www.mangomaterials.com/> (accessed on 10 September 2021).
46. Kovalick, A. Recent advances in 3D printing of polyhydroxyalkanoates: A review. *EuroBiotech. J.* **2021**, *5*, 48–55. [CrossRef]
47. Bio-On. Available online: <http://www.bio-on.it/> (accessed on 10 September 2021).
48. Kunststoff Web. Bio-On: Krisengeschtüttelter Biopolymer-Hersteller ist Pleite. Available online: https://www.kunststoffweb.de/branchen-news/bio-on_krisengeschtuetelter_biopolymer-hersteller_ist_pleite_t244145 (accessed on 10 September 2021).
49. Bio-On. Available online: <http://www.bio-on.it/biomedis.php?lin=inglese> (accessed on 10 September 2021).

50. GlobeNewswire. Bio-On Presents a Revolutionary New Technology to Eliminate Oil Pollution in the Sea within 3 Weeks. Available online: <https://www.globenewswire.com/news-release/2017/06/05/1008187/0/en/Bio-on-presents-a-revolutionary-new-technology-to-eliminate-oil-pollution-in-the-sea-within-3-weeks.html> (accessed on 10 September 2021).
51. Bio-On. Minerv Bio Cosmetics Formulation Type C1 Worldwide New Patent. Available online: <http://www.bio-on.it/minerv-cosmetics.php?lin=inglese> (accessed on 10 September 2021).
52. Bioplastics News. Bio-On and Unilever Revolutionise Sun Cream Industry with MyKai. Available online: <https://bioplasticsnews.com/2019/04/09/bio-on-and-unilever-revolutionise-sun-cream-industry-with-mykai/> (accessed on 10 September 2021).
53. Bio-On. Available online: <http://www.bio-on.it/minerv-supertoys.php?lin=inglese> (accessed on 10 September 2021).
54. Bio-On. Available online: <https://www.bioplasticsmagazine.com/en/news/meldungen/20191106Bio-on-patents-new-cigarette-filter-material-phi> (accessed on 10 September 2021).
55. Bio-On. Available online: http://www.bio-on.it/immagini/comunicati-finanziari/CS_82_BIO-ON_KARTELL_presenta_BIO (accessed on 10 September 2021).
56. Lemoigne, M. Études sur l'autolyse microbienne origine de l'acide β -oxybutyrique formé par autolyse. *Ann. Inst. Pasteur* **1927**, *41*, 148.
57. Wallen, L.L.; Davis, E.N. Biopolymers of activated sludge. *Environ. Sci. Technol.* **1972**, *6*, 161–164. [CrossRef]
58. Wallen, L.L.; Rohwedder, W.K. Poly-beta-hydroxyalkanoate from activated sludge. *Environ. Sci. Technol.* **1974**, *8*, 576–579. [CrossRef]
59. Findlay, R.H.; White, D.C. Polymeric beta-hydroxyalkanoates from environmental samples and *Bacillus megaterium*. *Appl. Environ. Microbiol.* **1983**, *45*, 71–78. [CrossRef] [PubMed]
60. Morikawa, H.; Marchessault, R.H. Pyrolysis of bacterial polyalkanoates. *Can. J. Chem.* **1981**, *59*, 2306–2313. [CrossRef]
61. Holmes, P.A.; Wright, L.F.; Collins, S.H. Beta-Hydroxybutyrate Polymers. European Patent EP0052459A1, 30 October 1981.
62. Luzier, W.D. Materials derived from biomass/biodegradable materials. *Proc. Nat. Acad. Sci. USA* **1982**, *89*, 839–842. [CrossRef]
63. Liggat, J. ICI's BIOPOL Cautionary Tales. Available online: <https://www.scotchem.ac.uk/wp-content/uploads/2019/02/Biopol-IBioC-compressed.pdf> (accessed on 10 September 2021).
64. Mirelplastics. Available online: <http://www.mirelplastics.com/> (accessed on 10 September 2021).
65. Lu, H.; Madbouly, S.A.; Schrader, J.A.; Kessler, M.R.; Grewell, D.; Graves, W.R. Novel bio-based composites of polyhydroxyalkanoate (PHA)/distillers dried grains with solubles (DDGS). *RSC Adv.* **2014**, *4*, 39802–39808. [CrossRef]
66. Mirelplastics. Available online: <http://www.mirelplastics.com/wp-content/uploads/2017/03/011212-MBLXAnnoucesTerminationTellesJV-1.pdf> (accessed on 10 September 2021).
67. Biokunststoffe.de. Available online: http://www.biokunststoffe.de/index.php?option=com_content&view=article&id=1598%3A009metabolixarticle&lang=de (accessed on 10 September 2021).
68. BIOCYLE—Sustainable Polymer from Sugar Cane. Available online: https://dc.engconfintl.org/cgi/viewcontent.cgi?article=1015&context=bioenergy_ii (accessed on 10 September 2021).
69. Rocha, R.C.; da Silva, L.F.; Taciro, M.K.; Pradella, J.G. Production of poly(3-hydroxybutyrate-co-3-hydroxyvalerate) P(3HB-co-3HV) with a broad range of 3HV content at high yields by *Burkholderia sacchari* IPT 189. *World J. Microb. Biot.* **2008**, *24*, 427–431. [CrossRef]
70. Ashby, R.D.; Solaiman, D.K.; Nuñez, A.; Strahan, G.D.; Johnston, D.B. *Burkholderia sacchari* DSM 17165: A source of compositionally-tunable block-copolymeric short-chain poly(hydroxyalkanoates) from xylose and levulinic acid. *Bioresource Technol.* **2018**, *253*, 333–342. [CrossRef] [PubMed]
71. Kovalcik, A.; Machovsky, M.; Kozakova, Z.; Koller, M. Designing packaging materials with viscoelastic and gas barrier properties by optimized processing of poly(3-hydroxybutyrate-co-3-hydroxyvalerate) with lignin. *React. Funct. Polym.* **2015**, *94*, 25–34. [CrossRef]
72. Modi, S.; Koelling, K.; Vodovotz, Y. Assessing the mechanical, phase inversion, and rheological properties of poly-[(R)-3-hydroxybutyrate-co-(R)-3-hydroxyvalerate] (PHBV) blended with poly-(L-lactic acid) (PLA). *Eur. Polym. J.* **2013**, *49*, 3681–3690. [CrossRef]
73. Montano-Herrera, L.; Pratt, S.; Arcos-Hernandez, M.V.; Halley, P.J.; Lant, P.A.; Werker, A.; Laycock, B. In-line monitoring of thermal degradation of PHA during melt-processing by Near-Infrared spectroscopy. *New Biotechnol.* **2014**, *31*, 357–363. [CrossRef]
74. Luo, S.; Cao, J.; McDonald, A.G. Esterification of industrial lignin and its effect on the resulting poly(3-hydroxybutyrate-co-3-hydroxyvalerate) or polypropylene blends. *Ind. Crops Prod.* **2017**, *97*, 281–291. [CrossRef]
75. Larsson, M.; Markbo, O.; Jannasch, P. Melt processability and thermomechanical properties of blends based on polyhydroxyalkanoates and poly(butylene adipate-co-terephthalate). *RSC Adv.* **2016**, *6*, 44354–44363. [CrossRef]
76. HelianPolymers. Available online: <https://helianpolymers.com/enmat-y3000p-phb-polymer-for-injection-molding-thermoforming.html> (accessed on 10 September 2021).
77. Meereboer, K.W.; Pal, A.K.; Cisneros-López, E.O.; Misra, M.; Mohanty, A.K. The effect of natural fillers on the marine biodegradation behaviour of poly(3-hydroxybutyrate-co-3-hydroxyvalerate) (PHBV). *Sci. Rep.* **2021**, *11*, 911. [CrossRef]
78. Genecis. Available online: <https://genecis.co/> (accessed on 10 September 2021).
79. Bioextrax. Available online: <https://bioextrax.com/wp-content/uploads/2020/04/Bioextrax-PHA-one-pager-April-20.pdf> (accessed on 10 September 2021).
80. Hall, E.; (CEO Bioextrax AB, Lund, Sweden). Personal communication, 2021.

81. Doi, Y.; Kunioka, M.; Nakamura, Y.; Soga, K. Nuclear magnetic resonance studies on unusual bacterial copolyesters of 3-hydroxybutyrate and 4-hydroxybutyrate. *Macromolecules* **1988**, *21*, 2722–2727. [CrossRef]
82. Utsunomia, C.; Ren, Q.; Zinn, M. Poly(4-hydroxybutyrate): Current state and perspectives. *Front. Bioeng. Biotechnol.* **2020**, *8*, 257. [CrossRef]
83. Kunioka, M.; Kawaguchi, Y.; Doi, Y. Production of biodegradable copolyesters of 3-hydroxybutyrate and 4-hydroxybutyrate by *Alcaligenes eutrophus*. *Appl. Microbiol. Biotechnol.* **1989**, *30*, 569–573. [CrossRef]
84. Cong, C.; Zhang, S.; Xu, R.; Lu, W.; Yu, D. The influence of 4HB content on the properties of poly(3-hydroxybutyrate-co-4-hydroxybutyrate) based on melt molded sheets. *J. Appl. Polym. Sci.* **2008**, *109*, 1962. [CrossRef]
85. Tjgreenbio. Available online: <http://www.tjgreenbio.com> (accessed on 10 September 2021).
86. Larsson, M.; Hetherington, C.J.; Wallenberg, R.; Jannasch, P. Effect of hydrophobically modified graphene oxide on the properties of poly(3-hydroxybutyrate-co-4-hydroxybutyrate). *Polymer* **2017**, *108*, 66–77. [CrossRef]
87. Khandal, D.; Pollet, E.; Averous, L. Elaboration and behavior of poly(3-hydroxybutyrate-co-4-hydroxybutyrate)-nano-biocomposites based on montmorillonite or sepiolite nanoclays. *Eur. Polym. J.* **2016**, *81*, 64–76. [CrossRef]
88. Made-in-China. Available online: <https://ecomann.en.made-in-china.com/> (accessed on 10 September 2021).
89. Coltelli, M.B.; Panariello, L.; Morganti, P.; Danti, S.; Baroni, A.; Lazzeri, A.; Fusco, A.; Donnarumma, G. Skin-compatible biobased beauty masks prepared by extrusion. *J. Funct. Biomater.* **2020**, *11*, 23. [CrossRef]
90. Wu, C.S.; Hsu, Y.C.; Liao, H.T.; Cai, Y.X. Antibacterial activity and in vitro evaluation of the biocompatibility of chitosan-based polysaccharide/polyester membranes. *Carbohydr. Polym.* **2015**, *134*, 438–447. [CrossRef]
91. CJ Bio. Available online: <https://www.cjbio.net/en/products/cjPha.do> (accessed on 10 September 2021).
92. ABC News. What to Know about PHA Biodegradable Plastic and How It Could Help Southeast Asia. Available online: <https://abcnews.go.com/Business/pha-biodegradable-plastic-southeast-asia/story?id=78859058> (accessed on 10 September 2021).
93. Yeld10 Bioscience. Yeld10 Bioscience Announces Achievement of Proof-of-Concept Milestone for Producing PHA Bioplastic in Field Grown Camelina Plants. Available online: <https://www.globenewswire.com/news-release/2021/01/19/2160613/0/en/Yeld10-Bioscience-Announces-Achievement-of-Proof-of-Concept-Milestone-for-Producing-PHA-Bioplastic-in-Field-Grown-Camelina-Plants.html> (accessed on 10 September 2021).
94. Tan, D.; Wu, Q.; Chen, J.C.; Chen, G.Q. Engineering *Halomonas* TD01 for the low-cost production of polyhydroxyalkanoates. *Metab. Eng.* **2014**, *26*, 34–47. [CrossRef]
95. Ye, J.; Hu, D.; Che, X.; Jiang, X.; Li, T.; Chen, J.; Zhang, H.M.; Chen, G.Q. Engineering of *Halomonas bluephagenesis* for low cost production of poly(3-hydroxybutyrate-co-4-hydroxybutyrate) from glucose. *Metab. Eng.* **2018**, *47*, 143–152. [CrossRef]
96. PHABuilder. Available online: <http://www.phabuilder.cn/> (accessed on 10 September 2021).
97. Chen, B.K.; Shen, C.H.; Chen, S.C.; Chen, A.F. Ductile PLA modified with methacryloyloxyalkyl isocyanate improves mechanical properties. *Polymer* **2010**, *51*, 4667–4672. [CrossRef]
98. Jun, C.L. Reactive blending of biodegradable polymers: PLA and starch. *J. Polym. Environ.* **2000**, *8*, 33–37. [CrossRef]
99. Rosa, D.S.; Guedes, C.G.F.; Bardi, M.A.G. Evaluation of thermal, mechanical and morphological properties of PCL/CA and PCL/CA/PE-g-GMA blends. *Polym. Test.* **2007**, *26*, 209–215. [CrossRef]
100. Martin, D.P.; Williams, S.F. Medical applications of poly-4-hydroxybutyrate: A strong flexible absorbable biomaterial. *Biochem. Eng. J.* **2003**, *16*, 97–105. [CrossRef]
101. Brigham, C.J.; Sinskey, A.J. Applications of polyhydroxyalkanoates in the medical industry. *Int. J. Biotechnol. Wellness Ind.* **2012**, *1*, 52–60. [CrossRef]
102. Tepha Medical Devices. Available online: <https://www.tepha.com/technology/overview/> (accessed on 10 September 2021).
103. Chen, G.; Zhang, G.; Park, S.; Lee, S. Industrial scale production of poly(3-hydroxybutyrate-co-3-hydroxyhexanoate). *Appl. Microbiol. Biotechnol.* **2001**, *57*, 50–55. [PubMed]
104. Kobayashi, G.; Shiotani, T.; Shima, Y.; Doi, Y. Biosynthesis and characterization of poly(3-hydroxybutyrate-co-3-hydroxyhexanoate) from oils and fats by *Aeromonas* sp. OL-338 and *Aeromonas* sp. FA440. In *Biodegradable Plastics and Polymers*; Doi, Y., Fukuda, K., Eds.; Elsevier: Amsterdam, The Netherlands, 1994; pp. 410–416.
105. Lee, S.H.; Oh, D.H.; Ahn, W.S.; Lee, Y.; Choi, J.I.; Lee, S.Y. Production of poly(3-hydroxybutyrate-co-3-hydroxyhexanoate) by high-cell-density cultivation of *Aeromonas hydrophila*. *Biotechnol. Bioeng.* **2000**, *67*, 240–244. [CrossRef]
106. Noda, I.; Green, P.R.; Satkowski, M.M.; Schechtman, L.A. Preparation and properties of a novel class of polyhydroxyalkanoate copolymers. *Biomacromolecules* **2005**, *6*, 580–586. [CrossRef]
107. Danimer Scientific. Available online: <https://danimerscientific.com/pha-beginning-of-life/> (accessed on 15 September 2021).
108. Bacardi Limited. Available online: <https://www.bacardilimited.com/media/news-archive/bacardi-first-in-fight-against-plastic-pollution-with-100-biodegradable-spirits-bottle/> (accessed on 15 September 2021).
109. Danimer Scientific. Kemira Announces Partnership with Danimer Scientific to Develop Biodegradable Coating for Paper and Board Industry. Available online: <https://danimerscientific.com/2020/12/09/kemira-announces-partnership-with-danimer-scientific-to-develop-biodegradable-coating-for-paper-and-board-industry/> (accessed on 15 September 2021).
110. Kaneka Biopolymers. Available online: <https://kanekabiopolymers.com/> (accessed on 15 September 2021).
111. Kaneka. Kaneka Biodegradable Polymer PHBH™ Applied to Straws for Seven Café's New Lineup. Available online: <https://www.kaneka.co.jp/en/topics/news/2020/ennr2005291.html> (accessed on 15 September 2021).

112. Kaneka. Kaneka Biodegradable Polymer PHBH™ Used in Shiseido's Cosmetics Packages. Available online: <https://www.kaneka.co.jp/en/topics/news/2020/ennr2008061.html> (accessed on 15 September 2021).
113. Global Bioeconomy Summit 2018. Marketing of Kaneka Biodegradable Polymer PHBH™ as a Solution to Plastic Waste Issues. Available online: <https://cupdf.com/document/marketing-of-kaneka-biodegradable-polymer-phbhtm-kaneka-biodegradable-polymer.html> (accessed on 15 September 2021).
114. Steinbüchel, A. Foreword. In *The Handbook of Polyhydroxyalkanoates*; Koller, M., Ed.; CRC Press: Boca Raton, FL, USA, 2020; Volume 1, pp. 13–15.
115. Bluepha. PHA Bioplastic. Available online: <http://en.bluepha.com/pha-bioplastic> (accessed on 15 September 2021).
116. RWDC Industries. Available online: <https://www.rwdc-industries.com/technology> (accessed on 15 September 2021).
117. TechInAsia. Does this \$133m Bet on Biodegradable 'Plastic' Hold Water? Available online: <https://www.techinasia.com/133m-bet-biodegradable-plastic-hold-water> (accessed on 15 September 2021).
118. Solon. Products & Applications. Available online: <https://www.solon.eco/products-and-applications> (accessed on 15 September 2021).
119. PolyFerm Canada. VersaMer™ PHAs. Available online: https://www.polyfermcanada.com/versamer_phas.html (accessed on 15 September 2021).
120. The Free Library. TerraVerdae Expands Elastomeric PHA Biomaterials Portfolio via PolyFerm Canada Partnership. Available online: <https://www.thefreelibrary.com/TerraVerdae+Expands+Elastomeric+PHA+Biomaterials+Portfolio+via...-a0439704651> (accessed on 15 September 2021).
121. Ramsay, B.; (Polyferm Canada, Kingston, ON, Canada). Personal communication, 2021.

MDPI
St. Alban-Anlage 66
4052 Basel
Switzerland
Tel. +41 61 683 77 34
Fax +41 61 302 89 18
www.mdpi.com

Bioengineering Editorial Office
E-mail: bioengineering@mdpi.com
www.mdpi.com/journal/bioengineering



MDPI
St. Alban-Anlage 66
4052 Basel
Switzerland

Tel: +41 61 683 77 34

www.mdpi.com



ISBN 978-3-0365-5040-4